A STUDY OF INTUMESCENT COATINGS

BY

MALKIT SINGH DEOGON

MATERIALS TECHNOLOGY DEPARTMENT

BRUNEL UNIVERSITY

UXBRIDGE

UB8 3PH

SUBMITTED FOR THE DEGREE OF DOCTOR OF PHILOSPOHY

MARCH 1989

TO

SUCHKHAND VASI SANT BABA PURAN SINGH JI

"we may read as long as we live and breath;

Yet, Nanak, there is only one truth that matters;

all else is vanity and vexation of spirit"

GURU NANAK

ACKNOWLEDGEMENT

I would like to thank the following people for their guidance, encouragement and continuous intrest and support which made it possible for me to carry out these studies:

1) Dr. G. Socrates for his unceasing encouragement and help

2) Dr. R. Hall for his help with the mathematics

3) all my colleagues at London Scientific Services

4) my family for their understanding and patience, particularly my wife Satinder.

I am sincerely indebted to Suchkhand Vasi, Sant, Baba Puran Singh Ji and Bhai Shaib, Naurang Singh Ji for their spiritual guidance and blessings, without which this task would have been impossible for me to achieve in the time limits set for the project.

INDEX

ABSTRACT

Intumescent coatings are used in the field of fire protection to prevent certain construction elements reaching the critical temperatures at which excessive damage would occur, thus avoiding premature structural collapse.

The studies presented in this thesis have been directed towards an understanding of intumescent coatings and the process of intumescence. The kinetics and mechanism of intumescence are discussed. The behaviour of the raw materials used in the preparation of intumescent coatings, was studied at elevated temperatures using thermal analytical techniques, and new formulations were developed. These formulations were examined in the laboratory using various screening tests and were also subjected to a large scale hydrocarbon fire test alongside other commercially-available coatings.

A simplified coating formulation with the minimum of ingredients required to produce good intumescent properties was developed. This formulation was subjected to various heat-radiation intensities using an ISO ignitability apparatus. The behaviour of the intumescence process observed was explained by a simple theoretical model. The model of Buckmaster, Anderson and Nachman was used and several new results were derived. In particular a relationship was derived giving the time taken for the temperature at the inner surface of the coating to reach a given value.

The durability of the newly-developed intumescent coatings, and methods of improving it, were also investigated.

SECTION 1

INTUMESCENT COATINGS

1.1 INTRODUCTION

Traditionally, fire protection of building elements has relied solely upon the ability of passive systems to provide the necessary insulation and fire retardation. Various types of fire-resisting materials are sold by manufacturers, along with accompanying test data on fire ratings. Modern technology has yielded new, lightweight materials, such as intumescent paints, which are superior to the older, masonry materials, and have greater or equivalent fire-resistance with a greatly reduced add-on weight to the construction.

Intumescent fire-proofing compositions are particularly effective as an active type of fire-protection system and provide thermal insulation with only a small increase in weight and thickness. Such fire-retardant coatings offer some significant advantages over passive types of fire protection:

1) They have many of the desirable features of traditional decorative coatings, viz, colour, finish, etc, which are architecturally pleasing.
2) They have an insignificant effect on the mass of the structure.
3) They do not occupy valuable floor space.
4) They can be applied to existing structures without loss of architectural detail, eg in historic buildings.
5) Because of ease of application, they are labour efficient.
6) Depending upon the individual formulation and thickness of application, they can be cost effective.

7) As the coatings are an integral part of the structure, they do not require any further fixtures or fixings.

8) Oxidation in a fire may cause failures well below the theoretically-critical temperature of metals and in such cases intumescent coatings are especially suitable since they evolve non-flammable gases when exposed to fire, thus preventing access of oxygen.

1.2 INTUMESCENT COATINGS

By definition, an **APHROGEN** is a substance that will be converted into a foam or a sponge when exposed to heat, a **PYROSTAT** is a substance that quenches a fire, and a **PYRO THERMAL INSULANT** insulates a substance from the heat of a fire. Thus an intumescent coating is an **APHROGENIC PYROSTATIC THERMAL INSULANT.**

Intumescent paint under normal conditions is a relatively thin coating which has the same protective functions as any other paint. In a thermal environment, it responds dynamically, decomposing and releasing gases - decomposition products - which can:

1) convectively and conductively block heat transfer to the substrate by the cellular structure evolved

2) suppress flames near the coating boundary layer

3) attenuate incident radiation

4) prevent oxygen getting to the substrate

5) prevent heat build up due to the endothermic nature of the reactions involved.

Generally, intumescent coatings are composed of the following basic ingredients:

1) An inorganic acid or an acid-yielding material at temperatures between 100°C and 250°C - **Catalyst.**

2) A polyhydric material rich in carbon - **Carbonific.**

3) An organic amine, amide or azo compound - **Primary Spumific.**

4) A halogenated material or other suitable material which can decompose and serve as a blowing agent - **Secondary Spumific.**

5) A synthetic resin which bonds the ingredients to each other and to the surface of the substrate when the paint is dry - **Binder.**

6) A hydrated salt to release the water of crystallisation (e.g. borax, sodium silicate, aluminum hydroxide, ammonium phosphate, etc.) - **Hydrated Salt.**

7) Smoke suppressant, nucleating agents, viscosity controllers, char surface tensioner, fibres, coalescents, thickeners, pigments, driers insulative materials, ablative materials etc. - **Agents/Fillers.**

Most formulations contain an example of each, although in some cases other ingredients are also included e.g. rare earth salts, organo-silicon compounds etc.

Over the last few years, a number of different systems have been developed which can be summarised as follows:

a) Elastomer-based polymeric compositions containing compounds which release large amounts of gases during heating and producing a charred foam which acts as a temporary barrier (1).

b) Elastomer-based compounds which rely upon hydrated salts to produce the intumescence (2).

c) Acetal binders such as melamine, phenol formaldehyde, urea formaldehyde etc., filled with intumescent ingredients (3).

d) Various binder compositions containing alkali silicates (4).

e) Aniline-bisulphite and related compounds which produce voluminous amounts of char upon heating (5).

When a coated substrate is subjected to intense heat, the coating protects the substrate in at least three separate ways:

1. The endothermic decomposition of the intumescent filler consumes energy.

2. Inert gases are evolved that expand the resulting carbonaceous char and drive back the convective hot-air currents.

3. The thick, expanded char layer which is permeated with entrapped, multi-cellular, gas pockets serves as an effective heat insulator.

In general, a low-density cohesive cellular char foam is formed when the coating, subjected to heat, decomposes and intumesces, that is, bubbles and grows from the surface of the coating (49), thus interposing a good thermal insulator between the heat source and the substrate (see Fig. 1). The char has a volume that is up to 400 times the original volume. The effectiveness of an intumescent protective coating or fireproofing is partly dependent on the physical properties of the char evolved. As the char develops, the surface emissivity (the total energy emitted via radiation) rises, rejecting heat rates proportional to the fourth power of the temperature in accordance with the Stefan's Law. Vandersall (49) reports that a suitable char consists of a system of closed cells between 30 to 50 μm in diameter. The rate of heat transfer through the char layer is dependent on the cell size. Theoretically, as the cell size increases above these values, internal cell circulation currents become greater and thermal conductivity is increased. Cagliostro and Riccitiello have estimated the effectiveness of insulation as a function of thermal conductivity (114). The insulation and protection offered by this char is of considerable value to structural fire protection, this being one of the major uses of such coatings.

The behaviour of intumescent coatings in real fire situations is not fully understood. Thus to be able to relate the theoretical aspects of the present study to an end application, the mathematical modelling has in the main taken into consideration the specifications given in BS 476 : Part 8, although exposure to other heating conditions has also been considered.

The aim of this thesis is to shed more light on the complicated reactions and mechanisms involved in the carbohydrate-phosphoric acid systems, as well as examining the theoretical aspects of intumescence in general.

It is important to state briefly the background to structural fire protection and the determination of 'fire resistance' given in BS 476 Part 8, before proceeding with the chemistry of the intumescence.

FIGURE 1A

A TYPICAL HOLLOW SECTION AFTER EXPOSURE TO FIRE

FIGURE 1B

A TYPICAL INTUMESCENT FOAM IN THE WEB OF AN I-SECTION BEAM

FIGURE 1C

INTUMESCENT COATING BEFORE AND AFTER EXPOSURE

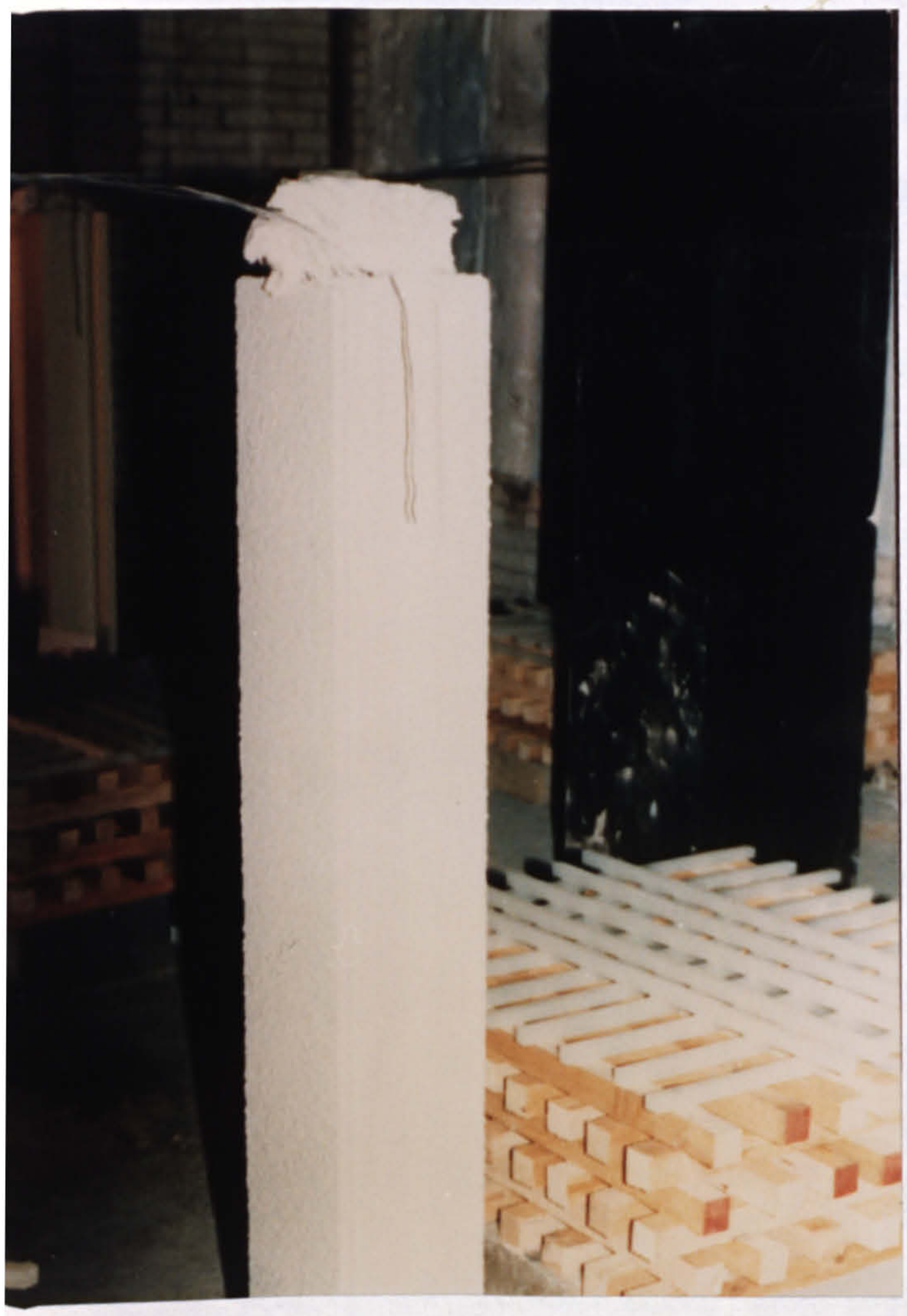

BEFORE EXPOSURE

AFTER EXPOSURE

SECTION 2

STRUCTURAL STEEL FIRE PROTECTION

2.1. STRUCTURAL FIRE PROTECTION - HISTORICAL BACKGROUND

The first recorded attempt of any significance to legislate for the control of fire spread seems to have taken place during the London Assizes 1189. The legislation laid down that the houses in the City were to be built of stone, thatched roofs were not to be permitted, and party walls were to be of a minimum height and thickness. However, there was no means of enforcing control of these requirements.

Modern and contemporary references (6-9) illustrate the progress of fire protection activity after the Great Fire of London (1667) which dramatically drew attention to the need for building control. Structural fire protection first began to be investigated seriously in the second half of the 18th century (9). Considerable advances were made in materials technology in the 19th century, making available substances such as concrete and rolled steel. This enabled the first 'fire proof' structures to be built.

2.1.2. EXISTING LEGISLATION AND REQUIREMENTS

It has been generally accepted that the primary purpose of the statutory requirements for structural fire precautions is to safeguard life, whereas the protection of the property is assumed to be covered by insurance interests. Thirty-nine statutory provisions relating to fire are listed in the 'Review of Fire Policy' published by the Home Office (10). For the fire brigades, there is the consideration that under fire conditions the structure, including floors, must have adequate load-bearing capacity.

Regulatory control is concerned with safeguarding occupants of buildings and minimising the risk to the adjacent buildings. Although the control is concerned with the behaviour of the building as a whole, the requirements apply to the individual elements of the construction as well.

Not only should all the main load-bearing members retain their stability in a fire but also those which provide structural support to them. If fire-resistance requirements apply to a floor, then the beam or column system or walls which are providing structural support to that floor must all have fire resistance not less than that expected of the floor itself.

2.1.3. METHODS OF COMPLIANCE

Currently, there are the following methods available to provide evidence of the ability of a construction to provide fire resistance:

a) standard tests to BS 476 : Part 8

b) alternatives to the standard test - 'deemed to satisfy' the regulations and by-laws

c) extrapolation and interpolation

d) analysis of structural performance.

In England and Wales the standard test means that when a specimen is subjected to the test specified in BS 476 : Part 8 : 1972 it should satisfy the relevant requirement of the test for not less than the specifed period.

The 'deemed to satisfy' data is an alternative to the standard test which is acceptable in regulations and by-laws. These are test data derived by various assessments.

There is no recognised technique at present for the extrapolation and interpolation of fire test data

The analysis of structural behaviour is not recognised at present by the authorities as a method of complying with the requirements for fire resistance.

2.1.4. ROLE OF STRUCTURAL FIRE PROTECTION

Structural fire protection may be defined as the application of structural design features which retard the spread of flame and the rate at which the effects of exposure to fire are felt by a building. The fire protection acts, basically, as a thermal insulation barrier for the steel, so increasing the time taken to achieve the critical temperature at which loss in structural strength occurs - 550°C for most mild steels (11-17,30). This also allows a longer period for the fire to be extinguished.

The fire protection may be either passive or active. The former is part of the built system and is functional at all times, while the latter comes into operation on the occurrence of a fire. Both systems serve to: a) prevent the initiation of fire, b) restrict the growth and spread of fire, c) maintain the integrity of safe areas in a building, d) prevent the building structure from becoming unstable.

2.2. FIRE PROTECTION AND PROPERTIES OF STEEL

The construction industry favours the use of steel over any other material in the fabrication of most structures; tall buildings are constructed with steel columns and beams, convention centres with steel trusses, and large parts of stadiums with cantilevered steel supports. There are two distinct ways in which steel is used in building construction - either as a structural

material or as reinforcement in concrete.

STRUCTURAL STEEL (BS 4360), grades 43 and 50 , have the following nominal properties (17):

GRADE	YIELD STRENGTH	ULTIMATE TENSILE STRENGTH	DESIGN STRENGTH
43A	250 N/mm^2	440 N/mm^2	165 N/mm^2
50B	350 N/mm^2	580 N/mm^2	230 N/mm^2

Figure 2 shows stress-strain curves for a mild steel and a cold drawn steel.

FIGURE 2

(Reference 16)

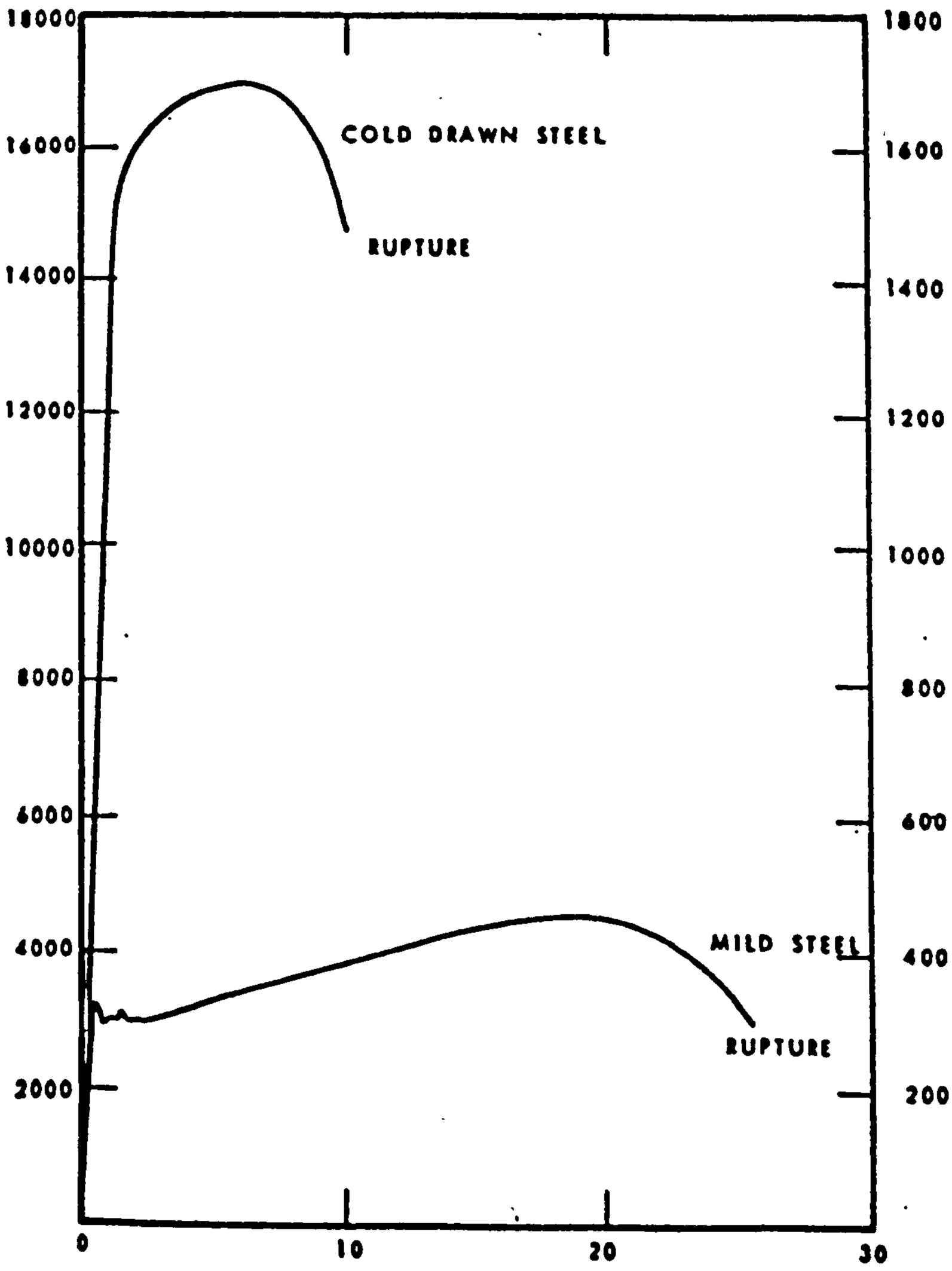

Although steel is non-combustible, and does not contribute fuel to the fire, it does lose its strength when exposed to the high temperatures of most fires. When steel reaches the critical temperature of 550°C its yield stress is approximately 60% of its value at room temperature (17). Another critical factor is that, during a fire, the large amount of heat generated causes steel to expand, which brings about the subsequent collapse of the walls.

Architects, designers and engineers tend to choose as light a steel as possible, bearing in mind cost, strength and safety factors required. In general, heavy, fire-resistant protection added to structures, requires heavy steel sections for support. Alternatively, a fire-protection system which is light may be used -namely, intumescent coatings.

The failure temperature of steel depends on the quality of the steel, its load, and structural features such as composite action, restraint and continuity. However, in this thesis, unless otherwise stated, a steel failure temperature of 550°C has been adopted as it is the temperature used by BS 476 Part 8. The effect of temperature on the properties of a mild structural steel and cold-drawn prestressed steel is given in Fig. 3 and 4.

2.3.1. DETERMINATION OF FIRE RESISTANCE

By the beginning of the century, technical criteria had been developed concerning a 'standard fire exposure' which could be used as a basis for rating building materials and constructions. Materials evaluated in this standard fire exposure were rated in terms of their capability to provide adequate insulation or structural integrity. Until recently, BS 476 Part 8 in the UK, and its equivalent ASTM E-119 in the United States (16), have been the only standards generally accepted for controlling the

FIGURE 3 (Reference 16)

ULTIMATE AND YIELD STRENGTHS OF A COLD-DRAWN PRESTRESSED STEEL AS A FUNCTION OF TEMPERATURE

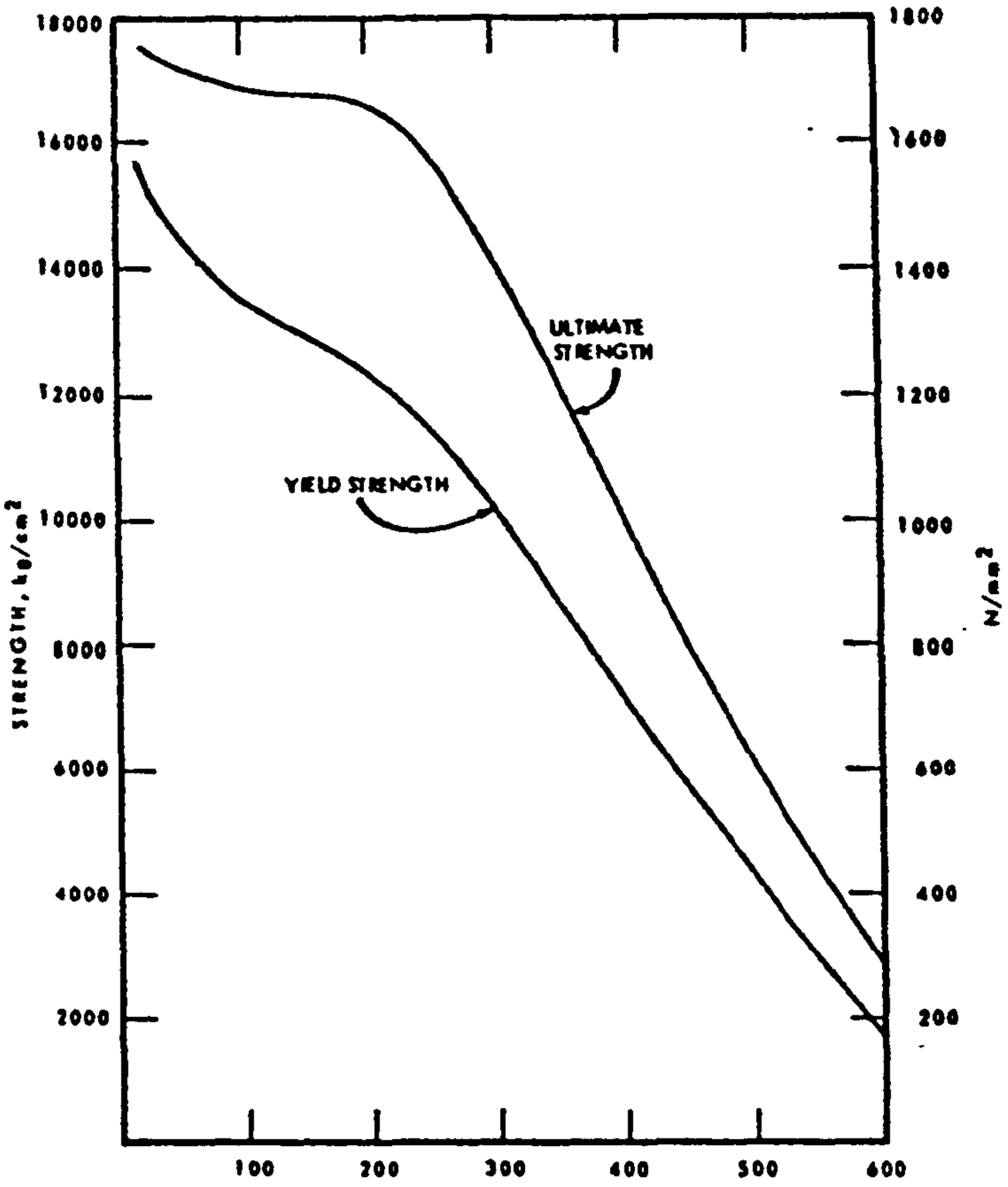

FIGURE 4 (Reference 16)

STRENGTH AND DEFORMATION CHARACTERISTICS OF A MILD STRUCTURAL STEEL AS A FUNCTION OF TEMPERATURE

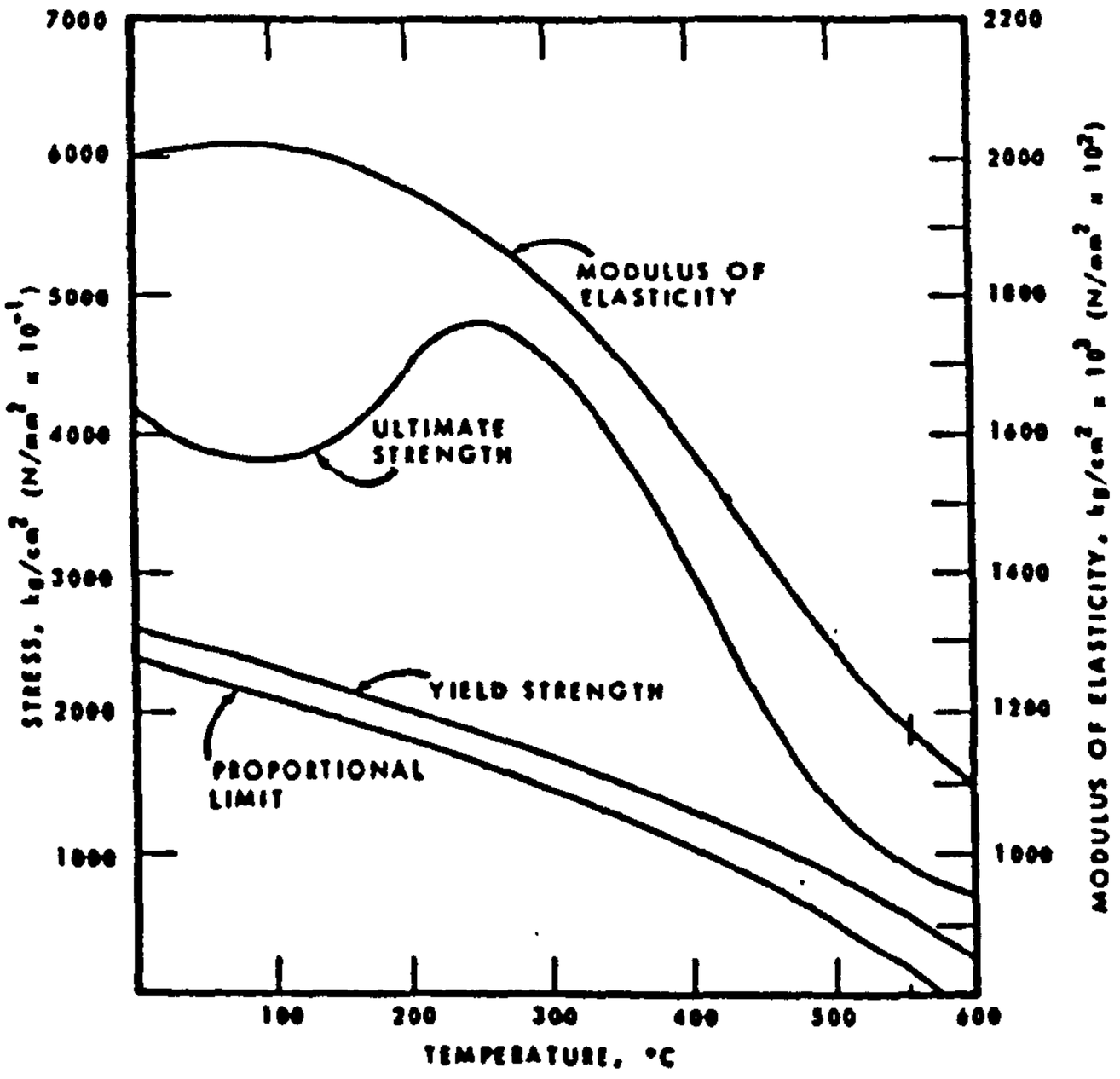

performance of intumescent coatings. This time-temperature exposure (Fig. 5) essentially defines the standard fire and was developed as a result of a series of experimental test fires in England and the United States between 1910 and 1930. Temperatures of up to 1000°C can be obtained after 90 minutes with maximum heat fluxes of up to 200 kW/m² (of which 42 kW/m² is conductive) may be achieved. Fig. 6 gives furnace temperatures (maximum and minimum) in a typical experiment conducted during this project.

FIGURE 5

STANDARD TIME TEMPERATURE CURVE FOR BS 476 : PART 8 : 1972

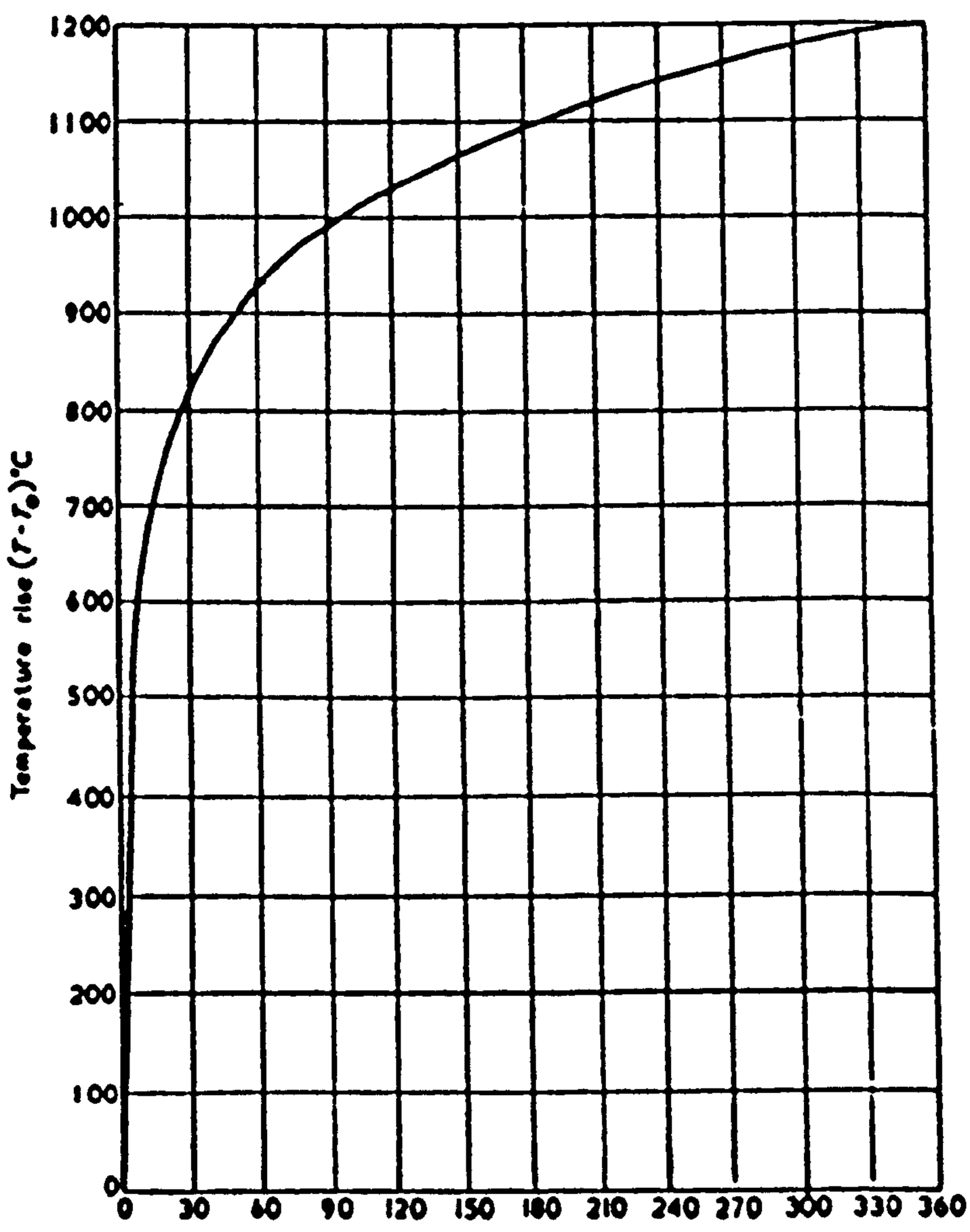

FIGURE 6

FURNACE TEMPERATURES

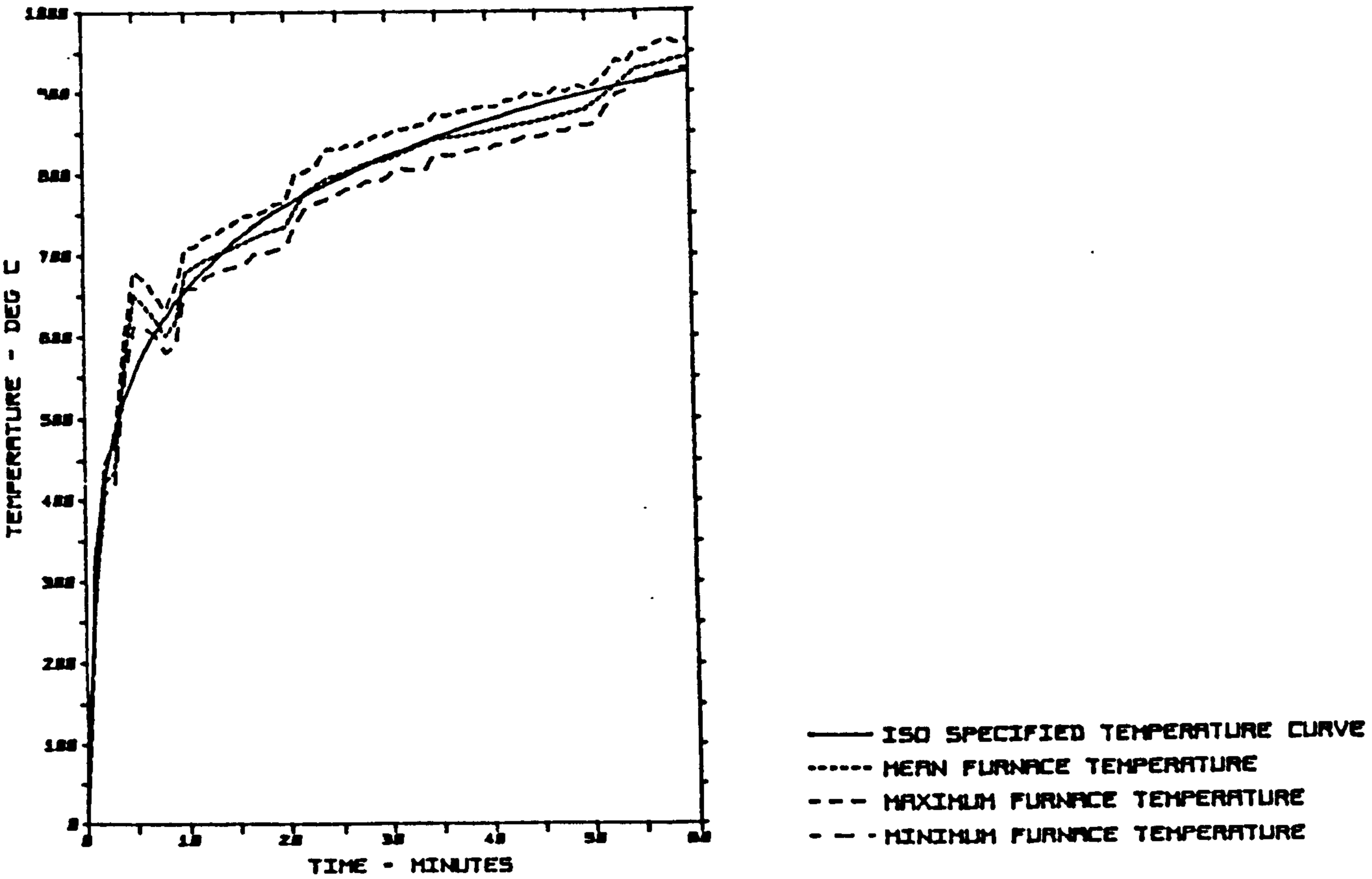

In the case of hydrocarbon furnace tests, heat fluxes of 226 kW/m² can be obtained of which 134 kW/m² is conductive. In 'pit' or 'pool' or 'design' tests (130), temperatures of 800-1000°C may be achieved with heat fluxes of up to 120-150 kW/m². Such tests are suitable for elements of plant or structure that would be completely engulfed by flame in a fire. They are not suitable for testing large elements. Pit and pool fires, while nominally being a better simulation of a real fire, are subject to problems of repeatability, mainly due to weather conditions. In addition, there may be environmental limitions on the use of pool fires for test purposes e.g. smoke pollution.

The temperature-time curves for various tests are given in Fig. 7.

The method of testing is, in principle, very nearly the same in all countries. Attempts have been made to harmonise these by the introduction of the international specification ISO - 834. During the test, the structure is exposed to heating in accordance with a standard time-temperature curve. The temperature of the structure is measured at various significant points. If the maximum permissible temperature is known, then from temperature measurements it is possible to deduce how long the structure can withstand a standard heating process. This length of time is called the fire resistance of the structure. However, the temperature curve and also the heat transfer that occur in a real fire may differ from those achieved under the standard heating conditions.

FIGURE 7

FIRE TESTS TIME-TEMPERATURE CURVES COMPARISON

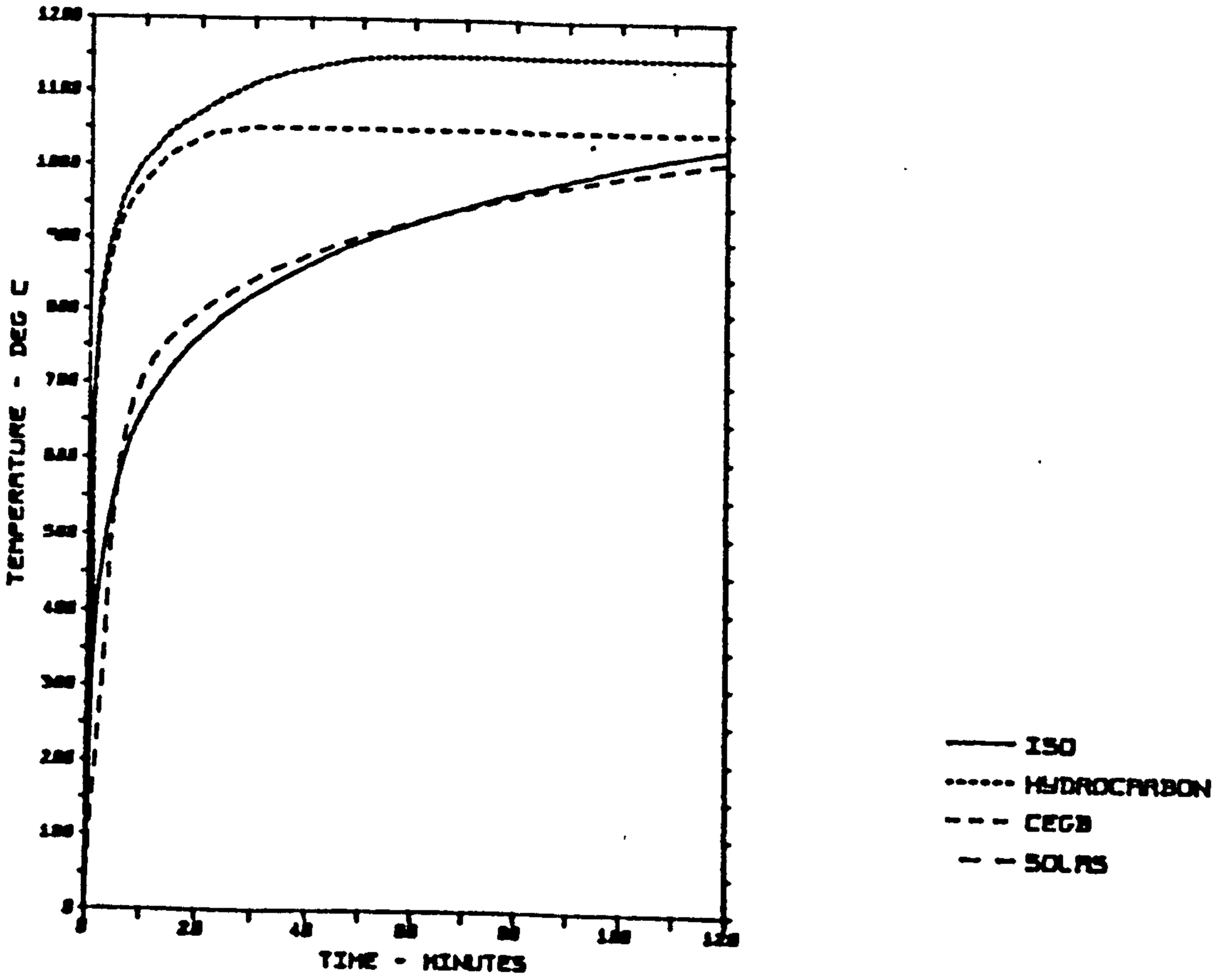

2.3.2 PERFORMANCE CRITERIA

Elements of building construction are required to satisfy various criteria according to their designed function in the event of fire. The criteria are:

a) 'stability' - resistance to collapse or excessive deflection

b) 'integrity' - resistance to penetration of flame and hot gases

c) 'insulation' - resistance to excessive temperature rise on the unexposed face.

The standard BS 476 Part 8 contains both beam and column tests - the column has to maintain stability, whilst the beam deflection must not exceed (test length)/30. Although the minimum useful period is a half-hour exposure, tests may continue for up to 4 hours. Intumescent coatings, however, are rarely subjected to anything more stringent than an exposure of two hours.

2.4. DESIGN METHODS

In the Draft BS 5950, Part 8: 1985 (the fire protection of structural steelwork (18) issued for public comment recently), three methods for determining the fire resistance of elements and sub-assemblies to meet the requirements of the building regulations were specified. These methods are currently in use and are:

1) the use of tabulated performance data for generic and proprietary fire-protection material applied to the surface of the steel sections, as determined by furnace tests in accordance with BS 476 : Part 8;

2) the use of calculation methods to determine the performance of elements and sub-assemblies were they to be subjected to the BS 476 : Part 8;

3) the use of calculation methods to determine the performance of the elements and sub-assemblies subjected to natural fires.

To date, the approach to structural stability has been based on the concept of 'fire resistance time'. This is the survival time of an element in the standard (BS 476 : Part 8) fire, and it can be misleading in a number of ways:

a) It gives the impression that a structure will survive for one hour if it has a 'one hour rating', whereas its real survival time will depend upon the severity of the real fire that the structure will experience.

b) Time has little meaning as a measure of structural stability. A structure will either survive a fire, in which case its real 'fire resistance time' is infinite, or it will not.

c) The 'critical temperature of 550°C' criterion applies a single fundamental failure limit.

The forthcoming structural steelwork code, BS 5950, Part 8, will introduce the concept of 'limiting temperature'. This is the temperature which the hottest part of the steelwork must reach at any given load, in order to cause failure of the member, e.g. the temperature of the lower flange of a beam supporting a concrete floor slab. This more realistic concept can be applied to natural as well as standard fires.

As mentioned earlier, intumescent coatings may play a very important role in the overall protection of the building. Although fire performance has been seriously considered for the last 100 years, it is only in the last 30 years that most of the developments in intumescent coatings have taken place.

2.5. MATHEMATICAL METHODS

The mathematical analysis developed to calculate the rate of temperature rise of steel requires information concerning the physical properties of steel and the insulating foam, in addition to their temperature dependence. Mathematical models offer a means of determining the rate of temperature rise of protected and unprotected steel members as a fire develops. At any time after initiation, the developing fire is considered to be instantaneously applied to the unprotected steel or insulating material. The rate of temperature rise of the steel is calculated progressively. The analysis can be used in reverse to represent the fire decay period and hence determine the theoretical maximum steel temperature.

2.5.1. EQUATIONS FOR THE DEVELOPMENT OF THE FIRE ENVIRONMENT TEMPERATURE

2.5.1.1. STANDARD TEMPERATURE/TIME RELATIONSHIP

In British Standard test BS 476 : Part 8 (ISO 834), the heating environment to which a sample is exposed is produced by specially-designed furnaces with controlled fuel inputs which allow a standard temperature/time relationship to be reproduced (Fig. 5). The relationship can be mathematically expressed (19):

$$T - T_o = 345 \log_{10}(8t + 1) \qquad (2.1.)$$

where t = time from the start of the test (minutes)

T = furnace temperature at time t (°C)

T_o = initial furnace temperature (°C)

Heating may be continued for up to 360 minutes.

2.5.1.2. HEATING BY A HYDROCARBON FIRE

The hydrocarbon fuelled fire environment requires the fire resistant materials to be subjected to a test as described in BS 476 : Part 21 (20). The temperature rise within the furnace is represented by the following equation:

$$T = 1100\,[1 - 0.325\,EXP\,(-0.167\,t) - 0.204\,EXP\,(-1.417\,t) - 0.471\,EXP\,(-15.833\,t)] \quad (2.2)$$

where T is the furnace temperature in degrees Celsius at time t in minutes.

The relationship expressed above gives the values shown in the following table:

TABLE 1

Temperature as a function of time	
Time, t	Furnace temperature, T
min	°C
3	880
5	945
10	1033
15	1071
30	1098
60	1100
120	1150
360	1190

The petrochemical industry has been increasingly concerned that the standard fire exposure test does not provide an adequate basis for evaluating materials especially when exposed to a hydrocarbon fire. Characteristically, hydrocarbon fires have a rapid rise in temperature during the initial stages and higher overall temperatures so the major difference between a 'hydrocarbon fire test' or 'high-rise fire test' (Fig. 7) and the standard test is the initial thermal shock experienced by the sample and the much higher final temperatures attained.

All tests expose intumescent materials to a fixed time-temperature curve. However, in a real fire not only can the temperature fluctuate but also there may be a rapid or a slow rise in temperature depending on the circumstances. Indeed, the intensity of a fire may vary with time and position.

To evaluate intumescent coatings thoroughly, tests should perhaps be conducted in a gas-fired furnace using a special slow heating rate for at least half an hour, a suitable equation being (18):

$$T - T_o = 154\,(t)^{0.25} \qquad (2.3)$$

this then being followed by a fast heating rate similar to that of the hydrocarbon fire test, for about the same period of time.

2.5.2. LINEAR REGRESSION ANALYSIS

A solution to the problem of how to specify the minimum protection thickness for steel members of different shapes and sizes in order to achieve a required fire resistance can be obtained by conducting fire tests with different thicknesses of protective coating on a range of sizes (i.e. different section factor values, H_p/A, where H_p = perimeter of the steel section exposed and A = its cross sectional area). See Appendix A.

FIGURE 8

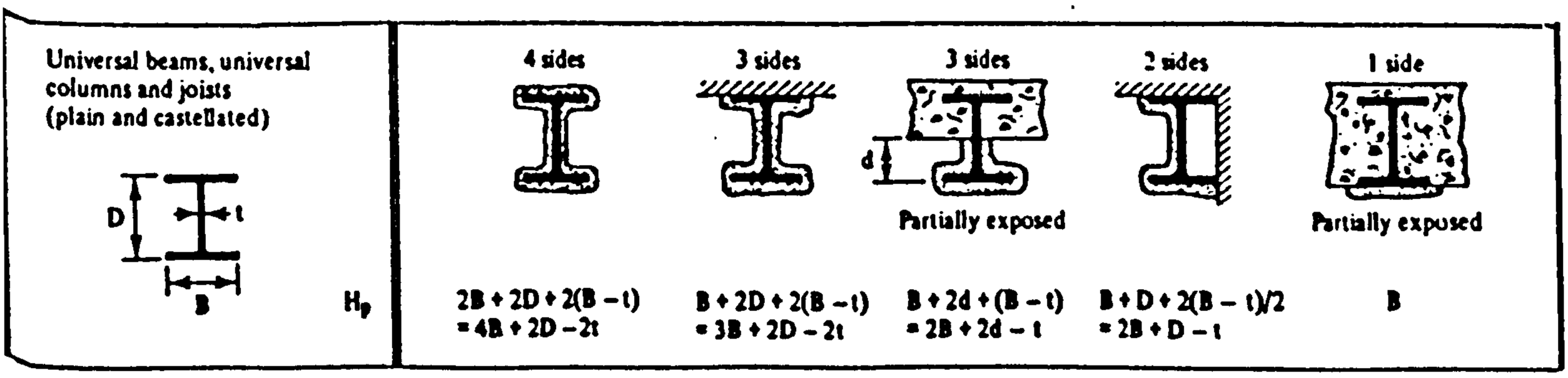

The thickness of material required to provide specific standards of fire resistance is derived by means of an empirical relationship:

$$\text{Fire Resistance Time (F.R.)} = K_1 + K_2 \,.\, W \,.\, A/H_p + K_3 \,.\, W \qquad (2.4)$$

where Fire Resistance Time is the time to achieve the failure temperature, K_1, K_2, K_3 are constants unique to each fire protective system (they are determined by means of multiple linear regression and are related to the thermal capacity and the elevated thermal conductivity of both the steel and the protective medium), W is the thickness of the protective coating and A/H_p is the reciprocal of the section factor.

By re-arranging the equation,

$$W = \frac{(F.R.) - K_1}{(K_2\ A/H_p + K_3)} \qquad (2.5)$$

With many fire protection materials it is possible to achieve a high level of agreement between test and predicted data.

It must be borne in mind that the above method is:

a) only applicable to the standard fire test

b) not suitable for extrapolation beyond the region investigated

c) restricted to insulated members.

However, this technique includes evaluation of adhesion and mechanical characteristics of the protective material as determined under the stress and thermal conditions encountered in the fire tests. The evaluation method can also be modified to assess insulation performance with higher (or different) failure temperatures.

2.5.3. RADIATIVE HEAT FLUX

To define the intensity of a fire, the gas temperature (T_f), the radiant heat flux (q_r), and the convective heat flux (q_c) are needed. T_f depends on the type of volatile hydrocarbons being oxidised, and q_r is defined as:

$$q_r = E_f \sigma T_f^4 \qquad (2.6)$$

where E_f is the effective grey body emittance of the fire.

and σ = Stefan-Boltzmann constant (5.67×10^{-8} W/m^{2}K^4)

and q_c is defined as:

$$q_c = h\,(T_f - T_o) \qquad (2.7)$$

where h is the convective heat transfer coefficient and T_o is the temperature of the object to which energy is transferred.

The heat transfer coefficient is dependent upon the gas transport properties (nearly the same for all fires) and the velocity of the gases. Slow-burning fires have low gas velocities (3-5 m/s) and consequently insignificant values of h, while free-burning liquid and gas fires have velocities of 30 m/s or more and hence very high h values. Radiation levels for both types of fire are equivalent. Thus high-temperature, high-velocity fires, such as pit or pool fires, produce conditions which are more onerous than furnace fires.

The total heat flux (q_T) of a fire can be defined as:

$$q_T = q_c + q_r \qquad (2.8)$$

A recent study by Castle (21) compared the heat transfer characteristics of three different furnaces by measuring the total heat flux and the radiative flux. It was shown that the heat received by a construction specimen differed, even though the standard temperature/time relationship was followed by the furnace thermocouples. This suggests that there should be a requirement for the measurement of convective and radiative heat flux. The heat flux data of a typical ASTM E-119 column test are given in Fig. 9. Similarly, results for a typical propane pit fire environment are given in Fig. 10.

FIGURE 9

HEAT FLUX DATA OF A TYPICAL ASTM 119 COLUMN TEST

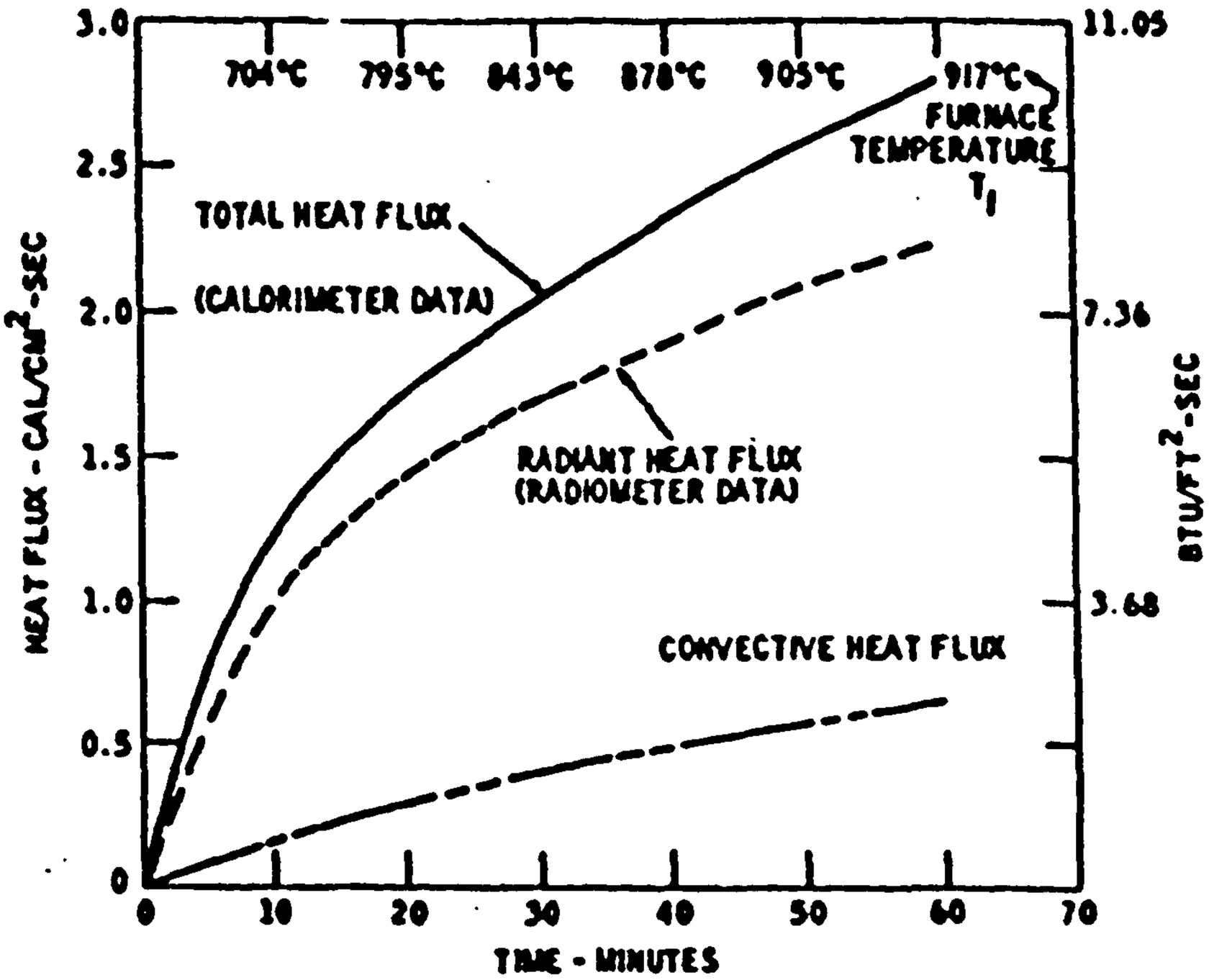

FIGURE 10

HEAT FLUX DATA OF A TYPICAL POOL FIRE

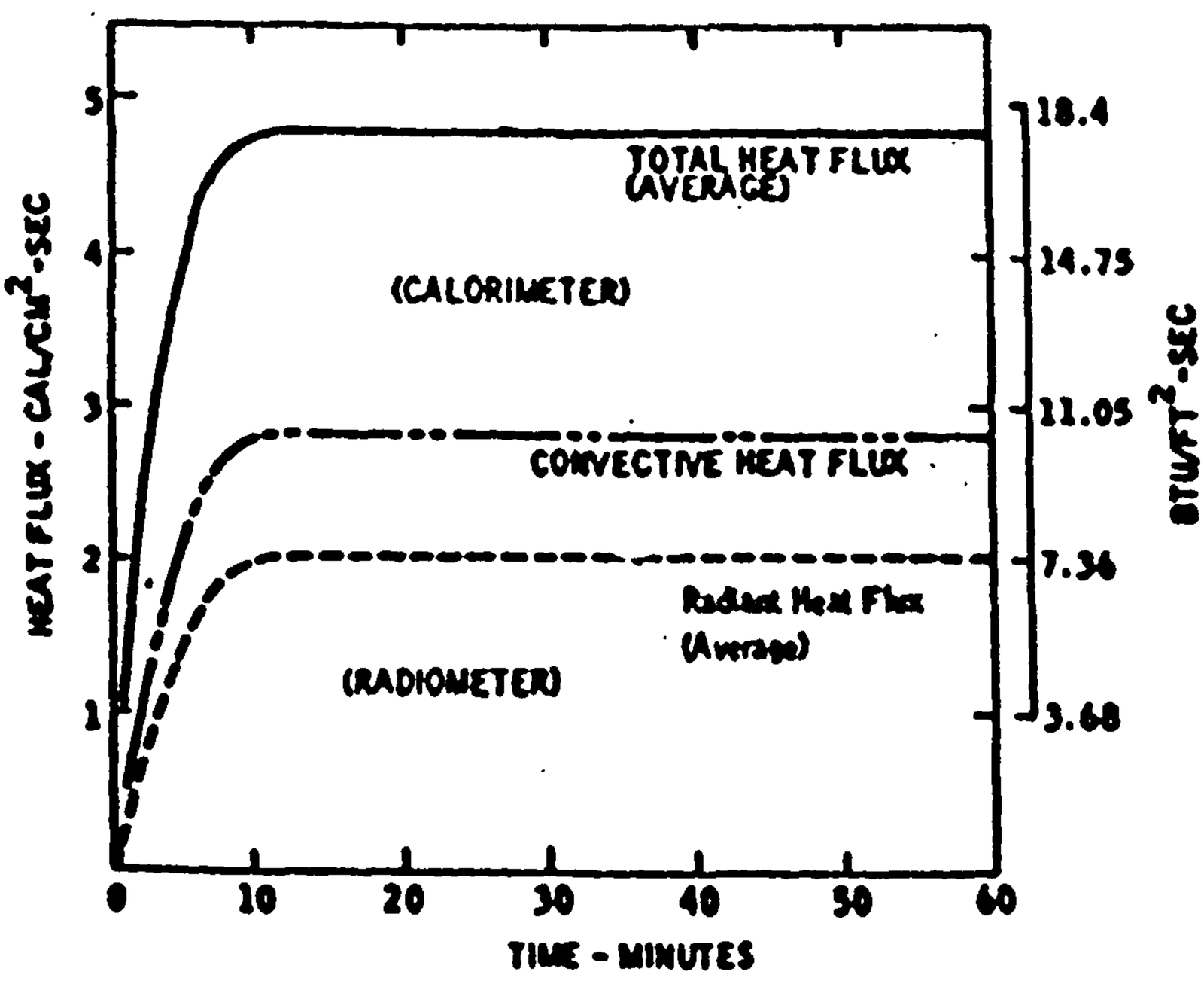

2.5.4. FIRE RESISTANCE AND FIRE SEVERITY

Mathematical modelling of fire severity was initiated by Fujita (22) and was continued by Kawagoe (23) and Sekine (24). Kawagoe demonstrated the effect of ventilation, i.e. the area and height of the openings through which air is made available to the fire. The rate of burning of fuel was found to be proportional to the area of the opening (A) and the square root of its height ($\sqrt{H}$). Extensive work was conducted by Heselden (25) and Law (26) on 'ventilation controlled fires' which led to the development of an equivalent fire resistance (t_e) concept. The relationship suggested was:

$$t_e = \frac{N}{A_F} \cdot \frac{A_F}{A_v(A_t - A_v)} \quad \text{(min)} \qquad (2.9)$$

where N = fire load, A_F = floor area (m^2)

A_v = area of ventilation (m^2)

A_t = surface area of the compartment (m^2)

Odeen (27) showed that the rate of burning was related to the 'opening factor':

$$\frac{A_v \sqrt{H_v}}{A_t} \qquad (2.10)$$

where H_v = window height.

Magnusson and Thelanderson (28) used the relationship to establish temperature-time curves for different opening factors and fire loads. A typical example, with different 'opening factors' and 'fire load densities' is shown in Fig. 11. Petterson (29) has used this approach and defined equivalent fire resistance by the following relationship which takes account of the thermal nature of the boundaries:

$$t_e = \frac{0.28N}{(A_t \cdot A_v\sqrt{H_v})^t} \quad \text{(min)} \qquad (2.11)$$

FIGURE 11

THEORETICAL TEMPERATURE-TIME CURVES FOR DIFFERENT FIRE LOAD DENSITIES AND OPENING FACTORS

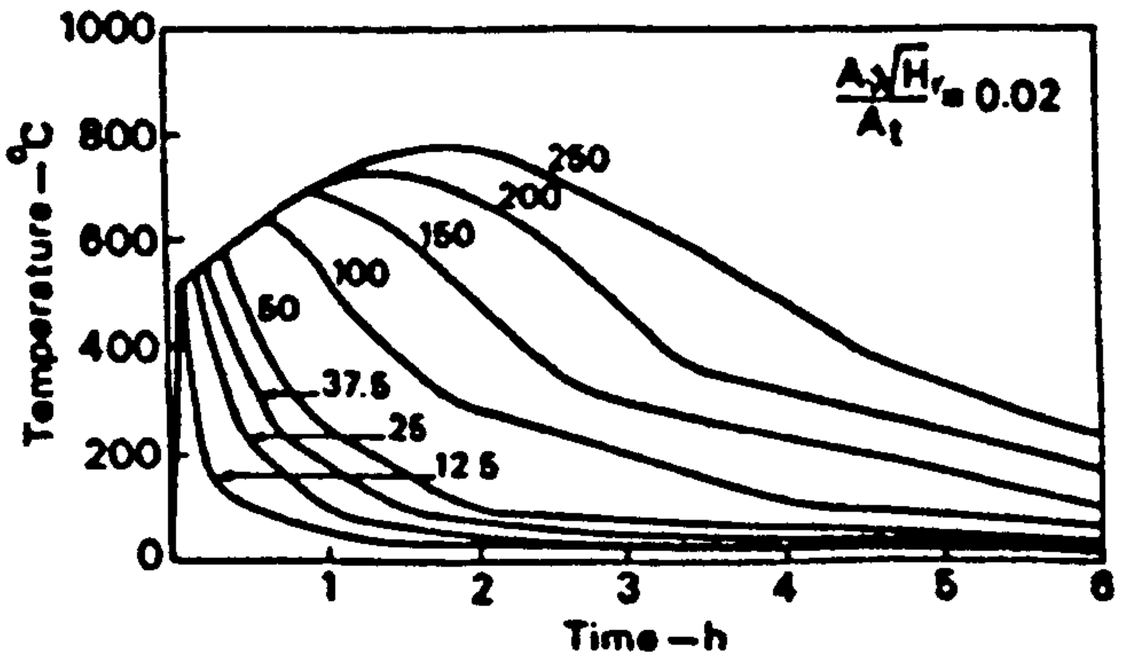

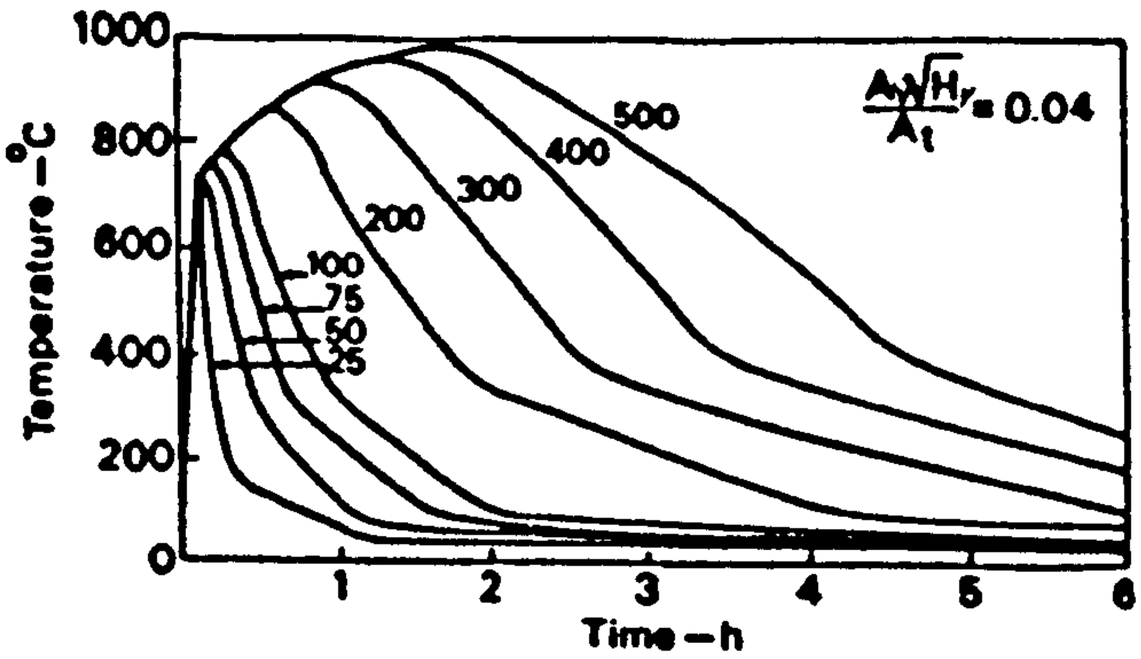

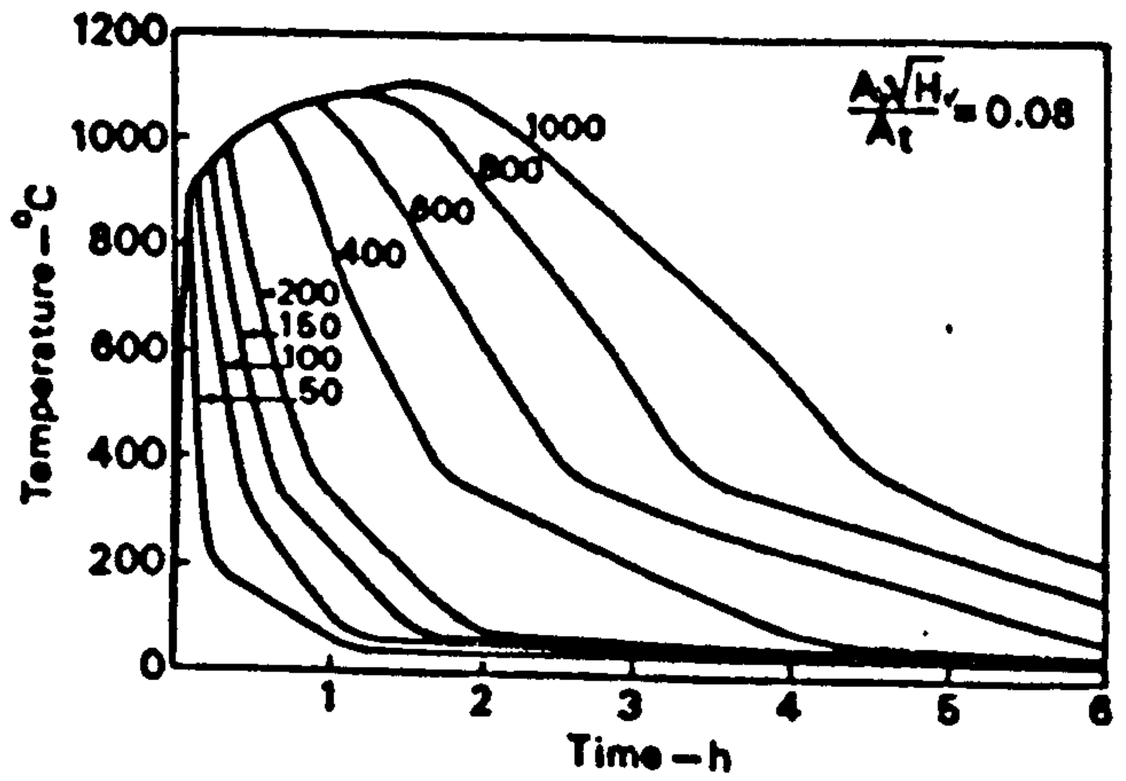

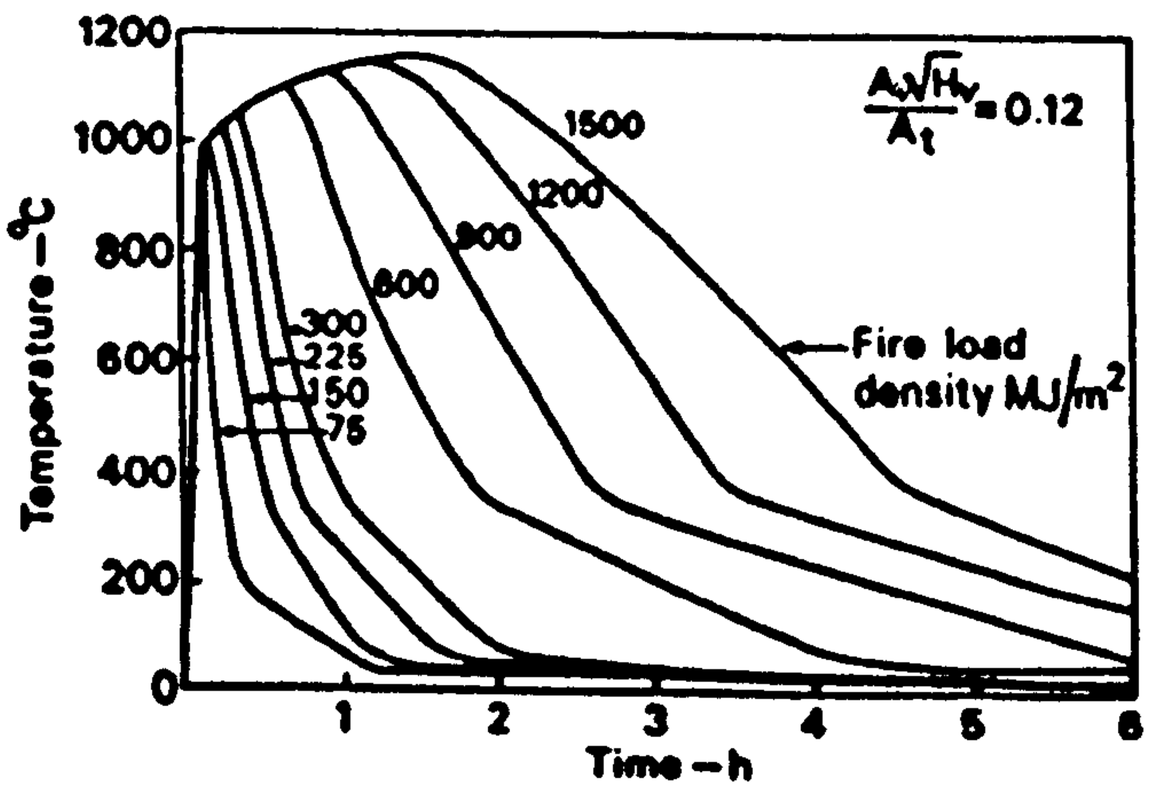

The fire load can be expressed as a density $q_f = N/A_t$, when the relationship becomes:

$$t_e = \frac{0.057\ q_f \cdot A_t}{\sqrt{A_v\ (A_t - A_v)}} \qquad \text{(min)} \qquad (2.12)$$

2.5.5.1. UNINSULATED STEEL STRUCTURES - HEAT BALANCE EQUATION

The heat flux transmitted to the unprotected structural member in a fire by convection and radiation depends on its exposed area, the temperature of the fire and the temperature of the steel.

FIGURE 12A

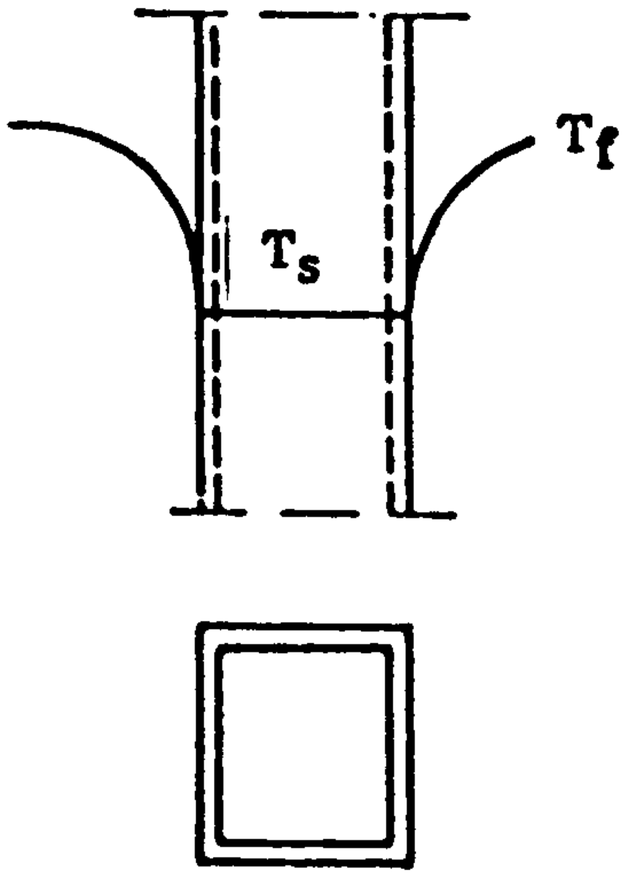

T_f = the gas temperature in the compartment

T_s = temperature of the steel section

The quantity of heat Q which passes through the boundary layer between the combustion gases and the steel section per unit length over a short interval of time Δt(s) can be written as:

$$Q = \alpha F_s (T_f - T_s)\ \Delta t \qquad \text{(J/m)} \qquad (2.13)$$

where α = surface coefficient of heat transfer (J m^{-2} K)

F_s = the surface area of the steel per unit length exposed to fire (m^2/m)

T_f = the gas temperature in the compartment at time t (°C)

T_s = the temperature of the steel section at time t (°C)

The heat Q supplied per unit length is equal to the heat required to increase the steel temperature by ΔT_s so that Q must also be given by:

$$Q = C_{ps} \Delta T_s V_s \rho_s \qquad (2.14)$$

where C_{ps} = the specific heat capacity of the steel (J/kg°C)

V_s = the volume per unit length of the steel section (m^3/m)

ρ_s = density of steel (kg/m^3)

Hence,

$$\Delta T_s = \frac{\alpha \quad H_p}{\rho_s \, C_{ps} \quad A} \cdot (T_f - T_s) \, \Delta t \qquad (2.15)$$

The assumptions made are:

1) the heat transfer through the steel member is uniform and instantaneous. (This becomes increasingly valid the thinner the cross section).

2) the heat flow is one-dimensional. (Hence, corner effects are ignored).

Owing to the high thermal conductivity of steel, these assumptions give satisfactory accuracy (except for extremely thick sections). If the gas temperature-time curve, and thus T_f, is known for a fire compartment, the maximum steel temperature can be determined by calculating ΔT_s for each time interval by means of Eq 2.15.

2.5.5.2. CALCULATION PARAMETERS

1) Since the gas temperatures T_f and the steel temperatures T_s vary with time, the accuracy of Eq (2.13) depends upon Δ t. For reasonable accuracy Δt should not have a value greater than:

$$\Delta t \leqslant \frac{25000}{H_p/A} \qquad (2.16)$$

2) The density of steel ρ_s is 7850 kg/m^3.

3) The specific heat capacity C_{ps} of steel varies with the temperature

and composition and lies in the range 0.482 kJ/kg °C (below 100 °C) to 0.682 kJ/kg °C (above 600 °C). See Appendix B.

4) The surface coefficient of heat transfer is the sum of a convection term, α_k which is approximately 23 W/m²°C and a radiation term, α_s which can be determined from the Stefan-Boltzmann equation :

$$\alpha_s = \frac{5.77\ E_r}{T_f - T_s}\left[\left(\frac{T_f + 273}{100}\right)^4 - \left(\frac{T_s + 273}{100}\right)^4\right] \quad W/m^2\,°C \quad (2.17)$$

where E_r is the resultant emissivity

E_r is dependent on the emissivities E_t and E_s of the flames and the steel structure respectively and is given by:

$$E_r = \frac{1}{1/E_t + 1/E_s - 1} \quad (2.18)$$

Eq (2.17) may be applied to a column placed in a fire compartment in which the flames completely surround the column. Since E_t varies with the size of the flames, but is usually in the range 0.6-0.9 (17), a value of 0.85 will be used for calculation purposes. Also E_s is approximately 0.8 (17) hence, E_r is about 0.7.

In the event of fire inside a building, a column placed outside the facade will be exposed to less radiation than a column placed on the inside. Furthermore, the cold outside air would retard the temperature rise of the column. This can be approximately taken into consideration by using a lower value for E_r than that applicable to an internal column. An analysis of the conditions shows that a value of E_r of 0.3 may be used in many cases (17).

2.5.6.1. FOR INSULATED STEEL STRUCTURES - HEAT BALANCE EQUATION

FIGURE 12B

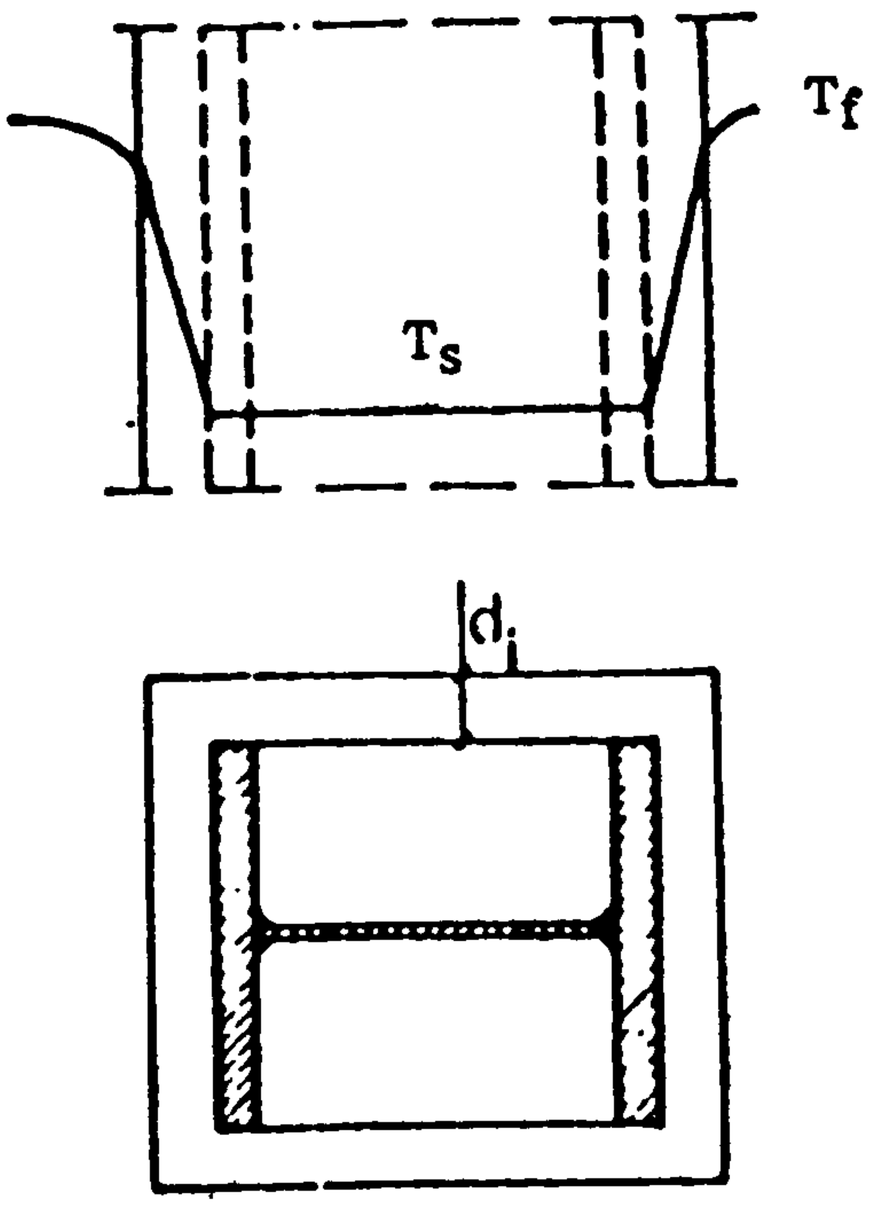

T_f = the gas temperature in the compartment

T_s = temperature of the steel section

The heat Q supplied per unit length to an insulated steel section (Fig. 12B) over a short time interval Δt is given by:

$$Q = \frac{1}{1/\alpha + d_i/k_i} . A_i (T_f - T_s) \Delta t \qquad J/m \qquad (2.19)$$

where d_i = thickness of insulation (m), k_i = thermal conductivity of the insulation and A_i = internal surface area of the insulation (m^2/m)

If the heat Q supplied per unit length raises the temperature of the steel section by ΔT_s, then Q is given by:

$$Q = C_{ps} \Delta T_s A_s \rho_s \qquad J/m \qquad (2.20)$$

when A_s = area of steel section (m^2).

If the heat capacity of the insulation by comparison with that of the steel is negligible, then it follows that

$$\Delta T_s = \frac{A_i}{(1/\alpha + d_i/k_i)\rho_s C_{ps} A_s} . (T_f - T_s) \Delta t \qquad °C \qquad (2.21)$$

2.5.6.2. CALCULATION PARAMETERS

The assumptions made are:

a) the temperature gradient in the insulation is linear, Fig. 12B;

b) that, at every point in time, the temperature is uniformly distributed over the whole cross section;

c) that, the heat flow in the steel section and the insulation is one-dimensional.

At the temperatures which occur during a fire, the thermal surface resistance $1/\alpha$ can normally be ignored by comparison with the thermal resistance d_i / k_i of the insulation.

In general, the heat capacity of the insulation may be ignored. However, if insulation with a large heat capacity is used, the mean temperature rise of the insulation over the interval Δt is equal to $\frac{1}{2}(\Delta T_f + \Delta T_s)$. The heat Q_i required per unit length to increase the mean temperature of the insulation by $\frac{1}{2}(\Delta T_f + \Delta T_s)$ is:

$$Q_i = \tfrac{1}{2} C_{pi} (\Delta T_f + \Delta T_s) d_i A_i \rho_i \qquad \text{J/m} \qquad (2.22)$$

where C_{pi} = specific heat capacity of the insulation (J/kg°C)

Hence, using (Eq 2.21), and Eq (2.22) the rise in temperature ΔT_s of the steel section in time interval Δt is found to be:

$$\Delta T_s = \frac{(T_f - T_s)\Delta t}{(1/\alpha + d_i/k_i)\rho_s C_{ps} \frac{A_s}{A_i}\left(1 + \frac{d_i k_i C_{pi} A_i}{2 \rho_s C_{ps} A_s}\right)}$$

$$- \frac{\Delta T_f}{\frac{2 \rho_s C_{ps} A_s}{d_i k_i C_{pi} A_i} + 1} \qquad (2.23)$$

Eq (2.23) may be further simplified by assuming that the effect of the heat capacity of the insulation can be simulated by increasing the heat capacity of the steel section by $\frac{1}{2}(C_i \rho_i d_i A_i)$:

$$\Delta T_s = \frac{k_i A_i}{d_i} \cdot \frac{(T_f - T_s)\,\Delta t}{A_s C_s \rho_s + \frac{C_i d_i \rho_i A_i}{2}} \qquad (2.24)$$

hence,

$$\Delta T_s = \frac{k_i A_i}{d_i A_s C_s \rho_s} \left[\frac{C_s \rho_s}{C_s \rho_s + \frac{C_i d_i \rho_i A_i}{2A_s}} \right] (T_f - T_s)\Delta t \qquad (2.25)$$

The expression in the square brackets is less than 1 and as a consequence delays the temperature rise. When the gas temperature T_f is known, the maximum steel temperature can be determined by means of Eqs (2.19) or (2.23).

SECTION 3

LITERATURE SURVEY AND HISTORICAL DEVELOPMENT

Scientific records mention the use of ammonium phosphate as early as 1786, when Arfrid (31) suggested its use as a flame retardant for cellulosic materials. It is still an important ingredient in many fire retardant compositions. In 1821, Gay-Lussac (32) published his study on fire-retarding cellulosics. The first reference to the use of inorganic salts as flame retardants in paints was in a patent taken out by Louis Paimboeuf (33) in 1837. It was claimed that the addition of lime, potash, alum and common salts to a water-based or linseed-oil paint would produce a fire retardant paint suitable for protecting buildings against fire. In 1948, Ware and Westgate (34) published a review of U.S. patent literature on fire-retardant coatings covering 111 years during which at least 330 patents were issued. The first patent to describe an intumescent coating was published in the 1930's (35). Tramm described a coating containing diammonium phosphate, dicyandiamide and formaldehyde that swelled to form a layer of carbon when heated. The term intumescent was used to describe the bubbling and foaming effect of phosphoric or sulphuric-acid-treated esters and alcohols in 1948, by Olsen and Bechle (36).

From 1948 to 1950, Jones, Juda and Soll (37) developed formulations with references to the words 'carbonifics' and 'spumifics.' These coatings possessed very little water resistance. In 1952, Nielson (38) developed a phosphorylamide complex by reacting phosphoryl chloride with ammonia. This complex is relatively insoluble in water and was mentioned in the literature for several years (39,40,41). However, it was never used commercially for economic reasons. Sakurai and Izumi (42) in their study

of urea formaldehyde, starch and diammonium phosphate, concluded that the optimum protection is not dependent upon the foam height. In 1953, Jones et al (43) discussed the use of melamine phosphate which is still used commercially. Christian et al in 1954 (44) reported the desirability of controlling the size of the cells in an intumescent char. They suggested the use of nucleating agents such as finely dispersed fillers. Wilson and Marotta (45) suggested the use of fibres to hold the char together. Cummings (46) described an intumescent formulation as a ternary system where the preferred composition was within the shaded boundaries shown in Fig. 13 below.

FIG 13

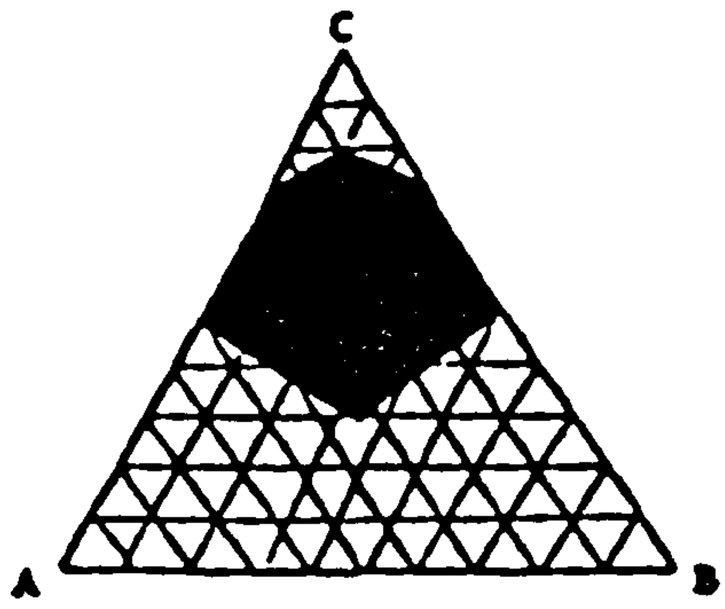

'A' is a non-resinous carbonific (dipentaerythritol), 'B' is an organic nitrogen compound (dicyandiamide), 'C' is a spumific (ammonium phosphate).

In 1961, Quelle (47) patented the first clear intumescent coating using a condensate resin formed from urea, formaldehyde, and phenol combined with butyl phosphate. In 1964, workers at the Southern Regional Research Laboratory of the USA (48) used melamine phosphate or halogenated phosphate esters, including a tung-oil-based alkyd resin. In 1965 (49,50) came the major breakthrough which led to the commercial introduction of the relatively insoluble ammonium polyphosphate which is now used extensively in many commercial formulations.

Durability to weathering and water soaking has been a major problem. Various attempts have been made to overcome the difficulty by selecting appropriate ingredients resistant to leaching. Fairly good water-resistant, oil-based, intumescing fire-retardant coatings may be achieved using isano oil, linseed oil, additives, pigments, driers and solvent (51,52). However, isano oil is obtained from the nut of the Onguekoa gore, native to Central Africa (53,61). This tree is not considered suitable for vegetative propagation or economic production (it takes about 20 years to produce oil-bearing nuts).

Isano oil is unusual since it contains mixed tri-glycerides having a large proportion of C_{18} diacetylenic acids (51%) (54,55) and their 8-hydroxy derivatives (22%), in addition to a small percentage of dihydroxystearic acid and the usual saturated and unsaturated fatty acids, such as myristic, palmitic, stearic, oleic and linoleic (56,57,58,60). One of the outstanding characteristics of isano oil is that it explodes and then carbonises when heated above 200°C (59).

Since the intumescing properties of isano oil are attributed to its conjugated diacetylenic and hydroxydiacetylenic moieties, research efforts were directed towards synthesising conjugated diacetylenic glycols (61) by oxidative coupling (62). However, although the paints formulated from the polyesters of these diacetylenic glycols were superior to those formulated from the isano oil vehicles (51,59), even better coatings were developed from chemically modified oil-based and water-resistant spumific and carbonific materials.

In 1969, an excellent intumescent agent, phosphoryl-trianilide (63) was

reported. Unlike most flame retardant additives, it is not a salt. This material has a high aromatic-ring content, is water insoluble and is not swollen by water. With proper formulation, very thin films of the coating material, approximately 1mm thick, can be made to intumesce forming a stable foam in excess of 25mm.

A comprehensive review of various formulations has been conducted by Vandersall (49). Other relevant references are (64-70), and reviews of patents are given by Williams (71), O'Neil (72) and Scruien et al (73). Work of recent origin is described by Kay (74,75) and Gannino et al (76).

Alternatives to the carbohydrate-phosphoric acid system have employed nitroaniline compounds such as nitroaniline bisulphate salts originally used by NASA (77) and more recently nitroaniline-sulphonic acids, quinonedioxime-acid mixtures, nitroanilinosulphones (78, 79). In the nitroaniline derivatives, the intumescence is modelled as a thermal self-polymerisation of the aromatic compounds passing through plastic states and being expanded by evolving gaseous products to form fine-textured, low-density foams. The resulting polymeric foams are polyheterocyclic structures similar to polyquinoxalines or polyphenoxazines. The intumescent reactions of nitro substituted aromatic amines and p-nitroaniline bisulphate are given in Figs. 14 and 15. A generalised mechanism for the polymerisation is discussed by Parker et al (78) and summarised in Fig. 16.

FIGURE 14

INTUMESCENT REACTIONS OF NITRO-SUBSTITUTED AROMATIC AMINES

THERMAL POLYMERIZATION PROCESS OCCURS WITH:

o-NITROANILINE
p-NITROANILINE
p-NITROACETANILIDE
5-NITROISATOIC ANHYDRIDE
etc

$$\xrightarrow[\text{CONCENTRATED SULPHURIC OR POLYPHOSPHORIC ACID}]{\Delta \; >200^{\circ}C}$$

SPONGY BLACK POLYMERIC FOAM + GAS

FIGURE 15

SYNTHESIS AND CHARACTERIZATION OF INTUMESCENT INTERMEDIATE p-NITROANILINE BISULPHATE

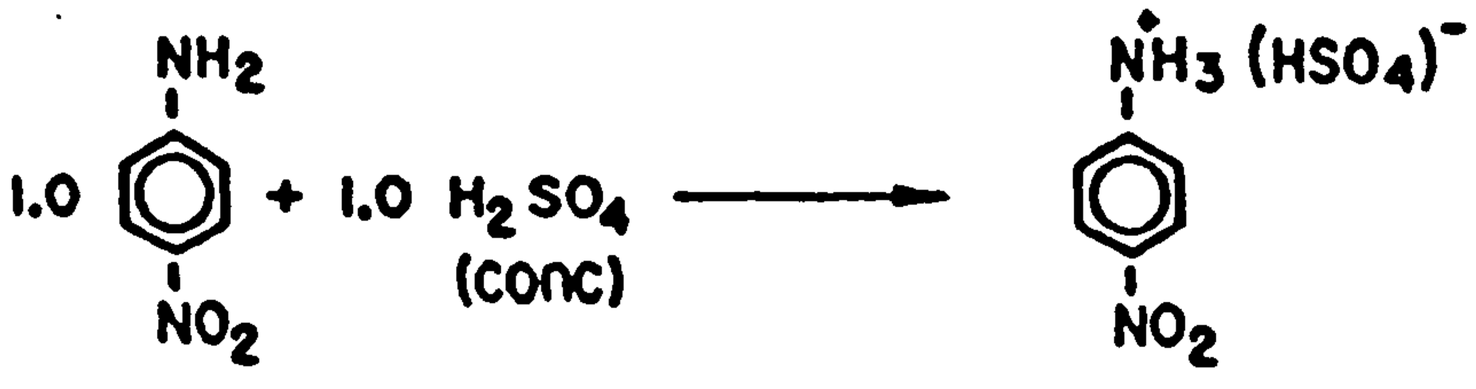

p-NITROANILINE — p-NITROANILINE BISULPHATE

145°C	MELT POINT	200°C (DECOMP)
138	MOL WT	236 (CALCULATED)
		236 (MEASURED)
YELLOW SOLID	APPEARANCE	LT YELLOW SOLID

(SOLUBLE IN ALCOHOLS, KETONES
INSOLUBLE IN BENZENE, TOLUENE,
ETHER

FIGURE 16

PROPOSED GENERALIZED MECHANISM FOR POLYMERIZATION

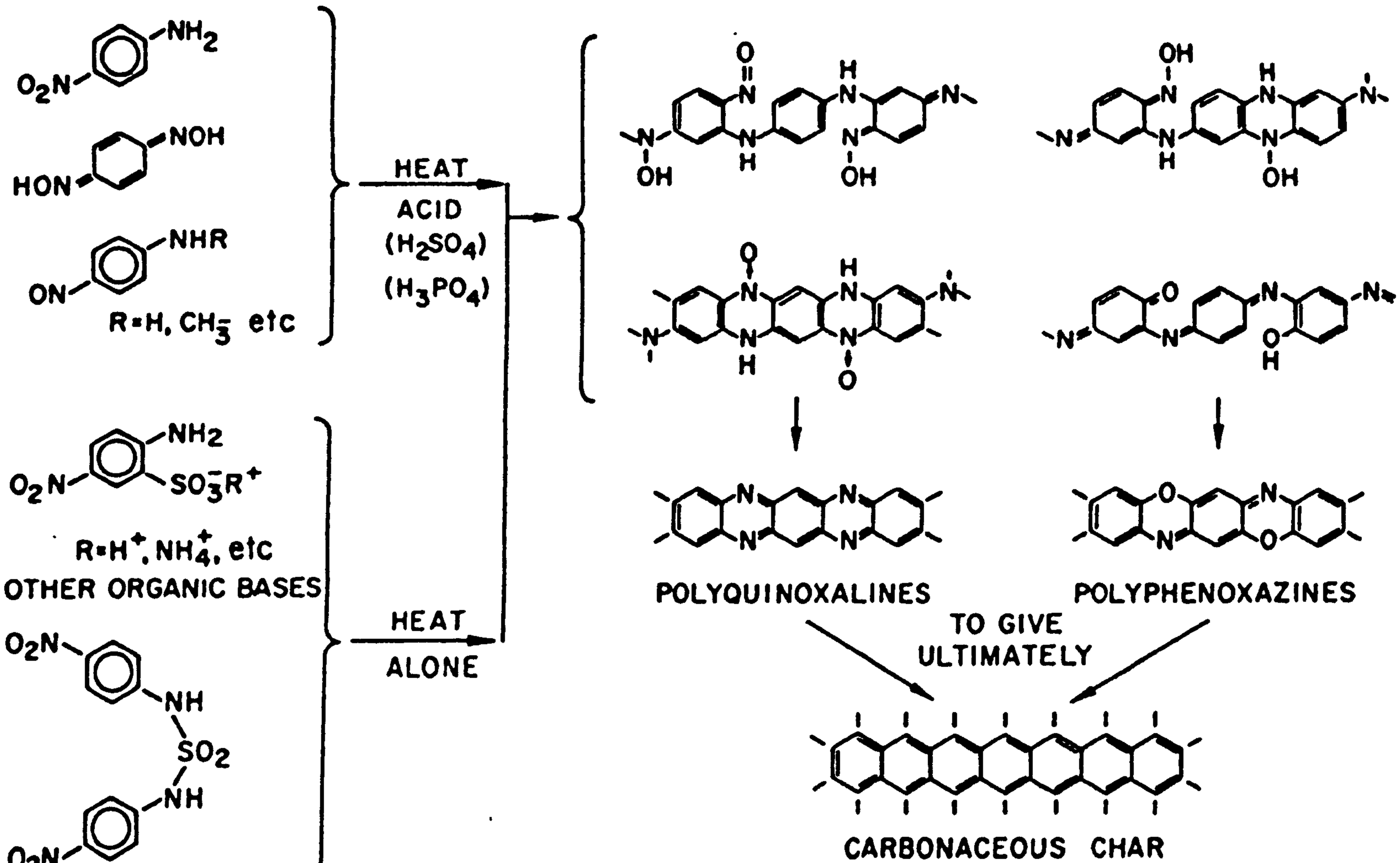

SECTION 4

4.1. EXPERIMENTAL METHODS AND TECHNIQUES USED

In the course of this study, intumescent formulations were developed using commercially-available materials. The relevant physical and chemical properties of all the individual ingredients were determined and the interactions between these ingredients were examined. Hence, subsequent formulations were improved by ensuring that decompositions, softening, interactions etc occurred when required in order to give the best performance. These formulations were analysed, the kinetic parameters being determined bearing in mind the following:

a) During combustion, the heating rate of a surface has been estimated (94, 95) to be between 10° /sec and 1000° /sec. These heating rates are significantly higher than those normally used in the study of polymer degradation. TGA, DSC, DTA, STA are rarely performed at greater than 20°/min. However, the kinetics and thermodynamics derived from such thermal analytical methods are used to interpret the results obtained from flammability experiments.

b) The effect of oxygen on the kinetic parameters is not known. The oxygen level at or near the surface of a burning polymer is greater than zero but often less than 5% (94).

Some of the analytical techniques and test methods employed are described below.

4.2.1. THERMOGRAVIMETRIC ANALYSIS (TGA)

Thermogravimetric analysis (TGA) provides a direct record of loss of weight of a material with temperature. TGA curves are characteristic for a given compound due to the unique sequence of physico-chemical

changes and the rate at which these occur with temperature change. Changes in weight are a result of the rupture or formation of chemical bonds which may lead to the evolution of volatile products. TGA curves give information concerning the thermal stability and composition of the original sample, its intermediate compounds, and the residue. The factors affecting the thermogram fall into two distinct categories, i) instrumental factors, and ii) sample characteristics.

The instrumental factors are a) furnace heating rate, b) recording or chart speed, c) furnace atmosphere, d) geometry of sample holder and furnace, e) sensitivity of recording mechanism, f) composition of sample container. The sample characteristics are a) amount of sample, b) solubility of evolved gases in sample, c) particle size, d) heat of reaction, e) sample packing, f) nature of the sample, g) thermal conductivity.

Factors such as sample holder geometry, recording speed, balance sensitivity and sample container air buoyancy are fixed for a given thermobalance. However, factors which are variable and difficult to reproduce are the sample particle size and packing, furnace convection currents and electrostatic effects.

Thermogravimetry is usually only concerned with a single substance and as such only two reactions may be observed:

i) reactions involving a decomposition such as:

$$A\ (solid) \longrightarrow B\ (solid) + C\ (gas)$$

and ii) reactions involving a solid and a gas:

$$A\ (solid) + B\ (gas) \longrightarrow C\ (solid)$$

In the main, the TGA experiments were conducted under dynamic temperature conditions (linear rate of heating) rather than isothermal.

One of the errors which can be encountered is due to the temperature of

the sample being taken as that measured by a thermocouple located either just above or below the sample container. However, the true temperature of the sample will either lag or lead the thermocouple temperature depending on the nature of the decomposition reaction (endothermic or exothermic), the heating rate, the sample thermal conductivity, the geometry of the sample holder etc. These factors were kept to minimum by selecting relatively low heating rates and long-stemmed quartz crucibles with a reasonable heat-transfer coefficient. In addition, instrument calibration was carried out before each run.

A Stanton-Redcroft analyser was used. From the TGA curves, data was obtained concerning the thermodynamics and kinetics of reactions. This technique was also used to complement differential thermal analysis (DTA) studies.

4.2.2. DIFFERENTIAL SCANNING CALORIMETRY (DSC)

A Perkin-Elmer (Model 2C) was used. The sample temperature is compared to a reference substance (or furnace block). The amount of heat required to maintain isothermal conditions is recorded as a function of time or, as in this case, temperature in Kelvin. A record of this balancing energy yields a direct calorimetric measurement of the enthalpy of the reaction transition. The instrument contains two control loops, one for the average temperature control, the other for the differential temperature control. In the former, a programmer provides an electrical output that is proportional to the required temperature of the sample and reference. This is compared with signals received from platinum-resistance thermometers permanently embedded in the sample and reference holders. In the differential temperature loop, a comparator circuit determines whether the reference or sample temperature is

greater. The power given to the reference or sample heaters is then adjusted to correct any difference observed.

Generally the heating rates used were kept low at 5-10°/min, although some experiments were conducted at 20°/min. The maximum temperature used was 750K.

4.2.3. DIFFERENTIAL THERMAL ANALYSIS (DTA)

A Perkin-Elmer (Model 1500) was used. DTA detects the physical and chemical changes occurring when a material is heated. Any transition which the sample undergoes will result in the liberation or absorption of energy, with a corresponding difference in its temperature from that of the reference substance. This difference in temperature (ΔT) and the programmed furnace temperature (ΔT) are measured. Reaction/transition temperatures and enthalpy changes (endothermic or exothermic) may be determined. The sample is tightly packed into a crucible to ensure good thermal contact, as is a reference material such as alumina, and both are heated at the same rate in a heating block. The temperatures of both are monitored by thermocouples in contact with their bases. Reactions/transitions are indicated by deviations on the resulting thermogram. When the change is complete, thermal diffusion brings the sample back to equilibrium. Hence, the peak (or minimum) temperature indicates when the change is completed. Degradation of the sample leads to a weight change which may cause base-line drift in the thermogram. The rate of heating and mass of the sample (and reference) also affect the thermogram.

4.2.4. SIMULTANEOUS THERMAL ANALYSIS (STA)

Thermal analysis under isothermal and non-isothermal conditions in the

form of DSC, TGA and DTA were found to be useful tools in the study of the thermal properties of the intumescent paints. However, some practical problems were experienced e.g. the crucibles available for DSC were unsuitable since on heating intumescent materials expanded to touch the lid of the crucible, hence giving erroneous results.

TGA and DTA are the two most important thermal techniques used. The two techniques complement each other, and when they are carried out simultaneously on the same sample the thermograms are readily compared and correlation is assured. This is particularly important when the reactions are complex.

In this study, simultaneous observation of mass and DTA was undertaken on a Mettler Thermoanalyser 2 system using a linear heating rate. A schematic illustration of the thermal analysis system is shown in Fig. 18. Simultaneous recordings of the sample mass M(t) (including expanded scale M*(t)), its time derivative $\dot{M}$*(t), the DTA response T(t), the sample temperature $T_s(t)$ and the furnace temperature T_F are obtained, Fig. 17. Sample masses of up to 100mg can be accommodated. In these investigations, due to the intumescence of the sample, masses of approximately 25mg were used in a long-stemmed quartz crucible without a lid. The measurements were conducted in air using a gas-flow rate of 60 cm^3 per min. An investigation of the heating rate revealed 20° per min produced the best differentiation between peaks and clarity in the thermograms Fig. 78-80. Schematic STA curves and the parameters measured from them are illustrated in Fig. 17. These include mass change W, rate of mass change R, heat of reaction H, TGA initiation temperature T_{gi} and peak temperature T_{gp}, and DTA initiation temperatures $T\Delta_i$ and peak temperature $T\Delta_p$.

FIGURE 17

TYPICAL SCHEMATIC STA CURVES

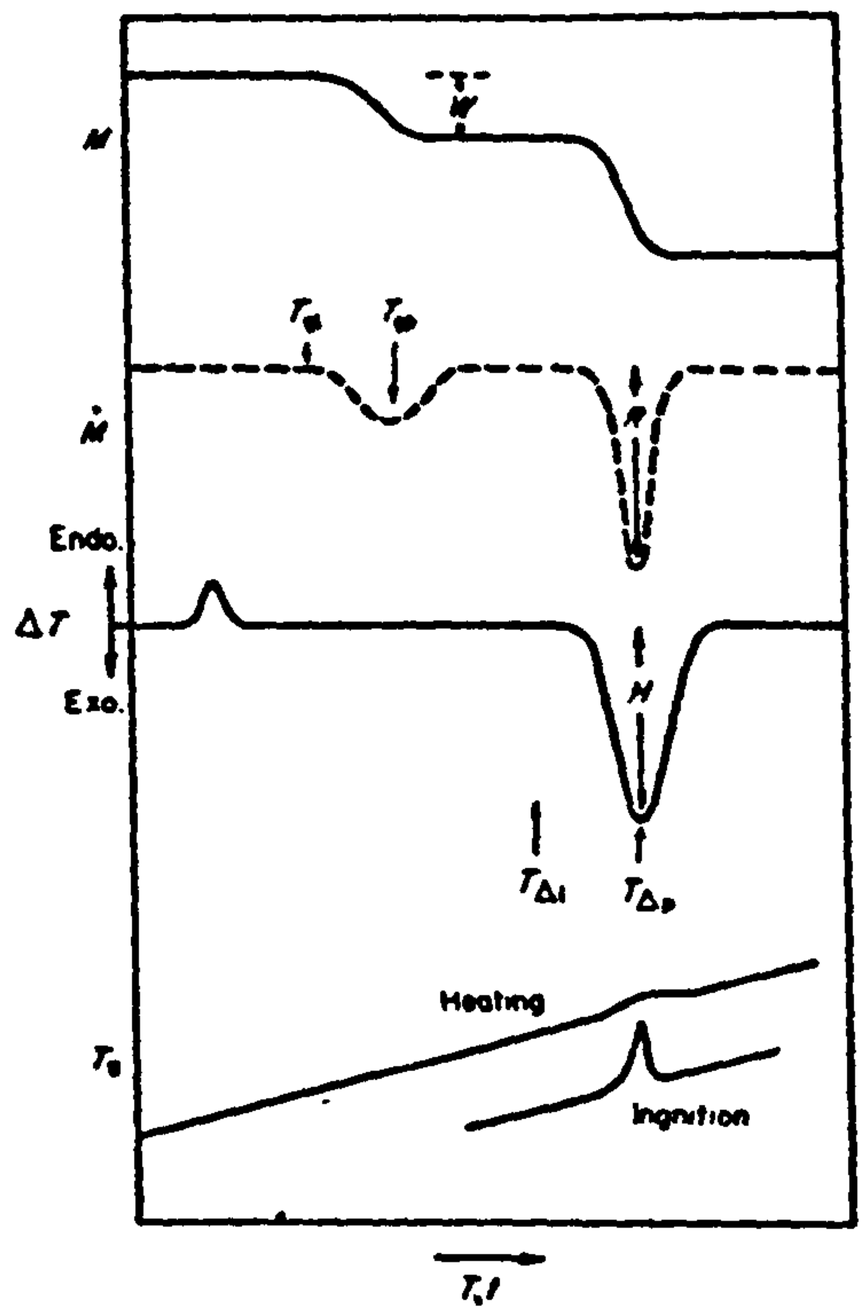

FIGURE 18

SCHEMATIC DIAGRAM OF THERMAL ANALYSIS SYSTEM

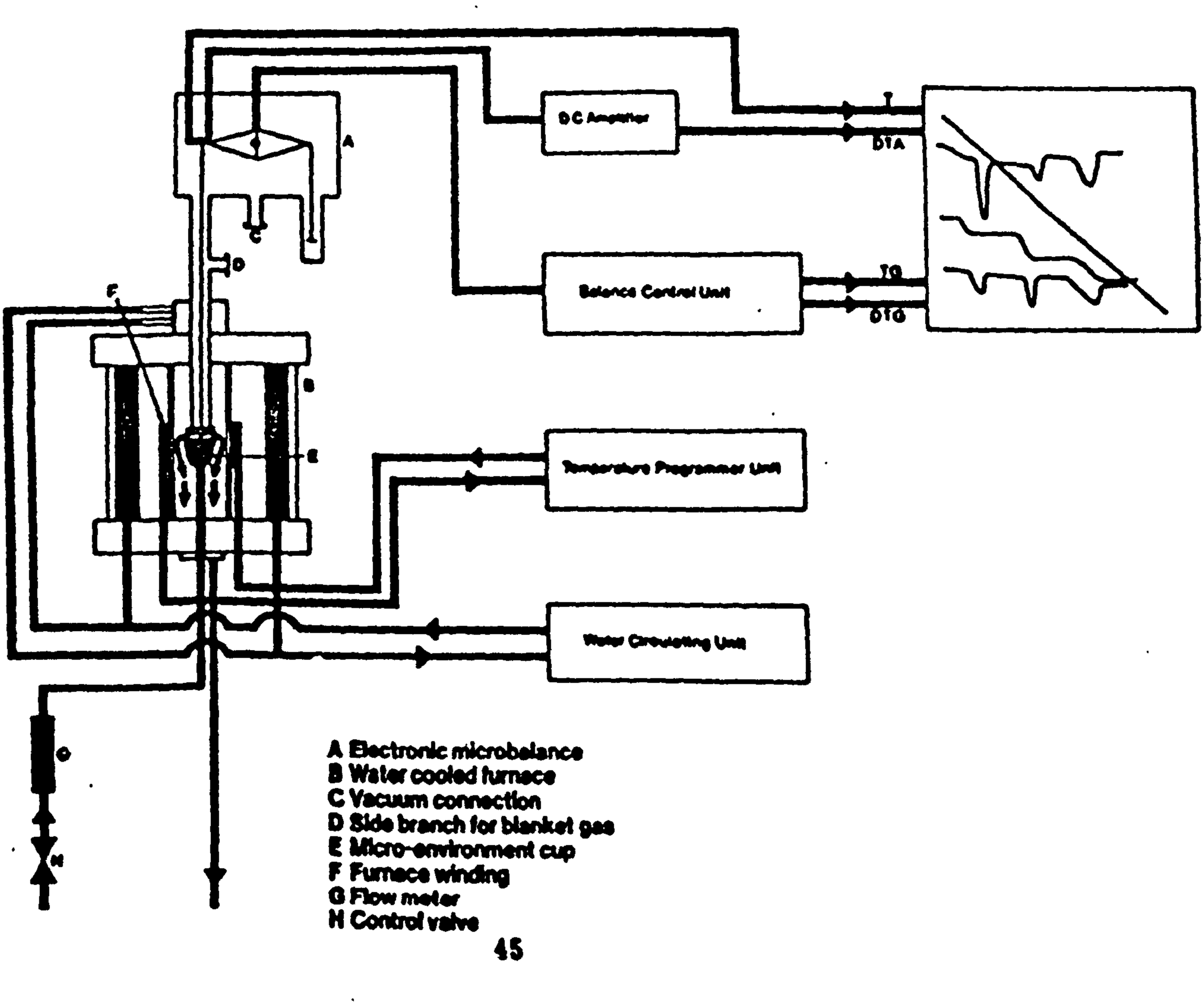

A Electronic microbalance
B Water cooled furnace
C Vacuum connection
D Side branch for blanket gas
E Micro-environment cup
F Furnace winding
G Flow meter
H Control valve

4.3. OTHER ANALYTICAL TECHNIQUES USED

4.3.1. INFRARED SPECTROSCOPY

The infrared instrument used in this study was a Perkin Elmer (Model 683) with data-station support. Potassium bromide dispersion discs were prepared using 1 - 10% of sample.

4.3.2. SCANNING ELECTRON MICROSCOPY (SEM)

A scanning electron microscope and microprobe (Hitachi HX 650) were used. In both techniques, the sample is irradiated with a finely-focused electron beam, which may be static or swept across the surface of the specimen. When the electron beam impinges on a surface, secondary electrons, back-scattered electrons, Auger electrons, characteristic X-rays, and photons of various energies may all be emitted and detected. These signals can be used to examine many characteristics of the sample (composition, surface topography, crystallography, etc.).

The signals of greatest interest in SEM are from the secondary and back-scattered electrons. The three-dimensional appearance of the images is due to the large depth of field as well as the shadow relief effect of the secondary electron contrast. Fig. 19 shows a typical photograph of a sample of coating material after being subjected to fire.

4.3.3. ELECTRON PROBE MICROANALYSIS (EPMA)

Electron probe microanalysis, developed by Casting (96) (1951), is a non-destructive method of elemental analysis of an area only 1 μm in diameter at the surface of a solid specimen. The beam is collimated into a fine pencil of 10 nm cross section and directed at the portion of the surface to be analysed. The electron bombardment excites characteristic X-rays which are then detected. Point-by-point microanalysis can be accomplished by translating the beam across the specimen. In addition,

EPMA has the capability of giving X-ray scanning pictures which show the elemental distribution in the area of interest. Figs. 20 and 21 show a typical elemental distribution and a mapping of phosphorus for an intumescent coating sample. Magnifications of up to 4000 times are possible without exceeding the resolution of the instrument, Fig. 19.

FIGURE 19

A TYPICAL PHOTOGRAPH OF AN INTUMESCENT CHAR

FIGURE 20

A TYPICAL ELEMENTAL DISTRIBUTION OF AN INTUMESCENT COATING

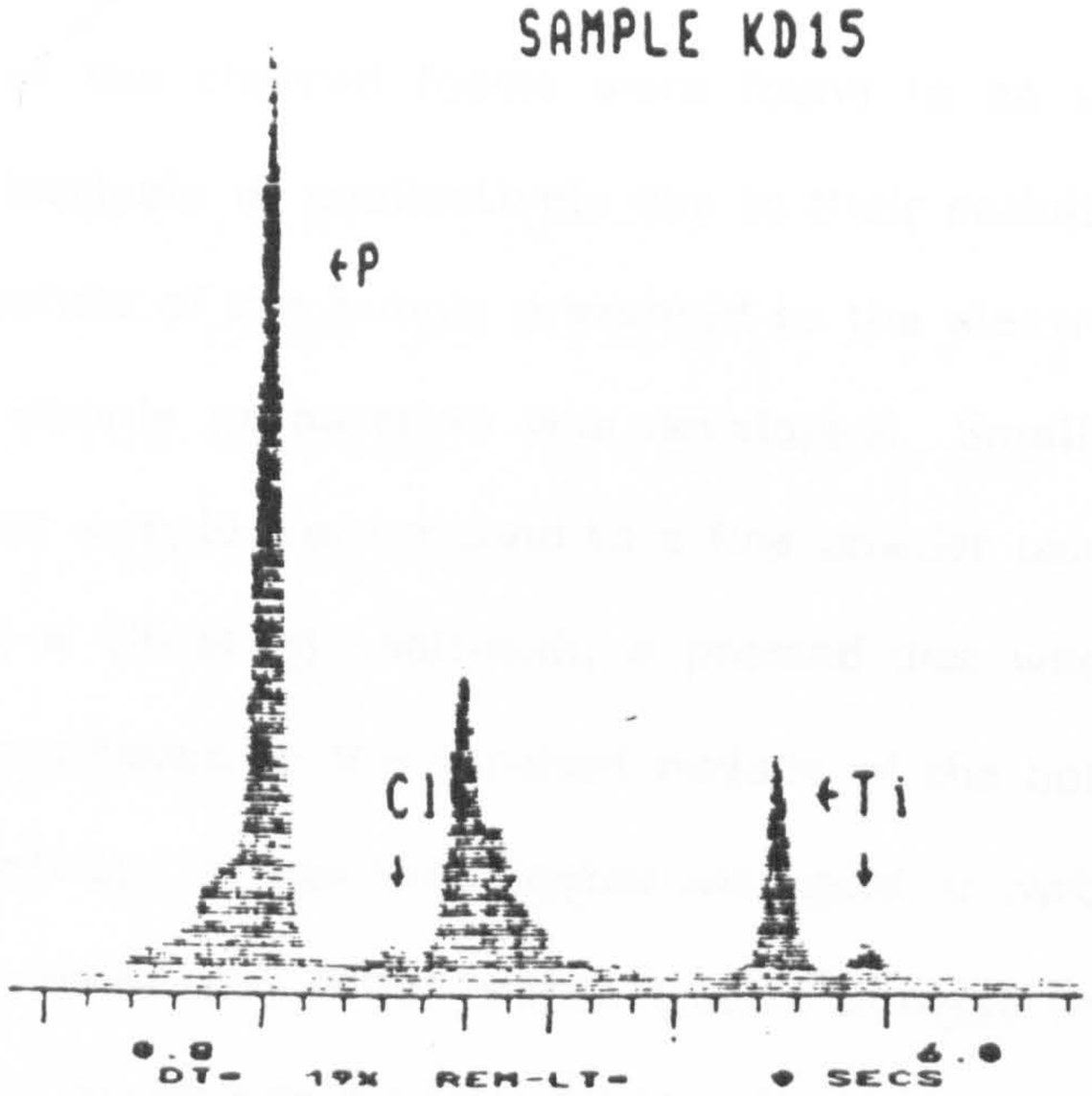

FIGURE 21

MAPPING PHOTOGRAPH FOR PHOSPHOROUS

FROM AN INTUMESCENT COATING

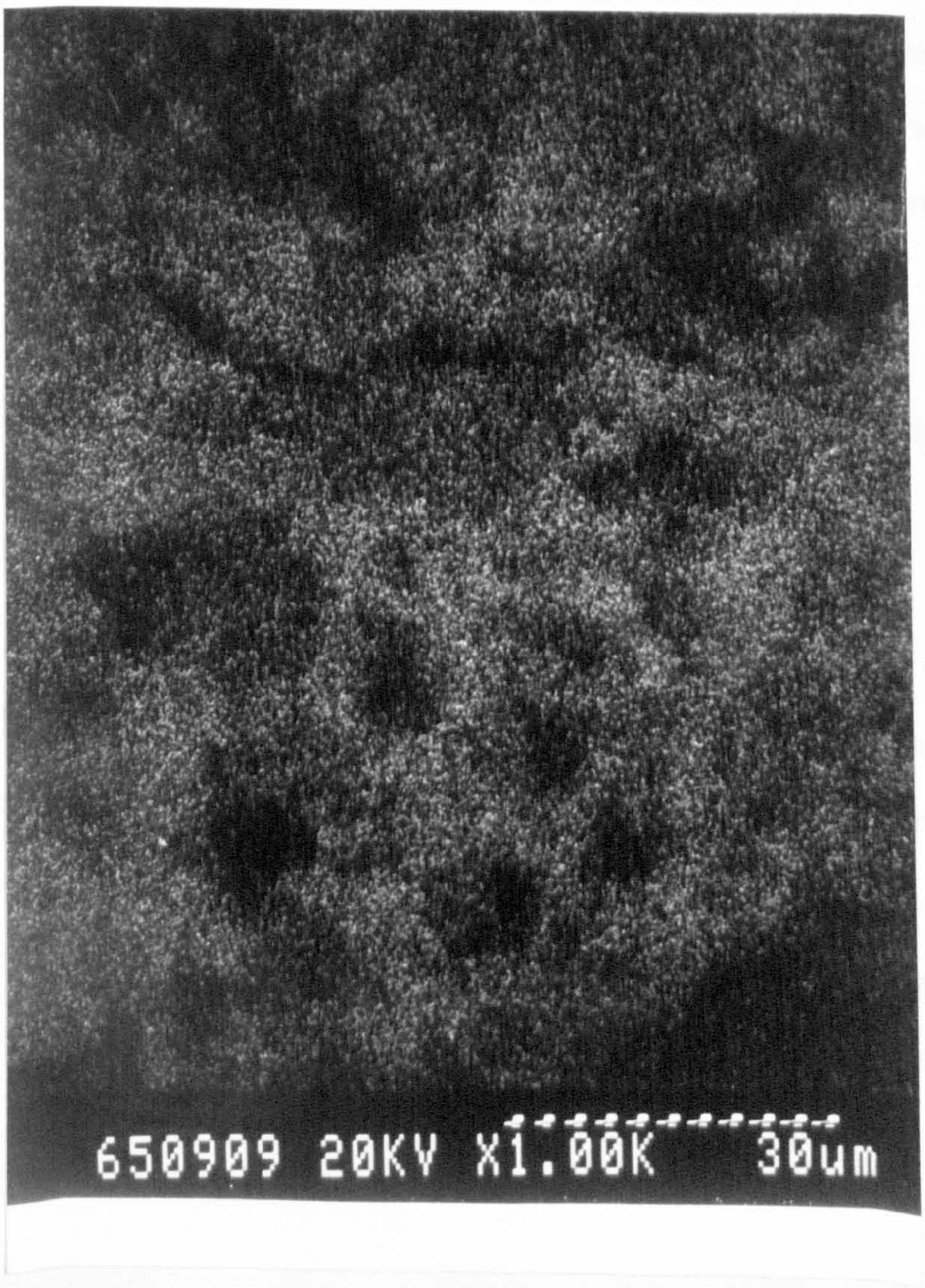

4.3.4. SAMPLE PREPARATION TECHNIQUE FOR SEM & EPMA

The samples of the charred foams were found to be very difficult to analyse quantitatively or qualitatively due to their cellular structure. To improve the nature of the sample presented to the electron probe, a new technique of sample preparation was developed. Small, representative portions of char sample were ground to a fine powder using a mortar and pestle. Using a vibrating ball-mill, a pressed disc was then prepared. Often the disc adhered to the polished surface of the bolt and had to be prised off carefully. It was then coated with gold or carbon as necessary using the high resolution E5400 Polaron Sputter Coater. In order to obtain high resolution, particular attention was paid to the composition of the conducting film. Thus the average grain size for a 7nm thick film was kept below 2-3nm. A gold/palladium target was used. For Energy Dispersive or Wavelength Dispersive Analysis, carbon coating of the specimen was used. The carbon coating attachment, comprising a top plate assembly, replaced the conventional sputter head. The coated sample was kept free of moisture in a desiccator. This technique was found to produce accurate results with good reproducibility.

4.4. TECHNIQUES USED FOR MEASUREMENT OF THE PHYSICAL PROPERTIES OF THE COATINGS

4.4.1. THICKNESS MEASUREMENTS

All the measurements of coating thickness and char height after exposure to the various thermal radiations were made using the Elcometer 256. This is a microprocessor coating-thickness gauge for ferrous, non-ferrous and ferrous/non-ferrous metal substrates. The gauge was used with a 25 mm diameter probe. For greater accuracy and verification of results in case of unevenly intumesced foams, 10mm diameter probe was also used.

A controlled oscillator produces a low-level alternating voltage which energises one coil in a multi-coil probe. This in turn induces a voltage in the coil in close proximity to the first. The magnitude of the induced voltage depends on the distance between the probe and the ferromagnetic substrate (coating thickness). This induced voltage is processed and displayed on a liquid-crystal display, reading directly in micrometres (μm).

Before using the gauge, the zero setting was adjusted using a thick polished-steel base plate. It was re-calibrated using precision calibration non-metallic foils of specific thicknesses. A graph was plotted of the thickness versus the display reading in microns.

The gauge was calibrated each time before use, using calibration foils of similar thickness to that being measured. An average of at least 20 readings was taken per sample. The datawerethen statistically analysed.

4.4.2. CHAR STRENGTH

The char strength was determined from its resistance to crush using an Instron Universal Testing Machine Model 1185 with a capacity of 0 to 100 kN. The Instron was calibrated using the procedures in BS 1610 : 1964, BS 3846 : 1970 and BS 5214 : Part 1 : 1975. The calibration was carried out in the static mode. The load cell used was 1 kN Instron Load Cell Type 2518-204. The crosshead speed and function controller (with push button speed selection over a wide range and in 1% increments), making use of a servo system, was employed.

The intumesced chars were tested either while still on the substrate plate or after removal from the plate. A graph of strain against cross-head speed was plotted. Due to the nature of the sample (cellular), troughs and peaks were observed. The average of these values was used as an

indication of the char strength relative to the control samples.

4.4.3. TEST FOR ADHESION OF THE CHARRED FOAM TO THE METAL PLATE

The adhesion of the charred foam to the metal substrate was recorded by subjective assessments. Observations were made to see if any peeling of the unintumesced paint layer occurred and the continuity of the layer was determined by flaking off the char. Further tests were conducted to determine the strength of the adhesion by using a sharp blade and traversing it across the surface of the char. Ratings ranging from 1 to 5 were used to assess the char strength:

1 - very easy to peel off or already delaminated

2 - easy to peel but with less than 50% continuity of the unintumesced paint layer

3 - char mainly in contact with the substrate

4 - char remaining in place by turning the sample plate upside down and gentle tapping

5 - char requiring a reasonable effort to remove using a scraper blade.

4.4.4. MEASUREMENT OF DENSITY OF THE PAINT

4.4.4.1. INITIAL, BULK DENSITY

The bulk density of the coatings can be determined from the densities of the individual constituents. The bulk density, $\bar{\rho}$, is defined by:

$$\bar{\rho}=\sum x_i \rho_i$$

where ρ_i and x_i are the density and percentage by volume of the total formulation of the i^{th} component.

Another method used involved the preparation of sample plates. The

plates were weighed before and after coating and the thickness of the dry coating and the cross-sectional area of the coatings determined. Density measurements using this method could be substantially less than the theoretical values due to entrapped air bubbles. Hence, great care was taken in the preparation of coatings to avoid air entrapment.

4.4.4.2. FINAL CHAR DENSITY

The final density is related to the total mass lost and the expansion of the coating. The initial mass, m_o, and the final mass, m_f, are given by:

$$m_o = \int_o^{X_o} \rho_o \, dx = \rho_o X_o$$

$$m_f = \int_o^{X_f} \rho_c \, dx = \rho_c X_f$$

where X_o and X_f are the original and final thicknesses of the coating respectively and ρ_o = initial paint density and ρ_c = final char density

$X_f = (E_f)_{max} X_o$ where E_f is the factor for linear expansion.

Hence, using conservation of mass, it may be shown that the char density is given by,

$$\rho_c = \frac{\rho_o (m_f/m_o)}{(E_f)_{max}}$$

$(E_f)_{max}$ is determined from the thickness of the coating before and after intumescence.

4.5. METHODS USED FOR EVALUATING FIRE PERFORMANCE

4.5.1. DEVELOPMENT OF SCREENING TESTS

A simple method to enable screening tests to be carried out rapidly was developed. A standard Bunsen burner with fully-open air intake, and a 25 mm perforated mouth attachment, was used together with a tripod to hold the coated plates face downward over the burner. A ceramic panel 100 mm by 150 mm and thickness 9mm, with an exposed Chromel-Alumel bead facing downwards was placed on top of the coated plate. To ensure adequate thermal contact, bulldog clips were used at either end of the plates. The perforated mouth attachment of the burner spread the thermal impact over the sample, thus avoiding a very concentrated flame impingement which would cause instantaneous intumescence/ablation at the point of contact. Coatings intumescing poorly allowed heat to reach the thermocouple rapidly. The time taken for the temperature of the thermocouple to reach 300°C was recorded and used to indicate the effectiveness of the coating. The char structure, strength, adhesion to the plate, and thickness were examined.

4.5.2. MORE SEVERE SCREENING TEST

A more severe screening test was required in order to differentiate between the good formulations. A laboratory muffle furnace heated to 900°C was used to produce heat fluxes akin to those of the standard BS 476 Part 8. The coated plate with the thermocouple in position was subjected to the furnace heat by placing it over the mouth of the furnace (see Fig. 22). The test was continued until the thermocouple temperature reached 450°C. As previously, the char thickness, structure and adhesion to the plate were examined. Due to the severity of this test, most of the initial formulations developed were found to produce a very friable char with little or no integrity and hence, the test proved very useful. The samples were found to oxidise very easily if left to stand overnight.

FIGURE 22

PHOTOGRAPH OF THE MUFFLE FURNACE TEST

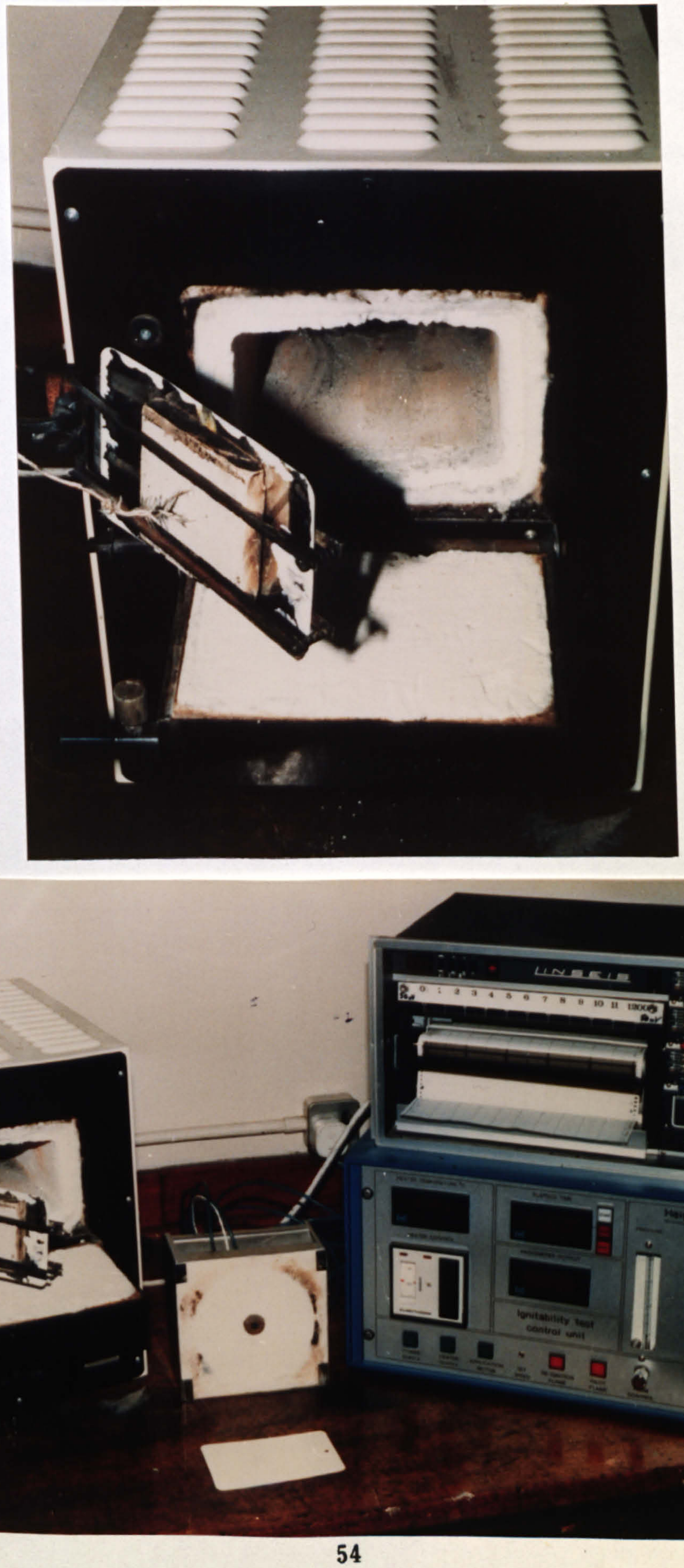

4.5.3. SEMI-CONTROLLED TEST METHOD FOR MODELLING EXPERIMENTS

The development of formulations which could withstand high and severe heat fluxes was accomplished using the above screening tests. These tests enabled the coatings to be subjected to different degrees of severity. The heater source from National Bureau of Standards (NBS) smoke density chamber was used to supply specific heat fluxes (Fig. 23). This allowed the rapid assessement of formulations using accurately-controlled heat fluxes and yet was simple to apply.

FIGURE 23

NBS SMOKE DENSITY APPARATUS HEATER TEST

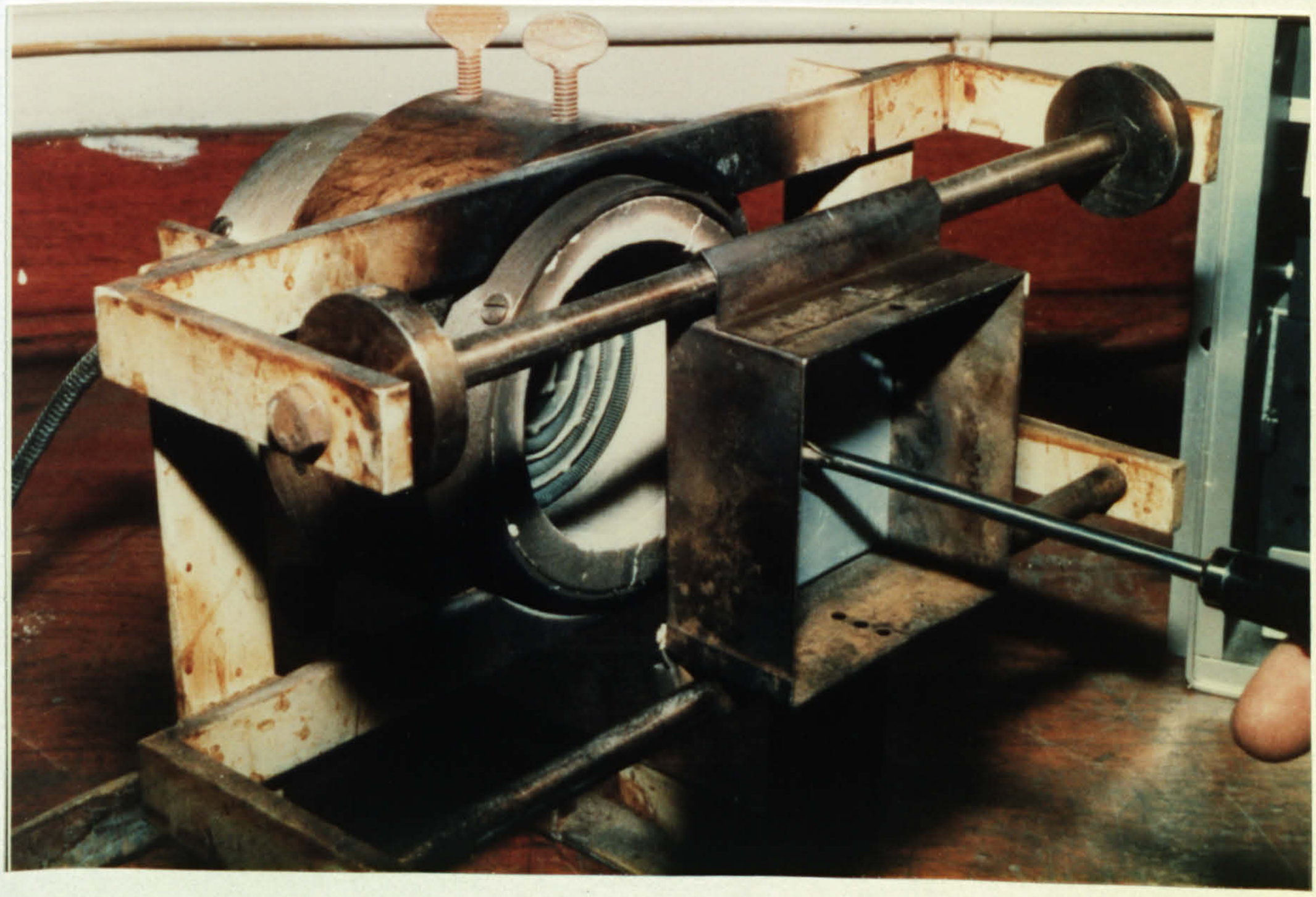

4.5.4. THE ISO IGNITABILITY APPARATUS

The ISO ignitability apparatus (97), as developed by the International Standards Organisation (ISO) for the testing of building materials, (Fig. 24), was also used for this research. The time to ignition of a sample when exposed to known radiation intensities is measured. The sample is placed horizontally and irradiated from above. A pilot flame is introduced at regular intervals at a position 10mm above the centre of the specimen in order to ignite any volatile gases liberated by the sample. The time taken up to the sustained ignition of the sample is noted. If the sample does not ignite within 15 minutes, the test is stopped. The time to ignition is plotted as a function of the radiation intensity.

The apparatus consists of a stainless steel support framework to which the test specimen is horizontally clamped between a pressing plate and a masking plate, such that a defined area of the upper surface of the specimen only is exposed to the radiation. Fig. 25 shows the general view of the apparatus. This radiation is provided by a radiator cone positioned above the specimen. The radiator cone consists of a heating element (Fig. 25) of nominal rating 3 kW contained within a stainless steel tube (4000 mm long and 8.5 mm diameter) which is coiled into the shape of a truncated cone and fitted inside a shade. The radiator is capable of providing radiation in the range 1 - 5 W/cm^2 at the centre of the aperture of the masking plate and in a reference plane which is parallel to the masking plate. The distribution of radiation over the reference plane is such that the variation within a circle of 50 mm diameter (drawn from the centre of the aperture) is within 2% of the radiation level at the centre and the variation within a circle of 100 mm diameter is within 2-10% of that at the centre. The cone is located and secured by vertical guide-rods, the lower rim of the radiator cone shade being 22 mm above the

upper surface of the masking plate.

An automated pilot flame application mechanism was used to bring the flame through a hole at the top of the radiator cone to a position just above the centre of the surface of the specimen. The mechanism was also capable of taking the pilot flame on through the aperture in the masking plate. The re-ignition point of the pilot flame was above the radiator cone and well clear of the smoke plume and combustion products which rose through the top of the cone. A specimen insertion and location tray was used to facilitate rapid and accurate positioning of the specimen in the apparatus. Initially, a screening plate shielded the specimen from radiant energy until the commencement of the test.

A single phase automatic voltage stabilizer with a nominal rating of approximately 3 kW was used, which was capable of maintaining the accuracy of the output voltage to within 1% over its entire range. The variable transformer was capable of handling a maximum of 3 kW and of regulating the voltage output linearly over the entire range.

The wattmeter used was capable of measuring up to 3 kW. The millivolt meter was compatible with the output from the radiometer. It had a sensitivity and accuracy which enabled the radiation to be determined to within 0.05 W/cm^2. Fig. 26 gives a diagrammatic arrangement of apparatus.

FIGURE 24A

ISO IGNITABILITY APPARATUS

FIGURE 24B

PHOTOGRAPH OF ISO APPARATUS SAMPLE BEING PLACED IN POSITION

FIGURE 25

GENERAL VIEW OF IGNITABILITY TEST APPARATUS

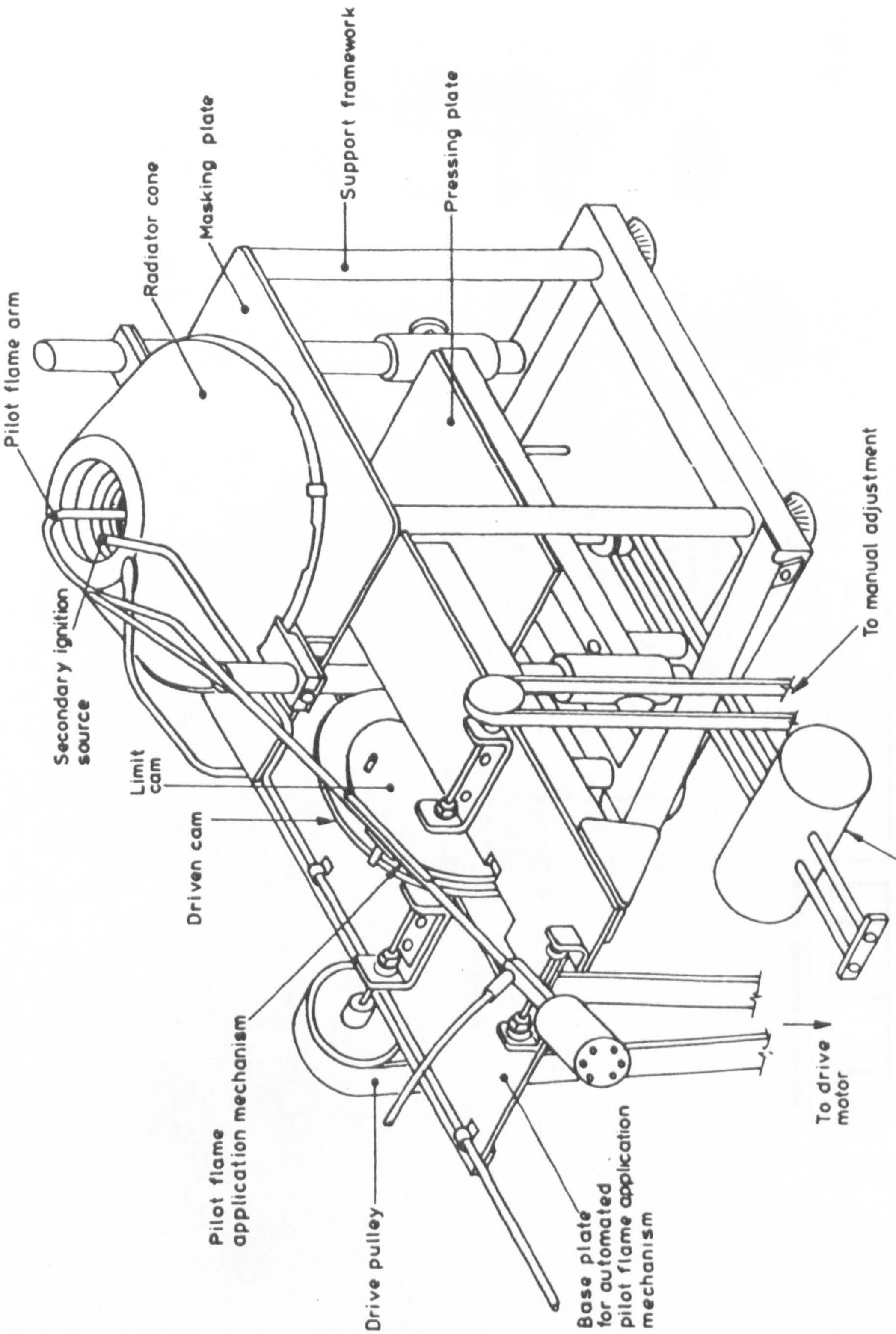

FIGURE 26

DIAGRAMMATIC ARRANGEMENT OF APPARATUS

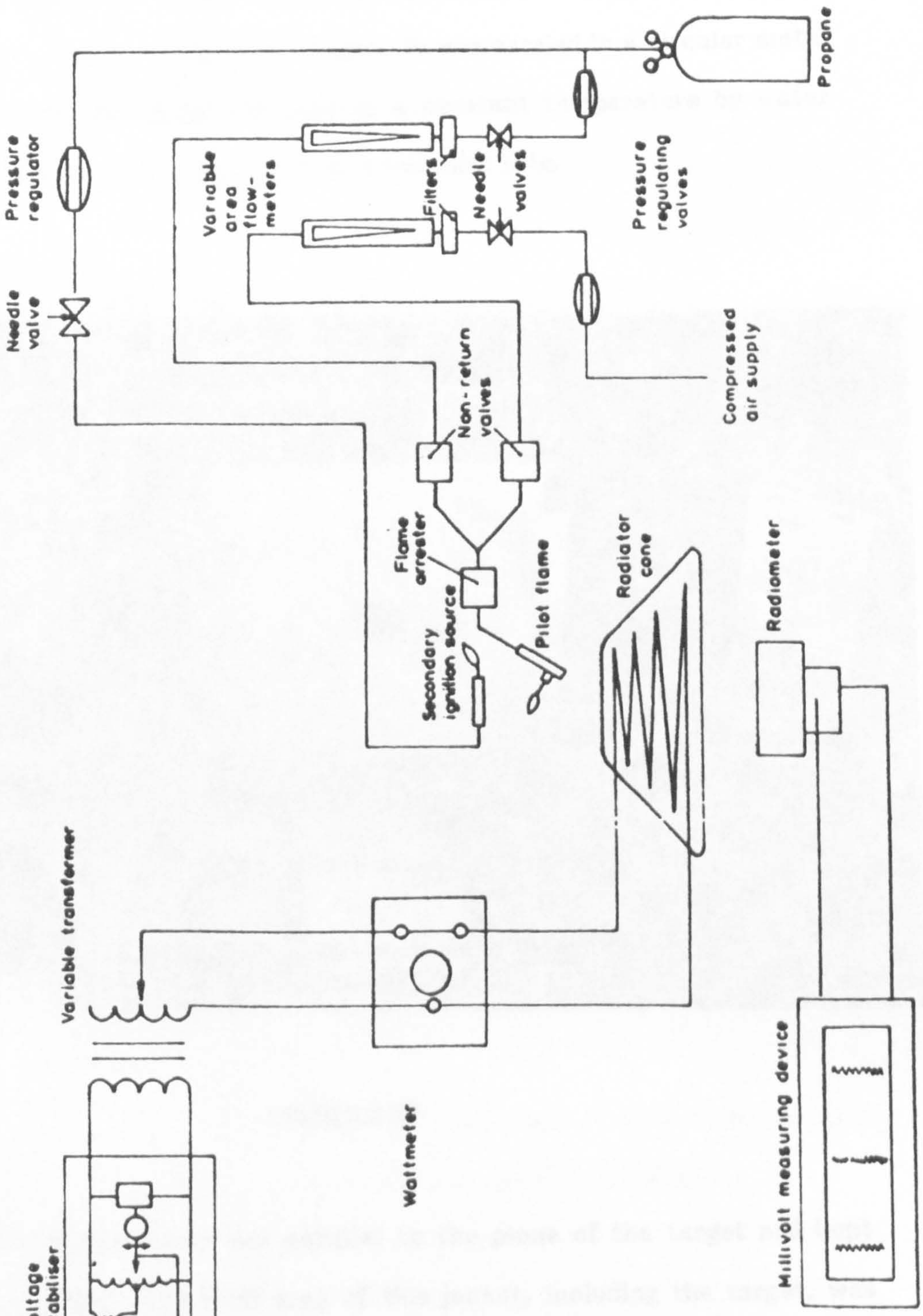

The radiometer used was capable of measuring radiation within the range 1 - 5 W/cm^2, Fig. 27 (98, 99). The time constant was not more than 3 s (this corresponding to about 10 s to reach 95% of the final output). The target receiving the radiation was circular, flat, 10 mm in diameter and coated with a durable matt black finish. It was carried in a circular metal jacket of diameter 25mm and kept at a constant temperature by water flowing through the cooling jacket at a constant rate.

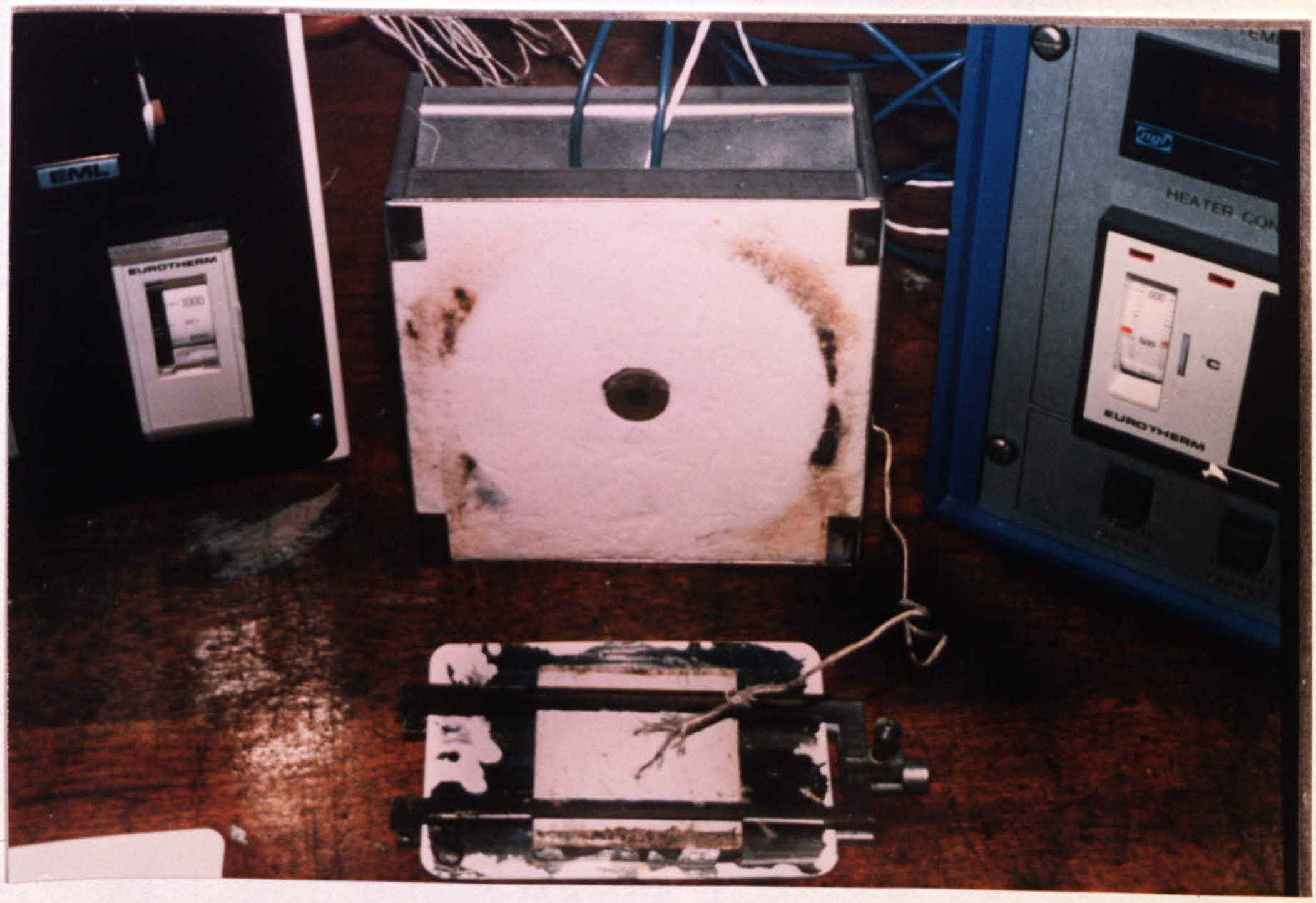

FIGURE 27

The face of the jacket was parallel to the plane of the target and kept highly polished. The total area of this jacket, including the target, was less than 80 mm^2. The radiometer was mounted in a calibration board held by a supporting framework which when placed on the pressing plate positioned the target centrally beneath the radiator cone. The calibration

board was made of 25 mm thick ceramic fibres of density 200 kg/m^3. Great care was taken, at all times, to ensure that the face of the radiometer was not scratched or damaged as this could significantly affect the calibration of the instrument. A protective cover was placed over the face of the radiometer when it was not in use.

The calibration of the radiometer (Fig. 28) was conducted using a radiation source at a temperature of approximately 850°C and against a reference instrument previously calibrated by the Fire Research Station, U.K. The sensitivity of the radiometer is known to alter slightly with use, therefore re-calibration was necessary before every test.

A calibration graph of the radiation measured at the centre of the surface of the specimen (W/cm^2) against the power input to the radiator (W) was made. Hence, the power inputs corresponding to levels of 1 W/cm^2, 2 W/cm^2, 3 W/cm^2, 4 W/cm^2 and 5 W/cm^2 were determined. The accuracy of the instrument was established by repeated calibration at increasing input levels and then at decreasing input levels. The values were repeatable to within 2% of the nominal radiation thus indicating that there were no defects in the control or monitoring equipment, and no significant changes in the test environment.

Figs. 29 - 32 show the graphs of the indicated temperatures on the equipment as a function of the radiometer output and irradiance.

FIGURE 28

DETAILS FROM CALIBRATION CERTIFICATE

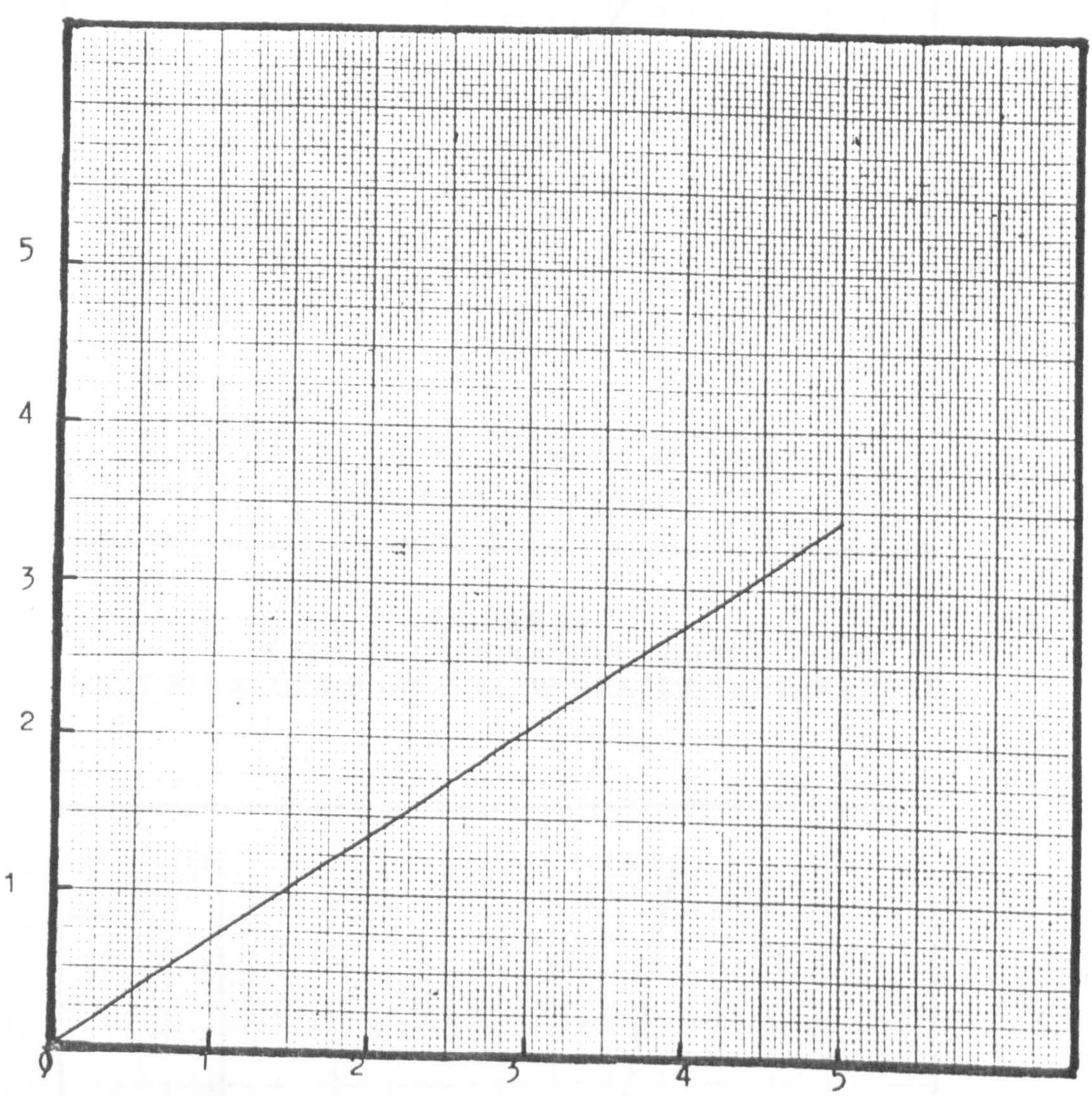

Sensitivity: 1 W/cm^2 = 0.686 mV

FIGURE 29
TYPICAL CALIBRATION CURVE
HEAT FLUX AS A FUNCTION OF HEATER SET POINT

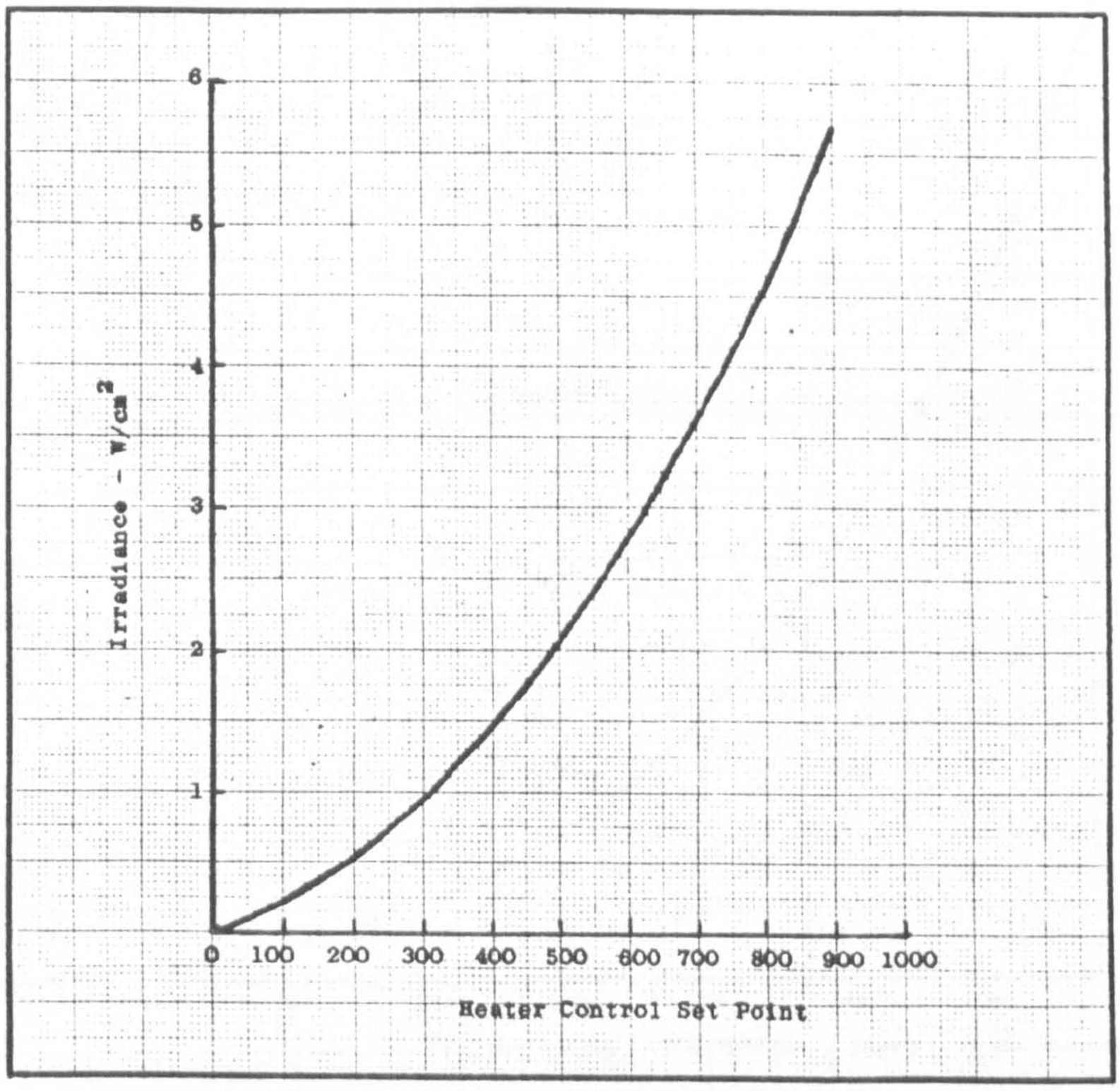

FIGURE 30
TYPICAL CALIBRATION CURVE
HEAT FLUX AS A FUNCTION OF HEATER TEMPERATURE

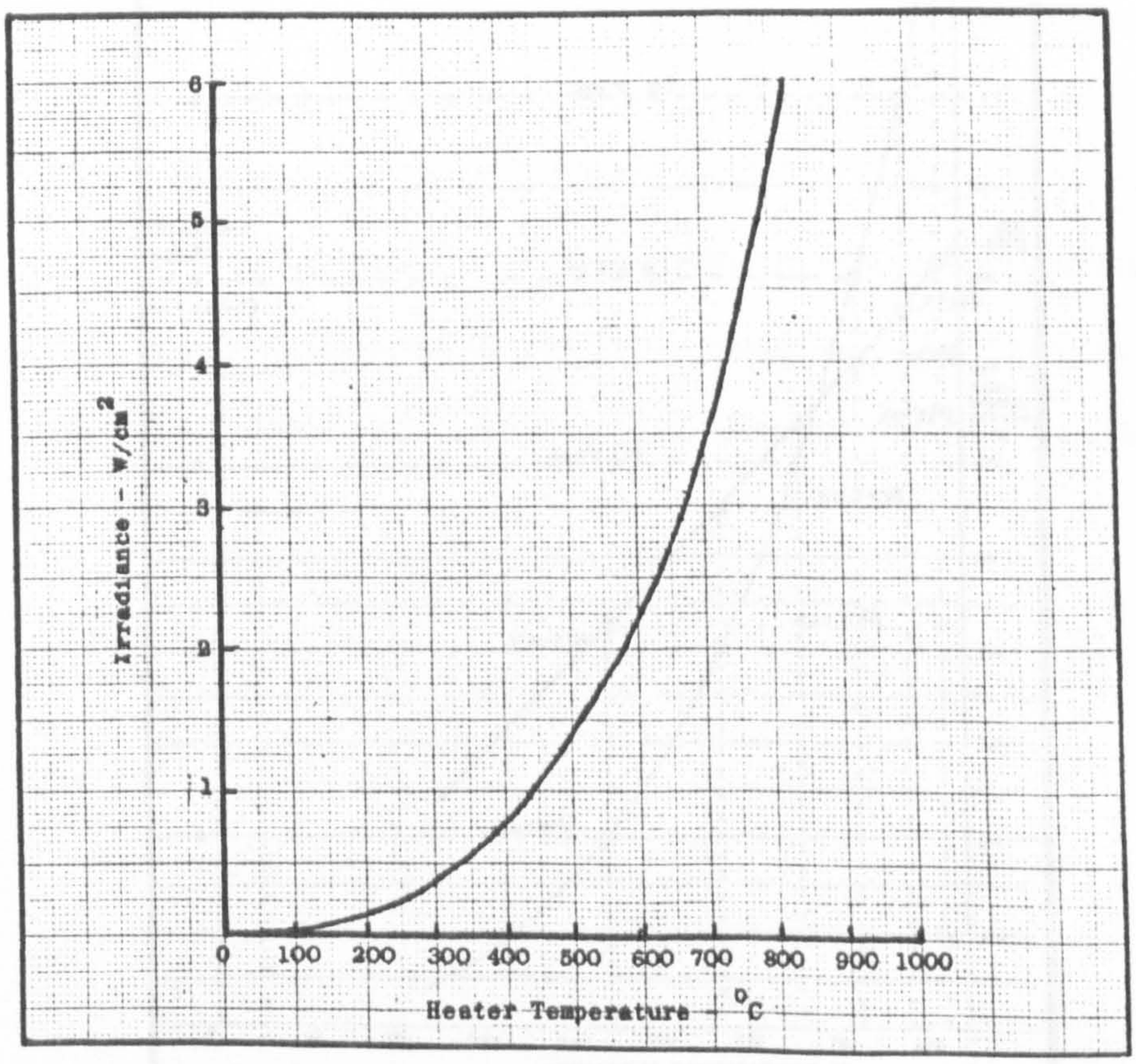

FIGURE 31
RADIOMETER OUTPUT AS A FUNCTION OF TEMPERATURE (SECONDARY THERMOCOUPLE)

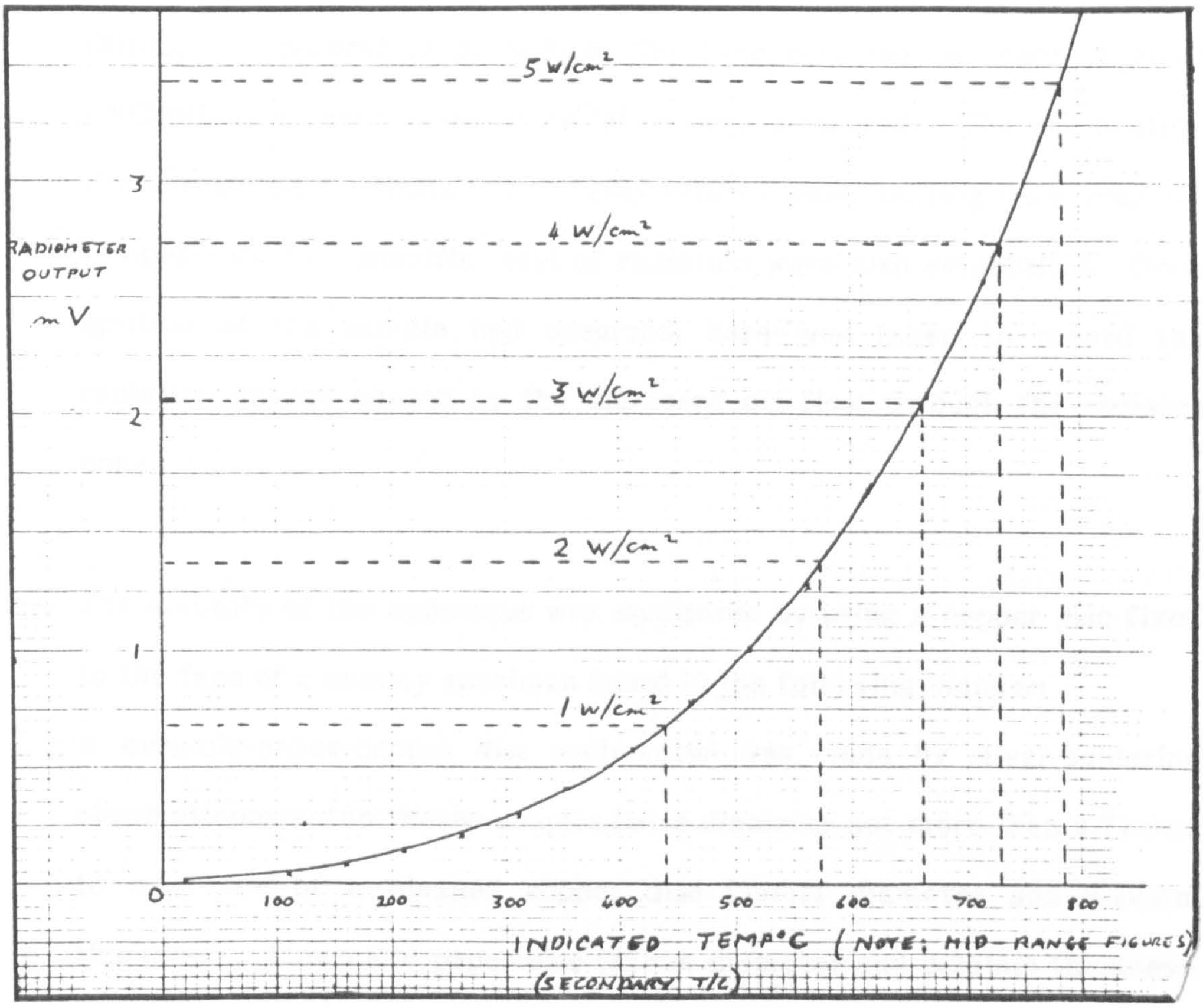

FIGURE 32
IRRADIANCE AS A FUNCTION OF MID-RANGE TEMPERATURE

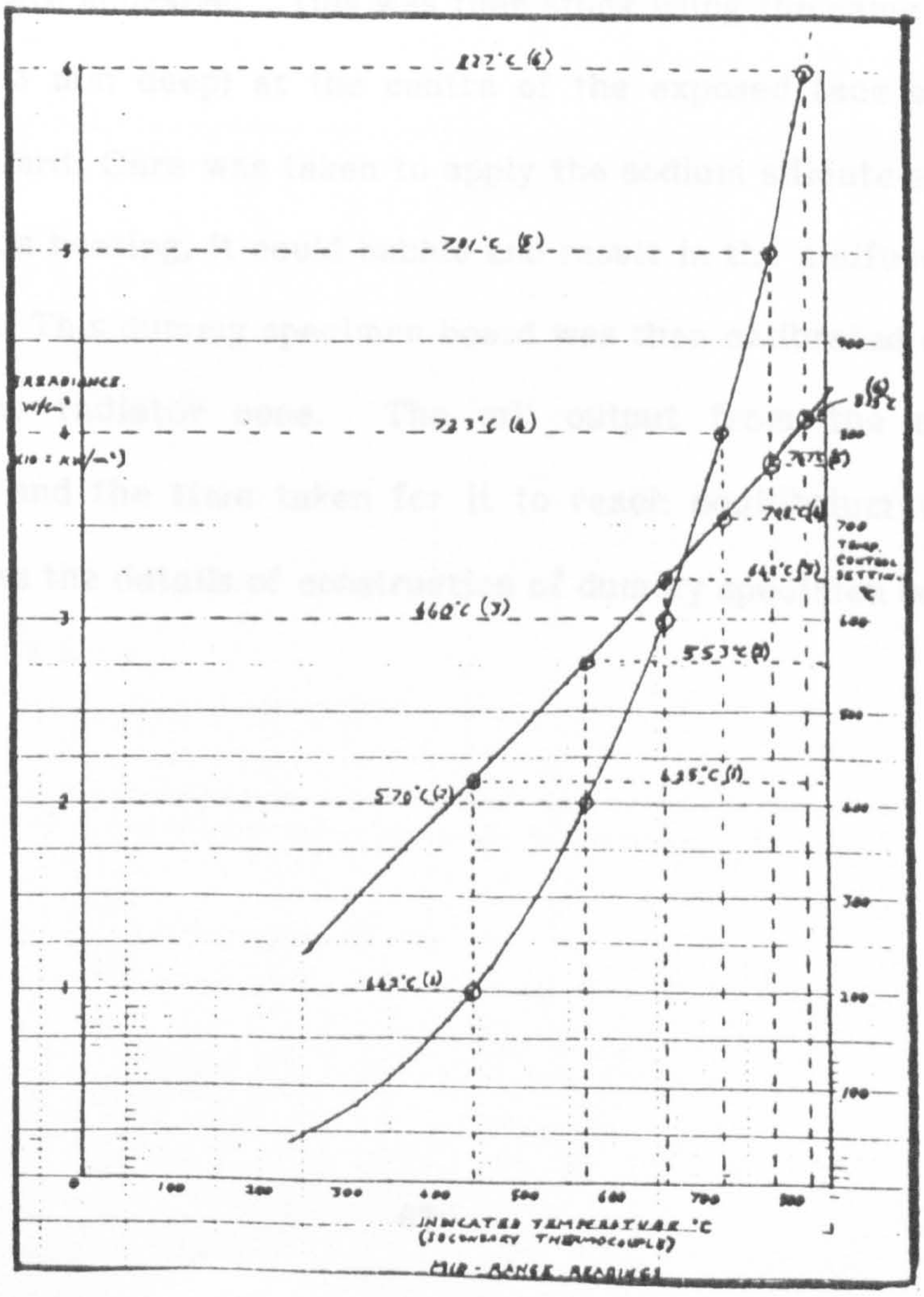

During the calibration procedure, the time required to reach thermal equilibrium at each level of radiation was measured. The pre-heating times required to obtain stable temperatures when heating from ambient temperature to a specific level of radiation were also established. Once ignition of the sample had occurred, care was taken to record the radiation change caused by the increased air flow through the radiator cone.

The stability of the apparatus was monitored by using a copper disc fixed to the face of a dummy specimen board in the following manner:

A ceramic-paper-copper disc radiometer was made by silver-soldering chromel/constantan thermocouples (wire diameter not more than 0.71mm) to one face of a cleaned copper disc (25mm diameter and 0.20mm thickness). A ceramic-paper disc (25mm diameter and 0.25mm thickness) was stuck to the same face of the copper disc as the thermocouple using a sodium silicate adhesive. This was then stuck using the same adhesive in a recess (0.3 mm deep) at the centre of the exposed face of a dummy specimen board. Care was taken to apply the sodium silicate sparingly, as otherwise, on heating, it could bubble and result in the malfunction of the radiometer. This dummy specimen board was then calibrated at the same time as the radiator cone. The mV output from the copper disc radiometer and the time taken for it to reach equilibrium were noted. Fig. 33 shows the details of construction of dummy specimen board.

FIGURE 33

DETAILS OF CONSTRUCTION OF DUMMY SPECIMEN BOARD

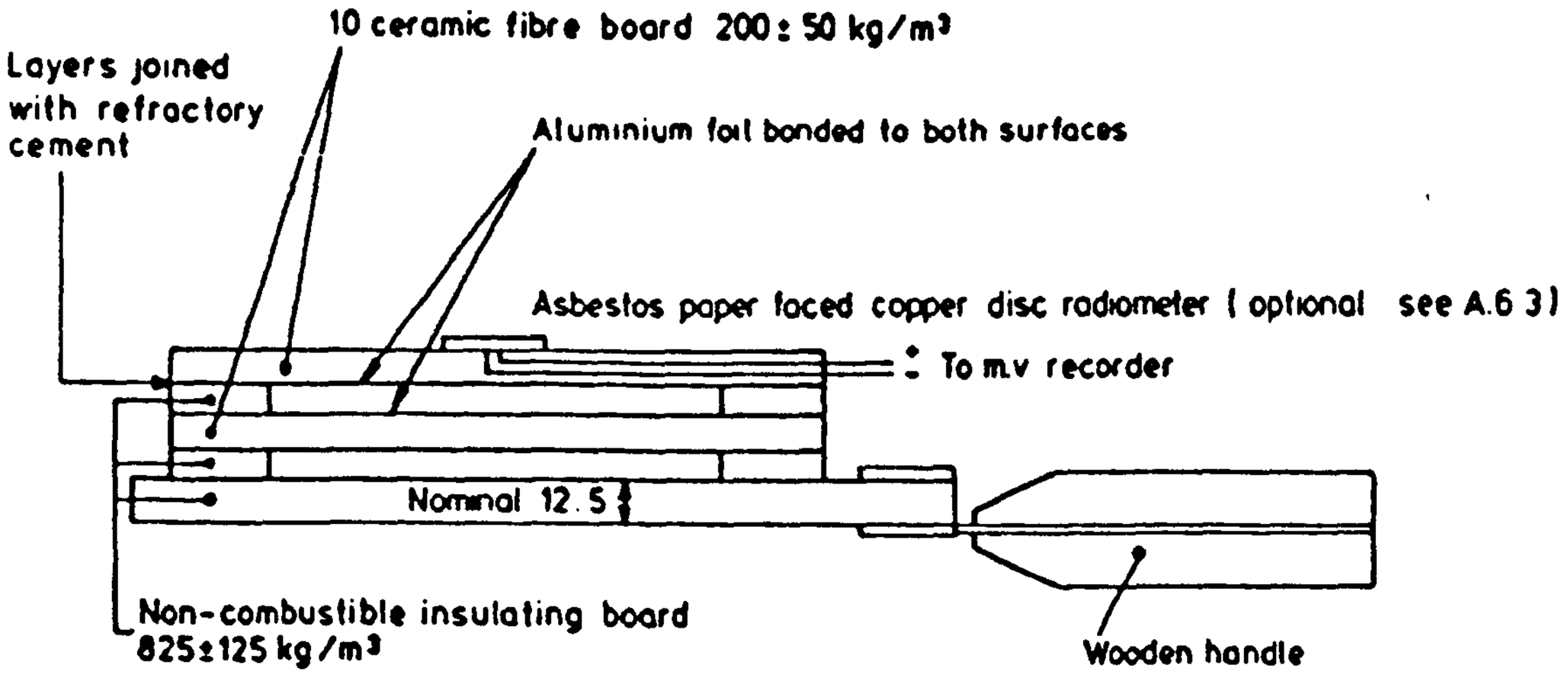

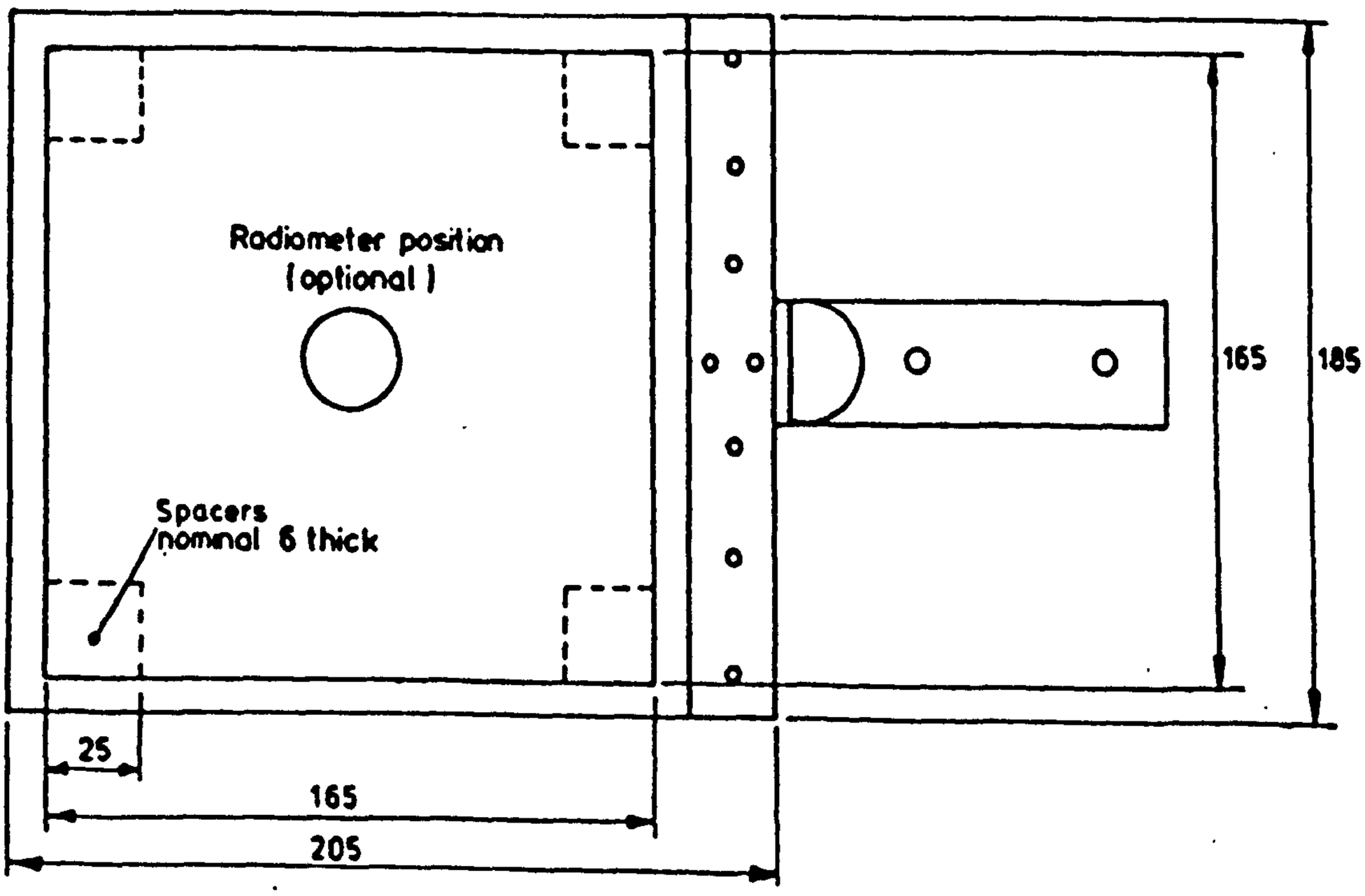

All dimensions are in millimetres.

The apparatus was set up in an unused fume cupboard with the extraction switched off and hence was essentially free of air currents and protected by a screen, as seen in Fig. 34. The screen was used to avoid any air turbulence which might occur during the emission of the effluent gases from the apparatus.

FIGURE 34

EXTRACTION HOOD AND DRAUGHT SCREEN

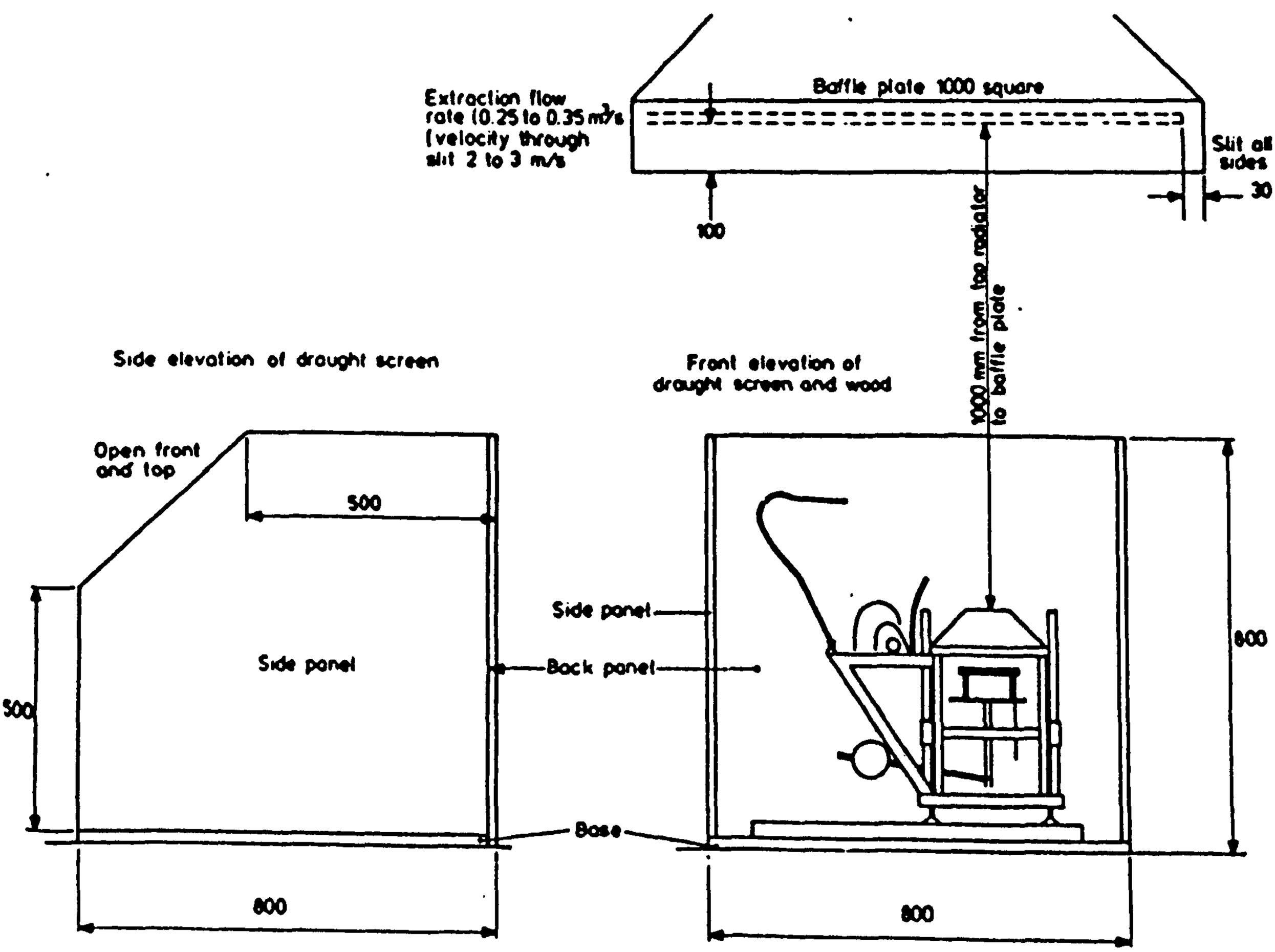

All dimensions are in millimetres.

SECTION 5

THERMAL ANALYSIS AND REACTION KINETICS

5.1. INTRODUCTION

The thermal behaviour of intumescent coatings, their ingredients, and mixtures of these, provides information relating to their reactions, mechanisms and kinetics of degradation.

In order to understand intumescence, it is helpful to know:

i) The change of molecular weight of the polymeric content as a function of temperature.

ii) The qualitative and quantitative composition of the volatile and non-volatile degradation products.

iii) The rates and activation energies of the degradation processes.

Unfortunately very little has been published on these. In general, it would appear that the molecular weight drops initially very rapidly during the first few per cent loss of weight, but beyond this it is slow (80, 86). Some polymers, for example polyvinyl chloride, on pyrolysis yield fragments not related in structure to the chain from which they are derived, along with fragments that are parts of the chain, whereas in the case of polyethylene pyrolysis yields a spectrum of hydrocarbon fragments (81, 82, 87-90). Most polymer pyrolysis studies reported in the literature (83-85) relate to temperatures up to about 400 - 500°C, although some experiments have been conducted up to 900°C. As expected, the results indicate that the higher the temperature the greater is the fragmentation. In general, the rate of degradation in the temperature range of 200-500°C tends to double for every 10 degree rise in temperature (94-95).

5.2. THERMAL ANALYSIS

A large number of compounds alone and in combination at a variety of concentrations were tested in various formulations in order to optimise the intumescent properties. Materials in each of the four major categories i.e. catalyst, spumific, carbonific, binder, were studied. Different vehicles and vehicle combinations were subjected to thermal analysis in order to determine their softening temperature, melting point, decomposition and char characteristics. Critical pigment volume concentration and pigment volume concentration were used. Thermal properties, such as softening, melting, etc. must be measured at a temperature lower than the decomposition temperature for the mixture. Very low levels of binder were found to affect the intumescence properties significantly. The decomposition temperatures and associated enthalpy changes are critical, as confirmed by the theoretical approach.

5.3.1. CHEMISTRY AND DEVELOPMENTS OF BINDERS

A large selection of polymers and their blends, especially with thermoplastic materials, has been mentioned in the literature. Use of rubbers such as nitrile, silicone are cited in the literature (100,101). Vinyl and vinylidene chloride copolymers were developed by Stilbert et al (102). A wide variety of resinous binders have been considered satisfactory, e.g. butylated melamine formaldehyde, epoxy-type polyesters, chlorinated rubbers, chlorinated and non-chlorinated alkyds, vinylidene chloride and the cellulose ethers. A systematic evaluation of organic-solvent soluble resins was made.

Binders can be divided into two general categories: non-convertible and convertible. Both types are dissolved in a suitable solvent. Upon application to a surface, the solvent evaporates leaving in the case of

non-convertible binders, a film which does not undergo any significant change on continued exposure. In the case of convertible binders, when the solvent evaporates the resin film hardens, primarily through oxidation and polymerisation induced by exposure to air.

The non-convertible resins form films which can be redissolved in the solvent initially used, whilst convertible resins form films which cannot be redissolved. Typical non-convertible binders are saturated-oil modified alkyds, e.g. castor, cotton, coconut etc; nitrocellulose; cellulose ethers; chlorinated rubber; reprocessed rubber; polyvinyl chloride; polyvinylidene chloride; acrylic and methacrylic esters and styrene butadiene.

Typical convertible resins are unsaturated-oil modified alkyds; phenolics; epoxies; chlorinated alkyds; some polyesters; polyamides; polyurethane and amine resins, melamine and urea formaldehyde.

In this study, it was found that, in general, thermosetting resins are to be avoided since they have a detrimental effect on intumescence after exposure to the atmosphere. In some cases, this effect was not observed until after several weeks or months. The use of a small amount of this type of resin, with the major component being a thermoplastic, was desirable in some formulations since superior water- and abrasion-resistance properties were exhibited.

The thermoplastic resins which have proved satisfactory are: styrene butadiene copolymers; vinyl toluene/acrylic copolymers; non -oxidising alkyds; acrylic solution polymers; ethyl hydroxyethyl cellulose and ethyl cellulose.

The higher molecular weight polymers were preferred since they imparted greater water, impact and abrasion resistance although a compromise between performance and resin-solution viscosity must be made. Chlorinated rubber resins included at low concentrations increased film serviceability. Although these resins are not recommended as the major binder, they can be used beneficially to improve the flame-retardant properties of intumescent coatings.

5.3.2. EXPERIMENTAL ANLYSIS OF BINDERS

Most of the polymers used in this study were obtained as commercial products. Most of the samples were in the form of powders.

Polyvinyl chloride - This was a sample of Corvic from Imperial Chemical Industries Ltd; Polyvinyl acetate - Distillers Ltd; Polyvinyl alcohol - Vinyl Products Ltd; Polyacrylonitrile - Imperial Chemical Industries Ltd; Chlorinated polyvinyl chloride - Rhenoflex - Dynamit Aktien Gesellschaft; Chlorinated rubber - Alloprene R 20 - ICI Ltd and Parlon S 20, Parlon VATCL - Goodyear Ltd; Ethyl cellulose - Monsanto Ltd and Polystyrene - Brunel University.

In the thermogravimetric analysis, samples were heated to about 850°C using an inert atmosphere and air. The appearance of the char residue was quantified by the following physical parameters: colour, lustre under UV light, relative compressibility, structural arrangement (fibrous, honeycombed, etc.), porosity, particle size etc.

5.3.3. RESULTS AND DISCUSSION

Typical of the thermal degradation pattern of a chloro-polymer are those observed for Alloprene R 20 and Parlon S 20 Fig. 35. There are two distinguishable stages which occur. The first is completed by about 300°C

and consists essentially of the loss of hydrogen chloride.

$$(\text{-}CH_2\text{--}CHCl\text{--})_n \longrightarrow (\text{-}CH{=}CH\text{-})_n + nHCl \qquad (5.1.)$$

Using the EPMA technique for elemental analysis, the loss of chlorine was followed, Fig. 36. The second stage, which occurs between 300°C and 500°C, is due to the loss of hydrogen, methane and other small hydrocarbons with predominantly carbon being left at 900°C.

FIGURE 35

TYPICAL THERMOGRAMS OF ALLOPRENE R20 AND PARLON S20

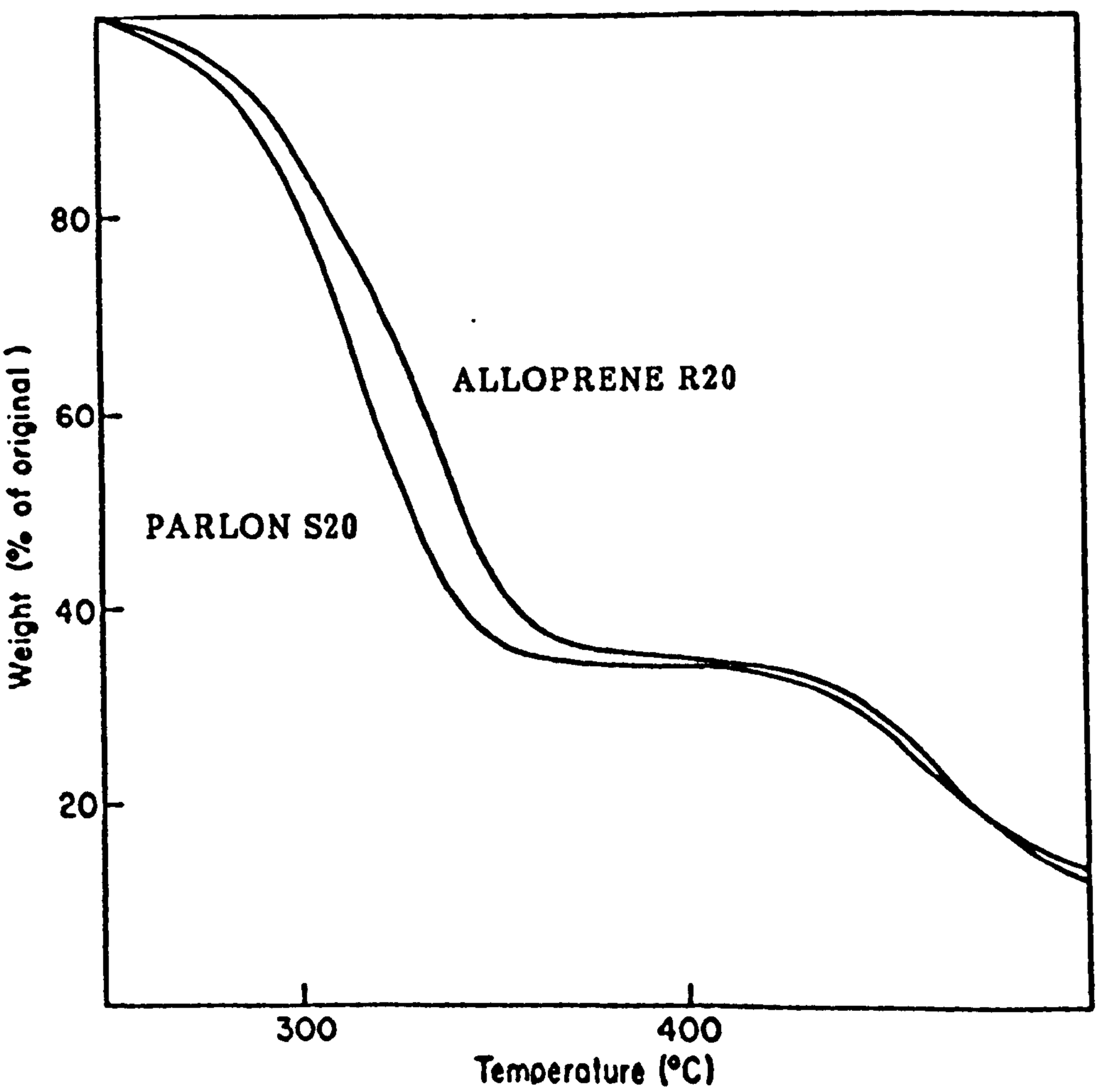

FIGURE 36

LOSS OF CHLORINE FROM ALLOPRENE BASED FORMULATION

AFTER EXPOSURE TO 20 KW/m^2

AFTER EXPOSURE FOR 5 MINUTES

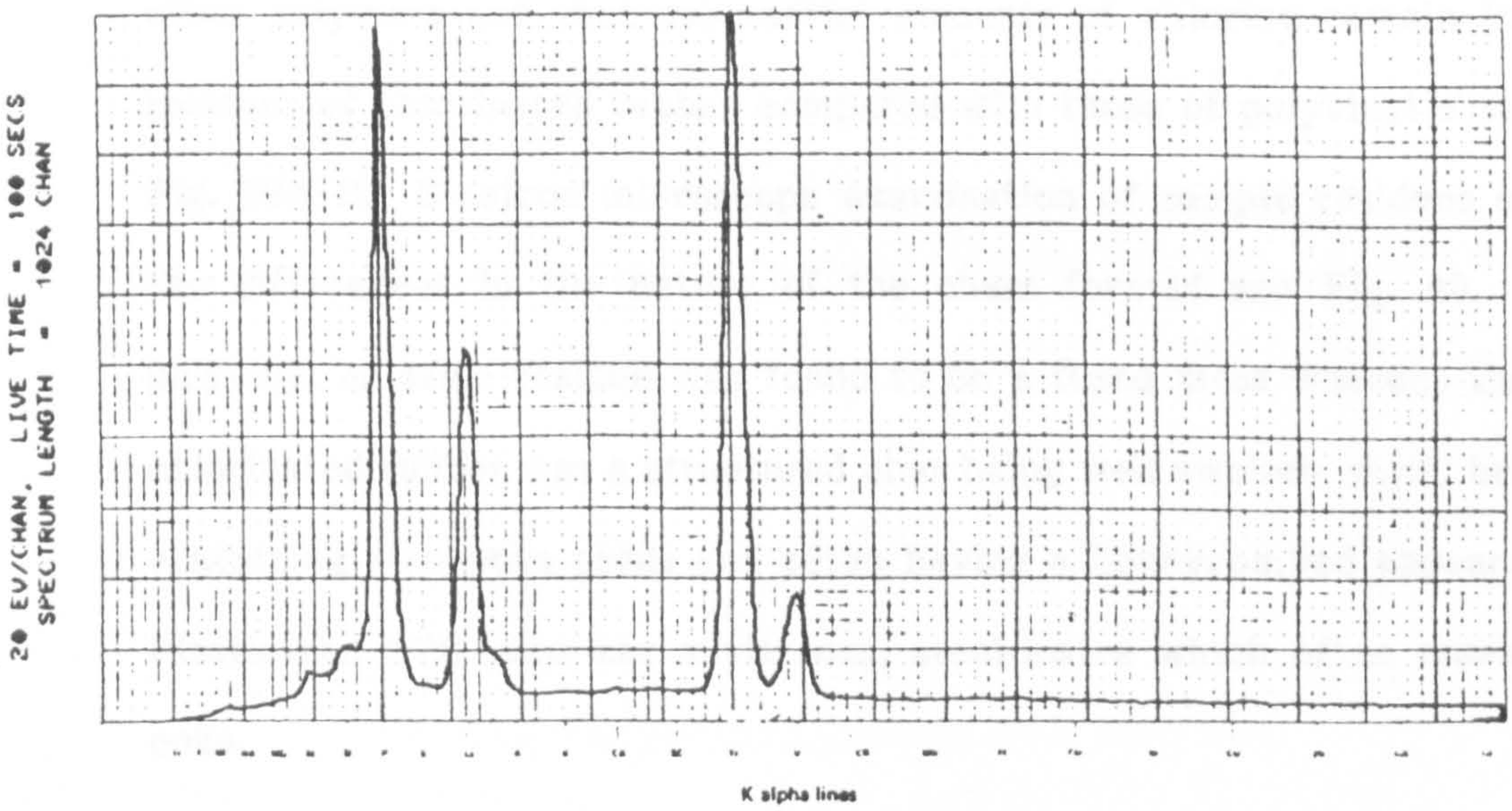

AFTER EXPOSURE FOR 10 MINUTES

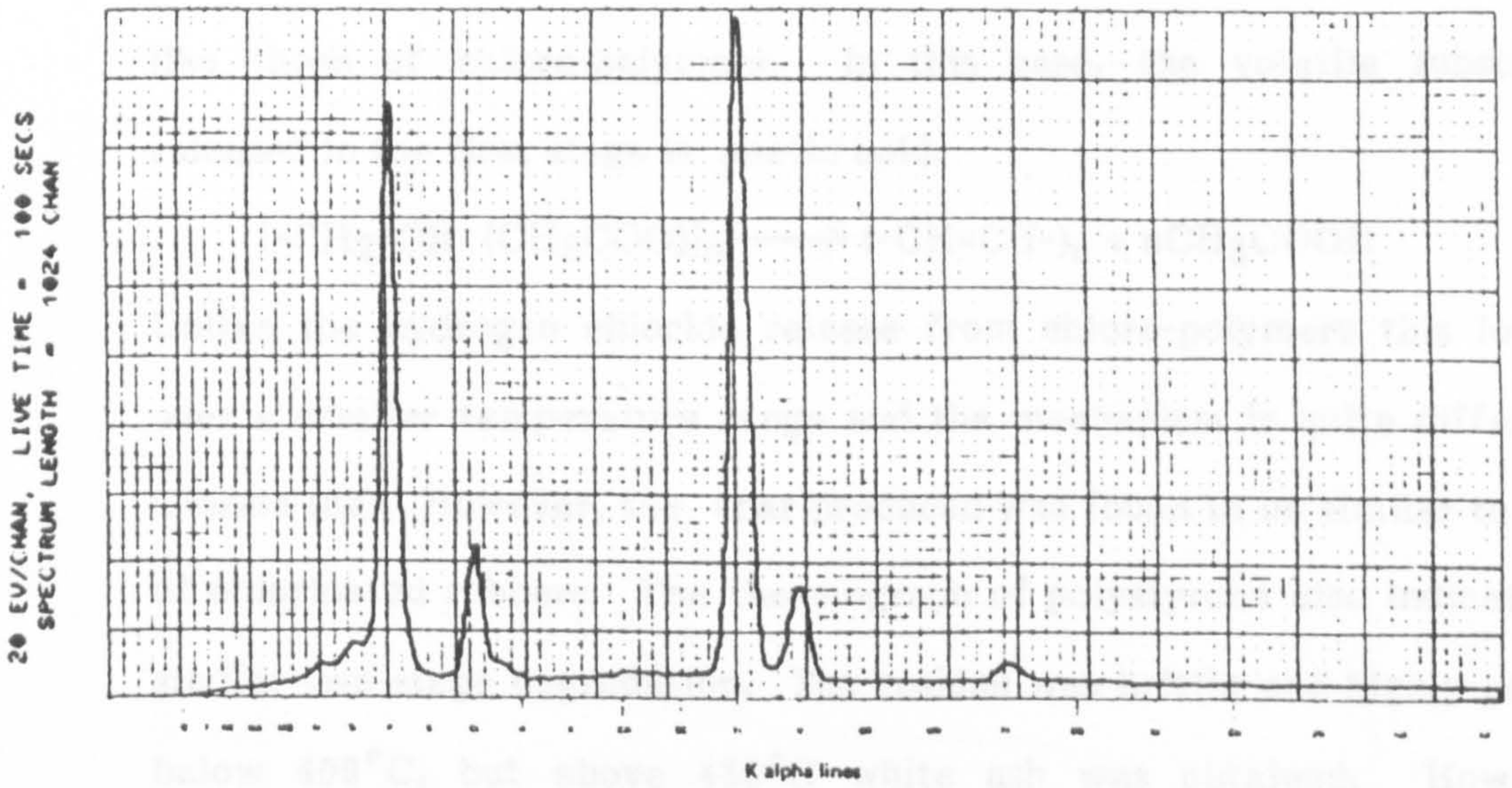

AFTER EXPOSURE FOR 20 MINUTES

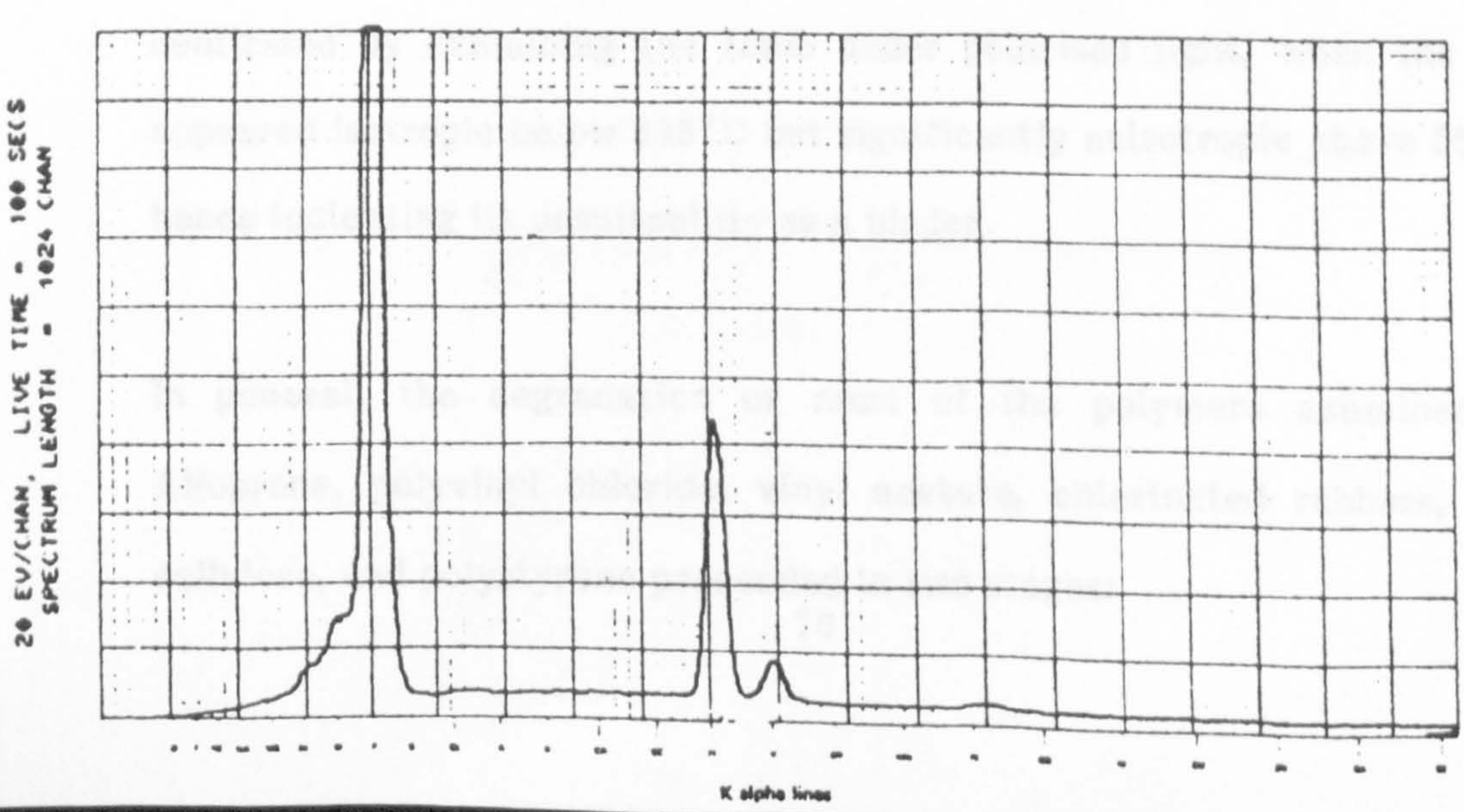

Comparison of the EPMA graphs of samples heated at 300°C suggests that chlorinated rubber loses chlorine at a lower temperature than any of the other polymers and that substantial amounts of chlorine remain in the residues of chlorinated rubber compared with those of polyvinyl chloride, Fig. 39A-B. Electron microscope examination of sample residues shows the differences in the nature of the chars formed see Fig. 40. The polyvinyl chloride residue was found to be a fused mass whereas that of chlorinated rubber was a structured char being well swollen, rigid, brittle, containing numerous pores and often having a honeycombed appearance. Plasticized PVC char has a vitreous, steel-lustre which often resembles coke.

The thermogram for vinyl acetate exhibits two well-defined stages Fig. 37 like those of chloro-polymers. In this case, the volatile substance released in the first stage is acetic acid:

$$[-CH_2-CH\ (CH_3COO)]_n \longrightarrow (-CH=CH-)_n + nCH_3COOH$$

Unlike the hydrogen chloride release from chloro-polymers this loss is over a smaller temperature range and the mechanism is quite different, Grassie (83). However, the char produced was found to be similar to that of chlorinated rubbers. The thermograph of polystyrene also indicated a similar two-stage degradation. The residue was brittle and highly-porous below 400°C, but above 450°C white ash was obtained. However, carbonisation did not occur below temperatures of 350°C. This was confirmed by examining the foam under polarised light, when the char appeared isotropic below 335°C but significantly anisotropic above 350°C, hence indicating its unsuitability as a binder.

In general, the degradation of most of the polymers examined i.e. Alloprene, polyvinyl chloride, vinyl acetate, chlorinated rubbers, ethyl cellulose, and polystyrene proceeded in two stages:

(1) The first stage begins in the temperature range 150 - 500°C. It is initially accompanied by melting, swelling and finally by the formation of a black/brown 'gooey' residue. In general, a char does not form unless a halogen is present in the polymer. When dehydrochlorination occurs the polymer begins to degrade at 125 -135°C.

(2) The second stage begins in the range 500-900°C. The primary residue (from the first stage) is carbonised into a final product which is rich in carbon.

FIGURE 37

TYPICAL THERMOGRAMS OF PVA AND PVC

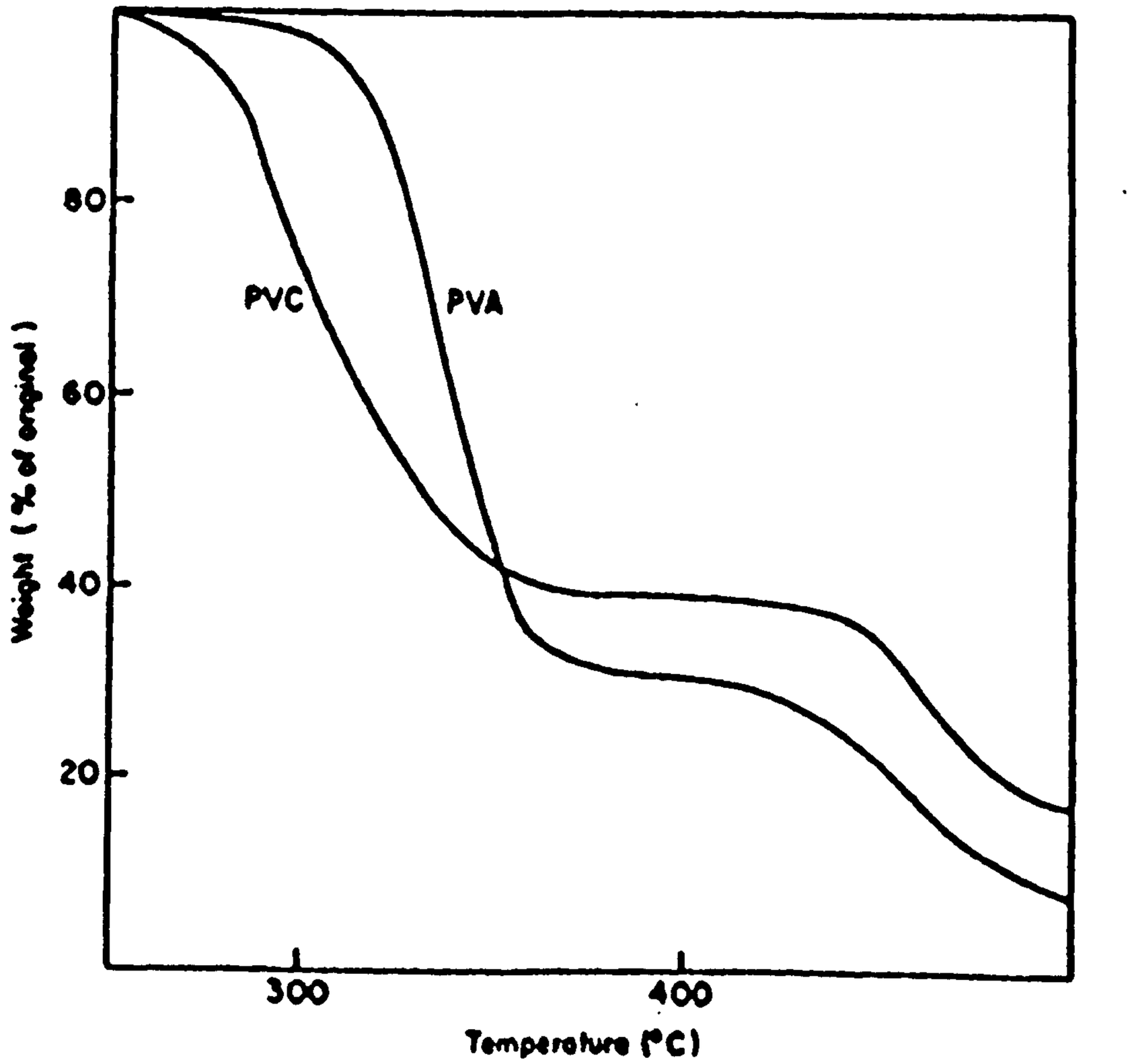

From Simultaneous Thermal Analysis and Differential Scanning Calorimetery, the decomposition temperatures were determined eg. chlorinated rubber 250-300°C (Fig. 38 & 41), styrenated acrylate, Parlon VATCL, 375-430°C. Fig. 42 shows a typical IR scan for a chlorinated polymer. Depending upon the type of intumescent system used, a high decomposition temperature could be a problem since, if the viscosity is too low, the resin may drip and the intumescent foam formed will be weak and porous see Fig. 97E. However, if the viscosity is too high , the gases will not be able to expand the melt into a foam.

TABLE 2

DECOMPOSITION TEMPERATURES OF THE VARIOUS BINDERS

BINDERS	TEMP. OF DECOMP. °C
CHLORINATED RUBBER	250 - 350
PVC	300 - 440
PARLON S16	280 - 340
PARLON S20	275 - 330
ETHYL CELLULOSE	310 - 340
PVA	250 - 320
POLYACRYLONITRILE	300 - 350
POLYSTYRENE	280 - 350
STYRENEACRYLATE	375 - 430

FIGURE 38

A TYPICAL TG THERMOGRAM FOR ALLOPRENE

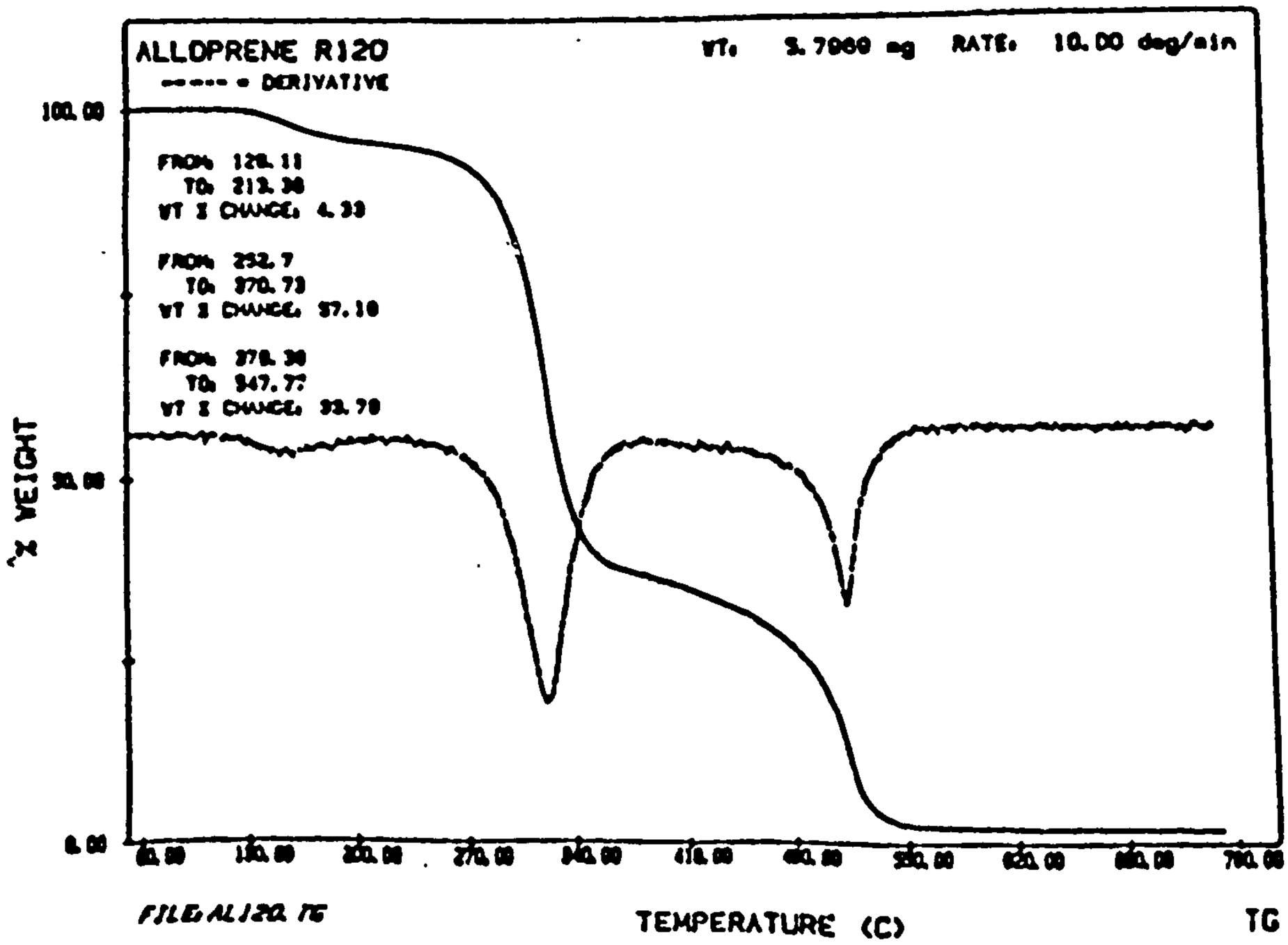

FIGURE 39A

PVC AFTER EXPOSURE AT 300°C FOR 15 MINUTES

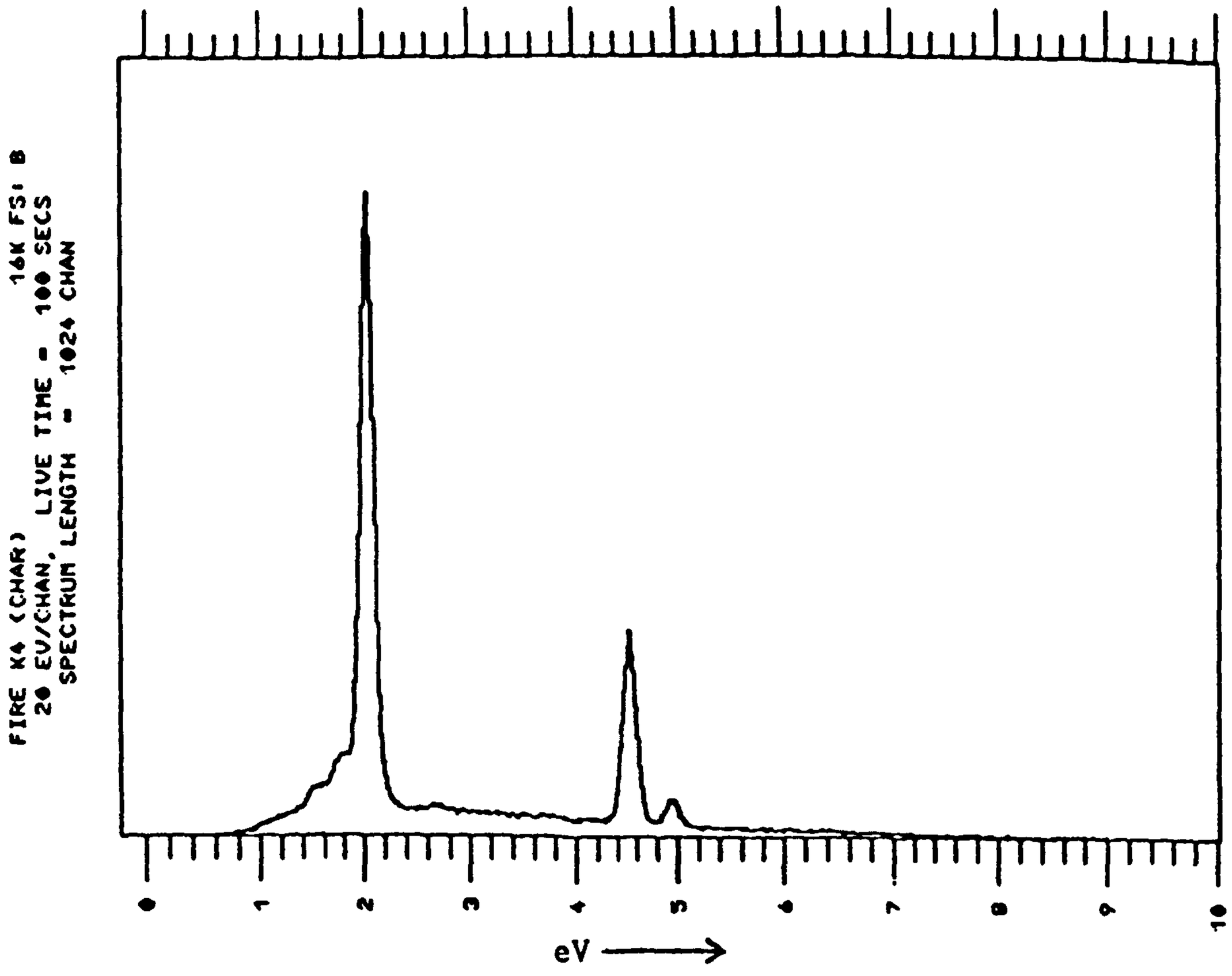

FIGURE 39B

CHLORINATED RUBBER AFTER EXPOSURE AT 300°C FOR 15 MINUTES

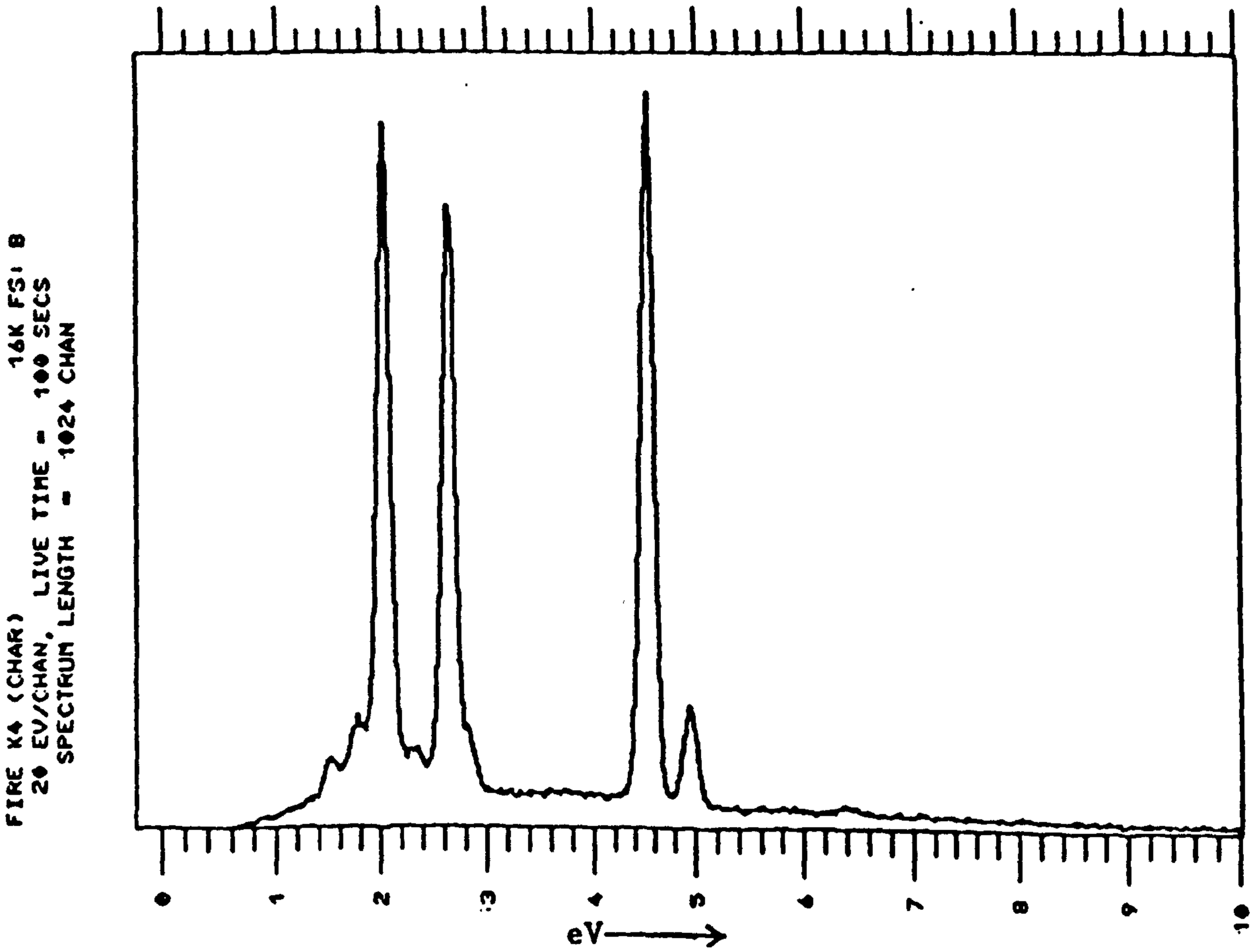

FIGURE 40

ELECTRON MICROSCOPY PHOTOGRAPHS OF THE CHARS FORMED

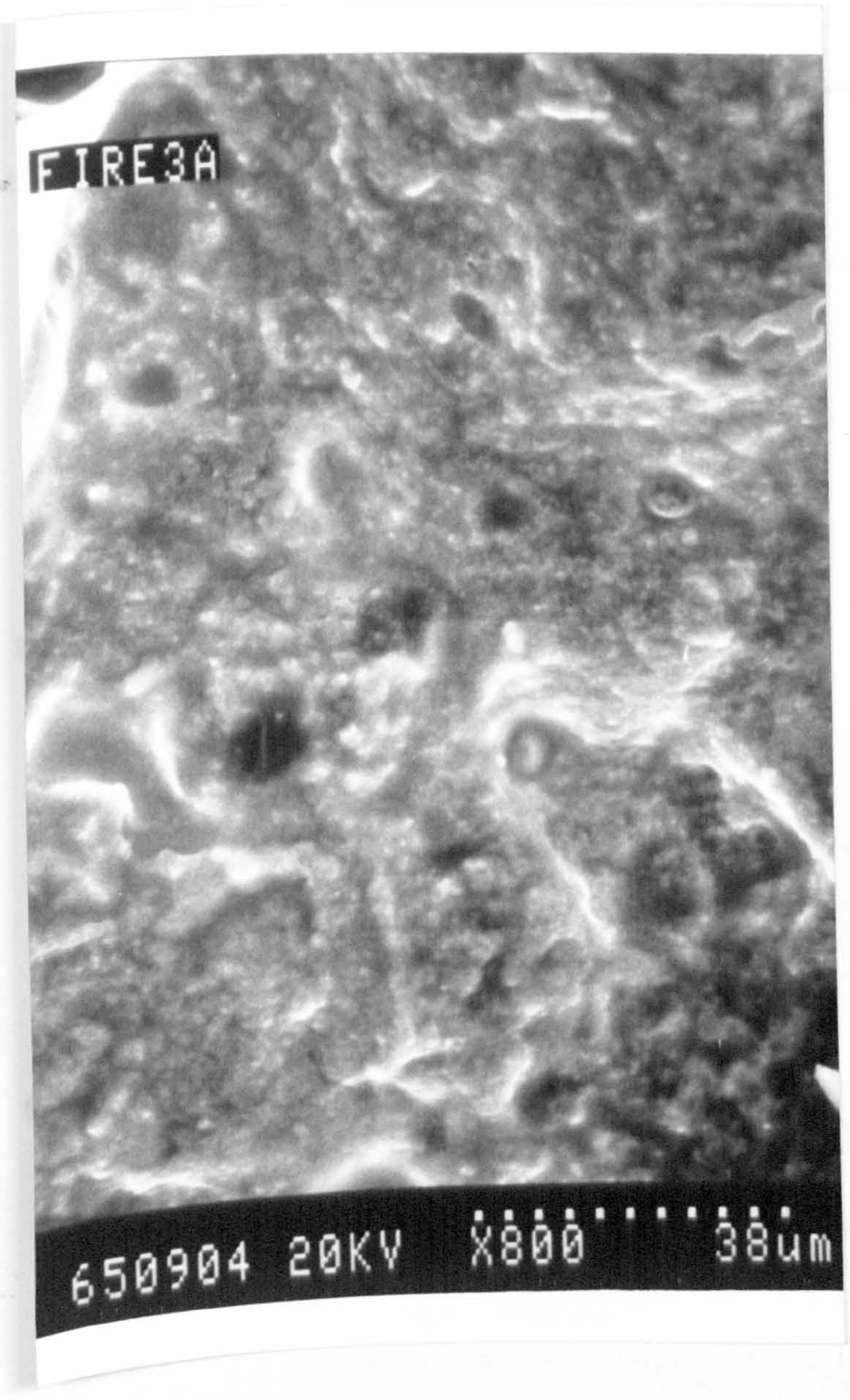

PVC RESIDUE

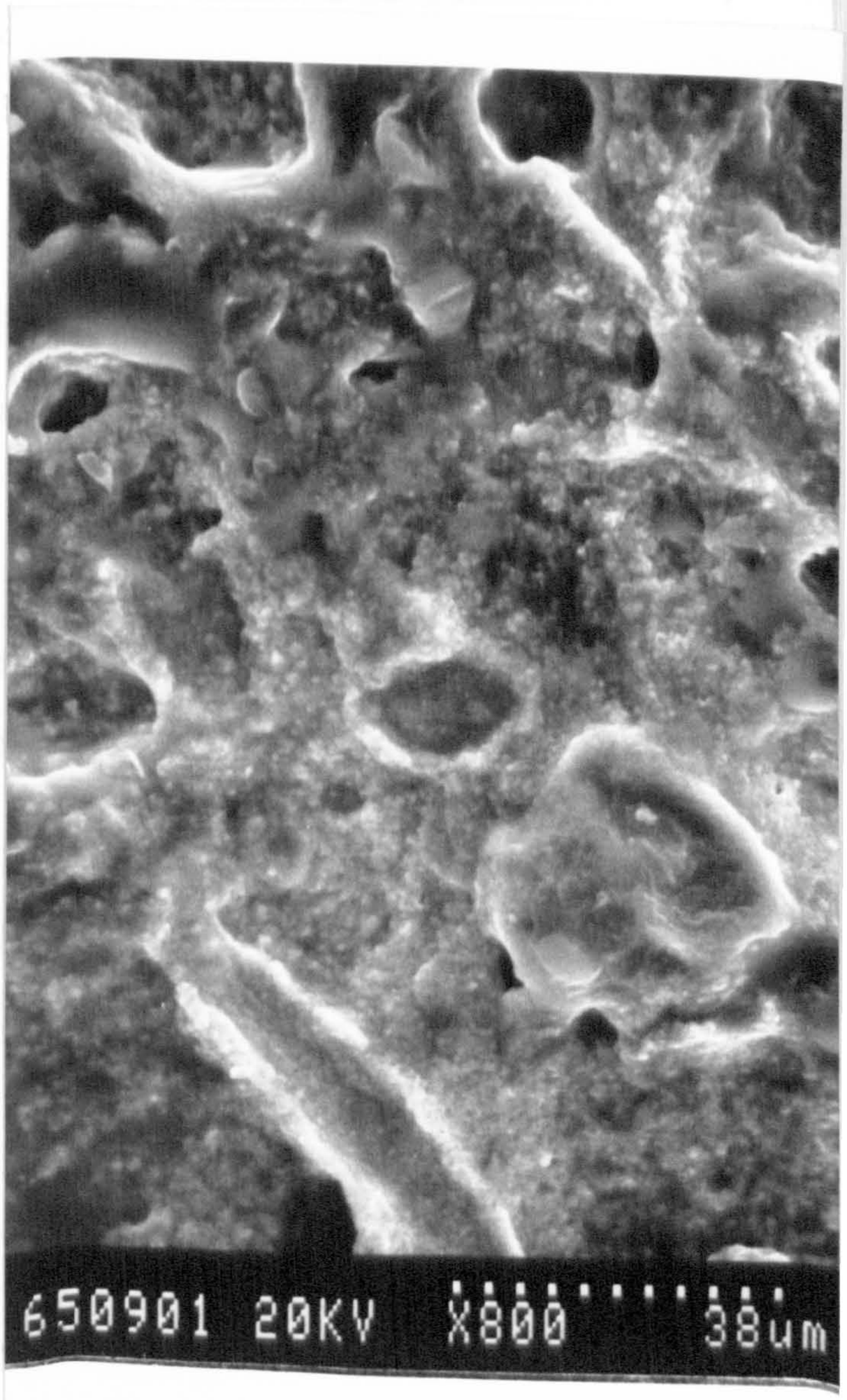

CHLORINATED RUBBER

FIGURE 41

TGA CURVE FOR ALLOPRENE R120

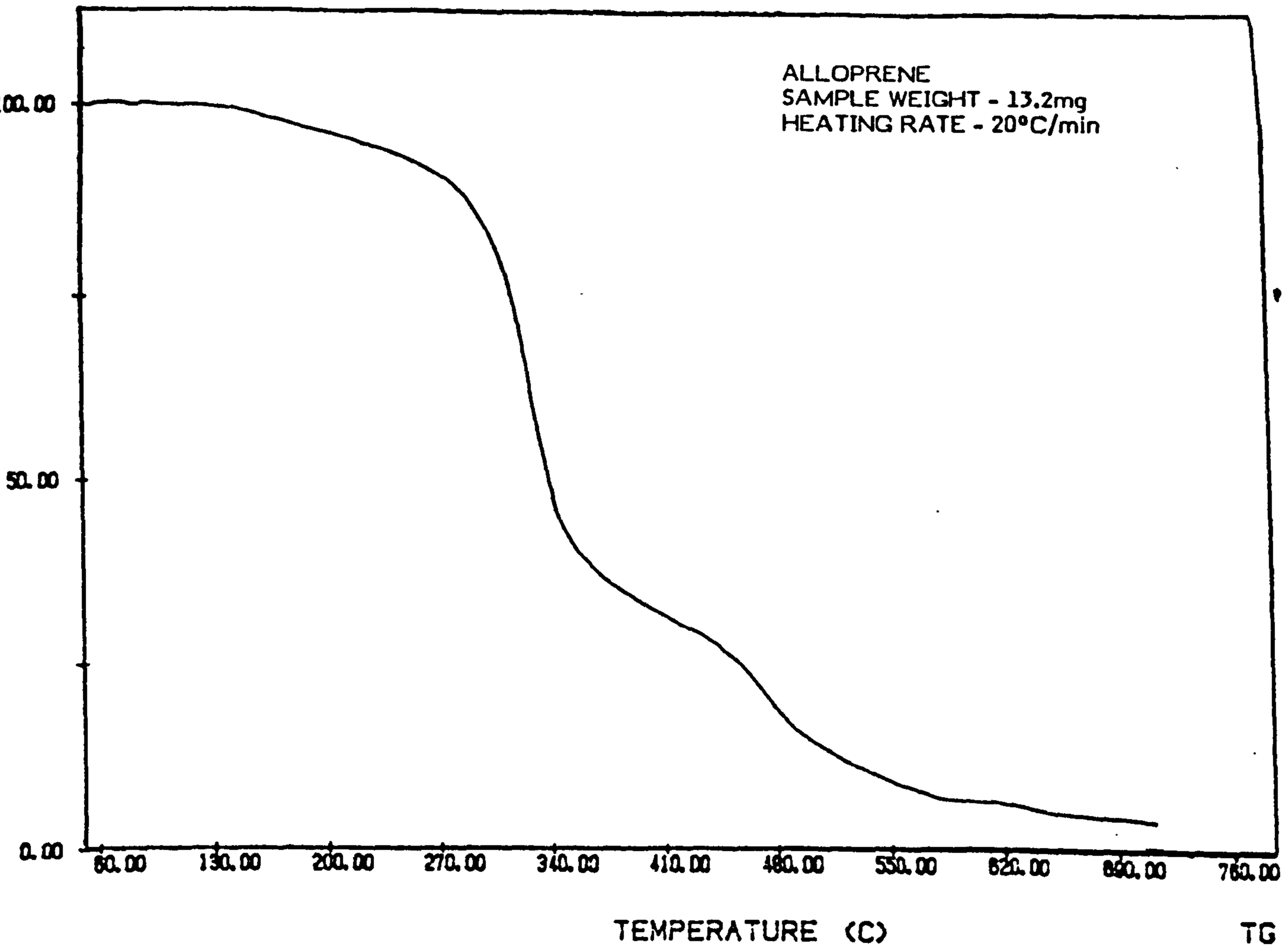

FIGURE 42

IR SCAN OF ALLOPRENE

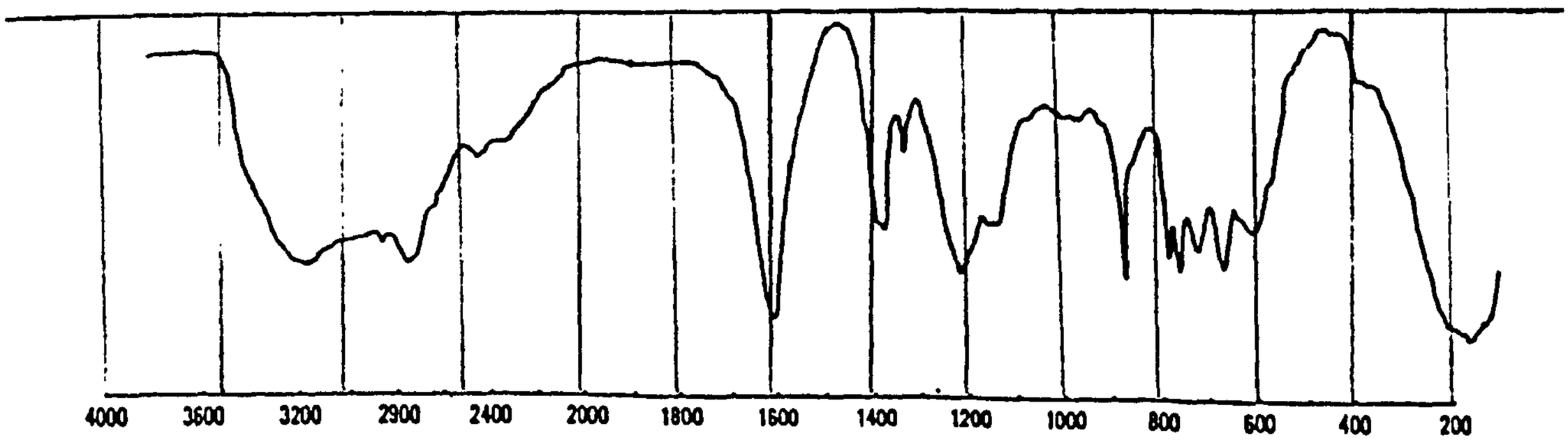

5.4.1. DEVELOPMENT OF ACID GENERATOR - CATALYST

Early attempts to produce ammonium polyphosphate (APP) varied from treating a copper or lead polyphosphate with ammonium sulphide (104) to tempering ammonium trimeta- or tetrametaphosphate at 200 - 250°C. The products from these approaches were impure (109). In 1941, a patent was published (110) which described the manufacture of APP by heating monoammonium phosphate (MAP) with ammonia under pressure. Water was eliminated according to the reaction below:

$$n(NH_4H_2PO_4) \xrightarrow{\text{heat}} (NH_4PO_3)_n + nH_2O \qquad (5.2.)$$

As a modification, the patent proposed the addition of phosphorus pentoxide to the MAP, in which case the removal of water was not required. The use of diammonium phosphate (DAP) instead of MAP was also suggested (110). Numerous patents have been published since, offering variations on this theme. For example, phosphoric acid can be used instead of P_2O_5, and urea instead of ammonia. In one patent (111), 20 parts of MAP and 11 parts of urea react at 275°C under pressure. The action of urea is illustrated below by the following equations:

$$NH_2CONH_2 + H_3PO_4 \longrightarrow (1/x)(NH_4PO_3)_x + CO_2 + NH_3 \qquad (5.3.)$$

$$NH_2CONH_2 + H_2O \longrightarrow 2NH_3 + CO_2 \qquad (5.4.)$$

$$2NH_4H_2PO_4 + NH_2CONH_2 \longrightarrow (NH_4)_4P_2O_7 + CO_2 \qquad (5.5.)$$

$$(NH_4)_4P_2O_7 + NH_2CONH_2 \longrightarrow (2/x)(NH_4PO_3)_x + CO_2 + 4NH_3 \qquad (5.6.)$$

In another publication (112), melamine phosphate is heated with urea to give a mixture of APP and melamine.

The choice of reactants and conditions determines the nature of the APP formed. Shen et al (103) found that APP has five different crystalline modifications, with varying solubility and thermodynamic properties. The grade of APP required should be designed to have as low a water solubility as possible while still remaining highly effective. APP starts to decompose endothermically at 275°C to form ammonia and polyphosphoric acid. Kay et al (75) investigated the crystalline structure of melamine phosphate and APP.

5.4.2. CHEMISTRY OF THE CATALYST

The acid generator is termed a catalyst since it is regenerated in the reaction and is available for reuse. The catalyst, which is a Lewis acid, may be strongly dehydrating. It may react to form an intermediate which then decomposes.

$$R(OH)_2 + ACID \longrightarrow [R(OH)_2 \cdot ACID] \longrightarrow RO + ACID \cdot H_2O \quad (5.7.)$$

The reuse of the acid in fact does not occur every time since these are heterogeneous systems where mixing does not occur during the reaction process. Therefore excess acid is required for reaction to occur with the majority of the polyol sites. The most commonly-used acid, phosphoric acid, is introduced as a salt or ester which then decomposes on heating to produce the acid. In the case of ammonium phosphate and simple polyols, the reaction sequence on heating is as follows:

$$x(NH_4)_2HPO_4 \xrightarrow{\text{heat}} HO\text{-}[\text{-}P(=O)(OH)\text{-}O\text{-}]_x\text{-}H + 2xNH_3 + (x-1)H_2O \quad (5.8.)$$

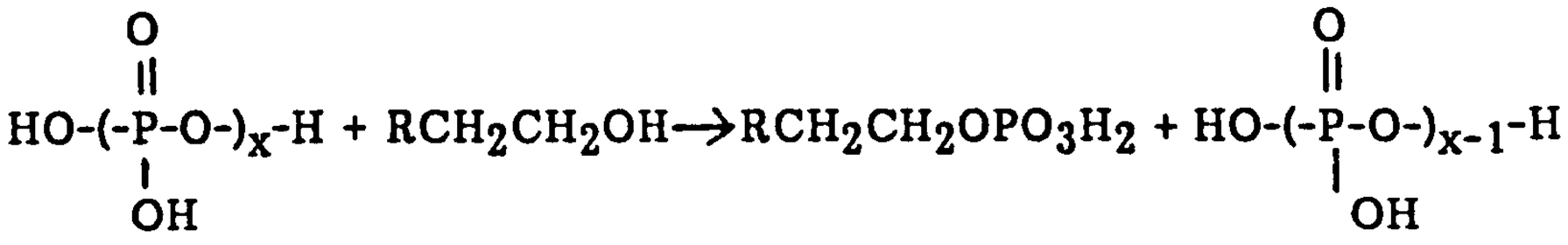

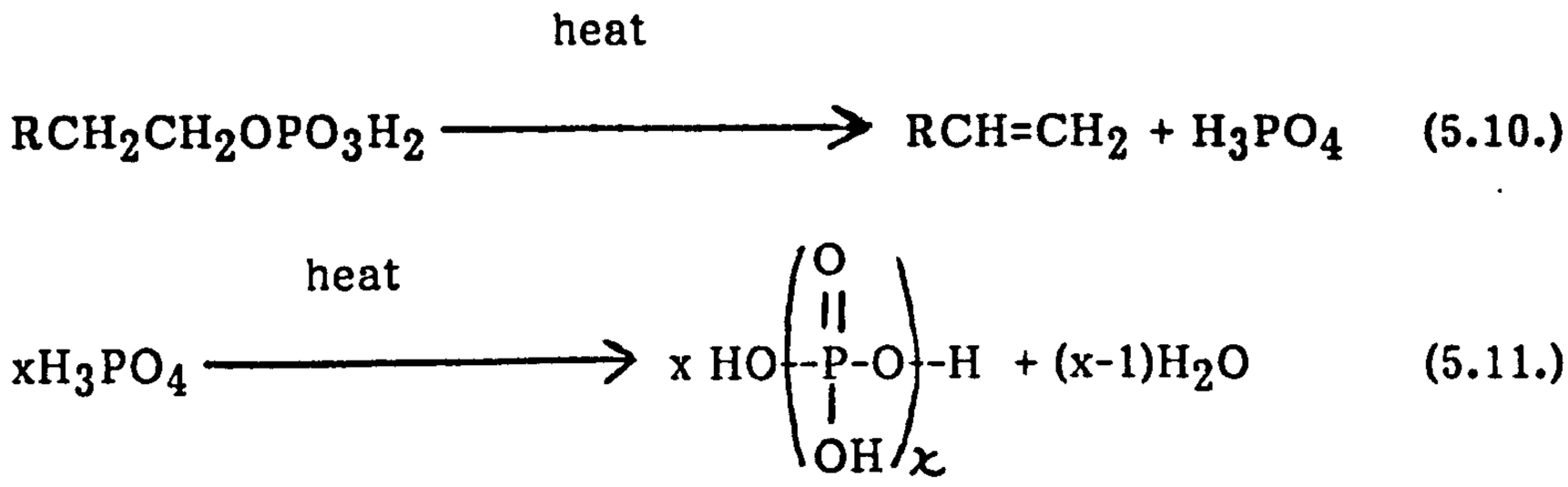

Monoammonium phosphate and ammonium polyphosphate are both used as catalysts. Although they are quite similar, the former has a significantly lower decomposition temperature (Table 3) and could, therefore, dehydrate a carbonific (such as starch) prematurely resulting in weak intumesence during the early part of an actual fire. In the course of this research project, it was found that the degree of intumescence and the height of foaming of a particular formulation is, to a large degree, related to decomposition temperatures and changes which occur when a number of multifunctional ingredients are used.

The effectiveness of the dehydrating agent depends partly on the amount of the 'active' component it contains. For example, ammonium polyphoshate contains approximately 32% phosphorus whereas ammonium phosphate has only 27% phosphorus, hence the former is more effective (Table 3).

Most of the formulations reported in the literature use phosphoric acid as the catalyst, although systems based on sulphuric and boric acid have been reported (105). The ability of the catalyst to dehydrate the carbonific is

the single most important criterion in its selection for a particular system. The acid must be combined with a volatile or thermally degradable cation so that the active component is released during pyrolysis. Ammonium and amine salts, the organic esters, amido and imido forms of the mineral acids may be used (Table 3). Evolution of the volatile component by the catalyst assists in dilution of the flammable gases and oxygen available for combustion. However, the release occurs prior to the decomposition of the carbonific and therefore before being really needed. Phosphoric acid has been found to be more effective than sulphuric acid, and nitric acid totally ineffective, in the production of intumescence. An apparent difference between these acids is their boiling points. Nitric acid is much more volatile than either sulphuric or phosphoric acids. The chemical reactions involving the acid catalyst are given in Fig. 43. Reaction for intumescence using ammonium polyphosphate is given in Fig. 44.

TABLE 3

POTENTIAL INTUMESCENT CATALYSTS

MATERIAL	%ACTIVE COMPONENT	DECOMPOSITION TEMP°C
MONOAMMONIUM PHOSPHATE	26.9% P	147
DIAMMONIUM PHOSPHATE	23.5% P	87
AMMONIUM POLYPHOSPHATE	32.0% P	325
MELAMINE PHOSPHATE	14.2% P	300
GUANYLUREA PHOSPHATE	15.5% P	191
UREA PHOSPHATE	19.6% P	130
AMMONIUM SULPHATE	24.2% S	-
AMMONIUM BORATE	16.3% B	-

FIGURE 43
CHEMICAL REACTION OF AN ACID CATALYST

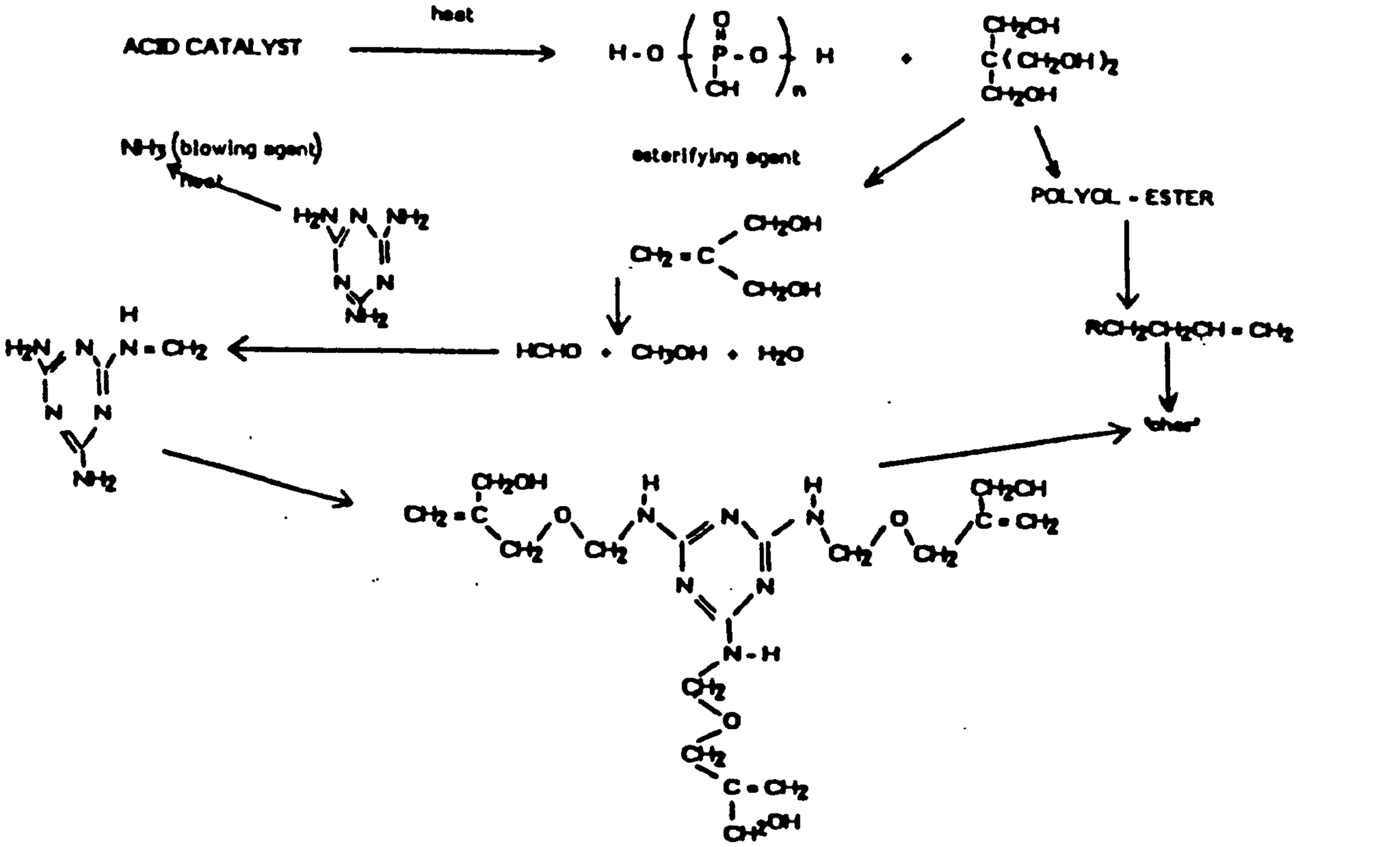

FIGURE 44
INTUMESCENCE USING AMMONIUM POLYPHOSPHATE

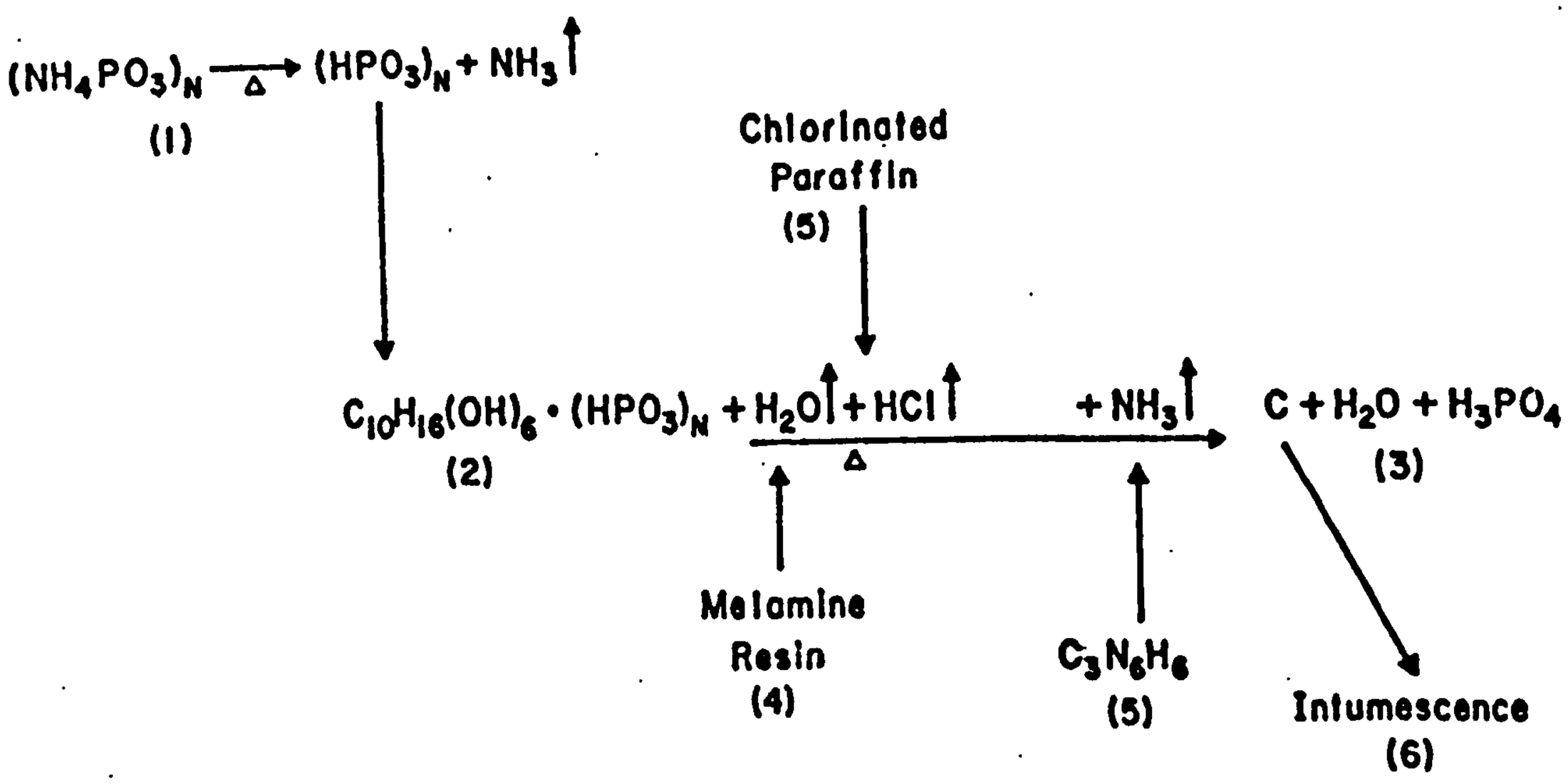

1. Catalyst decomposes to phosphoric acid and ammonia.
2. Acid reacts with carbonific.
3. Carbonific decomposes to carbon and regenerates acid.
4. Resin melts to form a film over the carbon.
5. Blowing agents release gases which cause the carbon to foam.

5.4.3. AMMONIUM POLYPHOSPHATE

This is a high-molecular-weight chain phosphate, the end groups of which can be disregarded, and the molecule can be treated as a straight chain polymer as shown below:

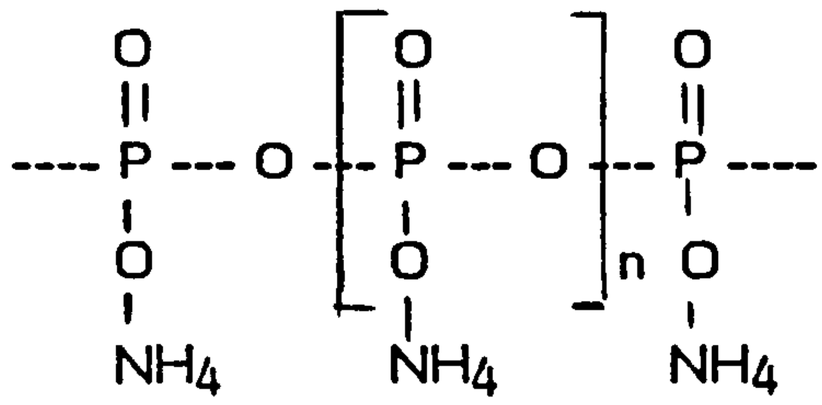

n = 1000 to 3000

The phosphate content was confirmed by acid hydrolysis, precipitation of the phosphate as Mg (NH_4) PO_4 . $6H_2O$, dissolution and titration with 0.1N HCl. APP can be regarded as essentially $(NH_4PO_3)_n$. The thermal characteristics of APP were determined using DSC, TGA and STA, Fig.45.

When heated APP decomposes to form metaphosphoric acid (HPO_3), ammonia and water through a series of steps. Decomposition was found to start initially at approximately 100°C Fig. 45.

$$2NH_4H_2PO_4 \longrightarrow 2H_3PO_4 + 2NH_3 \qquad (5.12.)$$

The ammonia gas escapes through the semi-char produced. In this endothermic decomposition, approximately 60 kilojoules per mole are absorbed.

The phosphoric acid produced decomposes at approximately 225°C.

$$2H_3PO_4 \longrightarrow H_4P_2O_7 + H_2O \qquad (5.13.)$$

During this reaction approximately 17 kJ mol^{-1} are absorbed.

The pyrophosphoric acid ($H_4P_2O_7$) decomposes further at approximately 290°C to produce metaphosphoric acid and water.

$$H_4P_2O_7 \longrightarrow 2HPO_3 + H_2O \qquad (5.14.)$$

This decomposition is also endothermic, approximately 24 kJ mol^{-1} being absorbed. The final product, a white material -metaphosphoric acid, is a vitreous compound which sublimes at about 900°C.

FIGURE 45

TGA THERMOGRAMS FOR AMMONIUM POLYPHOSPHATE - PHOSCHECK P30

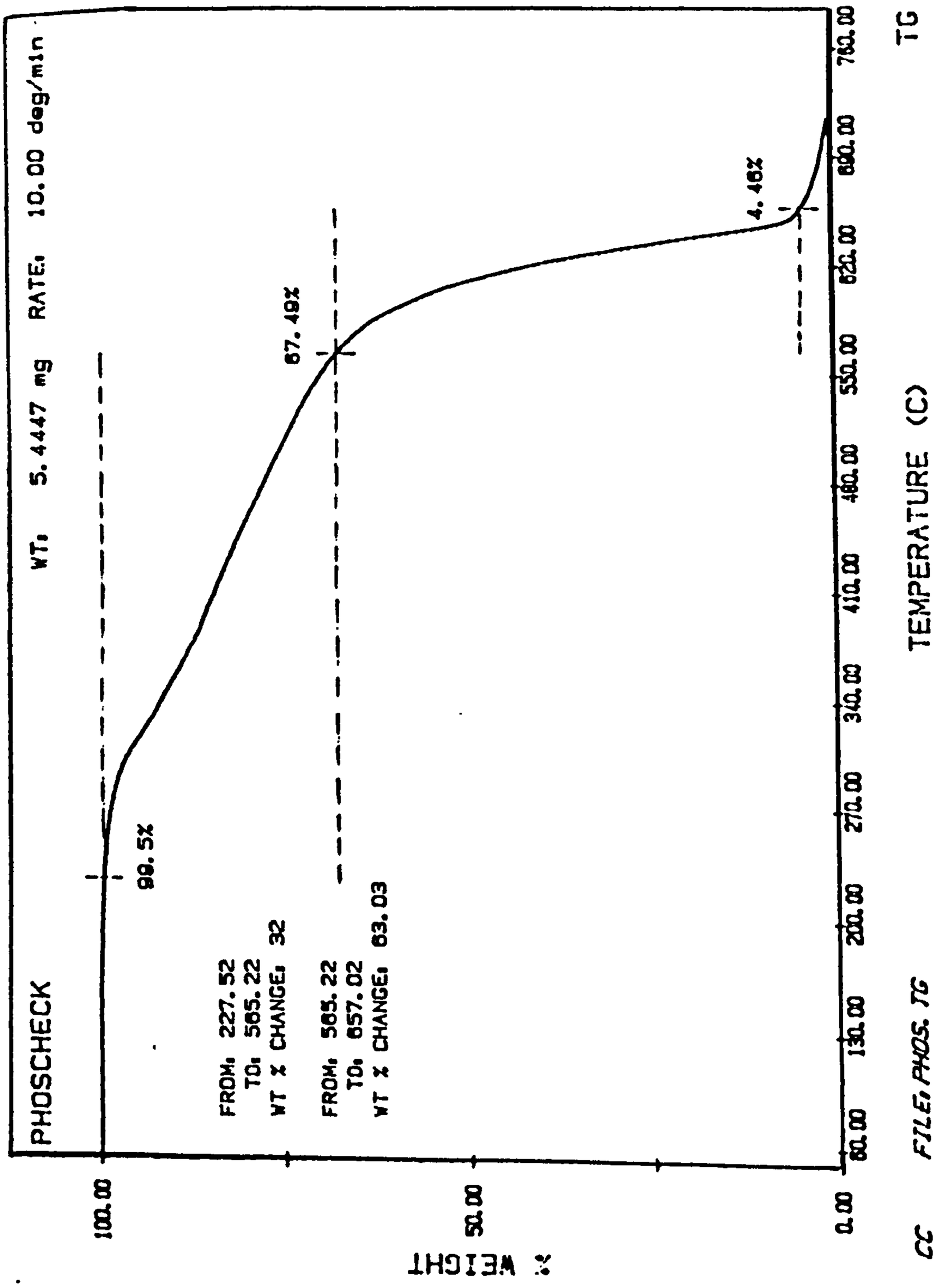

The other catalyst system investigated was based on the use of melamine phosphate. Melamine phosphate is less readily soluble in water and has thermal characteristics, see Fig. 47 which make it attractive for use. Formulations based on this catalyst system have some distinct advantages over the ammonium polyphosphate system, see Section 6.

FIGURE 46

DSC CURVE FOR AMMONIUM POLYPHOSPHATE

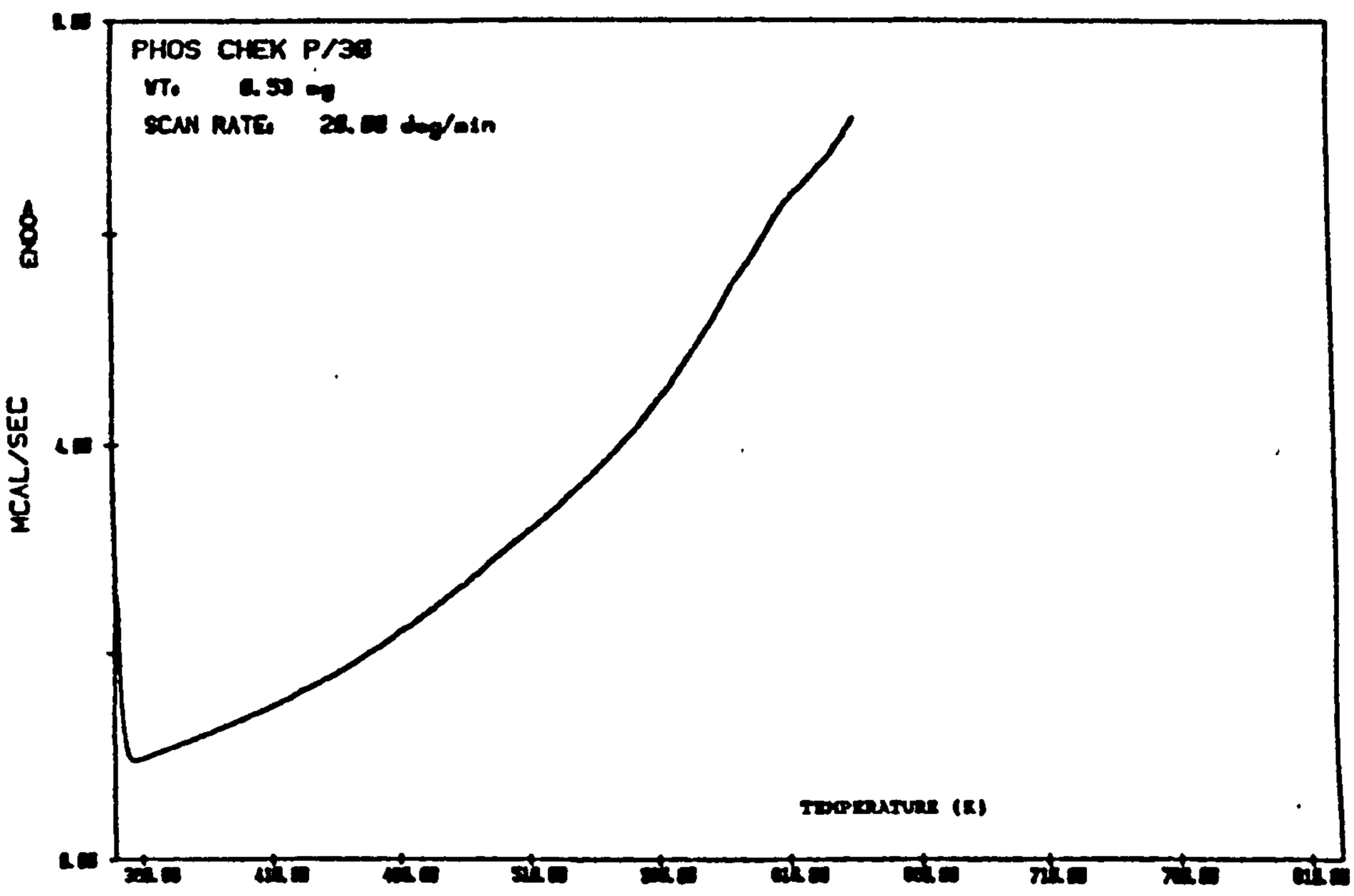

FIGURE 47

TGA **CURVE FOR MELAMINE PHOSPHATE**

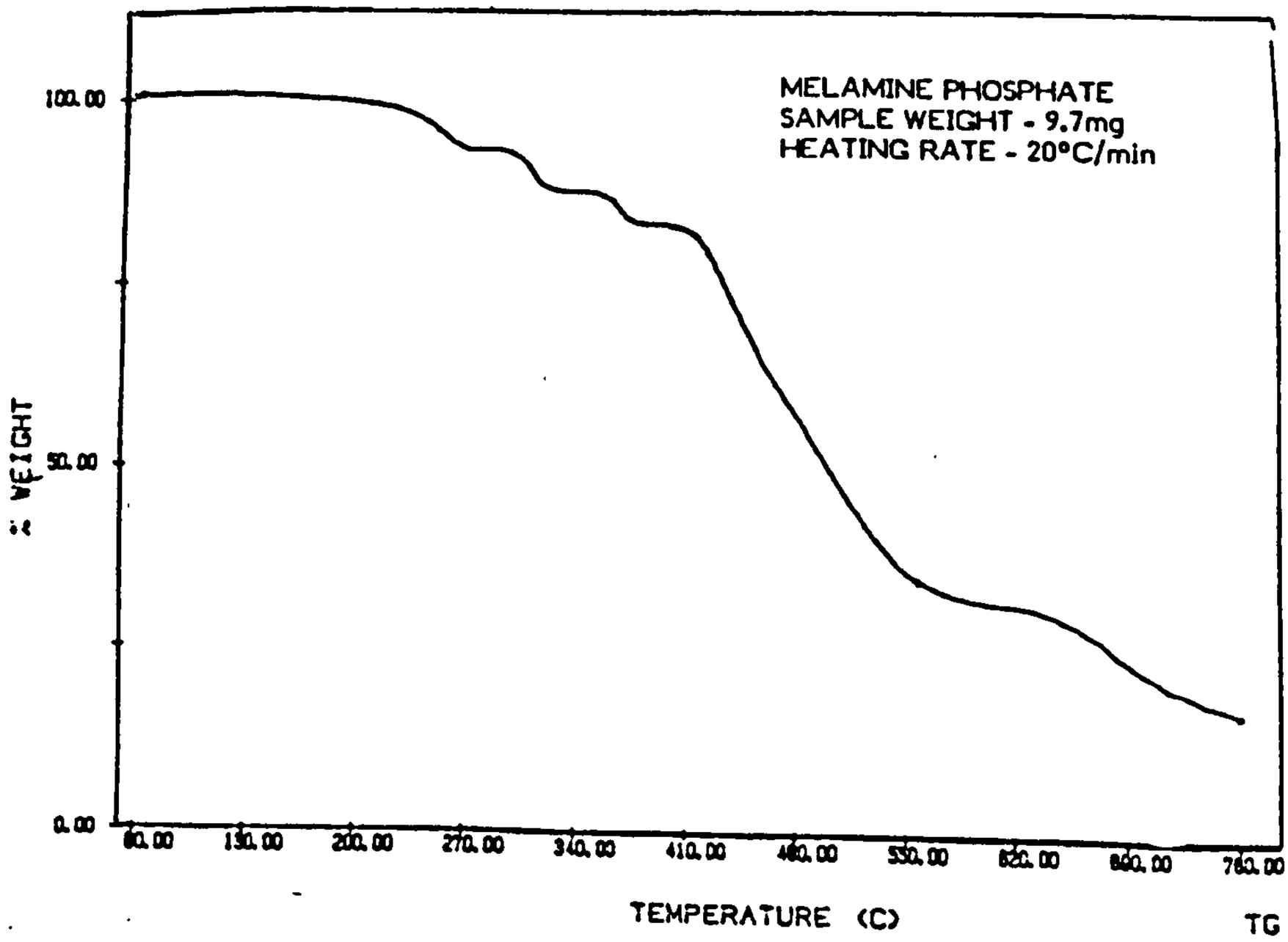

5.5. THE CARBONIFICS AND THEIR DEVELOPMENTS

Carbonific materials mentioned in the early patents and still in use are starch, pentaerythritol and its oligomers. Some of the patents mention the use of urea-formaldehyde as a 'resinous carbonific', meaning it acts both as binder and carbon source (106). Epoxy resins have also been extensively used (107, 108) although in general the carbonific is a carbohydrate, starches and polyhydric alcohols being used most frequently. The effectiveness of a carbonific is dependent on both the carbon content and the number of available reactive sites (Table 4). The amount of carbon determines the amount of char obtained, while the hydroxyl content determines the rate of dehydration and hence the rate of foam formation. In general, the higher the carbon content the lower will be the number of reaction sites available. In recent years, the erythritols (Fig. 48-50) and blends with starch (Fig. 51) have been extensively used. Other carbonifics investigated were glucose and sorbitol (Fig. 52 & 53).

TABLE 4

POTENTIAL CARBONIFICS

	FORMULA	% C	REACTIVITY SITES/100g
SUGARS			
GLUCOSE	$C_6H_{12}O_6$	40	2.8
MALTOSE	$C_{12}H_{22}O_{11}$	42	2.3
ARABINOSE	$C_5H_6O_4$	45	3.0
POLYHYDRIC ALCOHOLS			
ERYTHRITOL	$C_4H_6(OH)_4$	39	3.3
PENTA-"	$C_5H_8(OH)_4$	44	2.9
di," "	$C_{10}H_{16}(OH)_6$	50	2.5
tri," "	$C_{15}H_{24}(OH)_8$	53	2.4
ARABITOL	$C_5H_7(OH)_5$	39	3.3
SORBITOL	$C_6H_8(OH)_6$	40	3.0
INOSITOL	$C_6H_6(OH)_6$	40	3.0
POLHYDRIC PHENOLS			
RESORCINOL	$C_6H_8(OH)_2$	63	1.8
STARCHES	$(C_6H_{10}O_5)_n$	44	2.1

FIGURE 48

TG THERMOGRAMS FOR DI-PENTAERYTHRITOL

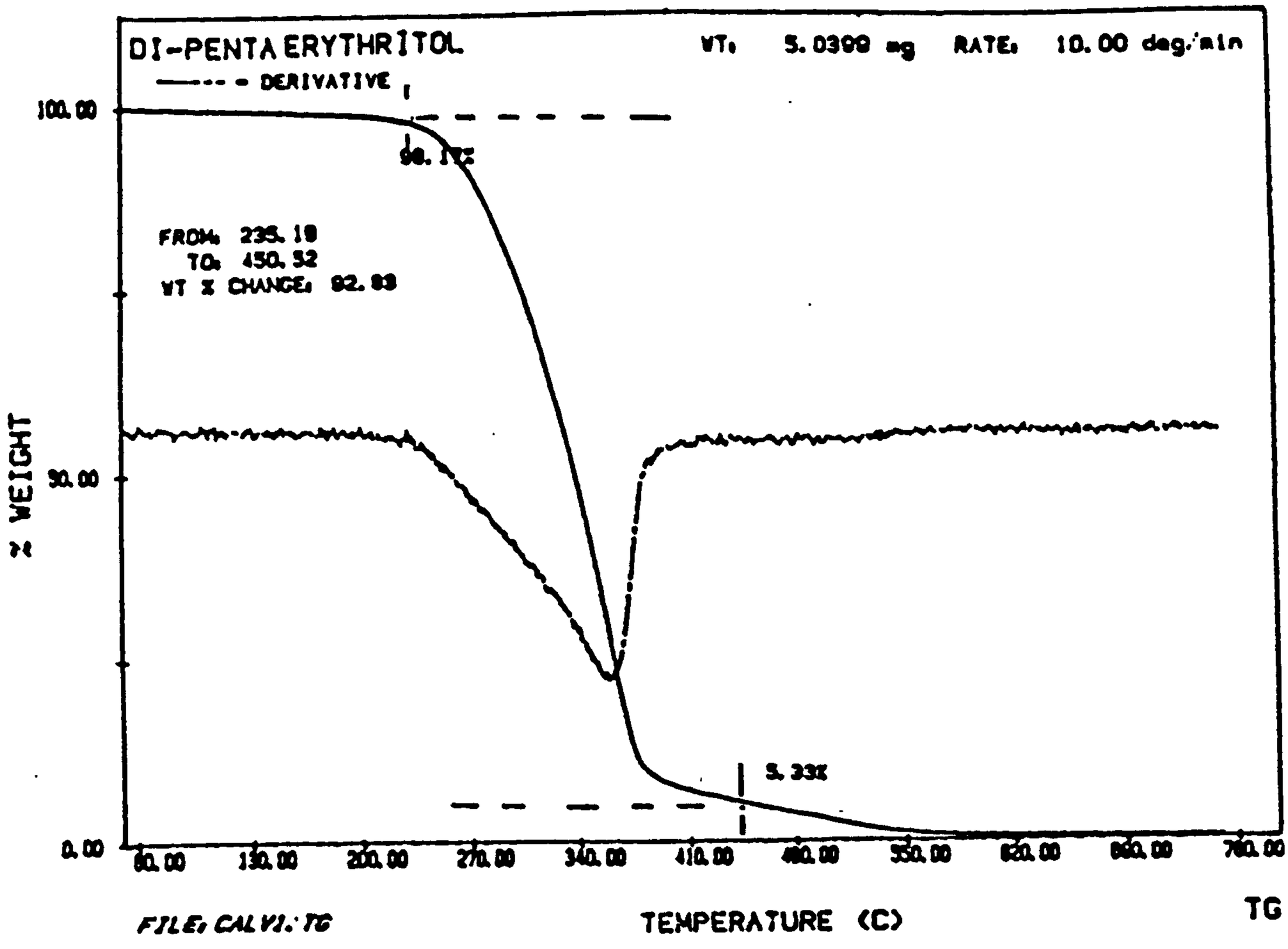

FIGURE 49

TGA THERMOGRAMS OF CARBONIFICS

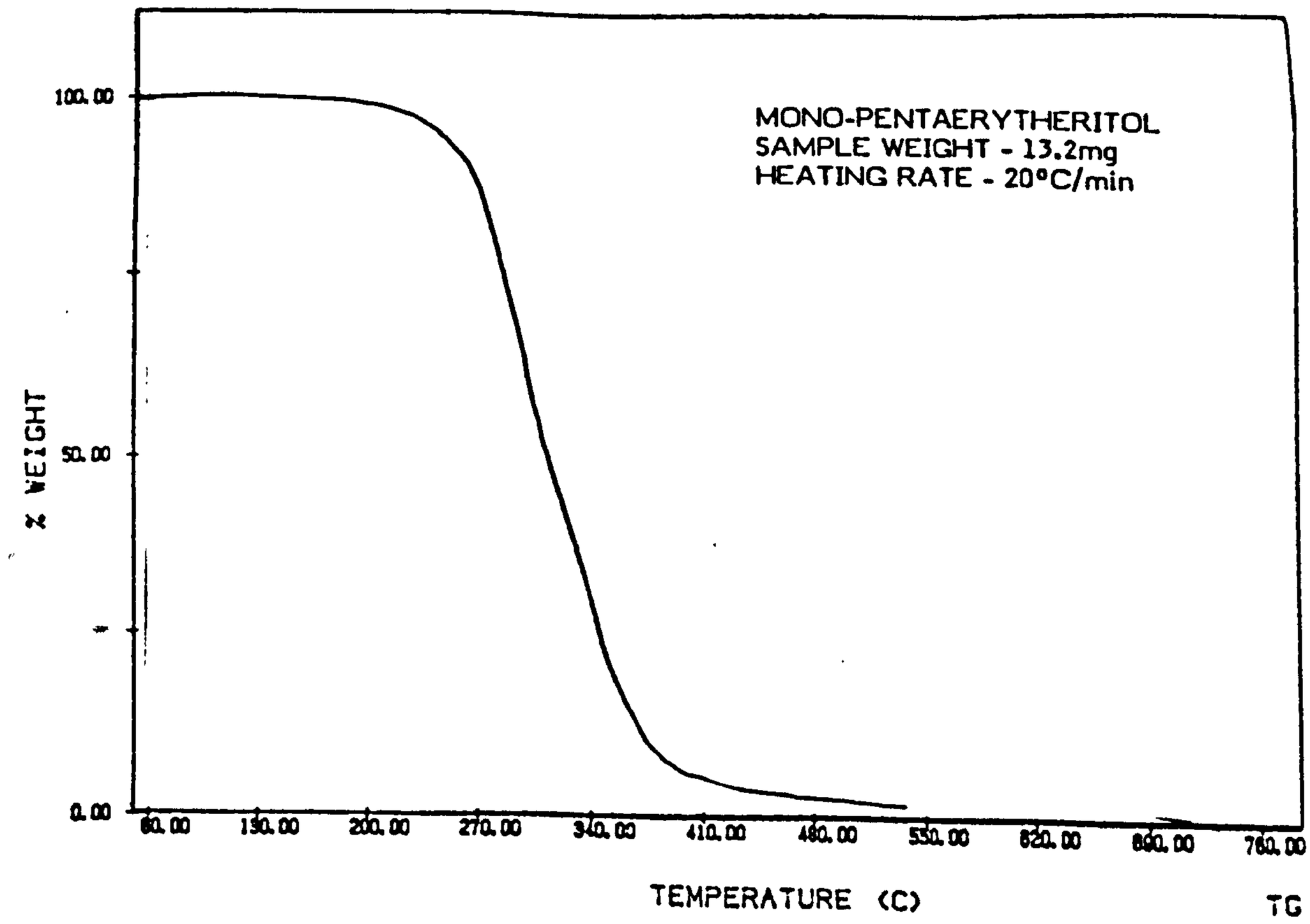

FIGURE 50

DSC CURVE FOR PENTAERYTHRITOL

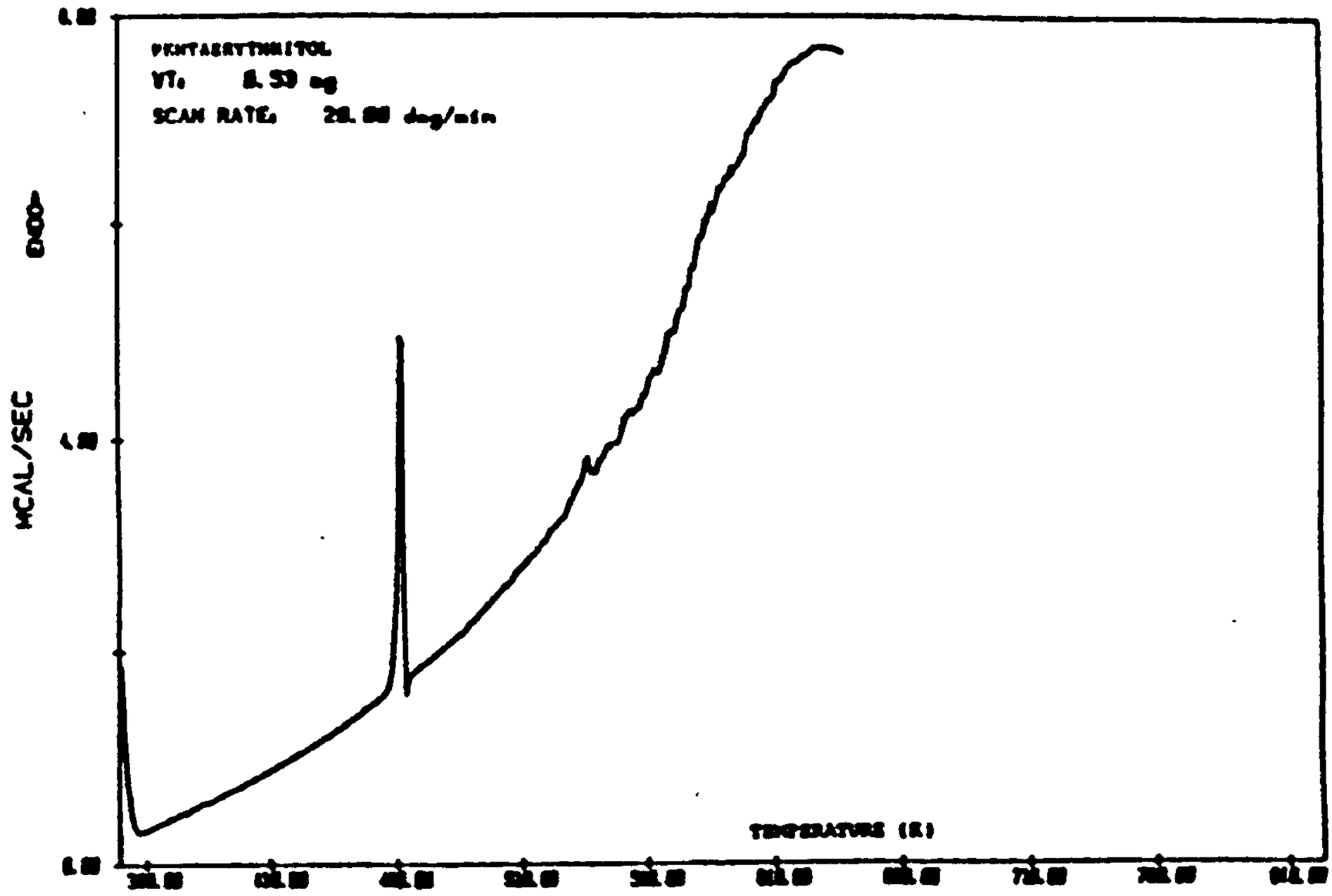

FIGURE 51

STA CURVE FOR WHEAT STARCH

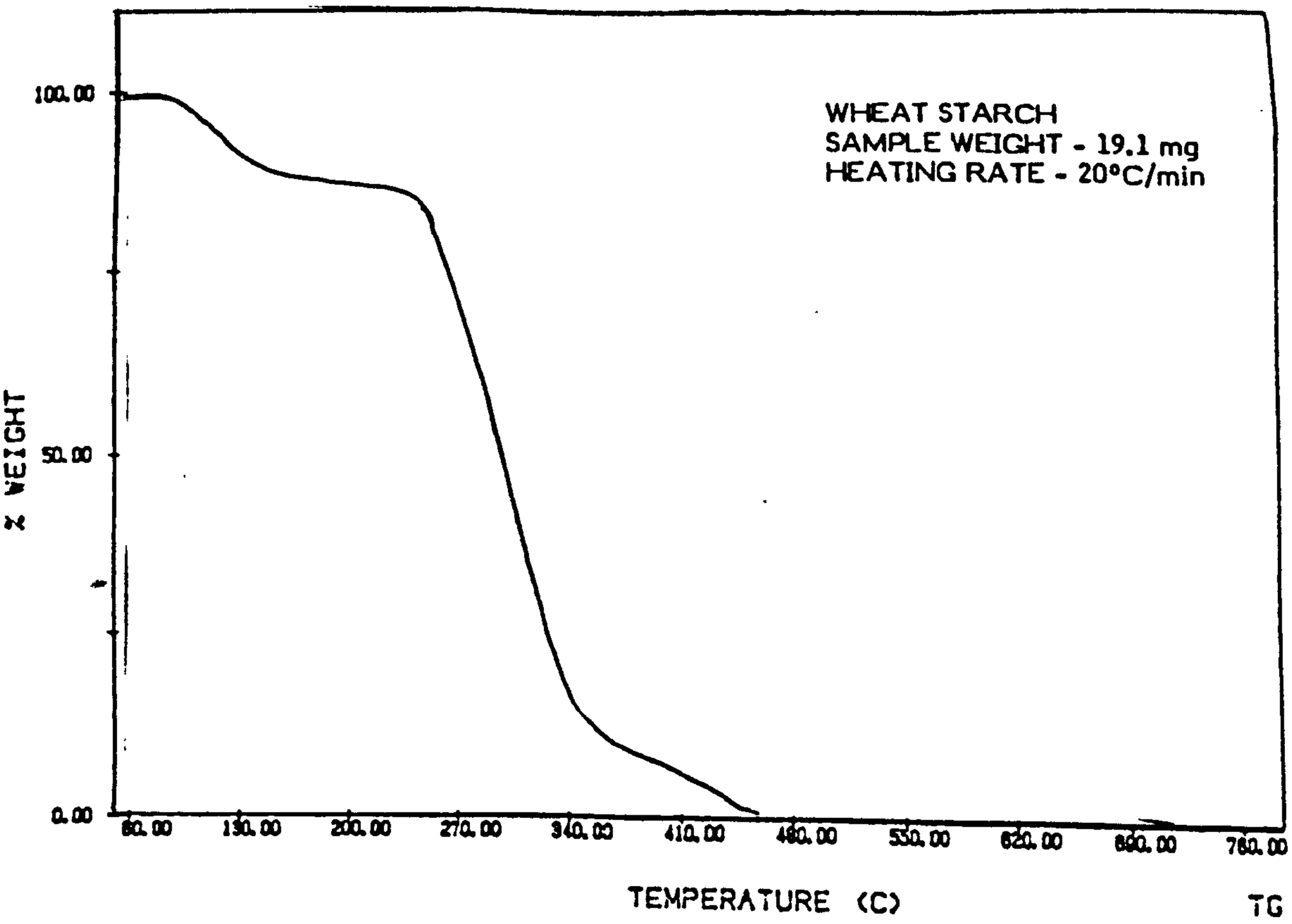

FIGURE 52

STA CURVE FOR GLUCOSE

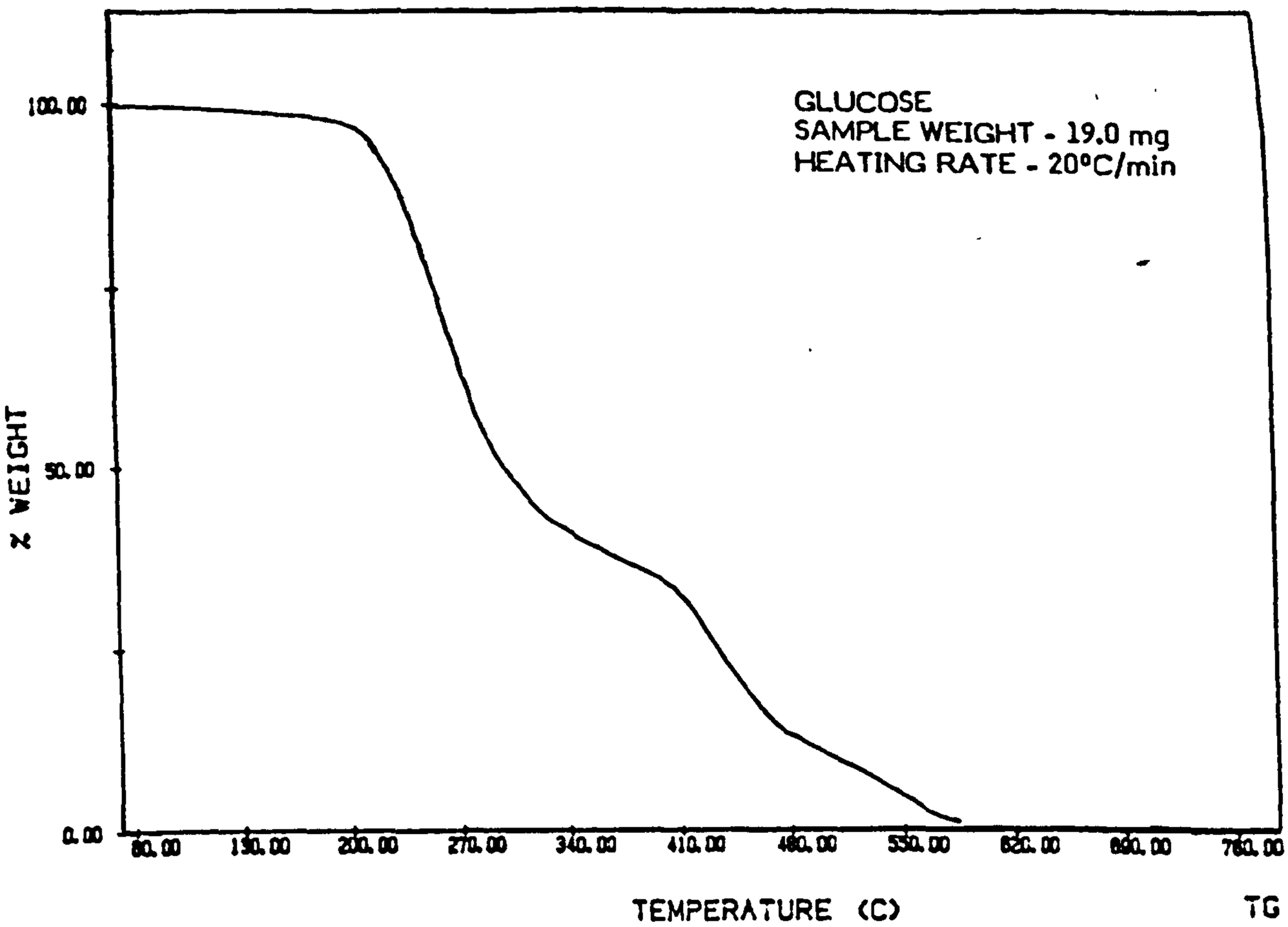

FIGURE 53

STA CURVE FOR SORBITOL

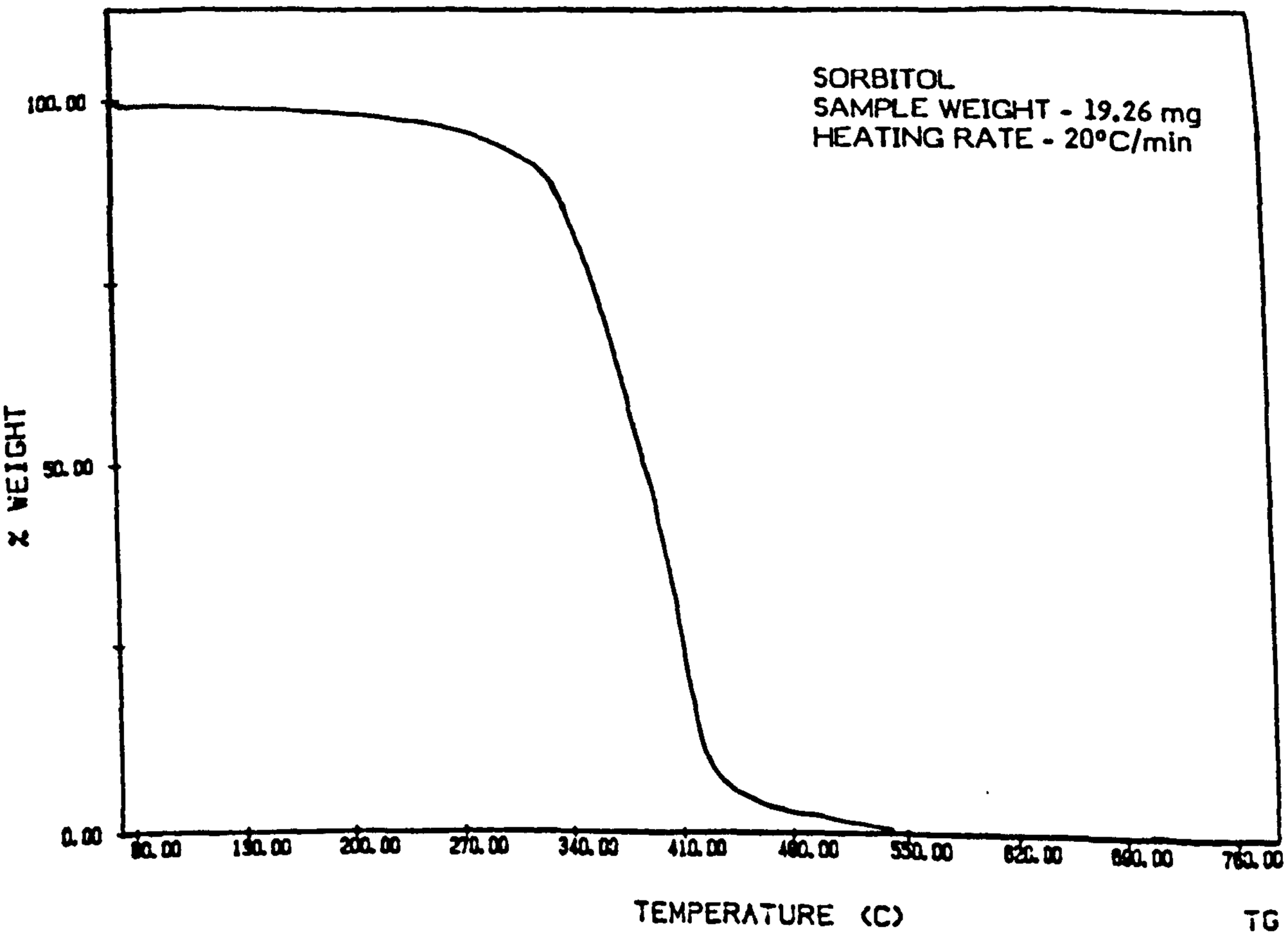

5.6.1. CHEMISTRY OF THE SPUMIFIC

At least two quite different classes of compound have been used as blowing agents, the organic amides and amines, and chlorinated paraffins. The common blowing agents are given in Table 5. In order to extend the temperature range over which gases are evolved, two or three agents are used, e.g. a combination of guanidine or chlorinated paraffin and melamine or dicyandiamide. Inorganic carbonates and bicarbonates and alumina hydrates have been used, but these agents are less effective.

Gas liberation should mainly occur after the melt forms and before gellation of the resin. While individual materials may be used to achieve a specific functional objective, most exhibit dual functionality. For instance, pentaerythritol is added to produce carbon, but in so doing it also releases gaseous by-products which also assist in blowing.

TABLE 5

POTENTIAL BLOWING AGENTS

MATERIAL	GASEOUS BY-PRODUCTS	DECOMPOSITION TEMP.°C
DICYANDIAMIDE	NH_3, CO_2, H_2O	210
MELAMINE	NH_3, CO_2, H_2O	250
GUANIDINE	NH_3, CO_2, H_2O	160
GLYCINE	NH_3, CO_2, H_2O	233
UREA	NH_3, CO_2, H_2O	130
CHLORINATED PARAFFIN	Cl_2, CO_2, H_2O	190

5.6.1. EXPERIMENTAL ANALYSIS OF SPUMIFICS

5.6.2. MELAMINE

Melamine (2,4,6-triazine) is sparingly soluble in water ranging from under 1% at 20°C to under 5% at 100°C. There are many publications about melamine, its salts and their crystalline forms (122 - 125).

The thermal decomposition of melamine in the range 200-500°C takes place in three stages, forming condensation products melam, melem, and melon in turn. The enthalpy of combustion was found to be 15.6 kJ/g, which is in agreement with the literature (122). During its decomposition, ammonia gas is released and a resinous residue is left (Fig. 54 & 55).

FIGURE 54

TGA CURVE FOR MELAMINE

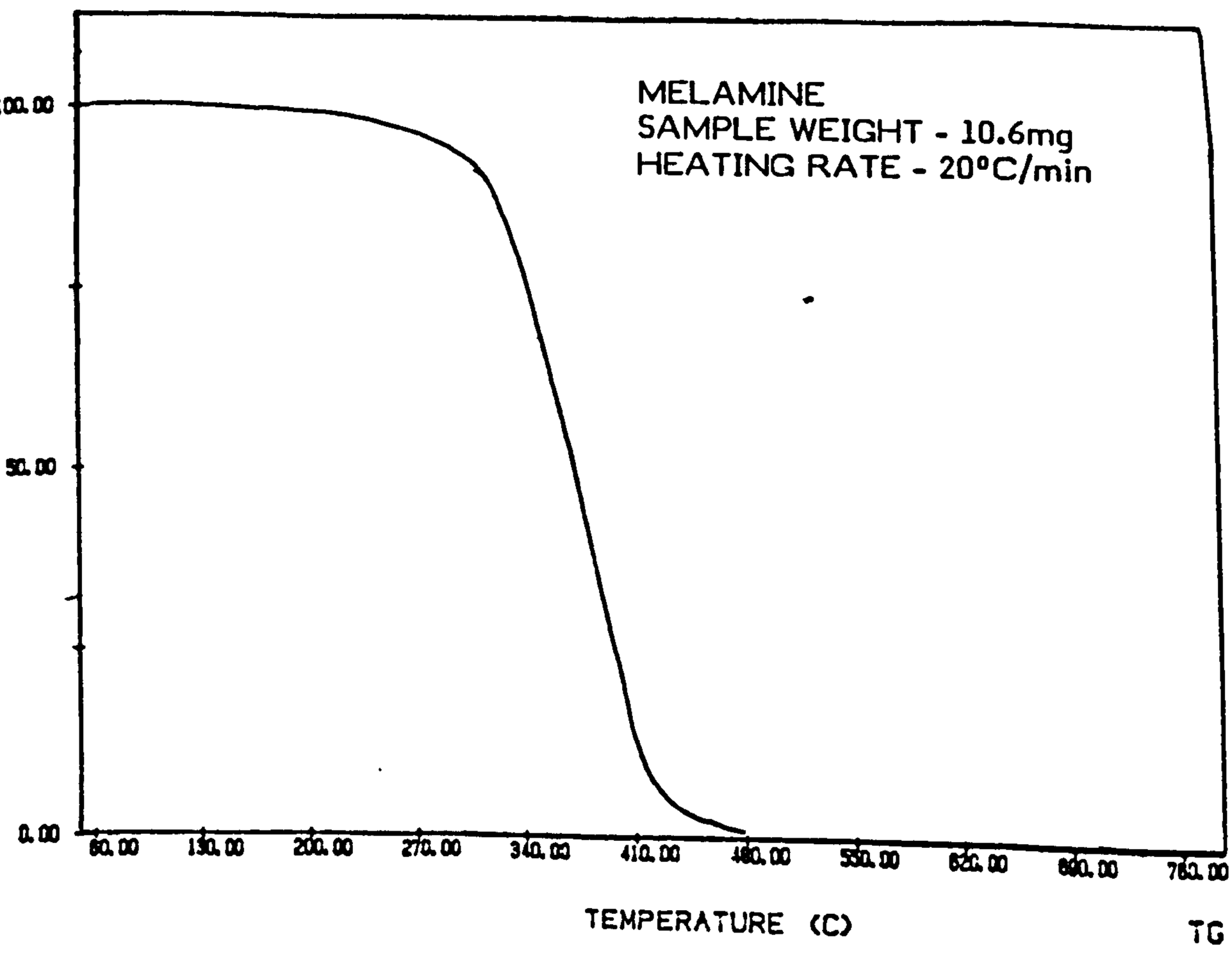

FIGURE 55

DSC CURVE FOR MELAMINE

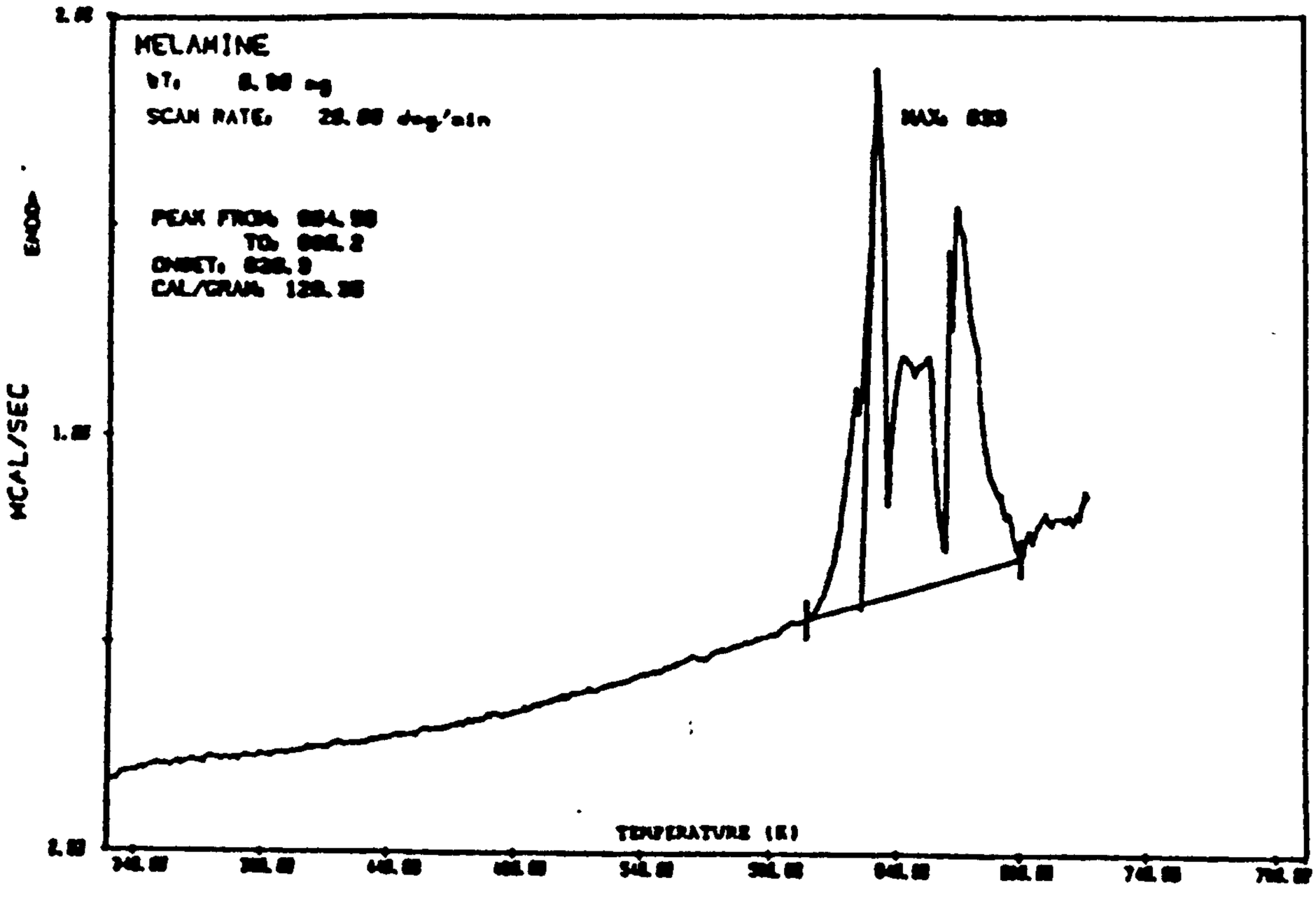

5.6.2.2. OTHER SPUMIFICS AND MIXTURES INVESTIGATED

Below are few examples of the various spumifics investigated.

FIGURE 56

STA CURVES FOR CERECLOR 42

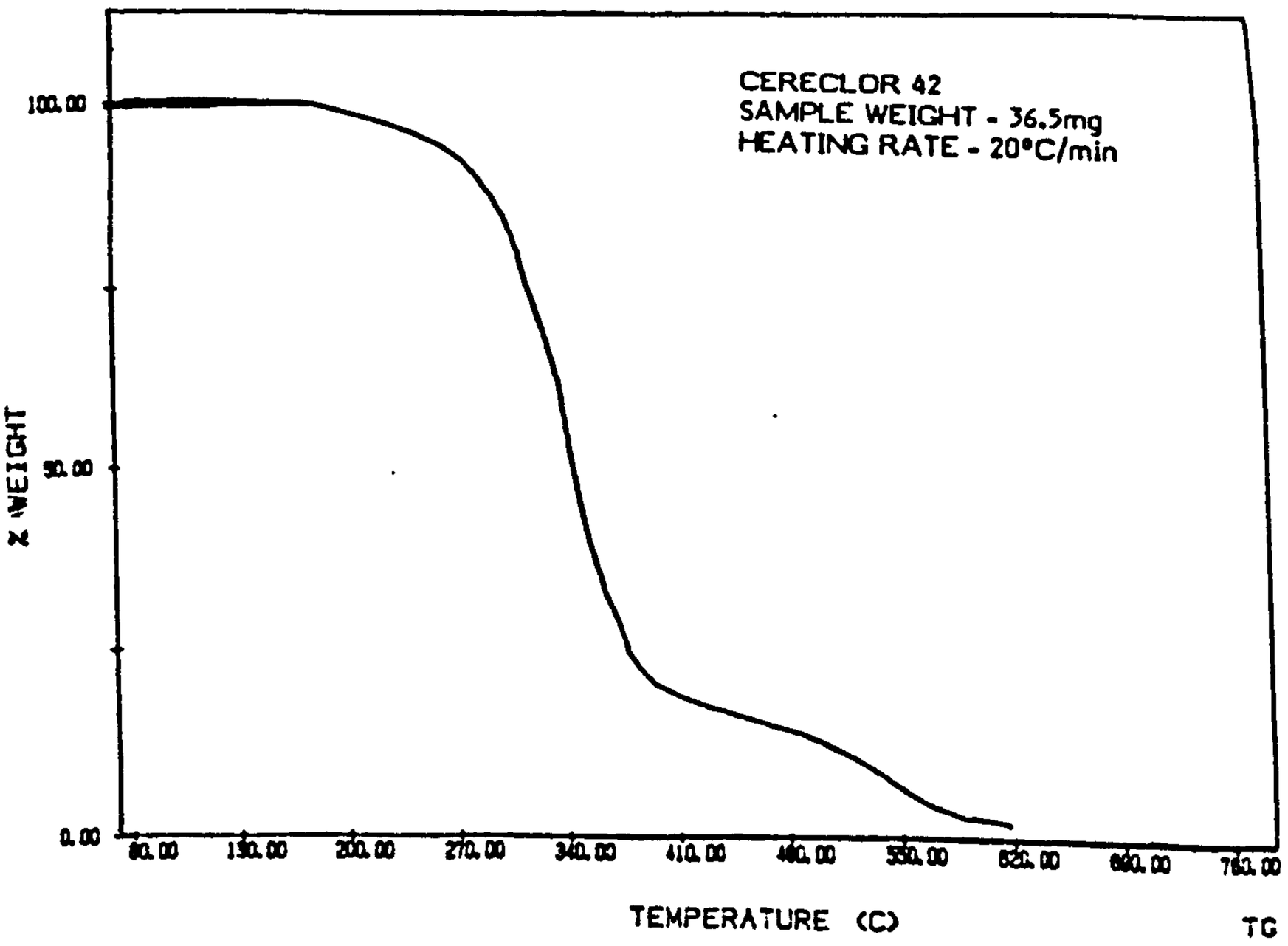

FIGURE 57

STA CURVE FOR CERECLOR 70

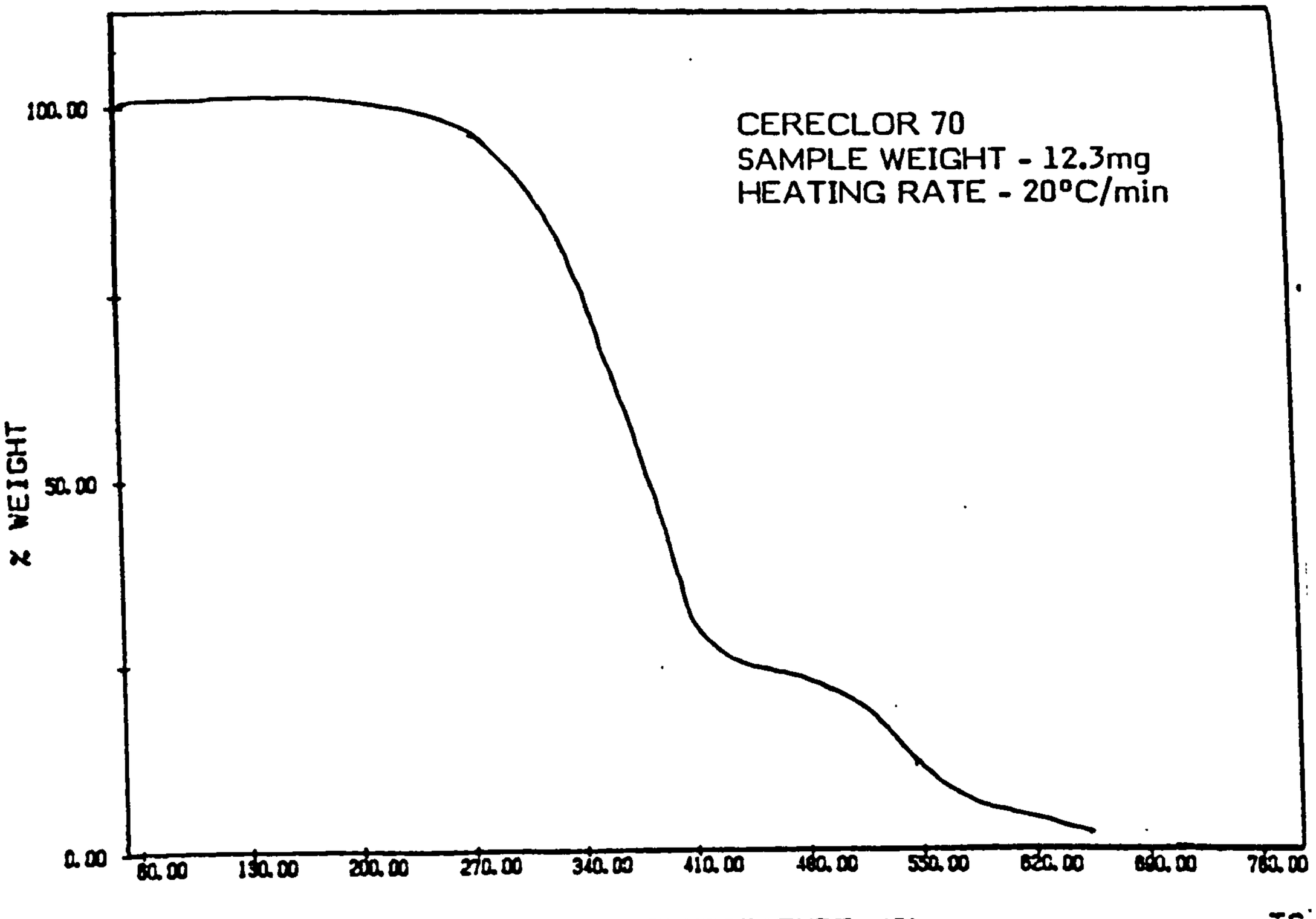

FIGURE 58

DSC CURVE FOR CERECLOR 70

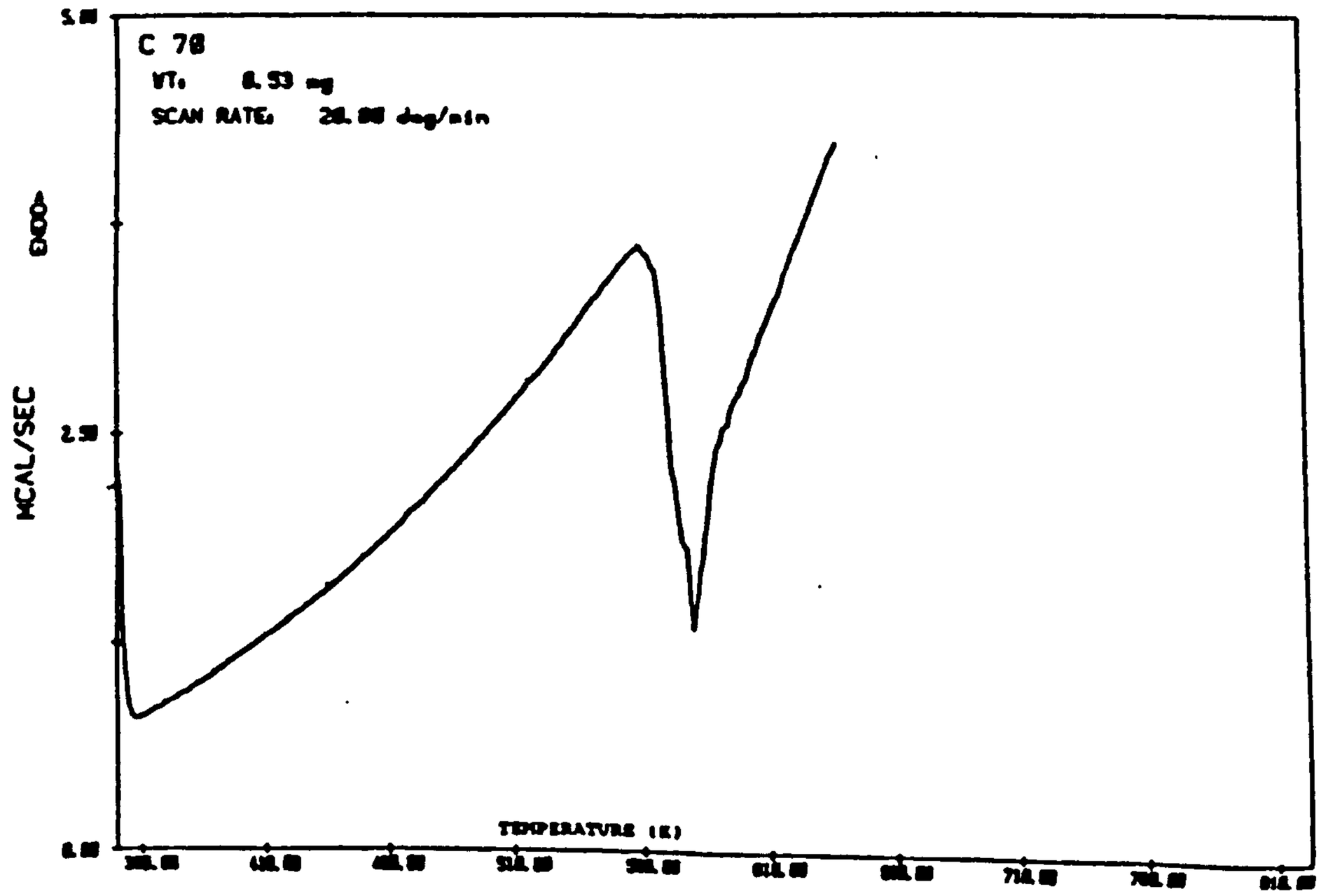

FIGURE 59

STA CURVE FOR DICYANDIAMIDE

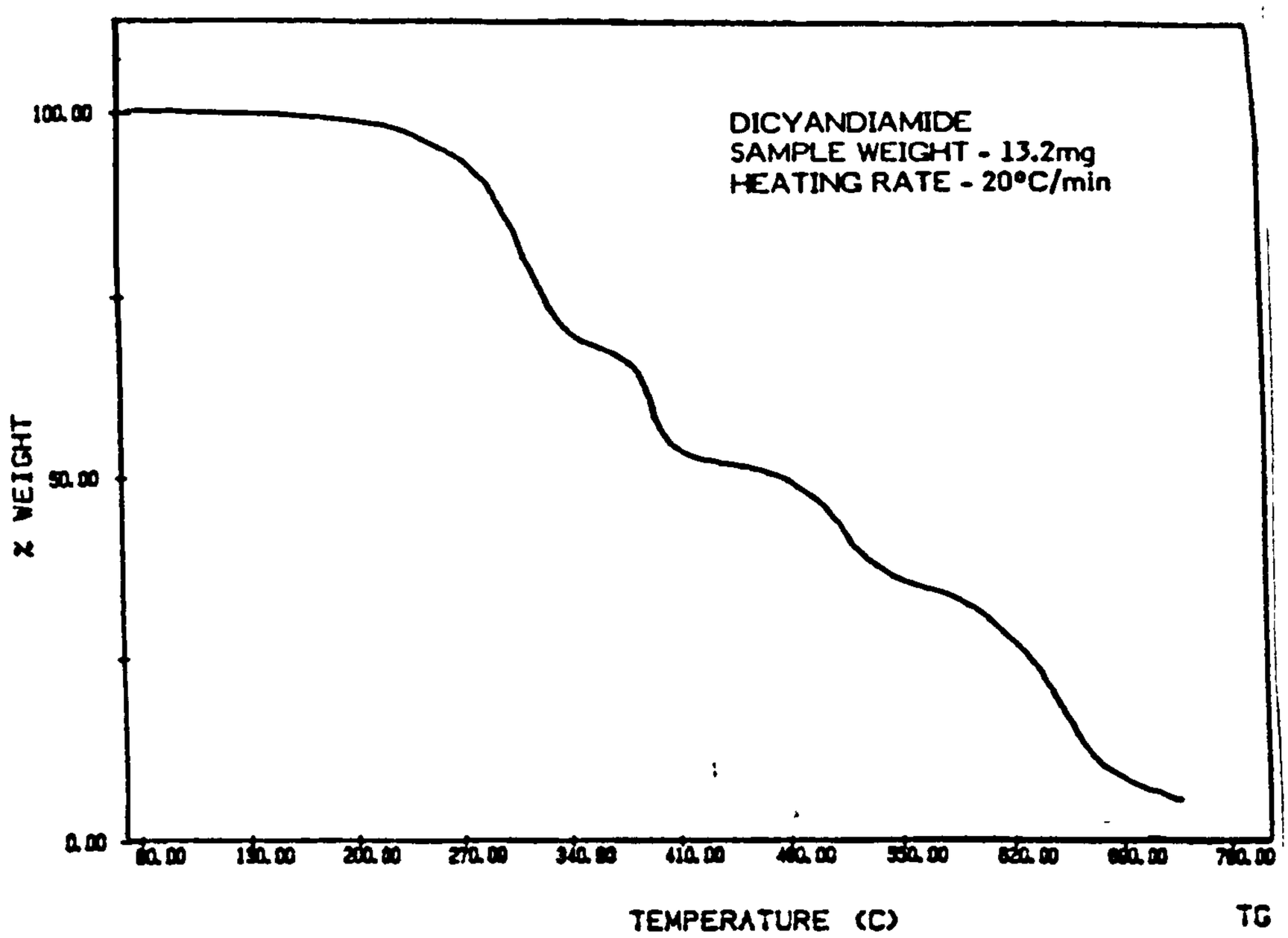

FIGURE 60

DSC CURVE FOR DICYANADIAMIDE

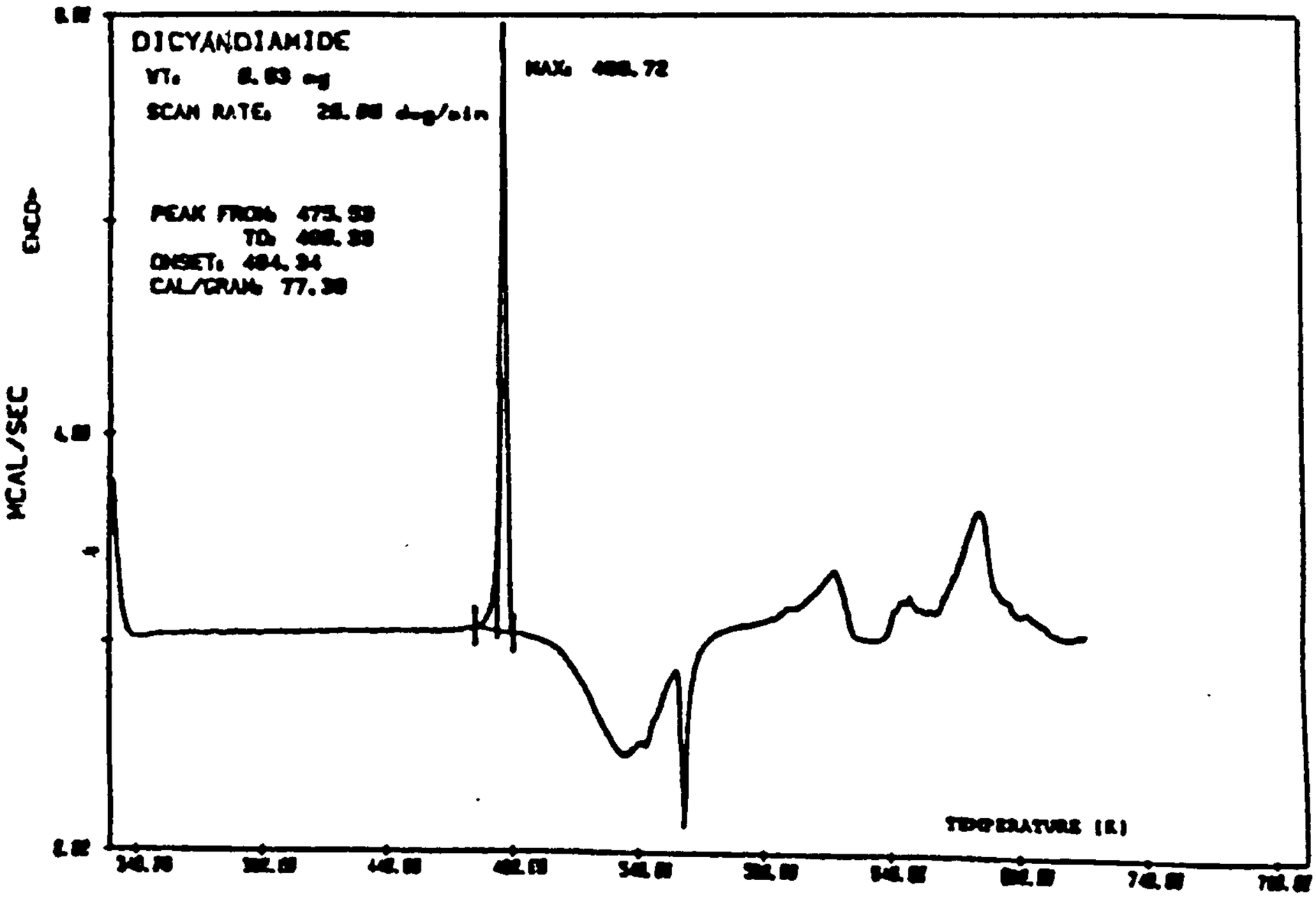

FIGURE 61

STA CURVE FOR UREA

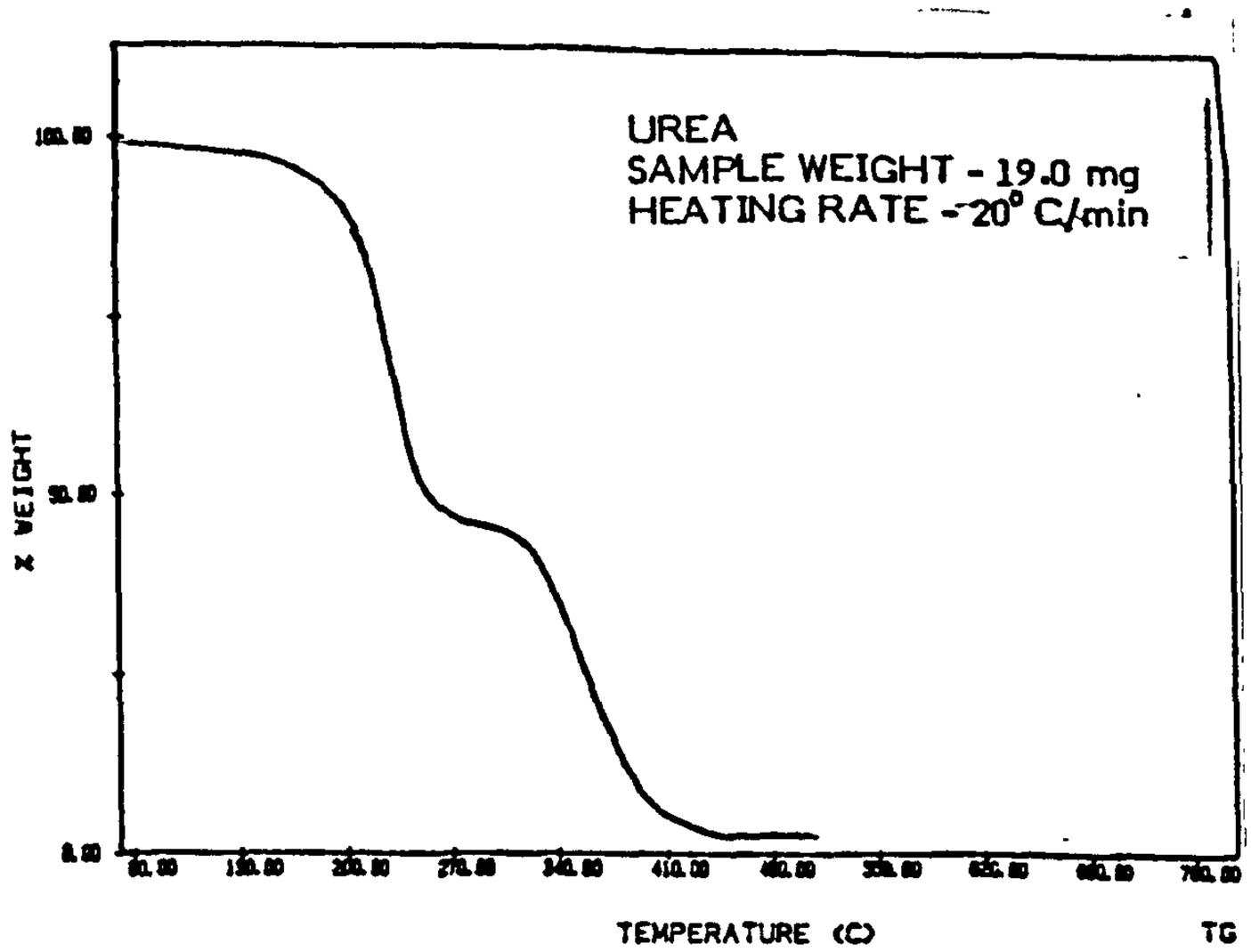

FIGURE 62

SUMMARY OF THE THERMOGRAVIMATRIC ANALYSIS OF INGREDIENTS IN INTUMESCENT PAINTS

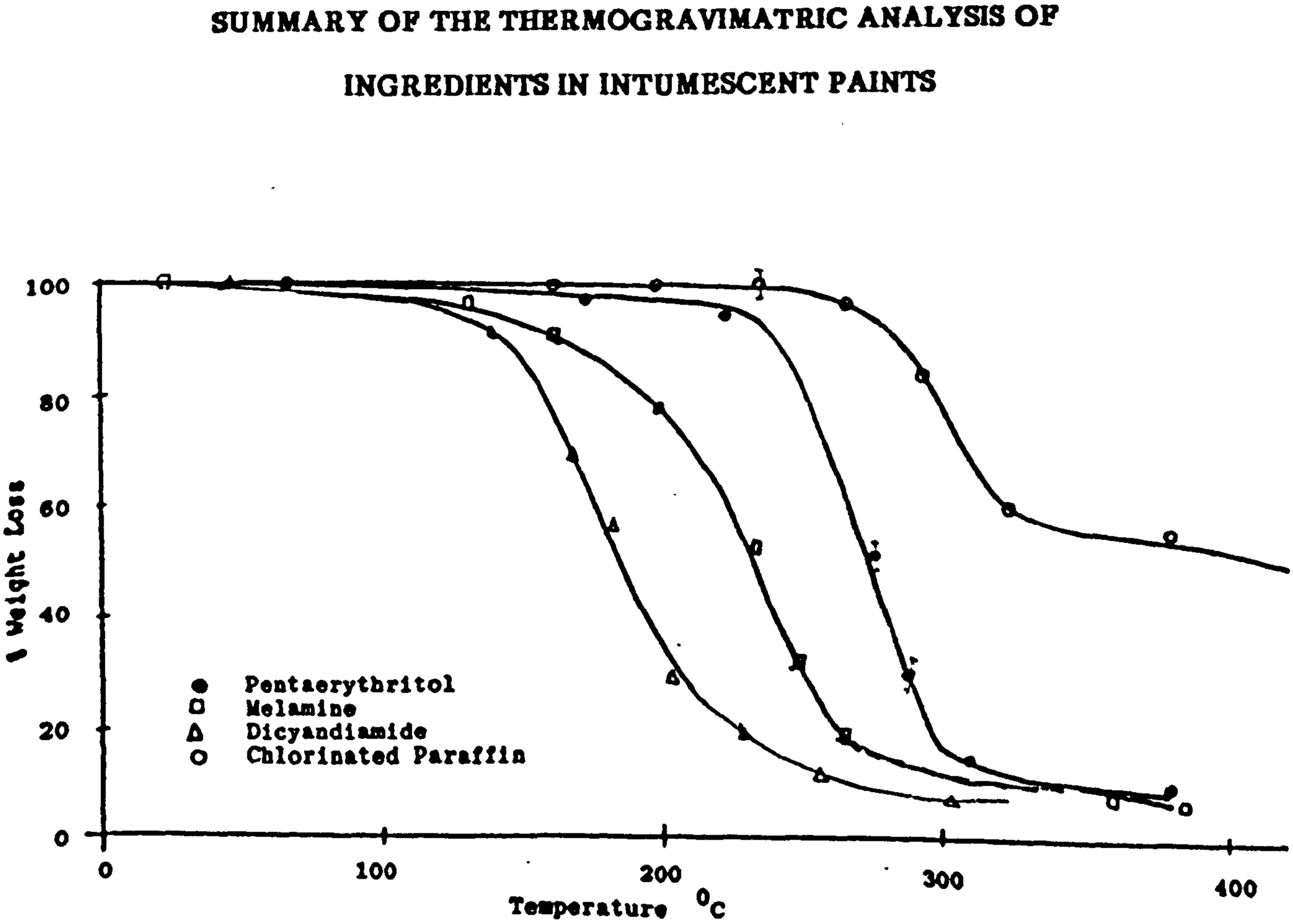

5.7.1. STUDY OF REACTION KINETICS

Let us assume that for heterogeneous solid-phase kinetics (113) the rate of reaction may be expressed as:

$$d\alpha/dt = k(1 - \alpha)^n \qquad (5.15)$$

where t is time, k is the rate constant, α is the degree of transformation or decomposition and n is the order of the reaction. Also let us assume that the temperature dependence of the rate constant is given by the Arrhenius equation,

$$k = B\, e^{-E/RT} \qquad (5.16)$$

where B is the frequency factor, E is the activation energy, R is the universal gas constant, and T is the temperature. Substituting for k into Eq (5.15),

$$d\alpha/dt = B \cdot e^{-E/RT}(1 - \alpha)^n \qquad (5.17)$$

Let $dT/dt = q$

Hence $$d\alpha/dT = (B/q) \cdot e^{-E/RT}(1 - \alpha)^n \qquad (5.18)$$

Thus $$\ln(d\alpha/dT) = \ln (B/q) - (E/RT) + n \cdot \ln (1 - \alpha) \qquad (5.19)$$

and on differentiation with respect to $\ln(1 - \alpha)$ we obtain

$$\frac{d \ln (d\alpha/dT)}{d \ln (1 - \alpha)} = -E/R \left[\frac{d (1/T)}{d \ln (1 - \alpha)} \right] + n \qquad (5.20)$$

which can be written in the form:

$$y = - (E/R) \cdot x + n \qquad (5.21)$$

Hence, plotting y against x, the activation energy E is found from the slope of the straight line obtained and the reaction order n is given by the intercept on the y-axis. The rates of reaction at different temperatures must be measured. From the TGA analysis, the loss of weight was plotted against time. The thermal degradation of some samples was found to involve two or more reactions which ran either concurrently or consecutively.

5.7.2. TYPICAL EXAMPLES OF REACTION KINETICS

5.7.2.1. A TYPICAL SPUMIFIC - MELAMINE

ENERGY OF REACTION

The energy of reaction was found by plotting

$$\frac{\ln dW/dt}{\ln W_r} \quad \text{against} \quad \frac{T^{-1}}{\ln W_r}$$

where dW/dt is the rate of weight loss, T is the temperature and $W_r = (W_c - W)$ where W is weight loss at time t and W_c is weight loss at completion of the reaction.

TABLE 6

TEMP. (K)	$\frac{\ln (dW/dt)}{\ln W_r}$	$\frac{T^{-1}}{\ln W_r}$
RESULTS FOR REACTION 1		
548	4.510	2.184×10^{-3}
598	3.931	1.958×10^{-3}
648	3.402	1.696×10^{-3}
698	2.616	1.351×10^{-3}
748	2.842	1.107×10^{-3}
RESULTS FOR REACTION 2		
848	2.720	8.565×10^{-4}
873	2.440	7.934×10^{-4}
898	2.251	7.170×10^{-4}
923	1.988	6.210×10^{-4}
948	1.446	4.399×10^{-4}

Energy of activation for reaction 1 = 43.7 kJ $mole^{-1}$

Energy of reaction 2 = 58.4 kJ $mole^{-1}$

For reaction 1, the order of the reaction was found to be = 9.50

For reaction 2, the order of the reaction was found to be = 4.86

FIGURE 63

GRAPH OF MASS VERSUS TEMPERATURE AND TIME FOR MELAMINE

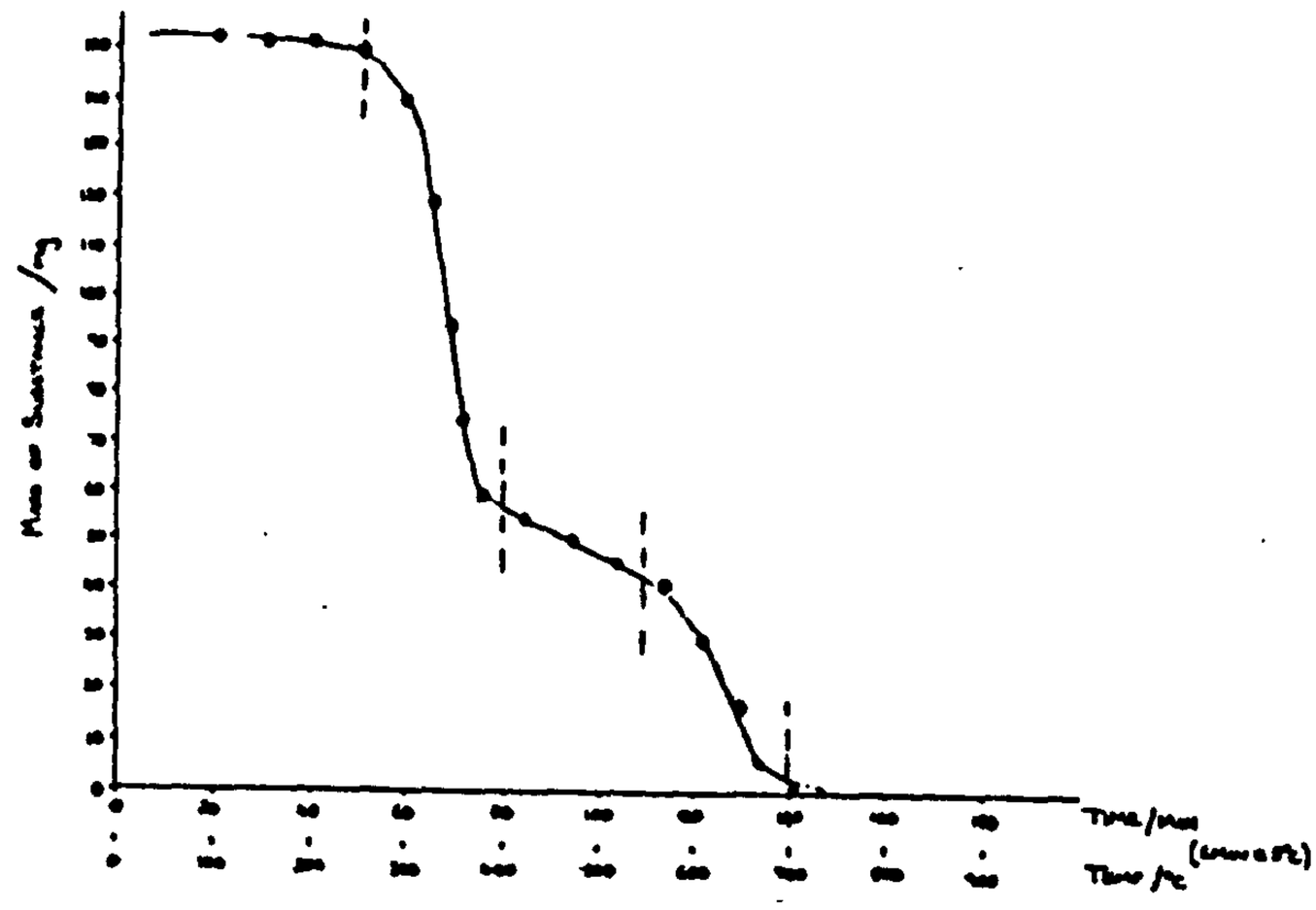

FIGURE 64A

MELAMINE - REACTION 1

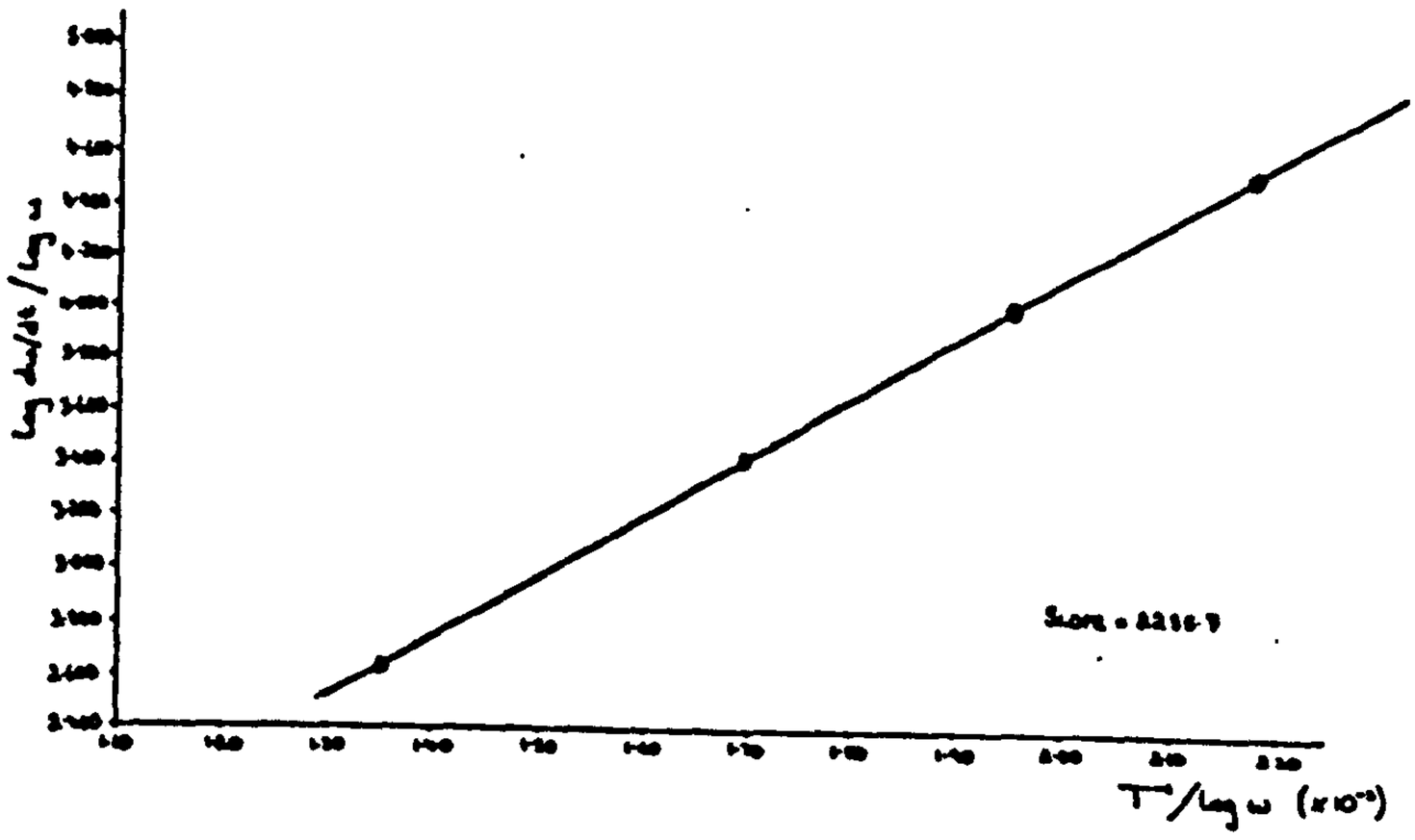

FIGURE 64B

MELAMINE - REACTION 2

5.7.2.2. REACTION KINETICS FOR A TYPICAL EXAMPLE OF THE INTUMESCENT PAINT (KD 23)

TABLE OF RESULTS

Temp.	ln (dW/dt)	T^{-1}
Reaction I	ln W_r	ln W_r
423	2.6948	1.268×10^{-3}
473	2.5000	1.125×10^{-3}
523	2.2900	0.992×10^{-3}
573	2.2100	0.865×10^{-3}
623	2.0900	0.749×10^{-3}
Reaction II		
673	2.2240	6.687×10^{-4}
723	2.2200	6.121×10^{-4}
773	2.1900	5.622×10^{-4}
Reaction III		
823	1.9330	5.044×10^{-4}
873	1.8600	4.514×10^{-4}
923	1.7350	3.981×10^{-4}

The results are plotted as three separate graphs, see Fig. 65-68 and the energy of reaction calculated as shown below:-

Therefore, energy for reaction I = 1012.5 x 2.3 x 8.314

$= 19.36 \text{ kJ mole}^{-1}$

energy for reaction II = 600 x 23 x 8.314

$= 11.47 \text{ kJ mole}^{-1}$

and energy for reaction III = 2333 x 2.3 x 8.314

$= 44.61 \text{ kJ mole}^{-1}$

For reaction I, (at 423 K), the order of reaction is 3.98

For reaction II, upto 673 K, the order of reaction is 2.63

For reaction III, upto 823 K, the order of reaction is 3.11

FIGURE 65

GRAPH OF MASS VERSUS TEMPERATURE AND TIME FOR INTUMESCENT PAINT

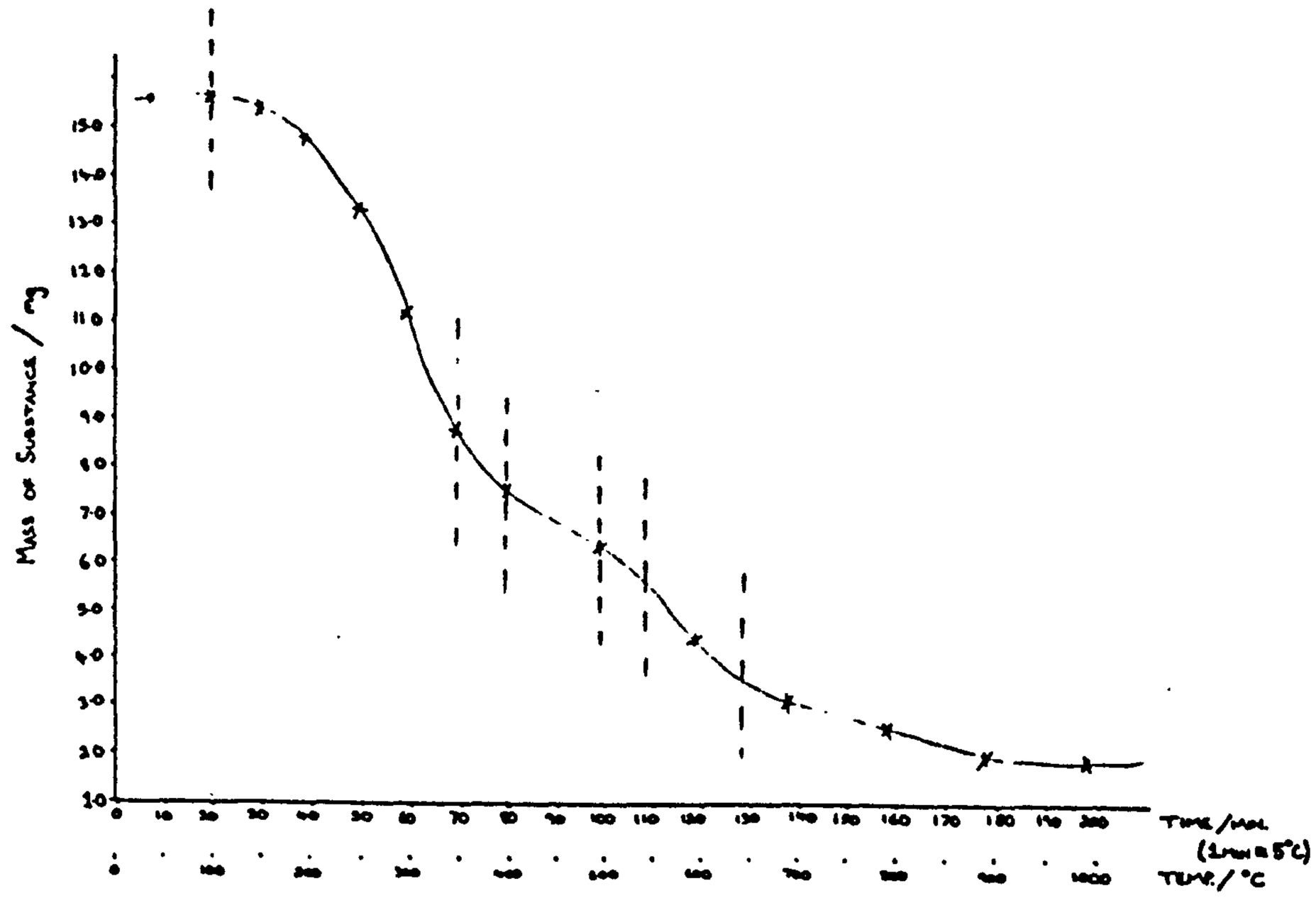

FIGURE 66

KINETICS OF REACTION I OF THE INTUMESCENT PAINT

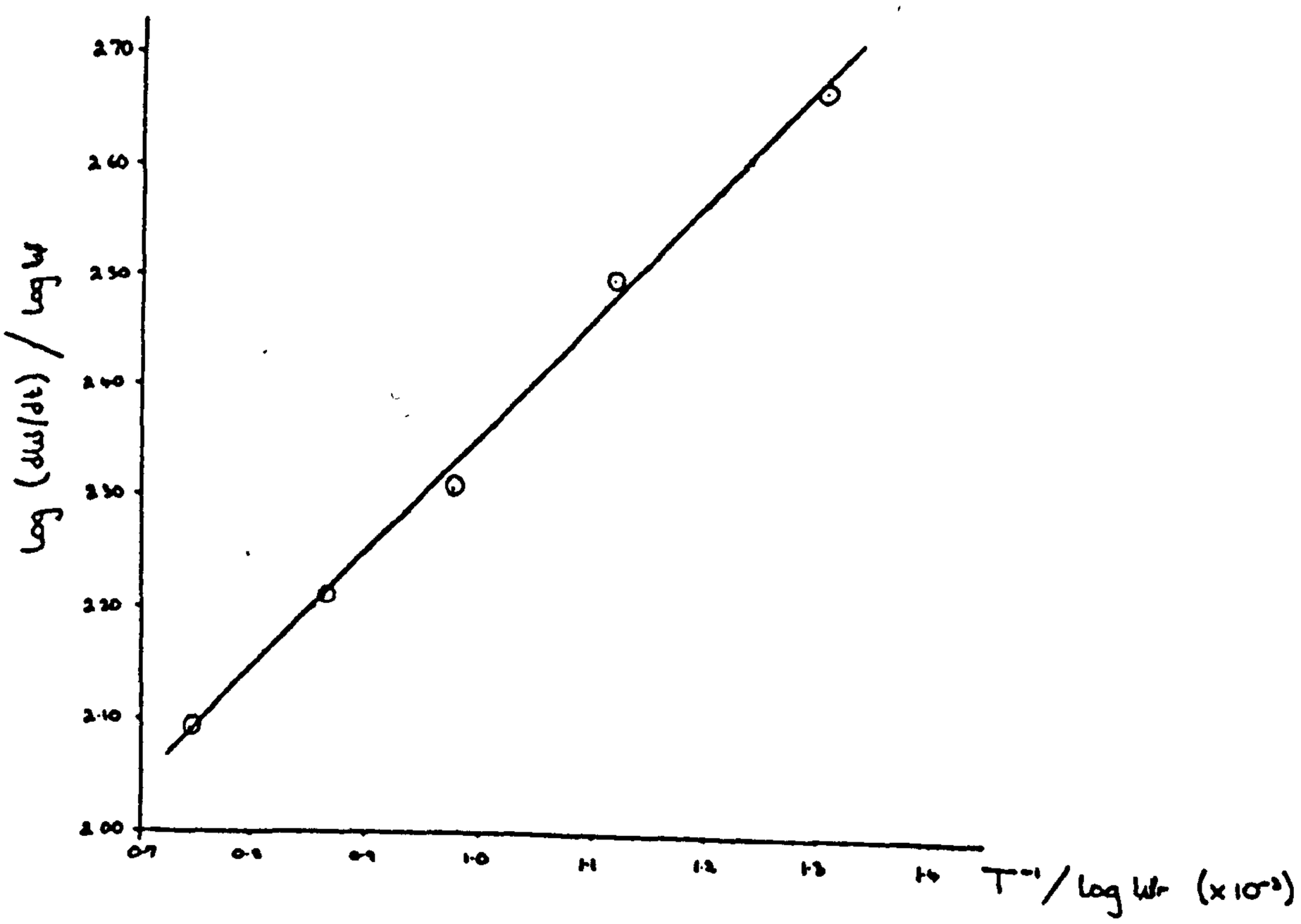

FIGURE 67

KINETICS OF REACTION II OF THE INTUMESCENT PAINT

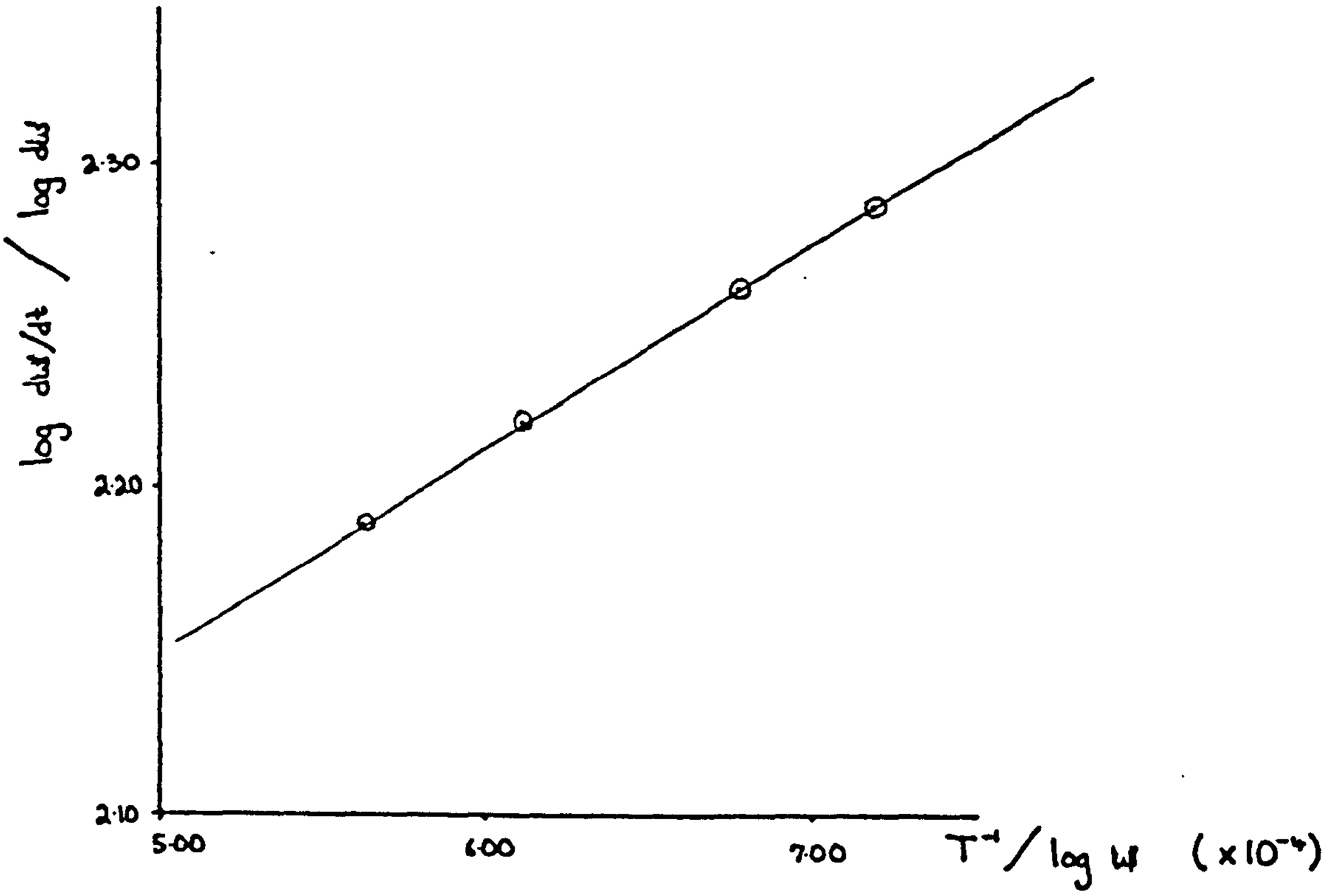

FIGURE 68

KINETICS OF REACTION III OF THE INTUMESCENT PAINT

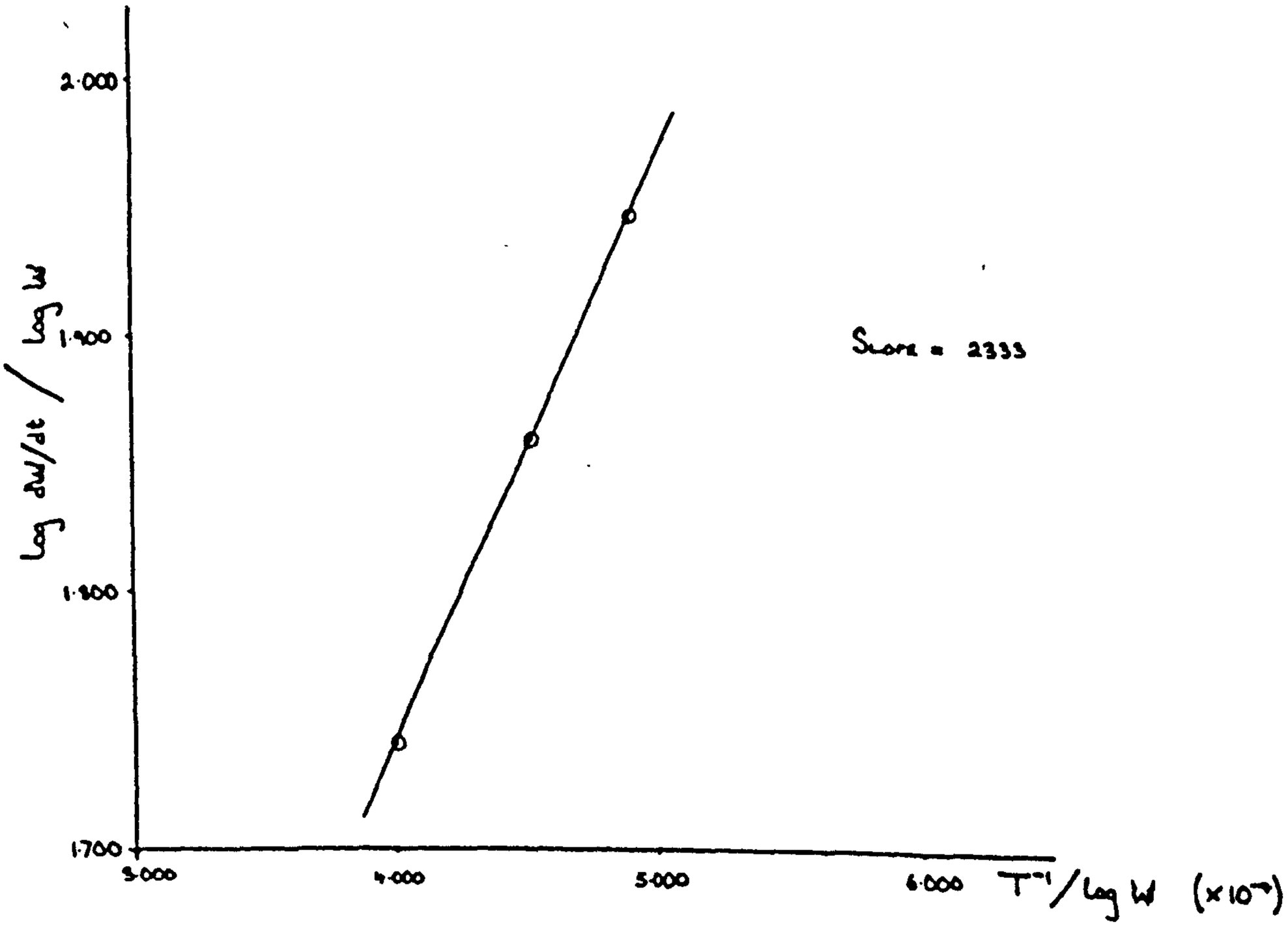

5.8.1. SUMMARY OF STA & DTA THERMAL DATA RESULTS

5.8.1.1. PAINT FILM (KD 23)

TEMP °C	ENDOTHERM/ EXOTHERM	SIZE OF PEAK	WEIGHT LOSS %
151	endo	average	<1
235	endo	average	≒5
275	endo	v/small	<1
295	endo	average	≒50
320	endo	average	
430	exo	med/small	≒10
662	exo	medium	≒5

Residual weight at end of reaction = 40%

5.8.1.2. PAINT FILM COMPONENTS AND THEIR MIXTURES

MELAMINE			
345	endo	large	≒100
POLY AMMONIUM PHOSPHATE (PHOSCHECK P 30)			
330	endo	average	15
650	endo	small	65
PENTAERYTHRITOL			
181	endo	average	0
340	endo	large	≒100
ALLOPRENE			
340	exo	average	50
512	exo	large	30
TITANIUM DIOXIDE			
No reaction			
AMMONIUM POLYPHOSPHATE + DIPENTAERYTHRITOL			
180	endo	average	0
240	endo	v/small	<5
345	exo	average	≒100
370	exo	small	
ALLOPRENE + DIPENTAERYTHRITOL			
186	endo	average	<2
237	endo	v/small	≒70
275	endo	average	
330	exo	shoulder	≒10
510	exo	large	

5.8.2. SUMMARY OF DSC THERMAL DATA

ETHYL CELLULOSE

An exothermic peak is observed between 328°C and 403°C with a maximum peak at 378°C.

CERECLOR 70 (CHLORINATED PARAFFIN)

Decomposition initially ranges between 100°C and 280°C.

There is a large exothermic peak observed between 280°C and 330°C with a maximum peak at 312°C.

PENTAERYTHRITOL

This shows a peak at 187°C with rapid decomposition occurring from 240°C.

CRYSTALLINE MELAMINE

This shows a melting point at 360°C followed by two main peaks at 380°C and 400°C.

CRYSTALLINE DICYANDIAMIDE

As expected, this shows a very sharp melting point at 209°C and several small endothermic and exothermic peaks.

PHOS CHEK P30 (AMMONIUM POLYPHOSPHATE)

No peaks were observed, just an overall decomposition initiating at 96°C.

5.8.3. SUMMARY OF THE KINETIC DATA OF THE PAINT & COMPONENTS

TABLE 8

REFERENCE SAMPLE	ACTIVATION ENERGY (kJ mole^{-1})		ORDER OF REACTION	
PAINT (KD23)	(AIR)	(NITROGEN)	(AIR)	(NITROGEN)
Reaction 1	19.36	20.5	3.98	4.1
Reaction 2	11.47	13.1	2.63	3.5
Reaction 3	44.61	46.5	3.11	3.9
ALLOPRENE	30.59		5.1	
AMMONIUM POLY-PHOSPHATE	61.2		8.96	
MELAMINE				
Reaction 1	43.7		9.5	
Reaction 2	58.4		4.86	
DIPENTAERYTHRITOL	25.8		1.72	
CERECLOR	17.53		2.03	

5.8.4. SUMMARY OF THE RESULTS

It can be seen from Table 8 that the activation energy for the decomposition of cereclor is much less than for either of the decomposition reactions of melamine, thus indicating that very much less energy is required for cereclor to act as a spumific than is required for melamine. What is more, the reaction does not occur with the same intensity, the order being much less than that for either of the melamine decompositions. Hence, cereclor would not only be expected to release volatile gases more easily but also the reaction would occur more steadily being a slower reaction in comparison.

The activation energy for the decomposition of ammonium polyphosphate is large, hence requiring a large amount of energy in order to intiate the reaction. However, once the reaction starts it is very fast. This would mean that the acid would be released over a relatively short period.

The first two intumescent reactions require only relatively small activation energies and are not particularly fast. Very fast reactions could result in poor and friable properties. The final reaction requires more energy to occur.

In general, the energies of activation for the various reactions were found to be low, with high order of the corresponding reaction.

SECTION 6

FORMULATION DEVELOPMENT

6.1. INTRODUCTION

The thermo-analytical information gained in the previous section was used to produce the initial formulations to be discussed in this Section. Formulations were prepared using a standard method, as described below, to enable a comparative study to be made using the relevant test methods given in Section 4.

The criteria used for the selection of the various materials were based on the decomposition temperatures and the softening temperatures, as determined by the thermograms. The properties of the formulation, such as flame retardancy, durability, dispersability, and characteristics of intumescence, were examined. The ability of the binder to remain fluid over a wide temperature range, and its softening temperature, are crucial factors in intumescence reaction and for achieving a reasonable foam height. Hence, a considerable effort was imparted to select a suitable binder.

An important criterion in the selection of the carbonific was its decomposition temperature - the higher the decomposition temperature, the wider the selection of catalysts and blowing agents that could be used. The carbonifics with a high carbon content produced large amounts of the char. Elemental analysis was used to ascertain the elemental/carbon content of each char. From the thermal behaviour of each spumific, the selection of the right combination of ingredients was made. The mixtures of the binders, carbonifics, spumifics and the catalyst in various combinations were examined.

6.2. FORMULATION DEVELOPMENT PROGRAMME

Each formulation was evaluated by subjecting coated steel plates to the screening tests described in Section 4. The char produced was analysed for its structure, strength, adhesion to the substrate, and its ease of oxidation with increased heat fluxes. The results for each formulation are tabulated in Table .

The criteria used to assess the suitability of the formulations were:

1) The foam height achieved by a 1mm (dry thickness) coating after exposure to various screening tests as described in Section 4.

2) The nature of the foam e.g. cell structure, evenness.

3) Strength of the char formed.

4) The total solids content value of the formulation, the maximum acceptable not exceeding 75%.

5) The viscosity of the formulation, the maximum acceptable being 100 Pa s. measured using a Brookfield spindle at 4/12 rpm.

6.3. PROCEDURE FOR MAKING THE FORMULATIONS

All the formulations were prepared using the following method. The binder was weighed into a stainless steel beaker. The solvent was added with slow stirring, using a variable-speed mixer with a propeller attachment. Once all the binder had dissolved or been dispersed, the chlorinated paraffin wax was added. The proper dispersion of the wax was found to take up to 30 minutes vigorous stirring. The carbonific was then added. The agitation speed was adjusted to create a vortex, the level of which was kept well above the propeller head to avoid aeration of the mix. The remaining ingredients were added one at a time. After each addition, the mix was stirred for at least 10 minutes, the speed of the mixer being adjusted to compensate for the increased viscosity. In some

formulations, further solvent was required to reduce the viscosity. Once all the ingredients had been added, the final mix was vigorously stirred for another 30 minutes whilst still avoiding aeration.

The dispersion was then milled on the two roller-mill. The rollers were set to produce a small nip and their speed was controlled to enable the mixture to be transferred equally to both the rollers. The nip was adjusted gradually to crush any lumps. These lumps were evident on the smooth surface of the steel rollers and the milling was continued until a smooth mixture was achieved. Some additional solvent was added occasionally at the nip to compensate for that lost by evaporation. The guides on the mill were set well in to avoid any contamination from the machine oil. The scraper blade was used regularly to remove the mixture completely from the rollers and reintroduce it at the nip.

For some experiments, the mixtures were further ball-milled using 5mm solid glass balls in a steel container. The ball milling was conducted for up to 6 hours although longer periods produced even finer products. The fineness of the mixture and degree of milling was determined using Hegmann apparatus.

6.4. PREPARATION OF TEST PLATES

In order to produce uniform coating thicknesses on steel plates, various methods of application were investigated. By regulating the viscosity, total solids and thixotropic properties of coatings, uniform thicknesses could be obtained by means of a fine brush. The final thickness was determined by the number of coats applied. This method was found to be adequate for the initial screening of formulations. Methods of producing coatings of accurately-known dried thickness (for mathematical model

experiments) were investigated. Padding with a cloth, spraying, dipping, flow coating, roller coating etc were found unsuitable.

6.5. PAINT COATING SPREADER

A method was developed which produced a uniform thickness and was easy to use. A stainless steel rod of 25 mm diameter was machined at three different positions around its circumference to produce smooth coating edges. Two stainless steel guide plates were fixed to opposite sides of the central rod to act as the base of the machined edges, thus producing gaps of 1, 2, and 3 mm respectively.

The spreader, with the required edge facing below, was placed on the sample plate to be coated, the paint being poured in front of it. Pulling the spreader gently produced an even coating on the base plate. It was important to keep the fluid at the nip rolling all the time. The curvature of the centre rod prevented both the formation of 'tram lines' and skinning of the paint surface. The overall thickness was determined by the number of applications and the characteristics of the paint formulation.

Samples were dried thoroughly in between coats and left in a standard atmosphere for at least two weeks before testing. The final thickness of the samples was recorded at different positions on the sample and statistically analysed. The samples which had low standard deviations in their measured coating thickness were used for the final testing.

6.6.1. DEVELOPMENT OF THE INITIAL FORMULATION (KD 1 - KD 7)

In the initial experiments, ethyl cellulose was used as the binder, the reasons for this being:

a) it is thermoplastic and has a decomposition temperature of about

380°C, although the softening point is well below this, starting at about 350°C (Fig. 69)

b) it easily dissolves in the common solvents used

c) it can be easily flame-retarded with a paraffin wax

d) it is readily available in powder form.

To determine the amount of paraffin wax required to impart the necessary flame retardancy to ethyl cellulose, thin films of ethyl cellulose were spread with various amounts of the wax. The use of the wax was considered advantageous since it could also act as a spumific. Due to its fairly low temperature of decomposition, 190°C (Fig. 69), it was expected to assist in initial foam development.

FIGURE 69

DSC CURVE FOR ETHYL CELLULOSE N10

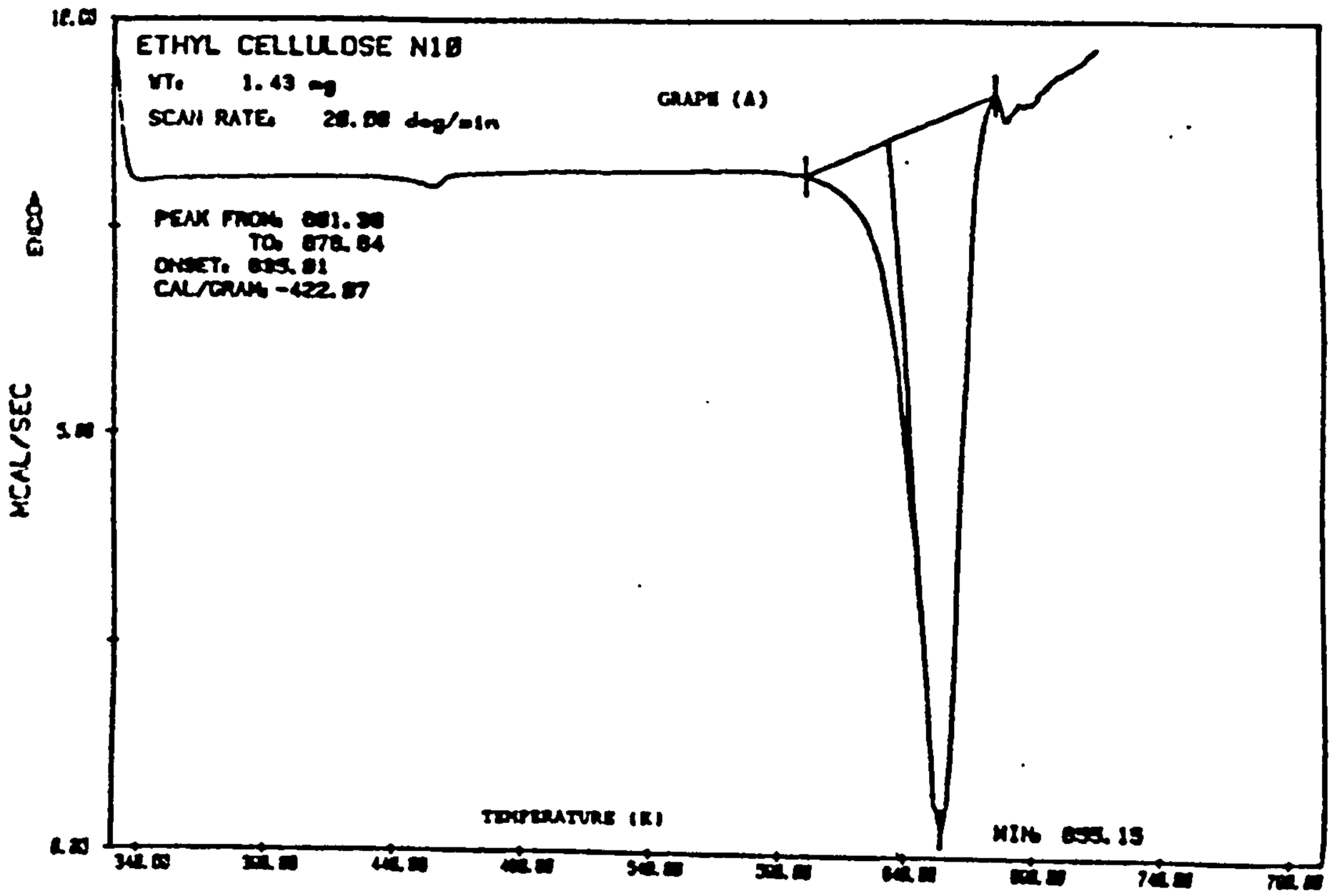

The carbonific selected was pentaerythritol as it is rich in carbon, has a decomposition temperature, of 350°C (Figs. 48), which is sufficiently high to allow the use of ammonium polyphosphate (Fig. 45), and is available in powder form. A very fine particle size (98% <100μm) was used, this being

an essential key factor in producing smooth, even paint films. Other carbonifics examined were erythritol, tripentaerythritol, resorcinol and various starches such as wheat and rice starch etc. Mixtures of carbonifics often made it difficult to determine the reasons for changes in the foam characteristics.

The spumific initially selected, melamine, has a decomposition temperature of 250°C (Fig. 54), the required amount of which was determined by a series of experiments. The other spumifics tried were glycine (decomposition temperature 230°C), dicyandiamide (decomposition temperature 210°C) and urea (decomposition temperature 130°C). Although urea had a decomposition temperature (Fig. 61)outside the range of that of the system, it did produce intumescence. A mixture of the blowing agents were also examined, Fig. 71.

The catalyst selected was ammonium polyphosphate (decomposition temperature 325°C, Fig. 45). It was found that the raw material varied between batches from the same manufacturer and in one extreme example no reaction was produced. Therefore, it was found necessary to confirm the chemical composition every time a new batch was used, DSC being used for the quality control. The other catalysts evaluated were monoammonium phosphate, urea phosphate, guanylurea and melamine phosphate and their mixtures. The monoammonium and urea phosphate were activated at temperatures below those required by the carbonific and often resulted in a black char without any significant intumescence. Melamine phosphate (Fig. 47B) was found to be a suitable alternative, but for the initial formulation APP was preferred.

FIGURE 70

A TYPICAL STA CURVE FOR A MIXTURE OF A CATALYST AND A CARBONIFIC

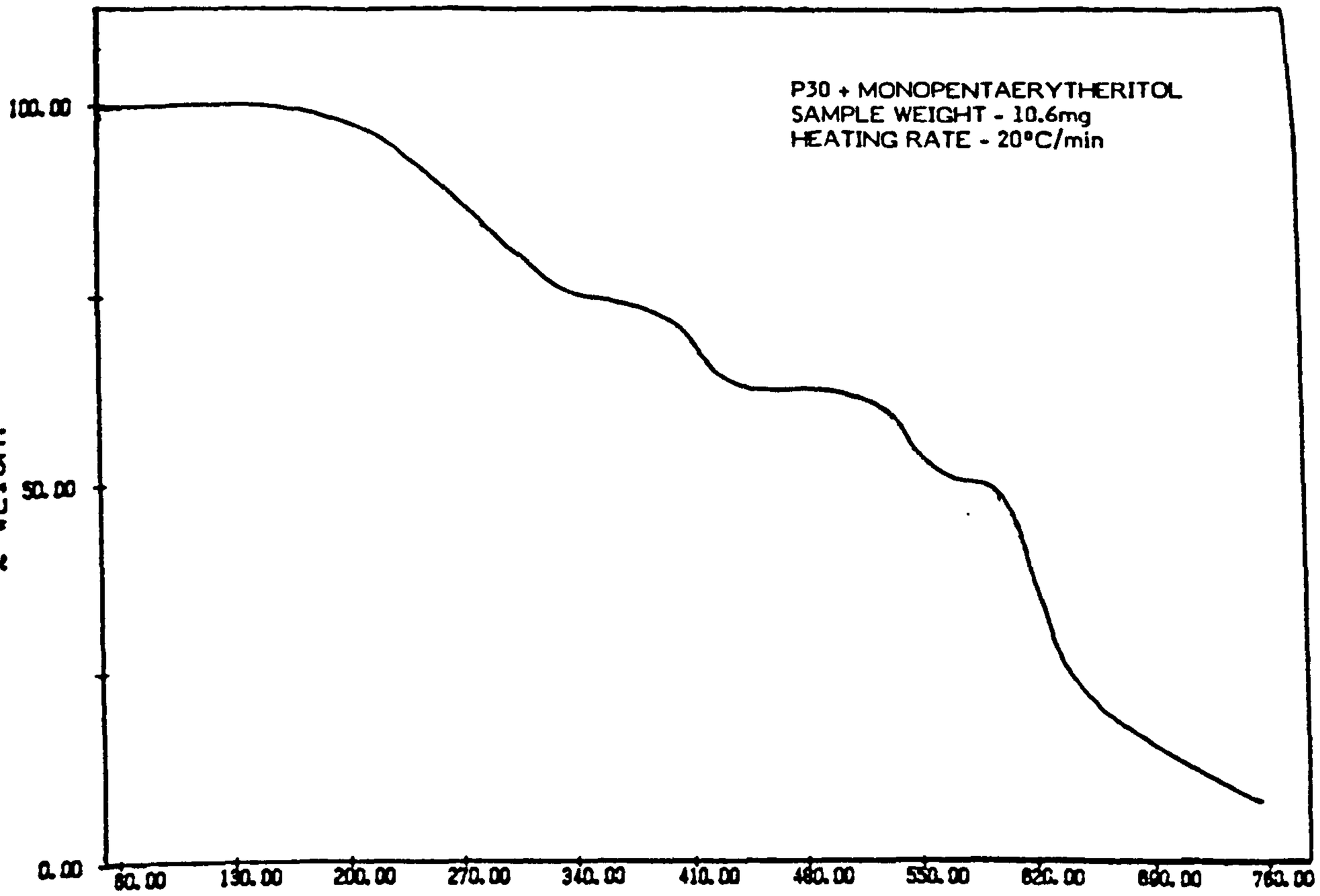

FIGURE 71

A TYPICAL STA CURVE FOR A MIXTURE OF SPUMIFICS

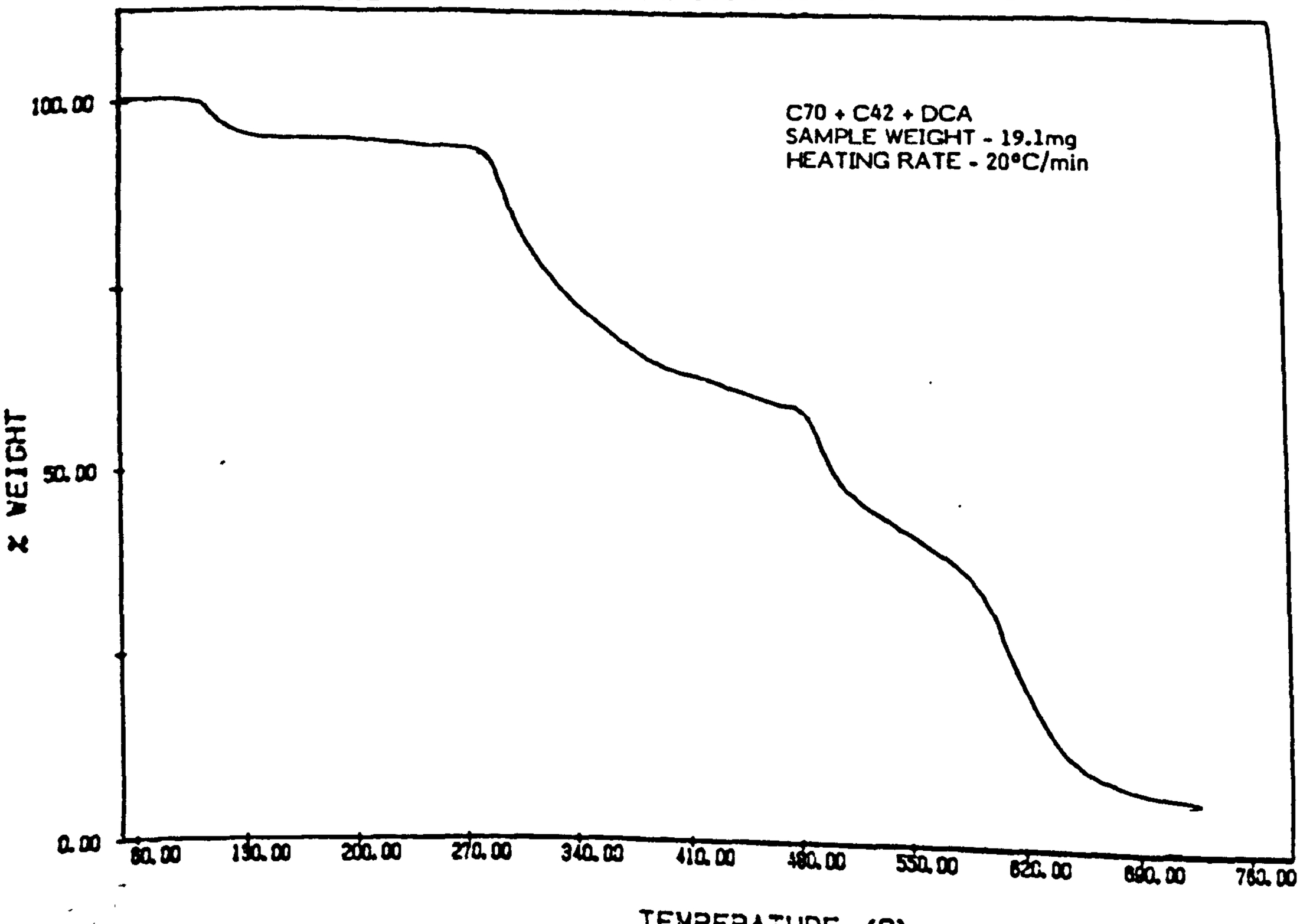

The formulations produced were tested using the screening test methods outlined previously. Those formulations which produced encouraging results were further improved by altering the proportions after bearing in mind the thermograms. The formulation given in table 9 produced the best results.

TABLE 9

FORMULATION REFERENCE KD 7

	% by weight	DECOMP. TEMP.°(C)
Ethyl cellulose	7.0	380
Cereclor 70	8.5	190
TiO_2	15.0	
Dipentaerythritol	8.5	350
Melamine	8.0	250
Ammonium polyphosphate	20.0	325
Toluene	35.0	

TSC% - 62

Viscosity spindle 4/12 - 35 Pa.s.

6.6.3. SUMMARY OF THE INITIAL FORMULATION RESULTS

The following observations were noted:

1) The level of APP is very critical. Levels below 15 parts cause a significant decrease in foam height, whereas levels of 30 parts or more produce little improvement in foam height or structure.

2) The use of dipentaerythritol instead of mono- or tri-pentaerythritol is preferable, according to literature (49). In practice very little difference, if any, was noticed in the foaming or other characteristics, Fig 72 & 73. However, using tripentaerythritol, it was possible to improve the TSC% content of the formulation. Furthermore, tripentaerythritol produced a slightly stronger foam. STA curves show the rate of weight loss for

tripentaerythritol at high temperatures is lower than for dipentaerythritol.

FIGURE 72

STA CURVE FOR DI PENTAERYTHERITOL

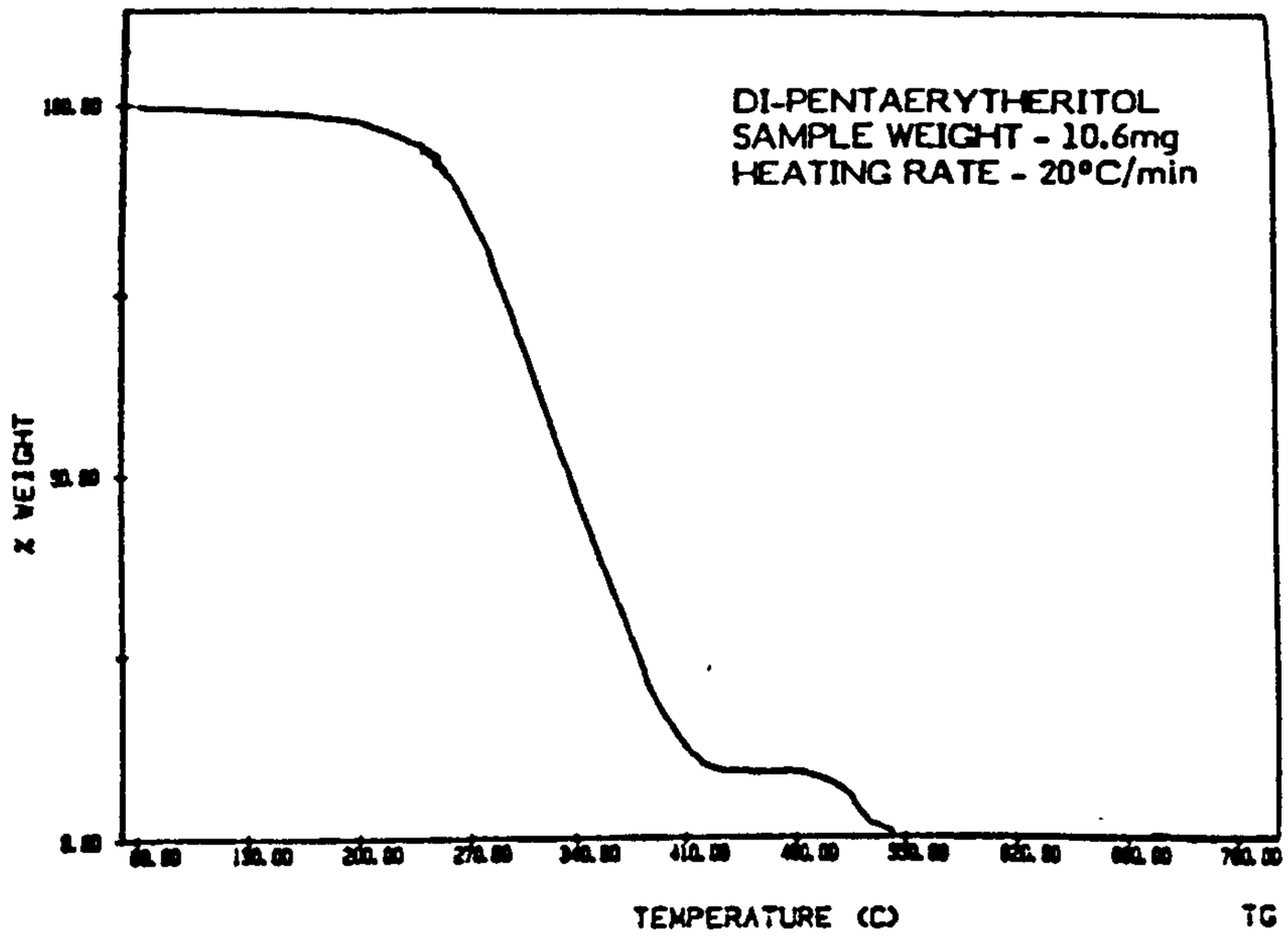

FIGURE 73

STA CURVE FOR TRI PENTAERYTHERITOL

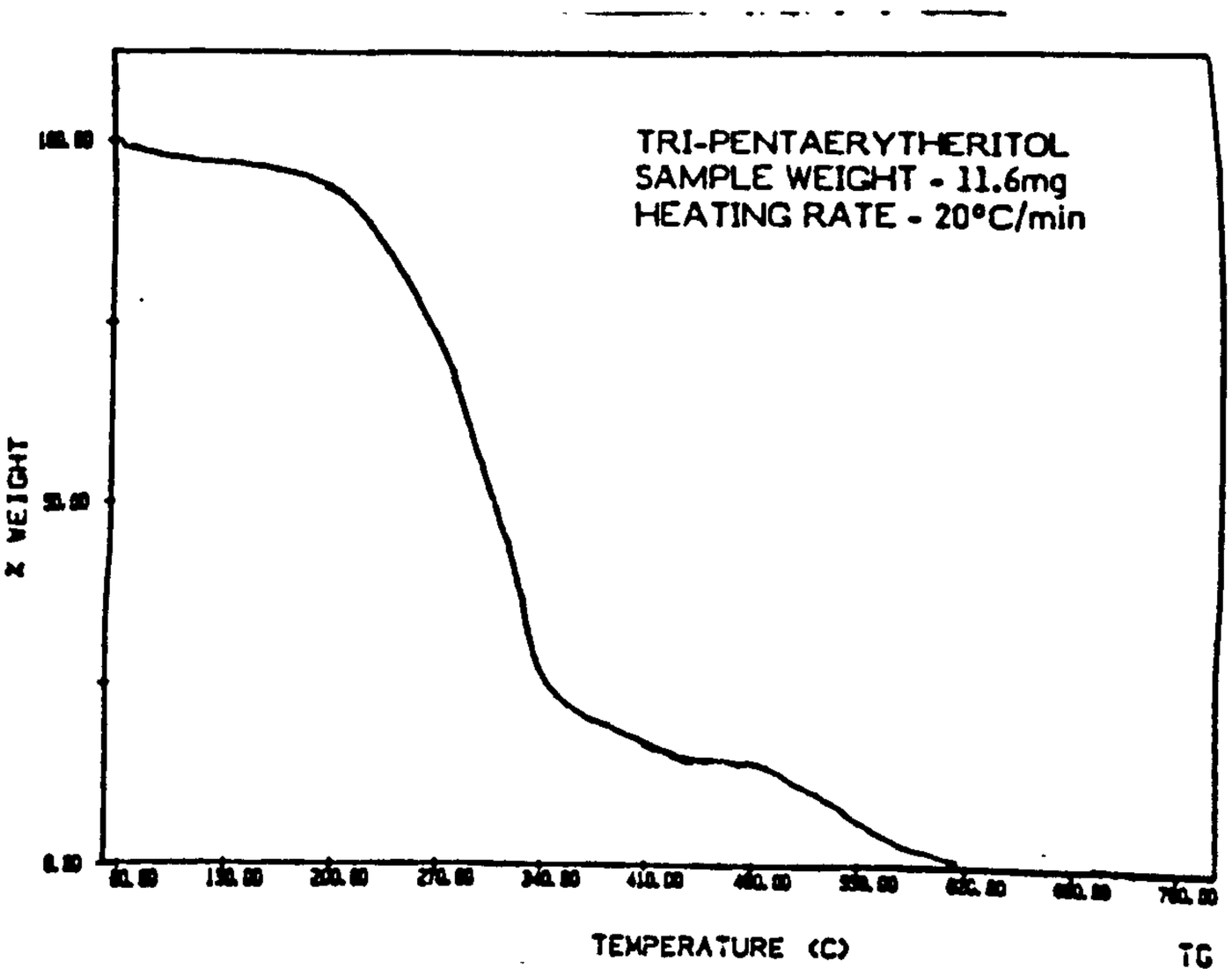

3) Blowing agents in large amounts have detrimental affects on the foam structure, in general resulting in a coarse foam structure which has poor strength and is fluffy, loose and friable, having poor adhesion to the substrate, Fig. 74A. Insufficient blowing agent resulted in poor foam height and a weak 'gooey' char which did however have good adhesion to the substrate.

4) Increasing the binder level to in excess of 20% reduced the foam height.

5) The inclusion of water-producing ingredients such as alumina trihydrate deactivated the system, producing little foam. This may be due to the dilution of the acid produced by the catalyst.

6) Titanium dioxide was used as the pigment. Although theoretically it should be inert in nature, in practice it was found to be beneficial when used in low quantities. The cell structure resulting from foams with titanium show a significant improvement, Fig. 74B and 74C. Excessive use of titanium dioxide resulted in adverse foam characteristics.

FIGURE 74A

PHOTOGRAPH SHOWING THE EFFECT OF EXCESSIVE SPUMIFIC

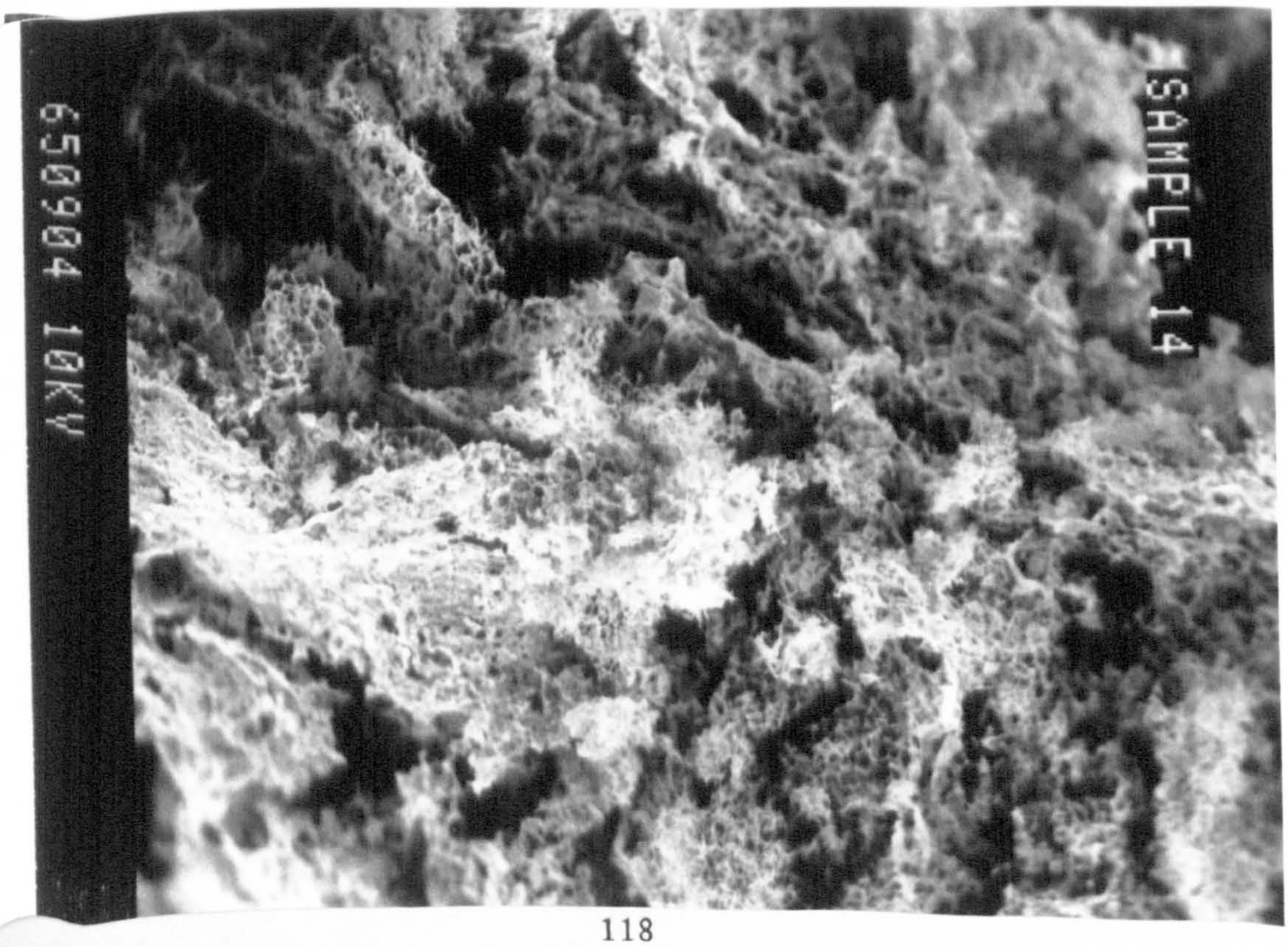

FIGURE 74B

IMPROVED CELL STRUCTURE WITH USE OF TITANIUM DIOXIDE

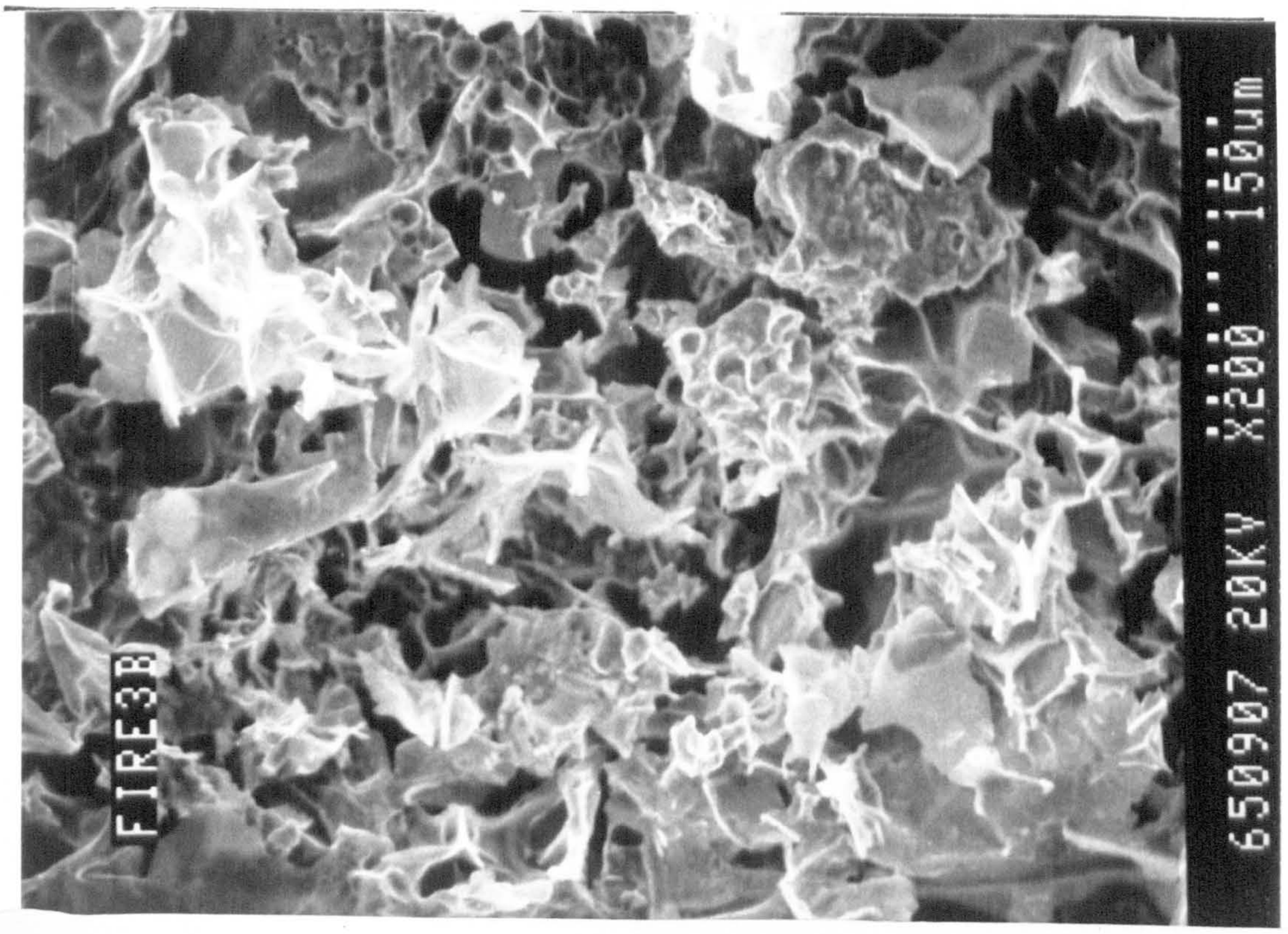

FIGURE 74C

MAPPING FOR TITANIUM

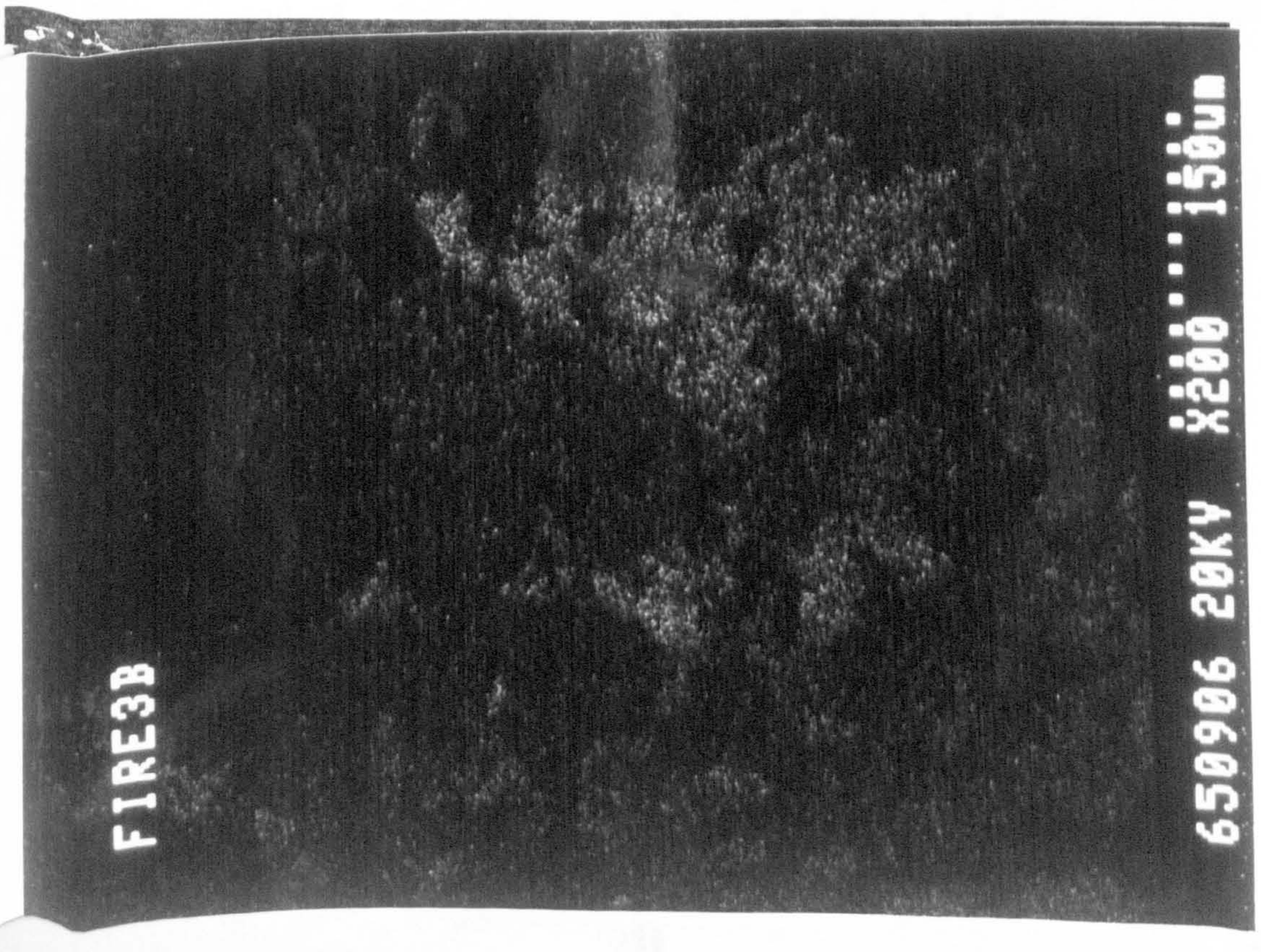

6.7.1. DEVELOPMENT OF FOAM CHARACTERISTICS (KD 8 - KD 17)

The improved formulation which was developed, as given in Section 6.6, had good foam height, adequate cell structure and was able to withstand exposure to temperatures in excess of 800°C. The next aim was to improve the foam characteristics such as, foam strength, density and integrity. The foams should hold their structure and integrity even after extensive exposure to temperatures and heat fluxes normally encountered in fire tests such as BS 476 : Part 7 : 1971 (Surface Spread of Flame) and BS 476 : Part 8 (Fire Resistance Test) or the Hydrocarbon Furnace Test where the temperatures can exceed 1100°C and the heat fluxes may be in excess of 130 kW/m^2.

A number of binders such as vinyl toluene/butadene copolymer resin (Pliolite VT), chlorinated rubber (e.g. Parlon S-10 ; Parlon S16; Alloprene R20), vinyl toluene acrylic co-polymer (VTACL), and many others, were examined. Thermo analytical data was used to select compatible and most suitable ingredients to produce the maximum intumescence effect, Figs. 75 and 76. For example mixtures of individual ingredients and a binder, and the combination of different spumifics and a binder were examined. Other paint characteristics such as viscosity and spreadability are also dependent on the binder used. Thickening agents and dispersants were required in some cases. It was found that each binder required a quite different formulation in order to achieve the best characteristics. In general the intumescence level was found to be inversely proportional to the level of the binder.

As a summary of this set of formulations, the following produced good end-results:

TABLE

6.7.2. FORMULATION KD 17

	% by weight
Alloprene R20	20.0
C70	2.3
C42	3.0
APP	25.0
TiO_2	5.0
Tripentaerythritol	15.0
Dicyandiamide	4.7
Thixomen	3.0 (dispersant)
Toluene	22.0

TSC % - 68 Viscosity 4/12 - 55 Pa.s

(Toluene level can be varied to give the necessary viscosity and paint characteristics). The foam produced had a reasonable structure and a height of at least 25mm (original coating thickness of 1mm).

6.7.3. SUMMARY OF THE RESULTS FOR IMPROVED FOAM CHARACTERISTICS (KD 18 - KD 20)

The following observations were made:

1) The foam height, cell structure and strength were better than attained by previous formulations, Fig. .

2) An increased amount of catalyst was required to produce the same foam height as KD/7.

3) The increased proportion of binder used produced good adhesion of the foam to substrate.

4) The spumific system developed, Fig , produced foams with good foam height. By increasing the amount of DCA in the system, it was possible to achieve coatings with intumesced foam heights in excess of 50mm. However, these foams lacked strength.

5) It was found necessary to add a dispersant to break down the agglomerates. This imparted some gloss to the coating surface and reduced the mixing time required significantly.

6) The binder level was increased to enable a higher proportion of

titanium dioxide to be used which improved the fire performance observed. This may be due to the titanium dioxide acting as a heat reflector at high temperatures.

FIGURE 75 AND 76

TYPICAL STA CURVES FOR THE COMBINATION OF THE CARBONIFIC AND THE SPUMIFIC PLUS THE BINDER SYSTEM

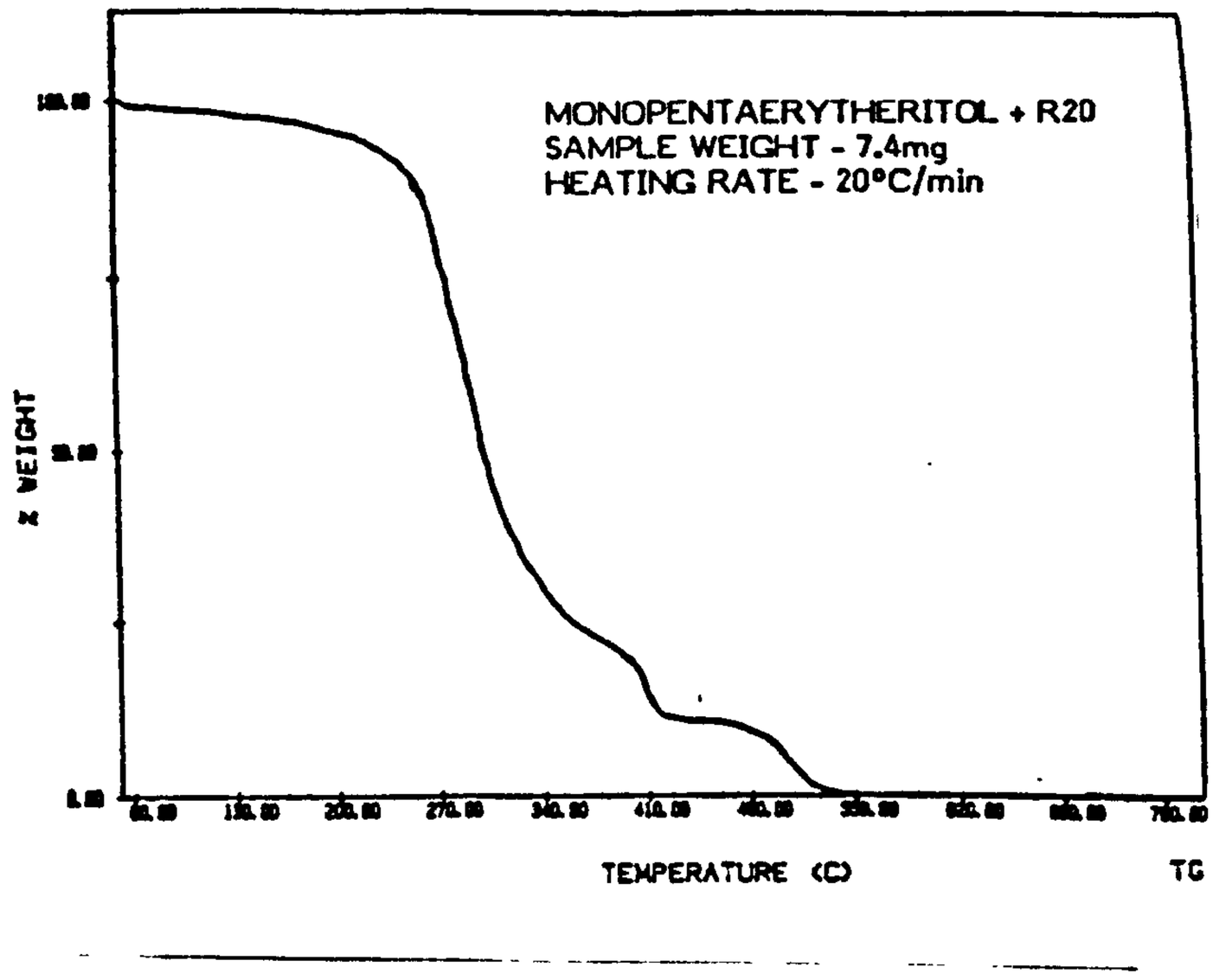

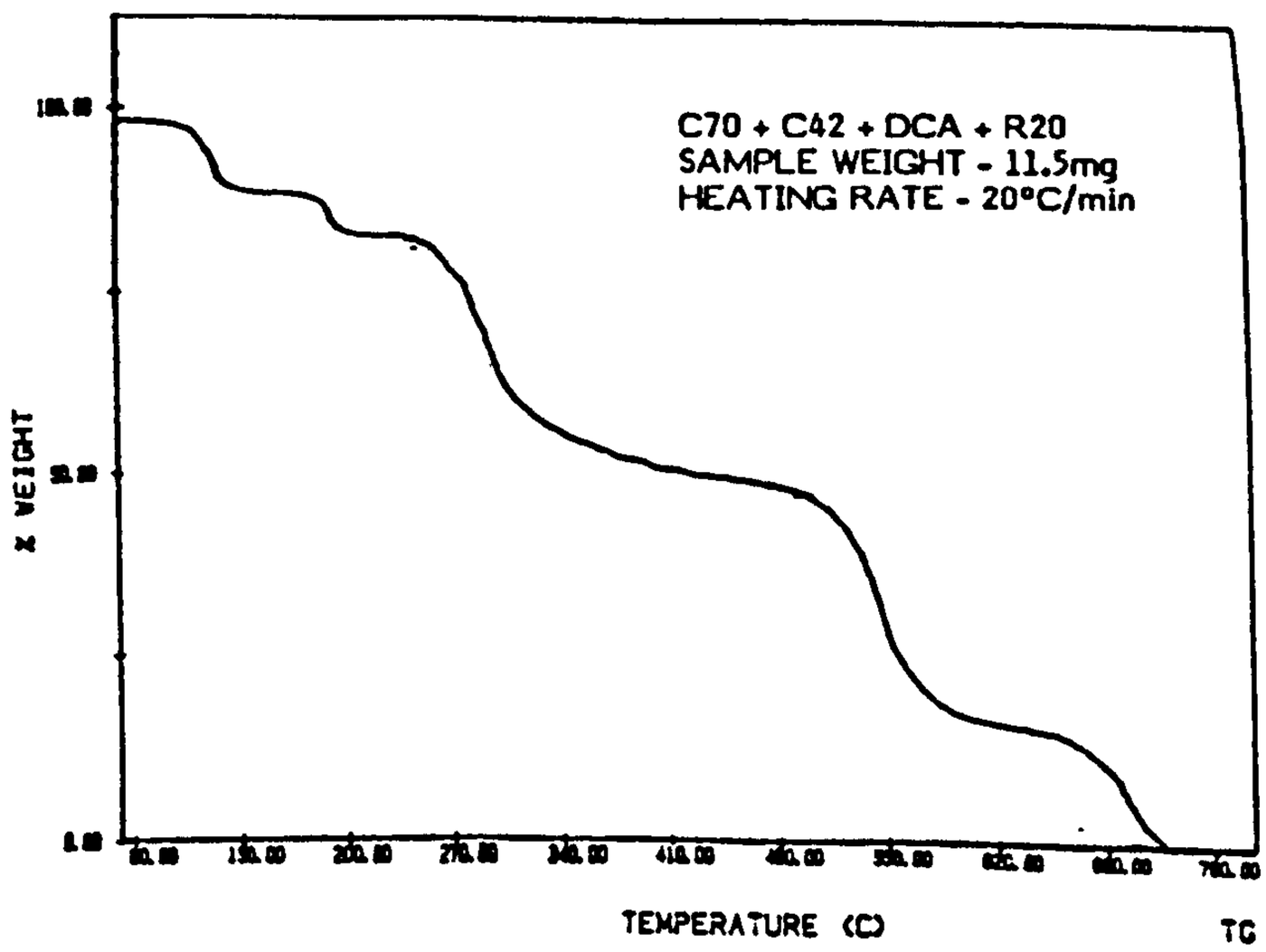

FIG 77

PHOTOGRAPH SHOWING IMPROVED CELL STRUCTURE

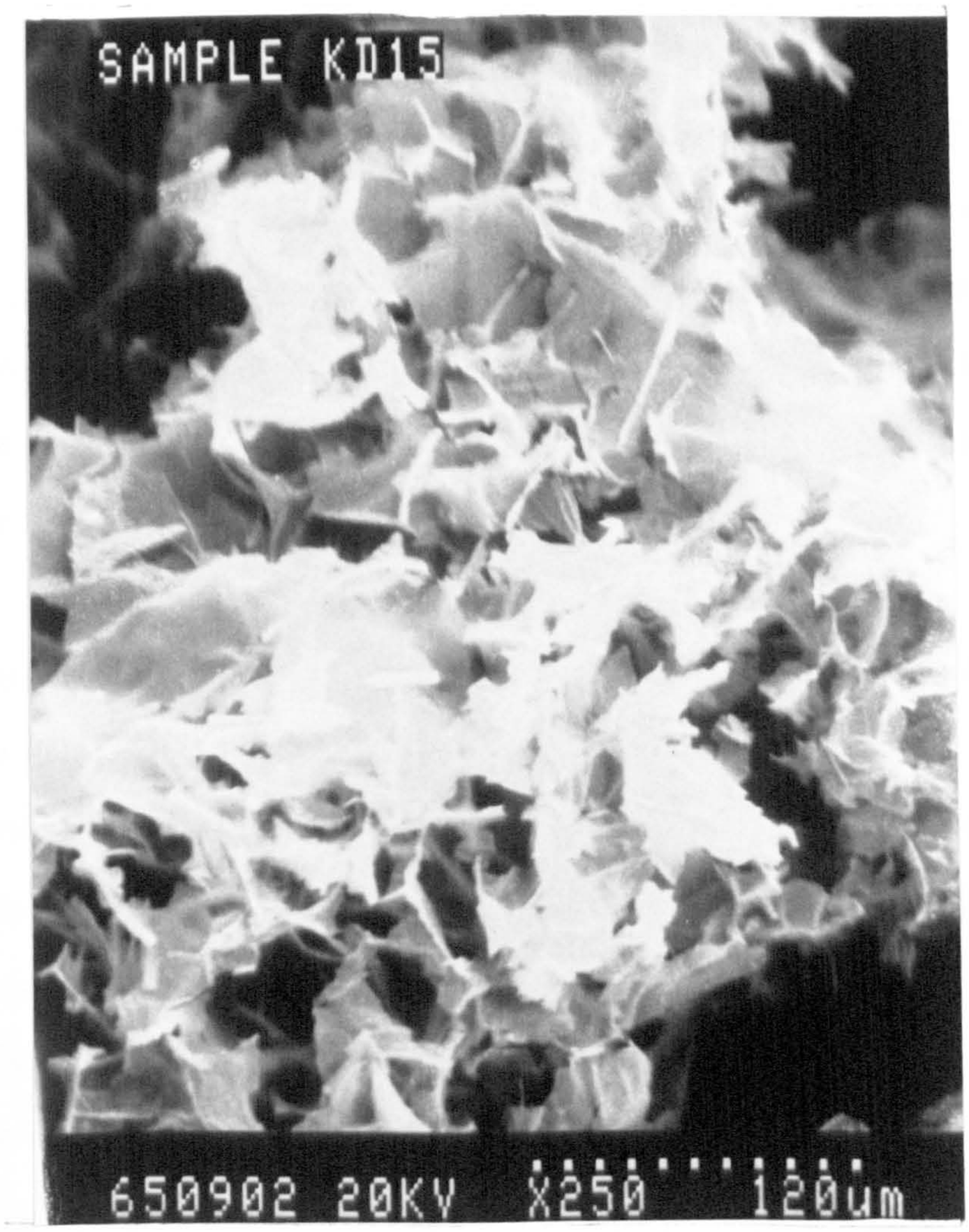

6.8.1. DEVELOPMENT OF A CHAR WITH IMPROVED PHYSICAL PROPERTIES (KD 18 - KD 20)

The formulation KD 17 developed in Section 6.7 was found to be suitable for applications of up to 1000°C for a limited period of time (e.g. 1 min). The formulation was considered adequate for protection of timber products and for less arduous applications. Since timber materials are normally only tested for surface spread of flame, the fire protection paints do not have to meet stringent requirements. For applications to steel and thin non-combustible building materials, further improvements in char properties were required to avoid the erosion which may occur in the test furnace due to the positive pressure exerted by the burning gases. The poor strength and adhesive properties of the currently-available

commercial coatings are a major drawback in achieving fire-resistance much in excess of one hour. In the new European fire tests currently being drawn up, the possibility of a specification relating to the ability of the intumesced foam to withstand hosing down is being considered - this is already a requirement of the French test. This would require the foams to have not only good thermal shock properties, adhesion and fire-resistance in excess of one hour, but also excellent strength after exposure to high temperatures.

To improve the foam strength, inorganic materials stable at high temperatures such as melamine phosphate were examined. Various proportions of the following ingredients were examined: zinc borate / sodium borate; magnesium silicate; zinc oxide; lead sulphate; lead carbonate; lead oxide;calcium silicate; borax; cerium and rare metal oxides; molybdenum oxide; fumed silica; titanium dioxide and fumed titanium dioxide; ferric oxide; various ceramic materials and mixtures of the above ingredients.

All the above ingredients resulted in some improvement in the properties of the foam char. The strength was greatly improved, in some cases by a tenfold factor. Also, the foam was not prone to damage even when pushed with a rod.

Increasing the amounts of the inorganic ingredients generally reduced the foam height observed. Usually, an improvement in one property was observed to be at the expense of another. The foam height was considered to be an important criterion (a minimum of 200% expansion was sought) and also a small closed-cell structure was preferred, Fig. 82. The addition of molybdenum oxide and other rare metal oxides (cerium

oxide in particular) greatly reduced the smoke emission and also contributed to the char strength. Calcium silicate and sodium borate were found to produce a glassy surface which resisted oxidation. A mixture of lead carbonate and lead oxide was found to enhance char strength and result in a good foam structure. However, due to the toxicity of lead, it was considered unsuitable. Fumed silica was found to be very advantageous -it reduced the tendency of the foam to 'slump' and again improved the foam structure. Melamine borate also produced similar results.

6.8.2.1. FORMULATION KD 20

The following formulation was tested in a full-scale fire test. It produced a very good fire performance in comparison to currently-available coatings.

TABLE 11

FORMULATION KD 20

	% by weight
PVC TYPE BINDER	7
C70	4.0
Tripentaerythritol	15
Dicyandiamide	10
P 30	30
Melamine	4.0
Zinc/melamine borate	15
Magnesium silicate	10
TiO_2/fumed silica	5

Toluene was added as required in order to give good viscosity characteristics.

Figures 78-81 give thermal data results for the above formulation.

FIGURE 78

STA CURVE FOR FORMULATION KD 20 AT HEATING RATE OF 4°C/min

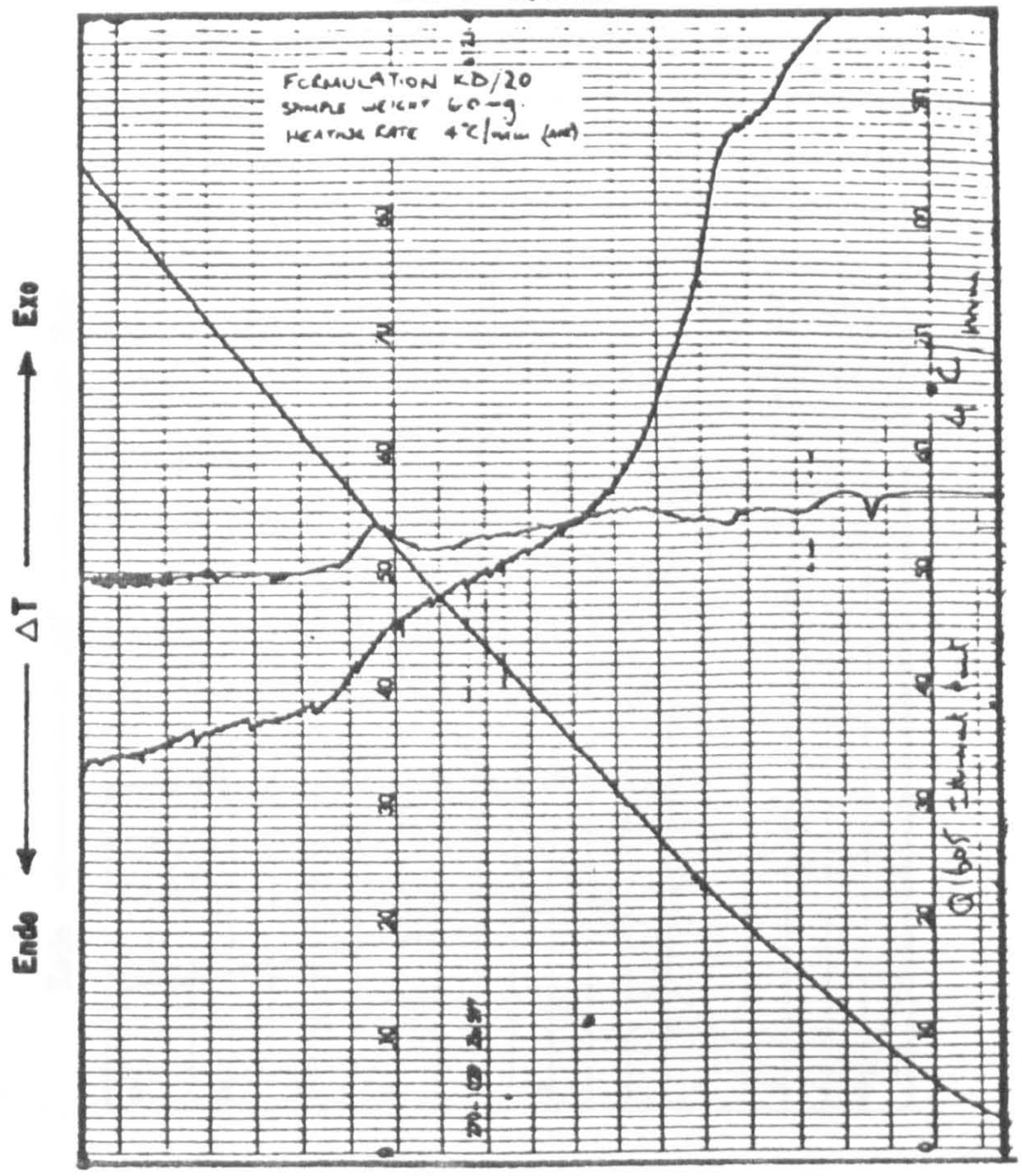

FIGURE 79

STA CURVE FOR FORMULATION KD 20 AT HEATING RATE OF 10°C/min

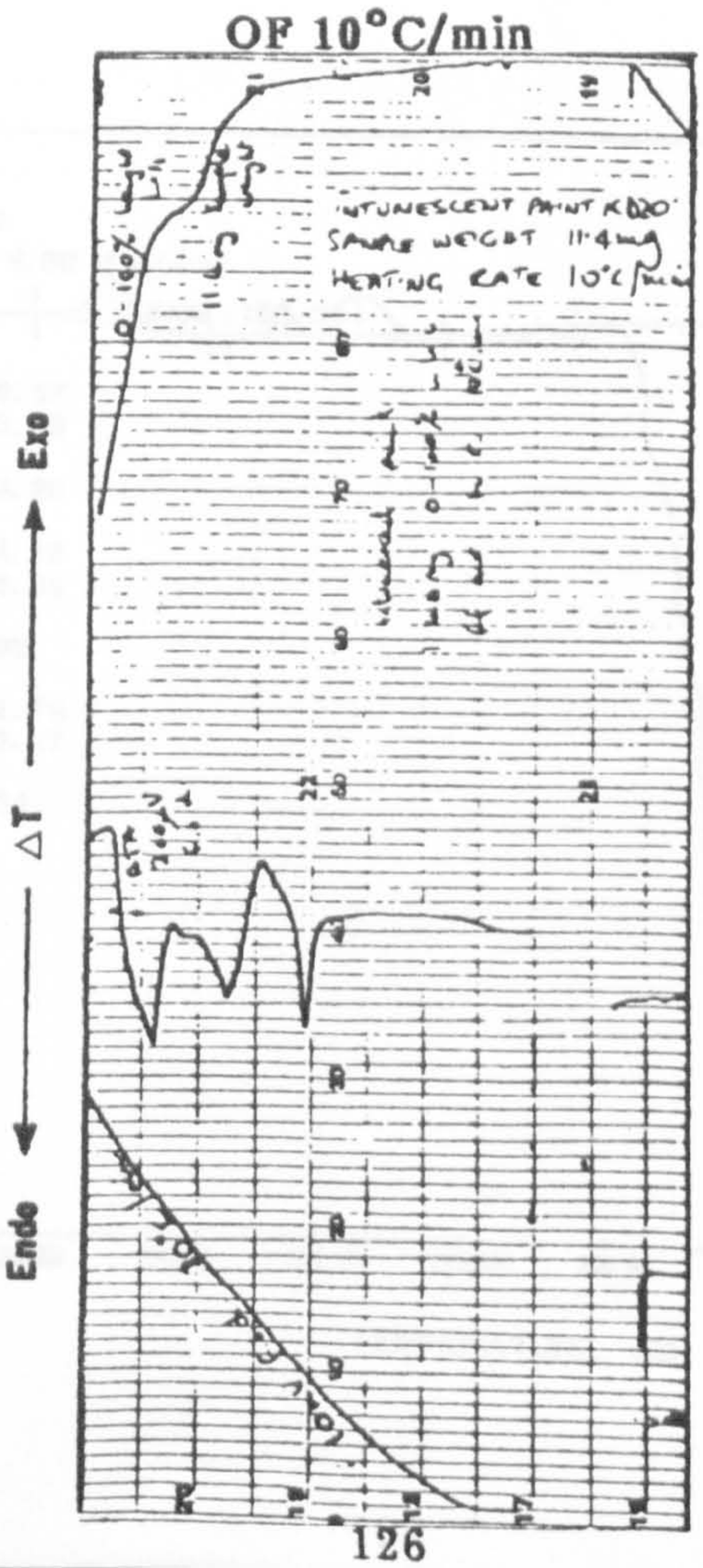

FIGURE 80

STA CURVE FOR FORMULATION KD 20 AT HEATING RATE OF 20°C/min

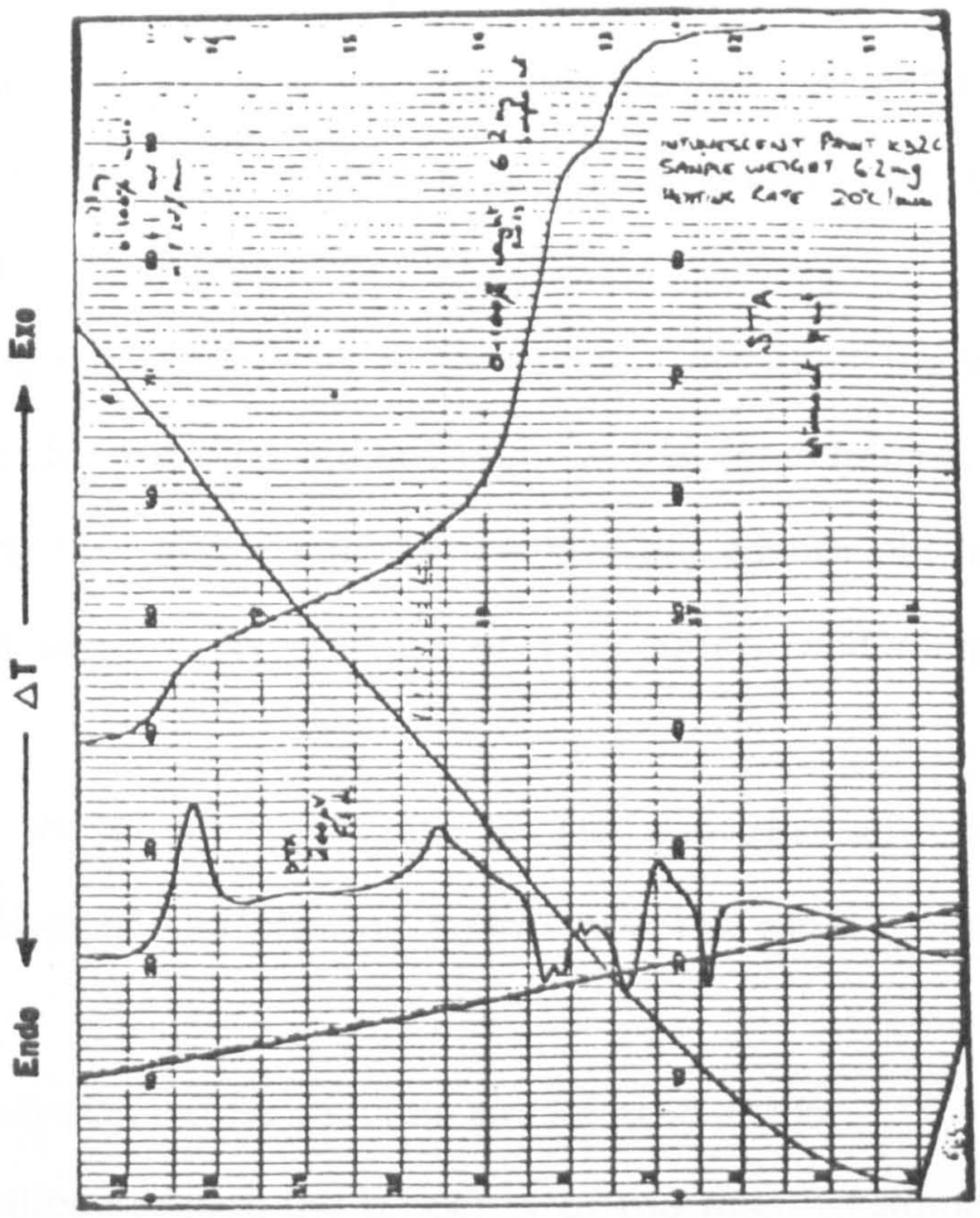

FIGURE 81

DSC CURVE FOR FORMULATION KD 20

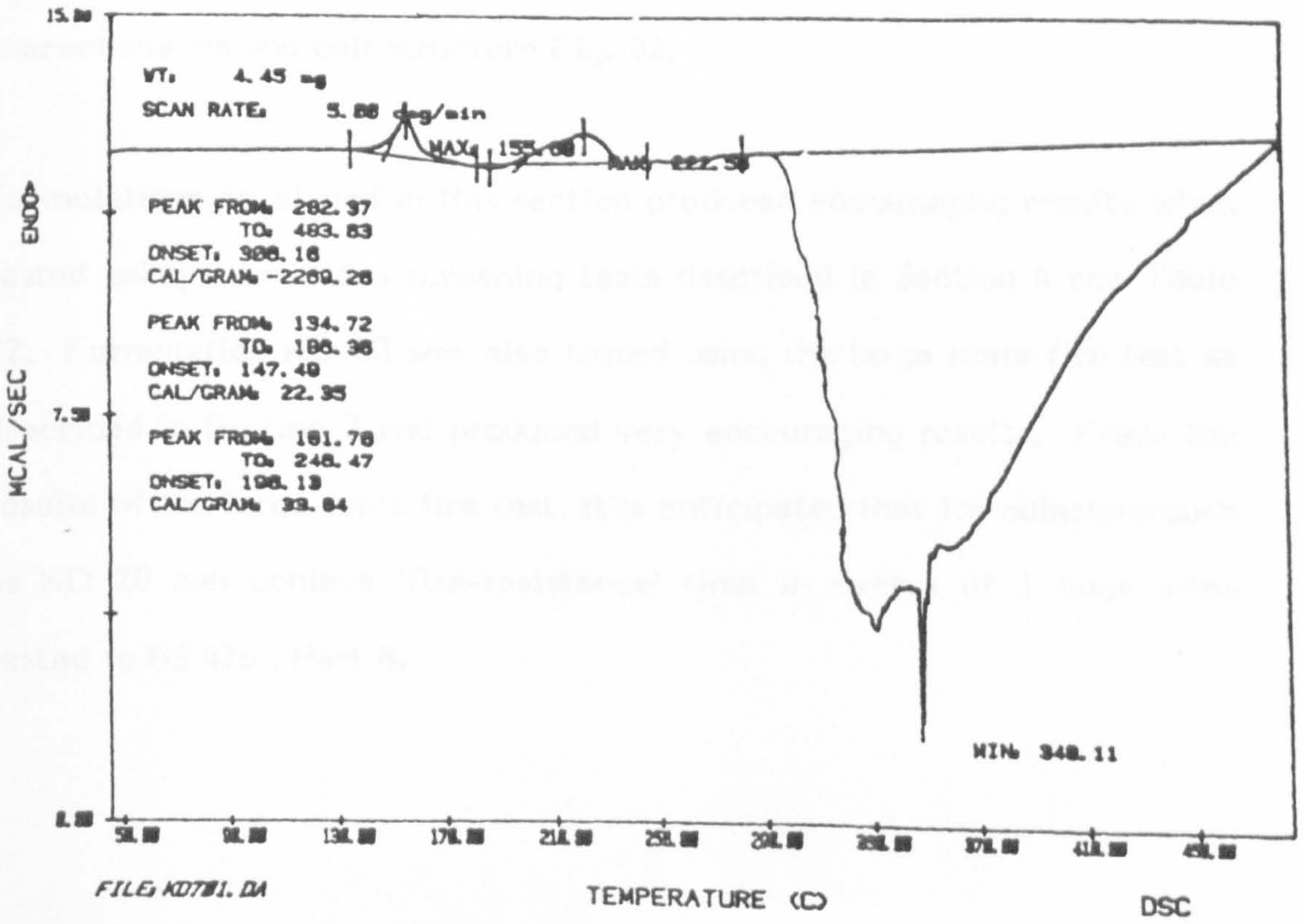

6.8.3. SUMMARY OF THE RESULTS

1) Zinc borate helps the char strength.

2) Magnesium silicate helps the char strength but reduces foam height.

3) A mixture of both produced a very crusty foam, but greatly reduced foam height.

4) Increasing the proportion of the binder improved the adhesion of the foam to the substrate but did not improve the foam height.

5) Increasing the proportions of the blowing agents did not improve the foam height when a 1:1 mixture of zinc borate and magnesium silicate was used.

6) Keeping the amounts of zinc borate and zinc silicate constant and increasing that of the blowing agents and the binder, reduced the foam strength.

7) The rare metal oxides reduced smoke production.

8) Fumed silica reduced the tendency of the foam to slump.

9) Melamine borate produced overall improvements in the foam characteristics.

10) The use of melamine phosphate as a catalyst produced better foam characteristics and cell structure Fig. 82.

Formulations developed in this section produced encouraging results when tested using the various screening tests described in Section 4 see Table 12. Formulation KD 20 was also tested using the large scale fire test as described in Section 7 and produced very encouraging results. From the results of the large scale fire test, it is anticipated that formulations such as KD 20 can achieve 'fire-resistance' time in excess of 1 hour when tested to BS 476 : Part 8.

FIGURE 82

TYPICAL EM PHOTOGRAPHS SHOWING THE DIFFERENCE IN THE CELL STRUCTURE OF FOAMS BASED UPON APP AND MELAMINE PHOSPHATE

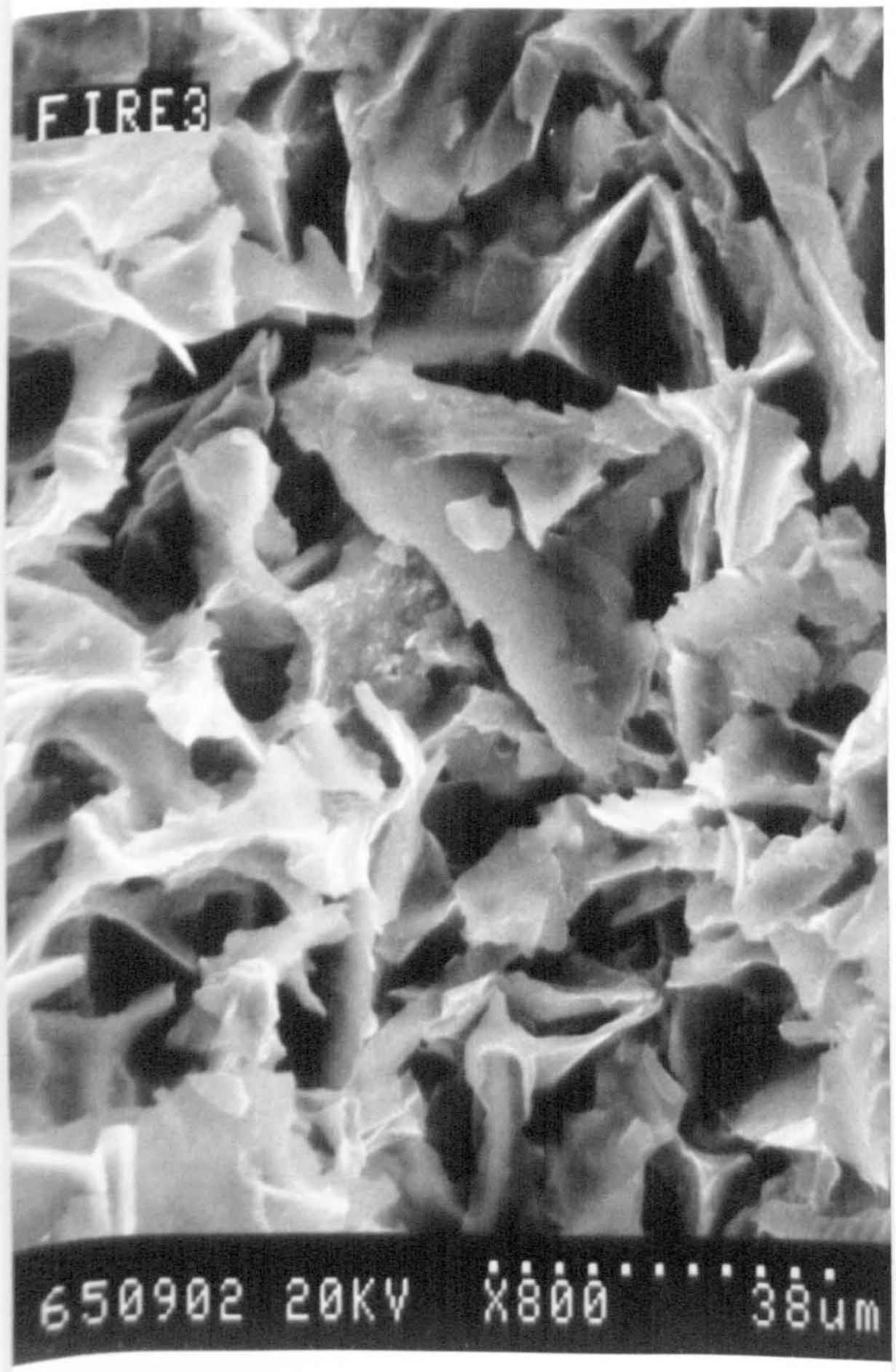

AMMONIUM POLYPHOSPHATE

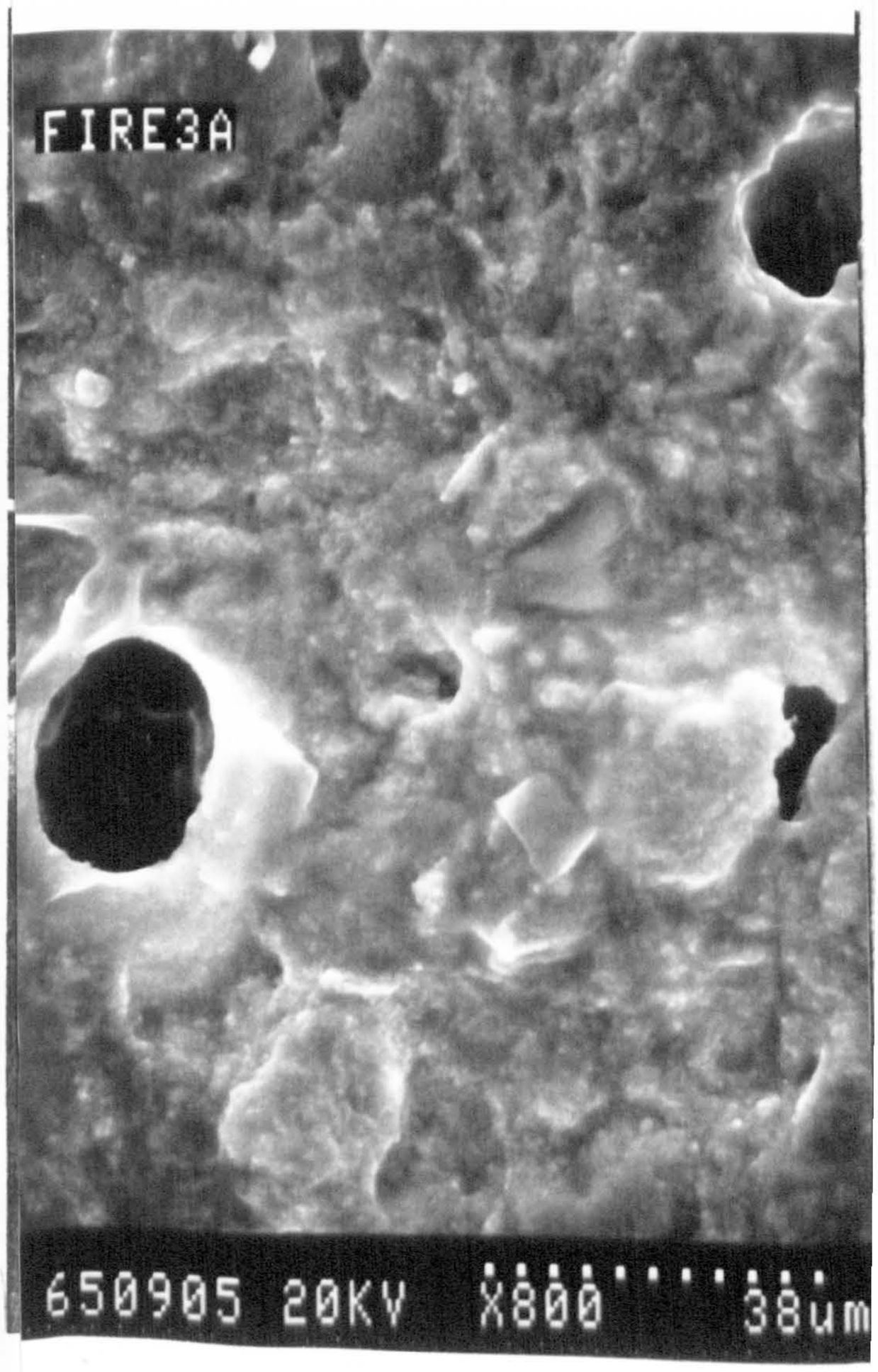

MELAMINE PHOSPHATE

6.9. EVALUATION OF EPOXY RESINS (KD 21 - KD 22)

The use of various epoxy resins cured with an amine-containing curing agent such as 2, 4, 6-Tri (dimethylaminomethyl) phenol were evaluated using a number of typical formulations (e.g. KD 7 and KD 20 - zinc borate/silicate mixture) and in general coating properties were greatly improved, very hard, glossy surfaces being produced. Initial results suggested that although the epoxy resins improve the properties significantly at levels above 15%, they reduced the foam height significantly. At levels above 5%, epoxy resins were difficult to cure and generally resulted in peeling of the coating. However, the char strength was significantly improved, at even a 3% level.

FIGURE 83

A TYPICAL INFRARED ABSORPTION CURVE OF EPOXY RESIN

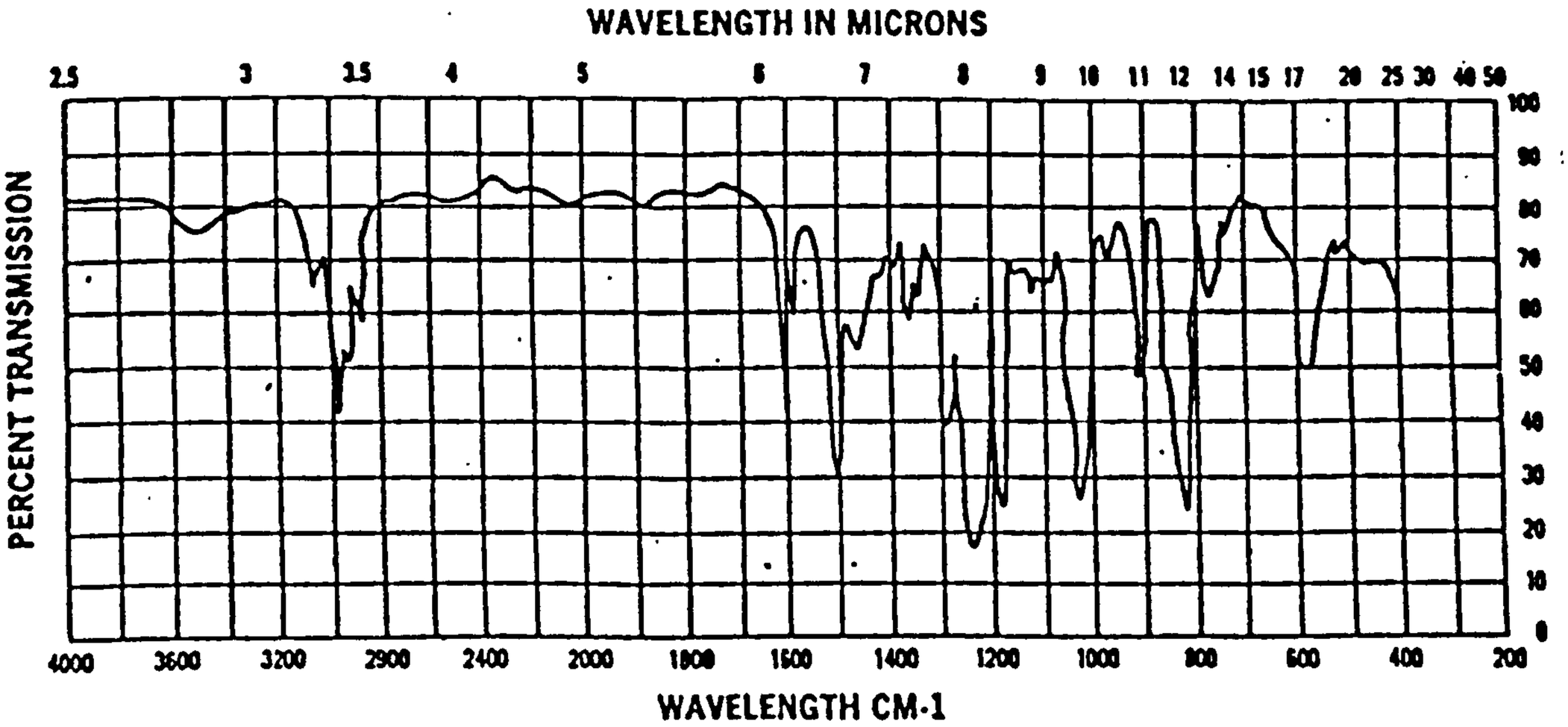

FIGURE 84

A TYPICAL INFRARED ABSORPTION CURVE FOR

2,4,6-TRI (DIMETHYLAMINOMETHYL) PHENOL

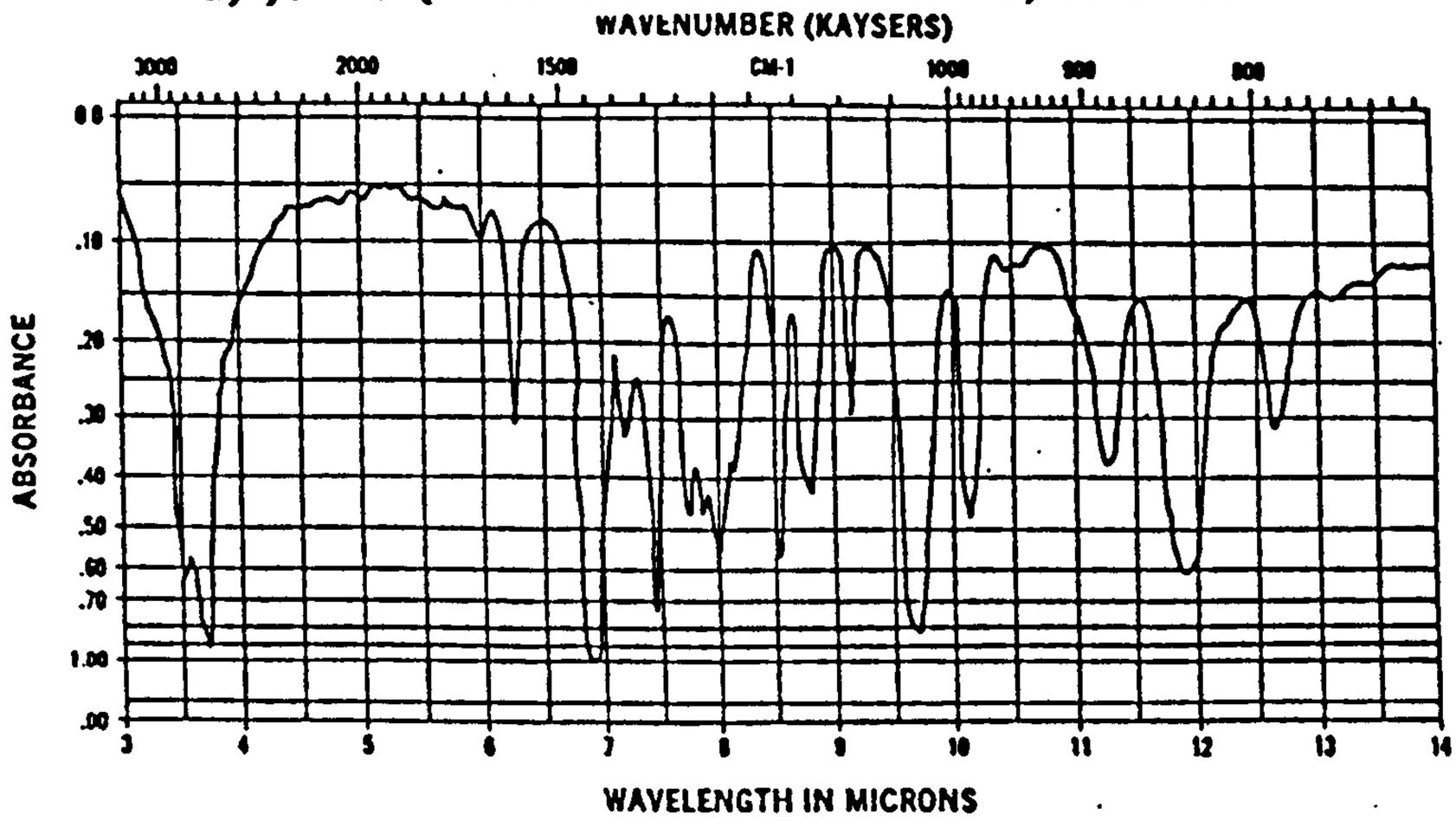

6.10. EVALUATION OF POLYSULPHIDES AND BLENDS WITH EPOXY RESIN

Polysulphides were found to be most beneficial in achieving good foam height. They made the coating more flexible, thus preventing any crazing or surface cracking. The inclusion of polysulphides in the formulation also produced a softer, more adhesive char. Some of the formulations developed were tested in a large-scale fire test. They produced excellent results compared with the commercially-available products.

FIGURE 85

A TYPICAL INFRARED ABSORPTION CURVE FOR POLYSULPHIDE POLYMER

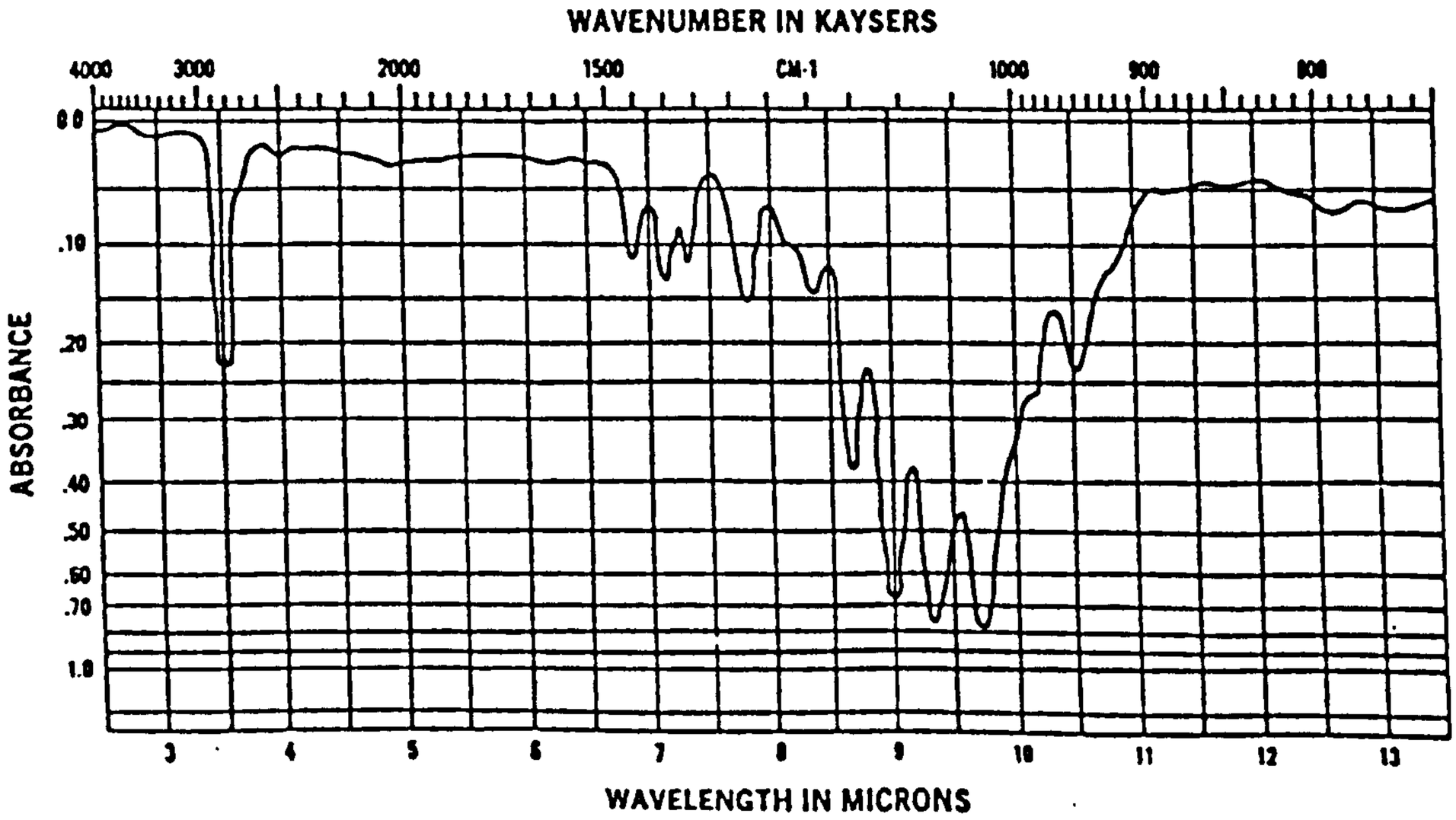

FIGURE 86

A TYPICAL TGA CURVE FOR EPOXY BASED FORMULATION

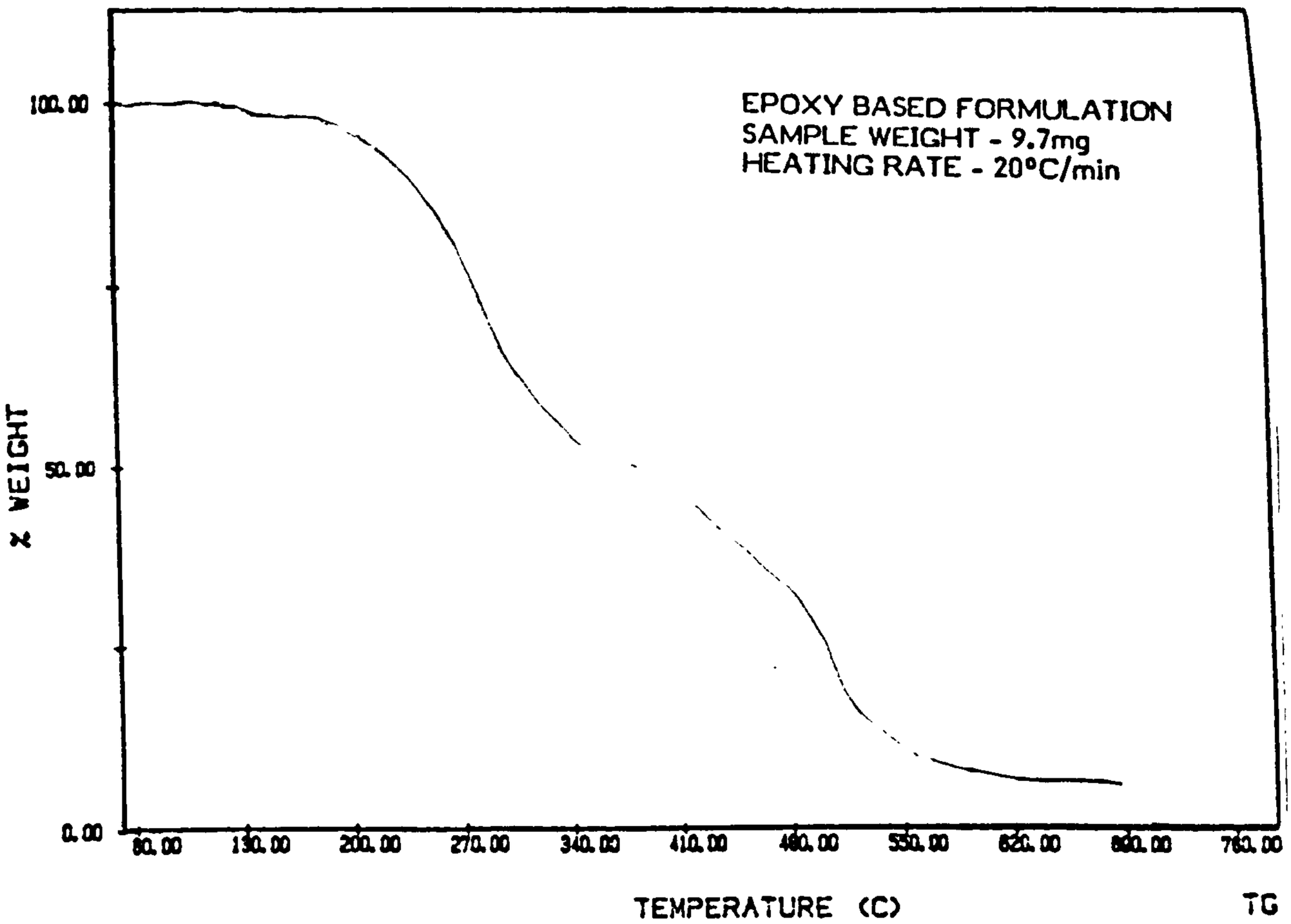

FIGURE 87

TGA CURVE FOR THE CONTROL SAMPLE USED IN THE LARGE SCALE FIRE TEST

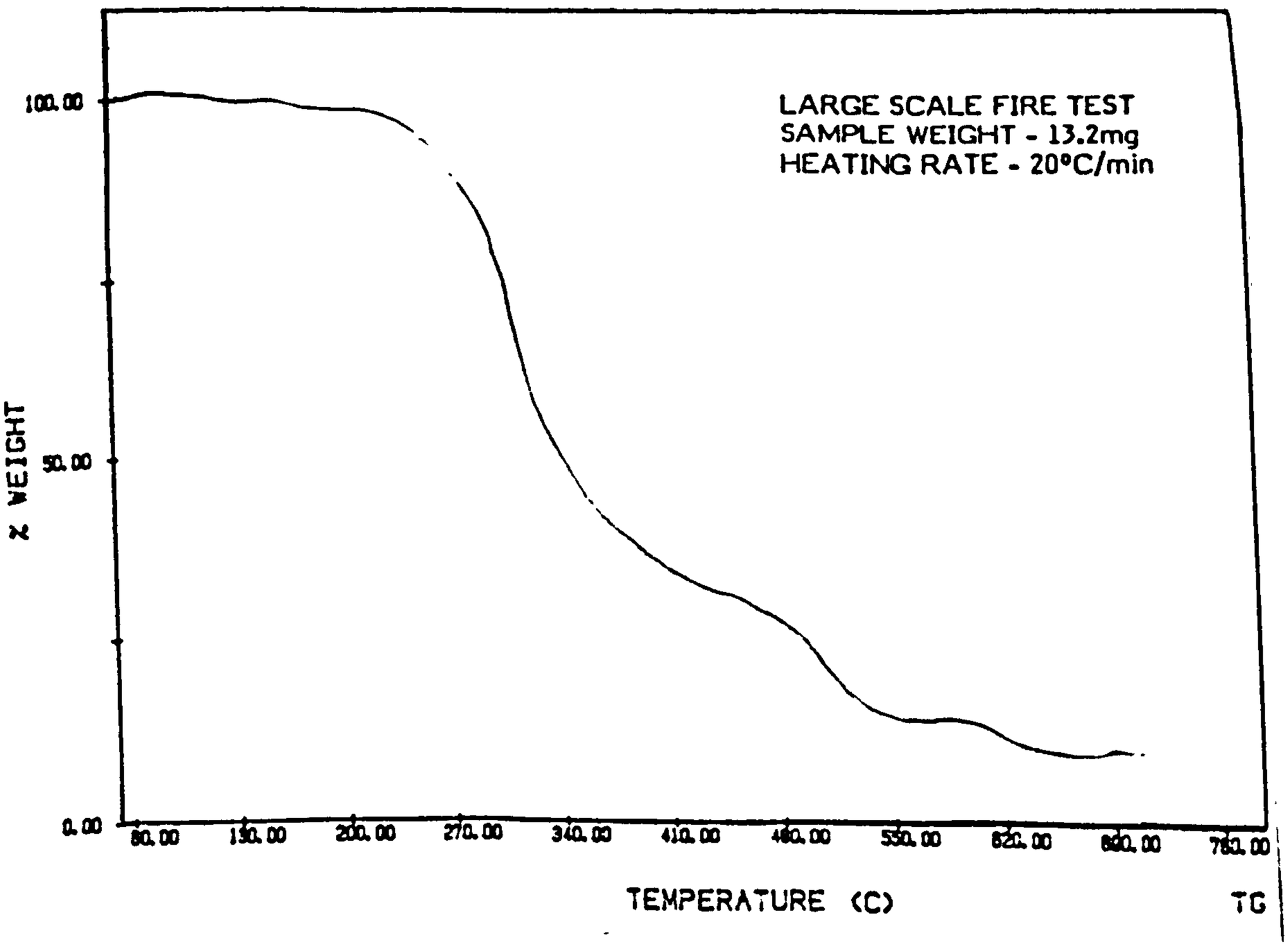

6.11. DEVELOPMENT OF THE FORMULATION FOR THE MODELLING EXPERIMENTS

Various formulations and their combinations were evaluated for their performance using the screening methods described in Section 4. Thermal analysis data was used to develop the final formulation with the necessary physical properties and a formulation which produced maximum height after exposure to various heat radiations. The coated steel plates were tested using the semi-controlled test method of NBS smoke density apparatus heater test method as described in Section 4. Figures 88-91 give a typical example of use of TGA analysis data for the optimisation of the spumific for the final formulation.

FIGURE 88

TGA CURVE FOR FORMULATION KD 22 USING 5% MELAMINE AS A SPUMIFIC

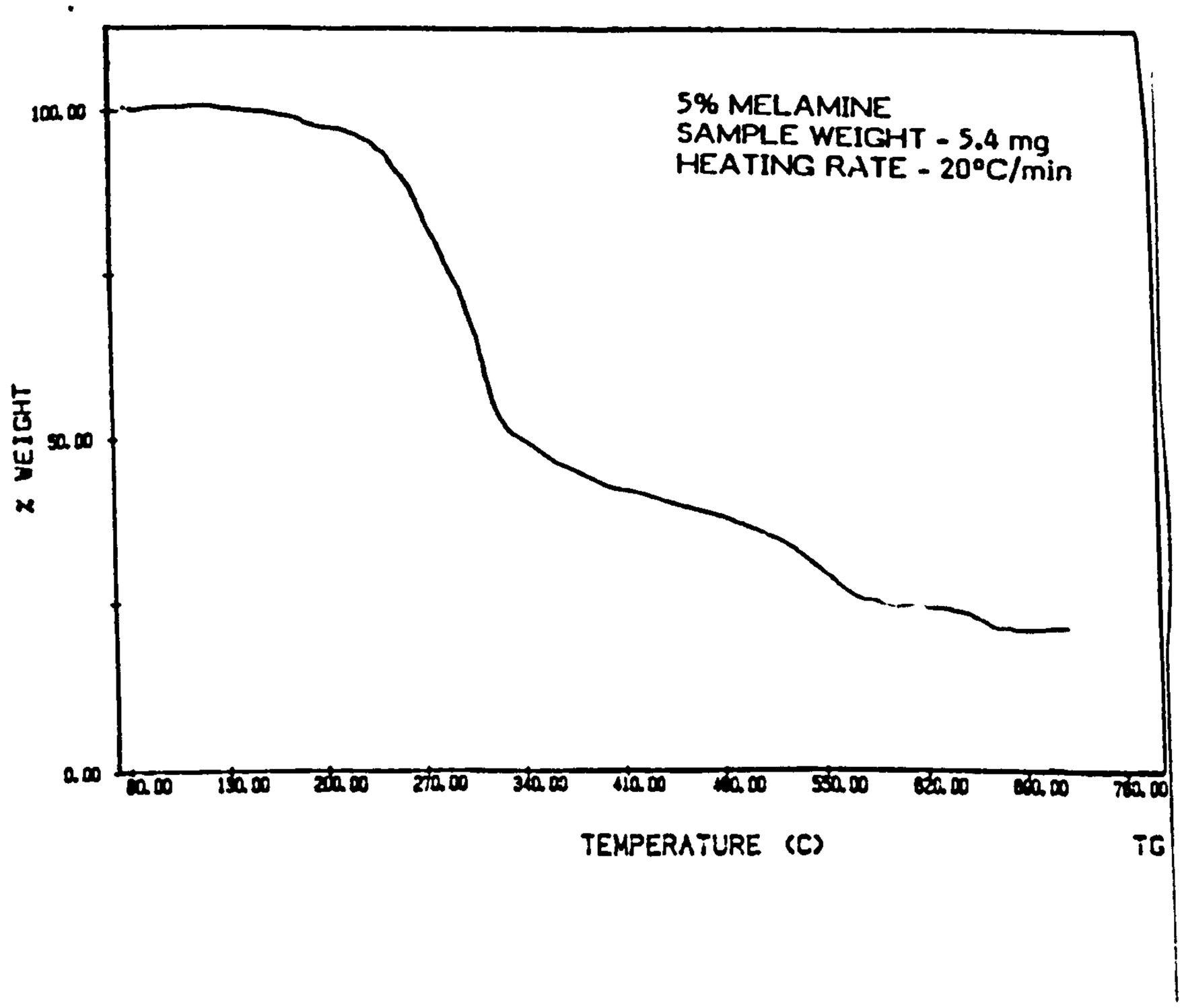

FIGURE 89

TGA CURVE FOR FORMULATION KD 22 USING 10% MELAMINE AS A SPUMIFIC

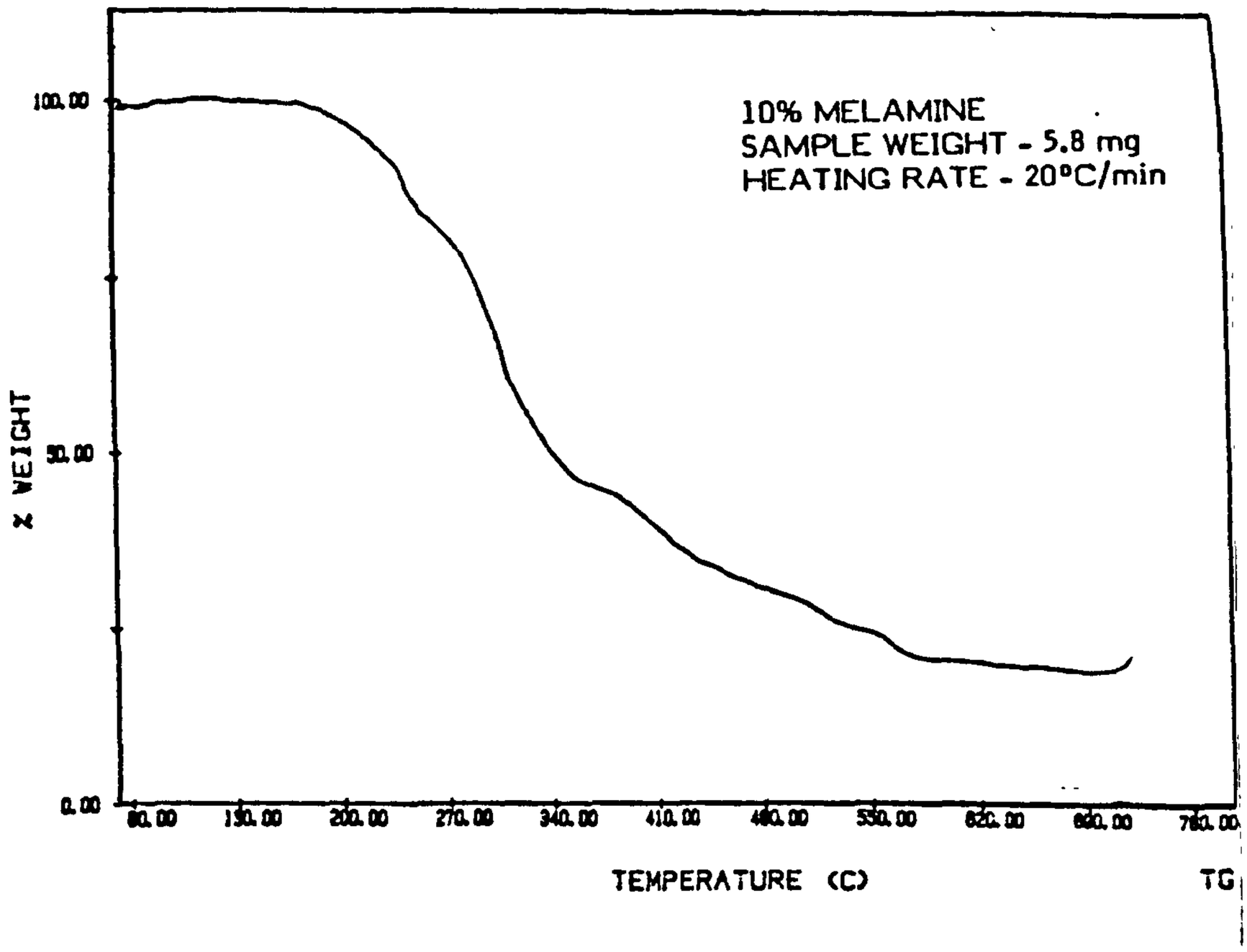

FIGURE 90

TGA CURVE FOR FORMULATION KD 22 USING 15% MELAMINE AS A SPUMIFIC

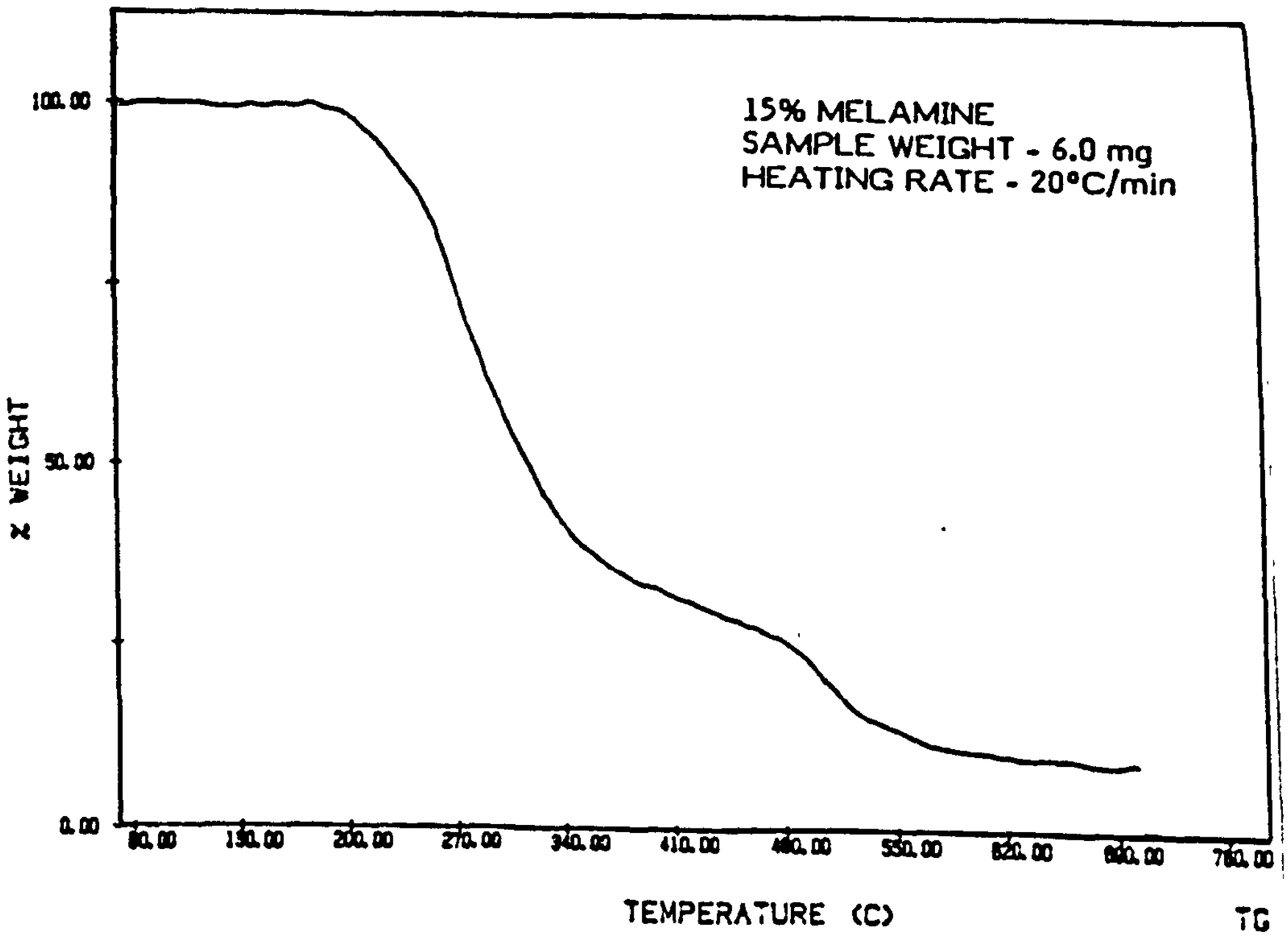

FIGURE 91

TYPICAL TGA CURVE FOR THE OPTIMISATION OF THE FINAL FORMULATION KD 23

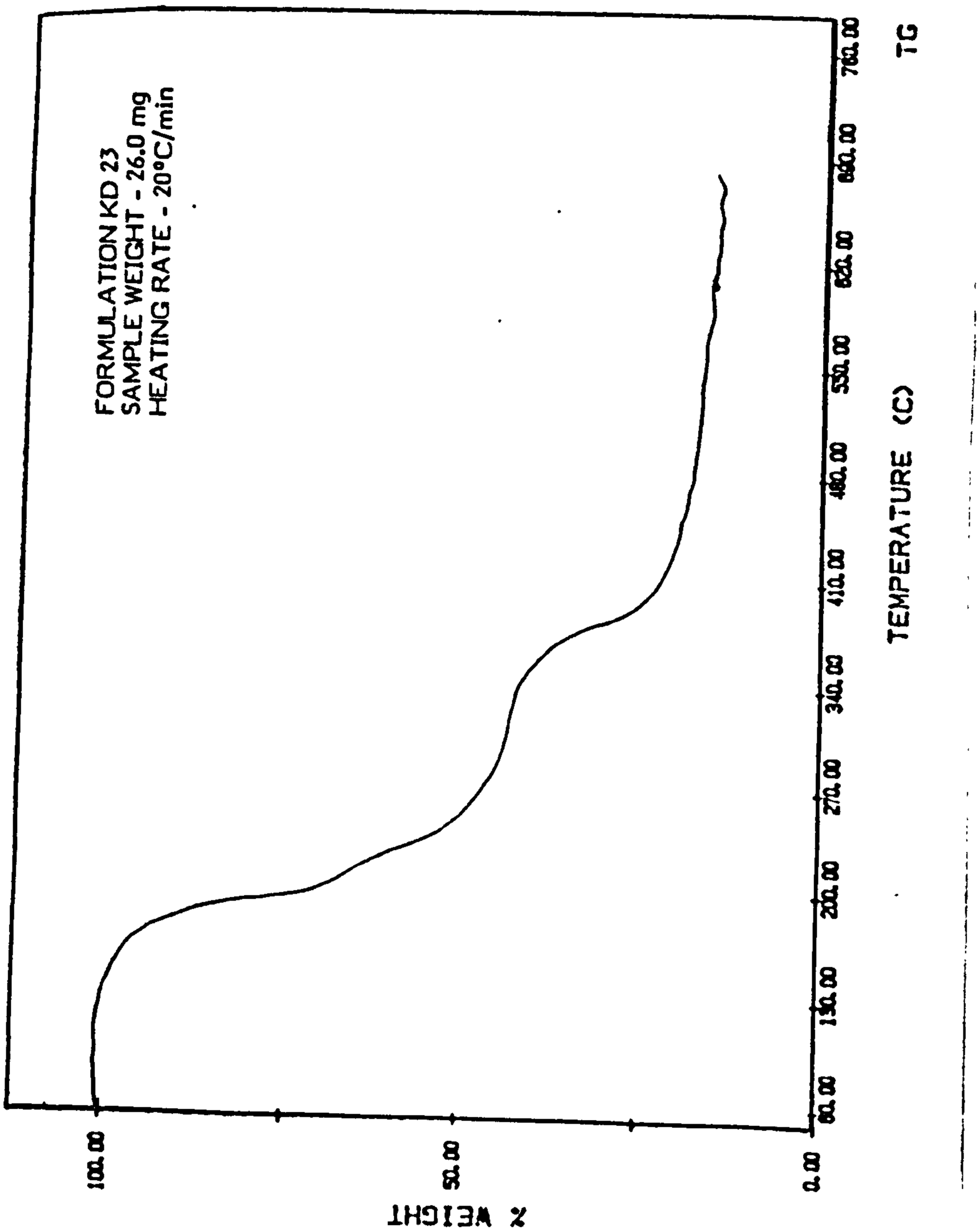

Formulation No.	Typical Expansion Ratio	Time to 300°C Simple Screening Test (Min)	Time to 450°C Muffle Furnace Test (Min)	Time to Ignition in ISO Ignitability (50 W/M²) Test (Secs)	Cell Structure *	Foam Strength **	Adhesion of the Charred Foam to Plate ***
KD1	6.5	1.50	2.20	17	2	1-2	1-2
KD2	4.8	1.35	2.00	15	1	1-2	1
KD3	5.2	1.40		18	3	2-3	2
KD4	14.8	3.50	3.50	Flashes only	2	2-3	1
KD5	12.6	2.40	3.20	25	3	3-4	1
KD6	20.5	5.10	5.00	-	4-5	3	1-2
KD7	21.0	5.30	4.75	-	5	3-4	4
KD8	18.4	5.00	4.95	-	3	3	3
KD9	26.0	6.00	7.00	-	3	2-3	2
KD10	17.5	4.30		30	4	2-3	2
KD11	29.5	6.15	10.00	-	4	2	1-2
KD12	16.0	5.12	8.60	-	3-4	2	1-2
KD13	18.3	5.00	7.30	Some Flashes	2	2-3	2
KD14	16.3	4.30	8.20	-	4	3-4	2
KD15	15.0	3.00	5.00	-	4	2-3	3
KD16	18.0	4.75	6.60	-	3	3-4	3
KD17	20.5	5.20	7.00	-	2-3	3-4	4-5
KD18	15.0	4.20	5.20	-	1-3	3-4	3-4
KD19	12.0	5.00	7.00	-	3	4-5	4
KD20	18.0	5.12	7.20	Some Flashes	4	4-5	4
KD21	10.0	4.12	4.30	Some Flashes	3	4-5	4-5
KD22/1	12.0	4.60	5.30	-	3	4-5	4-5
KD22/2	25	4.0	5.10		4	2-3	3-4
KD22/3	35	2.9	3.70		1-2	1-2	1

* Foam Strength
1) Fluffy/very weak
2) Weak
3) Crusty
4) Hard/crusty
5) Very hard

** Cell Structure
1) Very open
2) Coarse
3) Even but open
4) Even and fine
5) Even/regular and very fine

*** Adhesion of the charred foam to plate
1) Very easy to peel off or already delaminated
2) easy to peel but with less than 50% continuity of the unintumesced layer
3) char mainly in contact with the substrate
4) Char remaining in place by turning the sample plate upside down and gental tapping
5) char requiring a reasonable effort to remove using a scraper blade

TABLE 12

TEST DATA FOR THE FORMULATIONS

SECTION 7

7.1. LARGE-SCALE FIRE TEST

A natural fire test was carried out in the FRS hanger at RAF Cardington in order to study the behaviour of a number of intumescent fire protection systems in a real fire environment and to compare the formulations developed in the course of this research with the commercially-available materials.

A large compartment, measuring 8.6 m x 5.5 m x 3.9 m high, built by British Steel Corporation for the purposes of tesing unprotected steel beams and columns was used (Fig. 92). A mixed wood/polypropylene fuel was used with a fire load density of 20 kg/m^2 (360 MJ/m^2) and total fire load of 1330 kg timber equivalent (23900 MJ). The total internal area of the enclosure was 254 m^2.

7.2. SAMPLE PREPARATION

Steel plates 300 mm square and 15 mm thick were shot blasted using 1/4 sand grit. Chromel/Alumel (3mm diameter) type thermocouples with Inconel sheaths and insulated hot junctions were fixed to the back of the steel plates by drilling a hole 10mm long and inserting the thermocouple junction. A high-temperature epoxy was used to keep the thermocouple in position. The shot-blasted plates were coated with a standard zinc/chromium-rich primer coat and were allowed to dry for at least a week before further coating. Primed plates were brush coated with the test mixtures to the required thickness of approximately 1.2mm. The plates were allowed to dry between the coatings. The final coated plates were left to dry for at least 4 weeks before testing.

FIGURE 92

LARGE SCALE FIRE TEST RIG

The coated plates were placed in a specially-made box casing of 350 mm x 350 mm x 50 mm dimensions. The casing box was made of ceramic-type fibre-board nailed together. Ceramic felt of 96 kg/cm^3 density was used to insulate the rear of the plates.

Four plates were prepared and coated as follows:

1) control plate coated with a well-known, commercially-available product with 'fire-resistance' time in excess of 1½ hours when tested to BS 476 : Part 8

2) formulation based on non-epoxy-type binder

3) formulation based on epoxy-type binder

4) formulation developed to achieve the maximum char strength and fire performance.

The plates were then placed in the test rig alongside 11 columns of 1.5 m lengths with column sections of 203 mm x 203 mm x 52 kg/m coated with various commercially-available intumescent paints, protected using passive fire-protection systems and an unprotected control column.

The column sections protected to a one-hour standard of fire resistance were covered with the following types of material:

1) column I - plasterboard

2) column V - non-asbestos board

3) columns S, U - thick-film intumescents

4) columns T, W, X, Y and Z - thin-film intumescents.

Commercial products were tested both to determine their individual performance and as controls for formulations prepared in the course of this study. It was found that the formulations of this study gave an equal or better performance than the commercial controls Table 18.

FIGURE 93

A VIEW OF THE TEST COLUMNS AND THE FUEL CRIBS

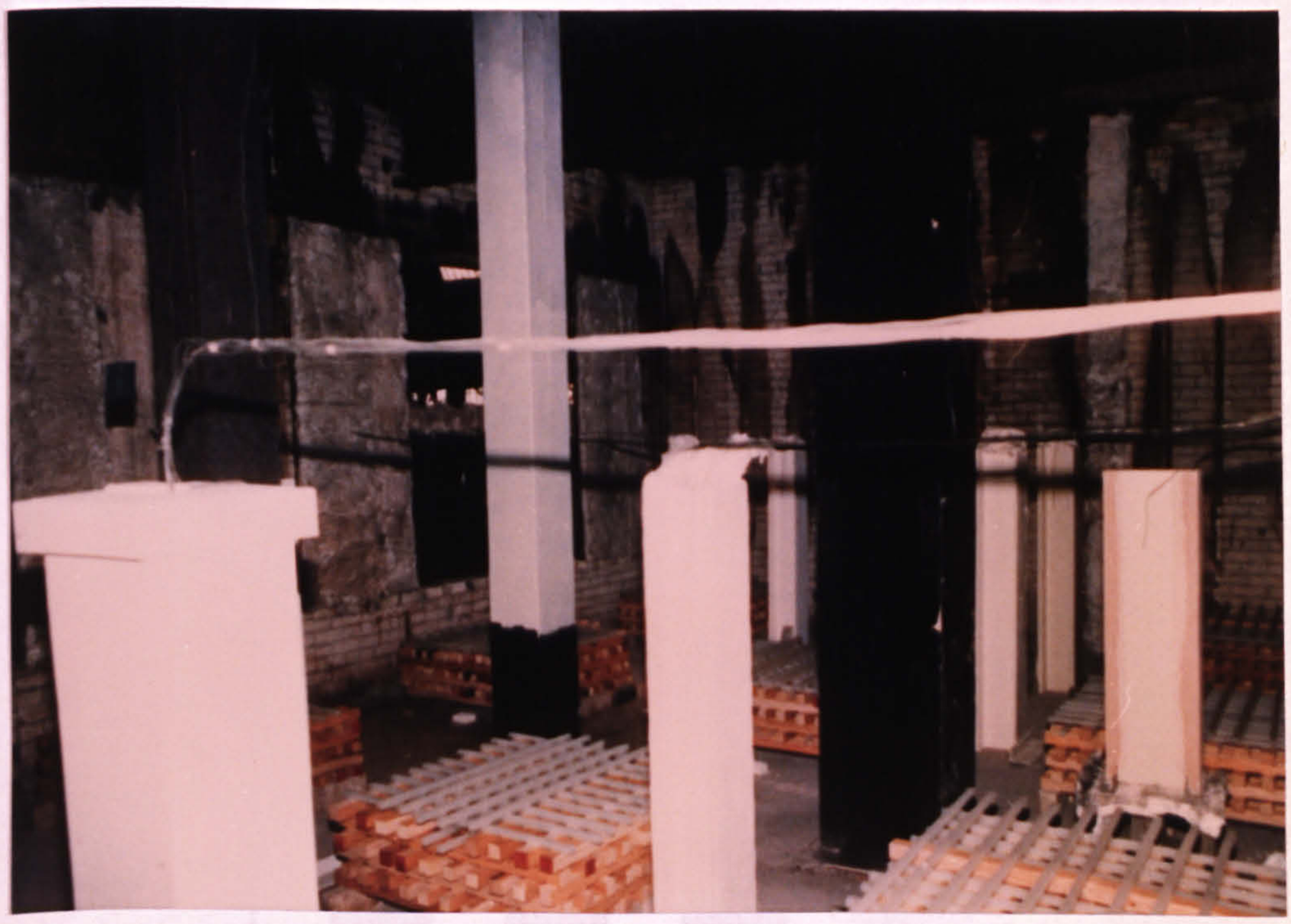

FIGURE 94

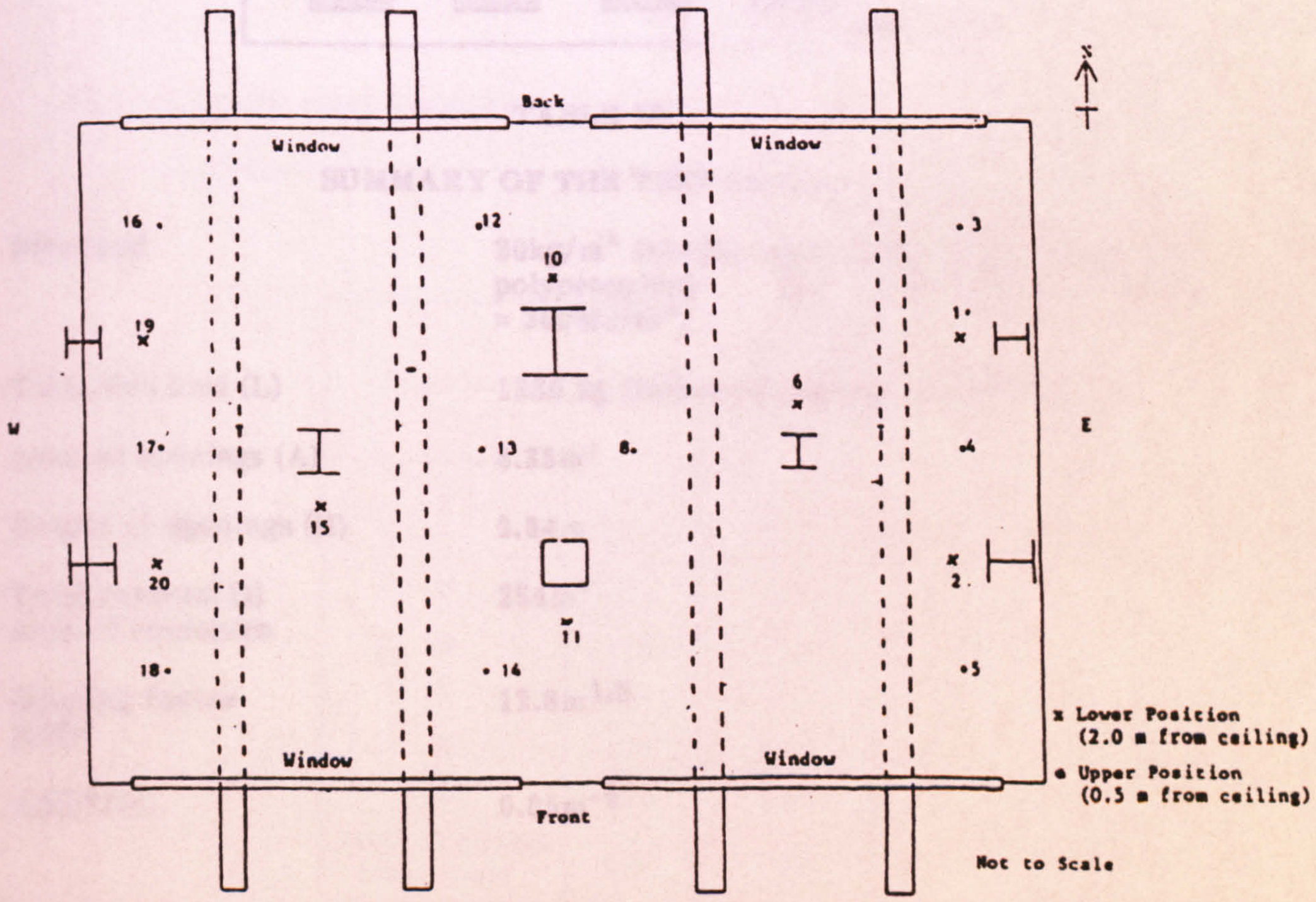

PLAN OF THE FIRE TEST COMPARTMENT SHOWING THE POSITIONS OF THE THERMOCOUPLES WITH RESPECT TO THE STEELWORK FOR MONITORING ATMOSPHERE TEMPERATURES

FIGURE 95

LAYOUT OF CARDINGTON FIRE TEST FACILITY

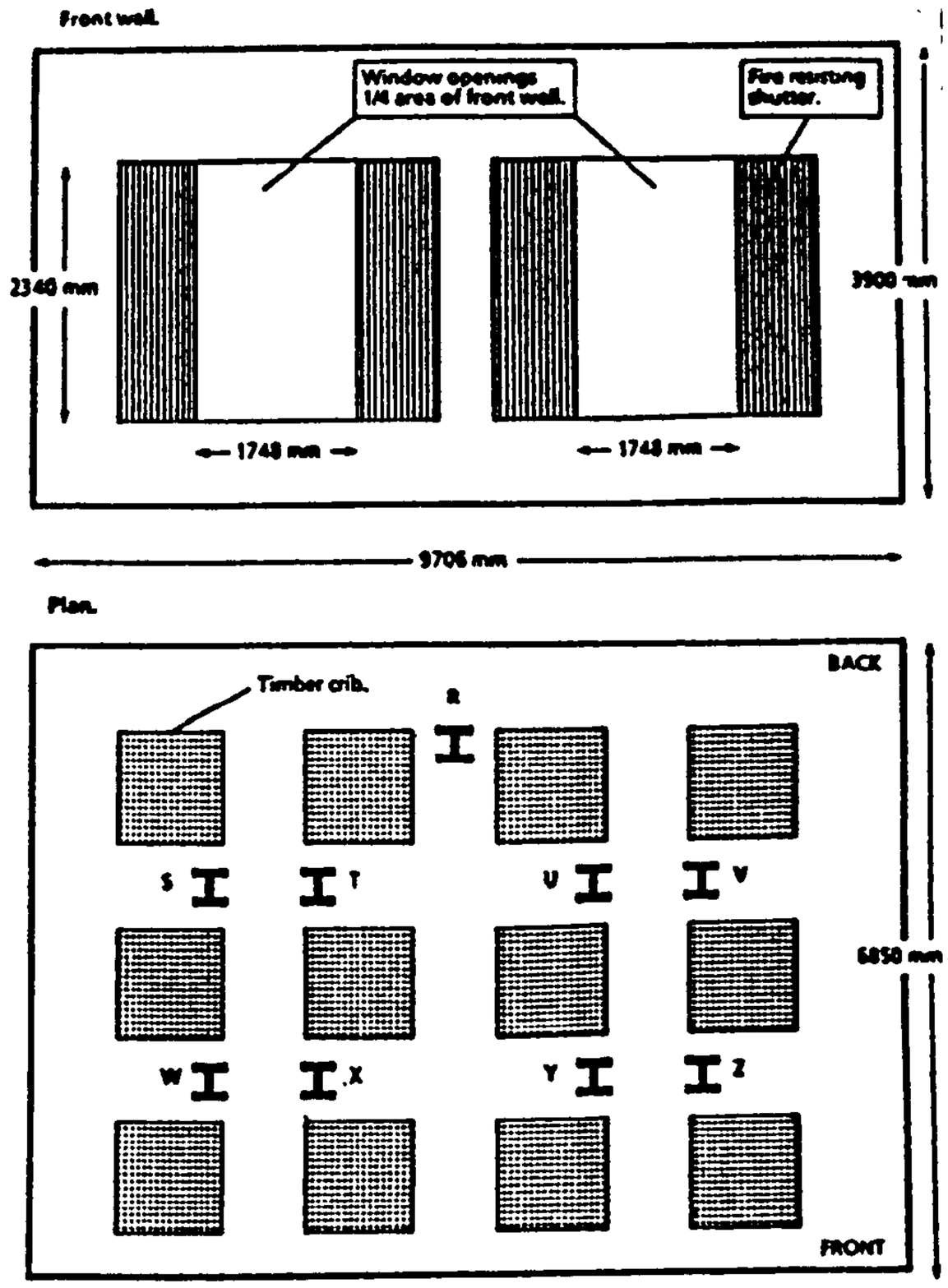

TABLE 13

SUMMARY OF THE TEST DETAILS

Fire load	20kg/m^2 (timber equivalent) 75% timber 25% polypropylene (by calorific value = 360MJ/m^2.
Total fire load (L)	1330 kg timber equivalent (23900 MJ).
Area of openings (A)	8.35m^2
Height of openings (H)	2.34m
Total internal (t) area of enclosure	254m^2
Opening factor $A(H)^2$	12.8m$^{1.5}$
$A(H)^{\frac{1}{2}}/A_t$	0.05m$^{-\frac{1}{2}}$

7.3. RESULTS OF THE FIRE TEST

Before the start of the test, precautions were taken to prevent draughts. All the cribs were ignited simultaneously. A considerable quantity of black smoke emerged from the compartment in the early stages of the test. Once the polypropylene had been consumed the amount of smoke produced was significantly reduced. The progress of combustion is shown in Figs. 96A-D.

The recorded atmosphere and steel temperatures are given in Fig. 99A-R and in Appendix C. A peak temperature of 1190°C was recorded after 6 minutes. The overall maximum average temperature was 938°C, achieved after 5 minutes. The temperature measurements were discontinued after 42 minutes.

The unprotected steel column reached a maximum average temperature of 785°C after 15 minutes.

The maximum steel temperatures recorded during the fire test for the columns protected with intumescent films are summarised in Table 14.

TABLE 14

Specimen	Max Steel Temp, °C	Max Ave Steel Temp, °C
S	278	258
T	372	354
U	267	259
W	458	430
X	461	433
Y	286	277
Z	388	379
Unprotected Specimen	802	785

TABLE 15

GENERAL OBSERVATIONS DURING THE FIRE TEST

Time (min):

0.00	All cribs ignited.
0.30	Flames beginning to develop to a height of 600mm above cribs.
2.00	Flames beginning to lick the ceiling no sign of intumescence or darkening of columns.
3.00	Flames rising with a cross sectional area similar to crib area and reaching ceiling height more consistently. Intumescent coatings starting to darken but no sign of significant intumescence.
3.30	Flames building up rapidly: some flames emerging from window openings.
4.00	Significant flaming from window openings. The fire is involving most of the compartments. The neutral plane is approximately 1/2 the height of the openings.
4.30	Large quantities of smoke and flame emerging from the test building. The fire is now very severe.
5.00	Neutral plane now appears to be at approximately 1/3 window height. The test columns are not now visible due to flame and smoke engulfment.
6.00	As 5.00.
7.00	As 5.00.
7.45	Neutral plane has risen to 1/2 window height and the fire now appears slightly less severe.
8.00	There is still substantial flaming outside the compartment. Neutral plane at approximately 1/2 height of window opening.
9.00	Columns are becoming visible as smoke production and flame engulfment reduces. Neutral plane 2/3 height of opening.
10.00	Fire dying down considerably. Flaming from the openings considerably reduced.
12.00	Flaming is now confined to the areas directly above the cribs and all columns are now clearly visible. Intermittent flaming emerging from window openings.
18.00	Flames now just licking ceiling of compartment.
21.00	Flames continuing to die down.
25.00	Cribs now little more than glowing embers with flames approximately 600mm high.
28.00	Combustion virtually ceased except for glowing embers and very slight flaming.

FIGURE 96A

PHOTOGRAPHS OF THE PROGRESSION OF THE FIRE TEST

5 minutes

10 minutes

FIGURE 60B

PROGRESSION OF THE FIRE TEST

20 minutes

25 minutes

FIGURE 96C

PROGRESSION OF FIRE TEST

30 minutes

45 minutes

FIGURE 96D

PROGRESSION OF THE FIRE TEST

60 minutes

AFTER THE FIRE TEST

FIGURE 97

PROGRESSION OF THE FIRE TEST

A TYPICAL COLUMN AFTER FIRE EXPOSURE

TOP OF THE COLUMN

BOTTOM OF THE COLUMN

FIGURE 98A

THE TEST PLATES AFTER EXPOSURE TO THE FIRE TEST

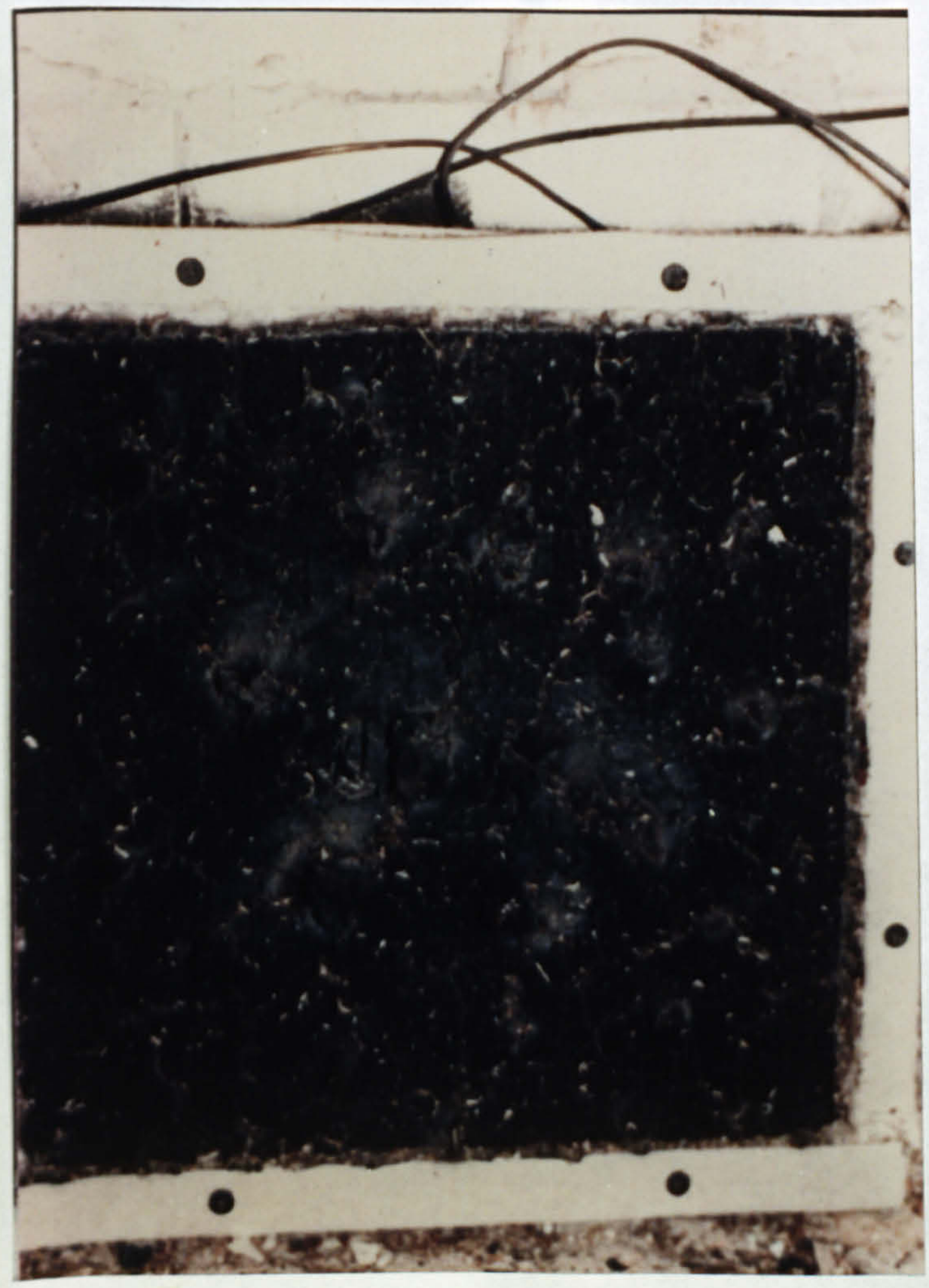

FORMULATION A

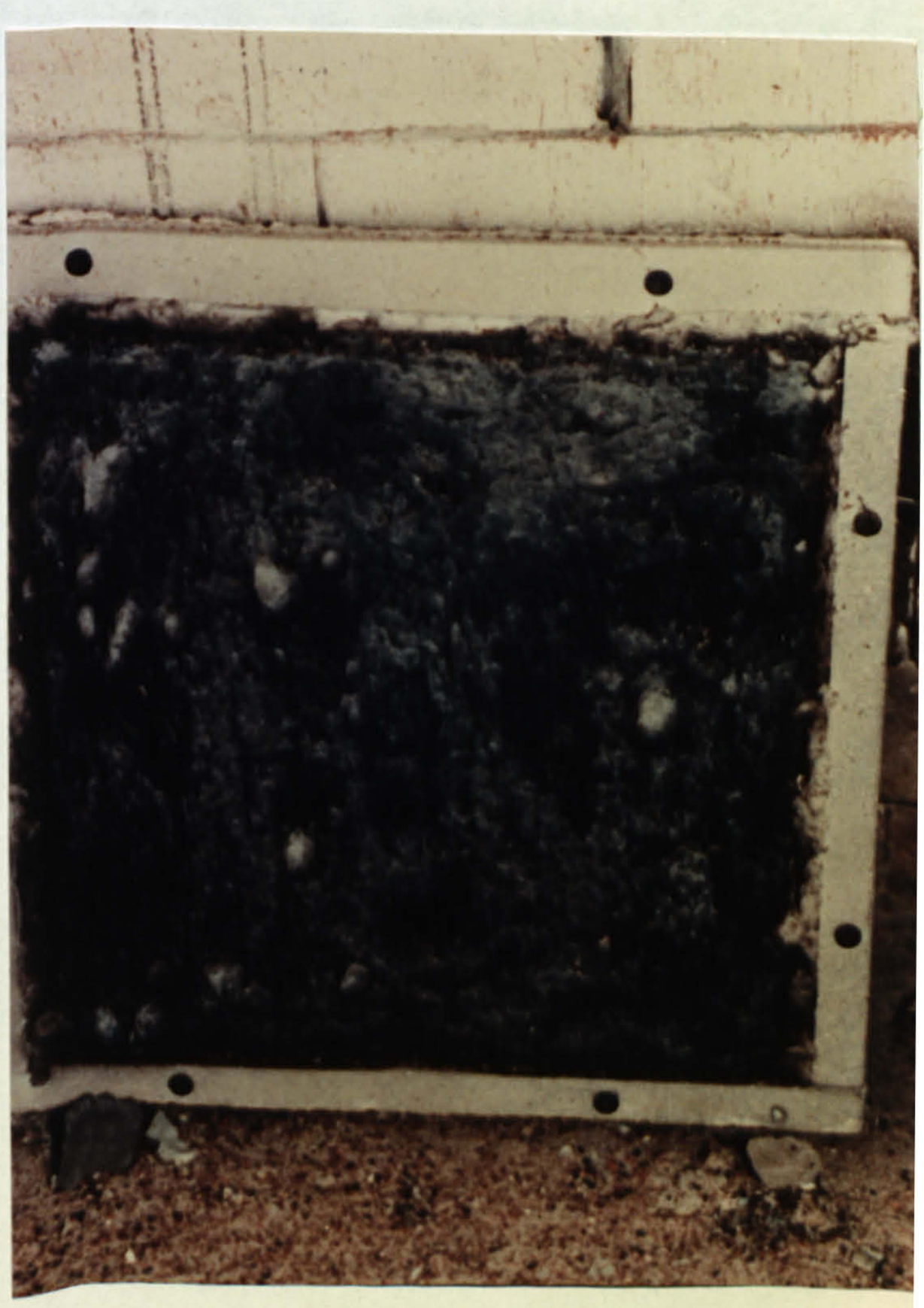

FORMULATION B

FIGURE 98B

THE TEST PLATES AFTER EXPOSURE TO THE FIRE TEST

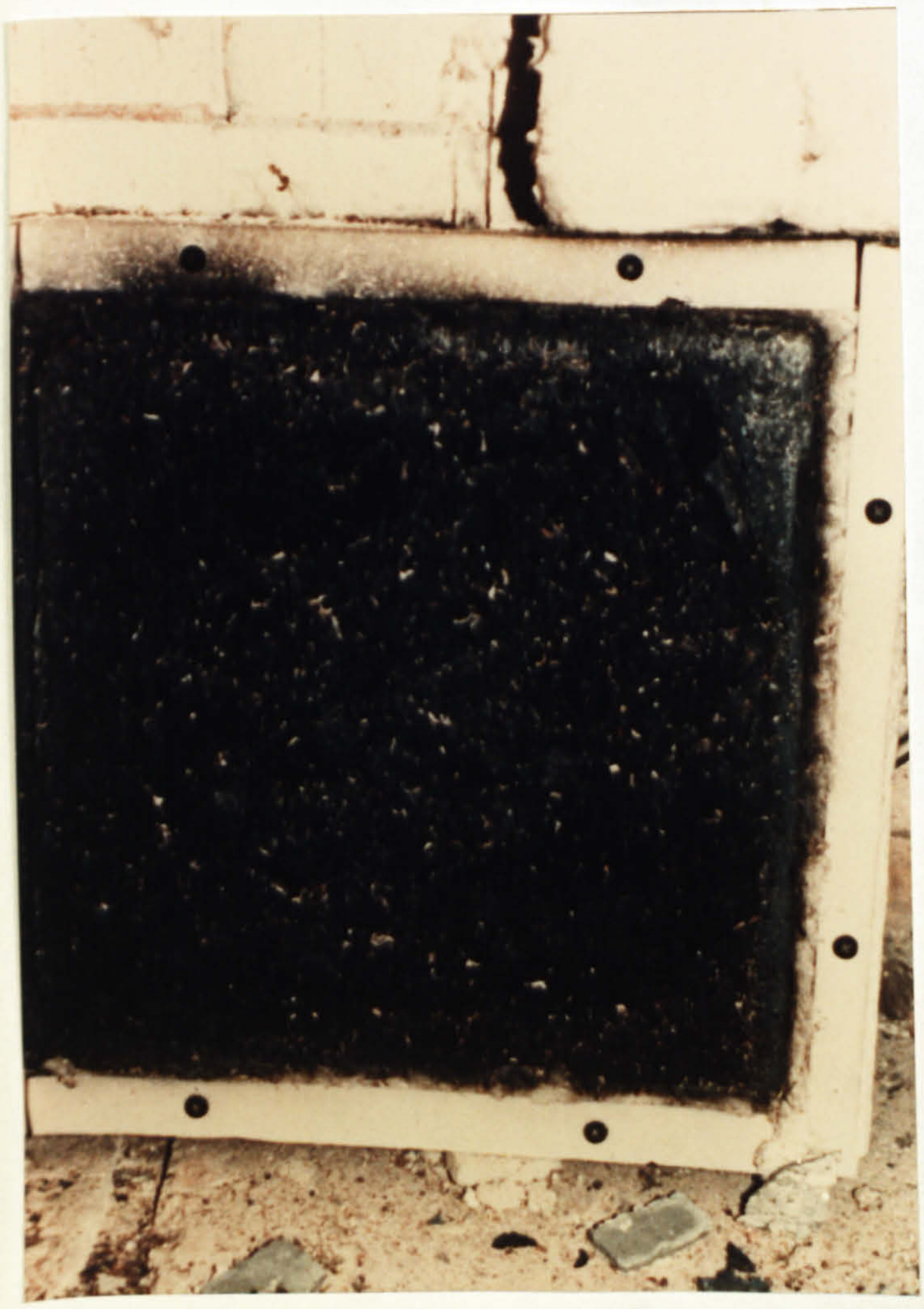

CONTROL FORMULATION

FORMULATION C

FIGURE 99A

ATMOSPHERE HEATING RATES RECORDED AT 0.5 m FROM ROOF IN THE EAST SIDE OF THE COMPARTMENT

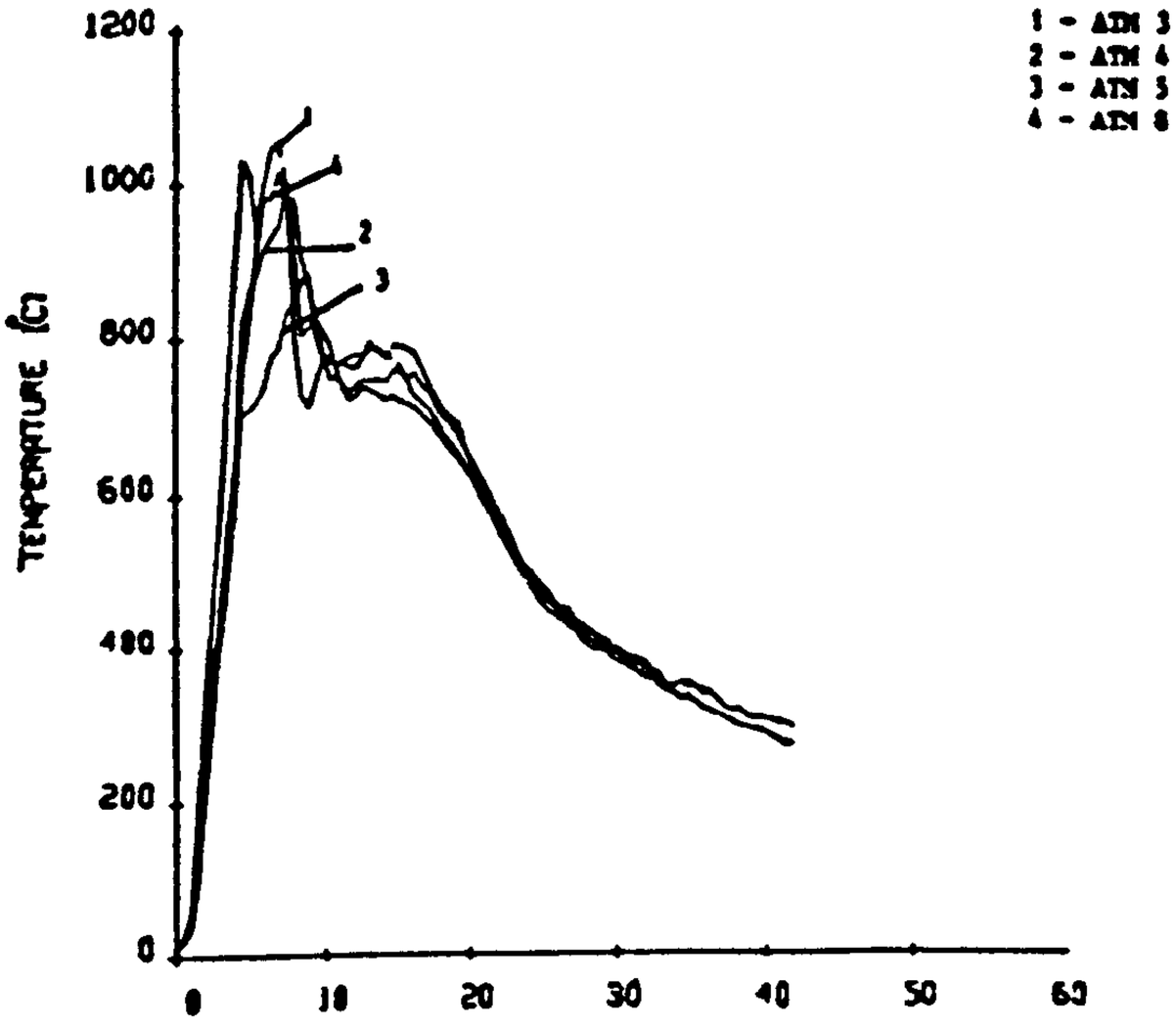

FIGURE 99B

ATMOSPHERE HEATING RATES RECORDED AT 2.0 m FROM ROOF IN THE EAST SIDE OF THE COMPARTMENT

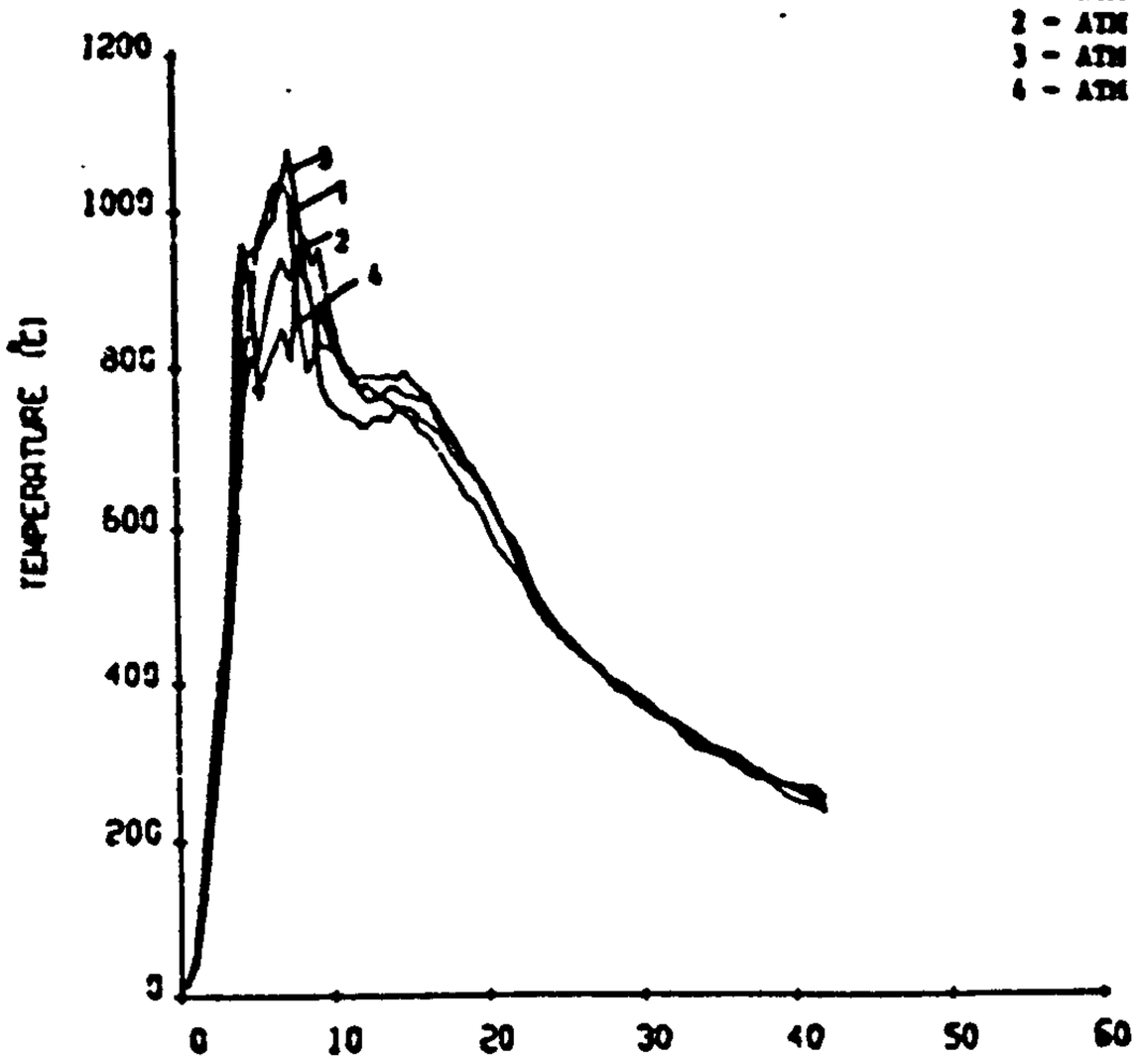

FIGURE 99C

ATMOSPHERE HEATING RATES RECORDED AT 0.5 m FROM IN THE WEST SIDE OF THE COMPARTMENT

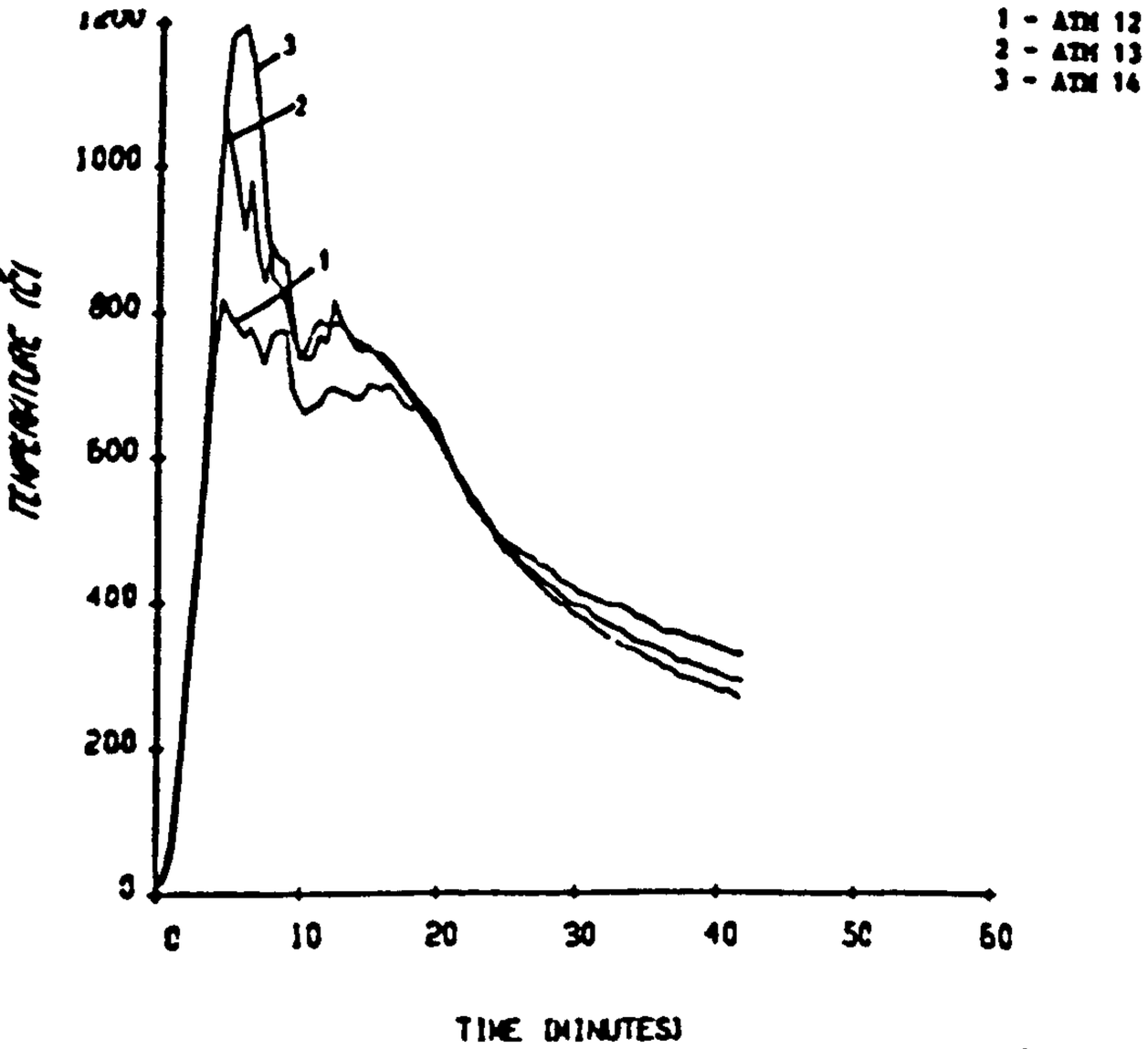

FIGURE 99D

ATMOSPHERE HEATING RATES RECORDED AT 2.0 m LEVEL IN THE WEST SIDE OF THE COMPARTMENT

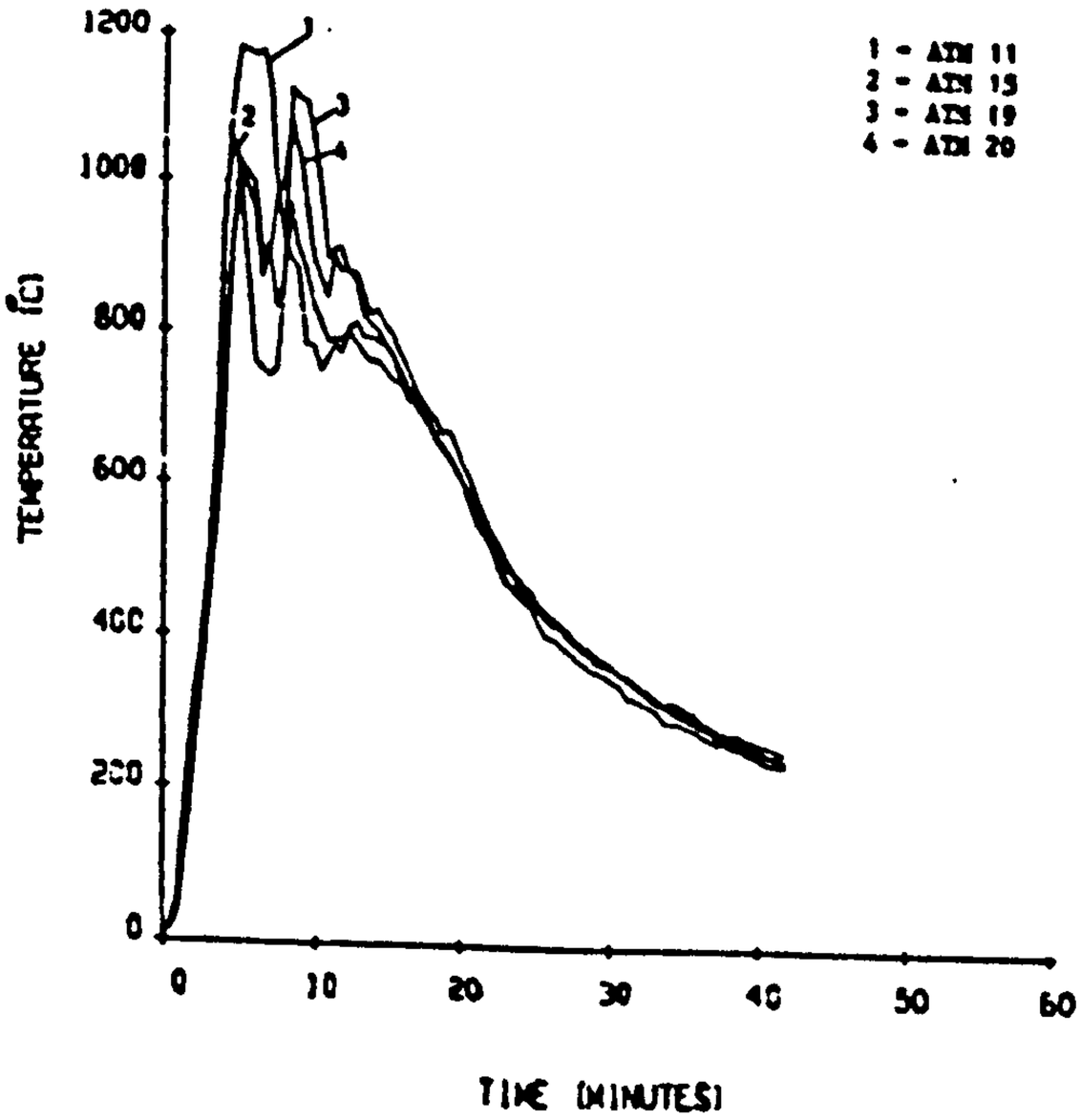

FIGURE 99E

ATMOSPHERE HEATING RATES RECORDED AT 0.5 m FROM ROOF IN THE WEST SIDE OF THE COMPARTMENT

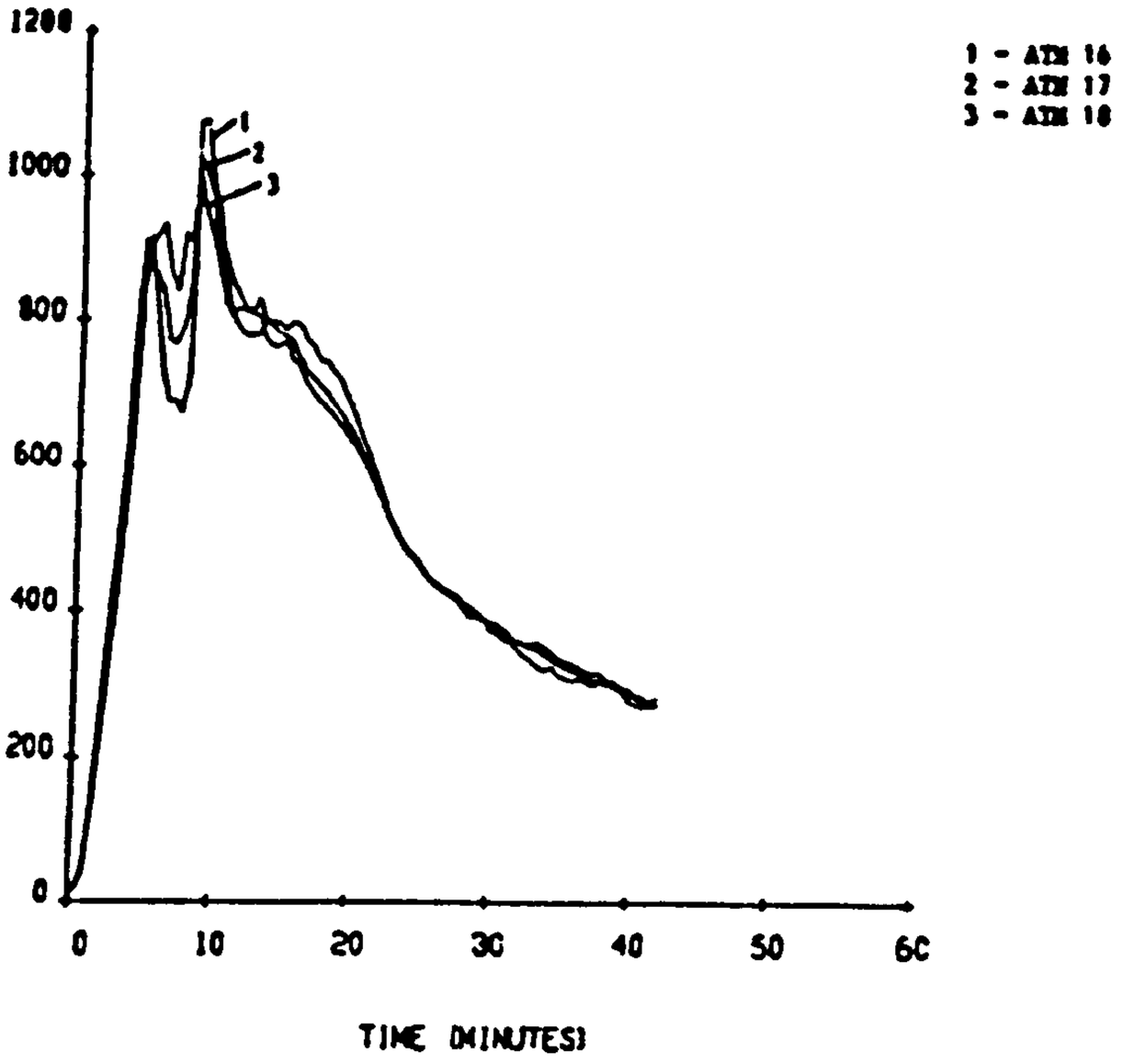

FIGURE 99F

STEEL AND ADJACENT ATMOSPHERE HEATING RATES RECORDED AT THE 2.8 m POSITION ON THE 203x203 mm x 52 kg/m COLUMN

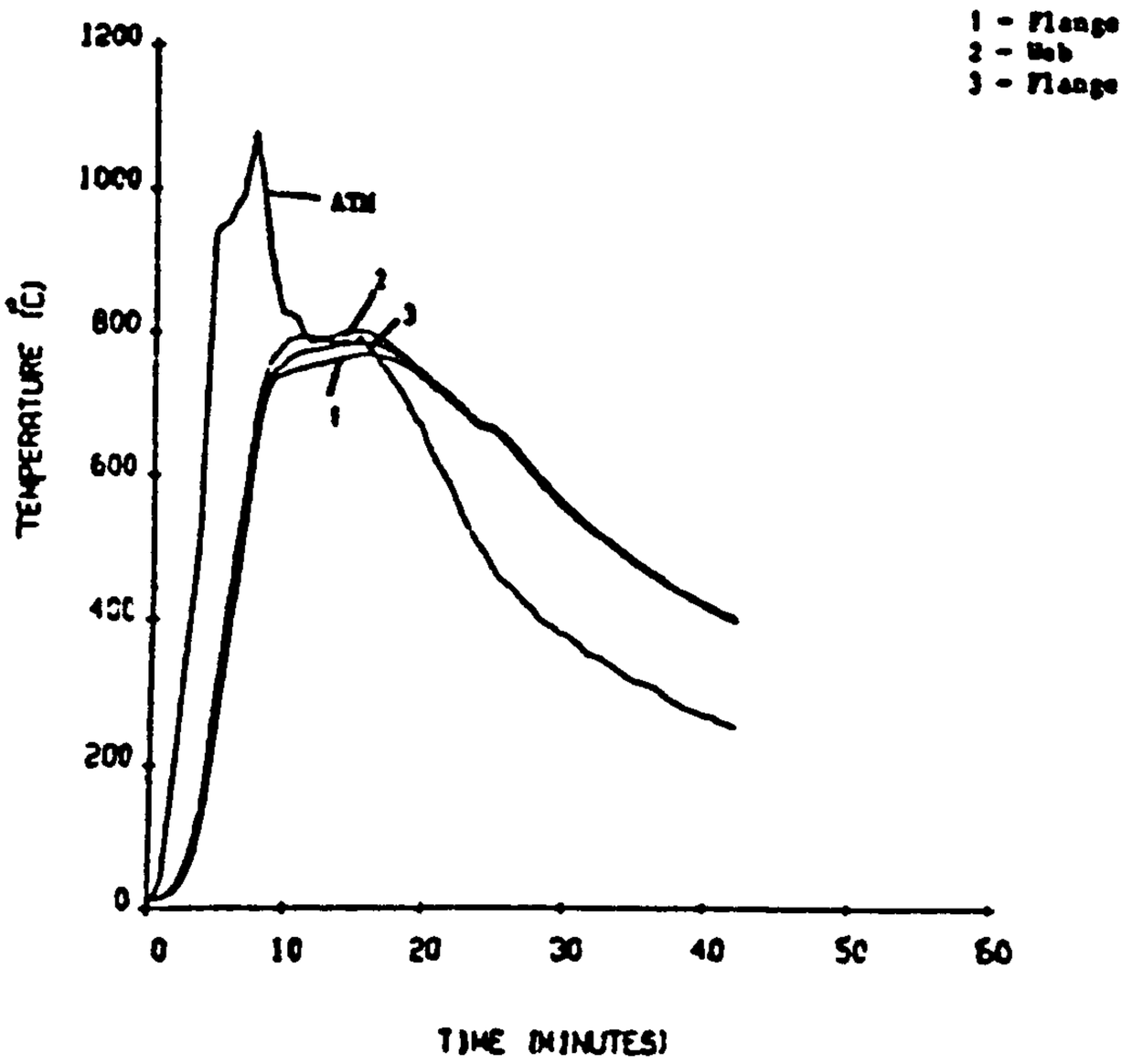

FIGURE 99G

STEEL AND ADJACENT ATMOSPHERE HEATING RATES RECORDED ON SPECIMEN 1

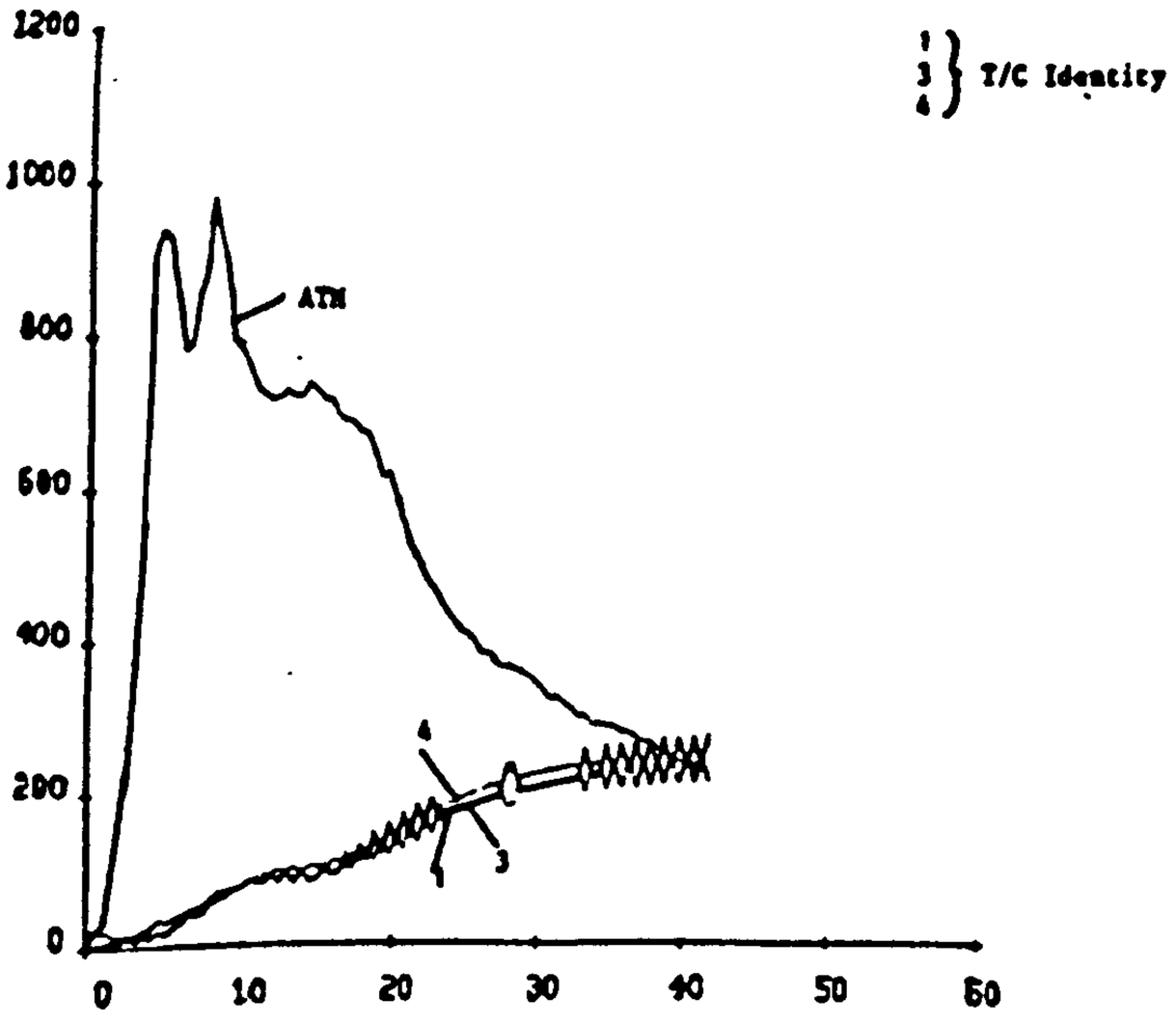

FIGURE 99H

STEEL AND ADJACENT ATMOSPHERE HEATING RATES RECORDED ON SPECIMEN V

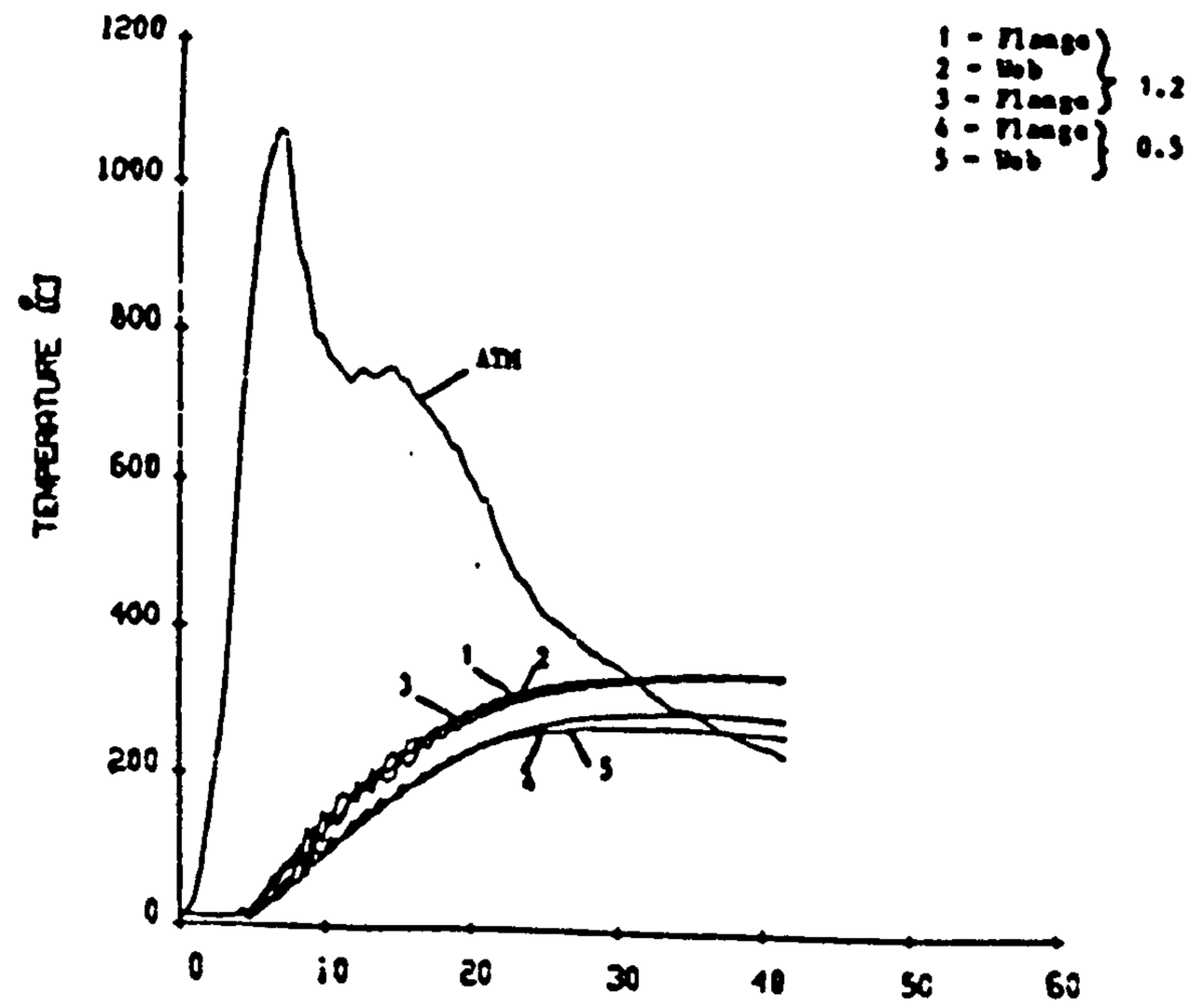

FIGURE 99I

STEEL AND ADJACENT ATMOSPHERE HEATING RATES

RECORDED ON SPECIMEN S

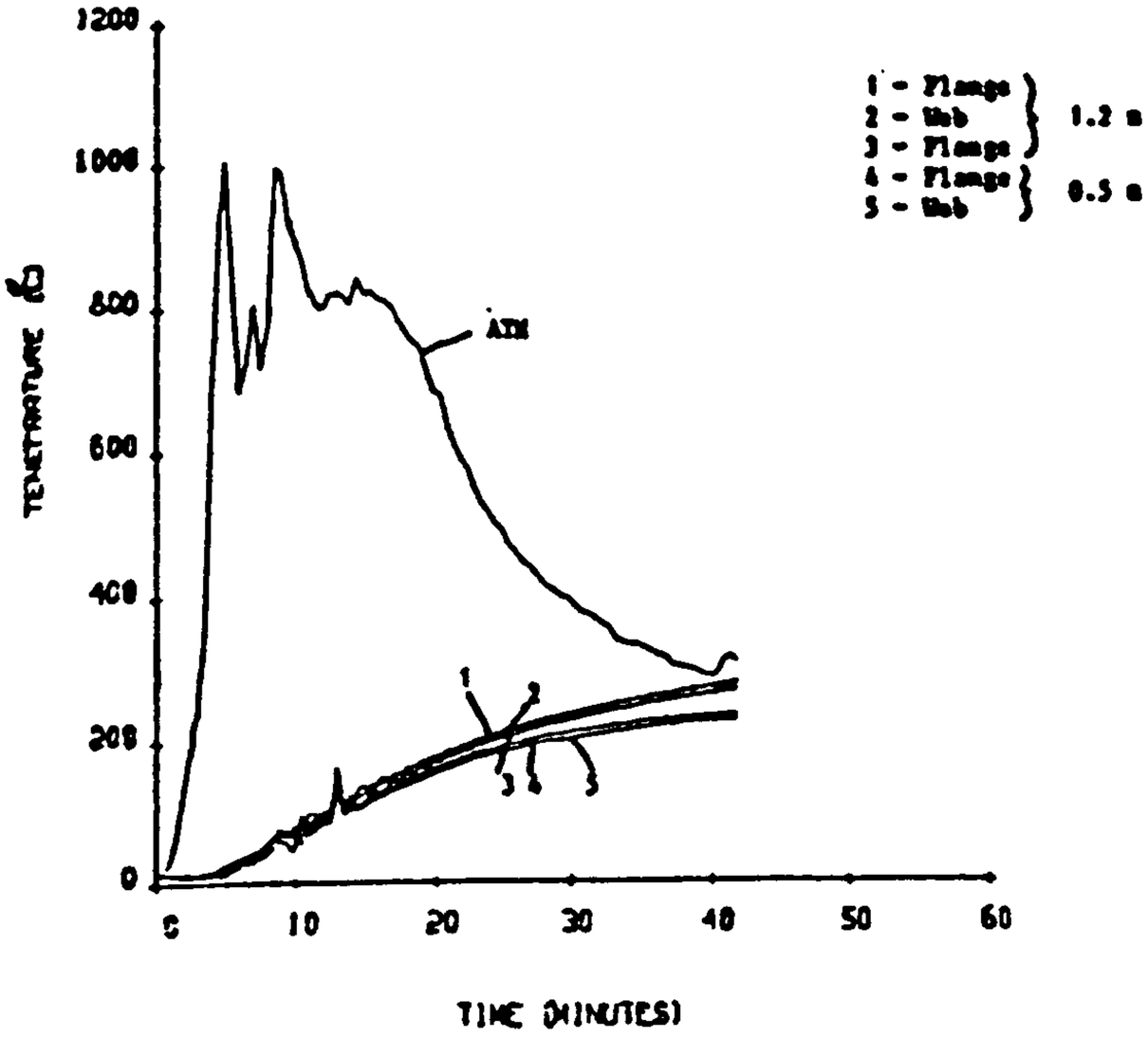

FIGURE 99J

STEEL AND ADJACENT ATMOSPHERE HEATING RATES

RECORDED ON SPECIMEN U

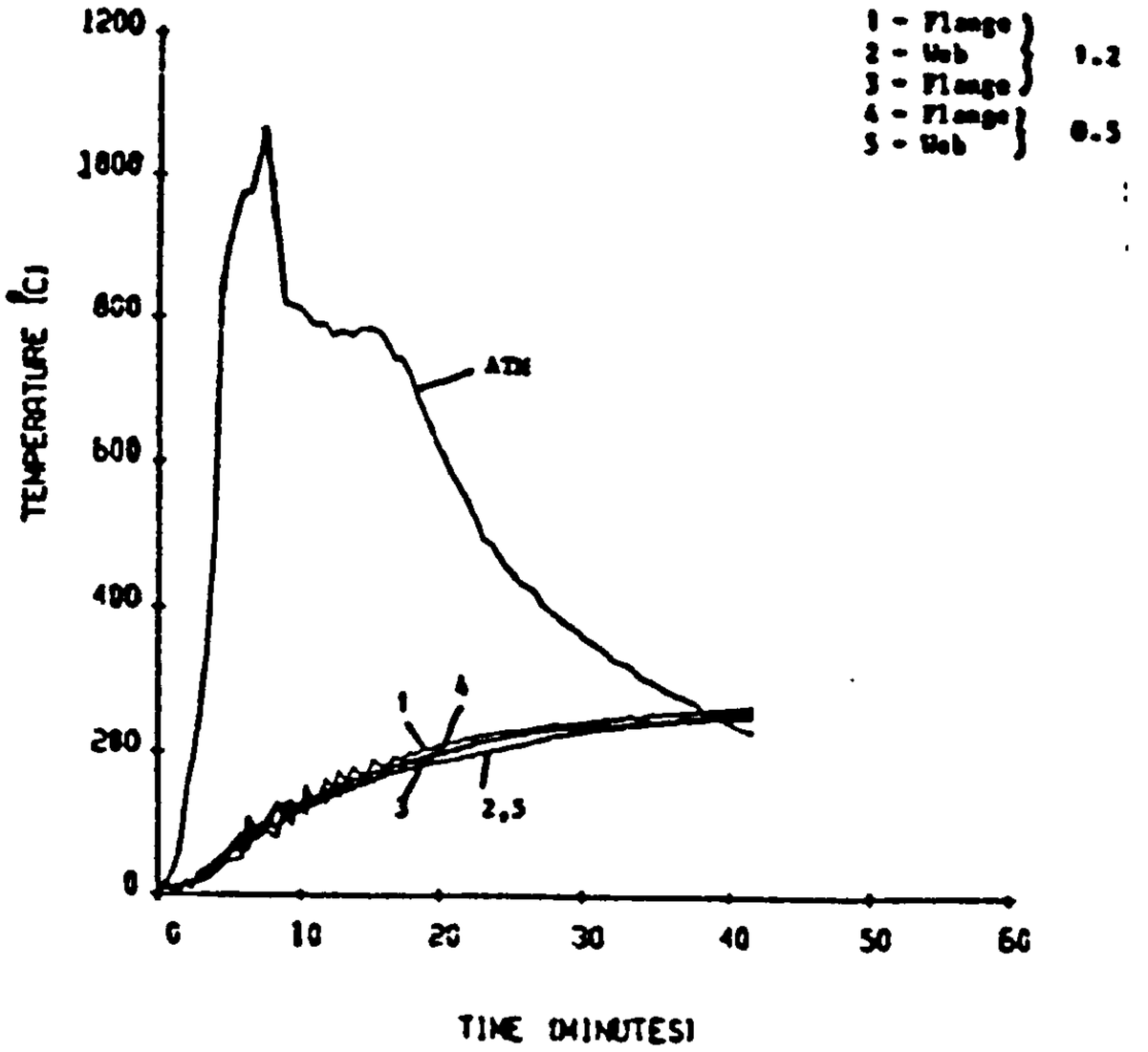

FIGURE 99K

STEEL AND ADJACENT ATMOSPHERE HEATING RATES

RECORDED ON SPECIMEN T

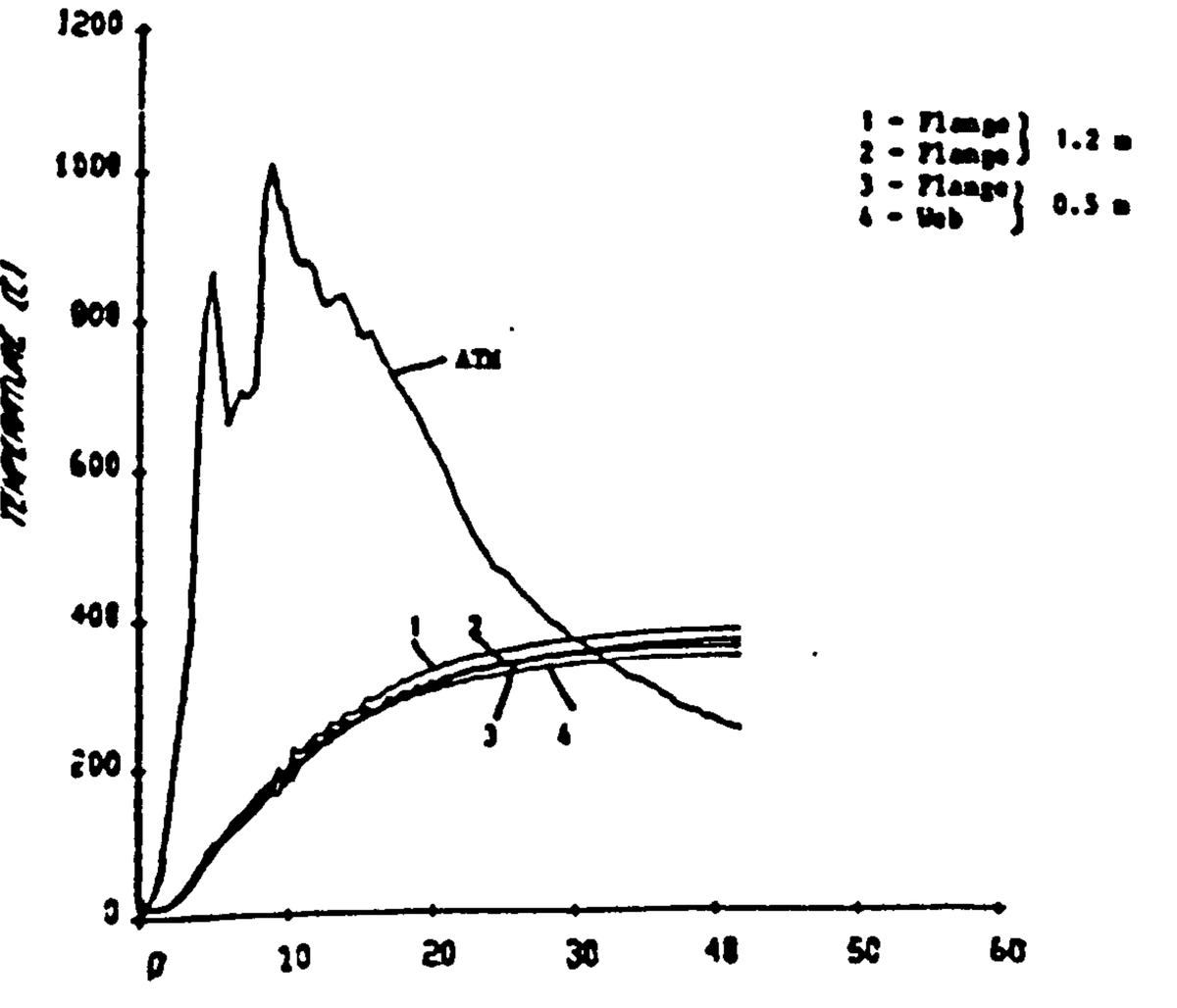

FIGURE 99L

STEEL AND ADJACENT ATMOSPHERE HEATING RATES

RECORDED ON SPECIMEN W

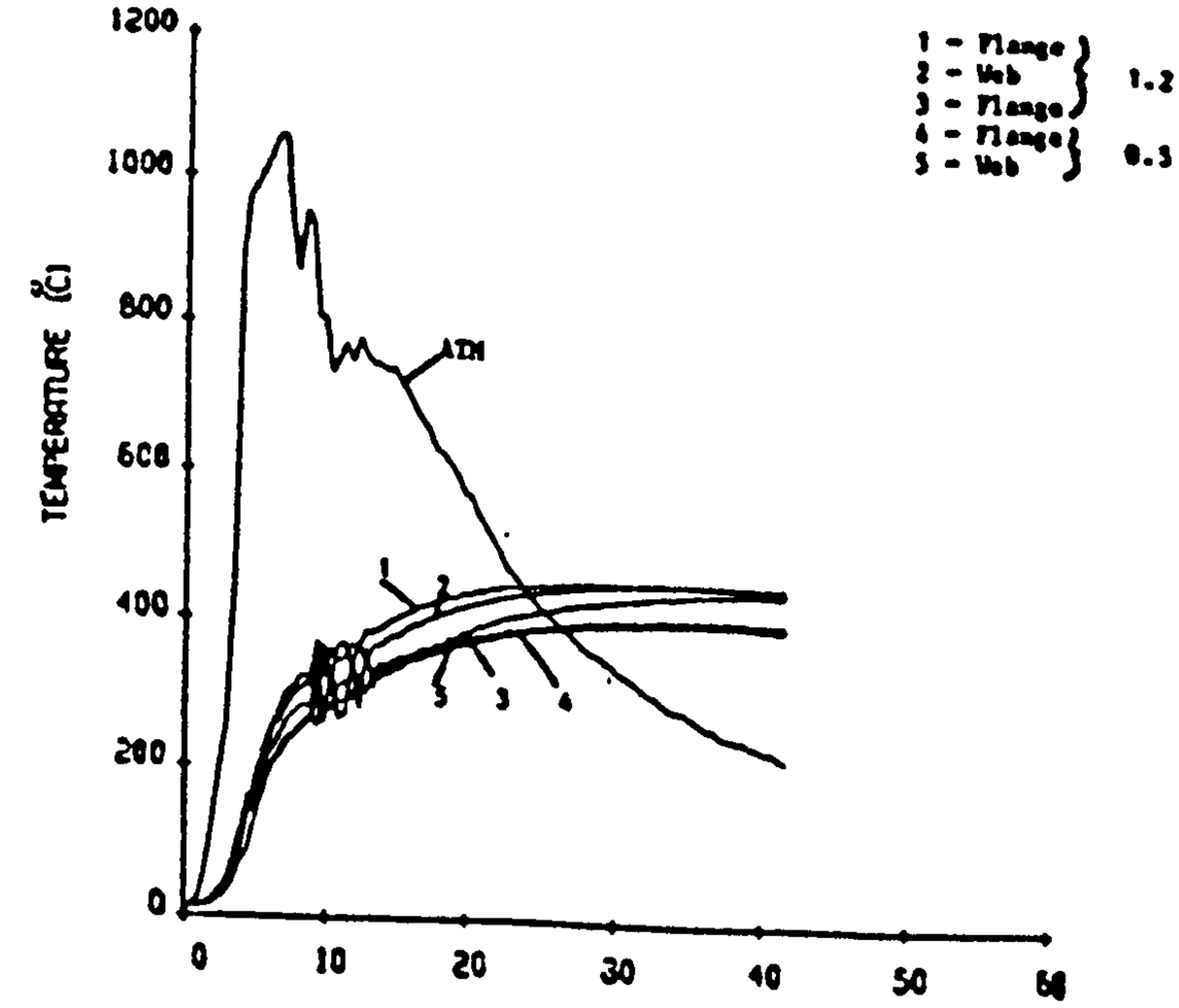

FIGURE 99O

STEEL AND ADJACENT ATMOSPHERE HEATING RATES

RECORDED ON SPECIMEN X

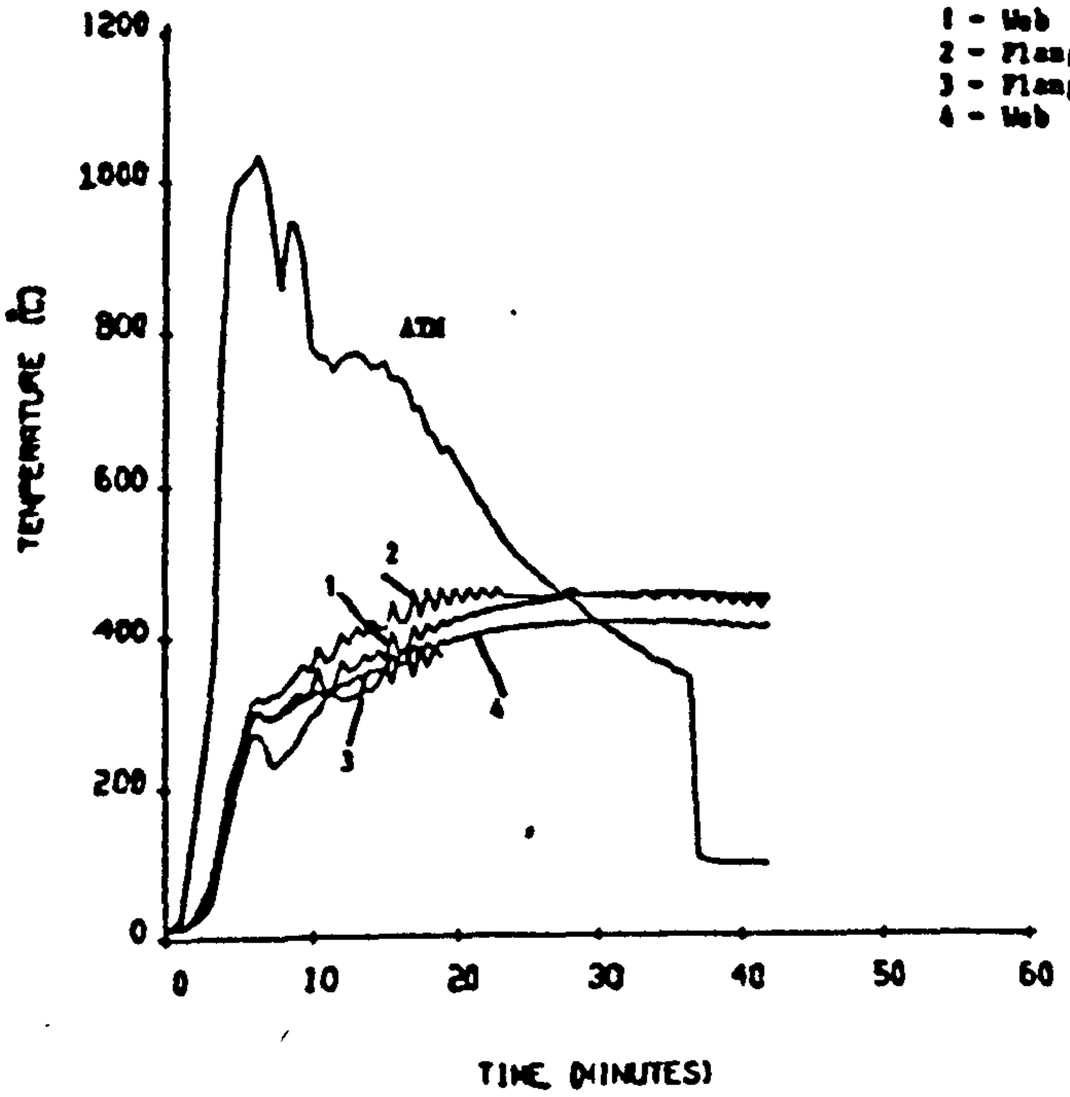

FIGURE 99P

STEEL AND ADJACENT ATMOSPHERE HEATING RATES

RECORDED ON SPECIMEN Y

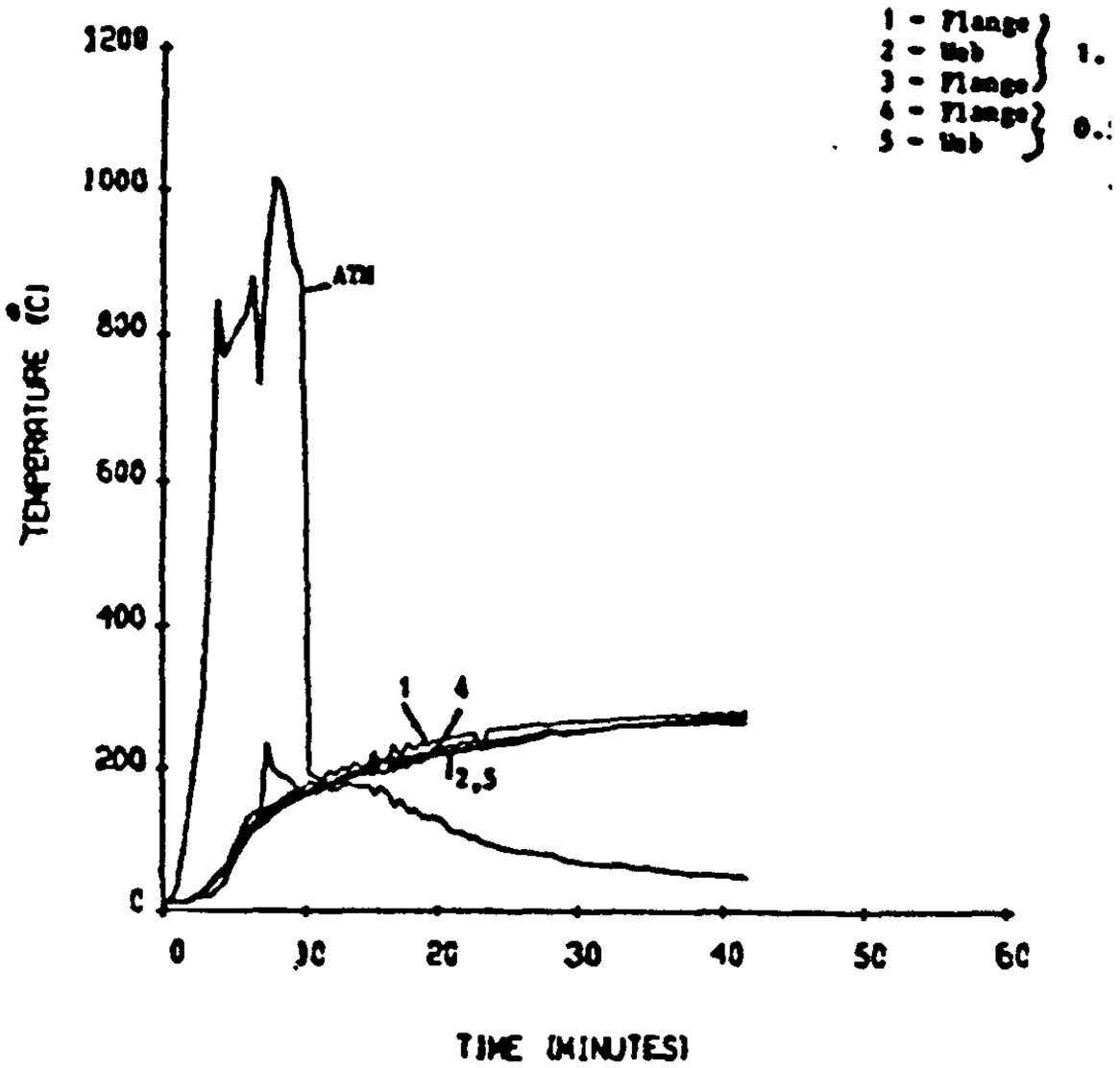

FIGURE 99Q

STEEL AND ADJACENT ATMOSPHERE HEATING RATES

RECORDED ON SPECIMEN Z

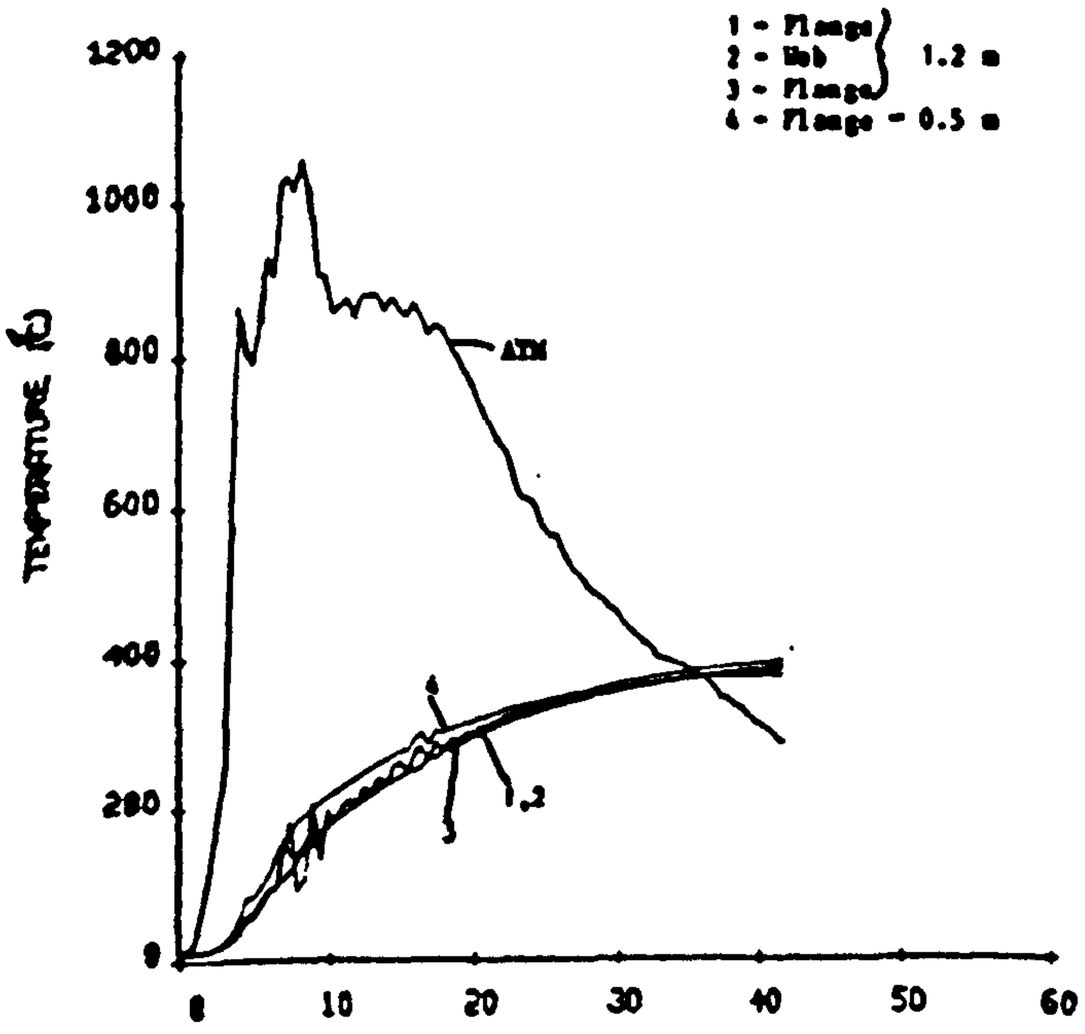

FIGURE 99R

STEEL HEATING RATES RECORDED ON THE PROTECTED

300 mm SQUARE PANELS

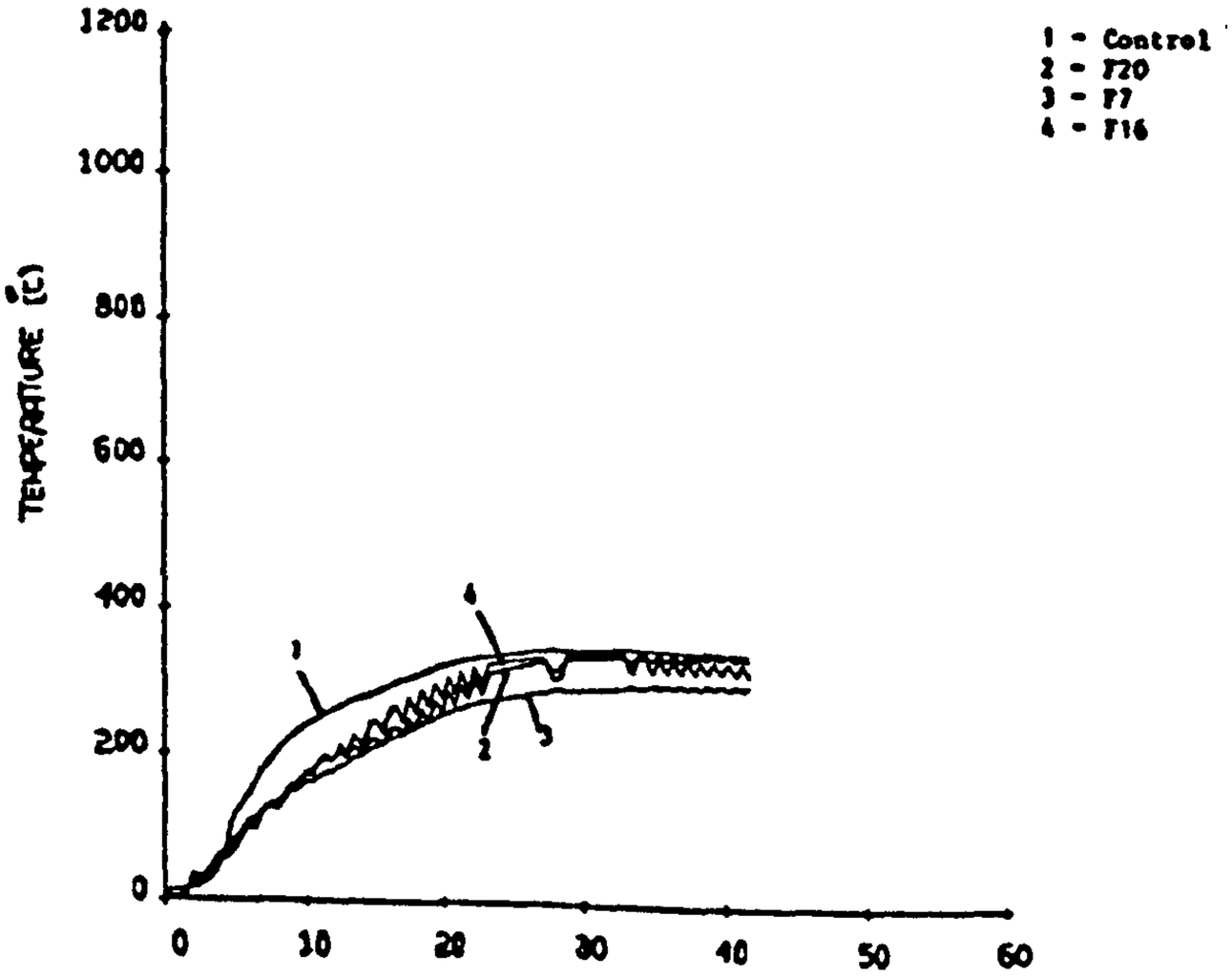

TABLE 16

OBSERVATIONS AFTER TEST ON THE COLUMNS

Coding Letter	Measured Thickness (total mm)	Yellow* Book Thickness for 1 hr	Observations After Test
R	12.5	12.5	Slight opening of joints. No obvious cracks in board or other signs of distress.
S	12.8	12.5	Thickness of char very variable. Thickness on flanges 10mm-130mm: web 10-100mm: lowest thickness at top and bottom of columns. Char crusty where material thin but friable where intumescence is thick.
T	2.64	1.8	Thickness on flanges 15-25mm: web 30-40mm. Very crusty layer over intumescent char.
U	5.62	6.0	Thickness on flanges 30-60mm: web 30-90mm. A number of small areas of steel visible around the arrisses. The intumescent char is slightly crusty. Some un-intumesced material approx. 1mm thick.
V	9.0	9.0	Each side of column protection contains approx. 12mm wide crack. Also 3 or 4 minor cracks on each face of the board.
W	1.58	2.3	Even firm intumescent char 10-20mm thick no bare steel very uniform crusty char.
X	0.78	1.3	Thickness on flanges 5-20mm: web 20-40mm. The char rather friable. Several small areas of steel exposed at top of column and over arrisses.
Y	5.28	-	Thickness on flanges 20mm: web 20-35mm. Fairly crusty char with some un-intumesced material in places.
Z	2.72	-	Thickness on flanges 15-20mm: web 20-30mm. Crusty uniform char.

*Published by: Association of Structural Fire Protection Contractors and Manufacturers Ltd.

7.4. CALCULATIONS FOR THE LARGE SCALE FIRE TEST

7.4.1. SEVERITY OF THE FIRE

The fire severity in the compartment is given by Eqs (2.11) and (2.12).

Compartment size: 8.6 m x 5.5 m x 3.9 m high

Area of openings (A) = 8.35 m^2

Fire load = 20 kg/m^2 (timber equivalent)

Window area A_v = 8.35 m^2

Window height H_v = 2.34 m

Total internal surface area A_t = 254 m^2

Calorific value of cellulosic content = 360 MJ/m^2 i.e. 360/20 = 18 MJ/Kg

Hence, the fire load density/unit surface area

$$q_f = 67.04 \text{ MJ/m}^2,$$

The equivalent fire resistance t_e given by Eq (2.11) is

$$t_e = 20.0 \text{ mins}$$

The equivalent fire resistance t_e according to Eq (2.12)

$$t_e = 22 \text{ mins.}$$

TEMPERATURE RISE OF THE UNINSULATED STEEL COLUMN

DETAILS OF THE COLUMN:

Size : 203mm x 203mm, I section column X 52 kg/m

Measured depth of section (D) = 206.2 mm

Measured width of section (B) = 203.9 mm

Measured thickness of web (t) = 8.0 mm

Measured thickness of flange = 12.5 mm

Calculated area of cross section = 6.747 x 10^{-3} $m^2 cm^2$

$$H_p = 1.212 \text{ m}$$

$$H_p/A = 179.6 \text{ m}^{-1}$$

The value of Δ t can be obtained by using Eq. 2.16

$$\Delta t = 25000/179.6 \quad = 139.2 \text{ sec}$$

Using Δt value of 120 sec in Eq. 2.15

$$\Delta T_s = \frac{\alpha \quad H_p}{\rho_s C_{ps} \quad A} \cdot (T_f - T_s)\, \Delta t \qquad (2.15)$$

i.e.

$$\Delta T_s = \frac{\alpha \times 120 \times 179.6 \quad (T_f - T_s)}{520 \times 7850}$$

$$\therefore \quad \Delta T_s = \frac{\alpha\ (T_f - T_s)}{189}$$

Ambient temperature during the large scale fire test was 13°C

Assuming emissivity $E_r = 0.5$, $\alpha_k = 23$ W/m^2°C.

The temperature rise within the test rig can be approximately represented by the following Equation See Fig. 100.

$$T = 1100\ [1 - 0.325\ EXP\ (-0.167\ t)] \text{ where t is in mins.} \qquad (7.1)$$

FIGURE 100

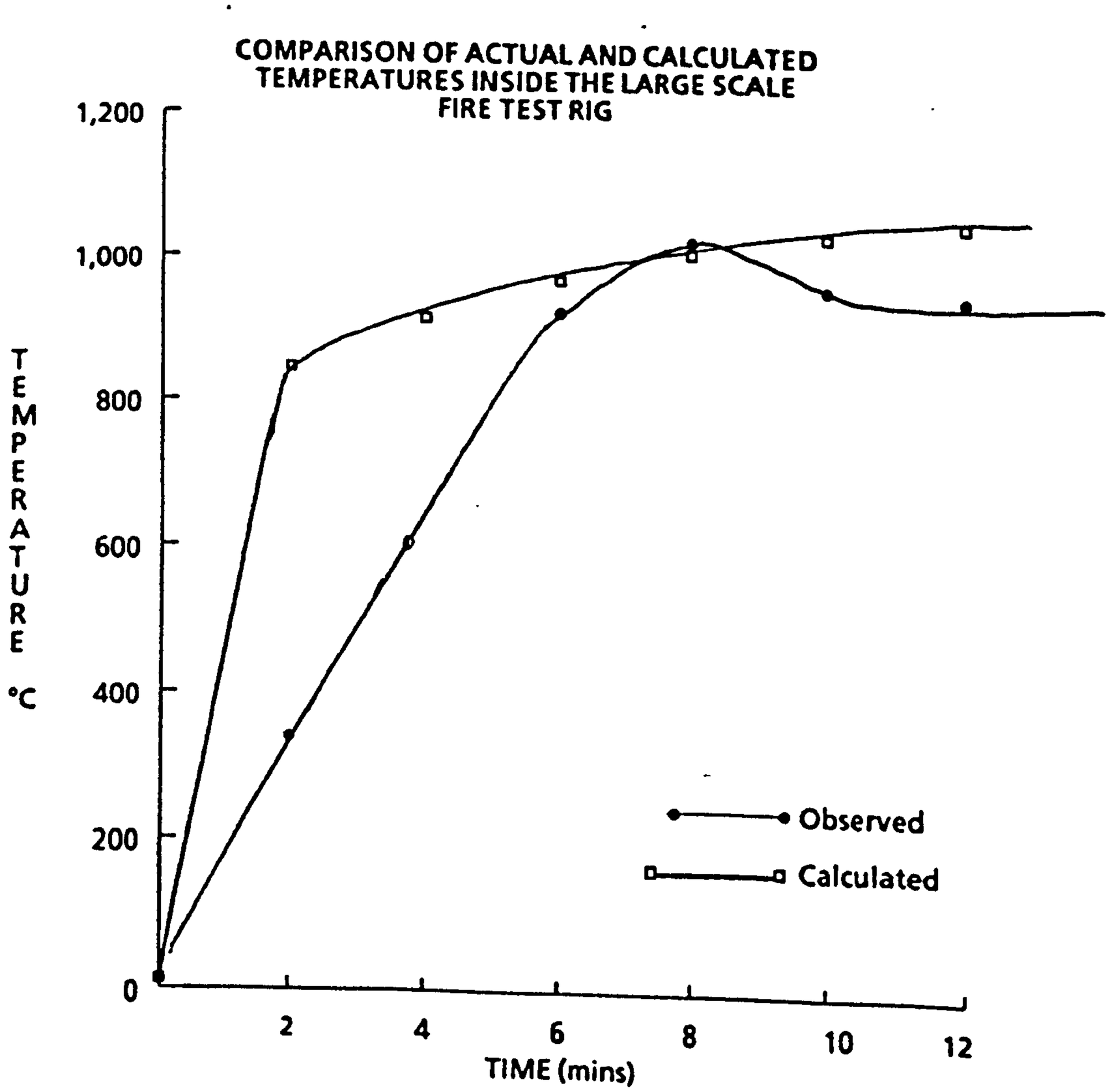

Using Eq. 7.1., the first value of T_f is obtained at 120 seconds

T_f at 2 mins = 844°C. T_s at 0 = 13°C

Therefore using Eq 2.17 the value of α_s can be obtained

$$\alpha_s = \frac{5.77\ E_r}{T_f - T_s}\left[\left(\frac{T_f + 273}{100}\right)^4 - \left(\frac{T_s + 273}{100}\right)^4\right] \quad W/m^2\ °C \quad (2.17)$$

$\therefore\ \alpha_s = 53.8$

Therefore $\alpha = \alpha_s + \alpha_k = 76.8\ W/m^2°C$

Substituting values of H_p/A, c_s and α_s in Eq. 2.15

$\Delta T_s = 337.7°C$

Therefore average steel temperature at 2 mins = 350.1°C

Similarly calculating the values of ΔT_s at intervals of 2 mins gives the temperature rise of the column as shown in Table 17 and Fig 101.

FIGURE 101

COMPARISON OF ACTUAL AND CALCULATED HEATING RATES OF AN UNINSULATED STEEL COLUMN DURING LARGE SCALE FIRE TEST

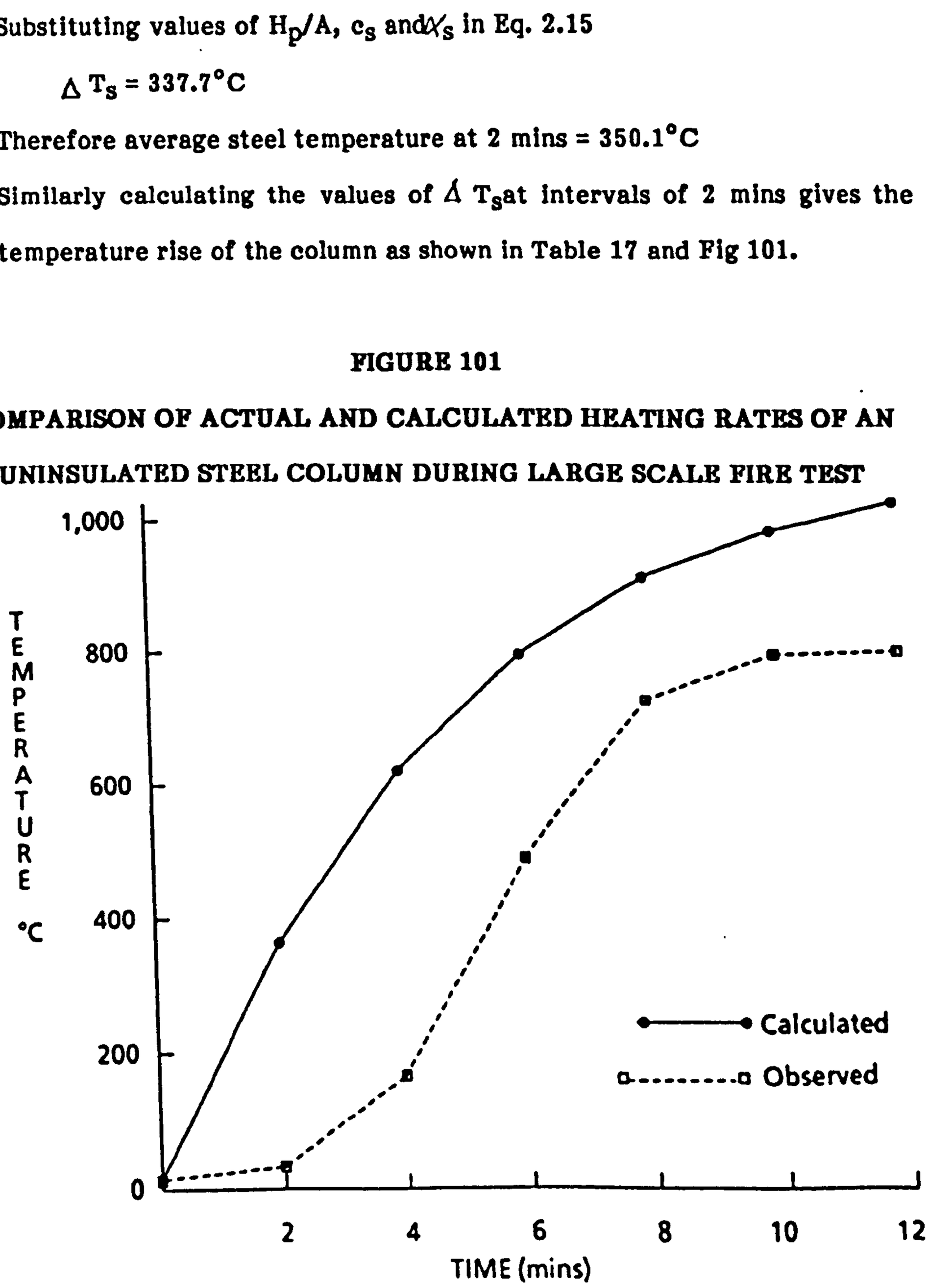

TABLE 17

TIME (min)	T_f °C	α W/m²°C	$(T_f - T_s)$ °C	ΔT_s °C	T_s °C
0					13
2	844	76.8	831	350	363
4	916	86.74	553.6	254	617
6	968	94.56	351.5	176	793
8	1006	100.6	212	113	906
10	1032	105.04	126.4	70	976
12	1052	108.4	75.23	43	1019
14	1065	110.8	45.8	26	1046
16	1075	112.6	28.8	17	1064

7.5. SUMMARY OF THE RESULTS

All the intumescent materials provided protection to the steel. The minimum rise in temperature was recorded on specimen S which reached an average of 258°C after 42 minutes, the maximum rise occured on specimen X which reached 461°C after 19 minutes. The steel plates coated with the developed formulation KD 20 reached an average of 242°C after 14.5 minutes while the control plate reached an average of 274°C after 13.5 minutes see Table 18.

The unprotected column reached a maximum average temperature of 758°C after 15 minutes. The maximum average steel temperatures for the columns protected by board materials were 247°C (specimen I) and 317°C (specimen V).

Table 18

Summary of Maximum Steel Temperatures and Times Recorded in the Fire Test on Specimens and steel plates Protected with Intumescents

Specimen	Max Steel Temp, °C	Time Achieved Min	Max Ave Steel Temp, °C	Time Achieved Min	Max Adjacent Atm Temp, °C	Time Achieved Min
S	278	42.0	258	42.0	1006	5.0
T	372	40.0	354	40.0	1004	9.0
U	267	42.0	259	42.0	1070	7.5
W	458	28.5	430	30.0	1059	7.0
X	461	19.0	433	23.0	1035	6.5
Y	286	41.0	277	41.0	1016	8.0
Z	388	42.0	379	42.0	1057	8.5
Unprotected Specimen	802	15.0	785	15.0	1078	7.5
Control Plate	348	35.0	274	13.5	1064	9.0
KD7	300	36.0	220	14.5	1066	5.0
KD16	344	35.5	250	19.5	1070	7.5
KD20	337	34.0	242	14.5	1057	8.5

SECTION 8

MODELLING EXPERIMENTS

8.1.TECHNIQUES & METHODS USED FOR MODELLING EXPERIMENTS

8.1.1. BASE LINE FORMULATION

For this series of experiments, a simple formulation was required with the least number of ingredients necessary to produce a good intumescent coating (foam height at least 20mm for a coating of thickness 1mm) while yet being strong enough to handle during testing. The formulation KD 23/3 (see below) was selected after extensive testing using screening tests such as the NBS smoke chamber test where the coated steel plates were irradiated with 2.5 watts/cm^2 of heat at a distance of 25 mm.

8.1.2. FORMULATION KD 23

	% by weight
BINDER (ALLOPRENE R20)	6.1
MELAMINE	5.0
DIPENTAERYTHRITOL	11.2
AMMONIUM POLYPHOSPHATE	24.6
TiO_2	12.6
TOLUENE	40.5

TSC % - 59.5

8.1.3. THERMAL ANALYSIS DATA FOR THE FORMULATION KD 23

The thermal analyses, using DTA, STA, DSC, and TGA, in air and nitrogen atmosphere, were conducted on the formulation before exposure to various heat radiations Fig. 102-105. IR absorption of the formulation was done before and after exposure to temperature of 100°C Fig. 107. Elemental analysis using EPMA was done Fig. 106.

FIGURE 102A

DTA CURVE FOR FORMULATION KD 23 IN NITROGEN ATMOSPHERE

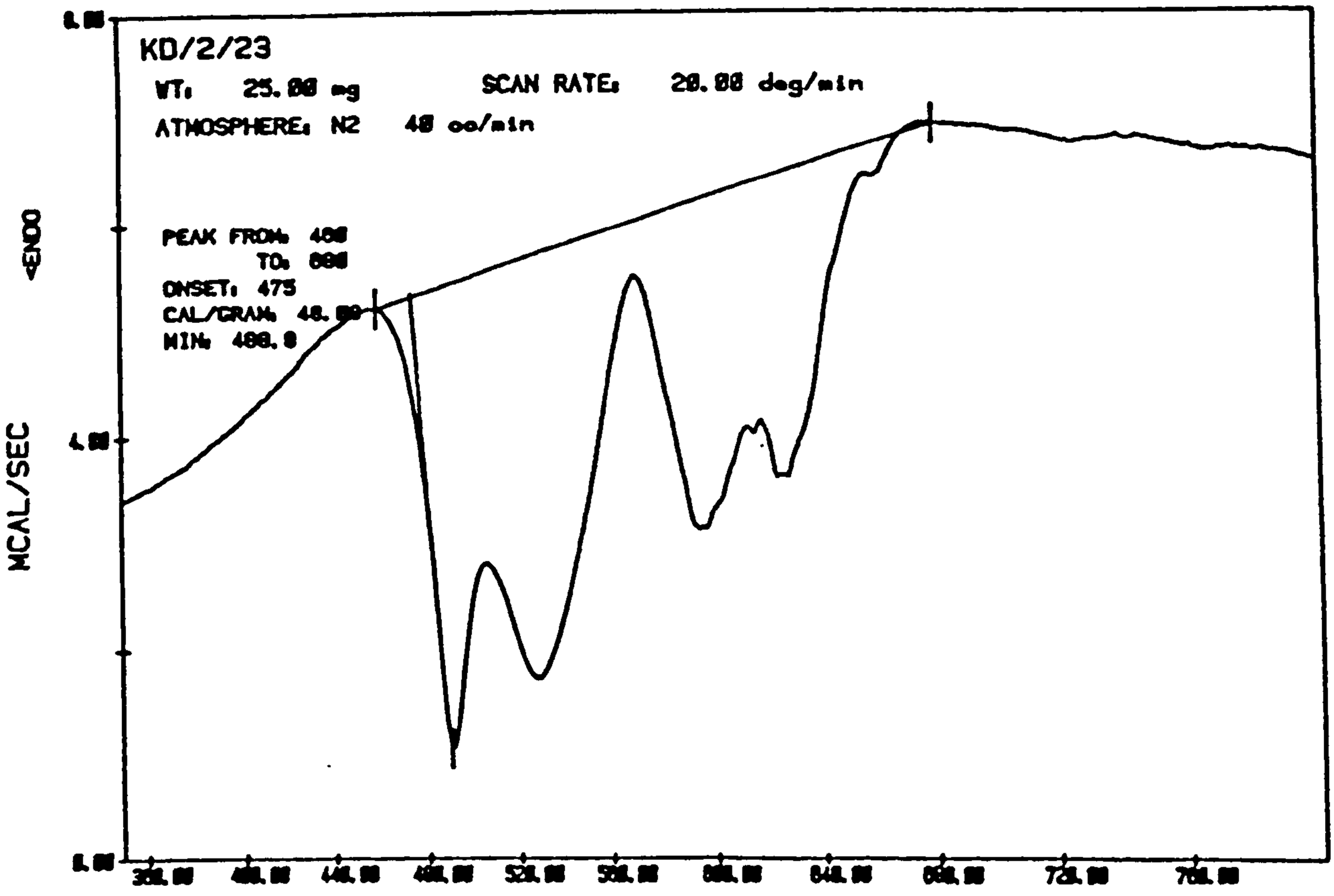

FIGURE 102B

DTA CURVE FOR FORMULATION KD 23 IN AIR ATMOSPHERE

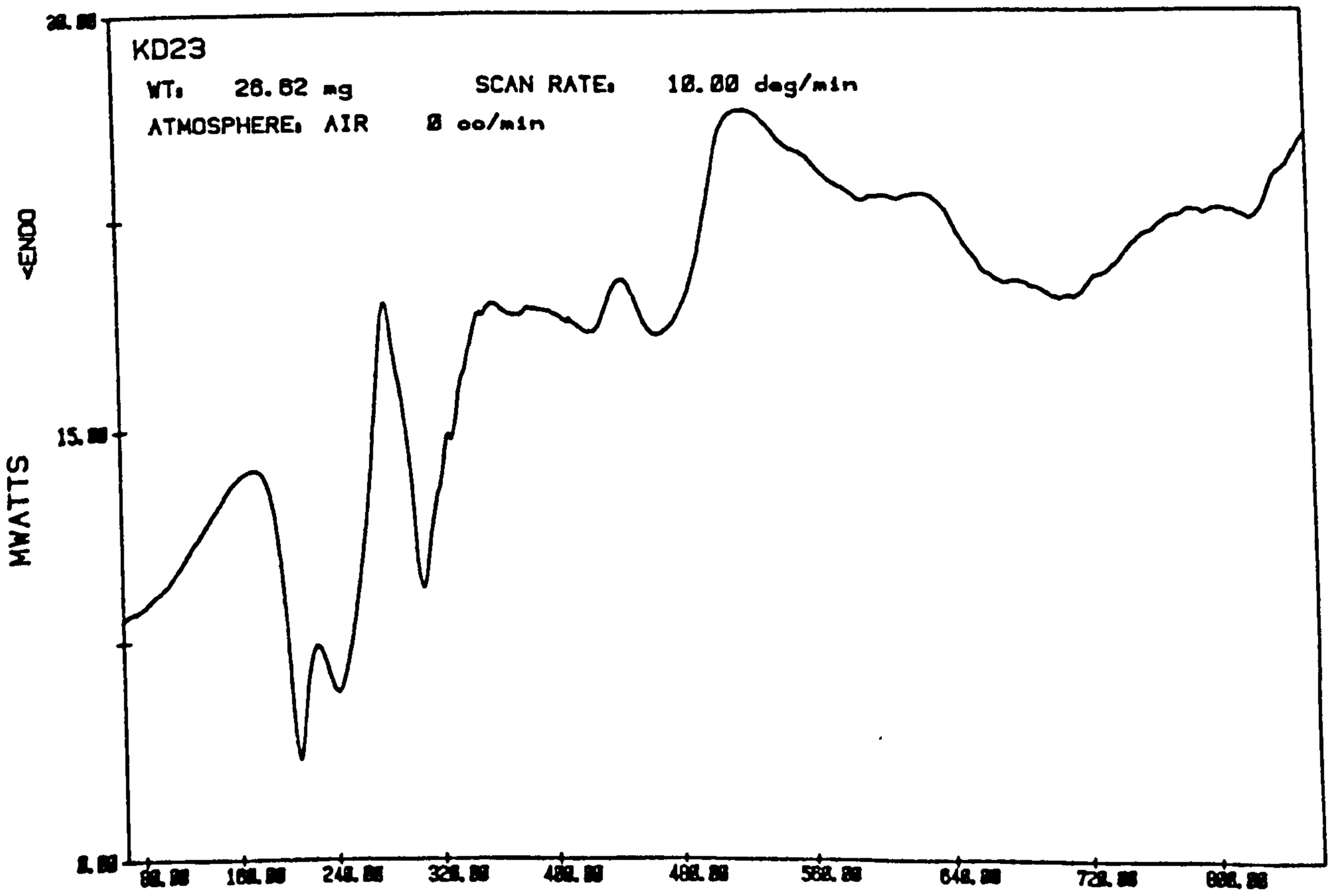

FIGURE 103A

STA CURVE FOR FORMULATION KD 23 IN NITROGEN ATMOSPHERE

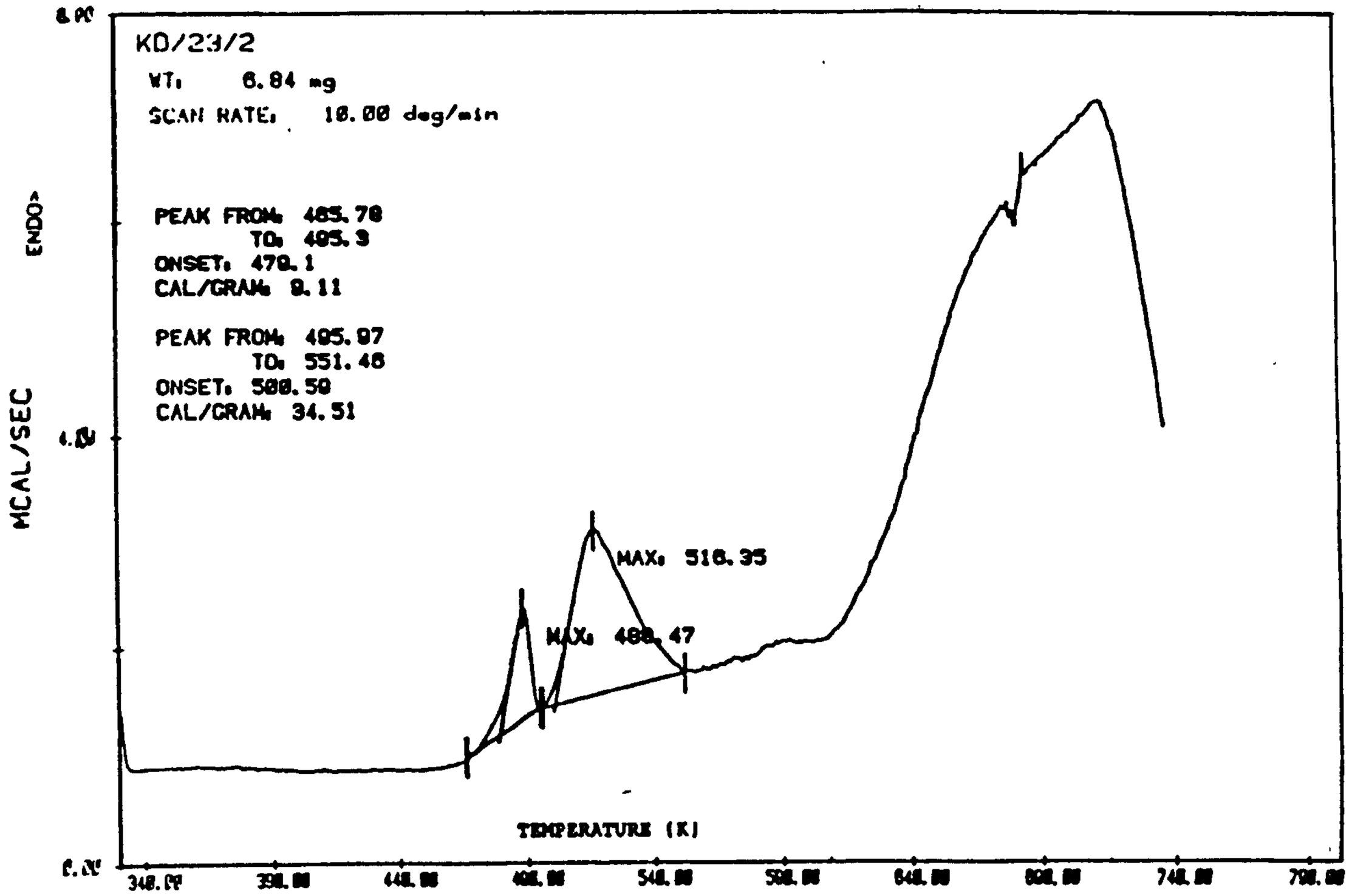

FIGURE 103B

STA CURVE FOR FORMULATION KD 23 IN AIR ATMOSPHERE

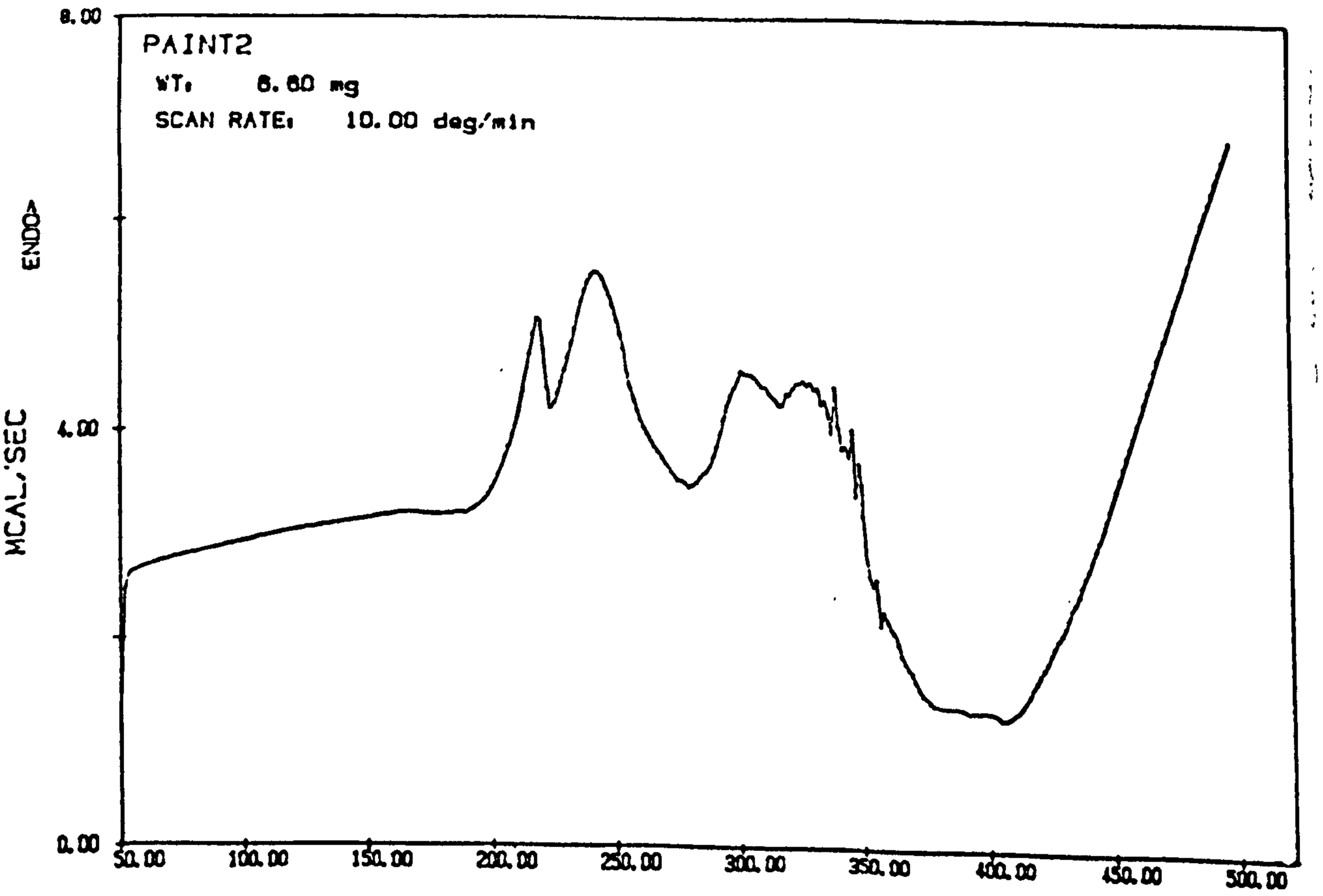

CC FILE: DSAVE.04

DATE: 88/01/08 TIME: 15:04

FIGURE 104

TGA CURVE FOR FORMULATION KD 23 IN NITROGEN ATMOSPHERE

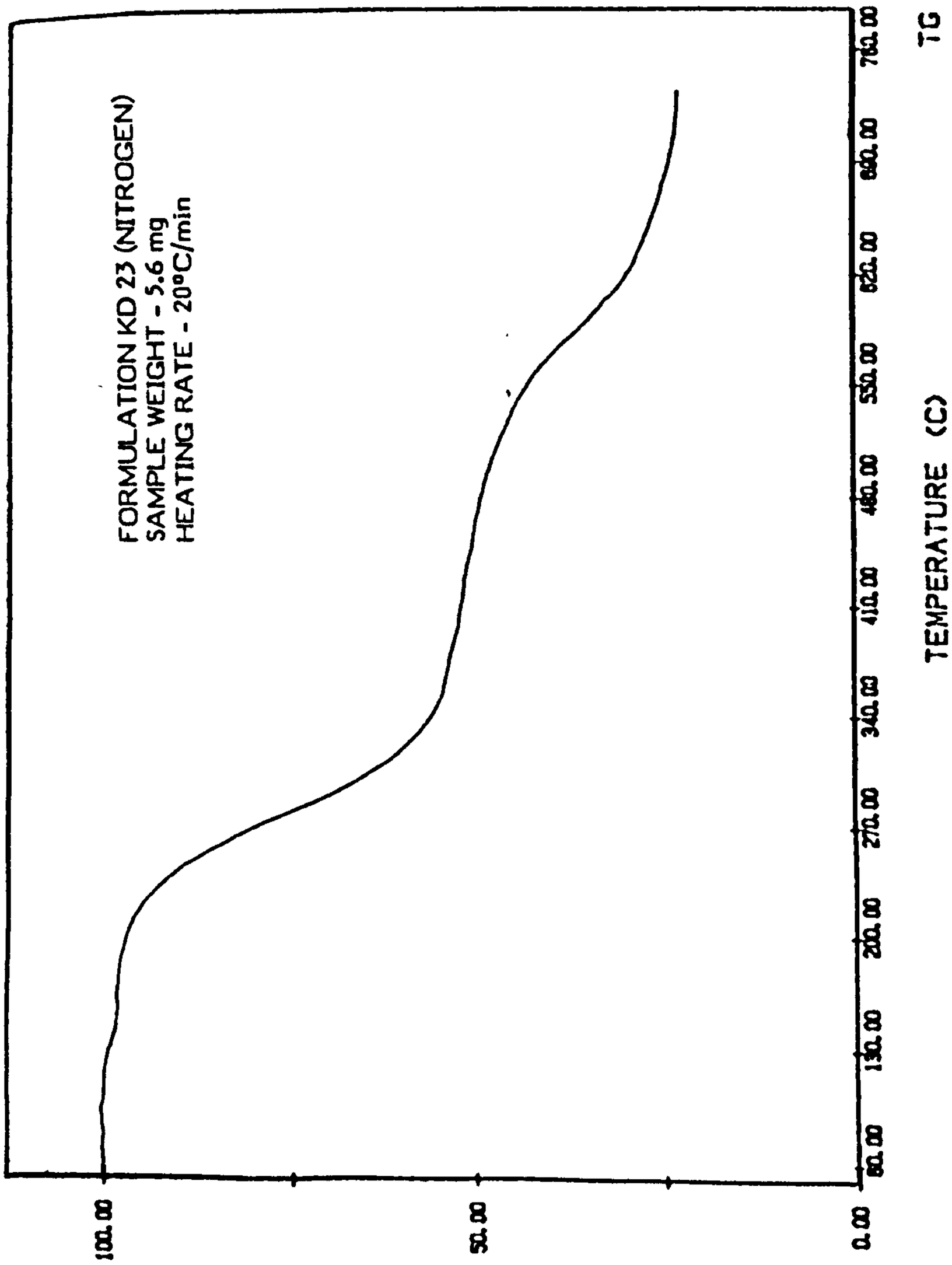

FIGURE 105

TGA CURVE FOR FORMULATION KD 23

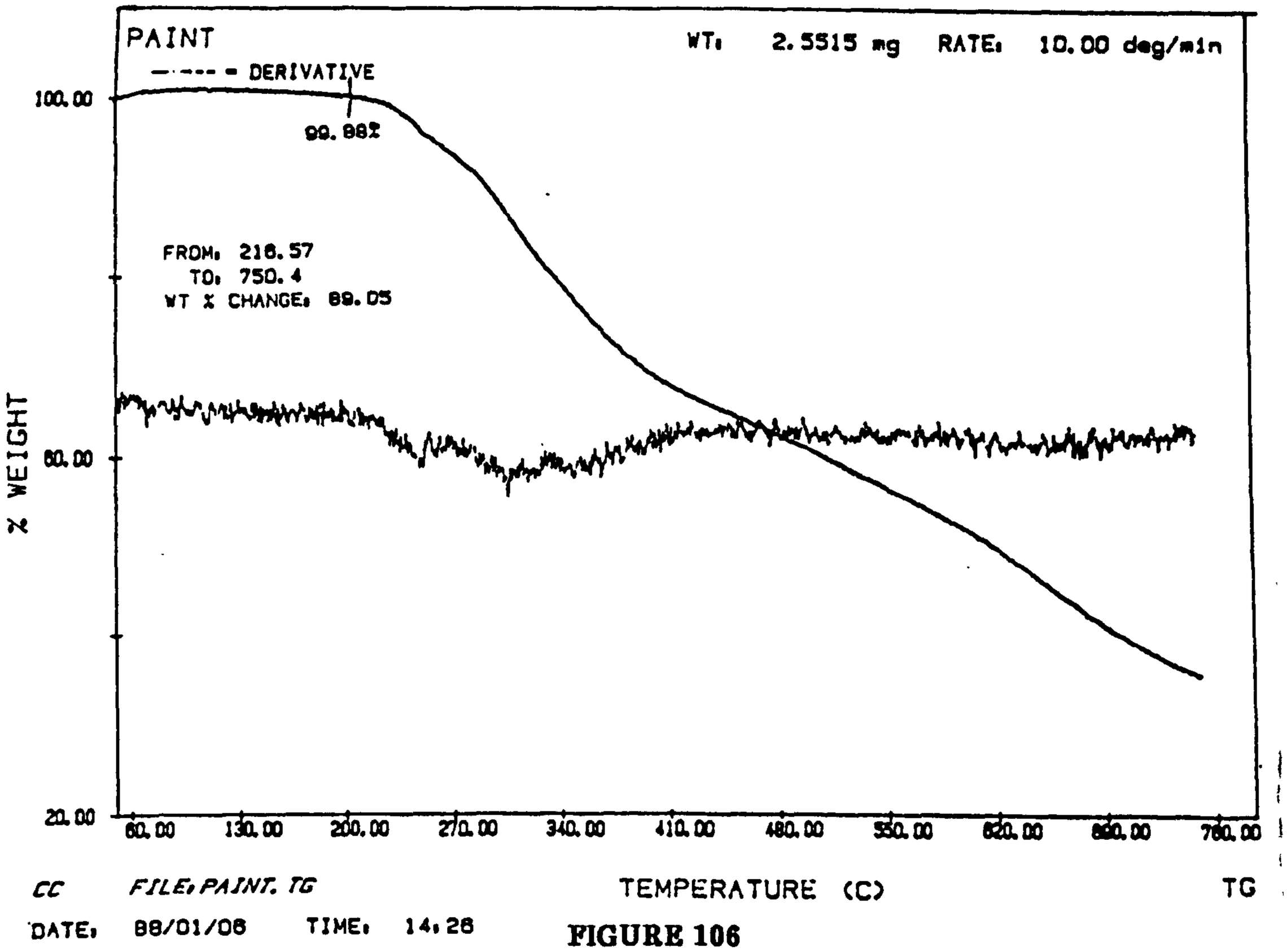

FIGURE 106

ELEMENTAL ANALYSIS FOR THE FORMULATION KD 23

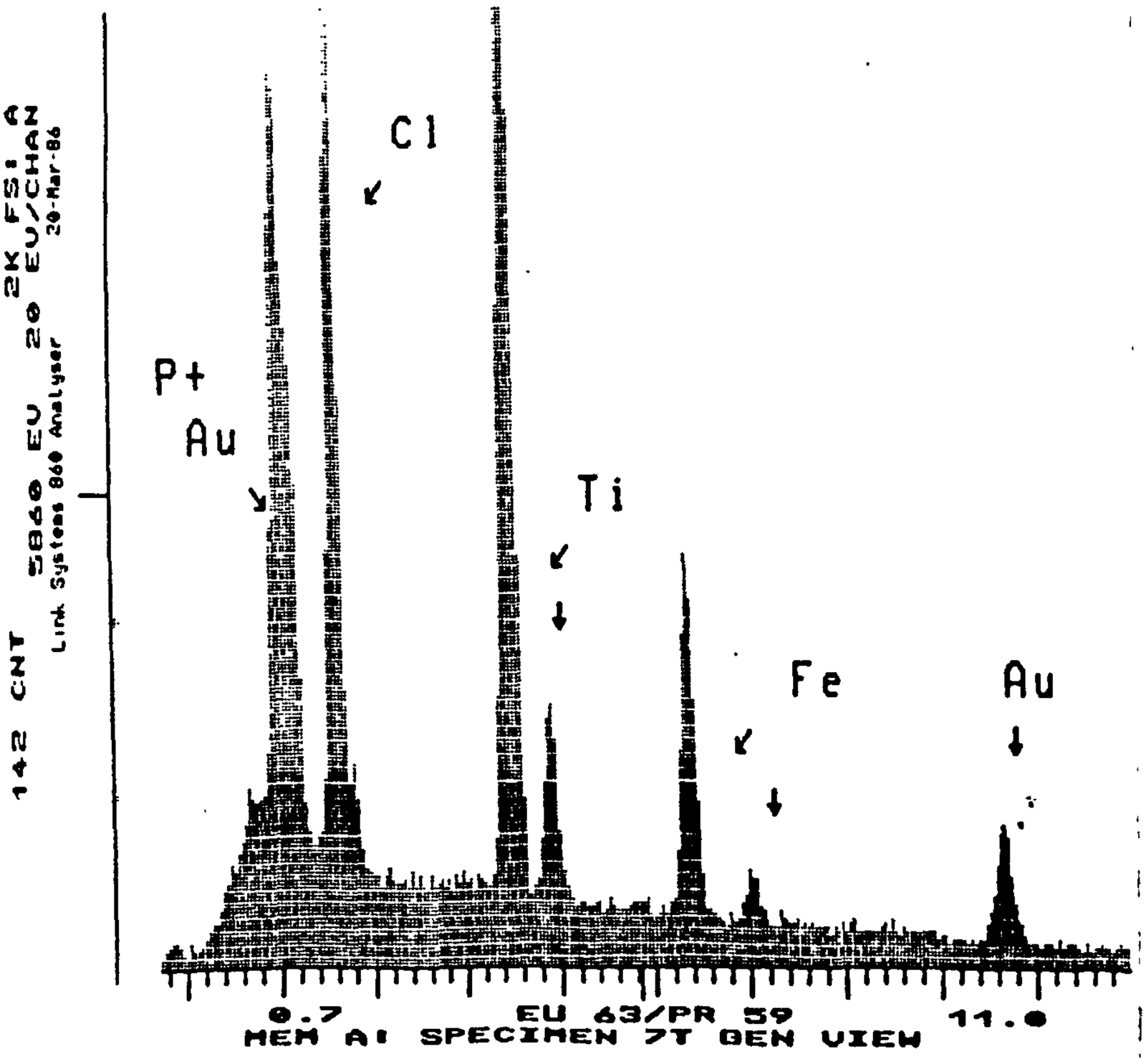

FIGURE 107A

INFRARED ABSORPTION OF A TYPICAL PAINT FORMULATION

BEFORE EXPOSURE

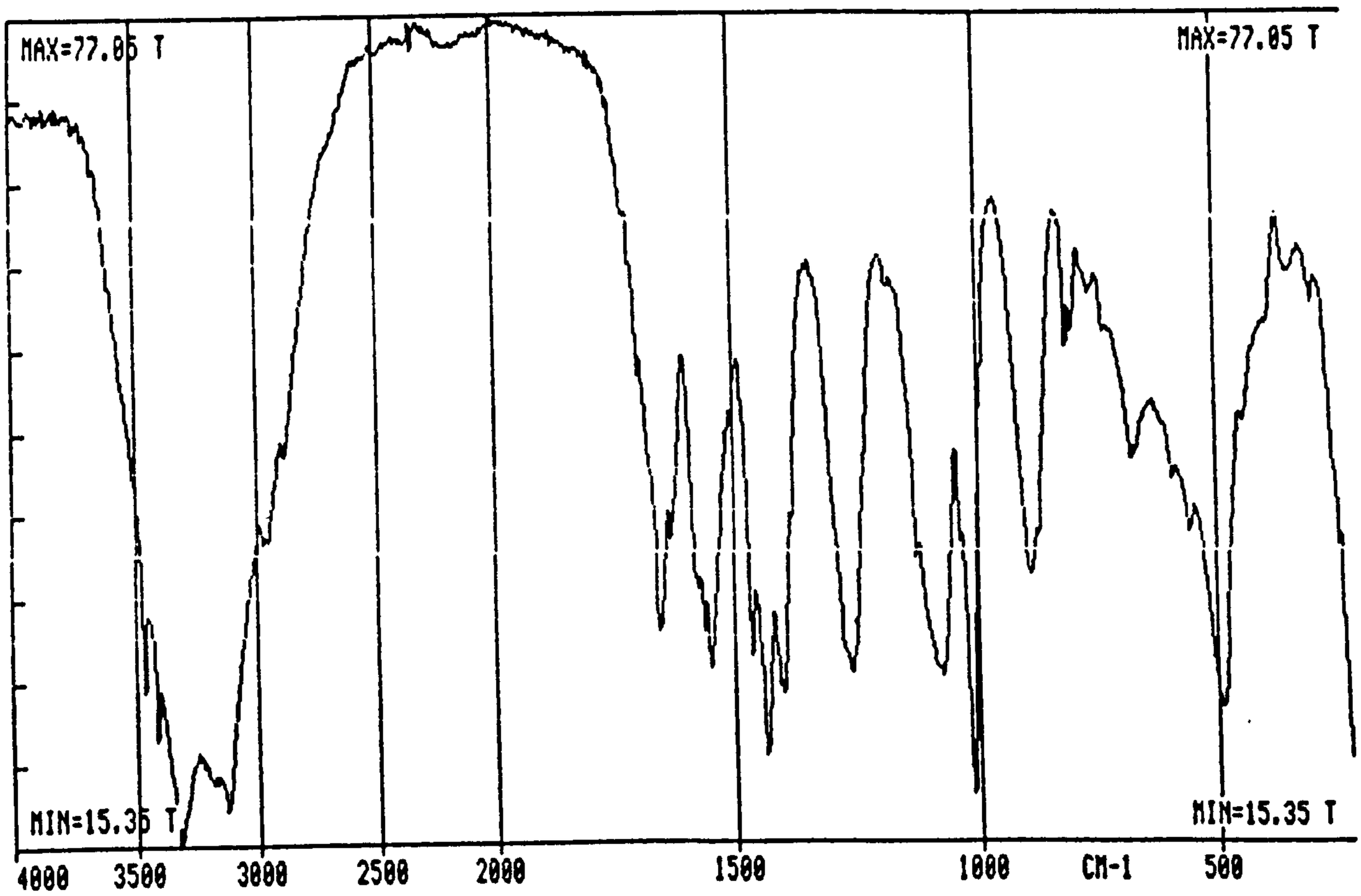

FIGURE 107B

AFTER EXPOSURE TO TEMPERATURE OF 100°C FOR 1 HOUR

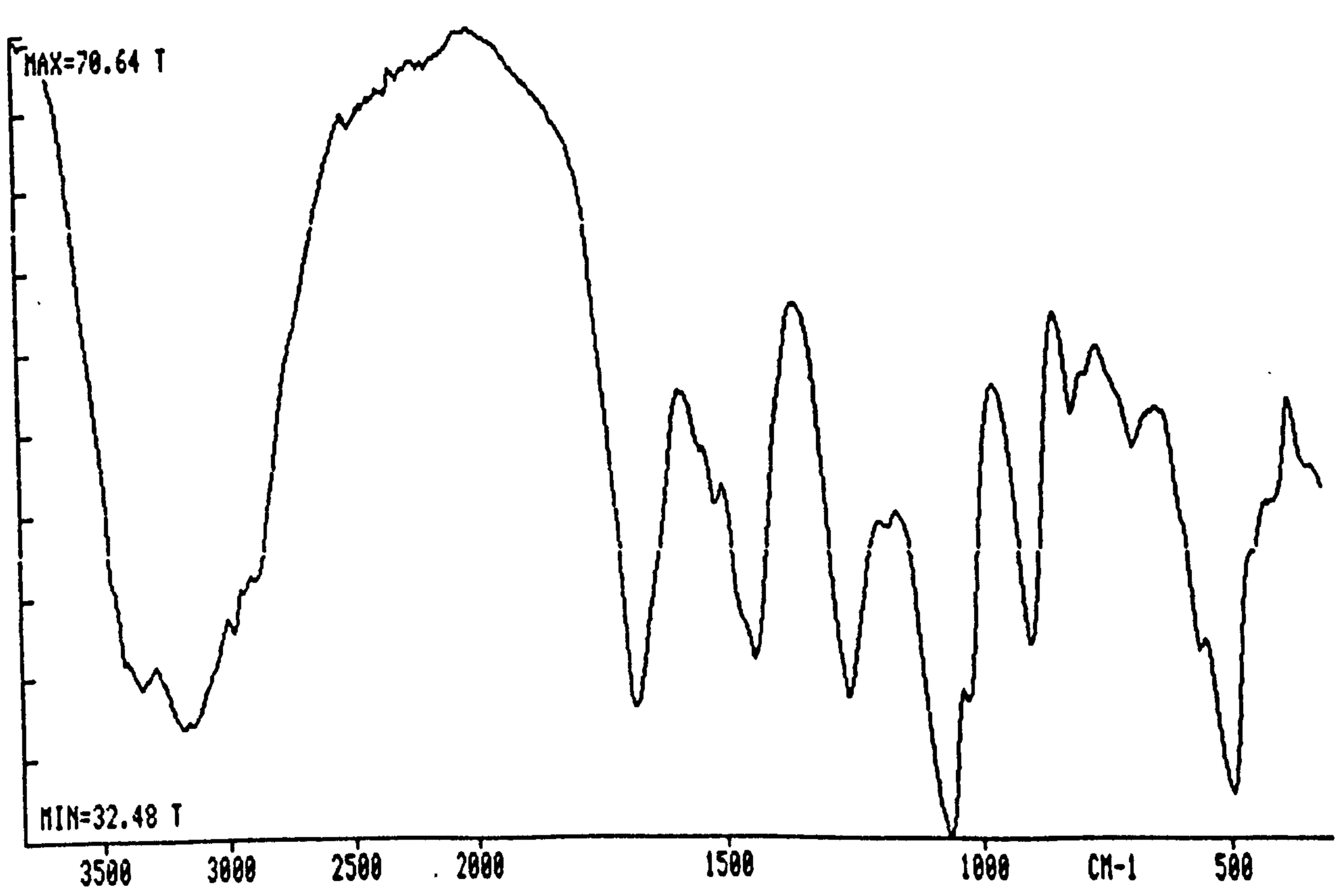

8.2. THERMAL EXPOSURE TEST

Steel plates were coated using the spreader technique described in Section 4 in order to make certain that the coating was of even thickness when dry. Before coating, all the steel plates were thoroughly cleaned using MEK/toluene mixture to remove any dirt or grease. The coated plates were left in a controlled atmosphere (20°C and 65% relative humidity) for at least 3 weeks before testing. The thickness was measured at various points over each plate and those whose thickness measurements had a standard deviation greater than 2 were rejected.

The coated test plates were weighed and then subjected to thermal radiation using the ISO ignitability apparatus described in Section 4. The coated steel plates were placed on a carrier plate with a Chromel/Alumel thermocouple attached to a copper disc, 5 mm diameter and 0.5 mm thick, at the centre of the test plate. The thermocouple was connected to a chart recorder which plotted the e.m.f. output against time. The thermocouple was calibrated using a standard system.

The following observations were recorded:

a) The time required for the onset of smoking.

b) The time taken to start bubbling (onset of intumescence).

c) The period of intumescence.

d) The time required for smoke evolution to stop.

e) The time required before oxidation of the char occurred.

After exposure, the plates were rapidly cooled, removed from the apparatus swiftly and placed in a freezer, this taking only a few seconds. The mass loss and thickness of the intumesced material were determined. Care was taken not to press the Elcometer gauge into the foam. The thickness of the char was recorded by taking 25 readings per plate, the maximum height was recorded.

Over a fixed proportion of each exposed plate, the top layer of char (black/grey material) was carefully removed and the weight and thickness of the coating remaining were recorded. Then the layer of partially charred material was removed, leaving the unreacted coating which was evident from its firmness and grey/white colour. The weight and thickness of this remaining material was also noted.

The material removed in both cases was carefully stored in glass bottles and kept for both elemental analysis and other analytical investigations (e.g. thermal analysis). The test plates were stored in sealed containers for further tests.

8.3. RESULTS OF EXPOSURE TO THERMAL RADIATION

8.3.1. ISOTHERMALLY TESTED PLATES

TABLE 19

PLATE NUMBER	EXPOSURE TIME/(min)	RADIATION LEVEL/($kW m^{-2}$)
1	1	20
3	10	20
4	30	20
5	3	20
7	2	20
8	5	20
10	4	20
11	6	20
12	7	20
14	5	60
15	2	60
16	1	60
17	60	60
18	1/2	60
19	3/4	60
21	30	10
23	1	40
24	3/4	40
25	2	40

8.3.2. CHAR THICKNESS OF THE PLATES EXPOSED TO VARIOUS RADIATIONS

NOMENCLATURE

N	number of readings taken
PN	plate number
BE	before exposure
AE	after exposure
AFR	after foam removal

8.3.2.1. CHAR THICKNESS OF THE PLATES EXPOSED AT 20kW/m²

TABLE 20

PLATE NO.		N	MEAN(mm)	σ_{n-1}	MAX.	MIN.
	BE	21	0.26	0.044	0.19	0.32
1	AE	20	0.228	0.064	0.40	0.15
	AFR					
	BE	20	0.268	0.029	0.34	0.23
3	AE	9	5.65	1.37	7.8	3.7
	AFR	6	0.05	0.011	0.06	0.03
	BE	21	0.263	0.028	0.34	0.22
4	AE	9	5.41	0.894	7.19	4.22
	AFR	11	0.035	0.016	0.07	0.02
	BE	20	0.25	0.04	0.31	0.17
5	AE	9	4.52	0.616	5.9	3.85
	AFR	7	0.063	0.029	0.11	0.03
	BE	17	0.17	0.032	0.24	0.10
7	AE	7	0.96	0.062	1.08	0.88
	AFR	8	0.088	0.039	0.18	0.07
	BE	18	0.196	0.029	0.3	0.15
8	AE	10	3.11	0.55	4.24	2.37
	AFR	11	0.033	0.014	0.07	0.02
	BE	20	0.192	0.047	0.33	0.15
10	AE	9	2.25	0.61	3.37	1.63
	AFR	11	0.108	0.031	0.18	0.08
	BE	18	0.199	0.042	0.33	0.13
11	AE	8	2.978	0.599	3.76	1.99
	AFR	9	0.046	0.019	0.08	0.02
	BE	20	0.187	0.023	0.24	0.14
12	AE	10	2.77	0.73	4.23	2.1
	AFR	10	0.074	0.023	0.11	0.04

8.3.2.2. CHAR THICKNESS FOR PLATES EXPOSED AT 40kW/m^2

TABLE 21

PLATE NO.		N	MEAN(mm)	σ_{n-1}	MAX.	MIN.
	BE	17	0.247	0.456	0.30	0.19
21	AE	18	0.226	0.045	0.30	0.16
	BE	17	0.205	0.070	0.34	0.13
23	AE	6	6.8	0.73	7.8	6.08
	AFR	5	0.16	0.005	0.02	0.01
	BE	17	0.15	0.035	0.21	0.09
24	AE	8	0.21	0.05	0.28	0.15
	BE	17	0.20	0.028	0.26	0.17
25	AE	6	6.1	0.727	6.90	5.14
	AFR	6	0.028	0.011	0.05	0.02

8.3.2.3. CHAR THICKNESS FOR PLATES EXPOSED AT 60kW/m^2

TABLE 22

PLATE NO.		N	MEAN(mm)	σ_{n-1}	MAX.	MIN.
	BE	17	0.17	0.022	0.21	0.13
(14)	AE	11	3.49	0.698	4.46	2.55
	AFR	8	0.026	0.005	0.03	0.02
	BE	17	0.198	0.018	0.23	0.17
(15)	AE	10	3.619	0.683	5.29	2.84
	AFR	8	0.095	0.017	0.12	0.07
	BE	16	0.233	0.036	0.30	0.16
(16)	AE	8	5.66	0.679	6.32	4.47
	AFR	7	0.054	0.011	0.07	004
	BE	17	0.246	0.030	0.29	0.20
(17)	AE	5	4.74	1.19	6.3	3.20
	AFR	7	0.007	0.0075	0.02	0.00
	BE	17	0.29	0.037	0.036	0.023
(18)	AE	6	2.10	0.117	2.30	2.01
	AFR	9	0.27	0.016	0.29	0.25
	BE	18	0.175	0.029	0.24	0.13
(19)	AE	6	2.755	0.581	3.66	2.18
	AFR	7	0.171	0.023	0.20	0.14

8.3.2.4. THERMAL DATA OF PLATES EXPOSED TO VARIOUS RADIATIONS

TABLE NO. 23

Plate Number	Exposure Time (mins)	Foam Height (mm)	Expansion Factor AE/BE	Expansion Factor BE-AFR / AE	Weight Loss (g)
20kW/m²					
1	1	0.228	0.88	0.88	0.06
7	2	0.96	5.6	11.7	0.25
5	3	4.52	18.1	24.17	0.52
10	4	2.25	11.72	26.78	0.32
8	5	3.11	15.90	19.08	0.40
11	6	2.978	14.96	19.46	0.52
12	7	2.77	14.81	24.51	0.62
3	10	5.56	21.10	25.92	0.78
4	30	5.41	20.60	23.73	0.78
40kW/m²					
24	½	0.21	1.40	1.4	0.01
23	1	6.81	33.17	151.1	0.60
25	2	6.1	30.5	35.47	0.61
60kW/m²					
18	0.5	2.10	7.24	105	0.22
19	0.75	2.755	15.74	688	0.24
16	1	5.66	24.29	32	0.60
15	2	3.619	18.29	35	0.54
14	5	3.49	20.53	24	0.98
17	60	4.74	19.27	20	1.08

FIGURE 108

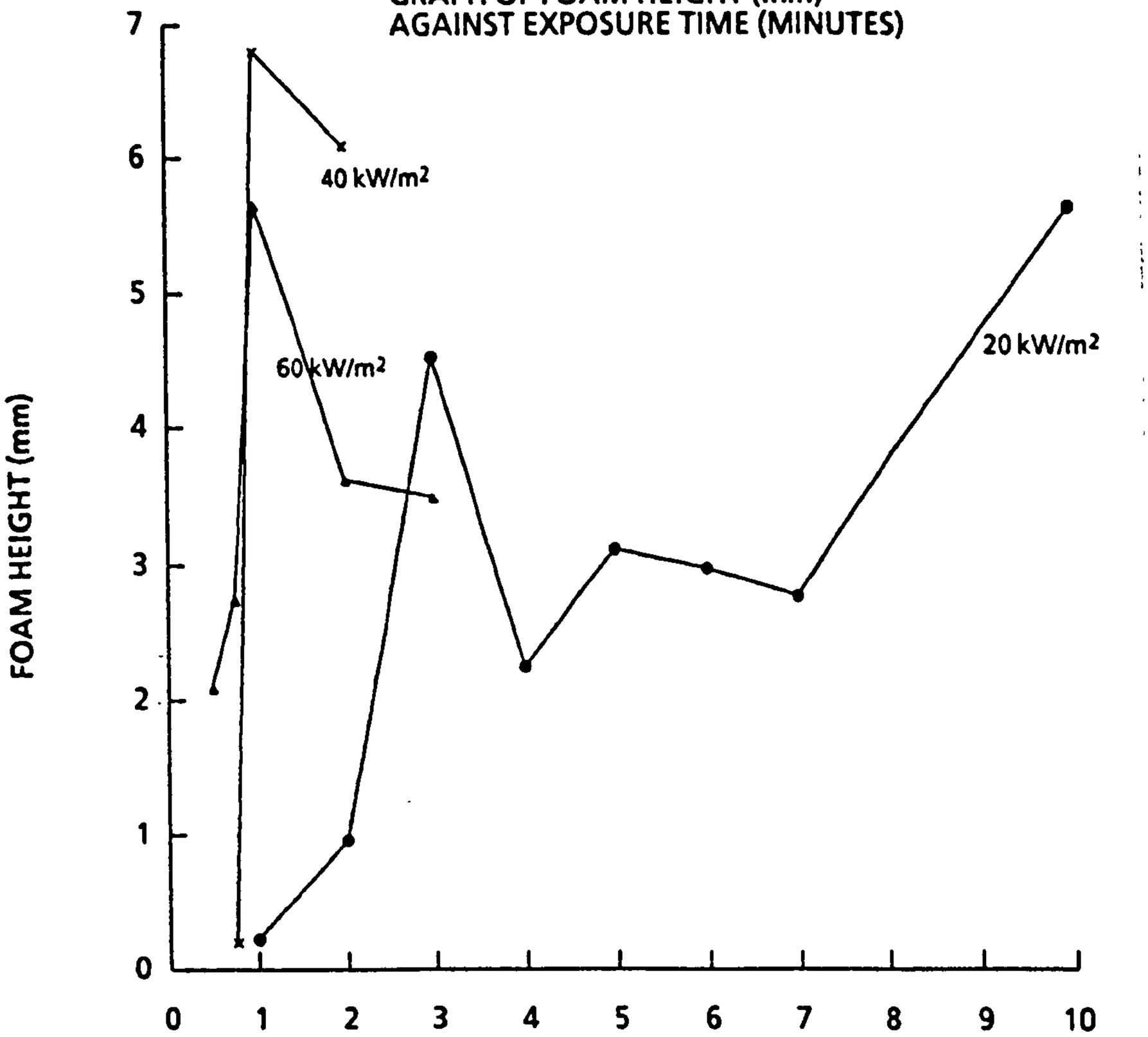

FIGURE 109

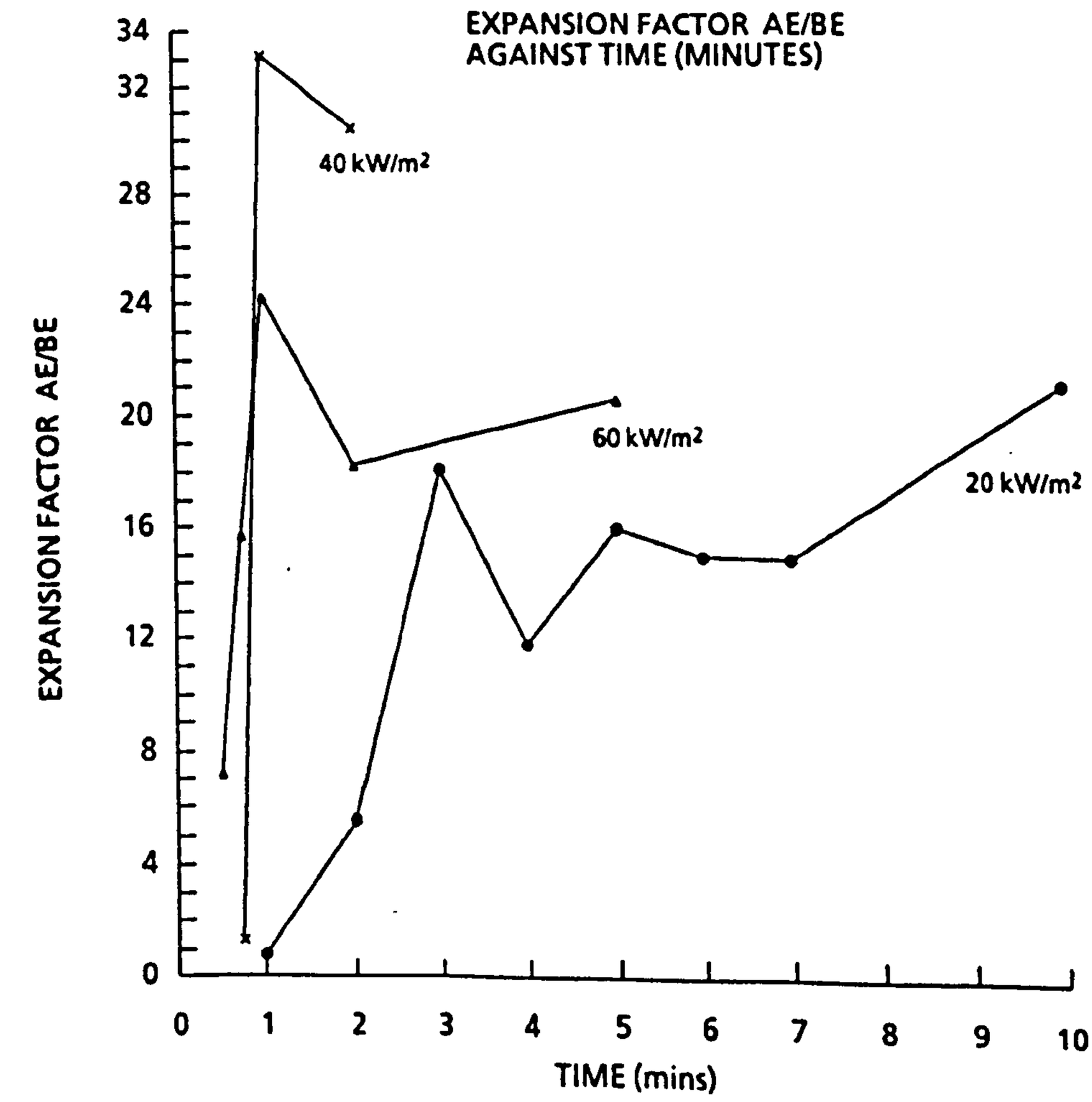

FIGURE 110

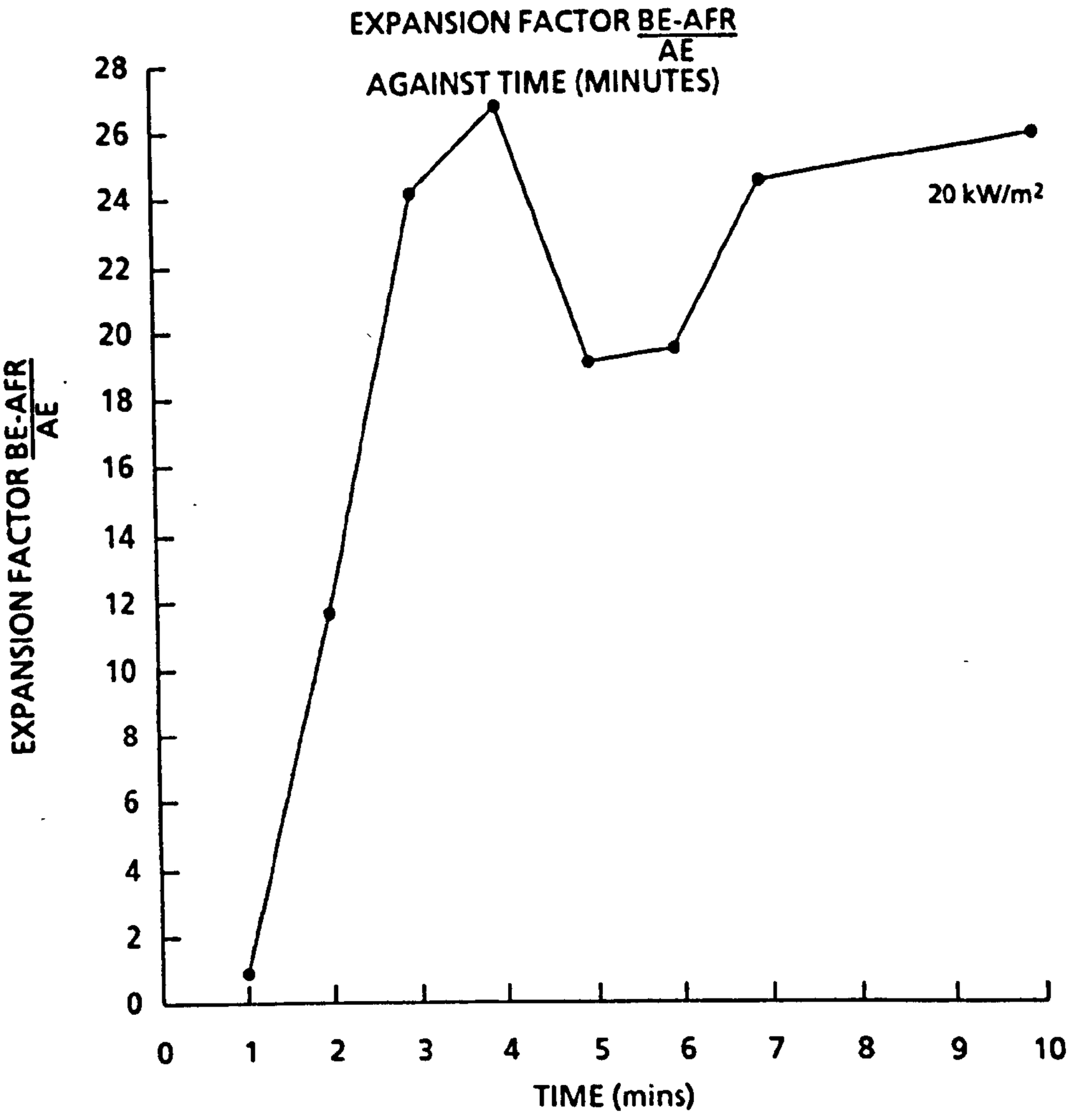

FIGURE 111

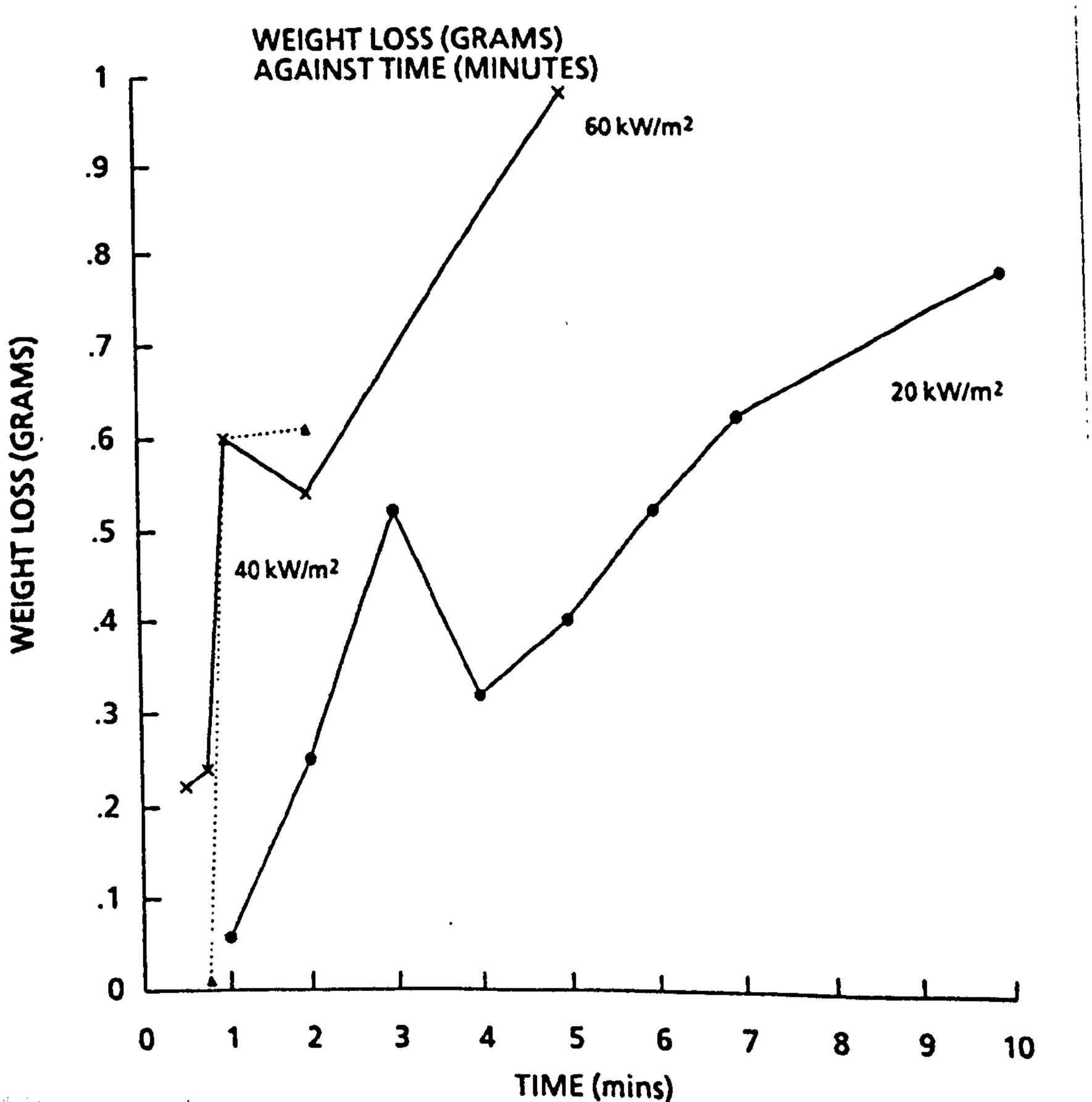

8.4. A TYPICAL SET OF RESULTS FOR A PLATE EXPOSED TO RADIATION

Plate No: 17

Radiation level 60kWm^{-2}, Exposure time: 60 mins

Heater Control Setting: 815, Heater temperature: 826°C

Indicated temperature: 831°C

Initial weight: 105.82 g, Final weight: 105.22 g

Initial thickness 0.205 mm, Final thickness 6.8 mm

Thickness after foam removal 0.16 mm

Observations during radiation of plate during exposure

TIME:	OBSERVATION:
20 seconds	Small bubbles begin to form on surface.
40 seconds	Slight smoke emission.
60 seconds	Large build up of smoke.
70 seconds	Paint begins to discolour, white to yellow/brown
90 seconds	Large bubbles form on surface.
110 seconds	Surface reaction occurs, considerable smoke emission and vigorous bubbling.
120 seconds	Black char forms.
140 seconds	Foaming along with continued smoke emission.
220 seconds	Foam formed. Reaction reaching completion.
10 minutes	The remaining foam is very even with no delamination. Surface of foam turning white.
15 minutes	Smoke gradually ceasing, foam surface completely white.
20 minutes	Foam at the edges showing signs of delamination.
25 minutes	Foam texture turning into a fluffy white ash with very little integerity and continuity.
30 minutes	Foam completely loose off the plate without any strength left.

FIGURE 112

SUBSTRATE TEMPERATURE - TIME HISTORIES FOR FORMULATION KD23 AFTER EXPOSURE TO VARIOUS HEAT RADIATIONS

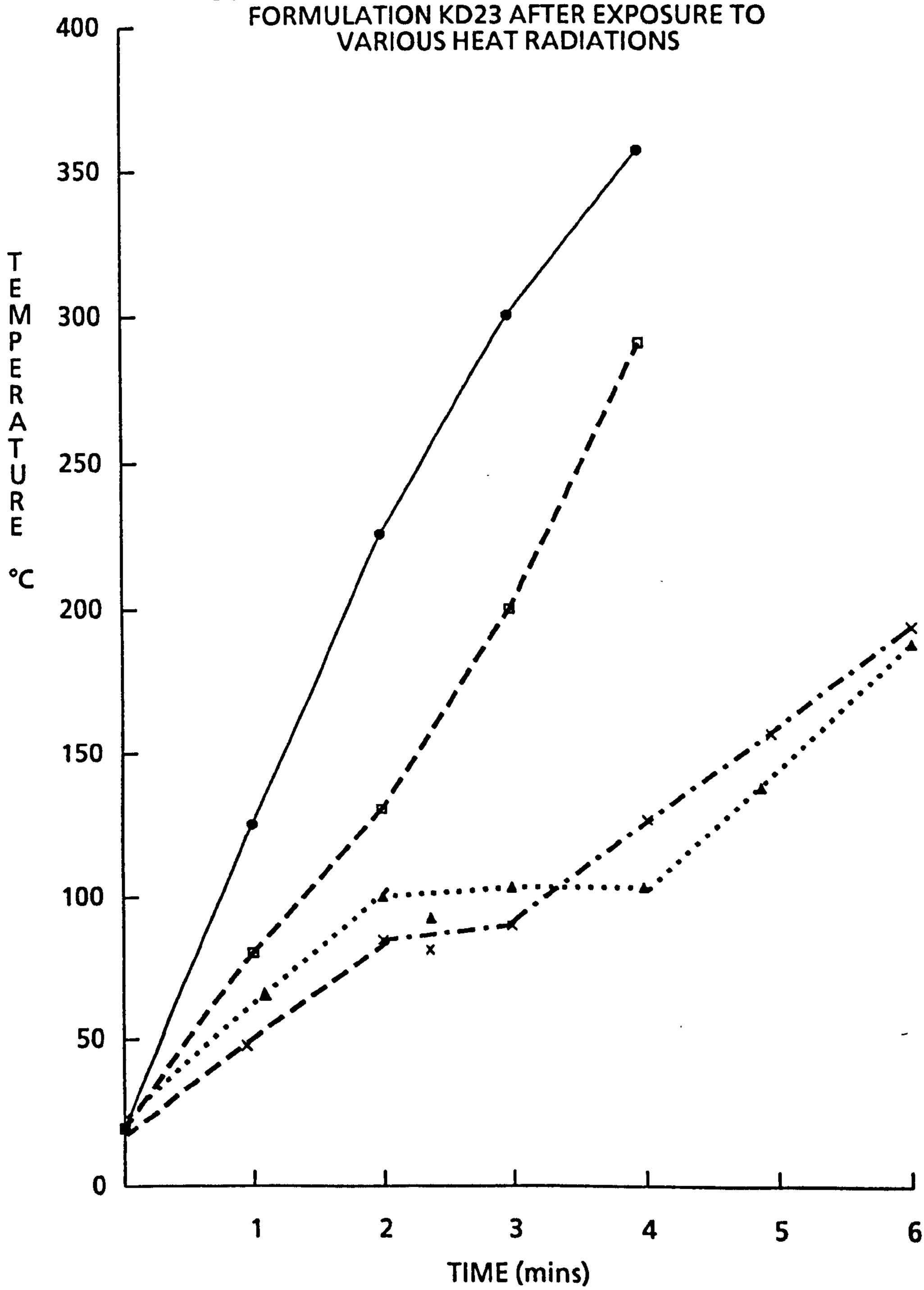

8.5. THERMAL ANALYSIS DATA FOR FORMULATION KD 23 AFTER EXPOSURE TO VARIOUS HEAT RADIATIONS

Thermal analysis using DTA, DSC and STA were conducted on the compound left after scraping off the top intumesced layer and on the material left at the bottom of the plates after further scraping off. Typical DSC and STA curves for the materials from the plates exposed to 20kW/m^2 for various periods are given in Fig. 113-121. Fig. 122-129 gives the typical curves for DSC and STA for the plates exposed to 60kW/m^2. Fig. 130 gives typical STA curves for top and bottom layers of intumescence from plate no. 11 after exposure.

FIGURE 113

PLATE NUMBER 1 AFTER EXPOSURE TO 20kW/m^2 FOR 1 MINUTE

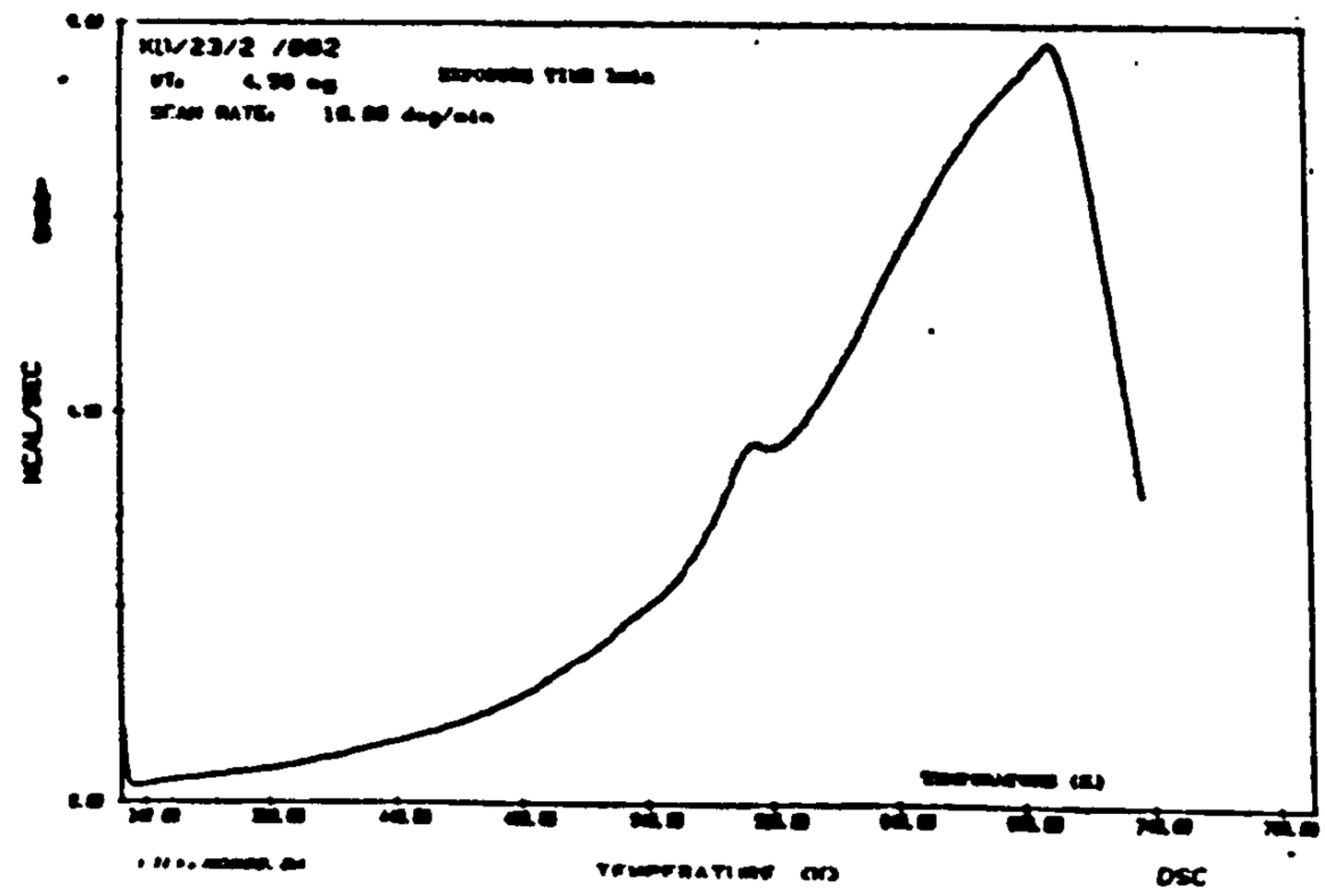

FIGURE 114

A TYPICAL TGA CURVE FOR PLATE NO. 1 AFTER EXPOSURE

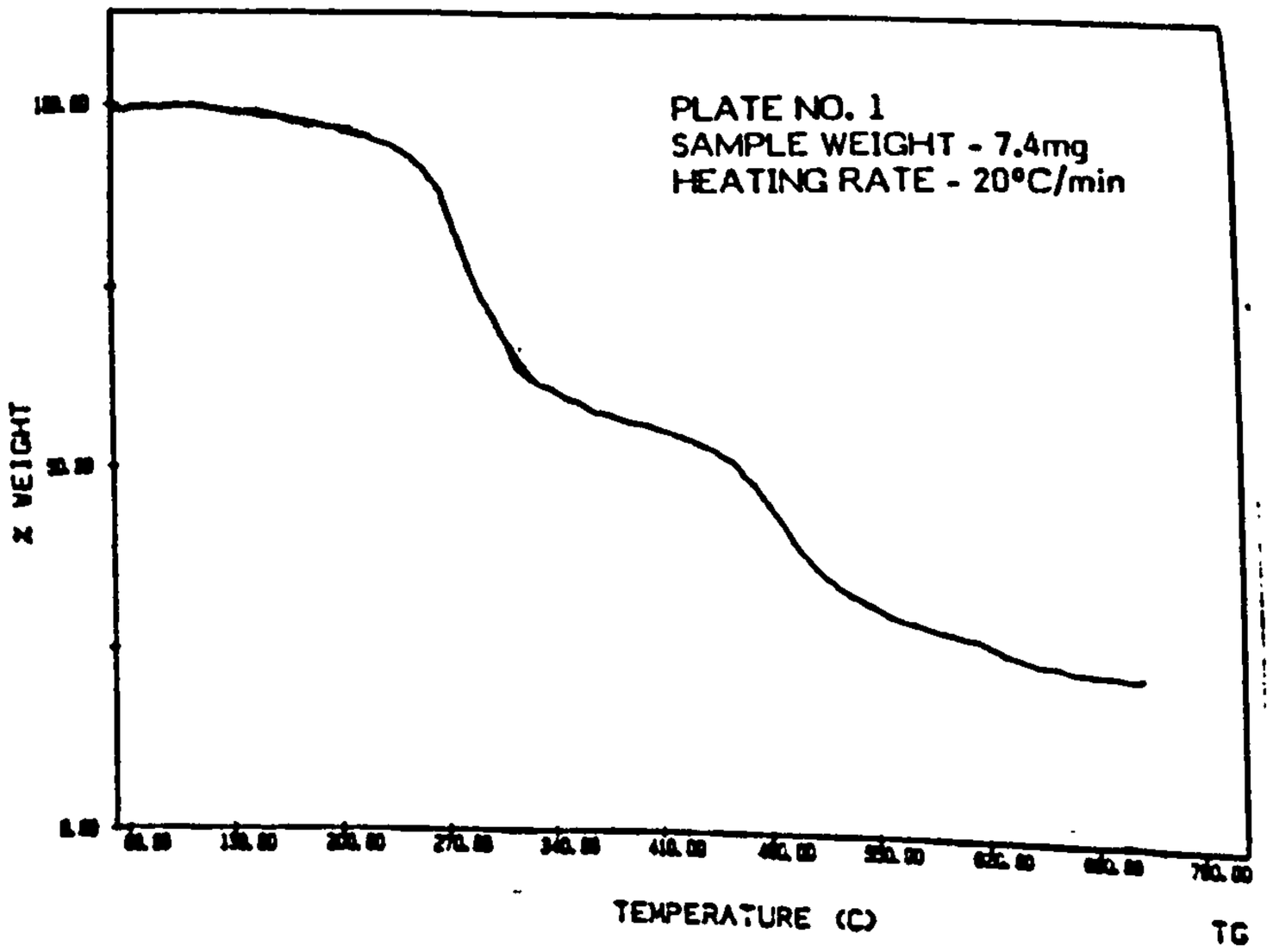

FIGURE 115

TOP LAYER OF INTUMESCENCE FROM PLATE NUMBER 7

AFTER EXPOSURE TO 20kW/m^2 FOR 2 MINUTES

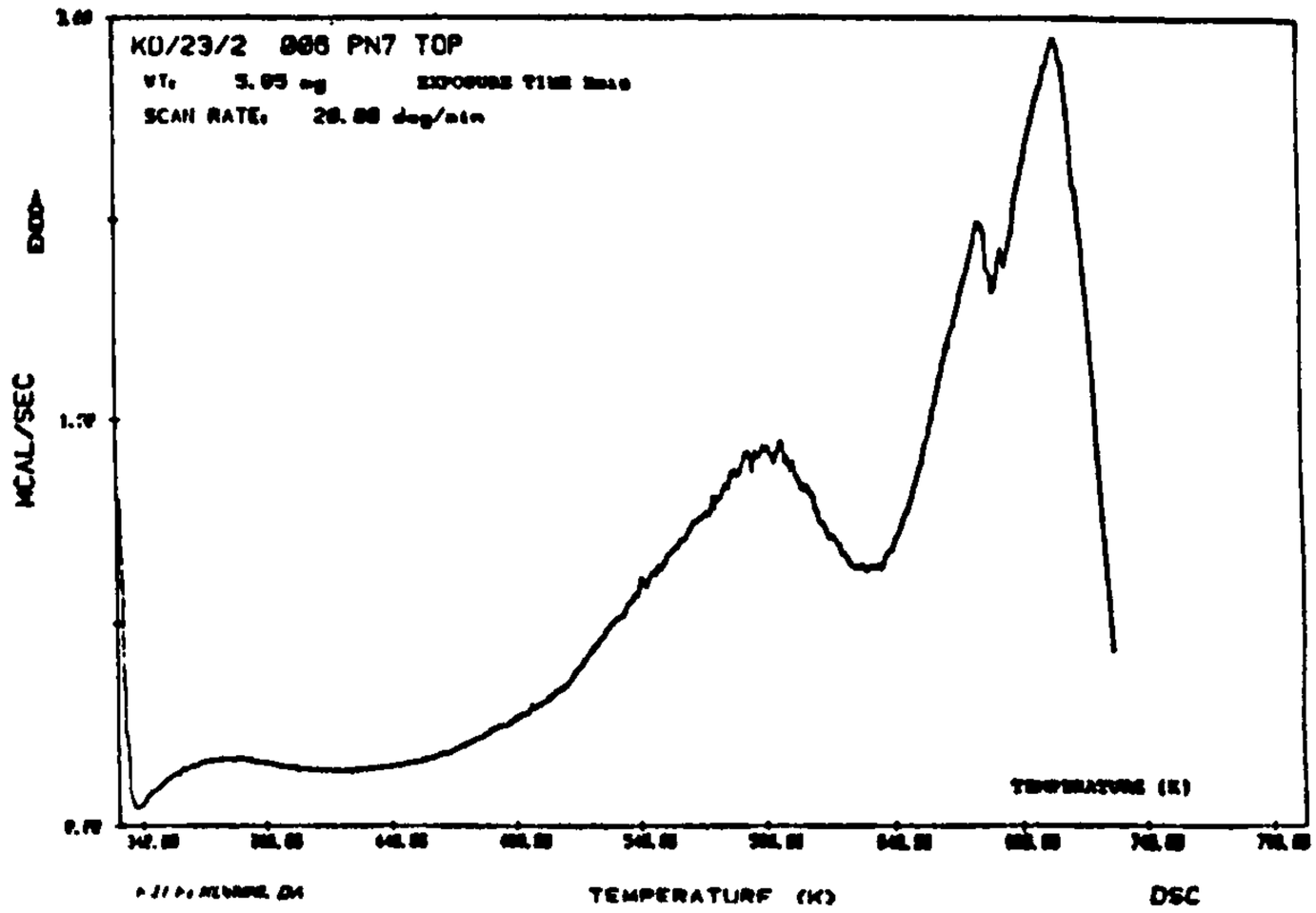

FIGURE 116

TOP LAYER OF INTUMESCENCE FROM PLATE NUMBER 10

AFTER EXPOSURE TO 20kW/m^2 FOR 4 MINUTES

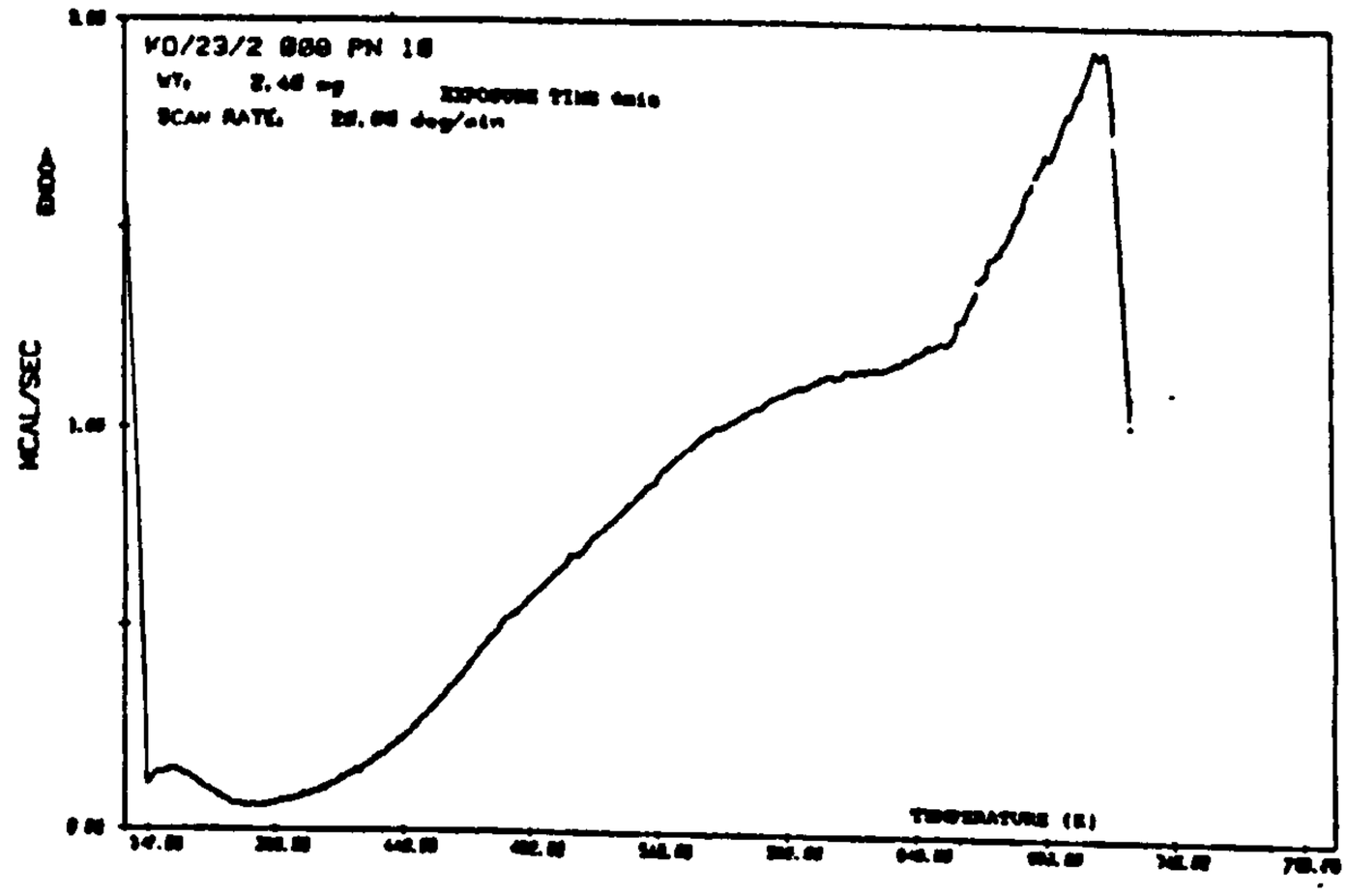

FIGURE 117

TOP LAYER OF INTUMESCENCE FROM PLATE NUMBER 11

AFTER EXPOSURE TO 20kW/m^2 FOR 6 MINUTES

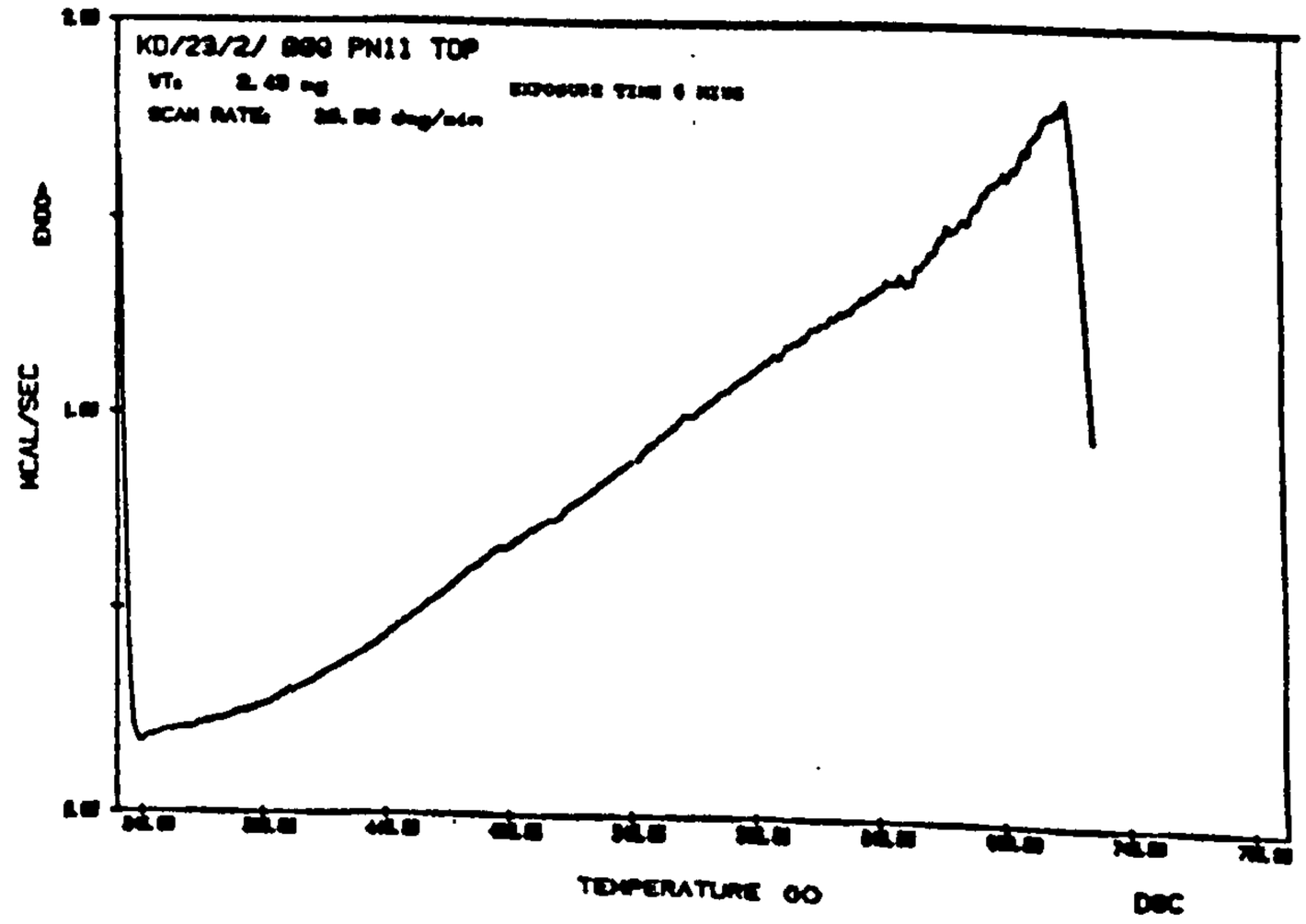

FIGURE 118

BOTTOM LAYER OF INTUMESCENCE FROM PLATE NUMBER 11 AFTER EXPOSURE TO 20kW/m^2 FOR 6 MINUTES

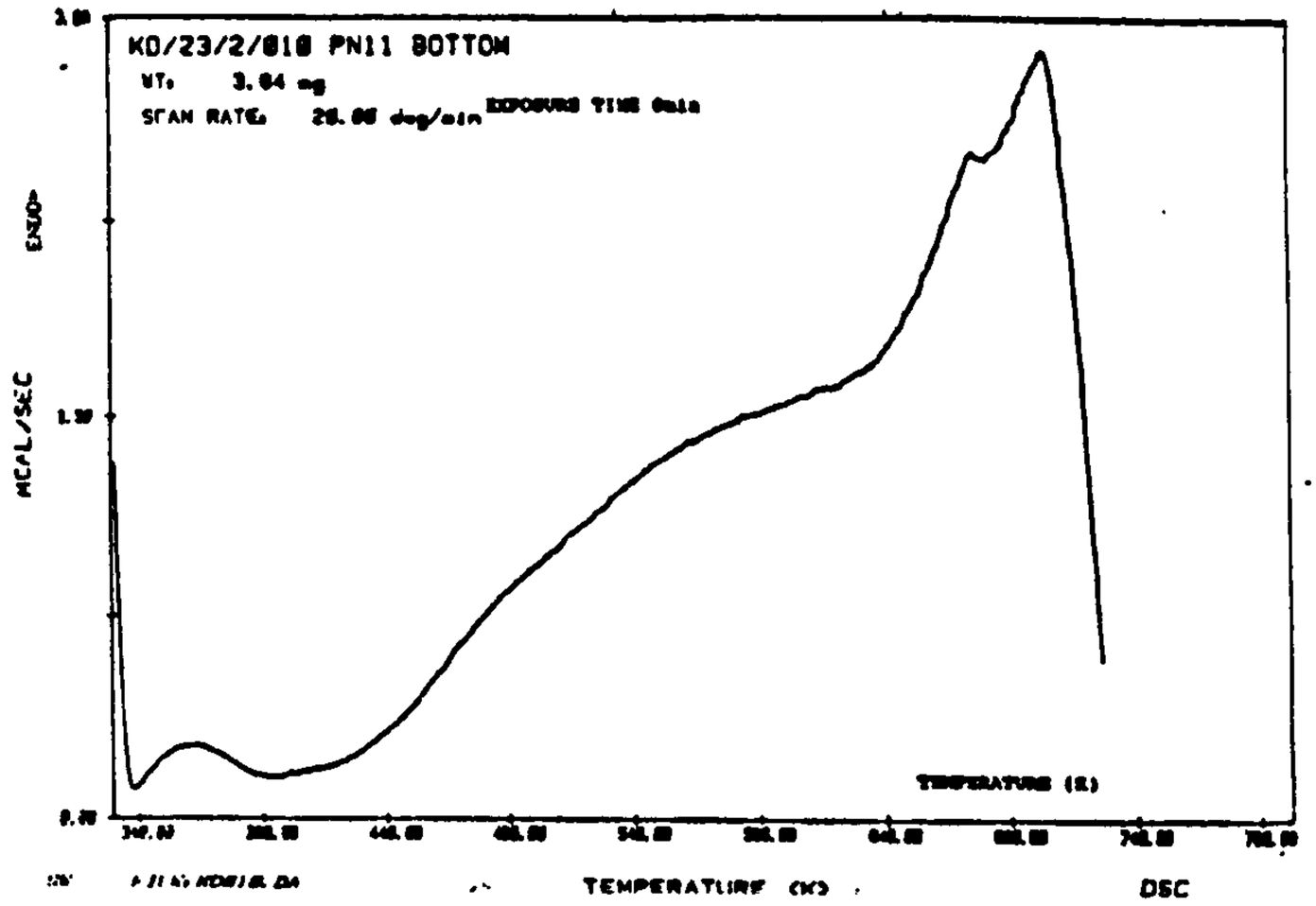

FIGURE 119

TOP LAYER OF INTUMESCENCE FROM PLATE NUMBER 12 AFTER EXPOSURE TO 20kW/m^2 FOR 7 MINUTES

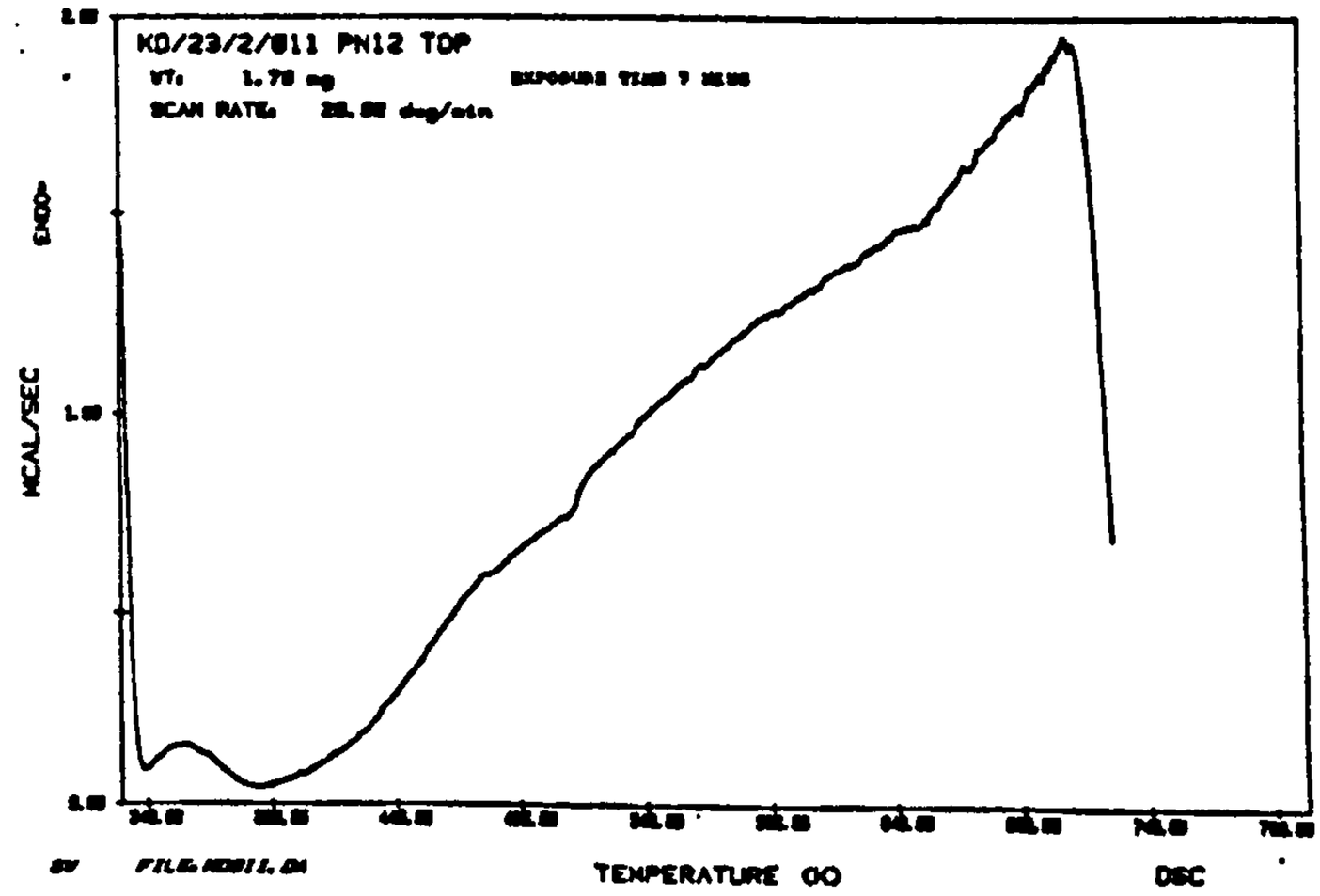

FIGURE 120

BOTTOM LAYER OF INTUMESCENCE FROM PLATE NUMBER 12 AFTER EXPOSURE TO 20kW/m^2 FOR 7 MINUTES

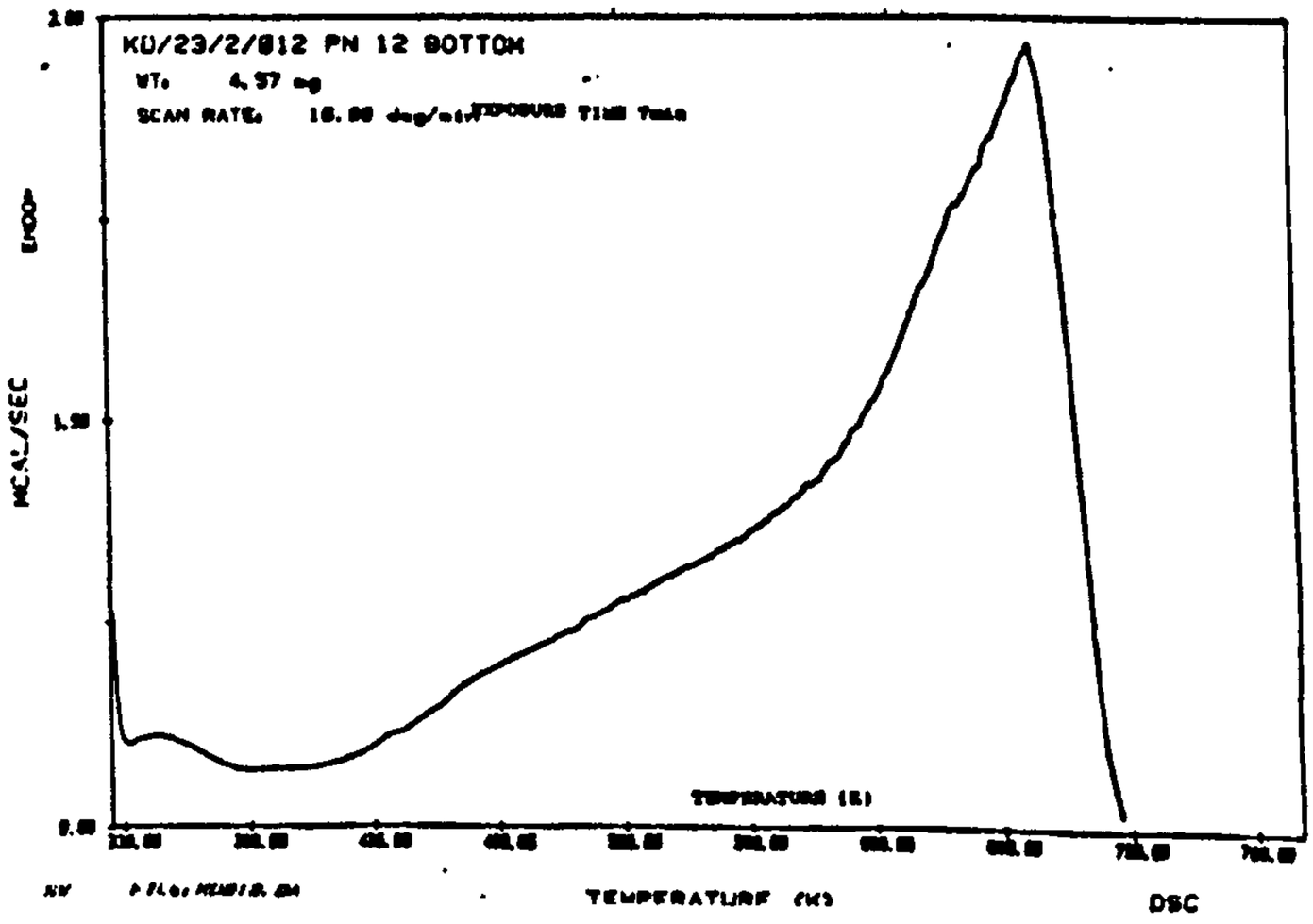

FIGURE 121

TOP LAYER OF INTUMESCENCE FROM PLATE NUMBER 4

AFTER EXPOSURE TO 20kW/m^2 FOR 30 MINUTES

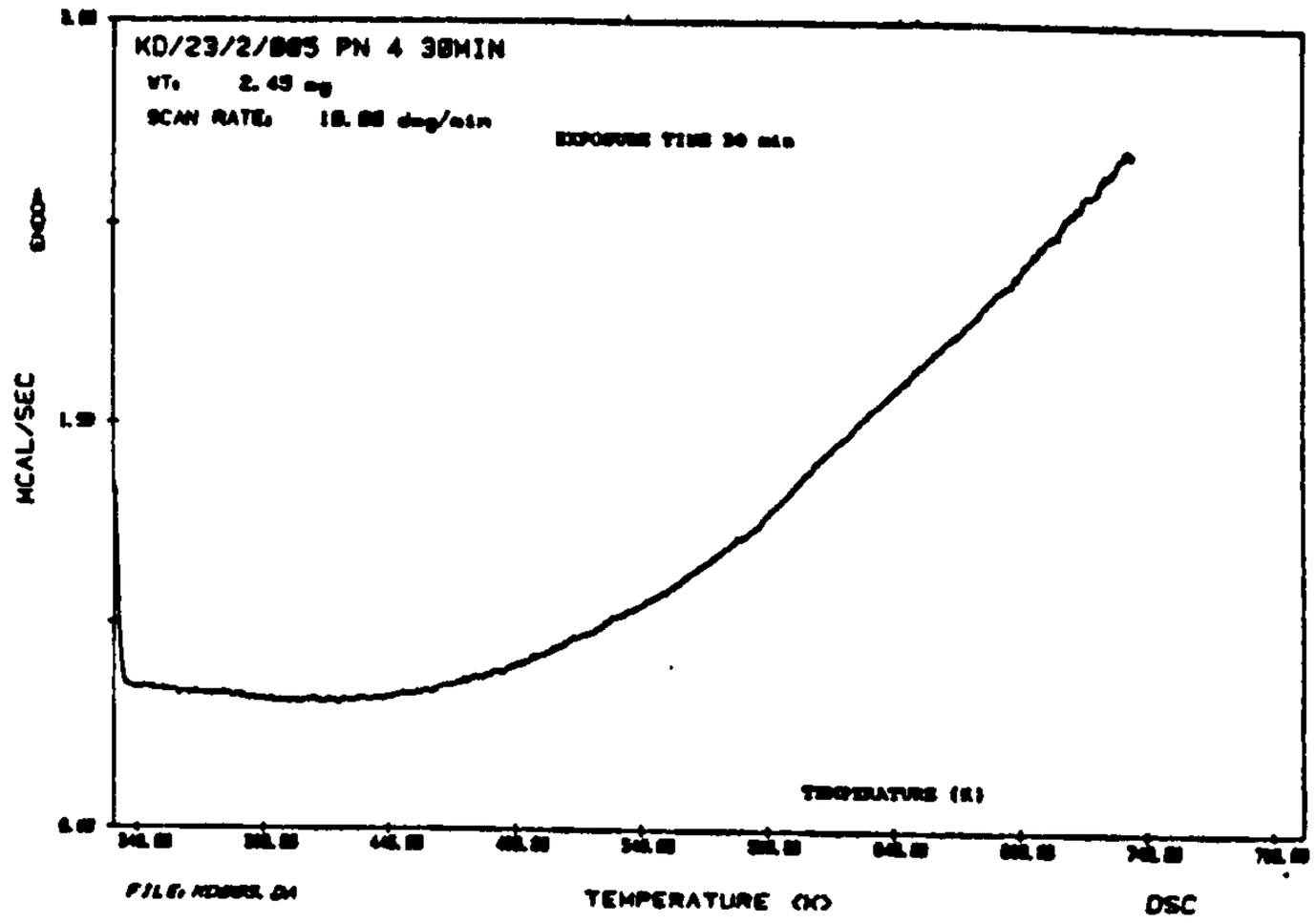

FIGURE 122

TOP LAYER OF INTUMESCENCE FROM PLATE NUMBER 18

AFTER EXPOSURE TO 60kW/m^2 FOR ½ MINUTE

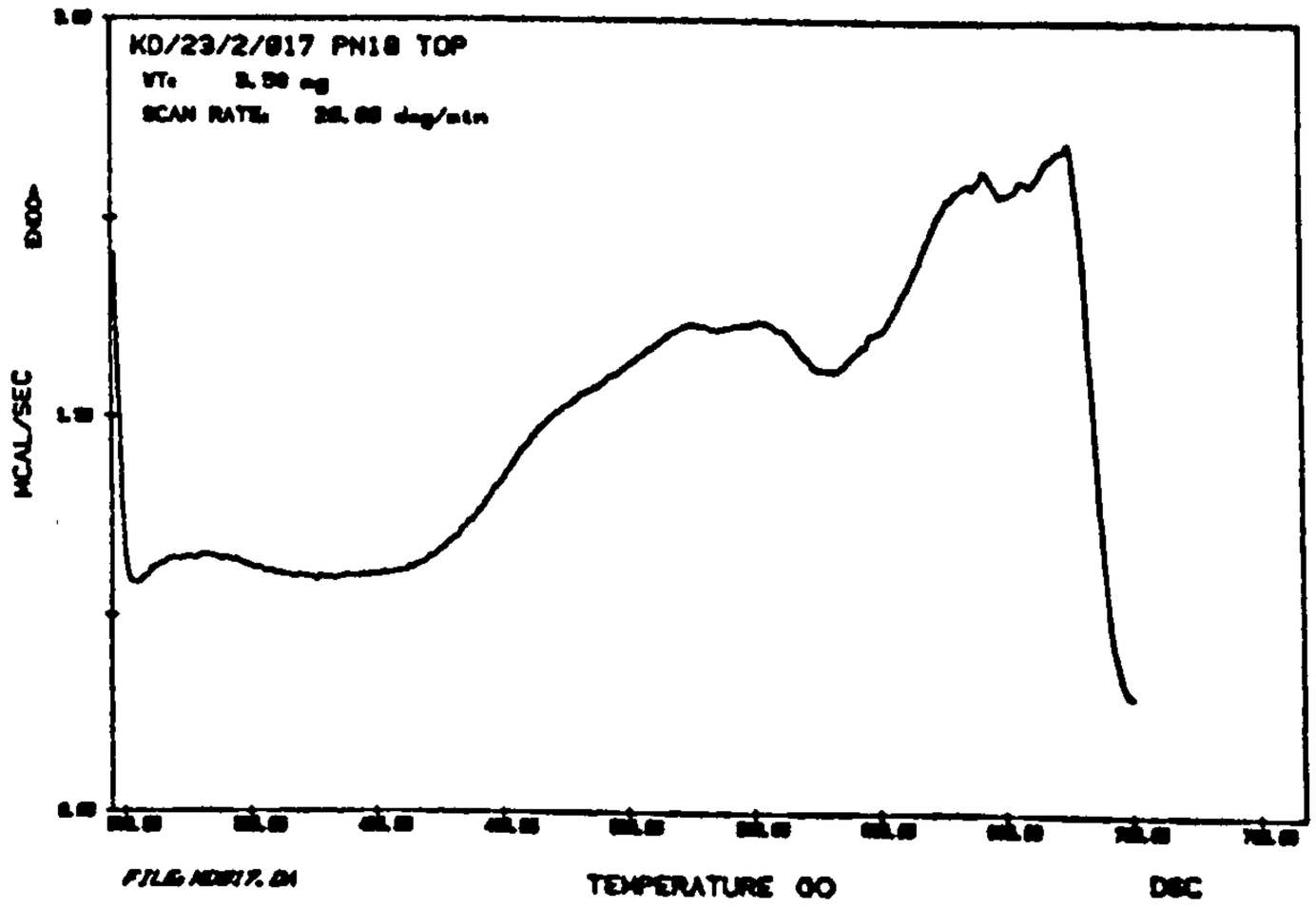

FIGURE 123

BOTTOM LAYER OF INTUMESCENCE FROM PLATE NUMBER 18

AFTER EXPOSURE TO 60kW/m^2 FOR ½ MINUTE

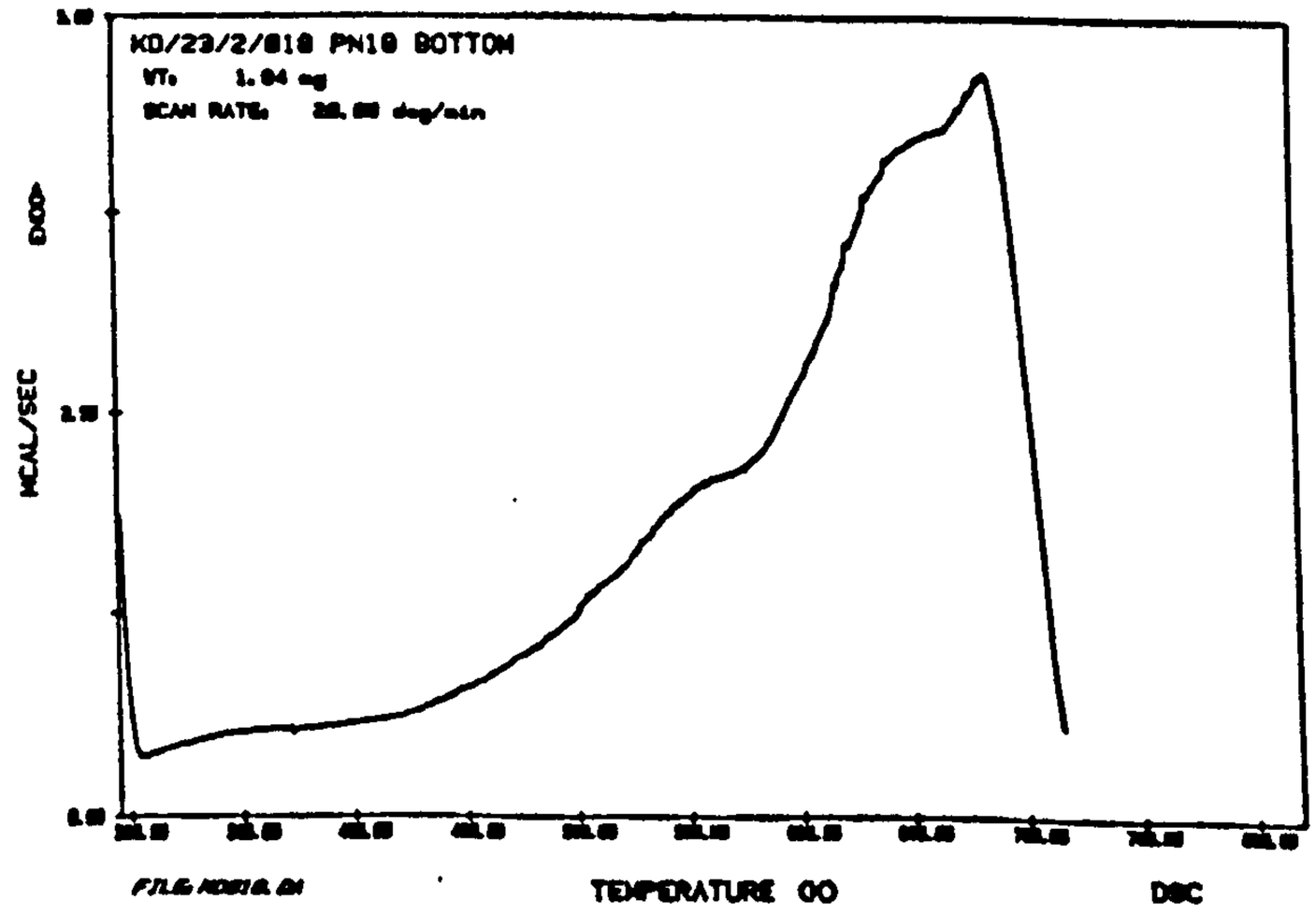

FIGURE 124

TOP LAYER OF INTUMESCENCE FROM PLATE NUMBER 19 AFTER EXPOSURE TO 60kW/m^2 FOR 3/4 MINUTE

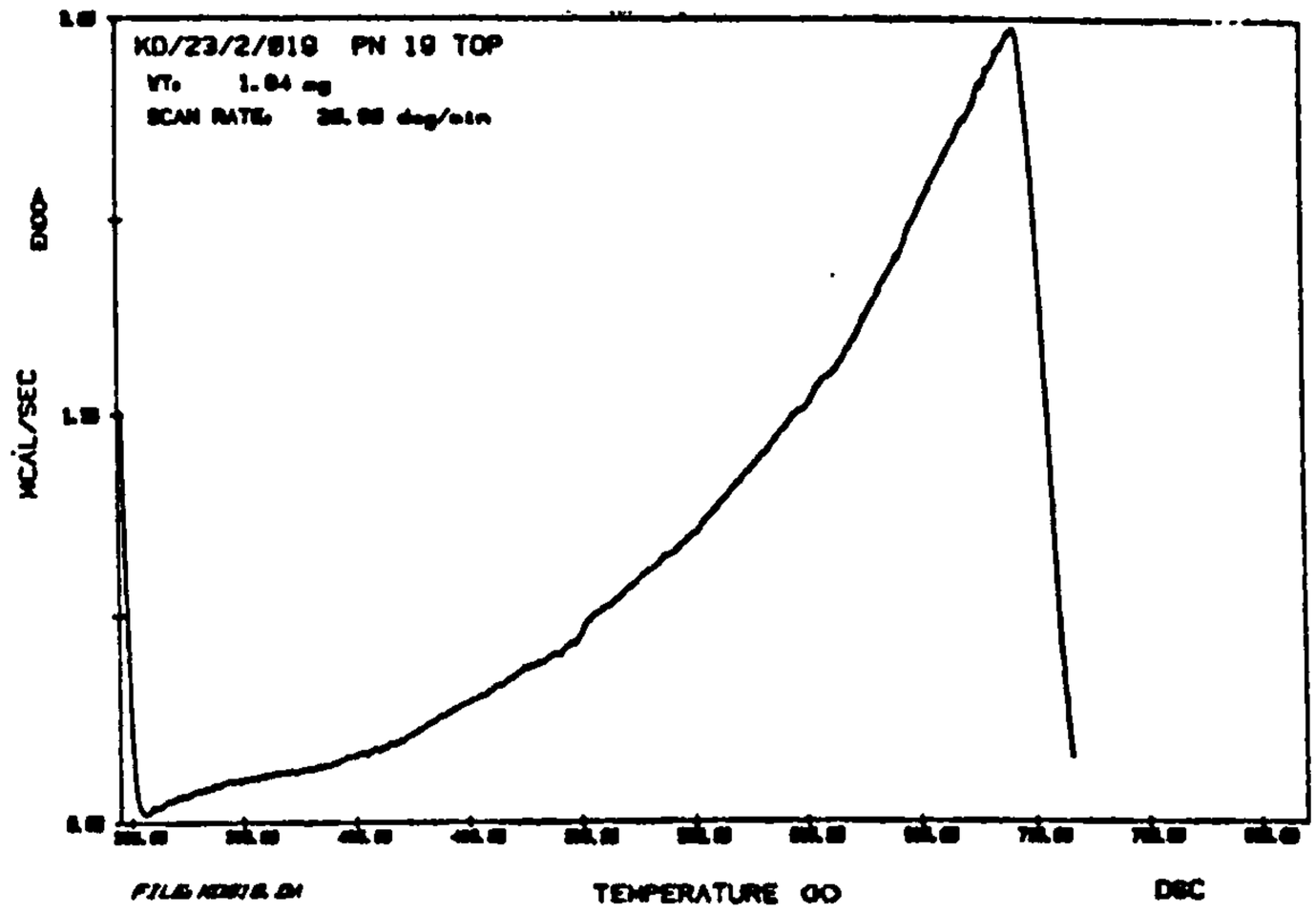

FIGURE 125

MIDDLE LAYER OF INTUMESCENCE FROM PLATE NUMBER 19 AFTER EXPOSURE TO 60kW/m^2 FOR 3/4 MINUTE

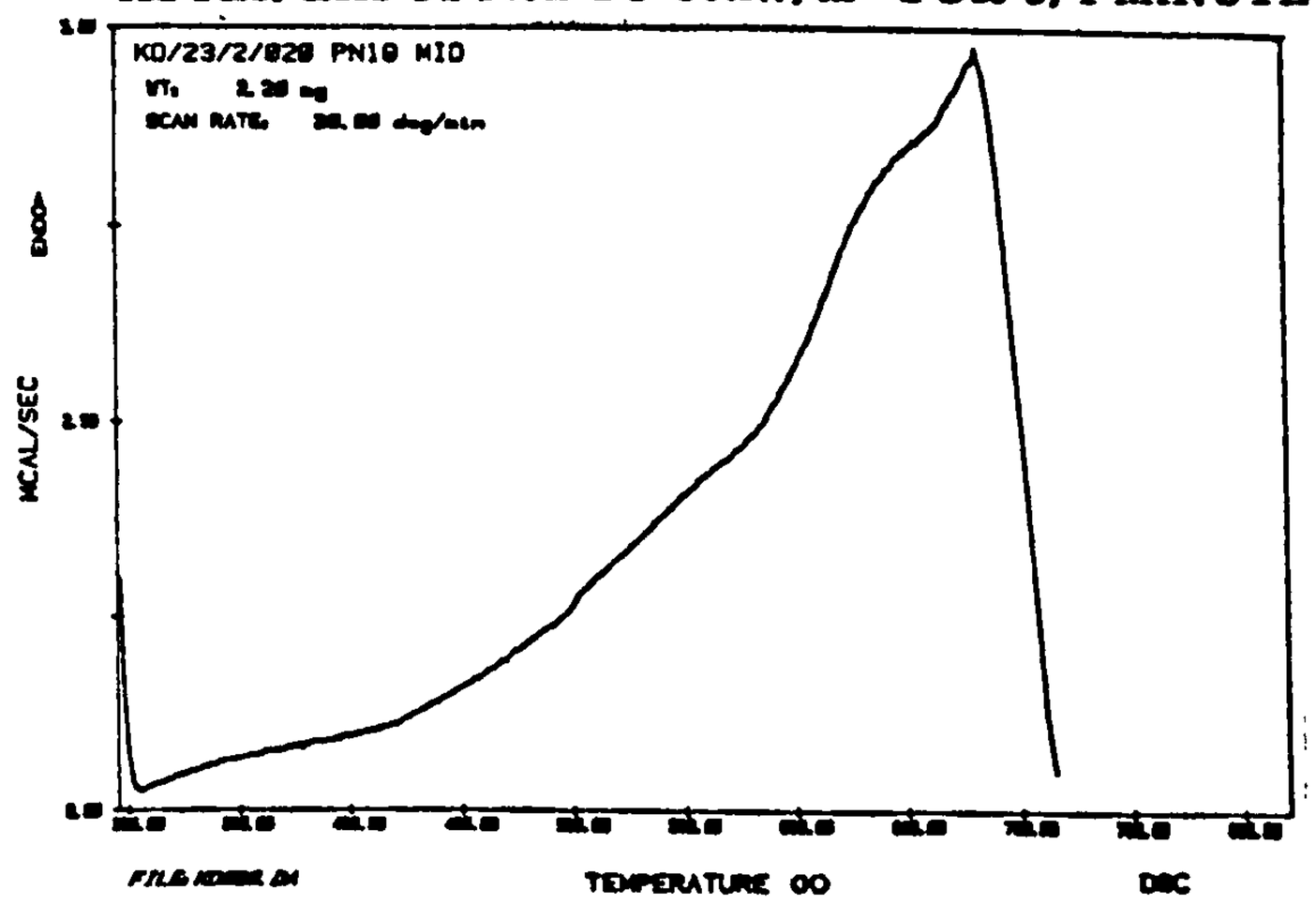

FIGURE 126

BOTTOM LAYER OF INTUMESCENCE FROM PLATE NUMBER 19 AFTER EXPOSURE TO 60kW/m^2 FOR 3/4 MINUTE

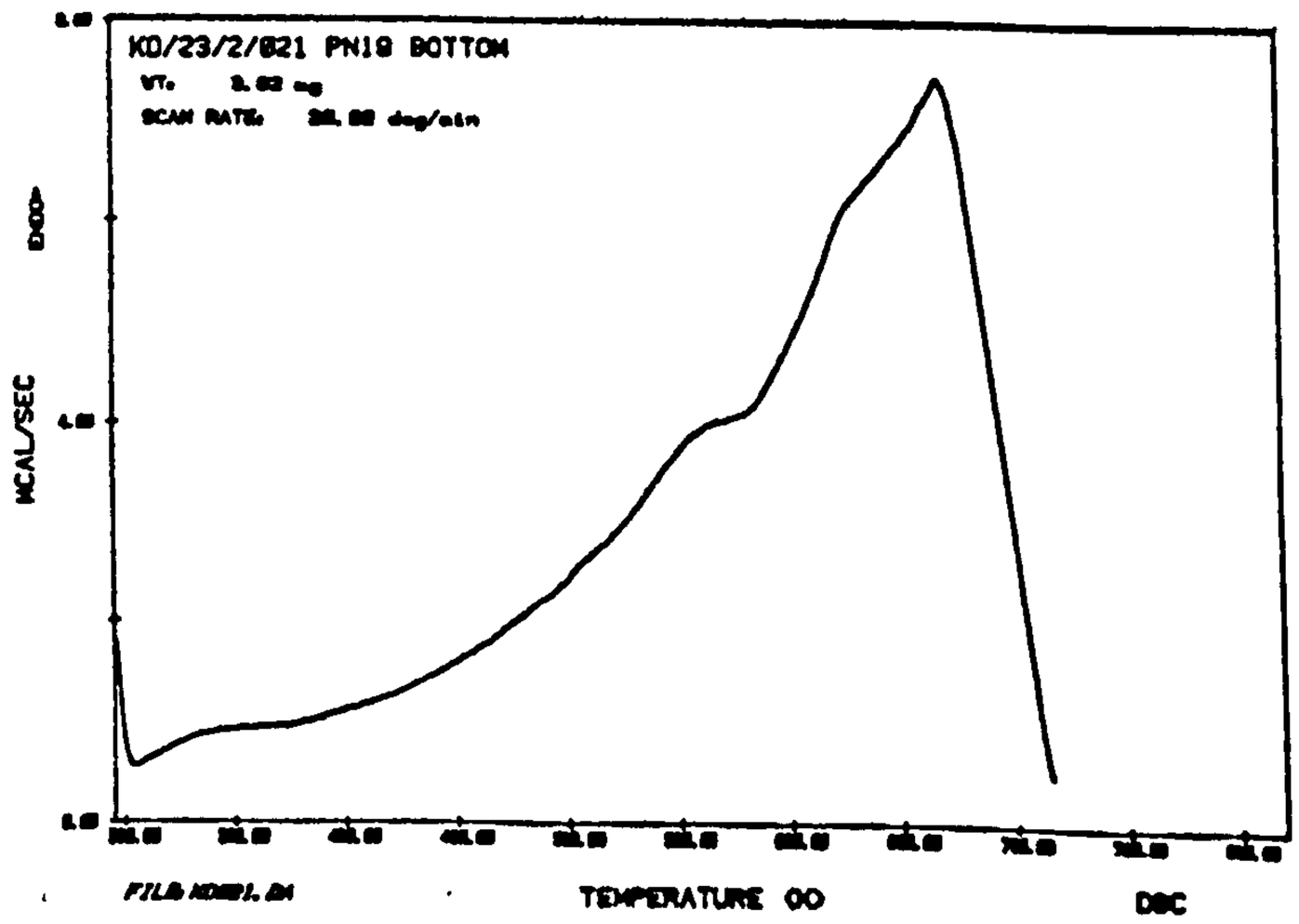

FIGURE 127

TOP LAYER OF INTUMESCENCE FROM PLATE NUMBER 16 AFTER EXPOSURE TO 60kW/m^2 FOR 1 MINUTE

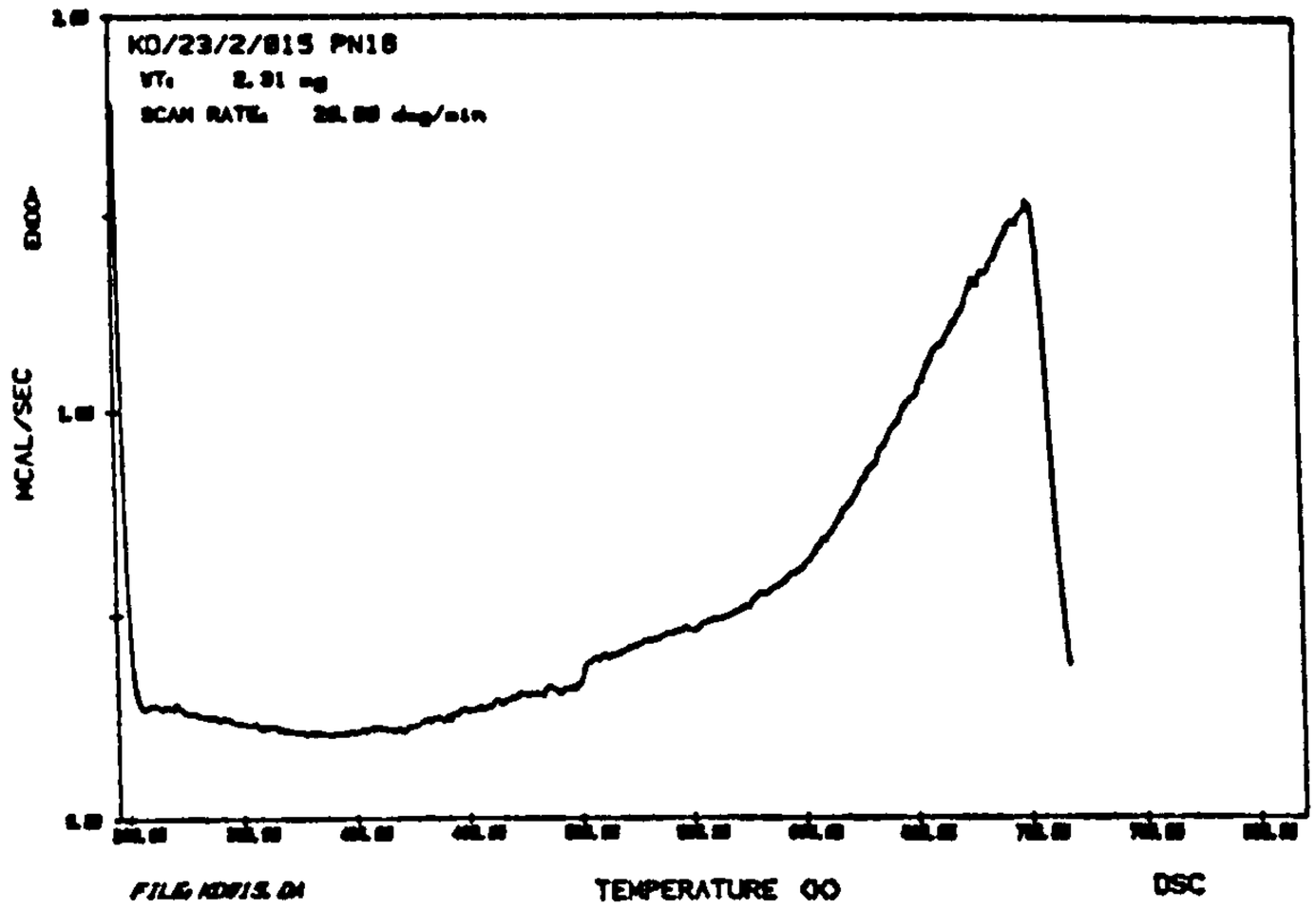

FIGURE 128

TOP LAYER OF INTUMESCENCE FROM PLATE NUMBER 14 AFTER EXPOSURE TO 60kW/m^2 FOR 5 MINUTES

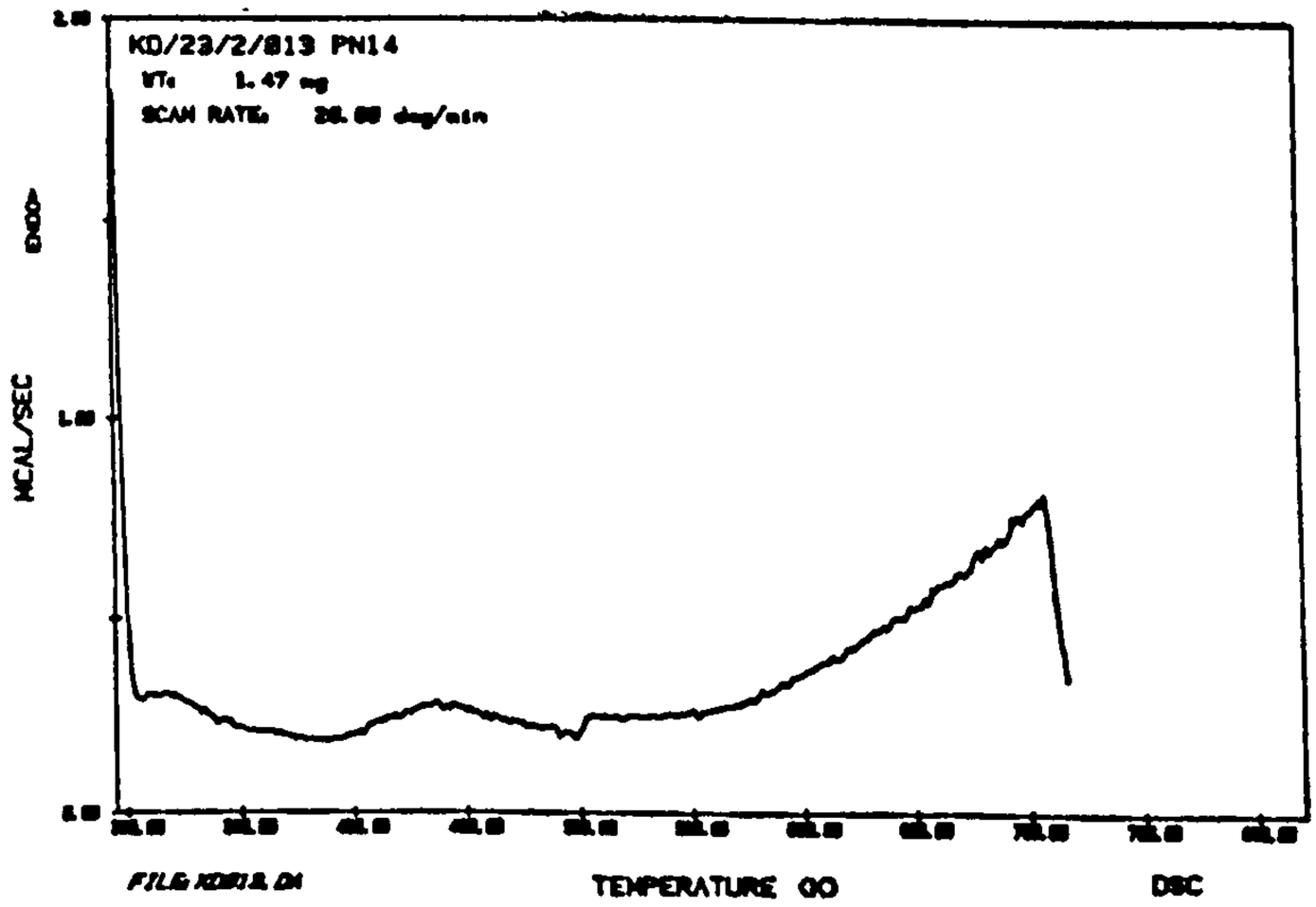

FIGURE 129

TOP LAYER OF INTUMESCENCE FROM PLATE NUMBER 17 AFTER EXPOSURE TO 60kW/m^2 FOR 60 MINUTES

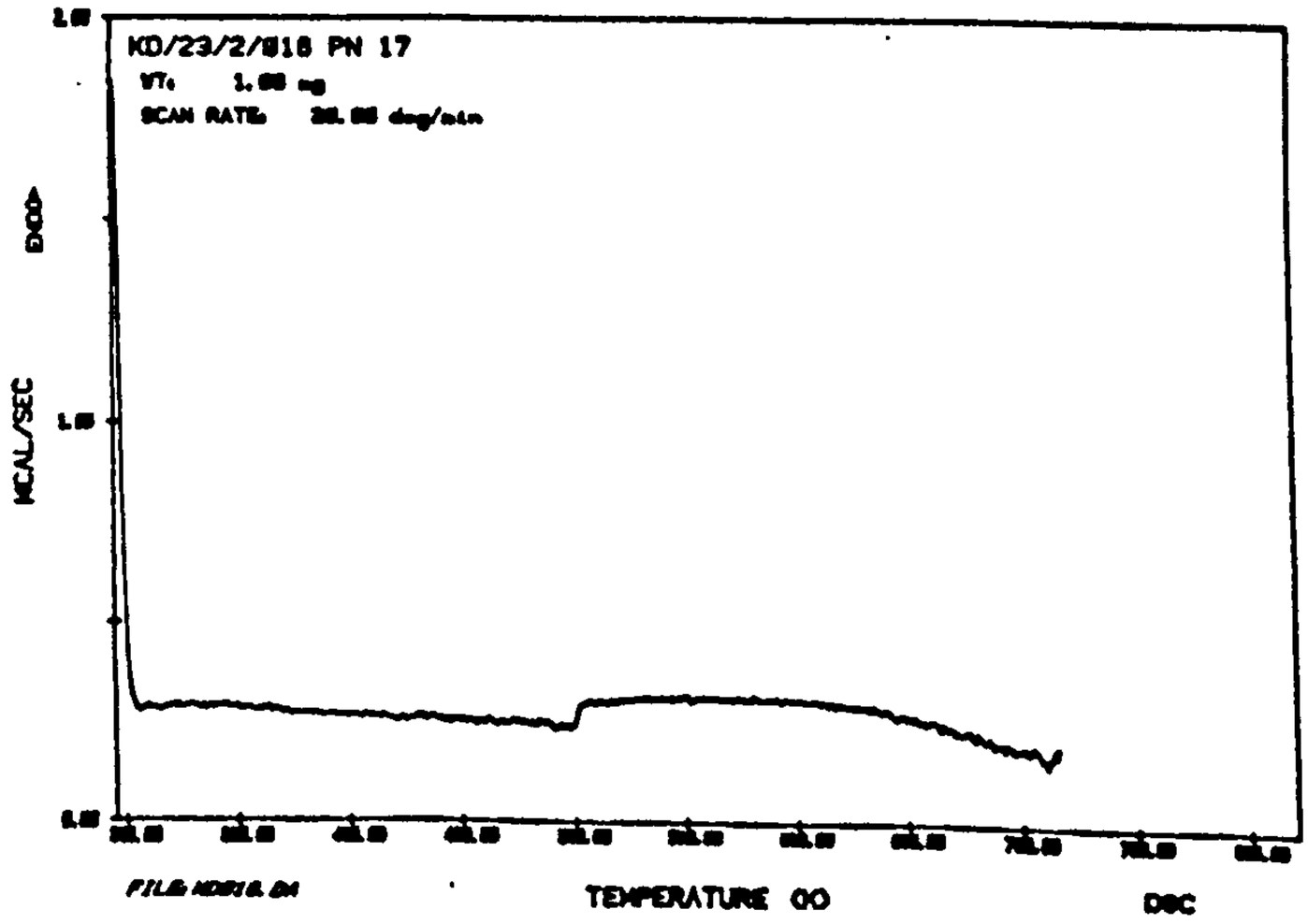

FIGURE 130A

TYPICAL STA CURVE FOR THE TOP LAYER OF INTUMESCENCE FROM PLATE NUMBER 11 AFTER EXPOSURE TO 20kW/m^2 FOR 6 MINUTES

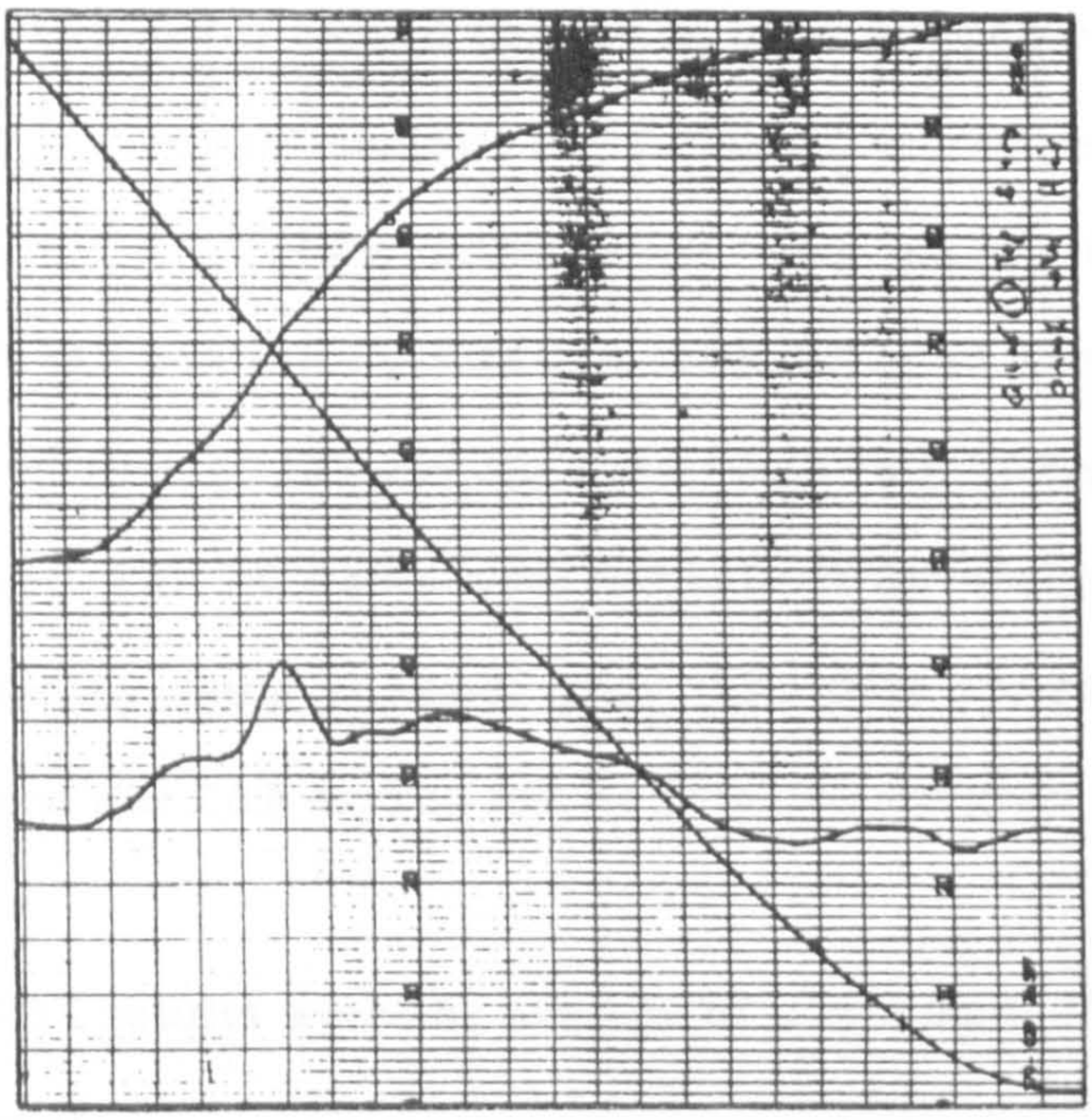

FIGURE 130B

TYPICAL STA CURVE FOR THE BOTTOM LAYER OF INTUMESCENCE FROM PLATE NUMBER 11 AFTER EXPOSURE TO 20kW/m^2 FOR 6 MINUTES

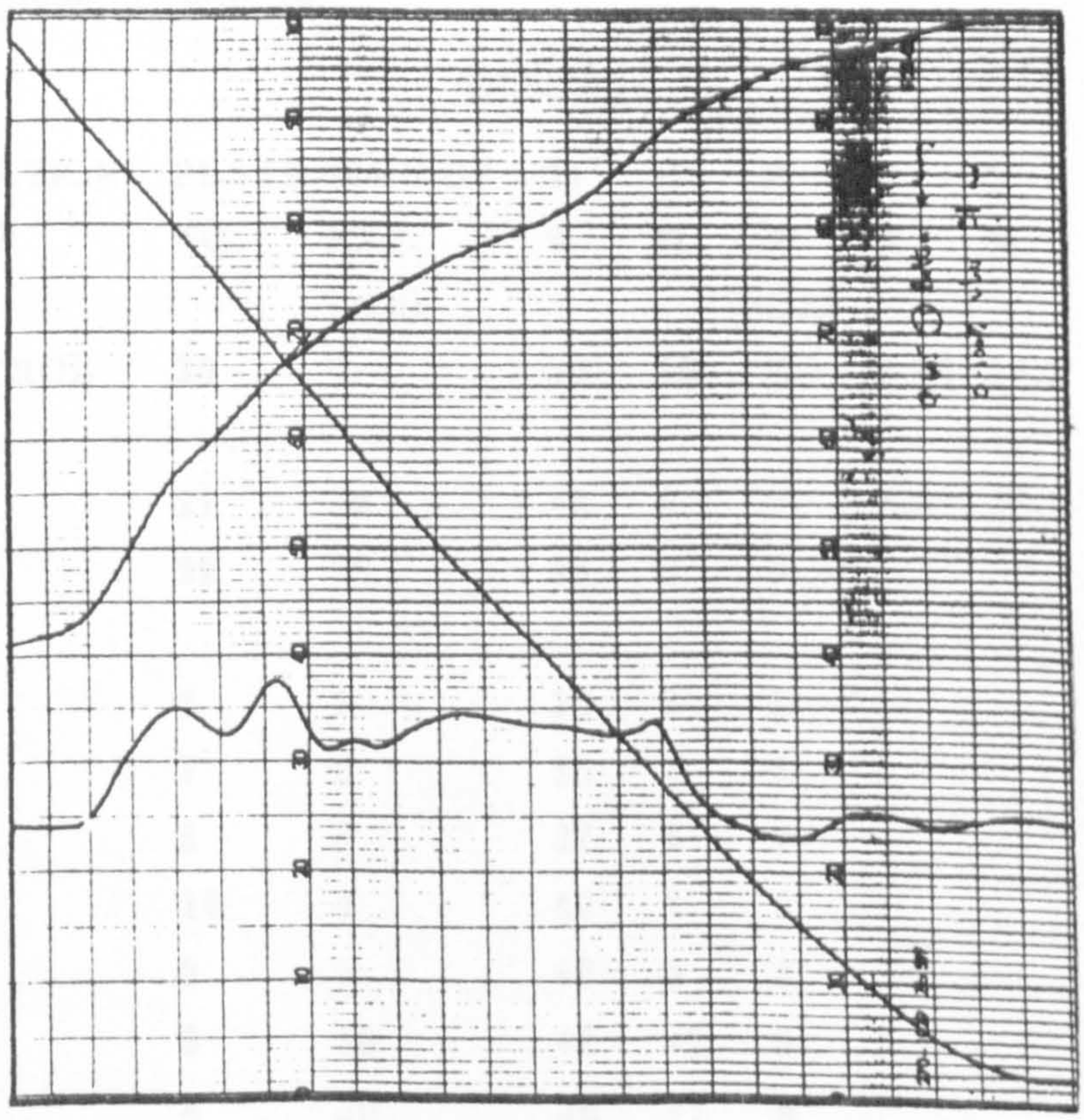

8.6. ELEMENTAL ANALYSIS OF COATED PLATES AFTER EXPOSURE TO VARIOUS THERMAL RADIATIONS USING SEM

Steel plates coated with intumescent paint (KD 23/3) were subjected to a range of radiations for various periods of time. The char so produced was analysed for elemental analysis for titanium, phosphorous and chlorine using a scanning electron miscroscope with energy dispersive X-ray analysis (EDX). Analysis by EDX was made using an electron gun EHT of 25kV, a count time of 100 seconds and a count rate of approximately 2000 counts/second. All elements were normalised for analysis. Calibration was achieved by using a copper grid. The data system used for these investigations was ZAF 4. The results obtained are given in Table 24.

The SEM-EDX results were the average of a minimum of 5 sets of typical samples per char.

The virgin material and char elemental compositions for carbon, hydrogen, nitrogen and phosphorous of the various coatings were found to be as given in Table 24.

TABLE 24

RADIATION kW/m^2	PLATE NO.	TIME OF EXP. (min)	Ti %	Cl %	P % (EDX)	P %	C %	H %	N %
CONTROL	30	0	38	10	6.0	5.66	14.2	3.98	11.6
10	21	30	42	8	7	5.8	15.4	4.12	10.6
10	22	60	35	6	6				
20	1	1	38	8	6				
20	7	2	35	7	6				
20	5	3	37	6	7				
20	10	4	40	6	5				
20	8	5	40	5	8				
20	3	10	41	<1	8				
20	4	30	38	<1	9				

RADIATION kW/m^2	PLATE NO.	TIME OF EXP. (min)	Ti %	Cl %	P % (EDX)	P %	C %	H %	N %
40	24	.75	40	12	7	6.34	14.4	3.5	8.7
40	23	1	38	8	6				
40	25	1.25	35	9	4				
40	26	1.67	38	7	7				
60	18T	.5	36	10	5	6.01	14.1	3.28	7.02
60	18B	.5	34	7	6	7.66	14.23	3.46	8.53
60	19T	.75	34	5	7	5.74	13.74	2.83	3.82
60	19M	.75	40	5	8	8.37	13.47	3.35	6.55
60	19B	.75		7	8	10.87	14.24	3.35	6.55
60	16	1	38	3	6		12.77	1.91	2.76
60	15	2	33	<1	6	8.21	12.2	1.95	2.72
60	14	5	27	<1	7	5.56	6.80	1.49	0.98
60	17	30	25	<1	6	4.17	<0.2	<0.2	<0.2

T = top M = middle B = bottom

FIGURE 131

TYPICAL MAPPING FOR CHLORINE FOR PLATE NO. 18

AFTER EXPOSURE TO 60kW/m^2

TOP LAYER

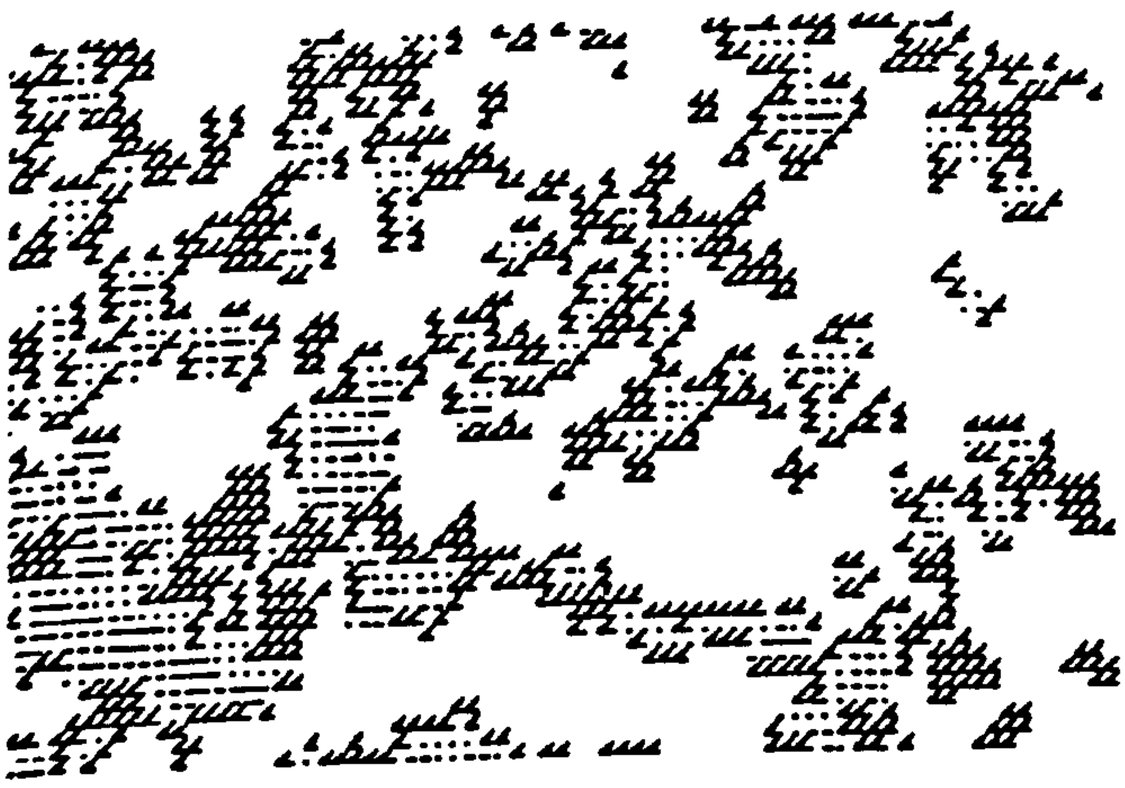

MIDDLE LAYER

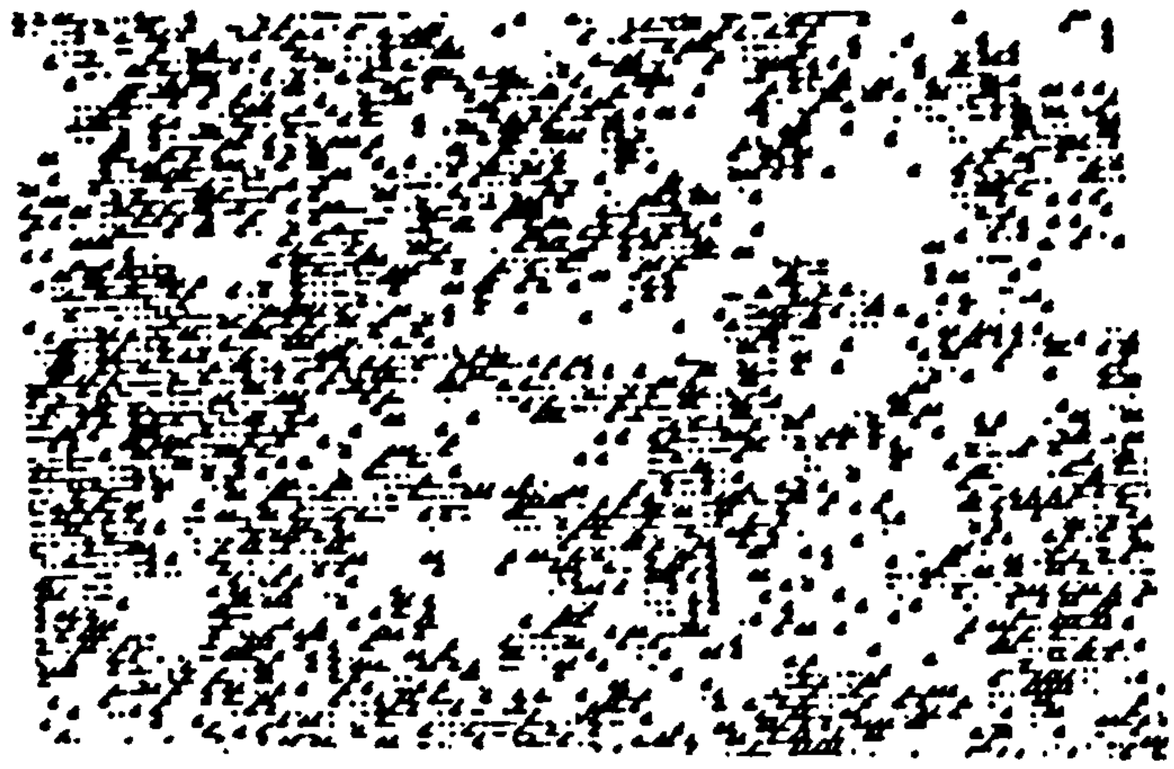

FIGURE 132

A TYPICAL ELEMENTAL ANALYSIS FOR INTUMESCENCE FROM THE TOP, MIDDLLE AND THE BOTTOM LAYERS OF PLATE NO. 19 AFTER EXPOSURE TO 60kW/m^2 FOR 3/4 MINUTES

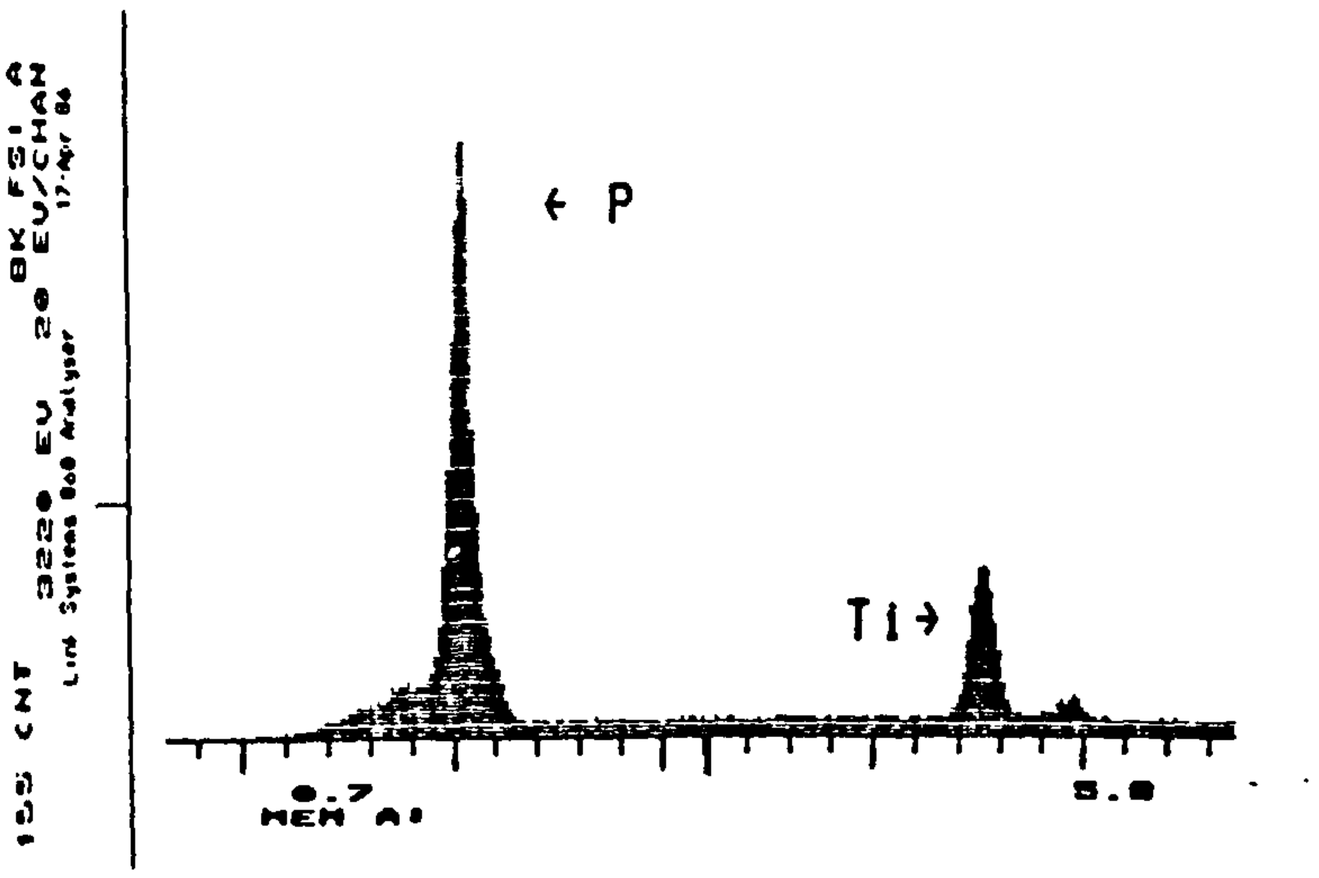

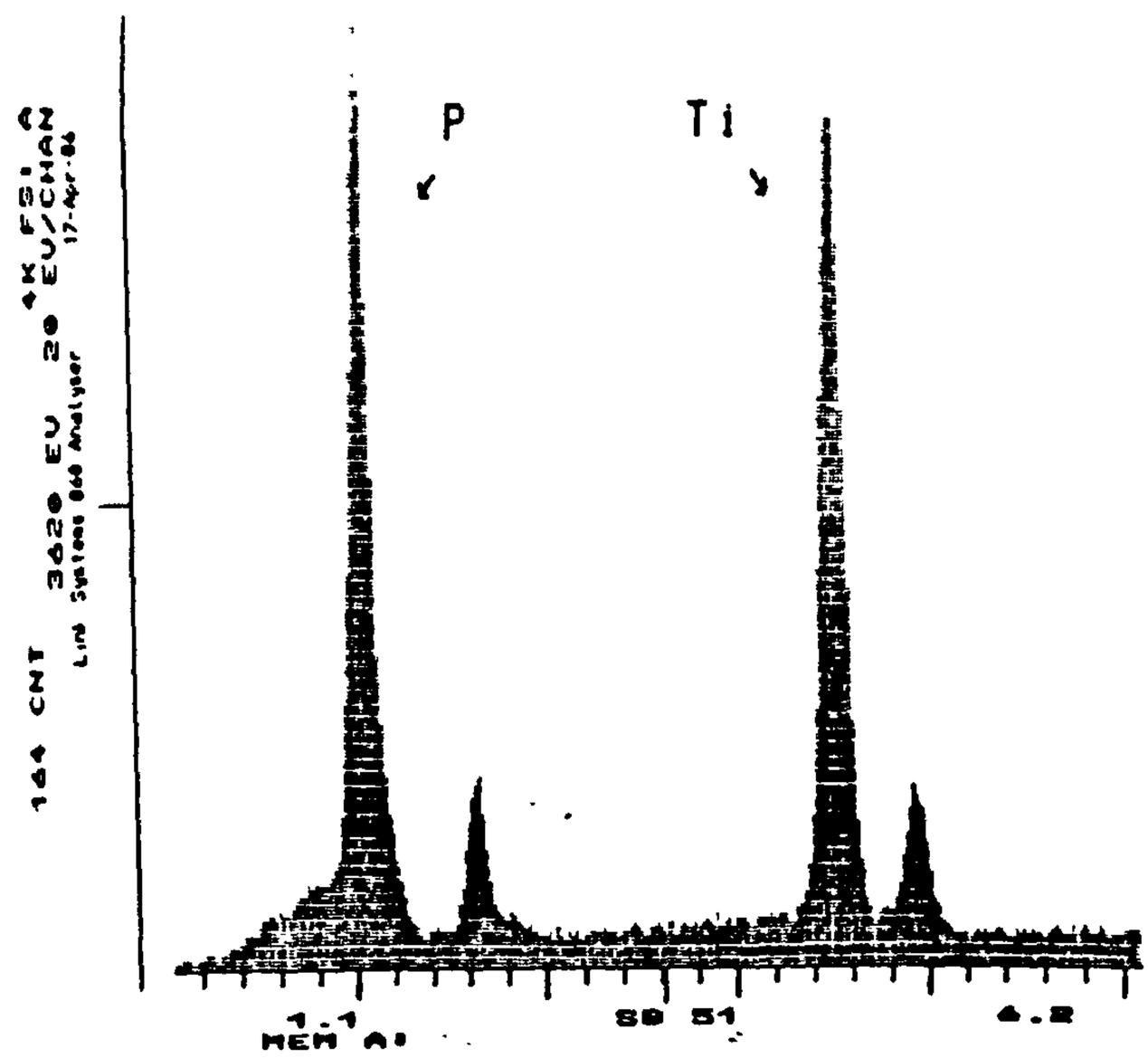

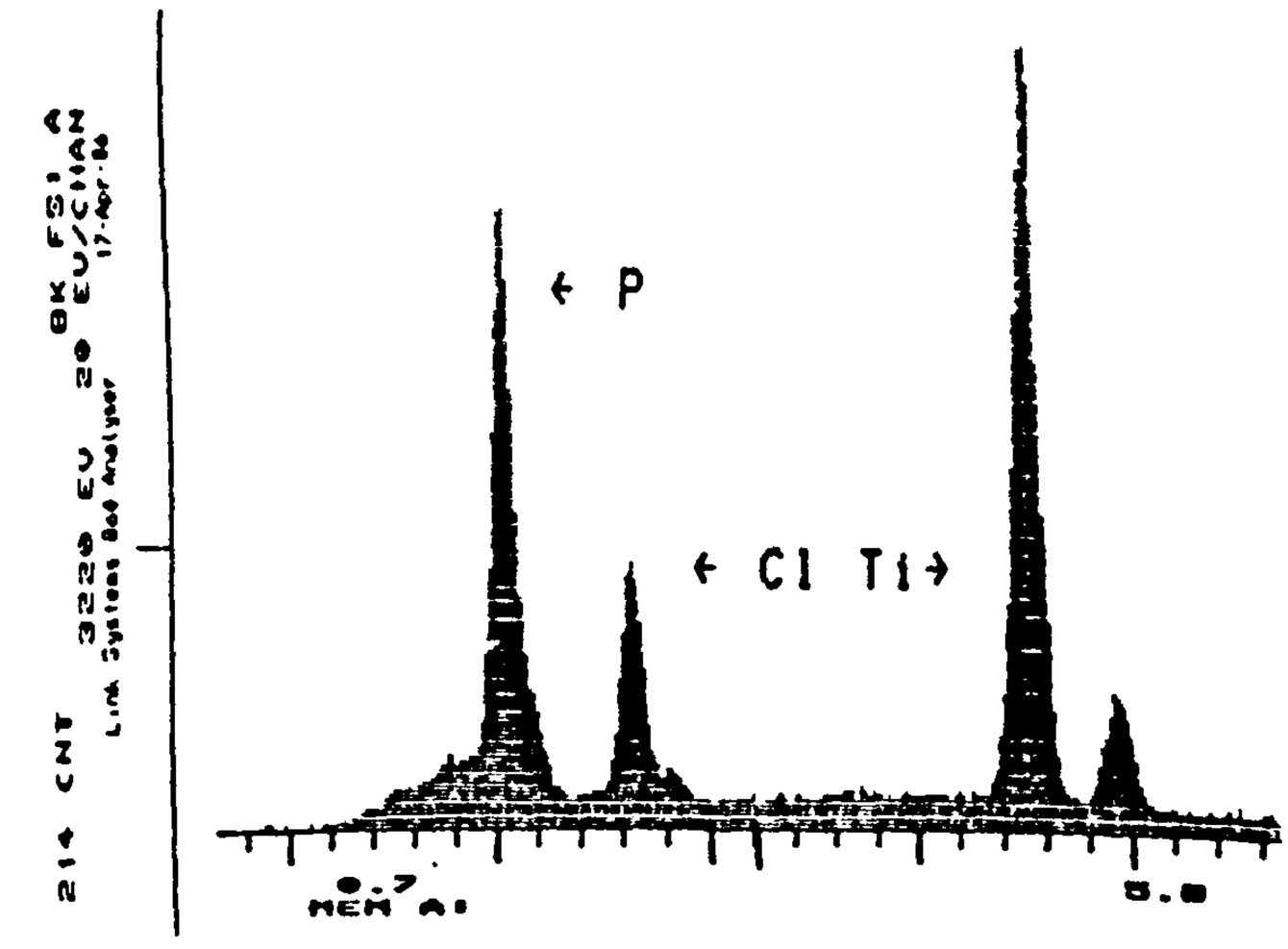

FIGURE 133

TYPICAL PHOTOGRAPHS SHOWING THE CELL STRUCTURE
FROM THE TOP AND THE BOTTOM LAYERS OF INTUMESCENCE
FROM PLATE NO. 18 AFTER EXPOSURE TO RADIATION

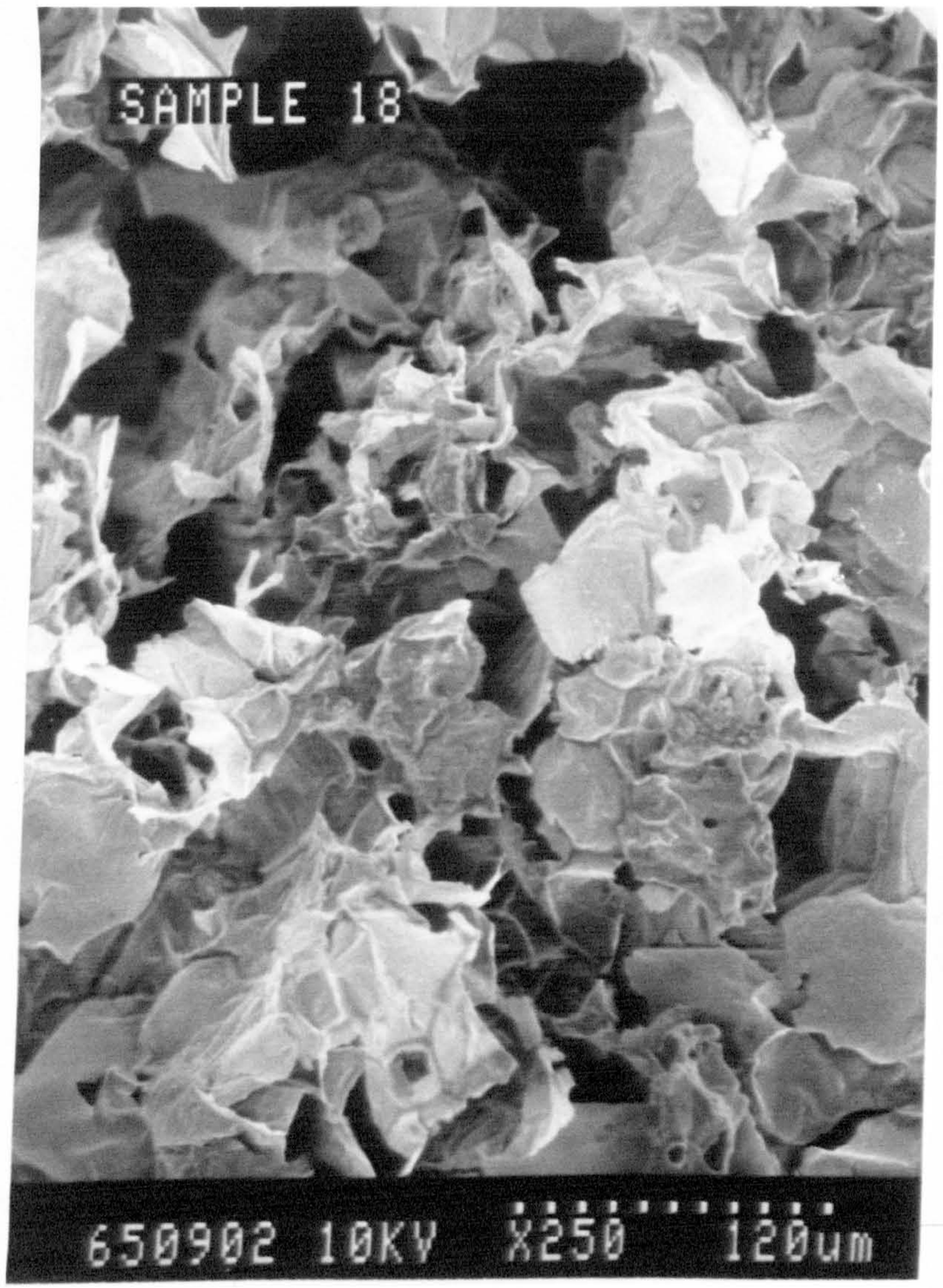

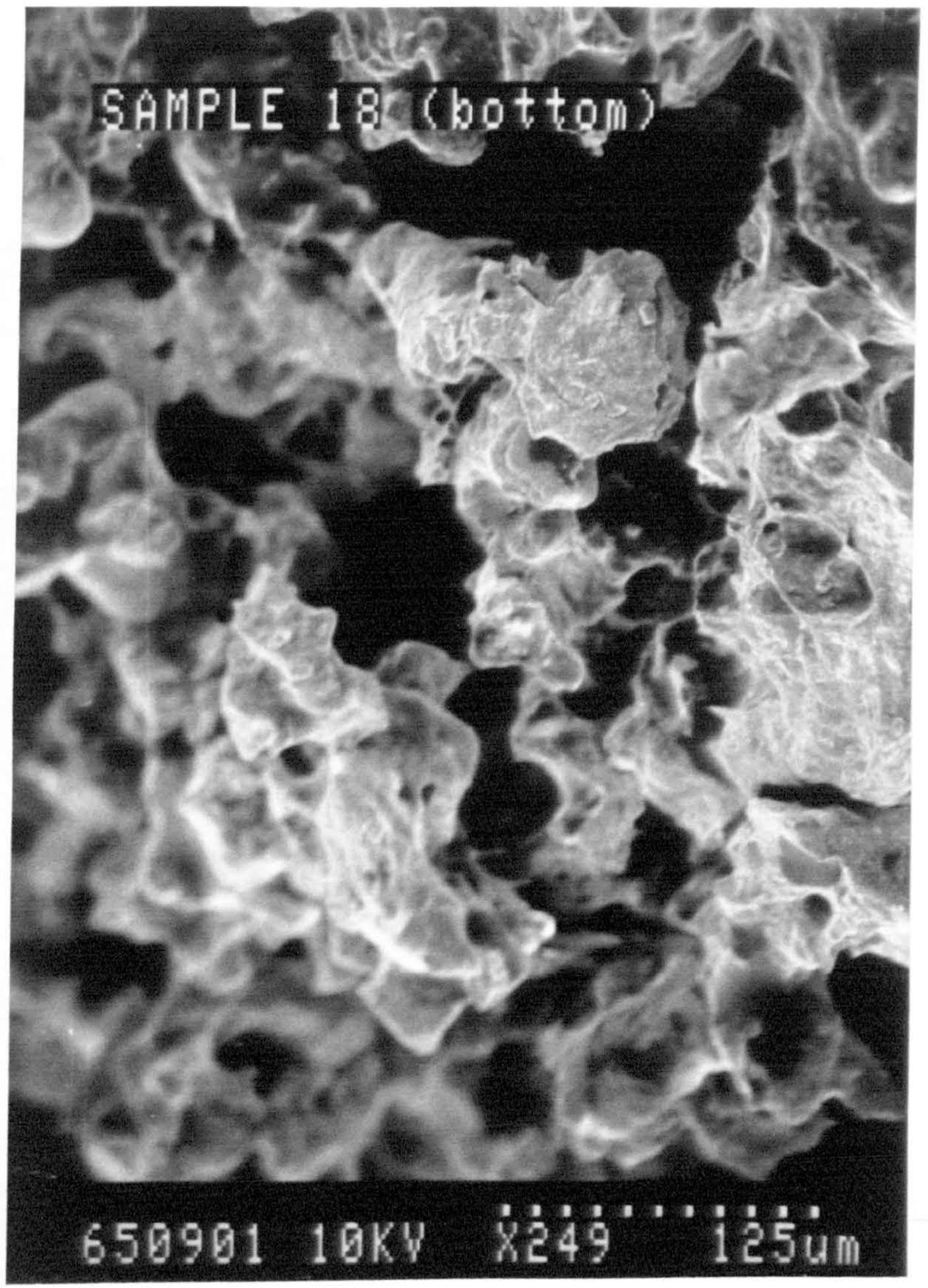

FIGURE 134

TYPICAL PHOTOGRAPHS SHOWING THE CELL STRUCTURE
FROM THE TOP AND THE BOTTOM LAYERS OF INTUMESCENCE
FROM PLATE NO. 18 AFTER EXPOSURE TO RADIATION

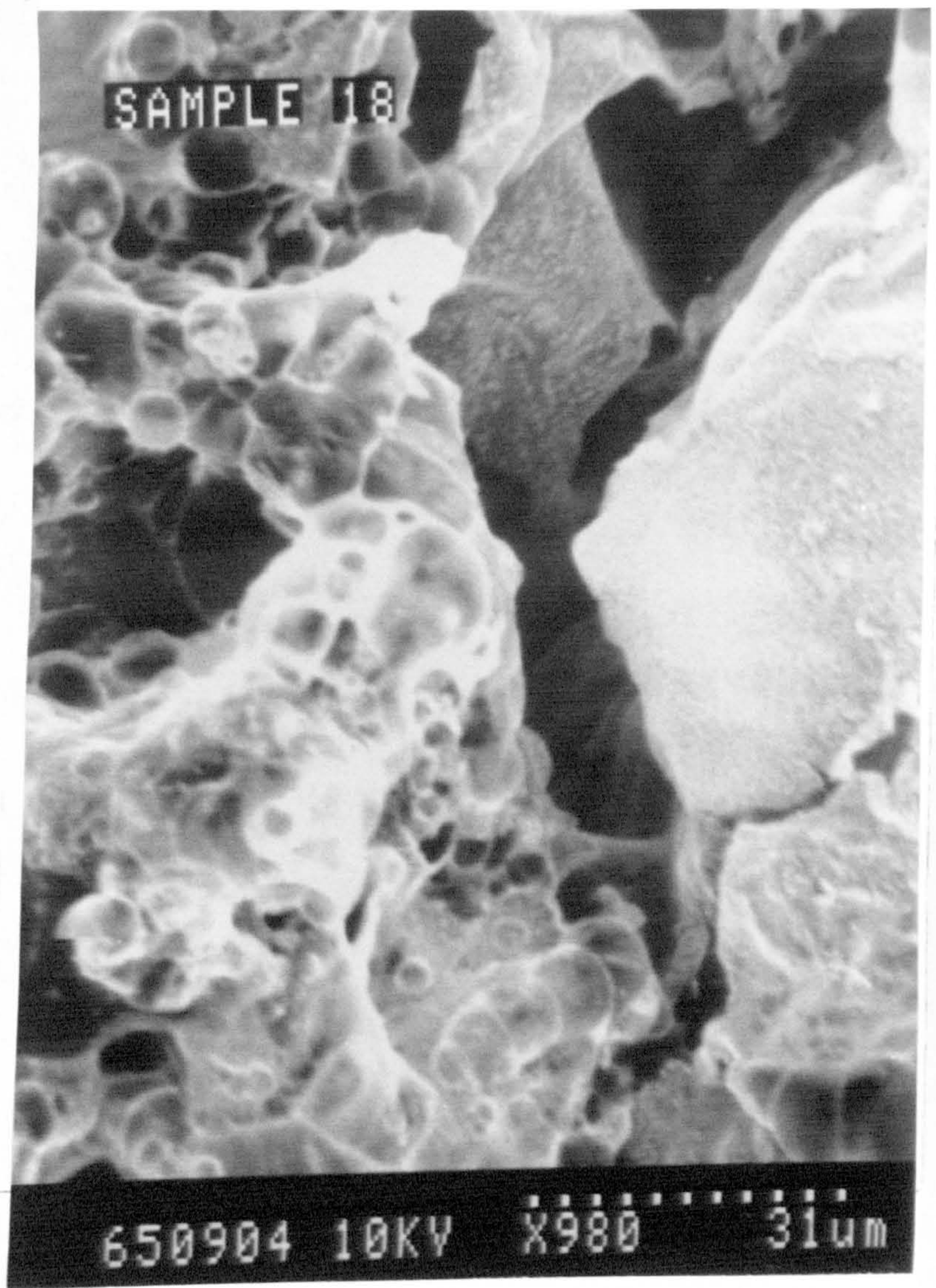

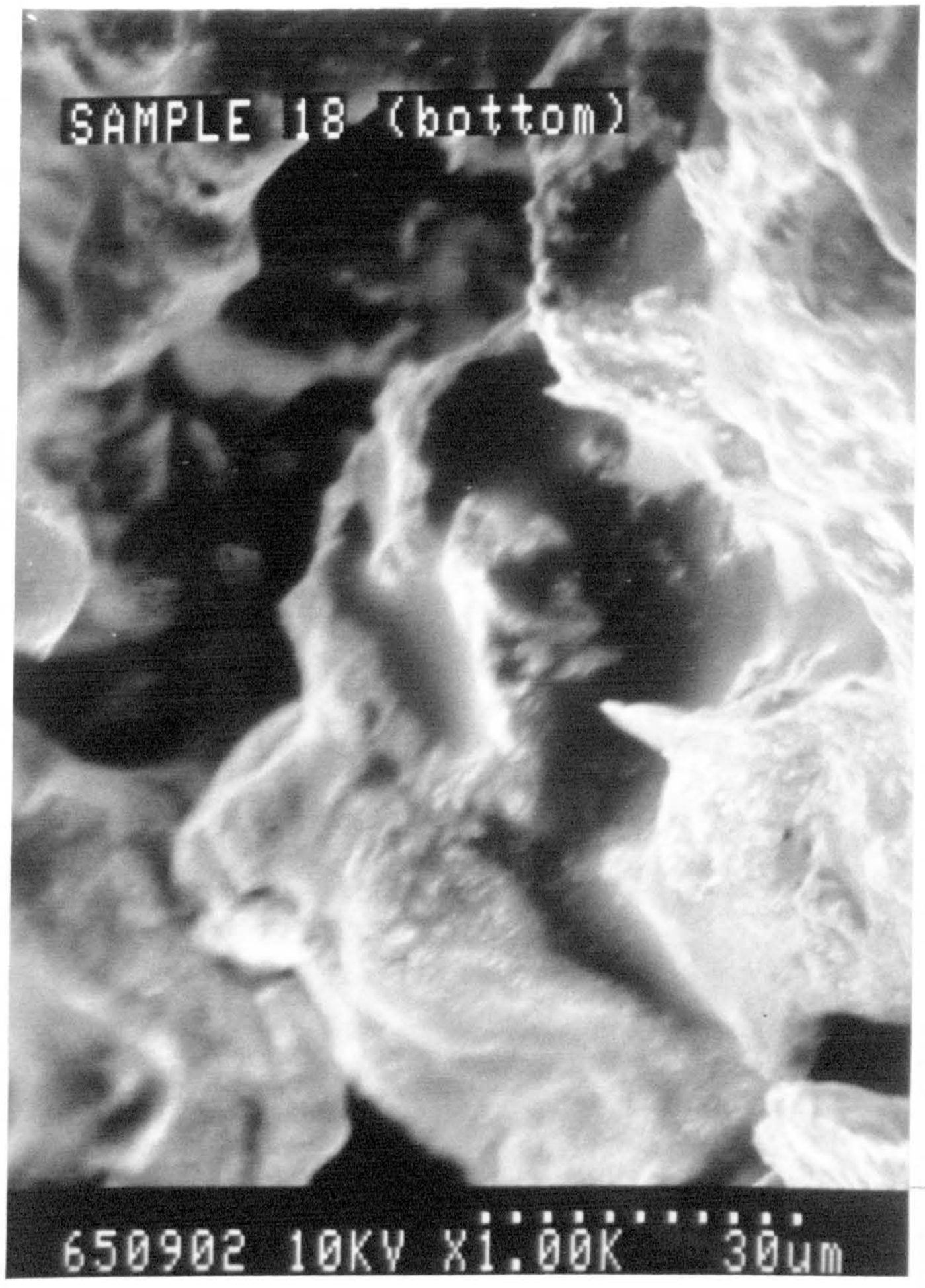

8.7.

Plate Number	Exposure Time (Min)	Radiation Level kWm^{-2}	Initial Coating Weight (g)	Final Coating Weight (g)	Ration of Remaining to Initial Weight	Initial Coating Thickness (mm)	Final Thickness mm	Ratio of Final to Initial Thickness	Time for Start of Intumescence (sec)	Time for End of Intumescence (sec)	Notes
1	1	20	109.49	109.43	.99	0.26	0.228	.877			No intumescence.
3	10	20	110.18	109.40	1.0	0.268	5.65	21.082	165	270	Good intumescence, crusty surface.
4	30	20	110.25	109.47	.993	0.263	5.41	19.543	168	270	Good intumescence crusty surface.
5	3	20	105.52	105.00	.995	0.250	4.52	18.08	165	-	Still intumescing at the end of test.
7	2	20	109.13	108.88	.998	0.17	0.96	5.647	-	-	Very short foaming.
8	5	20	105.56	105.16	.996	0.196	3.11	15.867	150	-	Still intumescing at the end of tests.
10	4	20	104.14	103.82	.995	0.192	2.25	11.728	170	-	Still intumescing at the end of tests.
11	6	20	105.53	105.01	.995	0.199	2.978	14.965	125	180	Good intumescence and cell structure.
12	7	20	106.35	105.73	.994	0.187	2.77	14.813	140	215	Good intumescence and cell structure.
14	5	60	103.26	102.28	.995	0.170	3.49	20.530	30	150	Very soft foam.
15	2	60	105.92	105.38	.995	0.198	3.619	18.278	27	140	Very soft foam.
16	1	60	106.56	105.96	.994	0.233	5.66	24.292	25	-	Slightly crusty surface.
17	60	60	107.73	106.65	.999	0.246	4.74	19.268	30	160	White oxidised fluffy foam.
18	½	60	104.62	104.40	.998	0.29	2.10	7.241	27	-	Very slight foaming in patches.
19	¾	60	109.53	109.29	.998	0.175	2.755	15.857	25	-	Slight foaming.
21	30	10	106.58	106.52	.999	0.247	0.226	0.915	-	-	Smoke only at 400 sec.
22	60	10	105.46	105.28	.998	0.245	0.220	0.898	-	-	Smoke only at 400 sec.
23	1	40	105.82	105.22	.994	0.205	6.8	33.171	25	-	Very even foaming.
24	¾	40	105.35	105.30	1.00	0.150	0.21	1.4	27	-	Very slight foaming.
25	2	40	103.87	103.26	.994	0.20	6.10	30.5	28		Very even foaming.

TABLE NO. 25.
GRAND SUMMARY OF THE MODELLING EXPERIMENTS.

SECTION 9

9. THEORY OF INTUMESCENCE

9.1. INTRODUCTION

Few theoretical models have been proposed for intumescent coatings which describe the observed physical behaviour. In the main, intumescent systems have been treated empirically. Cagliostro et al (114) developed a semi-empirical model to demonstrate the effectiveness of intumescent coatings. It took into account the heating environment (conduction), enthalpies of reaction, and the convection of the pyrolytic gases produced.

A study by Anderson and Wauters (115) proposed a mathematical model based on mass loss and energy absorbed. Intumescence was assumed to occur continuously as a function of mass loss. The best correlation between the model predictions and the experimental results was obtained when the expansion occurred early in the mass loss process. The authors suggested that a relationship which described the expansion as a function of not only total mass but also temperature and rate of mass loss could account for many of the anomalies observed between the model predictions and the experimental results.

Buckmaster et al (116) developed a theory which assumed that intumescence was completely confined to an infinitesimally-thin front whose temperature is a definite property of the coating. This front was assumed to travel through the coating from the surface to the substrate when heat was applied to the outer surface, leaving behind it swollen char. A one-dimensional model based upon energy conservation and heat diffusion was developed. As seen from Fig. 135, the coating is divided

into two regions separated by the front: 1) a region where the temperature is not sufficiently high to start intumescence so that this material has zero velocity; 2) a region behind the front where intumescence has occurred and the char is progressing with uniform velocity u_f from the substrate. Mathematically thermal diffusion is given by,

$$\rho c_p \left(\frac{\partial T}{\partial t} + u \frac{\partial T}{\partial x} \right) = \frac{\partial}{\partial x} \left(k \frac{\partial T}{\partial x} \right) \qquad (9.1)$$

where ρ, c_p, u, k are the density, specific heat, velocity and thermal conductivity of the material, respectively, T is temperature, t is time and x is distance from origin.

FIGURE 135

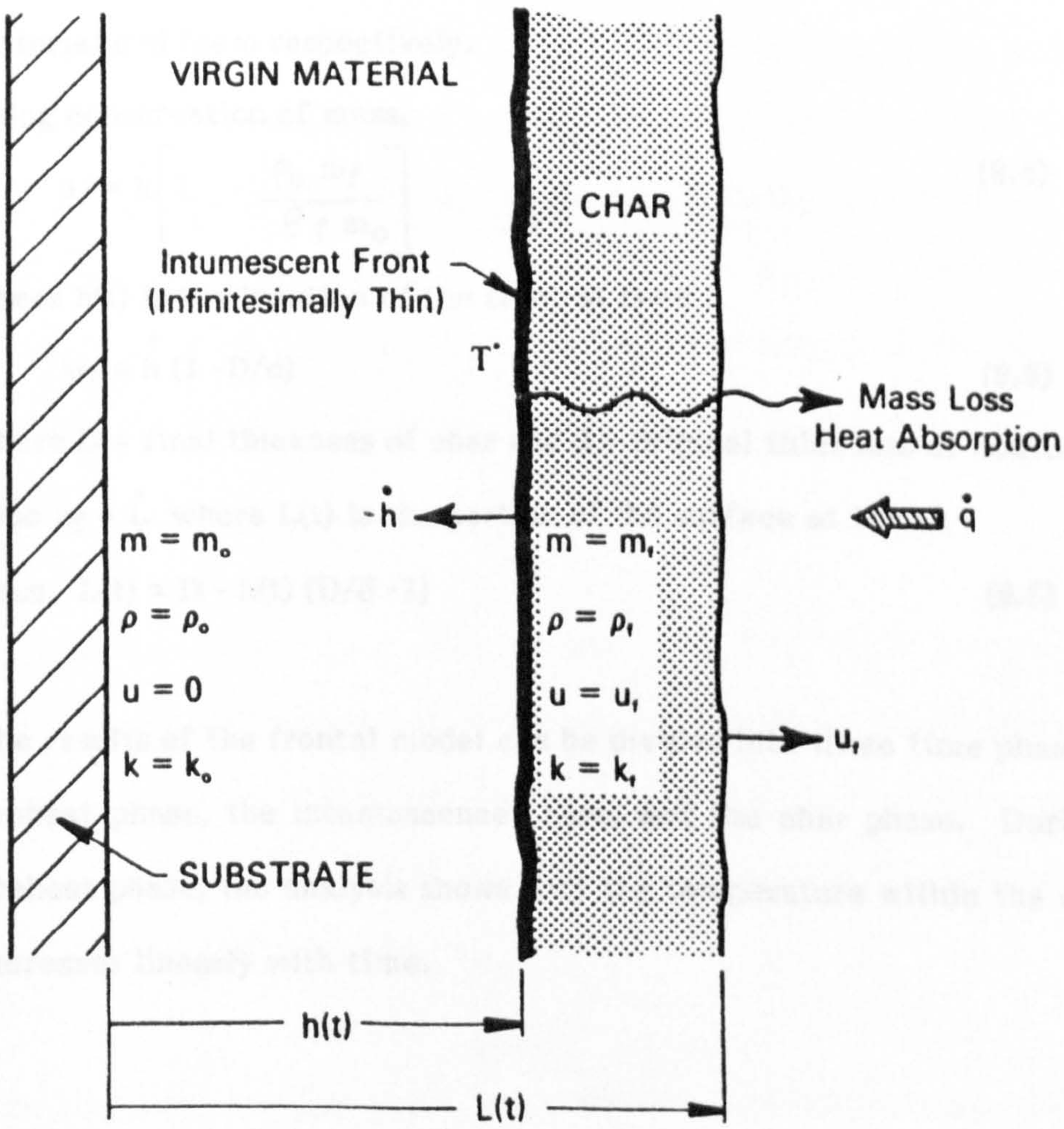

At t = 0, heat is applied to the surface. At t = t_1, the surface reaches the critical temperature T* and intumescence begins. The front then moves deeper into the coating while the free surface (foam) moves in the opposite direction, Fig. 135. Finally, at time t = t_2, the front reaches the substrate and intumescence is complete.

$$T^+ - T^- \equiv [T] = 0 \qquad T_{front} = T^* \qquad (9.2)$$

Eq. (9.1) is solved on both sides of the front with jump conditions to take into account the transition occurring across the front. These conditions specify the loss of mass, energy absorption and heat flux,

$$\left.\frac{k\partial T}{\partial x}\right|^+ - \left.k\frac{\partial T}{\partial x}\right|^- = \rho\dot{h}\,(Q - c_p T^*)\left(\frac{m_f}{m_o} - 1\right) \qquad (9.3)$$

where Q represents the energy absorbed by the overall endothermic reaction occurring, T* is the temperature at the front and m is the mass of material per unit length. Subscript o and f refer to the original (virgin) material and foam respectively.

Using conservation of mass,

$$u_f = \dot{h}\left[1 - \frac{\rho_o\, m_f}{\rho_f\, m_o}\right] \qquad (9.4)$$

where h(t) is the location of the front at time t.

$$u_f = \dot{h}\,(1 - D/d) \qquad (9.5)$$

where D = final thickness of char and d = original thickness of coating

Also $u_f = \dot{L}$ where L(t) is the portion of the surface at time t

Thus, $L(t) = D - h(t)\,(D/d - 1)$ (9.6)

The results of the frontal model can be divided into three time phases: the preheat phase, the intumescence phase, and the char phase. During the preheat phase, the analysis shows that the temperature within the coating increases linearly with time.

at $x = 0$

$$T \doteqdot T_o + \frac{\dot{q}_o}{\rho_o c_p d}\left(t - \frac{d^2 \rho_o c_p}{6k_o}\right) = T_o + \frac{\dot{q}_o (t - t_o)}{\rho_o c_p d} \quad (9.7)$$

where $\dot{q}_o$ is the heat flux applied at the surface T_o is room temperature and $t_o = d^2\rho_o c_p/6k_o$ is associated with the heating at short times, Eq. 9.7 is valid only for 'large' times, where large can be approximated by $t >> t_o$.

When the surface temperature reaches T*, the second phase, intumescence, begins. The time taken to initiate intumescence was shown to be

at $x = d$

$$t_1 = \frac{\rho_o c_p d}{\dot{q}_o}\left[T^* - T_o - \frac{\dot{q}_o d}{3k_o}\right] \quad (9.8)$$

The front moves through the coating, the temperature of the substrate remaining constant. This is indicated by a plateau on a graph of temperature of the substrate against time. This interesting feature predicted by the frontal model is due to the temperature of the front being fixed at T*. Hence, the substrate is shielded from the high temperature of the external heat source. The length of the plateau is dependent on the external heat flux and the enthalpy of the endothermic process.

The velocity of the front changes with position. It is greatest when intumescence just begins and decreases as the front moves toward the substrate. If a char does not form, that is, the char ablates away, the front will experience a larger heat flux and the time taken to reach the substrate would be much shorter.

Once the front reaches the substrate the temperature rises. From the

frontal model, Buckmaster et al derived the temperature at the substrate-coating interface(x = 0) as being given by:

$$T \doteq T^* + \frac{\dot{q}_0(t - t_2)}{\rho_f c_p D} \qquad (9.9)$$

Although good agreement between experimental and theoretical results may be obtained numerous assumptions are made in order for this to be achieved.

9.2. NUMERICAL VALUES

The numerical values which may be used for the various parameters describing the properties of the coating layer and the input energy flux are given below. Care must be taken in drawing detailed conclusions from these calculations because the values of the parameters are open to considerable uncertainity. The values used are listed below:

T_o = 130 K

L_o = 0.001 m

E = 1.13×10^5 joules/m²/s

$1 + R = 4.5$

k_1 = 0.23 joules/m/s/deg

k_2 = 0.084 joules/m/s/deg

c_1 = 2.5×10^6 joules/m³ K

c_2 = $(0.5 - 0.25) \times 10^6$ joules/m³ K

N = $(125 - 334) \times 10^6$ joules/m³

SECTION 10

10.1 A NEW THEORETICAL MODEL

In order to provide a framework for the development of more effective coatings and more stringent design criteria, a mathematical model was developed in the present study. The model is an extension of the frontal model developed by Buckmaster et al (116).

The theoretical description employs a one-dimensional model, Fig. 136, based on energy conservation. The energy absorbed at the surface of the coating may be equated to that diffusing through it. If a loss of mass occurs, as in the case of intumescent coatings, then this should be taken into account.

absorbed incident energy = energy dissipated

that is, A + B + C = D + E + F (10.1)

where A = the convective energy absorbed at the surface

B = the radiant energy absorbed at the surface

C = the energy absorbed at the surface due to oxidation

D = the radiant energy emitted from the surface

E = the energy absorbed by reactions/phase changes

F = the energy conducted into the material.

The in-situ formation of a char by intumescent coatings is beneficial in that they have low thermal conductivity. Thus,

Energy absorbed = Energy disipated

therefore, G + H = I + J (10.2)

where G = energy stored in the material layer

H = the energy of the pyrolysis gases diffusing through the char

I = net energy absorbed by thermal conduction

J = the energy absorbed due to phase changes, decomposition

reactions etc.

Hence, as much energy as possible should be taken up by endothermic reactions, phase changes and reflected away from the surface. Intumescent coatings having large endothermic changes, generating copious amounts of carbonaceous foam with good insulative properties, provide the most effective thermal protection in a fire.

FIGURE 136

ENERGY BALANCE

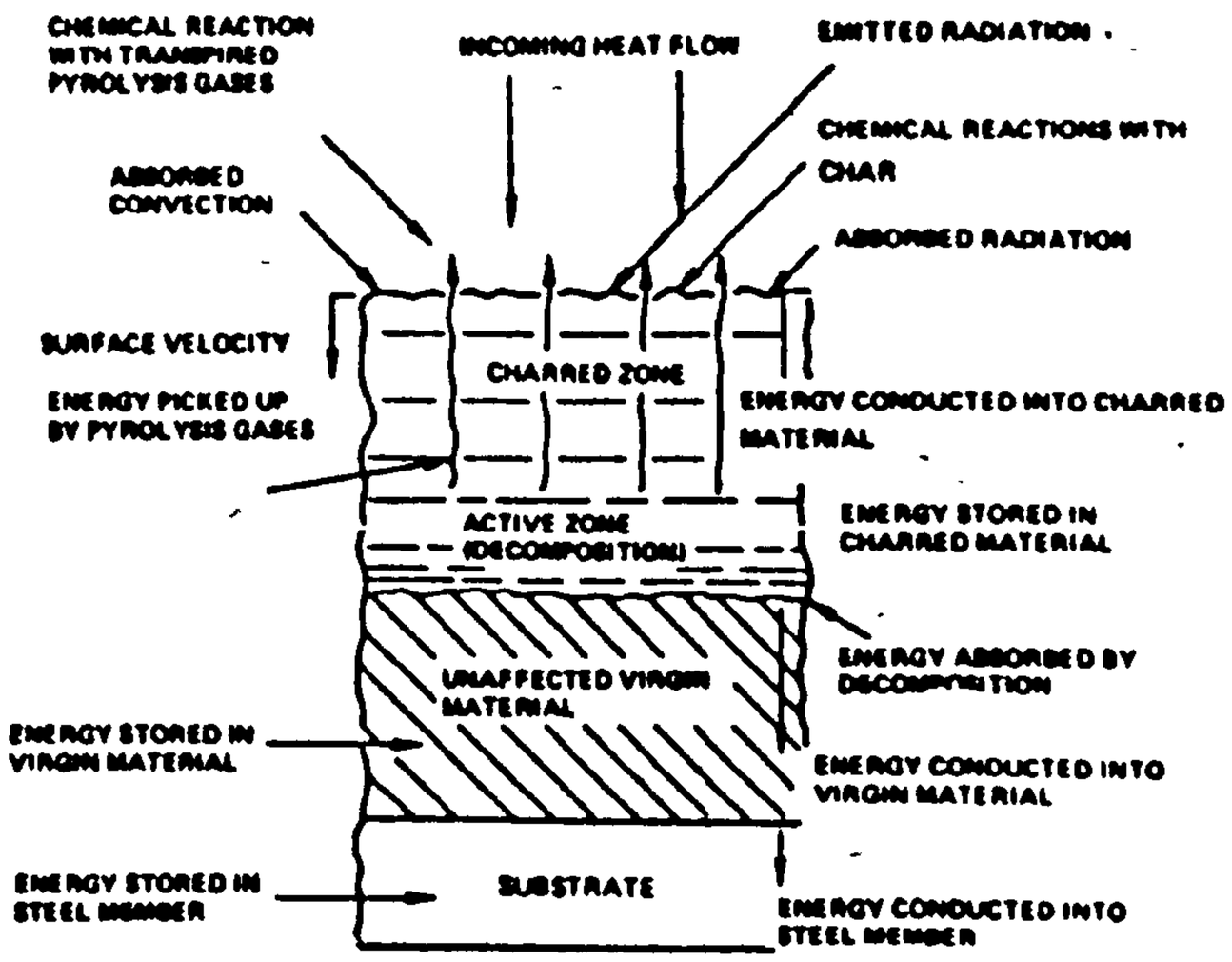

10.2. ENERGY CONSERVATION MODEL

Following the Buckmaster et al (116) approach, assume that when the coating is heated at the surface, intumescence only begins once a critical temperature T_o is reached. An infinitesimally-thin front, at which the reaction takes place, then moves through the coating. The temperature at this front remains constant. Behind the front the coating has formed a char. The temperature ahead of the front is less than T_o. When the front reaches the substrate, only a homogeneous char remains and all the intumescence has been completed. The process can be divided into three stages:

1) prior to the temperature of the surface reaching T_o (when normal

conduction takes place)

2) the period in which the front moves through the coating

3) the return to normal conduction.

The three stages are evident when the coated test plates are exposed to thermal energy and the temperature of the substrate is monitored with time (Fig. 137). Initially, a steady rise in temperature is observed, followed by a period of time when the temperature rises less steeply, and finally there is a steady increase in temperature once again. Some formulations display two clearly separated periods when the rise in temperature is less steep.

In the present model the continuous changes in the physical properties of the coating due to temperature, the evolution of gas etc. are ignored. It is assumed that a discrete jump in the properties occurs at the front.

FIGURE 137

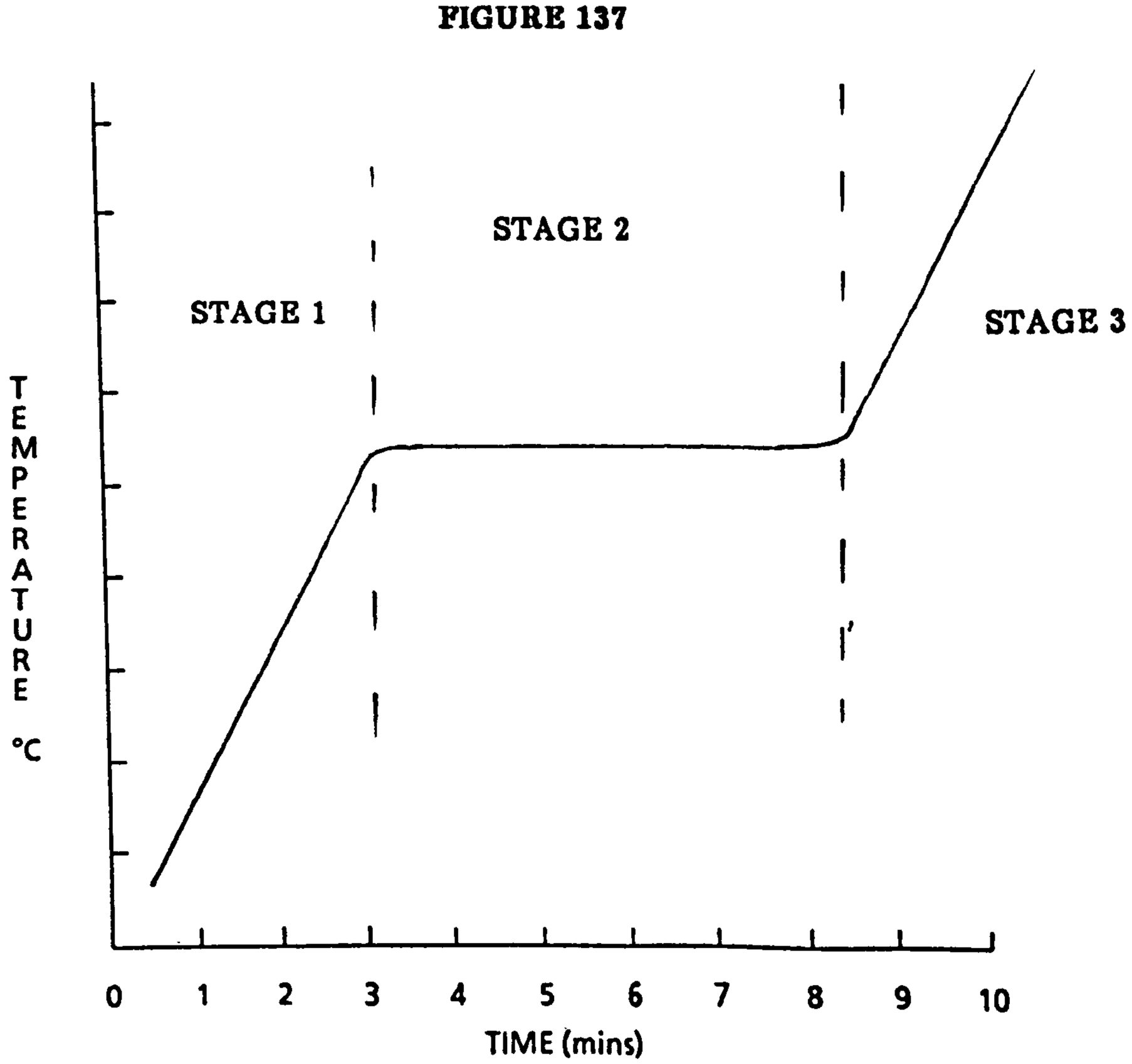

When the subscripts 1 & 2 are applied to properties, they indicate the coating in its virgin state and the char respectively. Let

k = coefficient of thermal conductivity

c = specific heat per unit length

ρ = density

$R = (\rho_1 - \rho_2)/\rho_2$

L_o = initial thickness of layer

L_1 = final thickness of layer = $(1 + R)L_o$

E = energy flux absorbed at outer surface

N = enthalpy of reaction per unit length

The effectiveness of a particular coating is measured by the time t taken for the temperature at the substrate (inner surface) to rise from room temperature to some temperature T_d that would be considered critical. We now derive an expression for t by applying the principle of energy conservation, with room temperature being set to zero. The more detailed model is described later in Sections 10.3.

During the time t, the energy absorbed by the coating is Et. In essence, this energy does three things, it provides (a) energy $c_1L_oT_o$ which raises the temperature of the coating to T_o, (b) heat for the reaction, NL_o and (c) provides energy to raise the temperature from T_o to T_d.

If it is assumed that the temperature profile of the expanded coating is purely governed by a simple relationship dependent on the thermal conductivity of the foam such that at point x within the foam the temperature is given by

$$T(x) = T_d + Ex^2/2k_2L_1 \qquad (10.3)$$

then the energy required to establish this drop is given by

$$Ec_2L_1^2/6k_2 \qquad (10.4)$$

Hence, the energy required to raise the temperature from T_o to T_d at the surface is:

$$(T_d - T_o)\, c_2\, (1 + R) L_o \quad + \quad \frac{E\, c_2\, (1 + R)^2\, L^2{}_o}{6k_2} \qquad (10.5)$$

Hence,

$$t = \frac{NL_o}{E} + \frac{T_o\, c_1\, L_o}{E} + \frac{c_2\, (1 + R)\, L_o\, (T_d - T_o)}{E}$$

$$+ \frac{c_2}{6k_2} \cdot (1 + R)^2 L_o{}^2 \qquad (10.6)$$

This expression leads us to the conclusions:

a) t is independent of the thermal conductivity of the coating, k_1.

b) the dependence of t on L_o is of the form

$$t = AL_o + BL_o{}^2$$

where A and B are positive parameters. Increasing the thickness of the layer will increase t by more than a linearly proportional amount.

c) the dependence of t on E is of the form:

$$t = \frac{A}{E} + B$$

where A and B are positive parameters. For a low input of energy, t becomes very large, but for a high input, t has a lower limit given by $c_2\, (1 + R)^2\, L_o{}^2 / 6k_2$. This is explained by the fact that when the inner surface reaches the temperature T_d, the outer surface is at temperature $T_d + E(1 + R)\, L_o / 2k_2$. In the event of a very fierce conflagration, this lower level for t may give a good indication of the delay time with its quadratic dependence on the final thickness of the layer.

d) t depends on N through the term NL_o/E. This could well be dominant if N is large compared with both $T_o\, [(c_1 - c_2\, (1 + R)]$ and

$T_d\ c_2\ (1 + R)$.

e) One expects t to depend upon the temperatures T_o and T_d through the combination $T_o + T_d$ but in fact T_o, and T_d occur in the form

$$c_1 T_o + c_2 (1 + R) (T_d - T_o)$$

If $c_2 (1+R) > c_1$, then t can be increased by having T_o as close to room temperature as possible, whilst if $c_2(1 + R) < c_1$, a temperature close to T_d is beneficial.

f) The dependence of t upon the extent to which the layer expands [(1 + R)] is not clear because both c_2 and k_2 depend on this factor in an unknown fashion.

10.3 GENERALISATION OF EQUATION

The expression for t, Eq (10.6), can be very easily generalised to the case of a coating which liberates several gases at various temperatures and with various enthalpies of reaction. To do this, let these components of the coating be labelled by the variable (α) so that their contribution to the specific heat per unit length of the unswollen paint is $c(\alpha)$ and

$$c_1 = \sum_{\alpha} c(\alpha) \qquad (10.7)$$

Also, component α liberates gas at temperature $T(\alpha)$, with enthalpy of reaction per unit length of the unswollen paint $N(\alpha)$, so that

$$t = \frac{L_o}{E} \sum_{\alpha} N(\alpha) + \frac{L_o}{E} \sum_{\alpha} c(\alpha)\ T(\alpha)$$

$$+ \frac{(T_d - T_o) c_2 (1 + R) L_o}{E} + \frac{c_2 (1 + R)^2 L^2_o}{6k_2} \qquad (10.8)$$

The comments made above apply equally well to this expression.

10.4. STAGE ONE OF INTUMESCENCE

During this stage the equation to be solved is:

$$\frac{\partial T}{\partial t} = \frac{k_1}{c_1} \frac{\partial^2 T}{\partial x^2} \qquad 0 < x < L_o \qquad (10.9)$$

subject to the conditions

$$\frac{\partial T}{\partial x} = 0 \qquad \text{at } x = 0,\ t > 0$$

$$\text{and} \qquad \frac{\partial T}{\partial x} = \frac{E}{k_1} \qquad \text{at } x = L_o,\ t > 0$$

In order to simplify the mathematics, room temperature is set to zero, so that $T = 0$, at $t = 0$

The solution is:

$$T(x,t) = \frac{E}{2k_1 L_o}\left[x^2 + 2\frac{k_1}{c_1}t\right] - \frac{EL_o}{6k_1} \qquad (10.10)$$

$$+ \frac{2\,EL_o}{k_1 \pi^2} \sum_{n=1}^{\infty} \frac{(-1)^{n+1}}{n^2} \exp\left(-n^2 \frac{k_1 \pi^2 t}{c_1 L_o^2}\right) \cos\left(\frac{n\pi x}{L_o}\right)$$

When the transient terms decay away, a steadily-rising parabolic temperature profile is observed. This stage finishes when the temperature at the outside surface reaches the value T_o. If we ignore the contribution from the transients, this takes a time

$$\frac{c_1 L_o T_o}{E} - \frac{c_1 L_o^2}{3k_1} \qquad (10.11)$$

This result is in excellent agreement with that derived by Buckmaster et al. Eq. 9.9. Using the data in Section 9 and Eq. 9.8. the outset of intumescence is found to be 2.1 seconds whereas using Eq. 10.10 the time was 3.1 seconds. At the substrate, the temperature increases linearly with rate of change given by $E/c_1 L_o$. Observation of this rising temperature can be used to decide whether it is justifiable to ignore the

transient terms. Using data given by Buckmaster et al (116), it can be shown that for a time of 2.5 s then the transient time is about 0.1 ns.

10.5. STAGE TWO OF INTUMESCENCE

During this stage, the equations to be solved are

$$\frac{\partial T}{\partial t} = \frac{k_1}{c_1} \cdot \frac{\partial^2 T}{\partial x^2} \qquad 0 < x < s \qquad (10.12)$$

$$\frac{\partial T}{\partial t} = - u \frac{\partial T}{\partial x} + \frac{k_2}{c_2} \frac{\partial^2 T}{\partial x^2} \qquad s < x < L \qquad (10.13)$$

where L(t) is the co-ordinate of the outer surface, u = dL/dt, and the front is situated at x = s(t). For mathematical convenience the temperature at which the reaction takes place is set to zero. The boundary conditions are

$$k_2 \frac{\partial T}{\partial x} = E \qquad \text{at } x = L \qquad (10.14)$$

$$T = 0 \qquad \text{at } x = s$$

and according to energy conservation

$$k_1 \left[\frac{\partial T}{\partial x}\right]_1 - k_2 \left[\frac{\partial T}{\partial x}\right]_2 = N \frac{ds}{dt} \qquad (10.15)$$

The initial conditions are determined by the temperature profile at the end of stage one.

The speeds at which the expanded coating and the front move are related. In this section, the density ρ_1 is the density of the virgin material excluding any volatile components. Then according to mass conservation,

$$\rho_1 L_o = \rho_1 s + \rho_2 (L - s) = \rho_2 L_1 \qquad (10.16)$$

Then
$$\frac{dL}{dt} = - R \frac{ds}{dt} \qquad (10.17)$$

The change of variable $y = x$ for $0 < x < s$

and
$$y = \frac{1}{1 + R} x + \frac{R}{1 + R} s \qquad s < x < L \qquad (10.18)$$

brings the outer surface to rest and yields

$$\frac{\partial T}{\partial t} = \frac{k_2}{c_2(1+R)^2}\frac{\partial^2 T}{\partial y^2} \qquad s < y < L \quad (10.19)$$

$$\frac{k_2}{(1+R)}\frac{\partial T}{\partial y} = E \qquad \text{at } y = L_o \quad (10.20)$$

$$T = 0 \qquad \text{at } y = s$$

$$\text{and} \quad k_1\left[\frac{\partial T}{\partial y}\right]_1 - \frac{k_2}{(1+R)}\left[\frac{\partial T}{\partial y}\right]_2 = \frac{N ds}{dt} \quad (10.21)$$

The diffusion equation and most of the boundary conditions are expressions of energy conservation at particular points. We can obtain a more useful expression if we consider the total energy of the system. The thermal energy contained in the region $s < x < L$ is $U(t)$ where

$$U(t) = c_2 \int_s^L T \, dx$$

$$= c_2 (1+R) \int_s^{L_o} T \, dy$$

$$\text{and} \quad \frac{dU}{dt} = c_2(1+R)\int_s^{L_o}\frac{\partial T}{\partial t}\,dy - c_2(1+R)\left[\frac{\partial T}{\partial t}\right]_s \frac{ds}{dt} \quad (10.22)$$

After some manipulation, this yields

$$\frac{dU}{dt} = E + N\frac{ds}{dt} - k_1\left[\frac{\partial T}{\partial y}\right]_1 \quad (10.23)$$

If the k_1 term is ignored, then integrating

$$U = Et + N(s - L_o)$$

Two times characterise the equations above, a lower boundary for the

transit time of the front

$$t_c = NL_o/E \tag{10.25}$$

and the diffusion relaxation time behind the advancing front

$$t_d = \frac{c_2 (1 + R)^2 L_\delta^2}{k_2} \tag{10.26}$$

One assumption we make in what follows is that

$$t_c >> t_d$$

(An assumption which holds in the case of the figures in Section 9.)

The diffusion relaxation time ahead of the front is considerably shorter than that which supports our last step in deriving equation (10.24).

Following Goodman (117), we introduce a parabolic temperature profile behind the front

$$T = A (y - s) + B(y - s)^2 \tag{10.27}$$

where A and B are possibly functions of time . Then

$$U = c_2 (1 + R)\left[\frac{A}{2} (L_o - s)^2 + \frac{B}{3} (L_o - s)^3\right] \tag{10.28}$$

and (10.24) becomes

$$t = t_{cp} + \frac{t_d k_2}{(1 + R) E}\left[\frac{A}{2} p^2 + \frac{B}{3} L_o p^3\right] \tag{10.29}$$

$$p = \frac{L_o - s}{L_o} \tag{10.30}$$

The boundary condition at $y = L_o$ gives

$$A + 2 B L_o p = \frac{(1 + R) E}{k_2} \tag{10.31}$$

Substituting the parabolic profile into the diffusion equation, we find that A and B must obey

$$\frac{dB}{dt} = 0,\ \frac{dA}{dt} + 2BL_o\frac{dp}{dt} = 0 \quad \text{and} \quad A\frac{dp}{dt} = \frac{2\,B\,L_o}{t_d} \qquad (10.32)$$

If the first of these equations is obeyed then the second equation follows from Eq. (10.31). Whilst

$$\frac{dp}{dt} < \frac{1}{t_c}$$

intimates that $A >> BL_o$

Expanding A, B and t in powers of p and substituting in the Eqs (10.29), (10.31) and (10.32) yields the results:

$$t = t_c p + t_d\frac{p^2}{2} - \frac{2}{3}\frac{t_d^2}{t_c}p^3 + \text{----} \qquad (10.33)$$

$$A = \frac{(1+R)\,E}{k_2}\left[1 - \frac{t_d\,p}{t_c} + 4\left[\frac{t_d}{t_c}\right]^2 p^2 + \text{---}\right] \qquad (10.34)$$

$$B = \frac{(1+R)}{2}\frac{E}{k_2 L_o}\left[\frac{t_d}{t_c} - 4\left[\frac{t_d}{t_c}\right]^2 P + 10\left[\frac{t_d}{tc}\right]^3 p^2 + \text{---}\right] \qquad (10.35)$$

These series are also in rising powers of $(\frac{t_d}{t_c})$, the ratio may be taken to be very much less than unity. The series for t describes how the front commences with a speed of $\frac{L_o}{t_c}$ but slows slightly to a speed of about $L_o/t_c + t_d$ by the time it has reached the inner surface. The transit time of the front is given by the expression:

$$t + \frac{t_d}{2} - \frac{2}{3}\frac{t_d^2}{t_c} + \text{-----} \qquad (10.36)$$

10.6. STAGE THREE OF INTUMESCENCE

This stage resembles the first stage, the primary differences being that the layer has expanded to width $(1 + R)\,L_o$ and the specific heat and thermal characteristics have reduced values. When the transients have died away the temperature profile has the form:

$$T(x,t) \doteqdot \frac{E}{2k_2(1+R)L_o}\left[x^2 + 2k_2/c_2 t\right] \qquad (10.37)$$

The temperature at the inner surface now rises at a rate

$$\frac{E}{c_2(1+R)L_o}$$

This is faster than the rise during stage one because c_2 is less than c_1 due to two factors, the expansion of the layer [a factor $(1+R)^{-1}$] and the loss of mass due to escaped gas. Using the data of the previous sections, the increase can be of the order of more than 100%. The transients during this final stage have decay periods given by the expression:

$$\frac{c_2(1+R)^2 L_o^2}{k_2 \pi^2 n^2}$$

This shows an increase over the decay periods during stage one, using the data given in Section 9, by a factor of 5 to 10. On the other hand the initial temperature is parabolic leading to the expectation that the transients have much smaller amplitudes.

10.7. COMPARISON WITH EXPERIMENT

The model presented above provides at least a qualitatively correct description of the heat conduction process through a layer of intumescent paint. In this section, we deal with the quantitative information about the layer that can be extracted from an accurate graph of the temperature at the inner surface against time.

(a) The stage one rate of rise of temperature yields a value of

$$\frac{E}{c_1 L_o}$$

(b) Similarly the stage three rate of rise of temperature yields

$$\frac{E}{c_2 L_1}$$

(c) For some layers, during stage three, the rate of rise of temperature gently decreases with rising temperature. This is probably due to the fact that the outer surface is reaching temperatures at which heat loss to the environment should be taken into account. This can be done by including an extra term into the boundary condition at $x = L_1$,

$$k_2 \frac{\partial T}{\partial x} = E - mT$$ where m is a constant for a given char

Hence, the curvature of the graph reveals information about m/E.

(d) If the graph for stage two has a clearly defined plateau, then it gives a value for T_o, the temperature at which the exothermic reaction takes place.

(e) The transient behaviour of the temperature at the commencement of stage two, if distinct enough, can yield a value for the principal decay time

$$\frac{\Pi^2}{4} \times \frac{c_1}{k_1 L^2_o}$$

(f) If the movement of the front is dominated by the enthalpy of reaction N, then the duration of stage two (t_o) gives the value for

$$NL_o/E$$

However, if the more complicated expressions for t_o derived in Section 10.5. needs to be used, the value obtained is

$$\frac{NL_o}{E} + \frac{c_2 L_1^2}{2k_2}$$

SECTION 11

DURABILITY OF COATINGS

11.1. INTRODUCTION

The formulations developed in this project were found to have significantly improved fire performance over the commercially-available materials when tested in a large-scale fire test, see Section 7. The formulations produced good films with excellent physical properties (hardness, impact resistance, scratch resistance, flexibility of the paint film and adhesion before and after exposure to fire). Only a few publications were found in the literature on the durability, i.e. resistance to water penetration, of intumescent coatings (118-119). This important aspect was examined in the present study in order to establish the principles involved and to develop a means of comparing the durability of formulations. A brief introduction to the theoretical principles involved is given below.

11.2. WATER PENETRATION - THEORETICAL CONSIDERATIONS

Water may permeate a paint film as a liquid or vapour by the mechanisms discussed below.

1) If a film with an open, continuous, connected structure is wetted, it may be penetrated by liquid water being drawn in by capillary forces. The depth of penetration depends on the capillary radius, the surface tension of the water and the temperature.

Liquid water will penetrate a film of any thickness if it has a pore structure. Wetting of a solid by a liquid can occur only when there is a decrease in Gibbs function of the system. If a drop of liquid is placed on a horizontal surface it may spread out indefinitely or only to a limited area,

in which case the edge of the drop meets the surface at the angle of contact. The smaller the contact angle, the easier it is to wet the solid and contact angles greater than 90° would result in no wetting occuring. Hence, to eliminate the possibility of water penetrating an intumescent film, the contact angle of water on the film must be greater than 90°. Two approaches were tried, (a) the incorporation of hydrophobic materials into the formulation (b) the application of hydrophobic paints to coatings. In an attempt to determine the effectiveness of these approaches the contact angle between water and film surface was measured.

2) Water in vapour form may penetrate a film, by Knudsen or Poiseuille flow through a connected, open pore structure, or by activated diffusion through the solid constituents (93, 120, 126).

If the channel radius is small compared with the mean free path of a gas molecule, Knudsen flow occurs. The convection velocity is given by

$$V = \frac{k'K}{\sqrt{\rho P}} \cdot \frac{\partial P}{\partial x}$$

where $k'K = \frac{r}{6}$

r is the pore radius

P is the vapour pressure

ρ is the vapour density

$\frac{\partial P}{\partial x}$ is the pressure gradient

For straight pores greater than 1 μm diameter, capillary flow occurs, and Poiseuille's equation applies, whereas Darcy's equation applies if the pores are tortuous and the penetration velocity is given by

$$V = \frac{k'}{n_g} \cdot \frac{\partial P}{\partial x}$$

where n_g is the vapour viscosity

$$k' \text{ (Poiseuille)} = r^2/8$$

k' (Darcy) is determined empirically.

This is likely to be the case with intumescent paint films.

As mentioned, in the absence of an open pore structure, water vapour may permeate a material by activated diffusion (ie. by solution in the film surface on the high concentration side) diffusion through the film by a series of activated steps, and evaporation at the low concentration side.

Simple diffusion, in which the diffusion coefficient is independent of the concentration of diffusing species, is described by Fick's first law (129):

$$F = -D \frac{\partial C}{\partial x}$$

where F is the diffusion rate

D is the diffusion coefficient

C is the concentration

x is the space coordinate normal to the section.

In many polymer systems, however, D depends markedly on the concentration(129), and Fick's second law applies:

$$\frac{\partial C}{\partial t} = D \frac{\partial^2 C}{\partial x^2}$$

where t is time.

Diffusion is a much slower process than capillary flow, as was demonstrated by Stannet (120).

Therefore, the water permeability of an intumescent coating should also be reduced significantly if a very thin polymer film with good barrier properties is applied.

Diffusion of water occurs through all polymers, but at rates which differ by many orders of magnitude, depending on the degree of chemical compatibility of the water and host molecules. For example, ethyl cellulose and cellulose acetate, which contain many hydroxyl groups, are poor barriers to water vapour, whereas polyvinylidene chloride and polytetrafluoroethylene, which contain none, are good barriers (121), (see Table 26).

The films tested in the present study were based on formulations using a copolymer of butadiene and vinyl toluene, both of which have a moderately high permeability to water.

11.3. EXPERIMENTAL WORK

11.3.1. PREPARATION OF PAINT FILMS

Preparation of detached coatings in a reproducible manner, without pin-holes or cracks, is very difficult. Due to the tendency of the 'fillers' to settle out and cause variations in viscosity, most of the formulations examined were adjusted to incorporate a small amount of wetting agent. The amount of settling is dependent on the time elapsed since manufacture. Before the coating specimens were cast, the sample was mixed thoroughly to produce uniform dispersion of the ingredients and a consistent viscosity.

Coating specimens were cast by pouring the paint onto a polyethylene-coated release paper which was in turn temporarily attached to a polished aluminium plate with a fine film of grease. A 'picture frame' made from a 1.5 mm thick aluminium was used to contain the paint, and enable the extra fluid to be screeded to the right thickness. The thickness of the aluminium 'picture frame' was selected in order to allow permeability within a reasonable time.

The films were allowed to dry in the laboratory under ambient conditions (approximately 20°C and 60% RH) for a number of days until they reached constant weight Fig. 138. It was found that films cast and allowed to dry for 2-3 days had sufficient strength and flexibility to allow sample preparation. Drying periods in excess of 3 days produced films which were very stiff and difficult to cut. The forced drying of films at 70°C for 4-5 hours produced samples which were flexible enough for handling. However, it was found that the higher the temperature at which the films were dried the faster they set and the greater was the variability of the results obtained from the permeability experiments.

FIGURE 138

WEIGHT LOSS AS A FUNCTION OF TIME

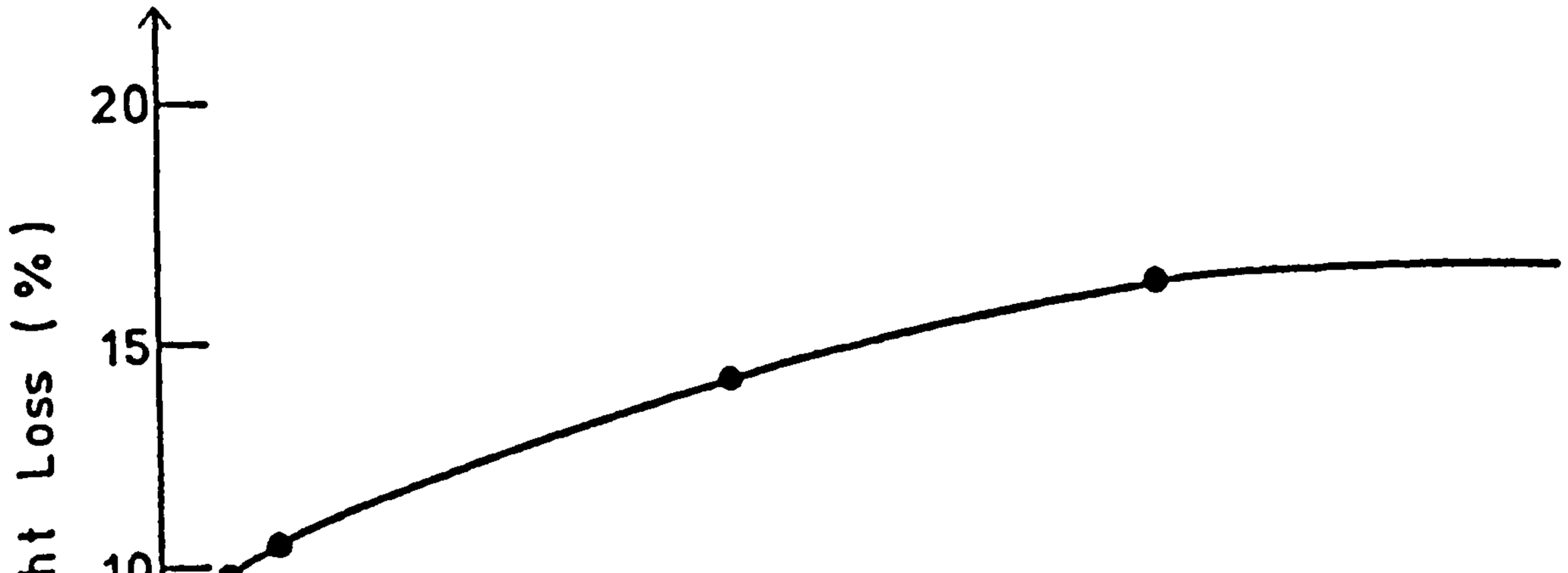

11.3.2. MEASUREMENTS OF WATER VAPOUR PERMEABILITY

The cast films were very carefully removed from the polythene coated release paper in order to ensure no tearing or cracking occurred. Circular discs, 50mm in diameter were cut from the cast films. Those discs which were free of visible pin-holes were selected for water vapour permeability measurements and other tests such as wettability and intumescent studies.

For the permeability tests, the selected discs were sealed by rubber bands across the mouths of aluminium cups filled with water, which were then placed in a desiccator containing phosphorus pentoxide. The cups were removed from the desiccator and weighed at regular intervals (every 24 hours) Fig. 139. A film of polyethylene was used used as a control. Water vapour permeabilities for all the films tested were calculated from the slopes of the linear portions of the curves, and average values are listed in Table 26 and 27.

FIGURE 139

WEIGHT LOSS OF CUPS AS A FUNCTION OF TIME

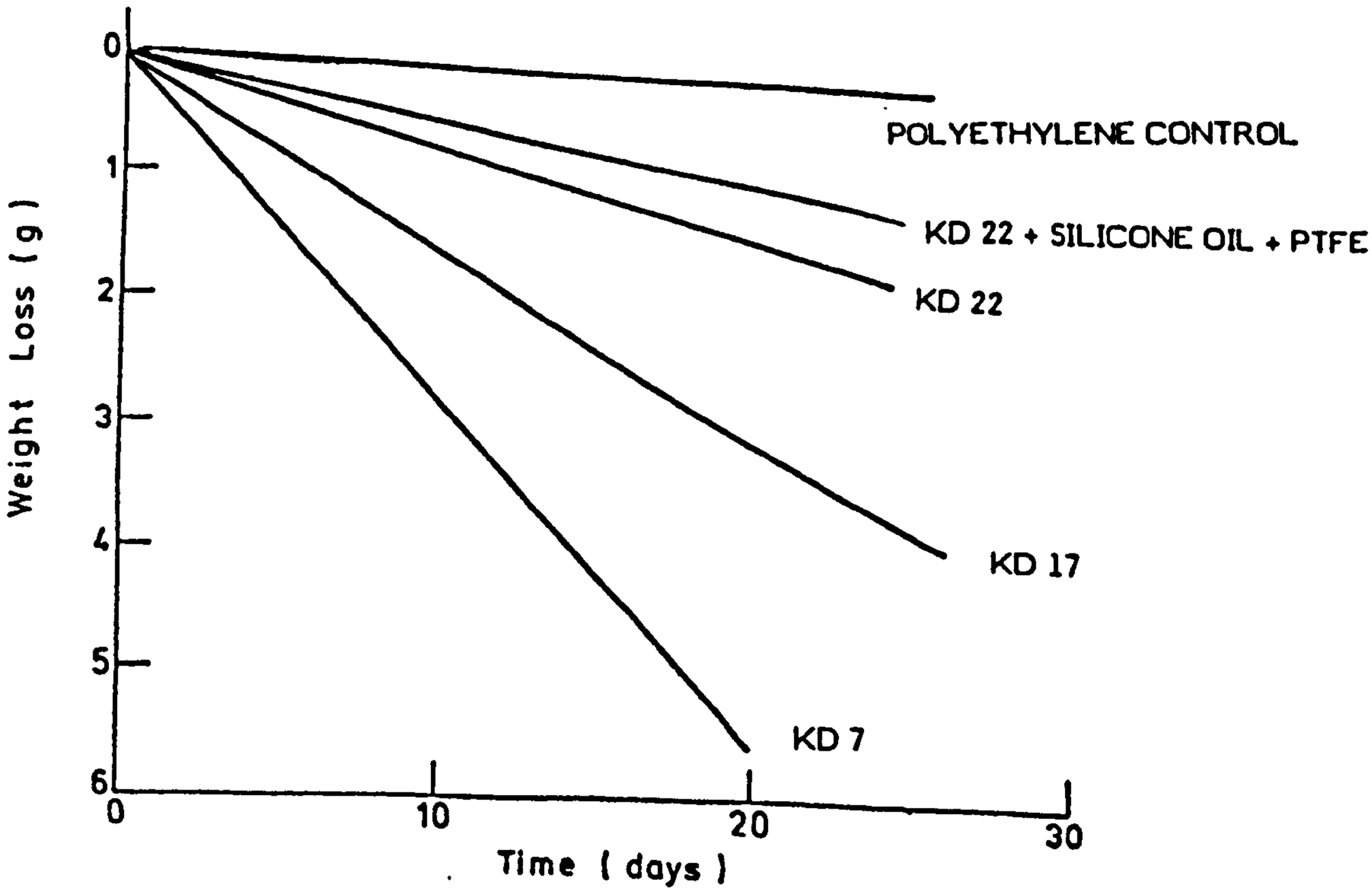

11.3.3. MEASUREMENT OF WETTABILITY BY WATER DROPLETS

A burette was used to produce water droplets of reproducible size (approximately 0.05 ml). This reproducibility was checked by weighing 50 individival drops. The average weight was found to be 0.047g, the standard deviation being 0.005g. Droplets of the same size were then placed on the cast films laid on a table. The time was noted for the droplets to be absorbed into the film. This technique was used to assess the various modified formulations.

Different formulations were assessed for wettability. Out of a large number of methods tried, the most effective treatments were found to be:

a) inclusion of silicone oil in the formulation,

b) a film of PTFE spray on the surface of a freshly applied coating

c) encapsulation of the catalyst in a water insoluble thermoplastic resin such as polyamide or polyester

d) replacing the water soluble components of the formulation with insoulble substitutes e.g. replacing APP by melamine phosphate

e) top coating with a sealer coat such as chlorinated rubber.

The addition of silicone oil to the formulations improved the wettability properties of the films significantly (Table 27). However, levels above 3% have an adverse effect on the intumescent properties. Coating the paint surface with a PTFE spray was found to be a temporary but very effective method of improving the wettability. Inclusion of the PTFE in the formulation was found to be ineffective and greatly reduced intumescent properties. Top coating of the paint with sealer coats was effective and the overall performance was dependant upon the system selected. In general, the best results were produced by the epoxy based sealer coats. However, the intumescent properties were greatly reduced. Systems based upon chlorinated rubber produced the best overall results.

Coating of the catalyst with thermoplastic resins was effective but the encapsulation technique was found to be extremely difficult. Total replacement of APP by melamine phosphate required a new formulation (Section 6) and produced good wettability results.

TABLE 26

POLYMER	PERMEABILITY ($mg/cm^2/mm/day$)
Ethyl cellulose	0.1 - 1.2
Cellulose acetate	0.12 - 1.0
Polybutadiene	0.4 - 0.6
Polyvinylidene chloride	1.16×10^{-4}
Polytetrafluoroethylene	3×10^{-2}

TABLE 27

Water vapour permeabilities and intumescence of the various formulations

FORMULATION NUMBER	PERMEABILITY ($mg/cm^2/mm/day$)	FOAM HEIGHT mm	
		BEFORE WVP*	AFTER WVP*
KD 4	35+	15	5
KD 7	28	24	10
KD 14	21	20	12
KD 17	16	22	15
KD 21	10	12	7
KD 22	8	25	18
KD 22 + 1% silicone oil	5	18	16
KD 22 + 3% silicone oil	3	10	9
KD 22 + PTFE (spray)	3	6	6
CONTROL (POLYETHYLENE)	.05	-	-

WVP* = water vapour permeability

11.3.4. MEASUREMENT OF INTUMESCENCE

All the formulations tested for water vapour permeability were further analysed to determine any change in the intumescence properties. This was done by comparing the thermal/thermogravimetric analysis measurements, using STA on the film samples before and after exposure to the permeability tests. However, no significant change was observed in the curves. The films tested for water vapour permeability test (WVP) were then subjected to $40kW/m^2$ radiation using ISO ignitability apparatus as described in Section 4. Results are given in Table 27.

SECTION 12

DISCUSSION

The chemistry of intumescence is very complicated and dependent upon the sequential interaction of various heterogeneously-dispersed ingredients. Because of these factors, the selection of ingredients is very critical, being dependent upon their thermal behaviour. Consequently, various raw material ingredients were fully examined for their thermal behaviour using a range of analytical equipment such as DSC, DTA, STA, DTG, TG etc. The information acquired from these analyses was used to develop new improved formulations of intumescent coatings. Initially, each formulation was tested for its fire performance using various laboratory-scale, screening test methods. Finally, the best three formulations were evaluated in a large-scale fire test, using commercially-available intumescent coatings as controls in a fire of hydrocarbon intensity.

The conclusions drawn from the experimental work done on the physico-chemistry of intumescence are important and form the basis for development of new formulations with greatly improved physical and fire-resistant properties. The studies of the kinetics and mechanism of intumescence which were undertaken for this research work resulted in a mathematical model which was used to explain the characteristics of intumescent coatings.

For intumescence to occur, the carbonific, catalyst and blowing agent must interact with each other in the fluid phase brought about by the melting of the binder due to an increase in temperature of the coating.

Hence, selection of a suitable binder is a very important factor and is the key for the intumescence process to occur. For example, thermal data from DSC and STA show that the mixture of the carbonific and the catalyst has an endothermic reaction at 240°C and exothermic reactions from 245°C to 370°C followed by an endothermic reaction from 370°C to 400°C. Thus, the binder selected should show thermal activity at a lower temperature than the decomposition temperature of the intumescent system. According to DSC, STA and DTA data, a chlorinated polymer binder softens at approximately 205°C and starts to decompose exothermically at 260°C-350°C, with a very exothermic reaction, possibly due to oxid ation of the carbon, occurring at about 512°C. The decomposition occurs in three distinct regions. In the region 130-240°C, the weight loss is about 5%. In the region 240-400°C, the weight loss is approximately 60% with activation energy of about 30kJ/mole and order of reaction at 300°C of 3.3. In the final region 400-600°C, the weight loss is about 35% with activation energy of approximately 50kJ/mole. This binder has activation in the region which is the preferred temperature range for the intumescent. A formulation based on such a binder system (KD 17) has been shown to produce coatings with good intumescent properties and above-average fire performance.

By comparison, a SBR type of binder system was found to have thermal activity at 340°C - 425°C, which is much higher than the decomposition temperature of the intumescent system. As predicted, formulations produced using this type of binder resulted in no intumescence and hence no fire performance.

The first stage of reaction is the acidic dehydration of pentaerythritol with ammonium polyphosphate. The thermal data for pentaerythritol

show a softening point at 181°C. The dehydration starts at about 240°C and is fully completed by 340°C, being a very large exothermic reaction Fig. 49 and 50. Under nitrogen, the process begins at 220°C and is complete at 330°C. It appears that the reaction follows 2/3 order kinetics with an activation energy close to 25-26 kJ/mole. In both cases, under air and nitrogen the STA and the DSC curves indicated a single endothermic reaction commencing near the beginning of the weight loss and having a minimum near the middle of the weight loss, see Fig. 49. Similarly, ammonium polyphosphate undergoes decomposition/volatilisation in three main steps with the weight loss being about 20% at a temperature of 400°C, and 60% at 750°C, Fig 45-47A. However, under nitrogen, the weight loss is only 15% at a temperature of 500°C. In both cases, ammonia and water are the gaseous products evolved in the first two steps. Phosphoric acid is released at approximately 200°C, this large endothermic decomposition being completed by 330°C. From STA experiments, the activation energy was found to be 60kJ/mole with an order of reaction of approximately 9 at 350°C. The high temperature region exhibits a decomposition curve having an activation energy of approximately 80kJ/mole.

Mixtures of the pentaerythritol and ammonium polyphosphate show a strong interaction, with esterification of the carbonific in two and possibly three main steps Fig. 70. The softening of the pentarythritol at 181°C, a new endothermic reaction at 240°C, with approximately a 5% weight loss, a number of exothermic reactions at 345°C to 370°C, with approximately 30% weight loss, and a series of very small exothermic reactions occurring at about 620°C, with a weight loss of 50-60%, are all observed, Fig. 70. The reaction of the mixture starts at about the same temperature as the main degradation of ammonium polyphosphate heated

alone under simlar conditions. However, the ester produced by the mixture decomposes thermally to produce acid and water. This is followed by further decomposition of the ester to produce a large amount of carbon, additional water, carbon monoxide, non-flammable gases and the release of acid for further esterification. The thermal data indicate that the ester begins to decompose at a temperature significantly lower than that of the 'non-esterified' carbonific.

The experimental work carried out in Section 6 on the development of various formulations revealed that selection of the acid generator is critical. Catalysts with phosphorylation temperatures above that of the carbonific decomposition produced char but no intumescence. In general, the ammonium orthophosphates have been used as catalysts, although the amine and amide phosphate reaction products, such as melamine phosphate (75) and polyphosphoryl-trianilide (127,128) have also been described in the patent literature. However, for the purposes of this research, the major catalysts investigated were ammonium polyphosphate 'Phoscheck P30' and melamine phosphate. The cell structure formed by the two catalysts and the degree of intumescence produced is a distinct feature of each catalyst. Fig. 83 shows the differences in the two cell structures - melamine phosphate producing a very aerated structure in similar conditions of exposure. In general, the earlier in the thermal process that phosphorylation can be induced, the greater is the chance for complete conversion of the polyol to char. This was demonstrated by the increased amount of char resulting from the use of equivalent amounts of melamine phosphate and ammonium polyphosphate in the same formulation. It was also noted that formulations produced from different batches of the catalyst resulted in varying degrees of intumescence. For example, in an extreme case, a batch of catalyst failed to give the

endothermic reaction peculiar to Phoscheck P30 and resulted in a formulation without intumescence.

The spumific selected for the final formulation was melamine. The decomposition of melamine occurred in two endothermic reactions at 345°C and 575°C with activation energy of 43.7kJ/mole and 58.4kJ/mole and orders of reaction at 275°C and at 575°C of 9.5 and 4.9 respectively. The other spumific investigated was a paraffin wax 'Cereclor 70' which appeared to show 2/3 order kinetics with activation energy of approximately 18kJ/mole. However, very strong exothermic reactions were observed at 350°C and 550°C which were found to have adverse effects on the backwall temperatures of the coatings.

As far as the mechanism of intumescence is concerned, it is generally accepted that the foaming action in the charring material is due to the gaseous degradation products evolved. It is also recognised that the final properties of the foamed carbonaceous residue are strongly dependent upon the matching of the temperatures affecting the gas evolution and the physico-chemical properties of the degrading mixture (Vandersall). During the 'esterification', the spumific also begins to decompose. This produces a large volume of non-flammable gases which cause the carbonaceous residue to foam. A thick, insulative, fine-textured, low-density foam should be formed. From the experimental work, it was found that a careful selection of the blowing agents is required. A range of spumifics and their mixtures were evaluated (Fig. 71). Each system produced a degree of intumescence and corresponding char strength. Fig. 88-90 show the effect of different amounts of melamine and Table 12 shows the change in the corresponding properties.

The large-scale fire test conducted at the RAF Cardington test rig gave some information on the behaviour of a number of intumescent fire-protection systems in a real, high-temperature, fire environment. A number of indicative column sections protected to a nominal one-hour standard of fire resistance using proprietary intumescent and passive systems were included in the test. The fire load density was very carefully selected to produce fire conditions more severe than those found in the normal BS 476 : Part 8 furnace and typified conditions encountered in a small office, but also represented the maximum quantity of fuel permitted by the Safety Committee. The severity of the fire was aimed at producing a maximum thermal shock to the intumescent systems and to represent partially the hydrocarbon fire intensity for an approximately 20 minutes period with maximum temperatures well in excess of 1000°C being achieved in a relatively short time. Consequently, wood/polypropylene fuel, based on 75% /25% balance of calorific value, was used, equivalent to a fire load density of 20 kg wood/m^2 and the 1/4 ventilation of one wall, a theoretical opening factor of 0.06 $m^{\frac{1}{2}}$. A peak temperature of 1190°C was reached after 6 minutes which reduced to approximately 850°C after 10 minutes and the test was discontinued after 42 minutes. The rapid rise in temperature, followed by a fall to a more conventional temperature, was characteristic of mixed wood/plastic fires. The unprotected column reached a maximum average temperature of 785°C this being achieved in 15 minutes. The temperature of the unprotected steel would have been reached in a BS476 : Part 8 test after 38 minutes. All the intumescent materials provided protection to the steel work with the maximum average temperatures ranging from 258°C to 433°C. The formulations developed in this research work produced maximum temperatures of 300°C for KD 7, 344°C for KD 16, and 337°C for KD 20 and 348°C for the control proprietary intumescent system.

Taking the virgin dry thickness into consideration, these results compared very favourably with all the intumescent coating systems investigated in this study. Fig. 100 represents a comparison with a typical hydrocarbon fire and Fig. 101 shows the predicted and actual temperatures attained. The accuracy of the results is dependent upon the the equation used.

The large-scale fire test showed the potential of the developed formulations and conclusively indicated their similarity to the commercially-available intumescent coatings from the point of view of fire performance. However, these formulations were rather complicated, with far too many interactions, to enable any meaningful investigation of the mechanism of intumescence to be undertaken. Hence, a simplified formulation KD 23, with the least number of ingredients and consequently with the minimum number of possible interactions, was developed. The new formulation was developed to produce a maximum height of intumescence at a relatively low level of heat radiation with maximum char strength and adhesion to the substrate. The formulation was thoroughly analysed using various thermal analytical techniques.

ISO ignitability apparatus was adapted to produce heat radiation equivalent to that attained in the furnace during tests to BS 476 : Part 8 and real large-scale fires. The equipment was fully calibrated at FRS. Steel panels coated with KD 23 were exposed to various amounts of radiation ranging from 10 kW/m^2 to 60 kW/m^2 for a range of time intervals from $\frac{1}{4}$ second to 60 minutes. The chars so produced were fully characterised for their physical properties i.e. intumesced height, weight loss, backwall face temperature etc. The chars were also analysed using thermal analysis.

The effect of radiation, as expected, was dramatic with lower radiations producing intumescence slowly. At 10 kW/m^2, no intumescence was observed. However, some loss of weight and thickness after exposure for periods of up to 10 minutes was noticed. Obviously, the temperature at the surface of the coating was below the temperature required for the intumescent reaction to take place. The loss in weight and thickness is possibly due to some of the polymer softening and release of some volatile decomposition products. Increasing the radiation to 20 kW/m^2 triggers the reaction in about 1.25 minutes. Initially, a slight weight loss was noticed, probably due to the degassing and release of decomposition by-products. The foam height and weight loss increased linearly for a period of up to 3 minutes after which a sudden reduction occurred. This reduction corresponds with the drop or stabilisation of the backwall face temperature. Exposure for a further period of up to 10 minutes produced a linear increase in foam height, weight loss and the backwall face temperature with maximum levels of foam height and weight loss occurring at 10 minutes. Further exposure for up to 30 minutes did not cause any further change in foam height or weight loss. Hence, this suggests that the whole reaction takes upto 10 minutes to complete. This is confirmed by the thermal data.

The residual thickness of the coating, after removing the intumescent foam contains almost virgin material, as shown by the thermal data. Hence, the 'active thickness' which has caused the intumescence to occur was found by deducting the residual thickness after exposure from the initial coating thickness. Expansion factors of the coatings were determined by 1) dividing the final intumesced thickness by the original thickness of the coating and 2) by dividing the final intumesced thickness by the 'active thickness'. The expansion factor calculated by method 2)

gives the true picture of the rate of foam production and its ability to insulate the coating underneath from further activation. This was clearly demonstrated on plates number 10, 23 and 19 and also by the peak in the graphs, Fig. 109-110.

The plateau in the backwall face temperature and the dip in the weight loss and foam height observed (Fig. 108 & 111) are all due to the thermal activity of the reactions involved. The duration of the plateau is partly dependent on the level of incident radiation, being almost negligible at high intensities, e.g. 60 kWm/m^2, whereas at 20 kW/m^2 it extends for almost 3-4 minutes. The length of the plateau indicates the extent of the reaction. If no intumescent reaction occurs the temperature-time relationship would be linear, that is, there would be no plateau. A simple mathematical model based on the physical model developed by Buckmaster, Anderson and Nachman was used to explain the temperature-time history of the behaviour of intumescent coatings. Several new results are derived from the infinitesimal-front model. In particular, a relationship was derived between the time taken for the temperature at the inner surface of the layer to rise to a given value and the parameters characterising the coating.

Intumescent protective coatings are usually applied as paints which have their own range of normal ingredients. An intumescent composition should provide all the functional requirements of a conventional paint, for example durability, scuff resistance, aesthetic appeal etc., plus the added benefit of fire protection. Most of the commercially-available products have properties which are a compromise between these requirements. For good fire-retardant paints, the proportion of intumescent ingredients required is so large that saturated solutions of the more soluble

components are formed. This results in poor 'can'-stability i.e. crystal growth, poor shelf-life and water sensitivity.

The search for improved weatherability has been a long and continuing one. A random sample of coatings tested after 5 - 10 years by O'Rourke (119) generated great concern due to the loss of fire retardancy. Durability of the coatings developed in this research work were examined for their water resistance. Some methods for reducing the water permeability were tested with good results.

As a fire-retardant coating, intumescent paints provide a very effective reactive fire barrier which allows time for active fire-fighting to be carried out. The use of these paints in the UK is growing, from £5 million in 1985 to £30 million in 1988. However, this growth is limited due to the scarcity of scientific information on intumescent coatings and the need for reasonable properties under all weather exposure.

The present research resulted in a number of formulations with good physical properties. The fire performance of these formulations has been determined by conducting large-scale tests of hydrocarbon fire intensity.

RECOMMENDATIONS FOR FURTHER WORK

A) Determination of the reaction kinetics of the various other formulations, their associated foam structure and the effect of greater endothermic reactions on the temperature-time plateau.

B) Determination of the effects of non - steady-state heating on the intumescing power of the ingredients, particularly small temperature rate changes as would occur in a slowly developing real fire.

C) The study of the effects of sudden changes of temperature, as could occur in a fierce conflagration, on the formation and erosion of foam, its stability and insulation.

D) The study of the mechanical properties of coatings exposed to long-term weathering and their fire performance with and without fibre reinforcement.

REFERENCES

1. Berger, Jensen and Nicholson Ltd., B.P. 935, 590.

2. Myers, R.E., Licursi, E., Evans, R.E., J. Fire Sciences, Vol. 3, 11/12/85.

3. Alim Corp., U.S. 2,881,088.

4. Albi Manufacturing Co., U.S. 2,452,054 (1948).

5. National Aeronautics and Space Administration U.S. 3,702,841, 1972.

6. Burnell, H.H., Description of the French method of constructing iron floors. RIBA Paper 1853.

7. Reddaway, T.F., The rebuilding of London after the Great Fire of London, Jonathan Cape, 1940.

8. Davidge, W.R., The development of London and the London Building Acts. J.R. Inst. Brit. Archit., 1914, 3rd Series, 21 (11), London.

9. Stanhope, Phil. Trans. (A), 1778, 884.

10 Review of fire policy, an examination of the deployment of resources to combat fire. London, H.O. 1980.

11. Skinner, D.H., Measurement of high temperature properties of steel. Melbourne Research Laboratories (MRL 6/10), May 1972.

12. Jerath, V., Smith, C.I., Elevated temperature tensile properties of structural steel manufactured by the British Steel Corp. Teeside Laboratories, Report No. T/RS/1189/11/80/C - July 1980; T/RS/1189/29/82/C - 1982.

13. Stirland, C., Steel properties at elevated temperatures for use in fire engineering calculations, B.S.C., Teeside Lab. Paper for ISO/TC92/WG15 Committee Oct. 1980.

14. Physical constraints of some commercial steels at elevated temperatures. The British Iron and Steel Research Assoc., Butterworth Scientific Publications, London, 1953.

15. Pettersson, O.; Magnusson, S.E.; Thor, J.; Fire engineering design of steel structures. Swedish Institute of Steel Construction, Publication 50, Stockholm, 1976.

16. Lie, T.T., Fire and buildings. Applied Science Publishers Ltd., London, 1972.

17. Malhotra, H.L., Design of fire-resisting structures, Surrey University Press 1982.

18. Draft BS 5950, Part 8: 1985.

19. Hamilton S.B. : A Short History of the Structural Fire Protection of Buildings, Special Report No. 27, Building Research Station, H.M. Stationery Office, London, 1958.

20. BS 476 : Part 21 : 1987.

21. Castle G.K., The nature of various fire environments and the application of

modern material approaches for fire protection of exterior structural steel. J. Fire and Flammability, 8, 1974 (American Institute of Chemical Engineers).

22. Fujita, K., Research report concerning characteristics of fires inside non-combustible rooms and prevention of fire damage. Building Research Institute Report 2N, Tokyo.

23. Kawagoe, K., Fire behaviour in rooms, Building Research Institute Project 7, Tokyo, 1958.

24. Kawagoe, K. and Sekine, T., Estimates of fire temperature/time curve in rooms. Building Research Institute Occasional Report 11 - 1963, Report 17 - 1961, Report 29 - 1967, Tokyo.

25. Heselden, A.J.M., Results of an international co-operative programme on fully developed fires in single compartments. Symposium No. 5: Fire Resistance Requirements for Buildings - a New Approach. H.M.S.O., London, 1971.

26. Law, M., Prediction of fire resistance (Ibid).

27. Odeen, K., Theoretical Study of fire characteristics in enclosed spaces. Bulletin No. 19, Division of Building Construction, Royal Institute of Technology, Stockholm, 1963.

28. Magnusson, S.E. and Thelanderssen, S., Temperature/time curves for the complete process of fire development. A theoretical study of wood fuel fires in enclosed spaces. Ci 65, Acta Polytechnica Scandinavia, Stockholm, 1970.

29. Pettersson, O., The connection between a real fire exposure and the heating conditions according to standard fire resistance test. European Convention for Constructural Steelwork, Chap. 11, CECM-111-74-2E.

30. Magnusson, S.E. and Petersson, O. : Kvalificerad Braudteknisk Dimensionering av Stalberwerk, Bulletin 11, Lund Institute of Technology, Lund, 1969.

31. Ward, F., J. Soc. Dyers Col., 1955, 71, 569.

32. Gay-Lussac, J.L. Ann. Chim. (Paris) 1821, 18, 211-7.

33. Paimboeuf, L., US patent 449, 11 Nov. 1837.

34. Ware, R.P. and Westgate, M.W., National Paint Varnish, Lacquer Assoc., Scientific Circular No. 727, 17-39 (1948).

35. Tramm, E. US Patent No. 2,106,938, Feb. 1938.

36. Olsen, J., and Bechle, C., US Patent No. 2,442,706, June 1948.

37. Jones, G., US Patent No. 2,452,054/5. Oct. 1948.

38. Nielson, W., US Patent No. 2,596,937, May 1952.

39 Marotta, R. US Patent No. 2,676,162, April 1954.

40. Wilson, I.V. and Marotta, R. US Patent No. 2,702,283, Feb. 1955.

41. Venable, J.M. US Patent No. 2,956,037, Oct. 1960.

42. Sakurai, T. and Izumi, T., J. Chem. Soc. (Japan) Ind. Section 56, (1953).

43. Jones, G., US Patent No. 2,628,946, Feb. 1953.

44. Christian, C., US Patent No. 2,681,326, June 1954.

45. Wilson, I. and Marotta, R., US Patent No. 2,702,283, Feb. 1955.

46. Cummings, I., Ind. Eng. Chem. 46, 1985 (1954).

47. Quells, G., British Patent 862,569, March 1961 and US Patent No. 3,077,458, Feb. 1963.

48. Verburg, G.B., Rayner, E.T., Yeadon, D. A., Hopper L.L., Goldblatt, L.A., Dollear, F.G., Dupuy, H.P., York, E., J. Amer. Oil Chem. Soc., 41,670 (1964); Yeadon, D.A., Rayner, E.T., Verburg, G.B., Hopper, L.L., Miller, H., Dupuy, H.P., Dollear, F.G., Official Digest, 37,1095 (1965); E.T. Rayner, J. Paint Tech., 38 (1951) 1966; G.B. Verburg, Ibid., 38,407 (1966).

49. Vandersall, H.L. Paper at the Wayne State University. Polymers Conference Series, Prog. 5, Detroit, Michigan, June 13-17, 1966.

50. H.L. Vandersall, Phos-chek P/30 Brand Fire-Retardant - Its use in intumescent Paint, Report No. 6512, Inorganic Chemicals Division, Monsanto Co., (Oct. 1965).

51. Vita-Car Corp., US 2,754,217 (1956).

52. Cumming, L., Offic. Dig. Federation Soc. Paint Technol. 33, 408-416 (1961).

53. Anonymous, Am. Paint J. 47, No. 32 (56-62) (1963).

54. Black, H.K. and B.C.L. Weedon, J. Chem. Soc. 1953, 1785-1793.

55. Steger, A. and J. van Loon, Rec. Trav. Chim. 59, 1156-1164 (1940).

56. Badami, R.C. and F.D. Gunstone, J. Sci. Food Agri. 14, 863-866, (1965).

57. Gunstone, F.D., Sealy, A.J., J. Chem. Soc. 1963, 5772-5778.

58. Kneeland, J.A., Kyriacou, D., Purdy, R.H., JAOCS 35, 361-363 (1958).

59. Anonymous, Ibid, 122, No. 9, 8-11 (1959).

60. Morris, L.J., J. Chem. Soc. 1963, 5779-5781.

61. Anonymous, Ind. Eng. Chem. 52, No. 11. 30A, 32A (1960).

62. Armitage, J.B., Cook, C.L., Entwistle, N., Jones, E.R., Whiting, M.C., J. Chem. Soc. 1952, 1998-2005.

63. R.R. Hindersinn and Co. Witschard, US. 3, 449,161 (June 1969).

64. Jones, D.J., Bibligraphics in Paint Tech. No. 22, R.H. Chandler Ltd. November 1973.

65. Lyons, J.W., The Chemistry and Uses of Fire Retardants, Wiley-Interscience, New York, 1970.

66. Brushwell, W., Am. Paint J., 1955, 39 (40).

67. Brushwell, W., Am. Paint J., 1972, 57, (10) 78-83..

68. Verburg, C.B., Yeadon, D.A., Rayner, E.T., Dollear, F.G., Dupupy, H.P., Hopper, L.L., J. of Paint Tech., 1966, 38, 105.

69. Bishop, D.M., JOCCA, 1983 (12) 373-396.

70. Verburg, G.B., J. of American Oil Chemists Soc. Vol. 41, Oct. 1964.

71. Williams, A., Noyes Data Corp. N.Y. (1974), Chem. Tech. Review 25.

72. O'Neil, L.A., Rev. Curr. Lit. Res. Assc. British Paint Colour Varm. Mfks. (39) 1966, 887.

73. Souien, R.L., Proc. Int. Symp. Flammability and Fire Retardants (1975), 187.

74. Kay, M., PhD. Thesis 1979, University of Aston.

75. Kay, M., Price, A.F., Lavery, I., J. Fire Retd. Chem. 1979, 6, 69-91.

76. Garnino, G., Costa, L., Trossarelli, L., Polymer Degradation and Stab., 6, (1984) 243-250; 7 (1984) 25-31, 7 (1984) 221-229, 8 (1984) 13-22.

77. Allyea, H., J. Chem. Educ. 3, 3 (1956).

78. Parker, J., Foflen, G.M., SAMPE Journal, Aug/Sept. 1968.

79. NASA, US 3,535,130 (1970).

80. Michael, A., Schmidt, G., Guyot, A., 1973, Polymer Preprints 14, 665.

81. Braun, D., and Quarg, W., (1973) Angew. Makromol, Chem., 29, 163.

82. Bereus, A.R., (1973). Polymers Preprints, 14, 671.

83. Grassie, N., Melville, H.W., 1970, European Polymer J., 6, 865.

84. McNeill, I.C., 1970 European Polymer J., 6, 373.

85. Grassie, N., (1952) Trans. Faraday Soc., 48, 379, (1953) 49, 835.

86. Bengough, W.I., and Varma, I.K., (1966) Eur. Polym. J., 2, 49, 61.

87. Crosato-Arnaldi, A., Palma, G., Peggion, E., Talamini, G., (1964), J. Appl. Polym. Sci., 8, 747.

88. Arlman, E.J., (1954), J. Polym. Sci., 12, 547.

89. Talamini, G., Pezzin, G., (1960), Makromol, Chem., 39, 26.

90. Braun, D., (1971), Pure Appl. Chem., 26, 173.

91. Shell Oil Co., US 3,449,375, 1969.

92. General Electric Co., US 3,723,481, 1973.

93. Geuskens, G., Degradation and Stablisation of Polymers, Applied Science Publishers, 1975.

94. Madorsky, S.L., Thermal Degradation of organic polymers, Interscience, New York, 1964.

95. Madorsky, S.L., Hart, V.E., Straus, S., Sedlak, V.A., J. Research Nat'l Bur. Standards, 51, 327 (1953).

96. Casting, R. Phd Thesis, University of Paris (1951).

97. Bluhme, D.A., Fire and materials, 11, 195-199, (1987).

98. McGuire, J.H., Wraight, H., J. of Sci. Inst. Vol. 37, 4, 1960, 128-130.

99. Wraight, H., Fire research note No. 790, FRC 11, 1969.

100. Sawko, P.M., US 3,702,841 (1972).

101. Dow Corning Corp., BP 1,255,132 (1970).

102. Silbert, E.K., Cummings, J.I., Guerrant, W.B., US 2,684,953.

103. Shen S., J. Am. Chem. Soc. 91 (1), 62, (1969).

104. Kiehl, S.J., J. Am. Chem. Soc. 49, 123 (1927).

105. Deutsche Gold-und Silber - scheide, BP 760,510 (1956).

106. The Gilden Co., US 2,722,523 (1955).

107. Rolls Royce Ltd., BP 1,215,286 (1970).

108. Monsanto Chem., Co., US 2,676,162 (1954).

109. Grunze, V.H., Anorg. Allgem. Chem., 281,262 (1955).

110. Klumpner, K. Ger. Pat. 742,256 (1941).

111. Neth. Appl. 6,603,408 (1966).

112. Jap. Pat. 80, 49,0004.

113. Freeman, E.S., and Carroll, B., J. Phys. Chem. 62,394 (1958).

114. Cagliostro, D.E., Riccitiello, S.R., Clark, K.J., Shmizu, A.B., J. Fire & Flamm. Vol.6, 205-220, 4, (1975).

115. Anderson, C.E., and Wauters, D.K., Int. J. Engng. Sci. vol. 22, 7, 881-889, (1984).

116. Buckmaster, J., Anderson, C., Nachman, A., Int. J. Engng. Sci. vol. 24, 3, 263-276, (1986).

117. Goodman, T.R., Advances in Heat Transfer (Eds. T.F. Ervin & J.P. Hartness), vol 1 p51, Academic Press, New York.

118. Pettit, M., Routley, A.F., Fire and Materials, Vol. 2, No. 4, 1978.

119. O'Rourke, J.F., JFF/Fire Retardant Chem. vol. 2, p48, (Feb 1975).

120. Handbook of Chemistry and Physics 58th Ed. (1977-78).

121. Hodgenson, P.A., Development of thermal coating for missile warhead fire protection, Natl. SAMPE Symp. Exhib. Proc. 24, 930 (1979).

122. Bann, K., Miller, S.A. Chem. Rev. 58 (1), Feb. 1958, 131-171.
123. Liberti, F., R. Am. Paint J., 1968, 53, (7), 96.

124. Allsebrook, W.E., Paint Manuf., 1972, 42, (11), 41-41, 44.

125. Sakurai, T., Derwant Jap. Pat. Rept., 1962, 1, (21)I, p1.

126. Burdon, R.S., Surface Tension and the spreading of liquids, 2nd Ed., Cambridge University Press (1949).

127. Hooker Chemical Corp., US 3,449,161 (1965).

128. Hooker Chemical Corp., U.S. 3,497,469 (1965).

129. Hindersinn, R.R., Flame Retard. Polym. Mater. 4, 1, (1978).

APPENDIX A

Steel section	Profile protection				
Universal beams, universal columns and joists (plain and castellated) 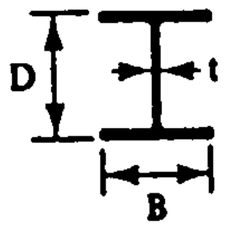 H_p	4 sides 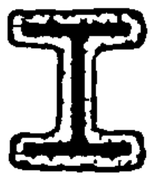 $2B + 2D + 2(B - t)$ $= 4B + 2D - 2t$	3 sides 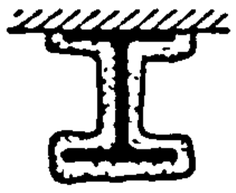 $B + 2D + 2(B - t)$ $= 3B + 2D - 2t$	3 sides 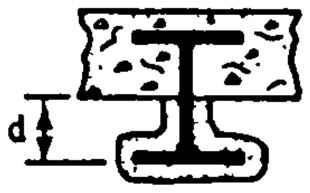 Partially exposed $B + 2d + (B - t)$ $= 2B + 2d - t$	2 sides 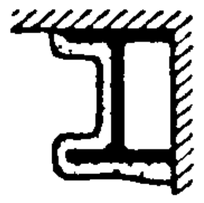 $B + D + 2(B - t)/2$ $= 2B + D - t$	1 side  Partially exposed B
Structural and rolled tees 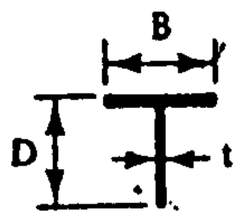 H_p	4 sides  $2B + 2D$	3 sides 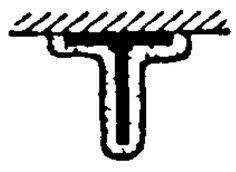 Flange to soffit $B + 2D$	3 sides 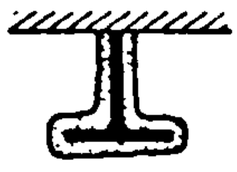 Toe of web to soffit $B + 2D + (B - t)$ $= 2B + 2D - t$		
Angles 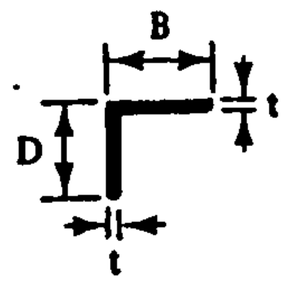 H_p	4 sides  $2B + 2D$	3 sides 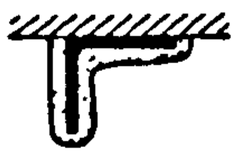 Flange to soffit $B + 2D$	3 sides 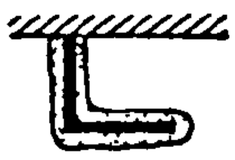 Toe of flange to soffit $B + 2D + (B - t)$ $= 2B + 2D - t$		
Channels 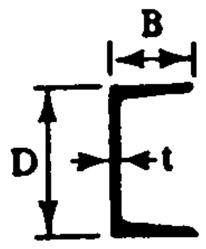 H_p	4 sides  $2B + 2D + 2(B - t)$ $= 4B + 2D - 2t$	3 sides 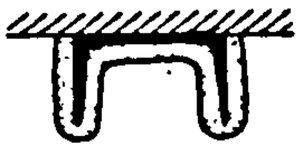 Web to soffit $2B + D + 2(B - t)$ $= 4B + D - 2t$	3 sides 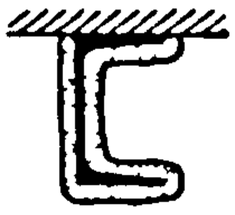 Flange to soffit $B + 2D + 2(B - t)$ $= 3B + 2D - 2t$		
Hollow sections, square or rectangular 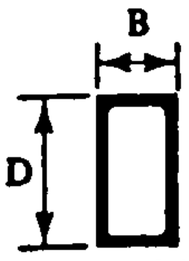 H_p	4 sides  $2B + 2D$	3 sides 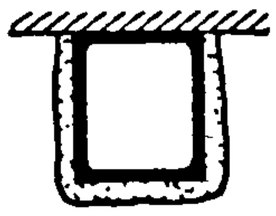 $B + 2D$			
Hollow sections, circular  H_p	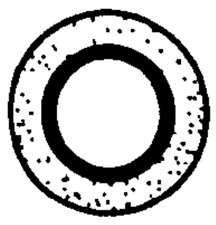 πD				
Example *using 203 x 203 x 52 kg/m universal column* B = 203.9 mm; D = 206.2 mm t = 8.0 mm. A = 66.4 cm^2	a) Profile protection – 4 sided exposure $H_p = 4B + 2D - 2t$ $\therefore H_p = 4 \times 203.9 + 2 \times 206.2 - 2 \times 8.0$ $= 1212\,mm = 1.212\,m$ $H_p/A = 1.212/0.00664 = 182.5\,m^{-1}$		b) Profile protection – 3 sided exposure $H_p = 3B + 2D - 2t$ $= (1212 - 203.9)\,mm = 1.208\,m$ $\therefore H_p/A = 1.208/0.00664 = 151.8\,m^{-1}$		

Protection configurations with values of perimeter H_p for use in the calculation of section factor, H_p/A

Note: The values are approximate in that radii at corners and roots of all sections are ignored

APPENDIX B

THE SPECIFIC HEAT C_{ps} OF STEEL

TEMP (C)	C_{ps}(kcal/kg C)	C_{ps} (kJ/kg C)
0	0.115	0.482
100	0.115	0.482
200	0.125	0.522
300	0.134	0.560
400	0.143	0.600
500	0.153	0.640
600	0.163	0.682
700	0.166	0.695

From reference Petterson et al 'Fire Engineering Design of Steel Structures' Publication No. 50 1976.

APPENDIX C

TIME (min)	TEMPERATURE (DEG C) PANELS Cont A	F20	F7	F16
0.0	12	2	12	4
0.5	12	3	12	4
1.0	13	4	13	3
1.5	15	6	14	2
2.0	16	24	16	32
2.5	21	17	19	31
3.0	26	33	25	40
3.5	36	44	33	52
4.0	53	57	46	66
4.5	82	71	65	56
5.0	114	84	79	68
6.0	150	110	108	103
6.5	164	111	110	97
7.0	179	123	120	119
7.5	192	132	127	127
8.0	203	134	129	121
8.5	212	143	135	134
9.0	223	157	151	152
9.5	232	162	151	154
10.0	239	175	162	173
10.5	247	178	162	172
11.0	251	189	171	192
11.5	256	194	176	200
12.0	261	191	177	191
12.5	265	205	185	215
13.0	270	196	188	201
13.5	274	212	196	229
14.0	279	202	199	212
14.5	282	220	206	242
15.0	286	224	211	249
15.5	291	213	215	229
16.0	294	236	221	262
16.5	297	241	225	267
17.0	302	226	230	245
17.5	304	252	234	279
18.0	309	238	239	256
18.5	311	263	243	290
19.0	315	246	247	266
19.5	317	275	250	299
20.0	321	257	255	275
20.5	323	287	257	308
21.0	327	267	262	283
21.5	328	296	263	315
22.0	331	275	268	290
22.5	333	305	270	322
23.0	336	282	274	297
23.5	336	313	275	326
24.0	337	315	276	327
24.5	339	318	278	329
25.0	340	320	280	331
25.5	341	323	281	332
26.0	341	324	282	332
26.5	342	325	284	333
27.0	344	329	286	334
27.5	344	330	287	335
28.0	346	306	291	317
28.5	346	307	293	319
29.0	346	333	290	338
29.5	346	334	291	338
30.0	346	335	291	337
30.5	347	335	292	340
31.0	347	336	293	340
31.5	347	336	293	340
32.0	347	337	294	341
32.5	347	337	294	341
33.0	347	337	295	342
33.5	348	316	297	331
34.0	347	337	295	343
34.5	347	337	296	343
35.0	348	317	300	333
35.5	346	337	296	344
36.0	347	317	300	333
36.5	345	336	296	345
37.0	346	317	300	332
37.5	345	336	296	344
38.0	345	316	300	333
38.5	344	336	295	343
39.0	345	316	300	334
39.5	343	333	295	342
40.0	343	315	299	334
40.5	341	332	294	341
41.0	342	313	299	333
41.5	340	331	294	340
42.0	340	312	298	333

STEEL TEMPERATURES RECORDED ON 300 mm SQUARE PANELS.

TIME (min)	TEMPERATURE (DEG C)						
	MID 1	MID 2	0.5 3	0.5 4	0.5 5	0.5 6	MID 10
0.0	13	10	13	13	12	13	12
0.5	15	15	17	17	18	19	17
1.0	38	55	35	47	44	59	45
1.5	119	170	101	136	171	210	136
2.0	209	295	187	227	272	339	248
2.5	296	396	294	308	355	431	353
3.0	384	453	401	397	414	543	466
3.5	495	581	483	498	539	674	639
4.0	614	635	573	613	627	887	900
4.5	806	766	757	817	701	1032	959
5.0	869	815	829	863	709	1012	907
5.5	967	812	959	885	720	913	760
6.0	997	879	1005	918	735	982	802
6.5	1031	915	1046	933	776	981	826
7.0	1035	941	1056	946	787	1015	851
7.5	1020	912	990	1005	834	980	807
8.0	875	949	799	898	844	981	942
8.5	793	968	724	803	873	904	916
9.0	810	931	711	814	883	872	878
9.5	883	953	745	826	827	804	777
10.0	846	881	777	777	813	771	757
10.5	818	846	777	747	792	767	748
11.0	808	798	764	751	764	767	738
11.5	778	796	770	739	735	768	736
12.0	770	770	761	729	720	775	726
12.5	779	758	762	740	725	779	723
13.0	769	759	777	746	737	777	735
13.5	763	764	788	743	732	795	736
14.0	776	757	786	747	726	780	732
14.5	773	749	772	742	719	779	749
15.0	764	750	789	756	724	772	742
15.5	763	746	790	760	719	765	731
16.0	758	733	786	745	715	746	717
16.5	767	727	780	755	710	724	713
17.0	733	719	760	737	701	716	697
17.5	719	709	738	729	691	707	682
18.0	708	691	720	708	677	692	668
18.5	693	679	705	696	667	675	654
19.0	679	670	695	685	654	663	634
19.5	666	661	687	671	642	650	629
20.0	654	653	657	656	629	634	613
20.5	633	631	636	642	617	618	590
21.0	612	610	620	621	595	599	569
21.5	591	591	600	603	578	581	561
22.0	583	567	582	581	558	560	545
22.5	563	547	565	560	540	544	533
23.0	534	525	543	533	520	524	508
23.5	511	503	522	516	502	512	490
24.0	488	493	506	493	490	496	474
24.5	472	478	497	490	474	485	463
25.0	460	460	483	465	459	475	454
25.5	448	444	474	460	447	461	445
26.0	439	436	459	453	441	452	437
26.5	430	430	448	449	433	440	431
27.0	421	421	436	449	426	431	424
27.5	411	410	434	433	419	425	410
28.0	395	394	427	420	405	413	395
28.5	388	388	421	416	396	408	384
29.0	386	384	410	415	396	401	384
29.5	383	381	400	411	393	392	372
30.0	378	376	394	399	392	383	367
30.5	370	365	390	396	387	378	361
31.0	360	353	387	387	381	373	356
31.5	354	351	368	385	380	369	358
32.0	350	344	363	380	372	360	349
32.5	340	334	361	371	369	357	340
33.0	335	322	348	367	358	353	335
33.5	327	314	343	352	347	348	317
34.0	317	310	338	350	348	343	318
34.5	317	309	330	353	353	336	315
35.0	313	305	338	347	355	332	318
35.5	307	302	328	349	348	327	305
36.0	305	294	317	337	345	322	304
36.5	303	290	317	342	338	315	293
37.0	295	282	312	328	332	311	291
37.5	287	276	305	321	319	307	278
38.0	283	277	304	315	317	299	276
38.5	279	273	296	319	320	294	277
39.0	273	266	293	307	309	292	276
39.5	266	257	290	304	307	291	269
40.0	264	252	290	306	308	287	270
40.5	260	248	280	303	304	284	266
41.0	254	246	275	298	304	277	267
41.5	253	243	268	299	301	273	262
42.0	243	237	271	293	294	271	255

TABLE 1 ATMOSPHERE TEMPERATURES RECORDED AT THE 0.5 m AND 2.0 m LEVELS IN THE EAST SIDE OF THE COMPARTMENT.

TIME (min)	TEMPERATURE (DEG C)									
	MID	BEAM 0.5M			MID	BEAM 0.5M			MID	MID
	11	12	13	14	15	16	17	18	19	20
0.0	13	13	13	13	12	13	13	13	13	13
0.5	18	19	19	16	15	21	20	17	17	16
1.0	39	72	51	54	35	51	52	44	44	38
1.5	210	173	149	166	126	130	150	148	127	123
2.0	315	285	296	283	241	239	285	264	237	231
2.5	398	407	423	390	355	345	414	390	342	339
3.0	518	519	529	503	465	434	512	507	457	448
3.5	651	634	703	624	620	539	610	622	539	567
4.0	914	750	893	890	924	669	749	801	665	707
4.5	1093	817	1064	1078	1057	831	885	911	881	878
5.0	1183	791	1023	1177	1024	917	886	903	1020	1027
6.0	1170	763	910	1190	959	736	842	931	959	996
6.5	1178	775	926	1149	868	687	792	862	749	896
7.0	1129	752	877	1072	915	689	768	840	739	896
7.5	992	725	837	936	829	673	792	920	747	978
8.0	930	763	888	945	860	718	849	910	846	996
8.5	896	770	870	832	969	1074	1024	998	1126	1082
9.0	881	779	965	807	910	1076	1006	947	1113	1037
9.5	781	689	790	763	883	985	971	908	1106	974
10.0	780	668	732	743	835	954	880	869	1052	899
10.5	746	655	744	731	810	856	894	822	982	867
11.0	765	663	770	734	785	808	855	809	894	843
11.5	785	668	783	765	791	792	835	816	908	902
12.0	772	687	776	754	788	779	816	813	912	880
12.5	801	699	777	810	802	778	811	809	879	877
13.0	786	684	779	783	812	781	830	805	877	866
13.5	772	682	766	766	793	802	799	776	847	820
14.0	761	674	747	756	792	798	793	764	821	810
14.5	761	677	741	752	788	797	782	763	828	800
15.0	749	693	748	742	782	787	777	771	808	784
15.5	735	691	736	739	767	798	771	745	795	768
16.0	732	686	736	724	748	793	748	735	772	739
16.5	709	694	727	713	726	772	730	713	753	721
17.0	705	682	714	703	716	763	720	700	730	703
17.5	690	667	699	689	697	743	709	689	712	695
18.0	677	658	685	677	685	741	700	678	696	679
18.5	658	660	672	662	662	727	685	667	688	665
19.0	646	648	662	647	653	717	673	655	666	650
19.5	634	641	651	636	637	695	657	643	670	639
20.0	620	642	634	620	621	670	642	627	650	615
20.5	601	612	613	605	603	643	619	610	628	601
21.0	577	586	591	587	586	621	602	594	611	572
21.5	548	566	571	570	567	596	579	574	587	558
22.0	535	547	558	556	554	567	558	553	563	541
22.5	519	527	539	541	532	535	539	530	541	521
23.0	497	516	528	524	515	515	512	513	525	490
23.5	476	502	511	508	495	497	495	496	504	472
24.0	462	495	499	490	485	483	479	483	487	470
24.5	451	484	483	475	468	468	469	473	475	463
25.0	443	476	474	462	453	454	455	457	467	456
25.5	423	470	463	455	441	441	442	443	449	444
26.0	406	464	450	444	434	432	433	435	440	431
26.5	403	457	440	435	426	428	424	428	431	420
27.0	395	452	435	426	418	424	419	424	423	419
27.5	386	442	426	416	409	414	411	419	414	404
28.0	377	441	419	408	401	400	406	410	401	396
28.5	370	434	414	399	394	390	403	405	394	388
29.0	361	423	405	392	386	392	390	397	390	381
29.5	359	419	396	387	379	387	387	389	380	379
30.0	354	413	389	377	372	373	379	384	375	369
30.5	346	405	389	373	365	369	379	381	367	364
31.0	341	404	385	368	357	360	368	374	357	357
31.5	326	398	374	360	350	358	360	365	355	351
32.0	324	394	368	359	343	347	360	358	348	345
32.5	319	389	363	345	336	340	356	355	339	337
33.0	315	389	358	341	330	332	355	349	334	327
33.5	310	388	355	335	323	324	352	347	326	319
34.0	296	383	347	331	318	319	352	341	319	316
34.5	293	373	340	328	313	324	343	333	321	311
35.0	294	371	337	323	312	312	335	328	318	304
35.5	287	366	335	315	304	309	330	323	311	299
36.0	284	359	330	312	297	306	328	319	307	295
36.5	277	352	326	304	291	309	323	314	296	288
37.0	272	352	321	303	289	304	318	312	292	287
37.5	266	353	312	293	282	300	315	307	284	275
38.0	266	348	313	290	276	304	316	306	281	272
38.5	262	343	309	287	270	302	307	303	279	268
39.0	259	343	307	284	270	299	305	298	278	264
39.5	253	338	301	280	264	293	296	293	272	260
40.0	250	336	299	278	264	278	294	290	270	257
40.5	244	331	295	279	257	273	287	284	265	253
41.0	240	327	289	274	252	270	284	278	263	251
41.5	239	322	287	267	248	271	277	274	258	247
42.0	238	323	286	262	245	272	281	274	253	242

TABLE 2 ATMOSPHERE TEMPERATURES RECORDED AT THE 0.5 m AND 2.0 m LEVELS IN THE WEST SIDE OF THE COMPARTMENT.

TIME (min)	TEMPERATURE (DEG C) T/C POSITION 1	3	4	FCE AIR
0.0	22	22	4	12
0.5	22	22	3	14
1.0	21	21	4	33
1.5	19	18	6	99
2.0	3	4	16	182
2.5	17	17	9	272
3.0	5	8	16	392
3.5	16	14	22	621
4.0	9	11	26	902
4.5	20	20	36	935
5.0	14	17	32	929
6.0	32	38	43	778
6.5	43	46	48	790
7.0	41	48	52	851
7.5	46	52	56	882
8.0	57	61	64	928
8.5	61	64	71	931
9.0	64	66	72	886
9.5	74	73	74	769
10.0	75	76	77	778
10.5	87	84	84	753
11.0	82	84	88	727
11.5	82	85	93	721
12.0	92	92	95	714
12.5	81	85	100	717
13.0	94	95	97	726
13.5	79	84	103	719
14.0	96	96	96	719
14.5	82	84	103	736
15.0	86	85	105	726
15.5	106	102	96	715
16.0	93	89	109	713
16.5	96	93	111	692
17.0	120	115	100	686
17.5	105	98	119	684
18.0	131	125	107	672
18.5	117	109	125	669
19.0	145	138	110	644
19.5	126	118	133	610
20.0	156	150	117	617
20.5	137	129	142	573
21.0	168	162	125	549
21.5	147	138	152	524
22.0	179	174	133	504
22.5	157	149	163	479
23.0	189	184	142	466
23.5	166	158	175	447
24.0	169	162	179	429
24.5	173	167	183	418
25.0	177	171	188	406
25.5	180	174	193	401
26.0	182	177	196	388
26.5	185	180	200	378
27.0	190	186	205	377
27.5	192	188	207	363
28.0	223	230	176	359
28.5	226	233	179	357
29.0	200	196	216	353
29.5	202	198	218	348
30.0	204	200	220	340
30.5	206	202	222	331
31.0	208	204	224	317
31.5	210	206	225	320
32.0	212	208	227	312
32.5	214	209	229	305
33.0	216	211	230	296
33.5	244	254	195	293
34.0	219	213	232	284
34.5	221	215	234	282
35.0	248	258	199	283
35.5	223	217	236	281
36.0	251	260	201	275
36.5	226	219	238	273
37.0	254	262	202	265
37.5	228	221	239	261
38.0	256	264	204	261
38.5	231	223	241	253
39.0	258	267	206	247
39.5	232	225	243	239
40.0	260	268	207	235
40.5	234	226	244	230
41.0	261	269	208	232
41.5	235	228	245	224
42.0	262	271	209	223

TABLE 3 STEEL AND ADJACENT ATMOSPHERE TEMPERATURES RECORDED ON SPECIMEN I

TIME (min)	TEMPERATURE (DEG C)					
	1.2m position			0.5m position		Fce Atm
	Flange	Web	Flange	Flange	Web	
0.0	12	12	12	12	12	12
0.5	12	12	12	12	12	15
1.0	12	12	12	12	12	30
1.5	11	11	11	11	11	78
2.0	10	10	10	10	10	142
2.5	11	11	11	11	11	210
3.0	10	10	10	10	10	276
3.5	12	12	11	11	11	381
4.0	12	12	12	11	10	527
4.5	20	16	18	12	15	688
5.0	17	18	14	6	9	807
6.0	41	44	39	23	27	1001
6.5	53	60	49	32	36	1042
7.0	61	68	60	36	47	1072
7.5	73	78	71	44	57	1065
8.0	83	87	79	55	63	976
8.5	102	84	103	59	87	903
9.0	85	128	79	82	65	874
9.5	127	105	130	78	103	793
10.0	114	150	108	93	87	799
10.5	146	131	149	96	116	766
11.0	141	167	132	109	110	755
11.5	153	175	144	117	120	740
12.0	173	166	172	122	137	729
12.5	173	191	163	133	137	742
13.0	192	180	191	137	153	748
13.5	189	209	176	149	150	737
14.0	209	196	205	152	167	739
14.5	206	223	192	163	164	748
15.0	213	232	198	171	170	752
15.5	234	217	229	173	187	735
16.0	229	246	213	184	184	731
16.5	236	251	221	190	190	713
17.0	254	241	245	194	203	703
17.5	251	260	237	202	203	694
18.0	266	255	256	206	213	677
18.5	265	270	252	214	214	666
19.0	277	270	265	218	223	646
19.5	278	279	265	225	224	641
20.0	288	282	275	230	232	612
20.5	289	288	276	236	234	598
21.0	297	292	284	241	241	575
21.5	299	296	286	246	242	573
22.0	306	301	293	251	248	540
22.5	308	305	295	255	250	514
23.0	314	309	301	260	255	495
23.5	316	312	304	263	257	473
24.0	318	315	307	266	259	464
24.5	321	317	310	269	261	451
25.0	324	320	313	272	263	433
25.5	326	322	315	274	264	421
26.0	327	324	317	276	265	414
26.5	329	325	319	278	266	408
27.0	332	328	322	281	268	399
27.5	333	329	323	283	269	392
28.0	334	331	324	283	271	382
28.5	336	333	328	286	272	374
29.0	336	333	328	286	271	370
29.5	337	334	329	287	271	362
30.0	338	335	330	288	272	359
30.5	339	335	331	288	272	351
31.0	339	336	332	289	272	345
31.5	340	337	333	290	272	338
32.0	341	337	334	290	272	329
32.5	341	338	334	290	272	322
33.0	342	338	335	290	271	314
33.5	343	340	337	292	273	309
34.0	342	339	336	291	271	300
34.5	342	339	336	290	271	296
35.0	344	341	338	292	272	295
35.5	343	340	337	290	270	293
36.0	344	341	338	291	270	287
36.5	343	340	337	289	269	280
37.0	344	341	339	290	269	276
37.5	343	340	337	288	267	269
38.0	344	341	339	289	268	268
38.5	343	339	338	287	266	262
39.0	344	340	339	288	266	257
39.5	342	339	337	286	264	252
40.0	343	340	338	286	265	249
40.5	342	338	337	284	263	245
41.0	342	339	338	285	263	243
41.5	341	337	336	283	261	236
42.0	342	338	337	283	261	232

TABLE 4 STEEL AND ADJACENT ATMOSPHERE TEMPERATURES RECORDED ON SPECIMEN V.

TIME (min)	1.2m position			0.3m position		FCB ALR
	Flange	Web	Flange	Flange	Web	
0.0	12	12	12	12	12	12
0.5	12	12	12	12	12	14
1.0	12	12	12	12	11	25
1.5	11	11	11	11	11	62
2.0	9	10	9	11	9	129
2.5	10	12	10	12	11	182
3.0	10	11	9	12	9	249
3.5	10	13	11	12	11	348
4.0	12	14	13	14	11	691
4.5	14	18	14	18	11	928
5.0	16	23	16	25	10	1006
6.0	30	34	26	30	21	682
6.5	38	34	35	35	28	723
7.0	40	42	36	39	29	807
7.5	45	46	42	44	34	716
8.0	55	50	51	50	41	775
8.5	64	65	59	59	50	999
9.0	73	75	66	67	59	991
9.5	73	69	67	66	56	932
10.0	67	70	63	79	44	896
10.5	95	66	89	53	87	870
11.0	81	97	70	81	65	824
11.5	90	98	79	83	72	807
12.0	101	87	96	87	82	801
12.5	101	106	90	91	93	819
13.0	160	157	150	128	136	823
13.5	111	118	100	99	94	818
14.0	123	105	117	104	104	807
14.5	120	130	108	106	104	843
15.0	125	137	112	113	109	821
15.5	138	119	133	116	119	824
16.0	137	144	125	120	120	814
16.5	141	147	130	124	124	810
17.0	150	140	143	129	133	801
17.5	151	153	140	131	134	781
18.0	159	152	151	136	142	765
18.5	160	160	151	139	144	752
19.0	167	163	158	143	150	745
19.5	169	167	159	147	152	713
20.0	175	171	166	151	158	683
20.5	177	175	168	154	160	680
21.0	184	180	174	158	165	638
21.5	185	183	176	161	167	607
22.0	191	187	182	165	172	589
22.5	194	190	184	168	174	576
23.0	199	195	189	172	179	553
23.5	202	198	192	174	181	531
24.0	204	201	195	176	183	517
24.5	208	204	198	179	186	501
25.0	211	207	201	181	189	494
25.5	214	210	204	183	191	472
26.0	216	213	206	185	193	463
26.5	219	215	209	187	195	450
27.0	223	220	213	191	199	443
27.5	225	222	215	192	200	435
28.0	228	226	218	194	203	423
28.5	231	228	221	197	206	414
29.0	232	230	223	197	207	409
29.5	235	232	225	198	208	401
30.0	237	235	227	200	210	398
30.5	239	237	229	202	212	386
31.0	241	239	232	203	213	378
31.5	243	242	234	205	214	376
32.0	245	244	236	206	216	369
32.5	247	246	238	208	217	362
33.0	249	248	240	209	219	353
33.5	252	251	243	212	221	340
34.0	253	252	243	212	221	336
34.5	254	254	245	213	222	332
35.0	257	257	248	216	225	333
35.5	258	257	249	216	225	329
36.0	261	260	252	218	227	323
36.5	261	261	252	219	227	318
37.0	263	264	255	221	229	315
37.5	264	264	255	221	228	303
38.0	267	267	258	223	231	302
38.5	269	268	258	225	230	300
39.0	270	271	261	225	232	297
39.5	270	271	261	224	232	290
40.0	273	274	264	226	234	284
40.5	273	274	264	225	233	278
41.0	275	276	267	227	235	309
41.5	276	276	267	227	234	317
42.0	278	279	269	228	236	310

TABLE 5 STEEL AND ADJACENT ATMOSPHERE TEMPERATURES RECORDED ON SPECIMEN S.

TIME (min)	TEMPERATURE (DEG C)					
	1.2m position			2.5m position		Fce Ata
	Flange	Web	Flange	Flange	Web	
0.0	12	8	12	12	12	13
0.5	12	8	12	12	12	14
1.0	12	7	12	12	12	31
1.5	13	0	12	12	12	53
2.0	13	21	13	13	11	147
2.5	18	7	18	17	14	190
3.0	22	30	22	19	16	256
3.5	30	35	29	25	20	341
4.0	39	42	40	33	26	425
4.5	49	52	50	43	36	842
5.0	59	62	60	53	46	907
6.0	68	88	64	83	80	97?
6.5	109	62	101	64	92	9?5
7.0	94	94	87	96	87	1014
7.5	96	98	97	109	27	1079
8.0	113	88	109	102	120	989
8.5	123	81	130	93	123	912
9.0	126	122	109	114	102	819
9.5	132	98	126	118	114	815
10.0	120	127	123	123	114	812
10.5	153	111	136	129	125	803
11.0	134	135	132	134	123	791
11.5	140	139	137	139	128	789
12.0	163	128	149	144	138	790
12.5	150	147	145	148	137	773
13.0	174	136	157	153	147	780
13.5	159	154	153	157	144	779
14.0	180	146	164	162	154	774
14.5	170	160	161	165	153	784
15.0	172	164	164	169	156	785
15.5	190	158	174	174	165	784
16.0	181	170	172	176	165	778
16.5	184	172	175	179	168	782
17.0	194	171	182	183	174	741
17.5	191	177	181	185	173	743
18.0	200	177	187	190	179	722
18.5	200	181	186	192	179	691
19.0	206	182	192	196	185	670
19.5	205	185	192	198	184	647
20.0	210	187	198	201	189	623
20.5	210	188	199	202	188	605
21.0	215	191	203	205	192	584
21.5	215	192	203	207	192	570
22.0	220	196	208	210	196	552
22.5	220	196	209	212	197	532
23.0	224	200	213	215	200	516
23.5	225	201	215	216	201	494
24.0	226	203	217	218	203	489
24.5	228	205	219	219	204	472
25.0	230	207	221	221	206	457
25.5	231	209	223	223	209	447
26.0	232	211	225	224	210	435
26.5	233	213	226	225	212	430
27.0	236	217	230	228	216	424
27.5	237	219	231	229	217	407
28.0	240	223	233	231	219	398
28.5	242	225	236	233	223	390
29.0	242	226	237	233	223	381
29.5	243	228	238	235	225	375
30.0	245	230	240	236	227	368
30.5	246	232	241	237	229	358
31.0	247	233	243	239	231	352
31.5	249	235	244	240	232	346
32.0	250	237	246	240	234	339
32.5	251	238	247	241	235	328
33.0	252	240	248	242	236	325
33.5	255	243	251	244	239	321
34.0	254	243	253	244	239	310
34.5	255	244	251	245	240	303
35.0	258	247	254	247	242	299
35.5	257	246	254	246	242	293
36.0	259	249	256	248	244	286
36.5	259	248	255	247	244	282
37.0	261	251	257	249	246	279
37.5	260	250	257	249	245	274
38.0	262	253	259	251	248	271
38.5	261	252	259	250	247	261
39.0	264	255	261	252	249	256
39.5	263	254	260	251	249	253
40.0	265	256	262	252	250	246
40.5	264	256	262	251	250	242
41.0	266	258	263	253	251	237
41.5	265	257	263	252	251	233
42.0	267	259	265	253	252	231

TABLE 6 STEEL AND ADJACENT ATMOSPHERE TEMPERATURES RECORDED ON SPECIMEN U.

TIME (min)	TEMPERATURE (DEG C)				PLT AIM
	1.2m Level		0.5m Level		
	Flange	Flange	Flange	web	
0.0	12	12	12	12	12
0.5	12	12	12	12	14
1.0	12	12	13	12	27
1.5	13	12	14	13	76
2.0	15	14	16	15	156
2.5	24	21	23	23	230
3.0	33	28	29	31	300
3.5	47	39	42	46	385
4.0	63	53	53	61	644
4.5	77	70	83	68	802
5.0	89	82	95	79	861
6.0	116	107	106	107	657
6.5	130	125	114	117	682
7.0	135	126	120	122	702
7.5	145	136	129	131	693
8.0	159	153	138	143	707
8.5	169	160	149	155	956
9.0	177	169	160	169	1004
9.5	197	189	159	185	950
10.0	183	180	193	171	938
10.5	222	207	177	200	895
11.0	214	202	198	197	872
11.5	223	211	206	206	872
12.0	237	229	213	219	859
12.5	237	224	224	222	818
13.0	252	244	226	235	813
13.5	250	237	238	235	823
14.0	265	256	239	247	823
14.5	263	248	249	247	802
15.0	269	254	255	252	780
15.5	284	273	256	262	768
16.0	282	266	265	262	775
16.5	287	271	268	267	749
17.0	297	286	274	274	730
17.5	297	280	278	275	712
18.0	306	293	285	282	698
18.5	306	288	287	282	683
19.0	313	300	293	288	668
19.5	314	296	295	288	648
20.0	320	306	300	293	626
20.5	321	303	302	293	613
21.0	327	311	306	299	592
21.5	328	310	308	299	566
22.0	333	316	313	303	539
22.5	334	317	314	304	524
23.0	338	322	318	308	502
23.5	339	323	319	309	485
24.0	341	324	320	310	472
24.5	343	326	322	311	456
25.0	345	328	325	313	452
25.5	346	330	326	315	445
26.0	347	331	327	316	431
26.5	349	332	328	317	419
27.0	352	335	331	320	411
27.5	353	336	332	320	400
28.0	354	338	335	322	391
28.5	356	340	336	324	382
29.0	357	341	336	324	378
29.5	358	342	338	325	370
30.0	359	343	339	326	359
30.5	360	344	340	327	357
31.0	361	345	340	328	350
31.5	362	346	341	329	345
32.0	363	347	342	329	335
32.5	363	348	343	330	327
33.0	364	347	344	331	323
33.5	366	351	345	333	317
34.0	366	351	345	332	309
34.5	366	351	345	333	305
35.0	368	353	347	334	304
35.5	367	353	346	334	297
36.0	369	354	348	335	293
36.5	368	354	347	335	294
37.0	370	355	348	336	280
37.5	369	355	347	335	270
38.0	371	356	349	336	267
38.5	370	355	349	335	262
39.0	371	357	349	337	262
39.5	370	356	348	336	255
40.0	372	358	349	337	254
40.5	370	357	349	336	247
41.0	372	358	349	337	241
41.5	371	357	348	336	240
42.0	372	358	349	337	238

TABLE 7 STEEL AND ADJACENT ATMOSPHERE TEMPERATURES RECORDED ON SPECIMEN T.

TIME (min)	TEMPERATURE (DEG C)					
	1.2m position			0.6m position		Fce Ata
	Flange	Web	Flange	Flange	Web	
0.0	13	13	13	12	12	12
0.5	13	12	12	12	12	13
1.0	13	13	13	13	13	23
1.5	15	15	14	13	13	60
2.0	20	20	18	15	16	123
2.5	30	32	28	21	24	190
3.0	42	46	38	29	32	258
3.5	67	78	61	42	49	453
4.0	110	113	84	71	85	891
4.5	159	136	162	85	145	925
5.0	168	181	139	127	155	989
6.0	239	232	195	183	217	1039
6.5	257	257	209	206	229	1058
7.0	281	267	225	217	246	1057
7.5	302	284	240	234	264	94?
8.0	310	299	248	246	275	870
8.5	327	308	260	256	285	953
9.0	322	319	269	271	282	916
9.5	373	291	291	258	341	808
10.0	321	369	262	296	266	806
10.5	363	306	335	277	335	733
11.0	343	366	268	311	288	750
11.5	349	371	274	319	291	772
12.0	369	335	352	293	336	749
12.5	365	372	282	329	306	779
13.0	386	338	362	302	349	755
13.5	385	367	309	331	333	745
14.0	389	367	345	322	338	744
14.5	395	375	327	335	342	737
15.0	401	381	332	339	346	739
15.5	406	383	353	336	351	722
16.0	411	392	346	346	353	710
16.5	415	396	352	349	356	689
17.0	421	398	363	350	361	672
17.5	422	405	362	356	361	659
18.0	428	407	371	357	367	633
18.5	429	412	371	362	367	627
19.0	434	414	380	364	373	614
19.5	434	419	380	368	373	600
20.0	439	421	388	370	379	577
20.5	439	425	389	373	379	570
21.0	443	427	395	376	384	549
21.5	443	429	396	379	383	531
22.0	447	432	401	381	388	514
22.5	447	434	403	384	388	498
23.0	450	437	408	386	392	477
23.5	450	438	409	388	392	464
24.0	450	440	411	389	393	452
24.5	451	441	413	391	395	440
25.0	452	443	416	392	396	429
25.5	453	444	418	393	397	418
26.0	453	445	419	394	398	410
26.5	454	446	421	395	399	400
26.5	454	446	421	395	399	400
27.0	455	448	425	396	401	393
27.5	456	449	426	397	402	384
28.0	456	450	428	398	403	372
28.5	458	452	430	400	405	363
29.0	456	452	430	400	404	360
29.5	456	453	432	400	405	354
30.0	456	453	433	401	406	346
30.5	456	454	434	401	406	337
31.0	456	454	435	402	406	332
31.5	456	455	436	402	407	327
32.0	456	455	437	402	407	317
32.5	456	455	438	403	407	309
33.0	456	455	439	403	407	305
33.5	457	456	441	404	409	294
34.0	455	455	440	403	408	288
34.5	455	455	440	403	408	286
35.0	456	456	442	404	409	284
35.5	454	455	441	403	407	276
36.0	455	456	443	403	409	271
36.5	453	455	442	402	407	263
37.0	454	456	443	403	407	263
37.5	452	454	442	402	406	253
38.0	453	455	444	402	408	251
38.5	450	454	442	401	406	248
39.0	451	454	444	401	407	249
39.5	449	453	443	400	405	241
40.0	450	454	444	400	406	240
40.5	448	452	442	398	404	234
41.0	449	453	444	399	405	234
41.5	447	451	442	397	403	229
42.0	447	452	443	397	404	221

TABLE 8 STEEL AND ADJACENT ATMOSPHERE TEMPERATURES RECORDED ON SPECIMEN W

TIME (min)	TEMPERATURE (DEG C)				
	1.2m Level		0.5m Level		FCE AIR
	Web	Flange	Flange	Web	
0.0	13	13	13	13	12
0.5	13	13	12	12	15
1.0	13	14	13	13	26
1.5	17	16	14	17	69
2.0	26	21	18	22	131
2.5	41	32	26	44	198
3.0	62	46	35	65	273
3.5	95	69	52	97	368
4.0	158	115	112	143	760
4.5	192	193	154	208	957
5.0	228	235	200	239	996
6.0	288	313	268	301	1017
6.5	303	320	271	297	1035
7.0	290	314	253	295	1006
7.5	292	323	226	290	930
8.0	303	329	237	296	853
8.5	311	338	247	302	946
9.0	325	350	257	311	941
9.5	320	362	275	316	896
10.0	326	354	292	319	780
10.5	360	385	300	329	766
11.0	322	365	324	320	765
11.5	334	373	323	325	747
12.0	368	402	315	338	763
12.5	353	389	316	338	769
13.0	359	412	321	348	771
13.5	374	399	331	346	766
14.0	367	421	327	356	752
14.5	379	408	337	353	750
15.0	367	408	359	354	759
15.5	403	444	337	374	735
16.0	375	415	374	361	737
16.5	380	417	379	363	728
17.0	411	459	346	387	696
17.5	391	424	384	371	698
18.0	414	461	358	389	669
18.5	402	432	382	380	662
19.0	418	461	372	391	640
19.5	412	439	*	383	648
20.0	423	461	*	394	630
20.5	420	443	*	394	616
21.0	427	461	*	397	599
21.5	426	445	*	399	580
22.0	431	460	*	401	566
22.5	432	447	*	404	549
23.0	436	460	*	404	538
23.5	437	449	*	407	524
24.0	438	449	*	408	512
24.5	439	449	*	409	502
25.0	441	449	*	410	493
25.5	442	449	*	411	484
26.0	443	449	*	411	475
26.5	444	449	*	412	467
27.0	447	451	*	413	461
27.5	447	450	*	414	451
28.0	449	457	*	412	447
28.5	451	457	*	413	440
29.0	450	450	*	415	431
29.5	451	450	*	415	421
30.0	451	450	*	415	415
30.5	452	449	*	415	409
31.0	452	449	*	415	403
31.5	453	449	*	415	399
32.0	453	449	*	415	390
32.5	453	448	*	415	383
33.0	453	448	*	415	320
33.5	155	454	*	415	374
34.0	454	447	*	414	366
34.5	453	446	*	414	361
35.0	454	453	*	415	359
35.5	453	445	*	413	350
36.0	454	452	*	414	345
36.5	453	444	*	412	341
37.0	453	452	*	414	100
37.5	452	442	*	412	97
38.0	453	452	*	414	95
38.5	451	440	*	409	94
39.0	452	451	*	413	93
39.5	450	438	*	408	94
40.0	451	450	*	411	93
40.5	449	436	*	406	94
41.0	450	449	*	410	93
41.5	449	434	*	405	93
42.0	448	447	*	409	92

* denotes thermocouple failure

TABLE 9 STEEL AND ADJACENT ATMOSPHERE TEMPERATURES RECORDED ON SPECIMEN X.

TIME (min)	TEMPERATURE (DEG C)					
	1.5m position			0.5m position		Fce Atm
	Flange	Web	Flange	Flange	Web	
0.0	13	13	13	12	13	13
0.5	13	12	12	12	13	14
1.0	13	13	13	12	13	30
1.5	13	12	13	12	13	82
2.0	15	13	15	14	13	153
2.5	22	18	22	19	18	220
3.0	29	23	28	24	21	311
3.5	39	38	39	42	21	553
4.0	49	48	49	52	31	847
4.5	59	58	59	62	42	768
5.0	78	68	89	71	66	794
6.0	115	100	129	100	105	829
6.5	124	115	138	122	116	881
7.0	134	120	142	123	129	731
7.5	145	127	235	131	130	922
8.0	149	142	201	142	137	1016
8.5	156	150	191	149	144	1009
9.0	165	153	188	150	151	961
9.5	171	162	173	161	157	900
10.0	174	168	*	163	160	884
10.5	185	163	*	168	172	195
11.0	179	177	*	177	166	188
11.5	184	178	*	180	171	185
12.0	198	174	*	181	184	169
12.5	194	182	*	186	182	170
13.0	202	184	*	190	191	175
13.5	199	190	*	194	188	180
14.0	208	190	*	196	197	175
14.5	204	196	*	199	193	175
15.0	204	202	*	205	193	177
15.5	223	191	*	200	211	163
16.0	207	210	*	212	195	175
16.5	210	213	*	214	196	165
17.0	233	196	*	207	217	146
17.5	216	214	*	217	201	156
18.0	236	202	*	215	219	139
18.5	226	215	*	219	209	143
19.0	237	210	*	223	219	131
19.5	233	218	*	222	215	132
20.0	239	217	*	228	221	130
20.5	239	220	*	226	220	126
21.0	243	221	*	233	224	115
21.5	245	222	*	230	225	110
22.0	247	225	*	238	227	110
22.5	250	225	*	234	230	104
23.0	250	230	*	242	231	104
23.5	225	229	*	238	235	97
24.0	256	230	*	239	237	95
24.5	257	232	*	241	239	92
25.0	259	234	*	242	241	89
25.5	260	235	*	244	243	87
26.0	261	237	*	245	244	84
26.5	262	238	*	246	245	83
27.0	264	242	*	249	249	83
27.5	265	243	*	250	250	80
28.0	264	249	*	256	249	81
28.5	265	251	*	257	251	80
29.0	268	249	*	253	254	75
29.5	269	250	*	254	255	71
30.0	270	252	*	255	257	70
30.5	270	253	*	257	258	68
31.0	271	255	*	257	259	67
31.5	272	257	*	258	260	66
32.0	273	258	*	259	261	66
32.5	273	260	*	260	262	65
33.0	274	261	*	261	263	65
33.5	275	265	*	265	264	65
34.0	275	264	*	262	265	62
34.5	276	265	*	263	266	61
35.0	278	268	*	266	267	63
35.5	277	268	*	264	267	60
36.0	279	270	*	267	270	59
36.5	277	271	*	266	268	57
37.0	281	272	*	267	272	57
37.5	278	274	*	267	269	56
38.0	282	273	*	268	273	53
38.5	279	276	*	268	270	55
39.0	284	275	*	268	275	53
39.5	280	278	*	269	271	53
40.0	285	279	*	269	276	52
40.5	280	283	*	268	272	53
41.0	286	279	*	269	277	50
41.5	281	281	*	269	273	52
42.0	286	280	*	270	277	49

* denotes thermocouple failure

TABLE 10 STEEL AND ADJACENT ATMOSPHERE TEMPERATURES RECORDED ON SPECIMEN Y.

TIME (min)	TEMPERATURE (DEG C)				
	1.2m position			0.3m	FCE AIR
	Flange	Web	Flange	Flange	
0.0	13	11	13	12	12
0.5	12	11	13	12	16
1.0	13	11	13	12	30
1.5	13	11	13	13	70
2.0	13	13	12	15	128
2.5	18	18	17	20	193
3.0	20	23	20	26	269
3.5	28	33	28	39	610
4.0	39	44	39	59	862
4.5	54	59	54	82	803
5.0	60	65	59	85	790
6.0	93	94	89	116	928
6.5	94	98	99	139	901
7.0	158	147	108	154	1023
7.5	138	129	118	166	1033
8.0	137	91	132	179	1012
8.5	151	105	143	189	1057
9.0	172	209	150	197	997
9.5	131	139	164	206	899
10.0	196	191	171	213	879
10.5	179	178	181	219	851
11.0	200	202	187	225	860
11.5	207	209	194	231	868
12.0	206	205	202	237	846
12.5	223	225	208	244	873
13.0	217	218	214	249	872
13.5	235	238	220	255	874
14.0	227	230	227	260	853
14.5	253	252	233	267	869
15.0	255	257	238	272	854
15.5	243	244	244	275	844
16.0	270	274	245	290	861
16.5	271	277	249	295	847
17.0	260	257	266	289	819
17.5	280	264	261	299	832
18.0	274	271	272	295	826
18.5	286	288	274	301	803
19.0	285	284	280	303	789
19.5	293	295	284	307	769
20.0	295	294	290	309	752
20.5	300	302	292	313	730
21.0	303	302	298	315	713
21.5	307	308	300	318	692
22.0	311	310	305	321	674
22.5	314	315	307	324	662
23.0	319	318	312	327	628
23.5	321	322	315	329	603
24.0	324	325	317	331	603
24.5	326	328	320	333	591
25.0	329	331	323	335	564
25.5	331	335	326	337	554
26.0	333	337	328	339	553
26.5	334	339	330	340	530
27.0	338	344	334	343	509
27.5	340	345	335	344	500
28.0	342	347	338	345	487
28.5	345	350	341	347	476
29.0	346	352	342	348	470
29.5	348	354	343	349	458
30.0	350	357	345	351	454
30.5	352	359	347	352	440
31.0	353	361	349	353	429
31.5	355	362	351	354	420
32.0	357	364	353	356	412
32.5	358	366	354	357	406
33.0	360	368	356	358	391
33.5	362	370	359	359	390
34.0	363	371	360	360	386
34.5	364	372	361	361	383
35.0	367	374	364	362	381
35.5	367	375	364	362	379
36.0	369	377	366	363	365
36.5	369	377	366	364	362
37.0	371	379	369	365	359
37.5	371	380	369	365	357
38.0	373	381	371	366	352
38.5	373	382	371	366	326
39.0	375	383	373	367	324
39.5	375	383	373	367	319
40.0	377	385	375	368	317
40.5	376	385	375	368	307
41.0	379	386	377	369	295
41.5	377	387	376	369	285
42.0	380	388	378	369	279

TABLE 11 STEEL AND ADJACENT ATMOSPHERE TEMPERATURES RECORDED ON SPECIMEN Z.

TIME (min)	TEMPERATURE (DEG C) FLANGE	WEB	FLANGE	AIM 6
0.0	13	13	13	13
0.5	13	13	13	17
1.0	14	15	13	41
1.5	17	20	17	139
2.0	24	31	24	231
2.5	35	47	34	332
3.0	51	69	52	428
3.5	75	104	82	529
4.0	124	165	134	729
4.5	200	248	195	939
5.0	284	330	263	946
5.5	365	405	334	953
6.0	442	485	413	976
6.5	511	549	485	989
7.0	575	612	557	1040
7.5	637	673	628	1078
8.0	688	721	682	1014
8.5	721	753	726	923
9.0	736	768	748	871
9.5	740	778	752	826
10.0	744	790	763	826
10.5	748	793	769	819
11.0	751	795	773	796
11.5	753	794	775	784
12.0	756	792	776	787
12.5	758	792	778	788
13.0	760	794	780	787
13.5	763	798	782	785
14.0	764	800	782	789
14.5	767	801	784	784
15.0	769	802	784	794
15.5	769	801	786	779
16.0	768	797	784	771
16.5	766	791	781	756
17.0	764	787	777	747
17.5	762	778	772	731
18.0	757	771	767	719
18.5	752	763	760	702
19.0	746	754	752	680
19.5	737	747	745	671
20.0	731	739	738	645
20.5	721	730	730	627
21.0	715	721	723	608
21.5	706	712	715	591
22.0	697	701	706	568
22.5	689	691	697	544
23.0	679	679	686	526
23.5	673	669	677	507
24.0	672	665	670	495
24.5	667	664	670	478
25.0	659	657	665	463
25.5	649	647	657	454
26.0	639	636	647	445
26.5	629	624	636	433
27.0	618	613	624	423
27.5	608	601	612	416
28.0	594	587	599	402
28.5	588	580	591	396
29.0	578	571	580	392
29.5	569	562	570	384
30.0	560	553	560	380
30.5	551	544	551	373
31.0	542	536	543	365
31.5	534	528	534	354
32.0	526	520	525	351
32.5	518	513	517	347
33.0	511	506	509	339
33.5	504	499	502	334
34.0	497	492	494	327
34.5	490	485	487	320
35.0	483	478	480	315
35.5	476	472	473	313
36.0	470	466	467	310
36.5	464	460	460	305
37.0	457	453	454	296
37.5	451	448	447	290
38.0	445	442	441	286
38.5	440	436	435	280
39.0	434	431	430	275
39.5	428	426	424	272
40.0	424	420	418	267
40.5	419	415	413	267
41.0	413	411	408	259
41.5	409	406	403	256
42.0	404	401	398	252

TABLE 12 STEEL AND ADJACENT ATMOSPHERE TEMPERATURES RECORDED AT 2.0 m LEVEL ON THE UNPROTECTED 203x203 mm x 52 kg/m COLUMN.